Advances in Heterocyclic Synthesis through Ring Expansions and Flow Chemistry

By

Manwika Charaschanya

Submitted to the graduate degree program in Department of Medicinal Chemistry and the Graduate Faculty of the University of Kansas in partial fulfillment of the requirements for the degree of Doctor of Philosophy.

Chairperson: Dr. Thomas Prisinzano

Co-chairperson: Dr. Jeffrey Aubé

Dr. Helena C. Malinakova

Dr. Stevan W. Djuric

Dr. Jon A. Tunge

Date Defended: April 27, 2018

The dissertation committee for Manwika Charaschanya certifies that this is the approved version of the following dissertation:

Advances in Heterocyclic Synthesis through Ring Expansions and Flow Chemistry

Chairperson: Dr. Thomas Prisinzano

Co-chairperson: Dr. Jeffrey Aubé

Date approved: April 27, 2018

Abstract

This dissertation comprises three chapters, which focus on the development of new synthetic methodologies and the construction of a screening collection.

An Application of the Schmidt Reaction: Construction of an Azasteroid Library. Ring expansion chemistry is a powerful way of introducing a heteroatom substituent into carbocyclic frameworks. However, such reactions are limited by the tendency of a given substrate to afford only one of the two rearrangement products or fail to achieve selectivity at all. These limitations may prove critical when seeking to carry out late-stage functionalization of natural products as starting points in drug discovery. In this chapter, a stereoelectronically controlled ring expansion sequence towards selective and flexible access to complementary ring systems derived from commercial or readily synthesized steroidal substrates of the A- and D-rings is described. A requisite intermediate in the reaction was leveraged to afford over one hundred isomerically pure analogs with spatial and functional diversity. This regiodivergent rearrangement, and the concept of using chiral reagents to effect regiocontrol in chiral natural products, adds value to late-stage natural product diversification programs.

New Variations of the Schmidt Reaction. A strong hydrogen-bond-donating solvent, hexafluoro-2-propanol (HFIP), was found improve the intermolecular reaction of ketones with trimethylsilyl azide and hydroxyalkyl azides. This study prompted the hypothesis for interrupting the classic Schmidt reaction with an added nucleophile reagent in HFIP. An extensive acid screen identified aluminum tribromide as a promoter for intercepting the Schmidt reaction iminium ion

intermediate and combining it with subsequent reaction with 1,3,5-trimethoxybenzene to form substituted imines, enamides, and amines. This new variation of the Schmidt reaction provided access to unique heterocycles.

Enabling Chemistry Technologies: High-Temperature and High-Pressure Continuous Flow Chemistry. The synthetic applications of a high-temperature and high-pressure flow reactor were investigated. The Gould-Jacobs reaction, nucleophilic aromatic substitution reaction with amine nucleophiles, and *tert*-butyloxycarbonyl deprotection in flow were explored. The protocols developed were applied to the high-throughput preparation of small-molecule libraries, as well as reaction telescoping, automation, and scaling.

Acknowledgements

First and foremost, I thank my advisor, Professor Jeffrey Aubé, for his unwavering support and mentorship over the past several years. Under his guidance, I have grown professionally, and he has inspired scholarly excellence, scientific creativity, and passion, which I hope to instill in my career. Professor Aubé's mentorship has reinforced my desired to perform scientific research and achieve my professional goals. I thank the entire faculty of the Medicinal Chemistry department for their teaching, expertise, and support throughout my graduate career. Particularly, I would like to thank the members of my oral and defense committees, Professors Thomas Prisinzano, Mike Rafferty, Jon A. Tunge, Helena C. Malinakova, and Blake R. Peterson, and Dr. Stevan W. Djuric, for their time and advice.

I would like to thank Norma Henley, Shelley Sandberg and Barbara Dearry for administrative assistance. I am also sincerely grateful to Drs. Victor W. Day, Patrick Porubsky, Ben Neuenswander, Justin Douglas, Karl Koshlap, and Brandie Ehrmann for their assistance with X-ray, NMR and MS analysis. I would like to acknowledge the University of Kansas at Lawrence and the University of North Carolina at Chapel Hill for financial support.

I would like to thank the staff in the high-throughput chemistry group, structural chemistry group, analytical and purification group of AbbVie for chemistry, purification, and analysis support of the studies carried out in Chapter 3. Specifically, I thank Drs. Andrew Bogdan, Ying Wang, Amanda Dombrowski, Jennifer Tsoung, and Justin Dietrich from high-throughput chemistry for collaborations and helpful discussions, as well as, Drs. Rick Yarbrough, Jan Waters, and Dave Whittern for structural chemistry support, Maurice Pheil for IR support, and Erin Jordan

for chiral chromatography support. I would like to acknowledge AbbVie for financial support of the studies carried out in Chapter 3.

I express my sincere gratitude to the former and current members of the Aubé group involved in fostering my research and laboratory skills, Drs. Hashim F. Motiwala, Sarah M. Scarry, Gurpreet Singh, Kevin Frankowski, and Mike Bovino. Also, I am grateful to my colleagues at KU and UNC for stimulating scientific discussion and my countless friends (especially Sarah M. Scarry and Molly Lee) for their continual motivation and support.

Finally, I would like to thank my parents, Suwanna and Suthep Charaschanya, my brothers, Manop and Nick Charaschanya, my sister-in-law, Manhar Sachasingh, and my cousin sister, Dr. Karampreet Sachdev, for their unconditional love, understanding, and support.

Table of Contents

List of Figures

Chapter 3

List of Schemes

Chapter 3

List of Tables

Chapter 3

List of Abbreviations

Abbreviation	Definition
[α]	Specific rotation (measured at 589 nm)
α	Alpha, stereodescriptor; below the plane of rings
Ac	Acetyl
AcBr	Acetyl bromide
AcCl	Acetyl chloride
Anal	Combustion elemental analysis
APT	Attached proton test
aq	Aqueous
β	Beta, stereodescriptor; above the plane of rings
bp	Boiling point
BOC, Boc	*tert*-Butoxycarbonyl
br	Broad signal (spectra)
n-Bu	Normal (primary) butyl
t-Bu	*tert*-Butyl
˚C	Degrees Celsius
^{13}C NMR	Carbon nuclear magnetic resonance
calcd	Calculated
CCDC	Cambridge Crystallography Deposit Center
CBZ	Benzyloxycarbonyl
cm^{-1}	Wavenumber(s)
COSY	Correlation spectroscopy (^1H-^1H)
CH_2Cl_2	Dichloromethane
m-CPBA	*meta*-Chloroperoxybenzoic acid
Cy	Cyclohexyl
EtOH	Ethanol
DCE	1,2-Dichloroethane
DIAD	Diisopropyl azodicarboxylate
DHT	Dihydrotestosterone

DMA	*N,N*-Dimethylacetamide
DMAP	4-(*N,N*-Dimethylamino)pyridine
DMF	*N,N*-Dimethylformamide
DMSO	Dimethyl sulfoxide
DoE	Design-of-Experiment
D_2O	Deuterium oxide
DPE	Diphenyl ether
DPPA	Diphenylphosphoryl azide
dr	Diastereomeric ratio
ee	Enantiomeric excess
er	Enantiomeric ratio
ESI	Electrospray ionization
Et	Ethyl
EtOAc	Ethyl acetate
equiv	Equivalent(s)
FTIR	Fourier transform infrared
g	Gram
h	Hour(s)
^{1}H NMR	Proton nuclear magnetic resonance
HESI	Heated electrospray ionization
HBr	Hydrobromic acid
HCl	Hydrochloric acid
HFIP	Hexafluoro-2-propanol or 1,1,1,3,3,3-Hexafluoro-2-propanol
HMBC	Heteronuclear multiple-bond correlation
HPLC	High-performance liquid chromatography
HRMS	High-resolution mass spectrometry
HSQC	Heteronuclear single-quantum correlation spectroscopy
Hz	Hertz (spectral)
IR	Infrared
J	Coupling constant (spectral)
L	Liter(s)

LAH	Lithium aluminum hydride in THF
LCMS	Liquid chromatography-mass spectrometry
LDA	Lithium diisopropylamide
m	milli; multiplet (spectral)
M	Molar; mega (spectral)
Me	Methyl
MeCN	Acetonitrile
MeOH	Methanol
min	Minutes
mmol	Milli-mole(s)
mp	Melting point
MS	Mass spectrometry
m/z	Mass-to-charge ratio
NaH	Sodium hydride 60% mineral oil dispersion
NOE	Nuclear Overhauser effect
NMR	Nuclear magnetic resonance
Nu	Nucleophile
PCC	Pyridinium chlorochromate
Pd/C	Palladium on carbon
Phenyl	Ph
i-Pr	Isopropyl
ppm	Part(s) per million
R	Stereochemistry element
R_f	Retention factor (in chromatography)
rt	Room temperature
s	Singlet (spectral)
S	Stereochemistry element
S_NAr	Nucleophilic aromatic substitution
S_N2	Bimolecular nucleophilic substitution
t	Triplet (spectral)
TBS	*tert*-Butyldimethylsilyl

TBAF	Tetrabutylammonium fluoride
TEA	Triethylamine
TFA	Trifluoroacetic acid
TFE	2,2,2-Trifluoroethanol
TfOH	Triflic acid or trifluoromethanesulfonic acid
THF	Tetrahydrofuran
TLC	Thin-layer chromatography
TMS	Trimethylsilyl
$TMSN_3$	Trimethylsilyl azide
TOF	Time-of-flight
t_R or RT	Retention time (in chromatography)
p-TsOH	*para*-Toluenesulfonic acid
μ	micro
UPLC	Ultra-performance liquid chromatography
UV	Ultraviolet

Chapter 1

An Application of the Schmidt Reaction: Construction of an Azasteroid Library

1.1 Introduction

1.1.1 Strategies Towards Development of Screening Libraries

Over the last two decades high-throughput screening (HTS) has become a staple in early stage drug and probe discovery.[1-5] The HTS format is a proven scientific toolkit for the identification of starting points for medicinal chemistry campaigns, and indeed has led to the development of many approved U.S. Food and Drug Administration (FDA) drugs (>19 drugs) such as imatinib (Gleevec), sorafenib (Nexavar), and maraviroc (Selzentry).[2-4] Although HTS is a highly effective strategy, the success of HTS in discovery is defined by a number of factors including the quality of targets, bioassays, detection techniques, compound screening collections, and others. In this section, I focus on the composition of compound screening collections as an essential aspect for the advancement of drug discovery and chemical biology programs.

The composition of compound collections has evolved from the early 1990s, where simply collections of chemicals and crude natural products were screened.[1, 3] Screening libraries continuously evolved because researchers have become more aware of the variable suitability of molecules for biological investigations. Modern efforts have focused on constructing chemical libraries that expand the traditional chemical space to consider physiochemical and diversity properties; e.g., to incorporate molecules with higher levels of sp^3-content and three-dimensionality (stereogenic centers) or filtered to comply with Lipinski's Rule-of-Five and drug-like properties. In this direction, numerous strategies have been devised to source molecules for HTS, which include among others, combinatorial chemistry, "diversity-oriented synthesis"

(Schreiber[6]), "biologically-oriented synthesis" (Waldmann[7]), and natural-product inspired libraries (Aubé[8] and Hergenrother[9]). Mindfully, these strategies are under constant revision as scientists continue to seek out collections that yield the most probable results for their biological inquisition.

First and foremost, the advent of combinatorial chemistry demonstrated the feasibility of synthesizing large compound collections. In fact, Merrifield's publication[10] on solid-phase peptide synthesis and Ellman's publication[11] on the library synthesis of 1,4-benzodiazepines paved the groundwork for combinatorial chemistry. However, early combinatorial libraries were predominantly peptide-centric, resulting in collections with poor physiochemical and diversity properties.[1] Moreover, in early combinatorial days, it became apparent that majority of biological targets could not be addressed through the use of common libraries comprising of structurally similar compounds. Thus, efforts were made to expand into new chemical space, which led to the renewed investments in natural products, development of new synthetic strategies, and contemporary late-stage functionalization (discussion in section 1.3).

Diversity-oriented synthesis (DOS), coined by Stuart Schreiber in the late 1990s, was developed to complement combinatorial chemistry namely by increasing complexity and diversity compositions within library collections.[6] The DOS program adopted a divergent synthesis approach, particularly employing organic chemistry that would achieve efficient generation of chemical scaffolds in a way that maximized diversity and provided appendages for post-screening optimization. Amongst these efforts were the execution of short syntheses guided by a build-couple-pair algorithm, and assessment of libraries by chemoinformatics determined the coverage of new chemical space.[12-14] Indeed, it has been shown that DOS collections aided in the discovery of antibiotics as well as molecules for challenging targets such as epigenetic

enzymes and protein-protein interactions.[13] Another complementary approach to combinatorial chemistry for library construction is biology-oriented synthesis (BOS), which was conceived by Herbert Waldmann.[7] The BOS program employed chemocentric analysis as a hypothesis-generating tool to identify compound classes based on the structural conservation stemming from the coevolution of proteins and natural products/ligands (e.g., hierarchical classification of compounds annotated by Structural Classification of Natural Products–SCONP, bioactivity, or target information).[7] Basically, BOS helped to identify scaffolds that are enriched in biological activity as starting points for medicinal chemistry research, and generally these scaffolds may be natural products or non-natural compound classes such as pharmaceutical agents. The conceptual framework of BOS is notable because the logic outlined a biological prevalidation of natural product structures as well as a guided basis of library design towards successful discovery of chemical tools for various biological targets.

In addition to Waldmann, other approaches were initiated in recent years that revisited natural products for library construction and synthetic tractability in medicinal chemistry. For example, Aubé and coworkers synthesized a compound collection resembling four families of biologically active alkaloids.[8] Using enabling azide chemistry, the diverse set of natural product-inspired compounds synthesized was comparable in structural complexity and sp^3 content to their guiding natural products. On the other hand, Hergenrother and coworkers started from commercially available natural products; they developed a divergent synthesis approach to systematically distort ring systems forming new scaffolds that were significantly more complex and diverse than those in the standard screening collections.[9, 15] Historically, natural products or their analogs were considered as end points in discovery research; however, Waldmann and other

researchers have shown how modern thinking can give rise to new and fruitful platforms for medicinal and chemical biology research.

In this chapter, the approaches discussed above are acknowledged in our library design and development of azasteroids—nitrogen-containing steroids. This library was designed to use readily available steroids as the starting point for systematic transformations to afford a diverse set of compounds in equal complexity. It is known that steroid-based analogs have continued to demonstrate biological importance, and the substructure is broadly considered as a successful drug and natural product chemotype. Despite this, there are only a few reports of steroid-based libraries for screening purposes.[9, 16-18] Herein, a re-imagination of the steroid substructure was conceived with enabling azide chemistry precedent within our research group. As such, an approach to a steroid-like screening library may become useful in the pursuit of new biology.

1.1.2 Steroids: Structure, Biosynthesis, and Implications in Drug Discovery

Steroids and related triterpenoids belong to a broad class of secondary metabolites called terpenes (terpenoids or isoprenoids). In this classification, the defining carbon skeleton of the substructure originates from the same 5-carbon building block, isoprene. Although the terpene structural feature does not resemble the 'typical' therapeutics (heterocycles or planar aromatics), as secondary metabolites terpenes have been tailored to interact with various biological targets.

Commonly, steroids have a tetracyclic molecular framework that consists of seventeen carbons arranged as four interconnected rings: three six-membered rings and a five-membered ring; formally denoted as A, B, C, and D ring respectively (Figure 1.1).[19-20] Steroids may contain additional carbons, functional groups, and a variety of oxidation states. There are fundamental structural properties of steroids: (1) in two-dimensional representation, the steroid scaffolds

appear planar and substituents on the carbon skeleta may be located above or below the plane, designated as α- and β-substituents, respectively, (2) in three-dimensional representation, the steroid rings are actually not planar, but generally exist in the preferred chair orientation; as a result substituents can be located in axial or equatorial positions, (3) steroids are generally rigid because they have at least one *trans*-fused ring system, and (4) commonly, two possible ring fusions are observed between A and B, where the ring junction can assume *trans*- or *cis*-isomerism, that is, 5α and 5β stereoisomeric forms.[19-20]

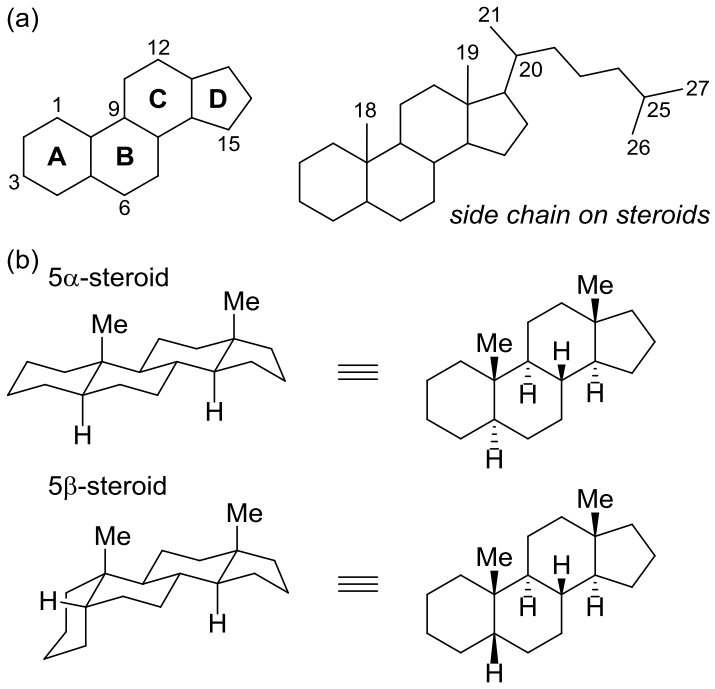

Figure 1.1. Introduction to steroids. (a) Representation of tetracyclic ABCD rings and numbering system. (b) Representation of *trans*- and *cis*-fused AB rings.

While the biosynthetic pathway of steroids is not universal to all organisms, they are typically biosynthesized by consecutive condensation of isoprene units. For example, the biosynthesis of cholesterol from isoprene can be outlined into two major stages: (a) conversion of acetyl-coenzyme A substrates to a C_{30} hydrocarbon squalene, and (b) the conversion of

squalene to cholesterol.[20] The rate-limiting step in cholesterol biosynthesis is the mevalonate pathway towards the synthesis of squalene epoxide. Specifically, the enzymatic step is irreversible (enzyme: hydroxyl-3-methylglutaryl-coenzyme A or HMG-CoA), and has become an important therapeutic target for the regulation of cholesterol biosynthesis. The second major stage is a well-known electrophilic cyclization the advances squalene to the preliminary steroid tetracycle. In general, cholesterol is an essential component of cell membranes, and a critical lipid-precursor to endogenous hormones, bile acids, and vitamin D.[20]

Numerous therapeutic agents and chemical probes are based on steroid skeleta, with new examples continuing to appear in the clinic (Figure 1.2a). In this field, discovery efforts have generated over 100 FDA approved steroidal agents as therapeutics and are prescribed for various indications including inflammation, pain, hormone therapy, cancer, and more (Figure 1.2b).[19-20] Arguably, steroidal analogs are one of the most successful classes of natural product-inspired pharmaceuticals, and deserve to be described as a 'privileged scaffold' for biomedical research. Since the early days, steroid modifications were based on semisynthesis strategies, whereby available natural steroids were chemically altered to provide new steroid collections. Historical examples include Merck's bile acid-to-cortisone process,[21] Marker's degradation from plant-derived steroid diosgenin into sex hormones,[22] and Djerassi's semisynthetic pursuit of the first oral contraceptive[23-24] (progestin, Figure 1.2b). While industrial access to important steroids via de novo syntheses remains an ongoing challenge, semisynthesis of steroids have continued to play a valuable role in both academic endeavors and commercialization of steroid-based medicines.[25-26]

There have been a number of investigations on the incorporation of nitrogen-heteroatoms as part of the steroidal framework with or without alterations of ring size, as well as attached as

part of functional groups, side chains, or additional fused ring systems.[27-28] The preparation of nitrogenous steroids has proven to be of biological interest, with two successful examples including dutasteride[29] and abiraterone acetate[30] (Figure 1.2c). The 4-azasteroids (e.g., dutasteride) have attracted interest because many exhibit strong inhibition of the enzyme 5α-reductase,[29] which catalyzes the conversion of testosterone to the more potent androgen dihydrotestosterone (DHT), as well as, inhibition of the androgen receptor.[31-32] This enzyme and receptor both serve as important regulators of male sex hormones, as a result have become clinical targets for the treatment of prostate cancer and male physiology-related diseases.[33-34] In 2001, dutasteride was approved by the FDA for the treatment of benign prostatic hyperplasia, and was found to be an irreversible inhibitor of 5α-reductase. Dutasteride is semisynthesized from testosterone-17-carboxylic acid as shown in Scheme 1.1.[35-36] In relation to prostate steroidogenesis, abiraterone acetate was marketed in 2011 for the treatment of metastatic castration-resistant prostate cancer. On the contrary, abiraterone inhibits cytochrome P450 C17A1 (CYP17α-hydroxylase and CYP17α-lyase) enzyme, another key enzyme involved in the biosynthesis of androgens specifically in the conversion of pregnenolone to dehydroepiandrostereone.[30, 34] The pyridyl-containing drug was synthesized from readily available dehydroepiandrosteron-3-acetate using a palladium-catalyzed cross-coupling reaction of 17-enol triflate.[37] Abiraterone is an effective binder of CYP17A1 because of the heterocyclic nitrogen that coordinates to the heme iron of the target enzyme, which also allows additional 3β-OH hydrogen-bonding interactions.[38] In searches for cancer therapeutics, other D-ring nitrogen-heterocyclic steroids have been shown to inhibit the CYP17A1 enzyme,[26, 38] as well as, to possess antiproliferative activities through other mechanisms of action (e.g., antiangiogenic activity of cortistatins[39]).[40-41]

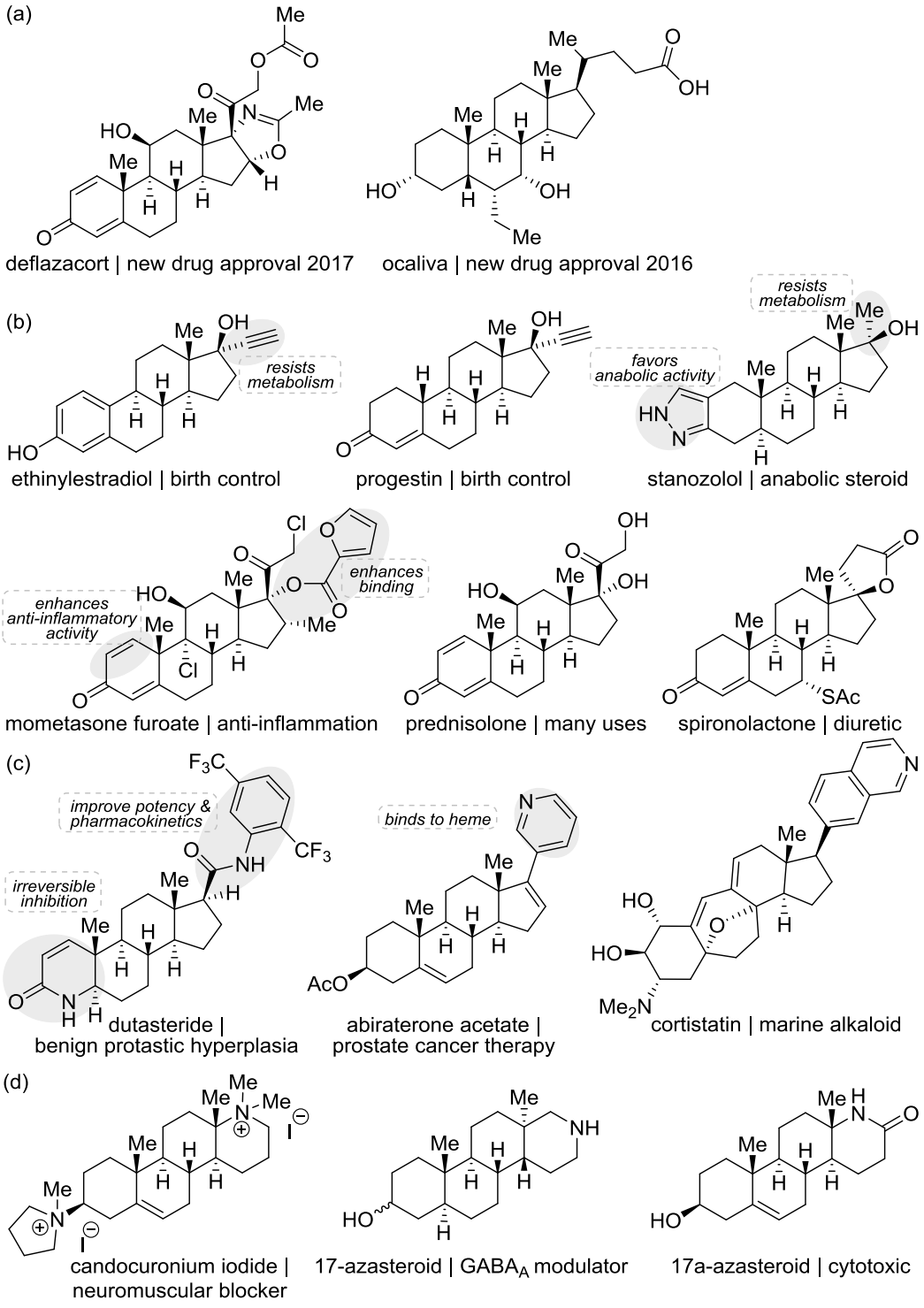

Figure 1.2. Representative examples of biologically important steroids. (a) Recent drug approvals. (b) Examples of common steroid therapy. (c) Examples of anti-cancer agents, (d) Examples of reported 17-azasteroids with biological activities. Agents are shown with emphasis on A- and D-ring structure-activity relationships.

Scheme 1.1. Synthesis of dutasteride.[a]

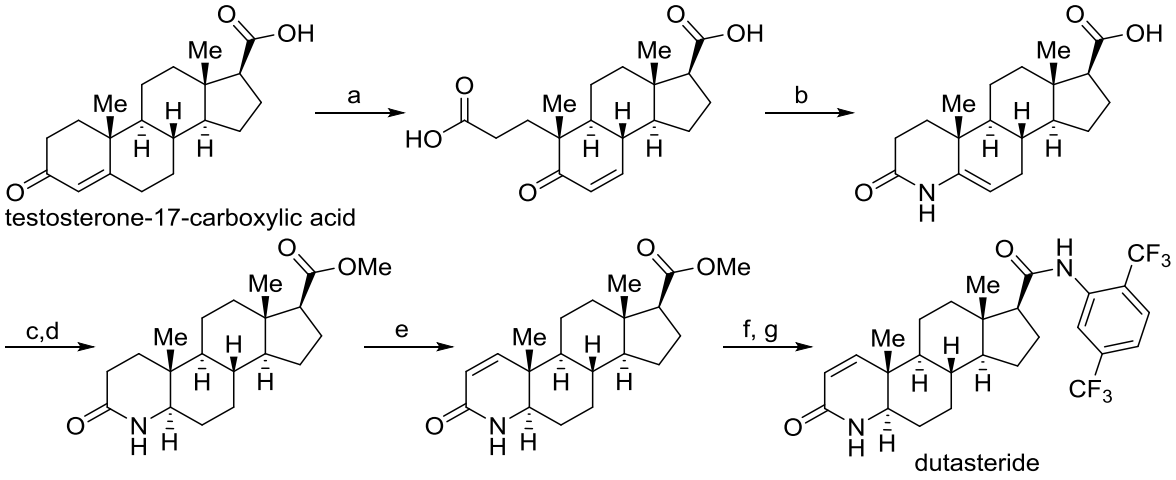

[a]Reagents and conditions: (a) aq. $NaMnO_4$, $NaIO_4$, *tert*-butanol, 75 °C, (b) ethylene glycol, NH_3, 180 °C, (c) acetic acid, PtO_2, H_2/50 psi, (d) MeOH, H_2SO_4, (e) DDQ, (f) MeOH, H_2O, (g) $SOCl_2$, aniline, toluene/CH_2Cl_2/THF, 70 °C.

Scheme 1.2. Synthesis of abiraterone acetate.[a]

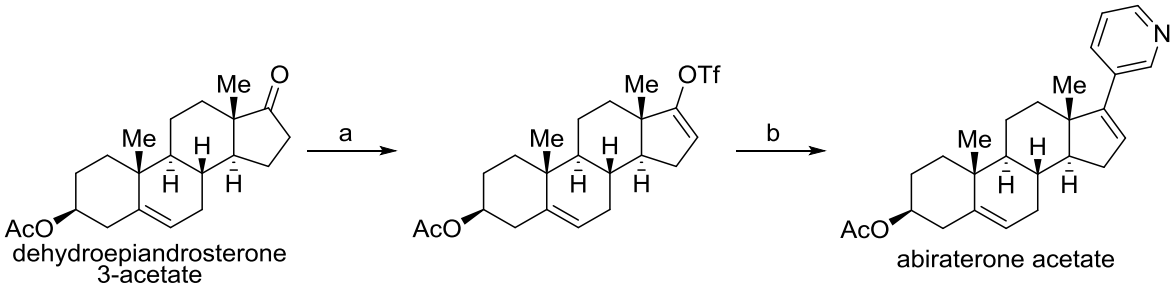

[a]Reagents and conditions: (a) Tf_2O, (b) 3-PyBEt_2, $Pd(PPh_3)_2Cl_2$, THF, H_2O, Na_2CO_3, (c) NaOH, H_2O, MeOH.

Candocuronium iodide is a potent neuromuscular blocker, exemplifying a bioactive 17-azasteroids.[42] Since its discovery, many 17-azasteroids have been investigated for potentially useful biological activities such as modulation of GABA receptors[43] and 5α-reductase enzyme, and for anti-cancer treatments[40-41, 44] (Figure 1.2d). These examples of nitrogen-containing steroids and related analogs can be found in review papers.[27-28] Although a number of nitrogen-

containing steroid analogs have been synthesized at various steroid positions, rarely have been developed into effective drugs.

1.1.3 Late-Stage Functionalization of Steroids

Late-stage functionalization has remained a long-standing and important paradigm in drug and probe discovery. The concept of late-stage functionalization is defined by the ability of a chemist to directly and selectively functionalize natural product-like and drug-like molecules in order to rapidly create new structures, and potentially alter their pharmacological profile. Particularly, this approach is suitable for research programs that involve rapidly accessing molecular diversity, exploring structure-activity relationships, and screening of library collections for biological activities.[45] Moreover, late-stage functionalization is useful because a synthetic route can efficiently generate analogs in few synthetic steps and without extensive redesign. However, there are many challenges associated with the direct functionalization of complex molecular structures, which include (1) carrying out reactions at one of the many identical functional groups (chemoselectivity, site selectivity), (2) controlling or overcoming dependence of the reactivity of one functional group, (3) controlling selectivity or overcoming substrate bias of product outcome, and (4) difficulty in isolation of pure products from mixtures.[46-47] Intrinsic to derivatizations of complex molecular frameworks are the numerous plausibility of stereoselectivity. In particular, within chiral molecular frameworks, diastereoselectivity and regioselectivity are inherent issues that require thoughtful considerations to overcome and achieve selective functionalization. Complex natural products continue to be quintessential in drug and probe discovery, as a result have been the cornerstone of studies for synthetic strategies, including that of late-stage functionalization. These efforts have been tried

on famous biologically relevant compounds such as erythromycin, vancomycin, amphotericin, digitoxin, and many more.[47] The application of late-stage functionalization to selectively modify steroids has historical prevalence, and as a biologically relevant framework steroid substrates remain under scrutiny to date.

Late-stage manipulation of steroid scaffolds is a worthwhile strategic advance for seeking new and more effective scaffold-related bioactivity, and accessing steroid-based natural products and drugs. In fact, the philosophical concepts and implications have been clearly demonstrated by early visionaries such as Breslow,[48] Barton,[49] Arigoni,[50] and Corey.[51-52] In the early 19th century, Corey and Arigoni independently applied the Hofmann-Löffler-Freytag reaction to aminosteroid synthesis. The Hofmann-Löffler-Freytag (HLF) reaction is the photochemical decomposition of *N*-haloamines that results in direct functionalization of distal unactivated aliphatic C-H bonds. Specifically, the N-X bond homolyzes to form a nitrogen radical capable of intramolecular hydrogen atom abstraction; this in turn, provides a carbon radical that recombines with the halogen species to undergo nitrogen-mediated nucleophilic displacement. A fundamental example by Corey in the total synthesis of alkaloid dihydroconessine showcased functionalization of C-18 via the *in situ* formation of free radical from the decomposition of *N*-chloro-20-aminosteroid (Scheme 1.3a).[53] Following Corey's and Arigoni's investigation on C-18 functionalization using the HLF reaction, Barton and coworkers reported the semisynthesis of aldosterone from corticosterone, the main mineralocorticoid steroid, using the Barton reaction (Scheme 1.3b).[54] Barton's work is a photochemical reaction that involves homolytic RO-NO cleavage of an alkyl nitrite, followed by hydrogen abstraction, radical recombination, and tautomerization to oxime.[54] While mechanistically similar to the HLF reaction, together Barton,

Corey, and Arigoni were influential in providing the first examples of C-H activation chemistry, as well as the concept of late-stage functionalization of bioactive molecules.

Scheme 1.3. Historical examples of late-stage functionalization of steroids. (a) A synthetic step from Corey's synthesis of dihydroconessine. (b) Aldosterone acetate synthesis using the Barton reaction.

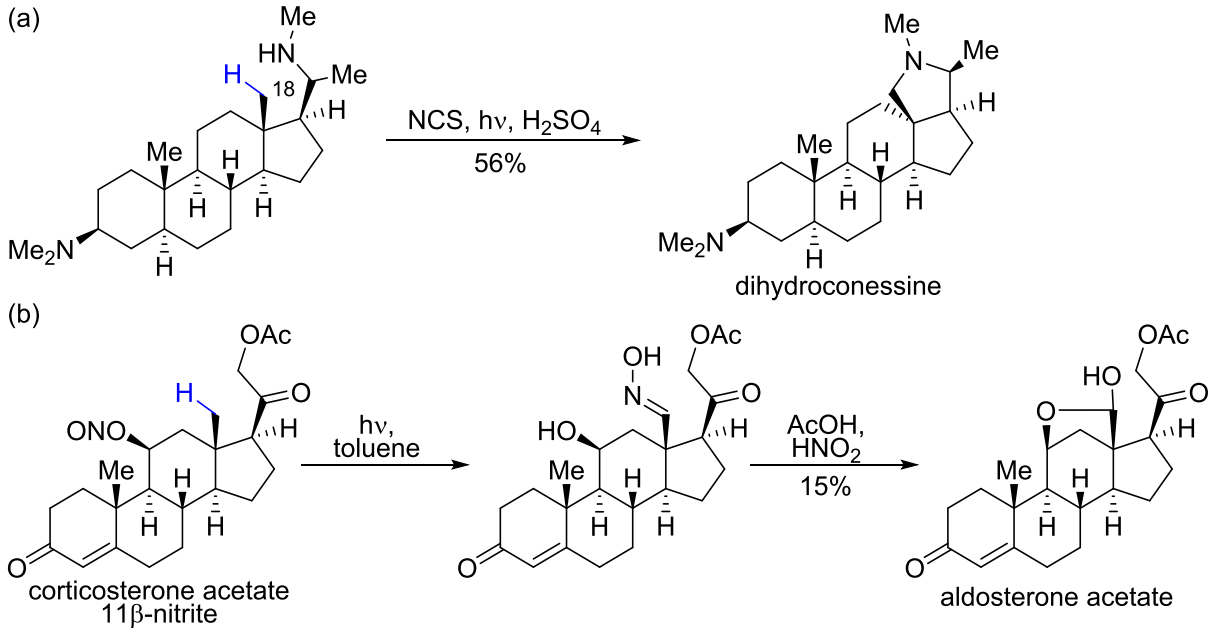

Furthermore, Breslow's research program pioneered a strategy to imitate nature's level of selective functionalization. Particularly, the concept posed mimicry of enzyme-substrate functional selectivity through appropriate geometry, which he termed the synthetic application as 'biomimetic'.[48] In this aspect, Breslow and coworkers used an oxidant (e.g., benzophenone) covalently attached to a substrate to mediate radical-driven functionalization (Figure 1.3). The site of C-H functionalization was dependent on the length and location of the tether, and such templates have been studied to catalyze remote functionalization at various positions of the steroid nucleus.[55] In the late 1990s, Breslow fostered the 'biomimetic' concept by development

of an artificial CYP450 enzyme (metalloporphyrin-based) that performed selective hydroxylations with catalytic turnover, unlike reagents that were originally designed and attached to the steroid nucleus.[55] Indeed, Breslow's excursion has inspired other researchers to develop biomimetic late-stage functionalization, such as Grieco's reports on related synthetic metalloporphyrins.[51, 56-57]

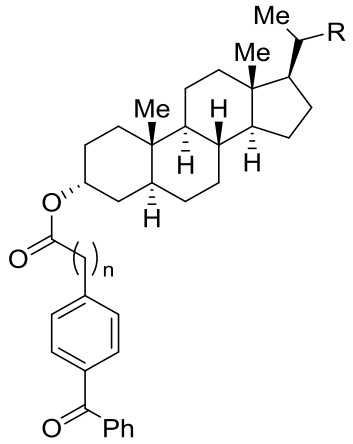

Figure 1.3. Functionalization of steroid nucleus using attached oxidants.

In recent years, contemporary C-H activation chemistry has exploded as a powerful approach to facilitate late-stage functionalization. In this context, C-H functionalization uses catalysts that exploit directing groups, or distinct differences in steric, electronic, or stereoelectronic properties of C-H bonds. In recent years, numerous research groups have developed a number of catalysts for this approach, which are based on small-molecules, transition metals,[58-59] peptides,[47, 60] or enzymes.[45, 61-62] Here, I will provide examples on recent efforts regarding the (1) late-stage introduction of nitrogen-substituents into complex molecules, and (2) late-stage functionalization of nitrogen- and heterocycle-containing substrates. Particularly, I will highlight papers that demonstrate modern examples of late-stage functionalization of steroid scaffolds.

Although the synthetic versatility of C-H activation chemistry is vast, the direct functionalization of natural product-like and drug-like molecules has been relatively limited. More promising methodologies further extend their applications towards complex bioactive molecules. For example, Hartwig[46] and Groves[63] have pursued the introduction of azides on representative complex molecules because this functionality can be easily converted to a range of nitrogen-containing functional groups, as well as, serve as attachment points for various probes through Huisgen "click" cycloadditions and Staudinger ligations (Figure 1.4a). Such reactions expand the chemistry toolbox for uses in medicinal chemistry settings. As a result, numerous developments of selective amination/amidation procedures with various catalytic systems have been a focus of intensive research.

One main issue in C-H functionalization is that nitrogen or heteroatoms present in substrates may bind preferentially to transition-metal catalysts rather than the desired directing group or site of functionalization for completion of the desired reaction.[64] This issue has hindered the application of C-H functionalization in late-stage derivatizations of nitrogen- and heterocycle drugs and probes. However, it must be noted that directing groups (including amides[65] and amines[66-67] directing groups) have been exploited as a major advantage and successful approach in this field (e.g., Baran, Figure 1.4b).[61] Because nitrogen and heterocycles are ubiquitous in drug discovery research, others have sought to find methodologies that tolerated the presence of such functionalities, and would allow modifications at different positions (especially, without the need to install and remove directing groups). For example, White and coworkers developed a nitrogen complexation strategy with strong acids, which enables remote oxidations of amine and pyridine-containing molecules.[68-69] Particularly, the authors showed that a salting strategy of amines (i.e., electronic deactivation) in conjunction with

iron catalysis effectively facilitates late-stage oxidation of medicinally relevant compounds (Figure 1.4b).[68-69]

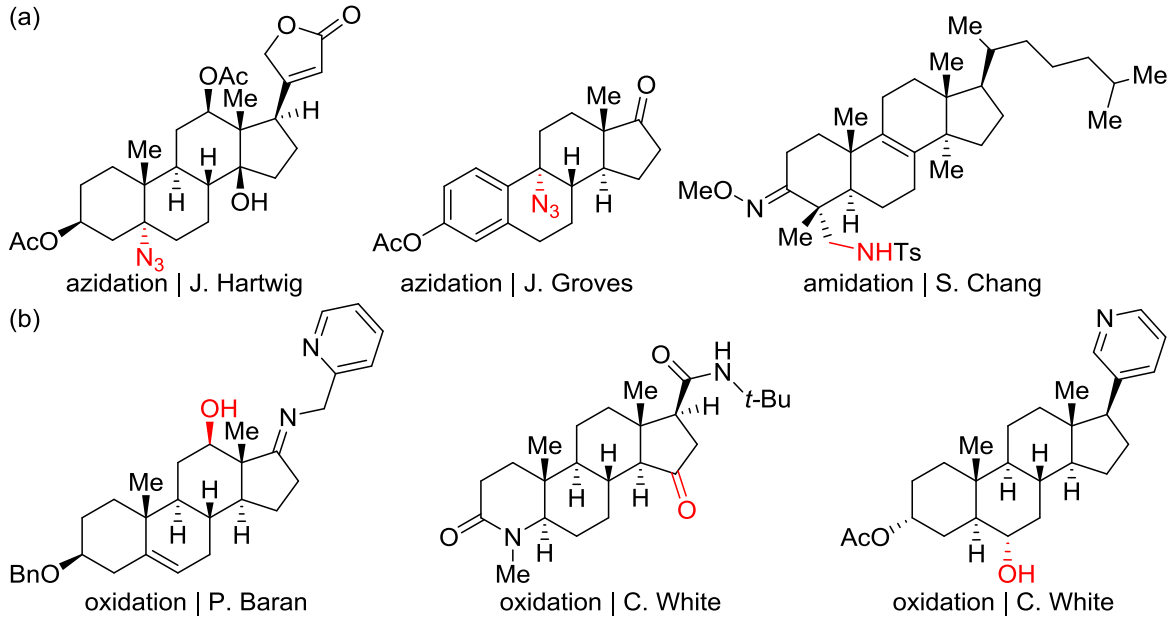

Figure 1.4. Modern examples of late-stage functionalization of steroids. (a) Late-stage introduction of nitrogen-substituents into complex molecules. (b) Late-stage functionalization of nitrogen- and heterocycle-containing substrates.

1.1.4 The Schmidt Reaction of Hydroxyalkyl Azides

The Beckmann rearrangement and the Schmidt reaction are two common ring-expansion transformations employed to insert a nitrogen heteroatom into a carbocyclic skeleton (Scheme 1.4). In 1886, the Beckmann rearrangement was discovered; it is a two-step transformation involving the conversion of a ketone to an oxime, followed by acid-mediated oxime rearrangement to afford an amide or lactam.[70] In contrast, the Schmidt reaction of ketones is a one-step transformation with azide reagents such as hydrazoic acid (HN_3) or sodium azide (NaN_3).[71-72] During the 1940–1950s, Briggs,[73] Smith,[74] and Boyer[75-77] individually investigated the use of alkyl azides in place of conventional HN_3 in order to extend the scope of the Schmidt reaction. However, Briggs and Smith failed to achieve the synthesis of *N*-substituted lactams in

this way. Later, Boyer disclosed a limited reaction series between aromatic aldehydes and alkyl azides using sulfuric acid (H_2SO_4) in benzene to afford *N*-substituted lactams in poor yields. Further, Boyer and coworkers discovered that by exchanging an alkyl azide for a hydroxyalkyl azide, this transformation provided an efficient route to oxazolines.[76] Boyer's proposed mechanism proceeded through intermediate **i** in Figure 1.5; formed by an initial attack of azide onto the activated carbonyl, accompanied by extrusion of molecular nitrogen and water to give the oxazoline product. While this finding was a significant advancement, the reaction was limited to the use of electron-deficient aromatic aldehydes.

Scheme 1.4. Common nitrogen-ring expansion reactions. (a) The Beckmann rearrangement. (b) The classic Schmidt reaction.

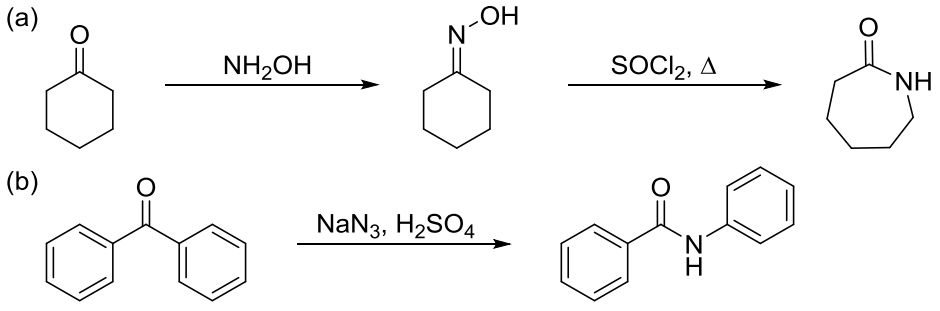

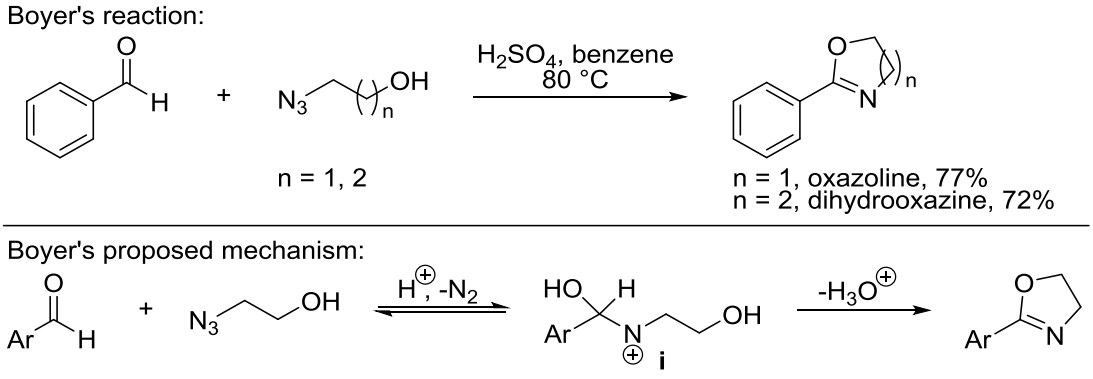

Figure 1.5. Boyer's reaction of aromatic aldehydes with achiral hydroxyalkyl azides.

In the early 1990s, Aubé and coworkers described the use of boron trifluoride diethyl etherate (BF_3•OEt_2) in dichloromethane (CH_2Cl_2) to promote the reaction between aldehydes or ketones with hydroxyalkyl azides (Figure 1.6).[72, 78-81] Compared to that of Boyer's work, Aubé reported superior yields, substantial scope extensions, and a modified mechanism proposal (e.g., of ketones; shown in Figure 1.6).[81] In this proposed mechanism, initial formation of oxonium ion is resultant from an initial attack of the hydroxyl group followed by the loss of water; instead of an initial attack onto the activated carbonyl by azide as speculated by Boyer. The formation of oxonium ion renders the azide addition intramolecular establishing an azidohydrin-like intermediate that rearranges due to extrusion of molecular nitrogen and results in an iminium ion intermediate as the primary rearranged product. In the case of an aldehyde, the initial intermediate was proposed as a related oxonium ion, and oxazoline or dihydrooxazine (n = 1 or 2, respectively) ensues from rearrangement and the loss of nitrogen.[78] Most often, the isolatable iminium ether intermediate from ketone is converted directly to an amide or lactam through an overnight stir in either an aqueous saturated solution of sodium bicarbonate ($NaHCO_3$) or 15% potassium hydroxide (KOH). Moreover, Forsee at el. showed that acyclic ketones or medium-sized ketone rings react with hydroxyalkyl azides to afford substituted esters or lactams (Scheme 1.6).[82] However, the outcomes of these reactions are highly dependent on substrate and base conditions, taking into account many factors including ring strain and the protonation state of reaction intermediates.

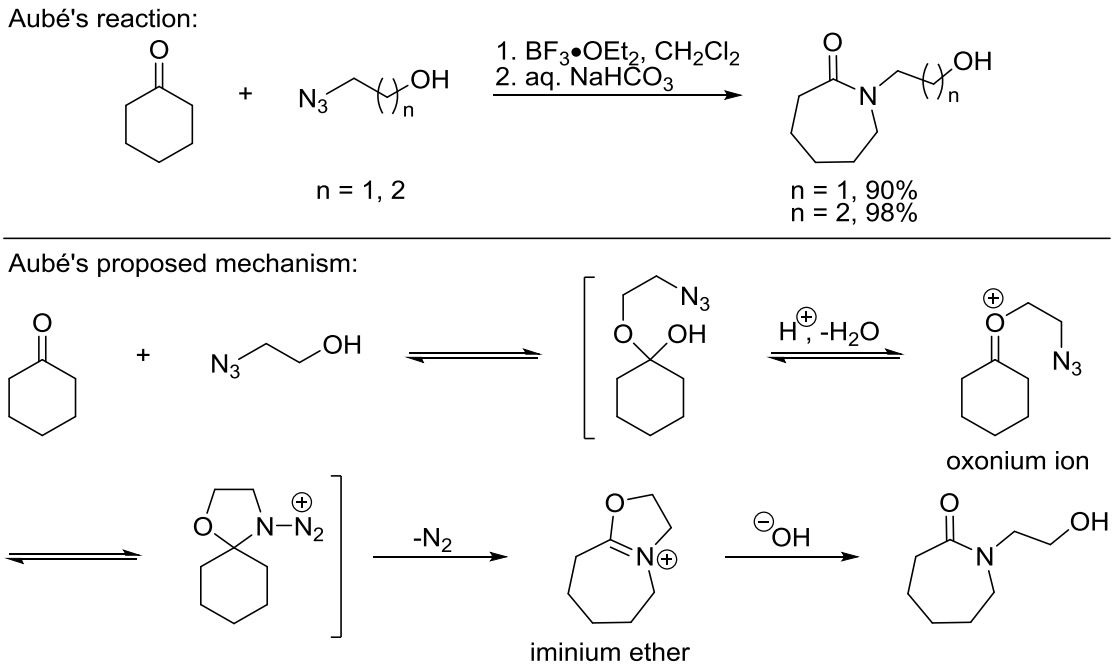

Figure 1.6. The Schmidt reaction of ketones with achiral hydroxyalkyl azides.

Scheme 1.5. The Schmidt reaction of medium-sized cycloalkanones with hydroxyalkyl azides.

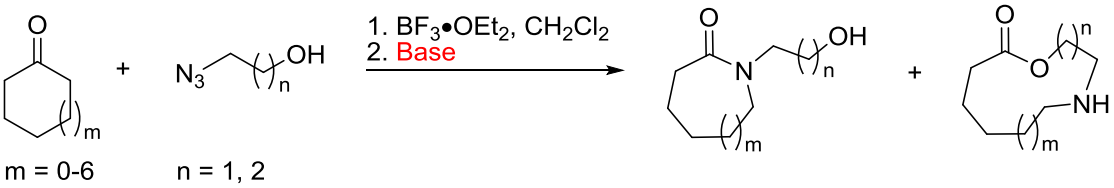

Particularly relevant to this chapter is the reaction of an iminium ether intermediate with various nucleophiles to afford functionalized *N*-alkyl heterocycles.[80, 83-84] In Figure 1.7, the iminium ether intermediate is shown to react with nucleophiles at two possible carbon sites, path *a* or path *b*. The selectivity for path *a* is rationalized based on the reversibility of the initial addition of nucleophile at the formal iminium carbon, which is dependent on the nucleophile. In path *a*, attack occurs at the sp^2 carbon (iminium carbon), forming a neutral intermediate that can either further convert to final product or revert back to the stable iminium intermediate. In this pathway, nucleophiles that behave reversibly ultimately attacks at the distal sp^3 carbon adjacent

to the oxygen atom in an S_N2 fashion (path *b*). For example, treatment of an iminium ether with aqueous hydroxide goes via path *a*; this was determined by Fenster el al., when the nucleophile was ^{18}O-labeled hydroxide showed enrichment of ^{18}O at the carbonyl.[84] Towards scope extension, Aubé studied a detailed range of nucleophiles in order to exploit the ambident electrophilicity of the primary rearranged product, and develop this chemistry as a tool for library construction. In these studies, two noteworthy heterocycles that were achievable from path *a* include amine and thioamide formation (under hydrogenation or sodium borohydride reducing conditions, and disodium sulfide workup, respectively). Other nucleophiles that add to iminium ether afford *N*-alkylated lactams include azides, sulfides, and halides (via path *b*). Since then, this reaction type has been applied towards library preparation, e.g., of γ-turn-like peptidomimetics based on 1,4-diazepin-5-ones.[83] Taken together, these protocols explored revealed the synthetic versatility and convenience of iminium ethers, which could either be deliberately isolated or chosen for maximal efficiency in a one-pot, three component sequence.

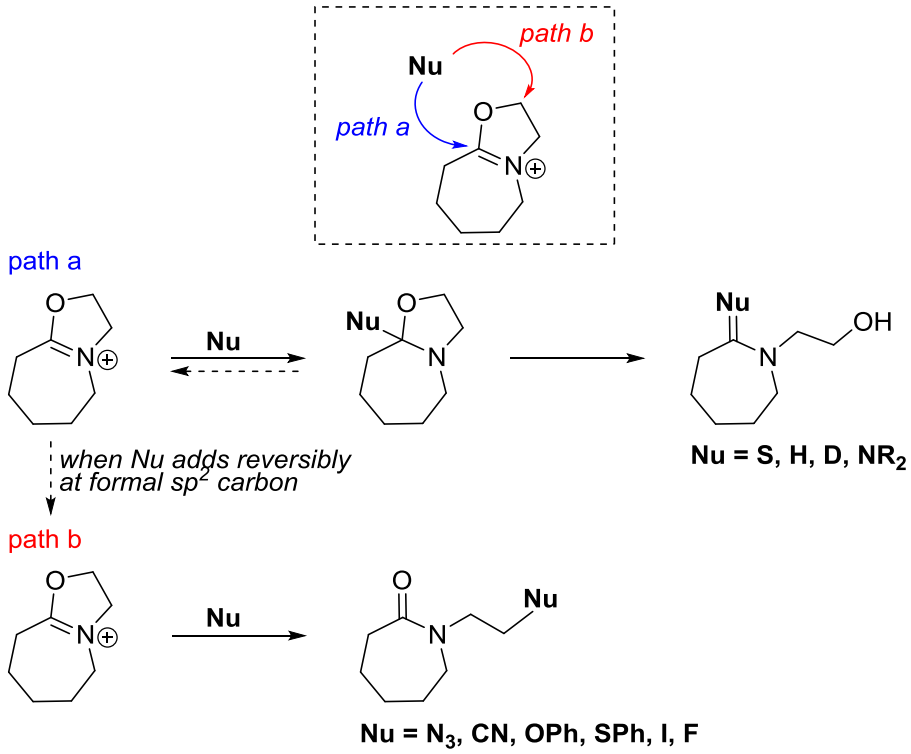

Figure 1.7. Nucleophilic addition reactions of iminium ethers.

The intermolecular Schmidt reaction between ketones and hydroxyalkyl azides has also been applied to the asymmetric synthesis of chiral lactams.[79, 85] As shown in Scheme 1.6, utilization of a chiral hydroxyalkyl azide afforded diastereotopic lactams in excellent yields and stereoselectivities. Sahasrabudhe et al. carried out a systematic study of chiral hydroxyalkyl azides in ring expansions of symmetrical cyclohexanones. In sum, many structure-selectivity analysis of various chiral azide reagents revealed diastereoselectivities up to 98:2 with substituted 3-azidopropanols. However, poorer selectivities were observed with substituted 2-azidoethanol reagents. The mechanism of the reaction (representative case shown in Figure 1.8), and the source of its stereoselectivity have been discussed.[85-86] The reaction has also been extensively studied by computational methods.[86] The specific features pertaining to stereocontrol are relevant to the present chapter. In brief, the product outcomes of the asymmetric reaction

depend on three following considerations: (1) direction of azide attack relative to pre-existing substitution on the ketone reactant, (2) selective formation and reaction of the most stable new heterocyclic ring (1,3-oxazinane from 3-azidopropanol, or oxazolidine from 2-azidoethanol), and (3) antiperiplanar C→N migration to afford the iminium ether intermediate. All steps prior to the actual migration are reversible; the iminium ether intermediate never reverses. In fact, supported by density functional theory (DFT) calculations, the barrier for C→N migration is only ca. 2 kcal/mol higher than reversion to azide and oxonium ion.[86]

Scheme 1.6. The asymmetric Schmidt reaction.

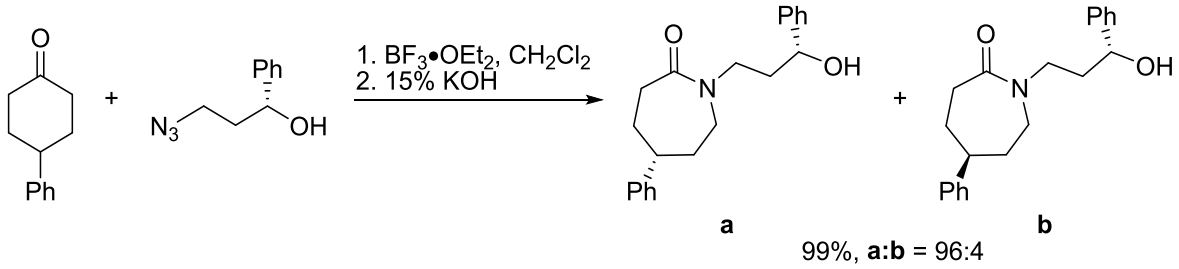

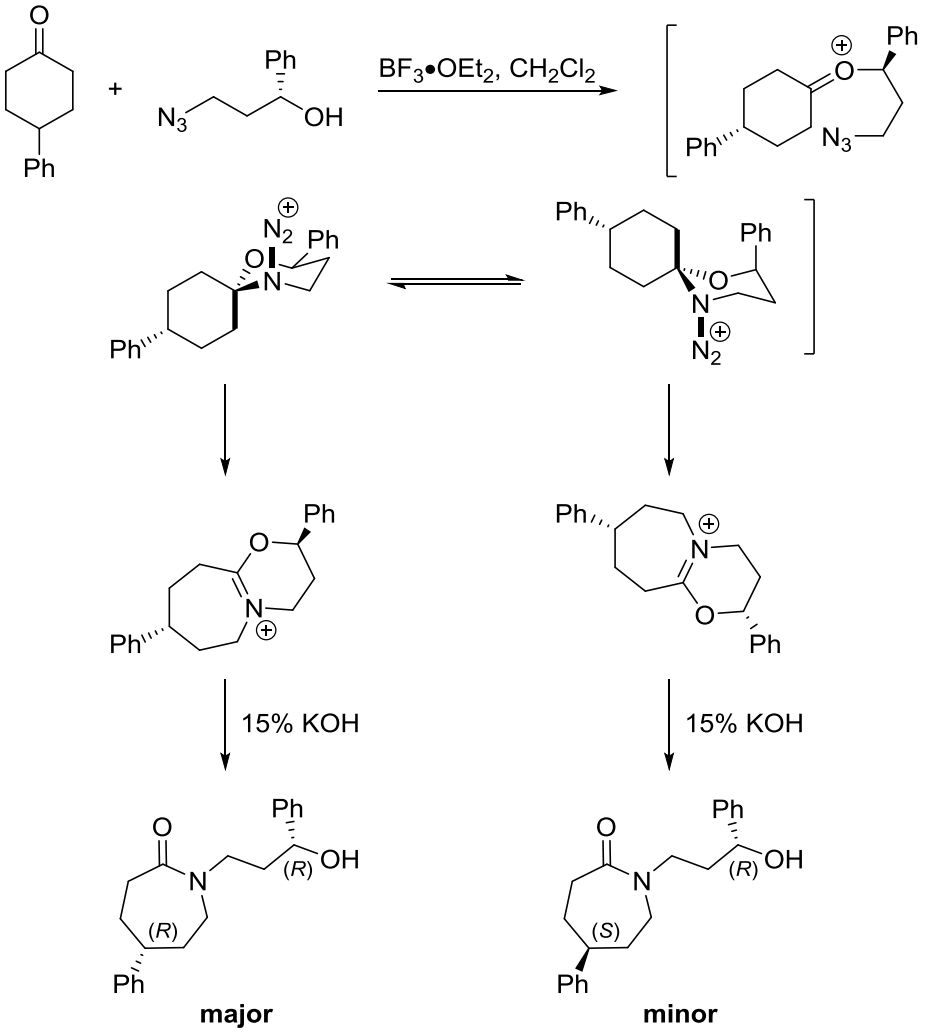

Figure 1.8. Proposed mechanism of the asymmetric Schmidt reaction. The figure was adapted from Sahasrabudhe et al.[85]

The following discussion focuses on the reactions of substituted cyclohexanones with 3-azidopropanols. The complex mechanism of this transformation results from a combination of three stereochemical and conformational factors (Figure 1.9):[85-86]

Factor (1): Direction of azide attack onto ketone. It has been proposed and supported by computational methods[86] that in the intermediates derived from six-membered rings, equatorial azide attack occurs onto the more stable cyclohexanone derivative; where stereoselectivity relates to the relative populations of the possible chair conformations of the

starting ketones. Attack onto ketones of other ring sizes depend on steric accessibility (specific to examples). Since it is not possible to directly observe the spirocyclic intermediate, the direction of attack in non-obvious cases may need to be inferred from analyzing the outcomes in the context of factors 2 and 3 below.

Factor (2): Selective formation and reaction of the most stable new heterocycle ring. In cases of intermediates derived from monosubstituted 3-azidopropanols, the major products afforded from spirocyclic 1,3-oxazinanes containing the substituent in an equatorial orientation. It has been reported that 2-aryl or 2-alkoxy substituted 3-azidopropanols lead to products arising from spirocyclic 1,3-oxazinanes having the substituent in an axial position. For example, due to a π-cation interaction between the aryl group and the N_2^+ leaving group, which is now in a 1,3-diaxial relationship.[87] In all cases, the heterocyclic ring is presumed to adopt the most stable chair-like conformation, and it is worth recognizing that the two chair forms can interconvert either by reversion to oxonium ion and azide, or by ring flip between the two chair forms.

Factor (3): Antiperiplanar migration. In all azido-Schmidt reactions, C→N migrations involve concerted antiperiplanar migration to the N_2^+ leaving group. For spirocyclic intermediates from hydroxyalkyl azides, the reaction goes through an axial N_2^+ group, since if this group is equatorial, the only possible antiperiplanar options are a C-O bond (unlikely to migrate as it would form a new and weak N-O bond), or a C-C bond (if broken, would lead to an unstabilized cation by neighboring an oxygen atom). Additionally, DFT calculations revealed that the N_2^+ is axial in the ground-state conformation.[86]

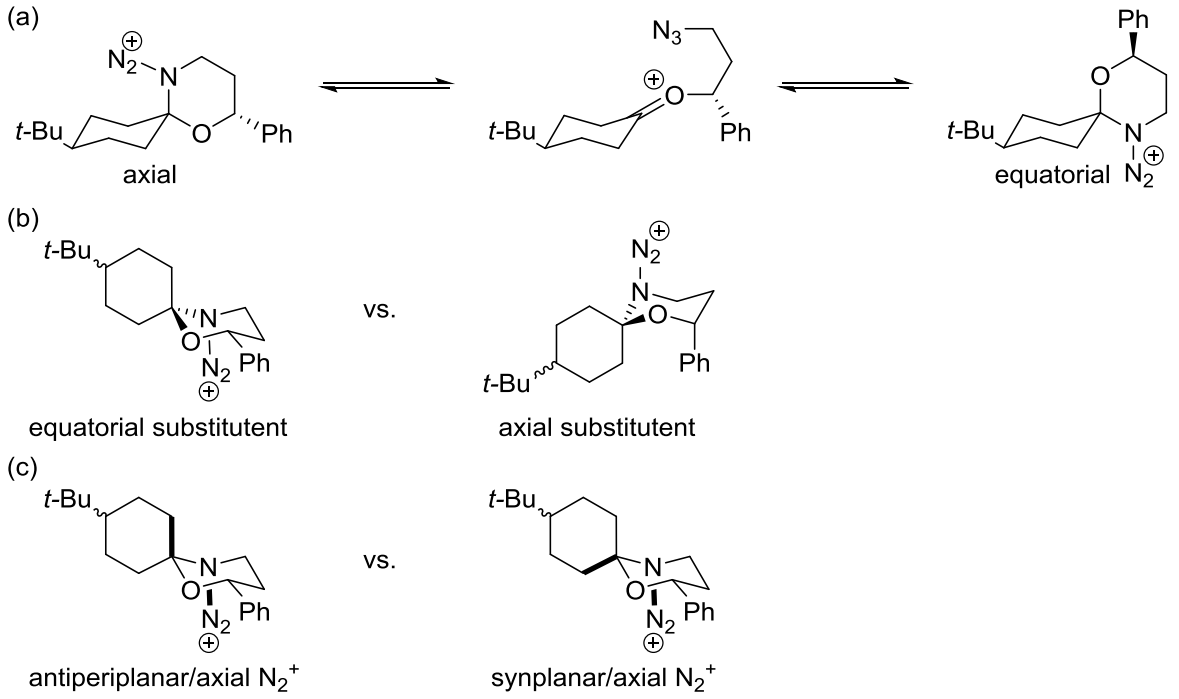

Figure 1.9. Factors that govern the asymmetric Schmidt reaction. (a) Direction of azide attack onto ketone. (b) Selective formation and reaction of the most stable new heterocycle ring. (c) Antiperiplanar migration.

1.1.5 Regiochemistry in Nitrogen Ring Expansions

Often in nitrogen ring-expansion chemistry of unsymmetrically substituted ketones two regioisomers are conceivable, and generally, the product outcomes are determined by electronic or steric preferences of the starting substrates. The classic Schmidt or Beckmann reactions preferentially proceed to ring-expanded isomers that result from the migration of the more substituted carbon, with few known exceptions.[70, 72] The regioselectivity of the Beckmann reaction generally arises from the preferential formation and regioselective rearrangement of one of the two possible oximes, (*E*)- and (*Z*)-isomer, as a result of steric interactions. Under acidic or protic conditions, interconversions of oxime isomers can take place, which may account for non-stereospecific rearrangements and failure to selectively achieve formation of one isomer over the other.

Alternatively, the photochemical rearrangement of oxaziridines entails a mechanism that establishes a stable nitrogen-centered stereoisomer en route to ring-expansion. In contrast to the traditional Beckmann, where the carbon anti to the hydroxyl group of the oxime undergoes migration, during oxaziridine photolysis the carbon anti the nitrogen lone pair of the oxaziridines undergoes migration. Moreover, Aubé has studied stereospecific ring expansions of chiral oxaziridines derived from α-methylbenzylamine (α-MBA).[88-89] Following stereoselective oxaziridine formation, photochemical rearrangement occurs under stereoelectronic control, in which the substituent anti to the nitrogen lone pair undergoes migration. Interestingly, by switching between (*S*)- and (*R*)-MBA reagents, the resultant oxaziridines contain nitrogen stereocenters with opposite configurations, thus allowing one synthesize selectively regioisomers.

Aubé has applied this reagent-directed strategy on simple unsymmetrically substituted ketones, as well as, on more challenging cases such as the Wieland-Miescher bicyclic ketone (Figure 1.10a).[90] In this work, the switchable access to regioisomeric lactams is a nice demonstration of group-selectivity concept in asymmetric synthesis. In asymmetric synthesis, tools that distinguish between enantio- or diastereotopic methylene groups are important methods for stereodifferentiation and stereoselectivity in chemical transformations. Herein, Aubé pioneered chiral oxaziridines as tool to differentiate between diastereotopic methylene groups in the migration step, thus enacting an asymmetric synthesis of seven-membered nitrogen ring-expanded products. Interestingly, only a few examples in the literature are reported that use asymmetric tools to effect regiochemical control (e.g., Jacobsen's work on Salen complexes, Figure 1.10b, and Miller's work on peptide catalysts, Figure 1.10c),[88, 90-92] and minimally has been repurposed for late-stage diversification and functionalizations.[47]

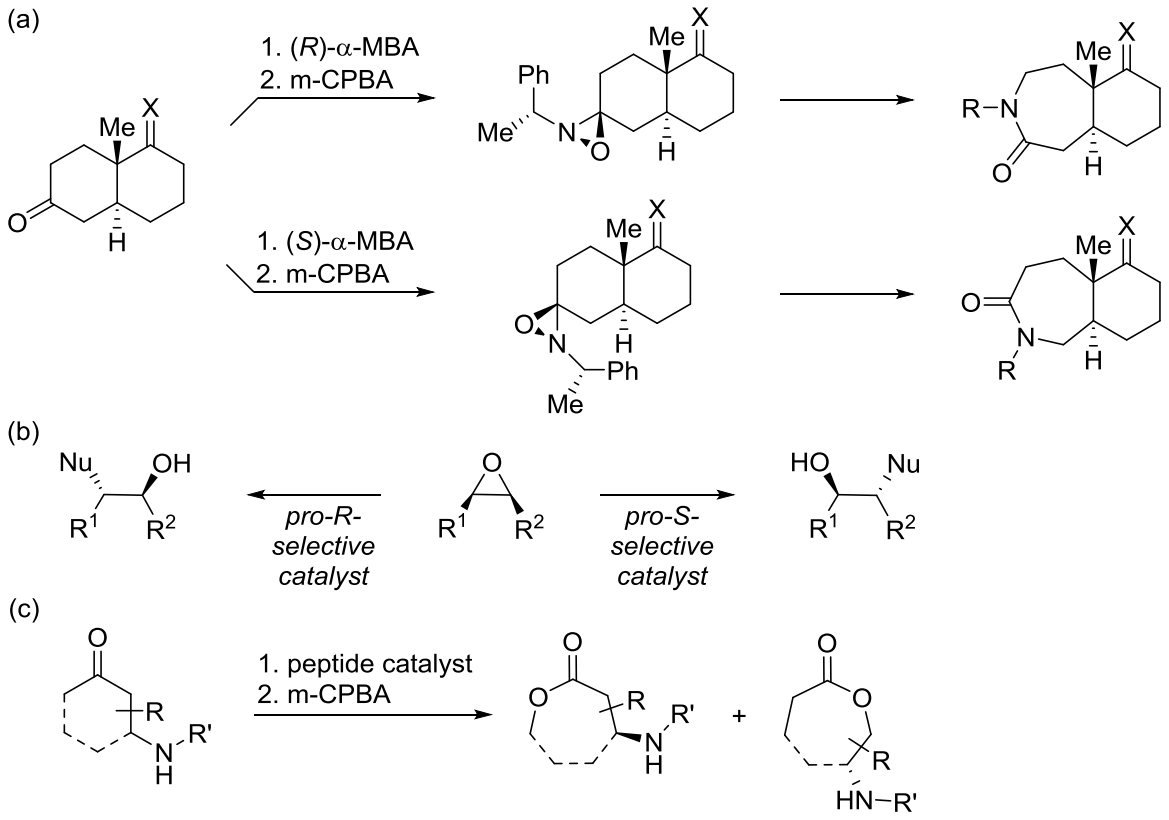

Figure 1.10. Regiochemical control using chiral reagents. (a) Chiral MBA reagents used in oxaziridine-photochemical ring expansion of substituted *trans*-decalone. (b) Jacobsen's regioselective ring opening of enantiomerically enriched epoxides using chiral salen complexes. (c) Miller's catalyst control in Baeyer-Villiger oxidation of functionalized ketones.

However, the above ring-expansion methods are not amendable to library preparation because they lack flexible and immediate access to functional diversity. On the other hand, the hydroxyalkyl azide variant of the Schmidt reaction encompasses features of functional diversity that is practical towards library development. However, this Schmidt reaction variant has not been extensively explored in the context of simultaneous regiochemical control and diversification.

The Aubé laboratory has studied the reaction between of 1,2- or 1,3-hydroxylalkyl azides with unsymmetrical cyclohexanones.[93] As shown in Figure 1.11, it was determined that the reactions of hydroxylalkyl azides with ketones containing methyl or ethyl groups are unselective,

however bulkier substituents on ketones may lead to preferential migration of the more substituted carbon (similar to the classic Schmidt trend). On the contrary, ketones bearing an electron-withdrawing group (e.g., bromine) afforded migration of the unsubstituted methylene group. The stereochemical analyses of these reaction intermediates are relevant to our understanding of selectivity. The effect of substituent size reflects the differences in the nonbonded interactions of the spirocyclic *N*-diazonium intermediates (Figure 1.11). On explanation is that the effect of steric bulk of the 2-substituent on regiochemistry is that the alkyl group and the N_2^+ leaving group experience varying degrees of steric interactions when they are in a syn versus anti orientation. Since the leaving group is small, there is not much difference between these forms for small alkyl groups, however for larger groups regiochemical preferences emerge. For example, presuming equatorial attack of azide on to the oxonium ion intermediate, the more substituted carbon (when R = *i*-Pr, *t*-Bu) occupies the anti-orientation leading to migration of the more highly substituted carbon. However, in the case of bromine, one possible explanation is that the electron-withdrawing group deactivates migration of that carbon and, in turn, favors migration of the less-substituted carbon.

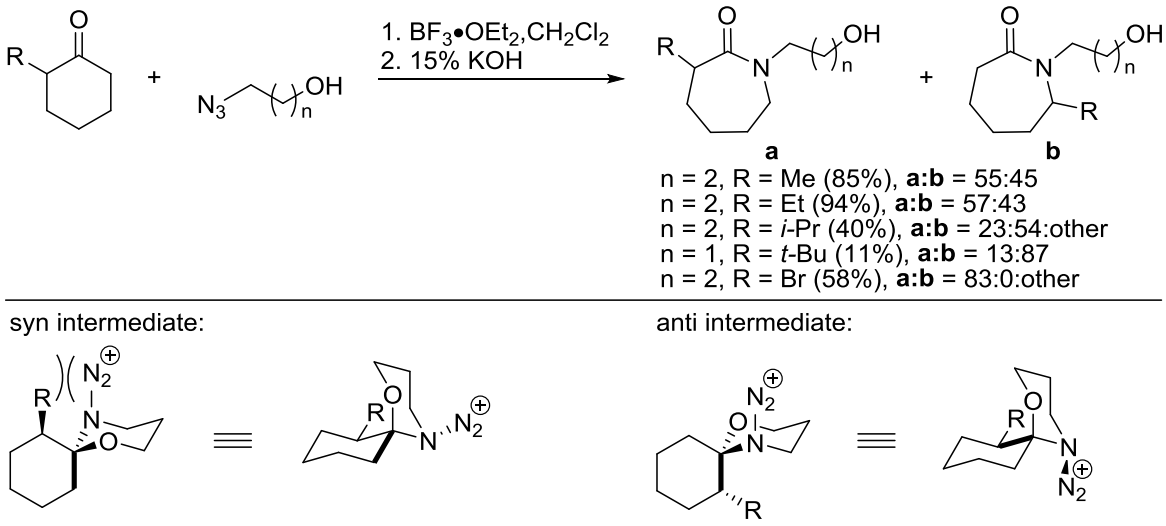

Figure 1.11. The Schmidt reaction of unsymmetrical cyclohexanones with achiral hydroxyalkyl azides.

1.1.6 Overview of our Library Design

Natural products represent valuable starting points for drug and probe discovery, with late-stage diversification as an attractive approach for generating new bioactive agents from complex starting scaffolds.[7-8] In recent years, relatively few approaches to *N*-containing steroid library collections have been reported.[9, 16-17] Because there is paucity of nitrogenous steroids for discovery research and these substrates prominently figure in both classic and contemporary synthetic approaches, we sought to develop a global approach to the late-stage introduction of nitrogen substituents by using ring expansion chemistry. To do so effectively, we needed to address the perennial problem of regiochemistry control that accompanies ring expansion chemistry, especially of complex structures where there is often substrate biases that dictate the regioisomeric outcomes. In this work, we aimed to describe a global approach that uses stereoelectronically controlled ring expansions to effect regiochemical control in a complex molecular setting, permit directed introduction of a nitrogen-containing group in settings where regiochemical control was previously not possible, and overcome strong substrate biases to

afford previously inaccessible constitutional isomers (Figure 1.12a). In this chapter, our regiodivergent rearrangement strategy describes the uses of chiral reagents to effect regiocontrol in chiral natural products, which should become applicable to late-stage natural product diversification programs.

We focused this chapter on ring-expansions of A and D-rings because the biological activities of steroids often depend on the structures of these ring systems. Unfortunately, modifications of B and C-rings proved to be relatively problematic (the challenges of these ring systems is be discussed in section 1.5). Thus, we present a stereoelectronically controlled ring expansion sequence towards selective and flexible access to complementary ring systems derived from common steroid substrates of A and D-rings.

The two limiting cases for regiochemical control are shown in Figure 1.12a. The nitrogen ring expansion of a 17-oxosteroid represents a classic case of unidirectional migration in an α-substituted ketone. Here, this corresponds to migration of the highly substituted C-13 carbon versus migration of the less substituted C-16 carbon. Both the Beckmann and Schmidt reactions have been carried out on this steroid system, and the standard outcome is the exclusive migration of the more substituted C-13.[27, 94-95] In contrast, migration of the C-16 carbon is unknown, except through multistep sequences.[27]

The challenges of A-ring rearrangement is more severe because the two methylene groups attached to the 3-oxosteroid are electronically and sterically similar enough that substrate bias may not come in play. In other words, this ketone is only non-symmetrical at a site distal from the actual point of chemical reactivity. In fact, reported ring expansion reactions at this ketone are known and poorly selective.[96-97] A potential solution to this problem is evident from previous Aubé laboratory endeavors in ring expansion chemistry. Conceptually, one may embed

an achiral cyclohexanone into the chiral context of the A-ring steroid (Figure 1.12b), which now renders the two potential migrating methylene groups that were enantiotopic in the monocyclic case, diastereotopic. This idea was previously explored in ring-expansion chemistry using chiral oxaziridines (Figure 1.10a).

As in all approaches for using an asymmetric reaction for the control of product regiochemistry (Figure 1.10), it is essential that the substrate be used in enantiomerically pure form. This is due to the fact that the stereodifferentiating reaction is designed to favor migration of a single enantiotopic methylene group when carried out on an achiral ketone. In a chiral ketone substrate, the relevant methylene groups are no longer enantiotopic and are chemically non-equivalent (Figure 1.12b). However, due to *local asymmetry*, they respond to the chiral reagent as if they were enantiotopic. Thus, if the reagent is able to distinguish between these chemically non-equivalent groups (through the same mechanism as if they were enantiotopic), it will afford a single isomeric product only if a given chemically non-equivalent methylene group in the molecule maps onto a single "enantiotopic" methylene group from the perspective of the added reagent. Another way of thinking about this is that just as the enantiomerically pure ketone reacts with racemic hydroxyalkyl azide to give two isomers in a 1:1 ratio because each isomer in the racemate enforced the formation of a single stereoisomeric product, a 1:1 mixture would also have to resulted if the substrate purities were reversed, i.e., if the hydroxyalkyl azide were enantiomerically pure and the ketone substrate were racemic. Therefore, in this work, we studied the regiochemistry of the Schmidt reaction between enantioenriched hydroxyalkyl reagents on complex chiral ring systems such as that of steroids (i.e., steroids that are in one enantiomeric pure form).

In this chapter, the library of azasteroids was devised in a systematic manner using the hydroxyalkyl azide variant of the Schmidt reaction: (1) I studied the use of achiral and enantioenriched hydroxyalkyl azides to effect ring expansion of 3- and 17-oxosteroids, (2) determined constitutional isomer selectivity by rationalization of reaction mechanisms, and (3) functionalized iminium ether intermediates with various nucleophiles to afford analogs with spatial and functional diversity. The main sections in this chapter are separated by A- and D-ring modifications.

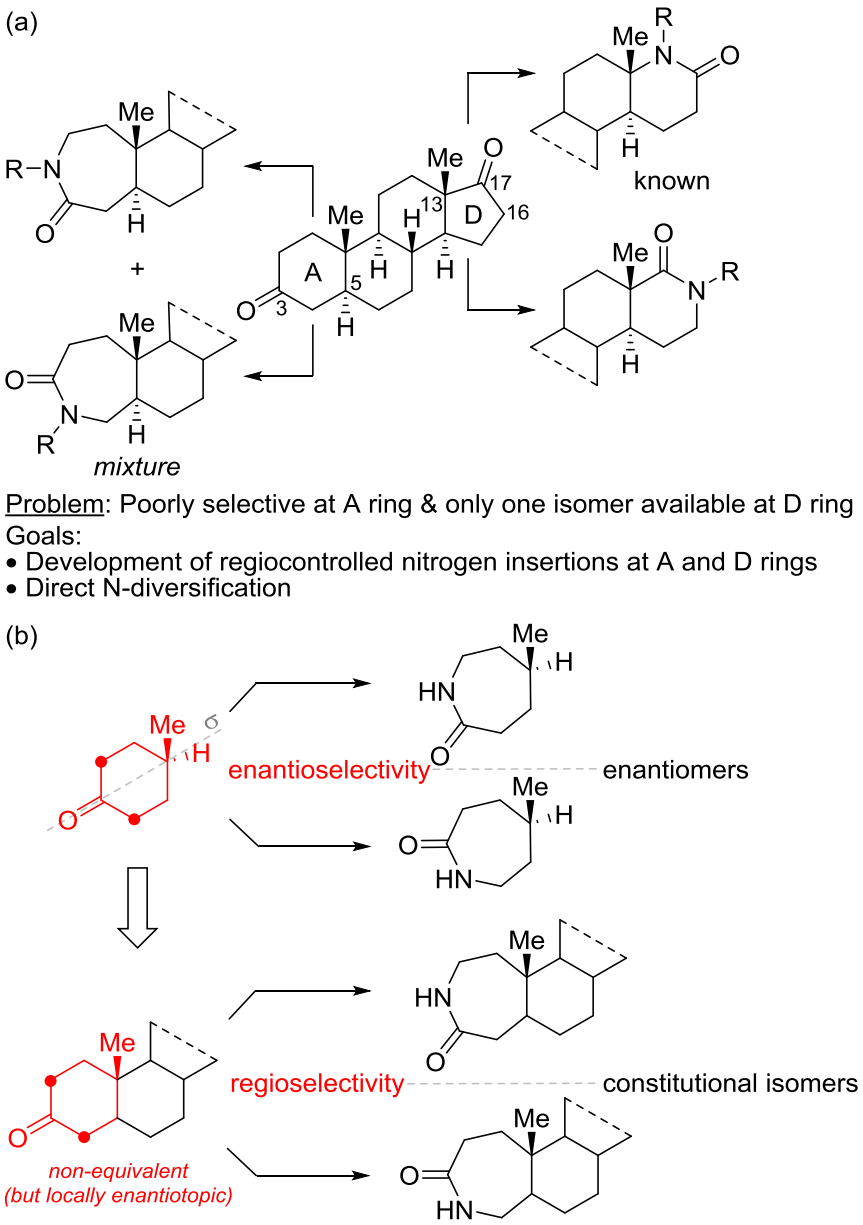

Figure 1.12. Rationale of the project and challenges associated with A- and D-ring late-stage functionalization using ring expansion chemistry. (a) Regiochemical issues accompanying ring expansion reactions of 3- and 17-oxosteroids. (b) The relationship between enantiotopic group migration selectivity in substituted cyclohexanones and regioselectivity in a 3-oxosteroid.

1.2 Synthesis of Hydroxyalkyl Azides

A variety of 1,2- and 1,3-hydroxyalkyl azides were synthesized for this study; two reagents were achiral and eighteen reagents were pairs of enantiomers (Figure 1.13). An

attractive aspect of the proposed ring-expansion study was the ready availability of hydroxyalkyl azides from commercial starting materials using simple chemical transformations.

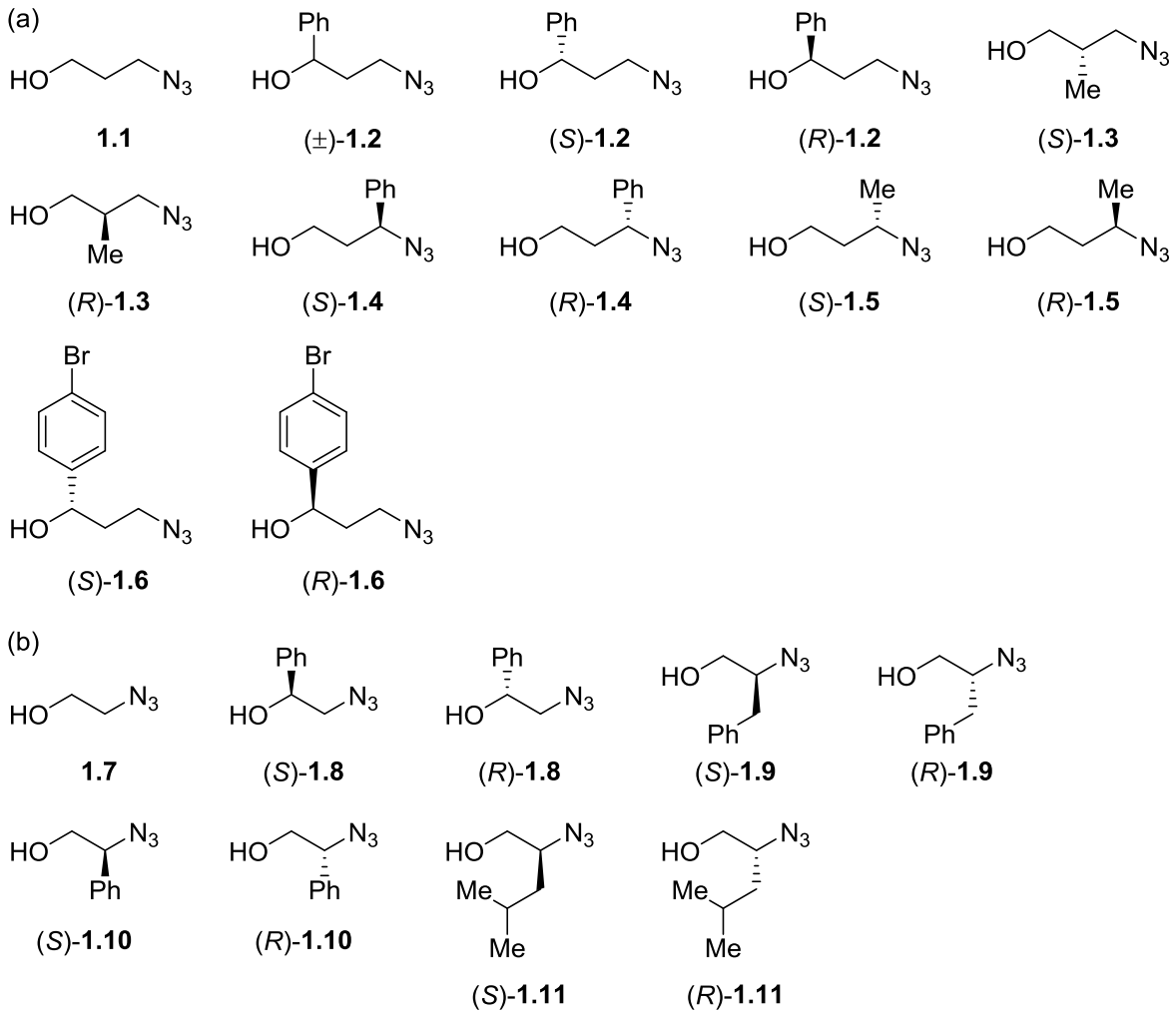

Figure 1.13. Chiral and enantioenriched hydroxyalkyl azides for library preparation. (a) 1,3-Hydroxyalkyl azides. (b) 1,2-Hydroxyalkyl azides.

In general, a simple S_N2 reaction of alkyl halides with NaN_3 was used to prepare seven azide-reagents, which included achiral azides **1.1** and **1.7**, racemic azido-1-phenylpropanol **1.2**, (*S*)- and (*R*)-**1.2**, and (*S*)- and (*R*)-3-azido-2-methylpropanol **1.3** (Figure 1.13; representative S_N2 reaction shown in Scheme 1.7). In other cases, the synthesis of enantioenriched 1,3-substituted azides required multistep reactions as shown in Scheme 1.7. In one case, enantioenriched 3-

chloro-1-phenylpropanols were converted to phenyl-containing (*S*)-**1.4** and (*R*)-**1.4** following three synthetic steps—displacement of chloride with acetate, Mitsunobu azidation with inversion of the benzylic center, and hydrolysis of the acetate protecting group. Similarly, a Mitsunobu transformation was used to prepare (*S*)- and (*R*)-3-azidobutanol **1.5** following *tert*-butyldimethylsilyl (TBS) protection of the less hindered alcohol on the 1,3-butandiol starting material. All Mitsunobu procedures were carried out using diphenylphosphoryl azide (DPPA)[98] because this reagent is readily available, nonexplosive, and more stable than HN_3.

The synthesis of a bromophenyl-substituted 3-azido-propanol was desired because of potential downstream diversification applications. The enantiomers of **1.6** were synthesized from an asymmetric Corey-Bakshi-Shibata reduction[99] of 4'-bromo-3-chloropropiophenone and subsequent displacement of chloride by NaN_3 (Scheme 1.7). Enantioselective reduction was achieved using an oxazaborolidine catalyst (Me-CBS) and *N,N*-diethylaniline borane (DEANB), which gave secondary alcohols with selectivity in the range of 96–97% enantiomeric ratio (92–94% ee). In a similar manner, enantiomers of 2-azido-1-phenylethanol **1.8** were synthesized in 98–99% enantiomeric ratio (96–98% ee).

In general, enantioenriched 1,2-hydroxyalkyl azides were prepared from the corresponding amino acids by carbonyl reduction and conversion of the α-amino group to an azide.[100] In particular, the amino acids leucine, phenylalanine and phenylglycine were reduced using refluxing lithium aluminum hydride (LAH) and the resulting amino alcohols were converted to the corresponding azides via a diazo transfer using freshly prepared trifluoromethanesulfonyl azide (TfN_3) (Scheme 1.8). In this way, enantioenriched hydroxyalkyl azides **1.9**–**1.11** were easily prepared.

Scheme 1.7. Representative synthesis of 1,3-hydroxyalkyl azides.

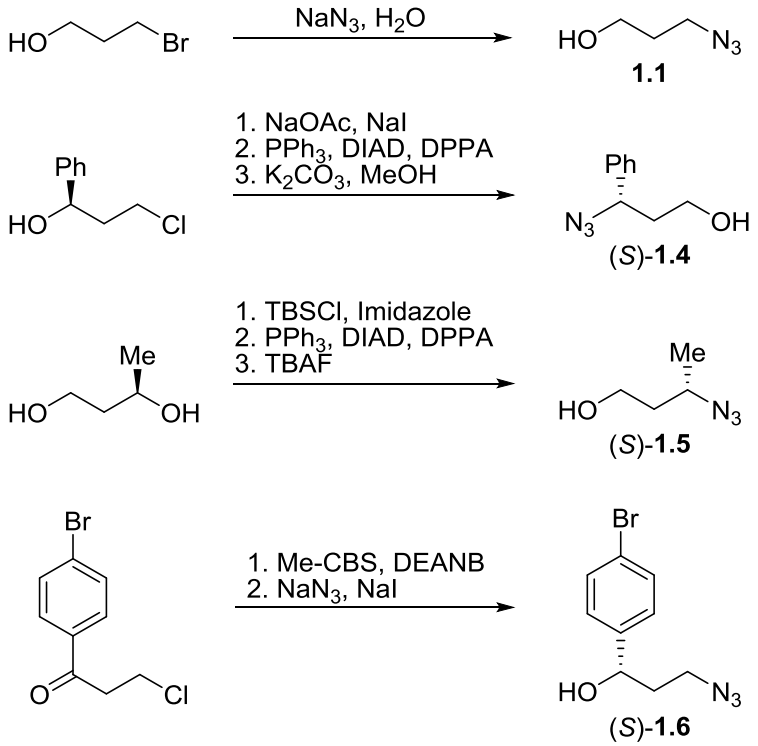

Scheme 1.8. Chiral pool synthesis of 1,2-hydroxyalkyl azides from amino acids.

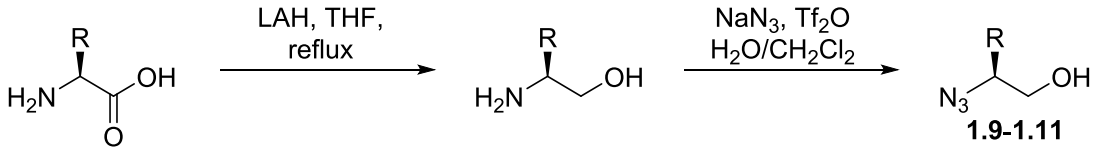

1.3 A-Ring Modifications

1.3.1 Synthesis of 3-Oxosteroids

An attractive aspect of the proposed library preparation was the ready availability of steroids from commercial sources in enantiopure forms. In the A-ring series, three steroidal ketones (3-oxosteroids) were synthesized in one or two steps from either commercial cholesterol or testosterone, respectively (Scheme 1.9). We focused on the preparation of 3-oxosteroids for several reasons. Firstly, the ketone handle could be easily secured by using straightforward

chemistry, which included olefin reductions and oxidation of a secondary alcohol. Secondly, the three substrates prepared, 5α-cholestan-3-one **1.13** (3-cholestone), 5α-dihydrotestosterone **1.14** (5α-DHT), and 5β-dihydrotestosterone **1.15** (5β-DHT), are structurally diverse containing variable C-17 side chains and AB junctions. It is interesting that the stereochemical preferences of the olefin reduction are sensitive to the steroid substrate and strongly influenced by the reducing systems. The stereoselectivity of α,β-unsaturated testosterone is a classic example (Figure 1.14). As shown in Figure 1.14, the selectivity of the dissolving metal reduction (lithium in ammonia) is under thermodynamic control, whereas Pd/C hydrogenation proceeds with kinetic control. In the former case, the *trans*-product formed is the more stable isomer, and the stereochemical outcome is governed by "axial protonation" as originally discussed by Barton[101] and Stork.[102] They proposed that the resulting hydrogen is axial because the transition state for protonation of the carbanion species has considerable tetrahedral character that allows the carbanion orbital to overlap in the unsaturated system; this transition state characteristic is favorable in the *trans*-fused AB ring conformation and not in that of a *cis*-fused AB ring.

Scheme 1.9. Synthesis of 3-oxosteroids from commercial steroids. (a) Synthesis of 5α-cholestan-3-one. (b) Synthesis of 5α-dihydrotestosterone and 5β-dihydrotestosterone.

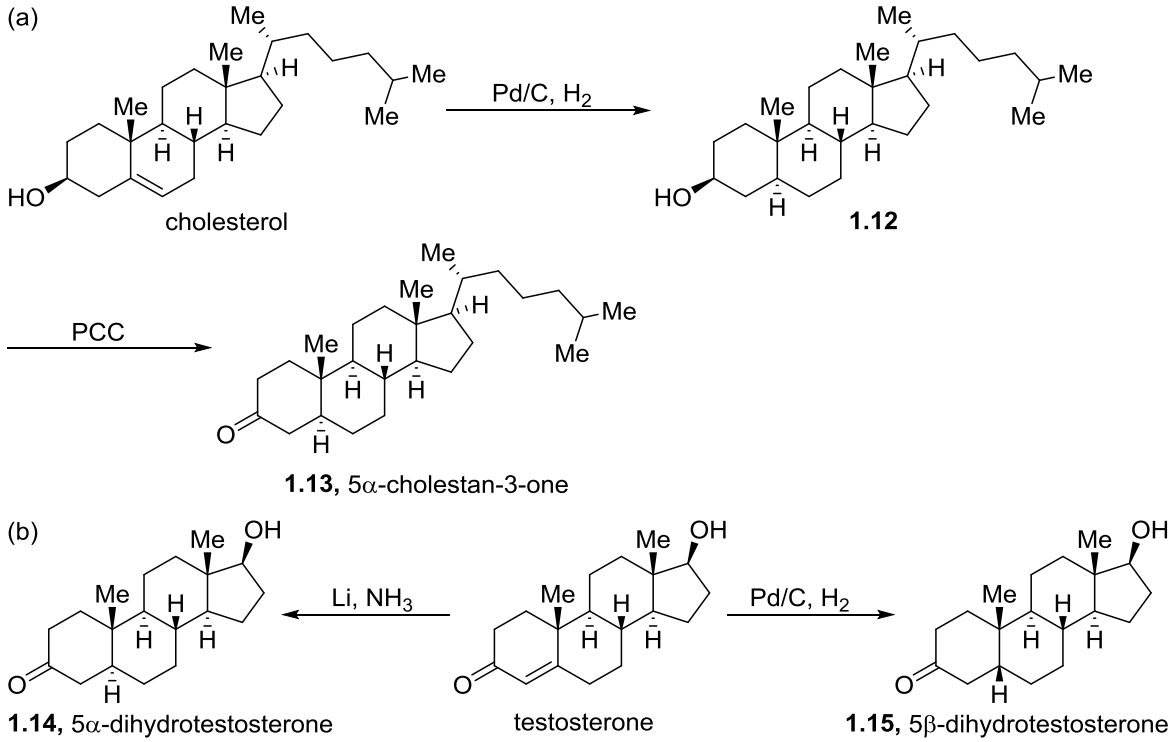

Figure 1.14. Kinetic versus thermodynamic hydrogenation. The figure was adapted from Shenvi and coworkers.[103]

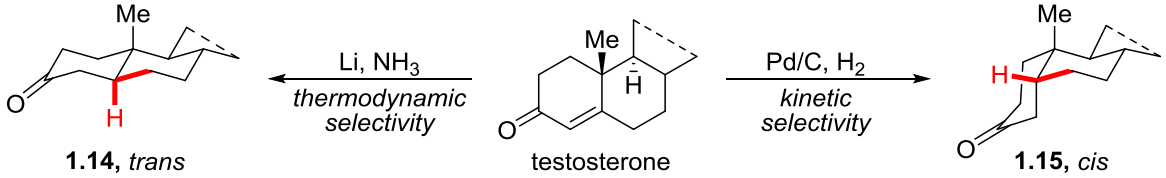

1.3.2 A Study on the Use of 1,3-Hydroxyalkyl Azides to Effect Ring Expansion on 3-Oxosteroids, Determination of Constitutional Isomerism Control, and Rationalization of Mechanism

We aimed to address the problem of A-ring selectivity using a stereocontrolled ring expansion to influence the regioselectivity of the *N*-side chain installation. In this study, readily available 3-oxosteroids **1.13**–**1.15** were reacted with hydroxyalkyl azides **1.1**–**1.6** (Table 1.1). As

expected, the ring expansion of 3-cholestone **1.13** with achiral 3-azidopropanol **1.1** gave little selectivity for one ring expansion outcome over the other; **1.16** and **1.17** were observed as a 38:62 mixture by ^{1}H NMR, and were inseparable by normal phase column chromatography (entry 1, Table 1.1). In order to surmount this problem, a reagent control approach was tested with a variety of chiral azide reagents **1.2**–**1.6**. For example, enantioenriched (*S*)- or (*R*)-3-azido-1-phenylpropanol, (*S*)- or (*R*)-**1.2**, were reacted separately with 3-cholestone **1.13** and afforded spectroscopically pure lactams **1.19** and **1.18**, respectively. In each case, the reaction demonstrated high regiochemical control (>95:5) and gave excellent yields 88–89% (entries 3 and 4). As expected, the reaction with racemic 3-azido-1-phenylpropanol (±)-**1.2** gave an equimolar mixture of **1.18** and **1.19** (entry 2). Compared to the achiral reactant (entry 1) where a modest inherent substrate bias was observed, the racemic reactant (entry 2) influenced the non-selectivity. In this case, each half of the racemate provided a specific regioisomer with high selectivity, thus an equimolar mixture of **1.18** and **1.19** was obtained. Generally, the reaction was carried out in CH_2Cl_2 and promoted by 5.0 equiv of BF_3•OEt_2. These conditions were adapted from the asymmetric Schmidt reaction variant.[85] However, substantial optimization study was carried out for D-ring modifications, which was not done for A-ring modifications. This is because A-ring substrates (6-membered ring ketones) readily reacted with azide reagents under the standard conditions, while D-ring substrates (5-membered ring ketones) did not proceed in high conversions.

Table 1.1. Reaction of 3-oxosteroid **1.13**–**1.15** with 1,3-hydroxyalkyl azides **1.1**–**1.6**.[a]

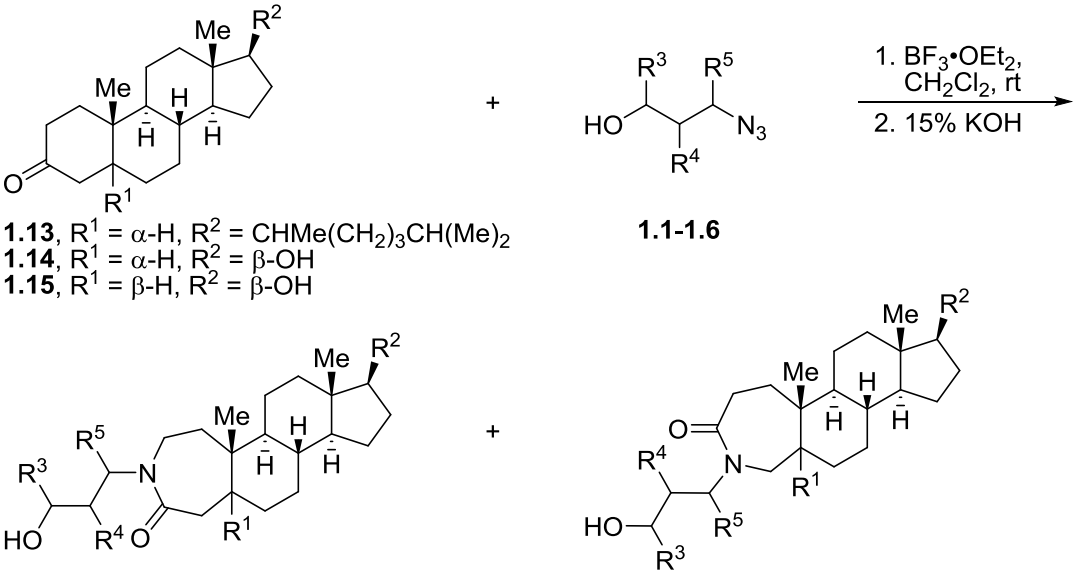

entry	steroid	azide	R^3	R^4	R^5	3-aza: 4-aza ratio[b,c]	product(s)		isolated yield (%)[d]
							3-aza	4-aza	
1	**1.13**	**1.1**	H	H	H	38:62[e]	**1.16** + **1.17**		92[f]
2	**1.13**	(±)-**1.2**	(±)-Ph	H	H	50:50[e]	**1.18** + **1.19**		92[f]
3	**1.13**	(*S*)-**1.2**	(*S*)-Ph	H	H	5:>95	-	**1.19**	88
4	**1.13**	(*R*)-**1.2**	(*R*)-Ph	H	H	>95:5	**1.18**	-	89
5	**1.13**	(*S*)-**1.3**	H	(*S*)-Me	H	10:90[e]	-	**1.20**	84
6	**1.13**	(*R*)-**1.3**	H	(*R*)-Me	H	87:13[e]	**1.21**	-	71
7	**1.13**	(*S*)-**1.4**	H	H	(*S*)-Ph	>95:5	**1.22**	-	88
8	**1.13**	(*R*)-**1.4**	H	H	(*R*)-Ph	5:>95	-	**1.23**	87
9	**1.13**	(*S*)-**1.5**	H	H	(*S*)-Me	5:>95	-	**1.24**	89
10	**1.13**	(*R*)-**1.5**	H	H	(*R*)-Me	>95:5	**1.25**	-	92
11	**1.14**	**1.1**	H	H	H	40:60[e]	**1.26** + **1.27**		95[f]
12	**1.14**	(*S*)-**1.2**	(*S*)-Ph	H	H	5:>95	-	**1.28**	88
13	**1.14**	(*R*)-**1.2**	(*R*)-Ph	H	H	>95:5	**1.29**	-	84
14	**1.14**	(*S*)-**1.6**	(*S*)-(4-Br)Ph	H	H	5:>95	-	**1.30**	86
15	**1.14**	(*R*)-**1.6**	(*R*)-(4-Br)Ph	H	H	>95:5	**1.31**	-	83
16	**1.14**	(*S*)-**1.3**	H	(*S*)-Me	H	13:87[e]	-	**1.32**	87
17	**1.14**	(*R*)-**1.3**	H	(*R*)-Me	H	87:13[e]	**1.33**	-	85
18	**1.14**	(*S*)-**1.4**	H	H	(*S*)-Ph	>95:5	**1.34**	-	89
19	**1.14**	(*R*)-**1.4**	H	H	(*R*)-Ph	5:>95	-	**1.35**	90
20	**1.14**	(*S*)-**1.5**	H	H	(*S*)-Me	5:>95	-	**1.36**	85
21	**1.14**	(*R*)-**1.5**	H	H	(*R*)-Me	>95:5	**1.37**	-	85
22	**1.15**	(*S*)-**1.2**	(*S*)-Ph	H	H	>95:5	**1.38**	-	89
23	**1.15**	(*R*)-**1.2**	(*R*)-Ph	H	H	5:>95	-	**1.39**	83
24	**1.15**	(*S*)-**1.4**	H	H	(*S*)-Ph	5:>95	-	**1.40**	87
25	**1.15**	(*R*)-**1.4**	H	H	(*R*)-Ph	>95:5	**1.41**	-	90

[a]See Sections 1.7.2 for reaction protocol. [b]Ratio of 3-aza- and 4-aza-*A*-homo-steroid lactam was determined by ^{1}H NMR of the crude reaction mixture. [c]Only one regioisomer was observed by ^{1}H NMR

of the crude reaction mixture, unless otherwise noted. [d]Isolated yields of only the major regioisomer, unless otherwise noted. [e]Mixture of regioisomers observed by ^{1}H NMR of the crude reaction mixture. [f]Isolated yields of a mixture of regioisomers.

Representative mechanisms explaining the regiocontrol for the reaction between 3-oxosteroid with (*R*)- or (*S*)-3-azido-1-phenylpropanol **1.2** are illustrated in Figures 1.15 and 1.16, respectively. The mechanism first involves the formation of a pair of spirocyclic 1,3-oxazinanes that readily equilibrate prior to rearrangement.[85-86] The outcome of the rearrangement is governed by three principles: (1) equatorial attack of azide upon the initial oxonium species to establish the stereogenicity of the spirocyclic carbon, (2) preferential reaction of the newly formed 1,3-oxazinane conformer with the phenyl group in an equatorial position, and (3) the stereoelectronically enforced migration of a carbon antiperiplanar to the N_2^+ leaving group (which is axial to allow appropriate arrangement between the migrating and leaving groups). All three factors combine to enforce migration of one diastereotopic methylene group over the other, which was experimentally observed (Table 1.1). In fact, regiochemical outcome switches when the opposite enantiomer of hydroxyalkyl azide is used.

It is revealed in Table 1.1 that 3-oxosteroids **1.13**–**1.15** can be regioselectively converted into either desirable lactam in excellent yields by the expedient choice of (*S*)- or (*R*)-azidopropanol reagents. A prominent trend is that the best regioisomer ratios were obtained from reactions containing alkyl or aryl substitutions at either the 1 or 3 positions of the hydroxyalkyl side chain, whereas a slight erosion in regioselectivity was observed when the 2 position of the hydroxyalkyl side chain is substituted. Particularly, in the cases of (*S*)- or (*R*)-3-azido-2-methylpropanol, (*S*)- or (*R*)-**1.3**, 90:10 regioisomer ratios were observed (entries 5 and 6). It should be noted that azide reagents substituted at the 2 position (whether 2-alkyl or 2-aryl) have been shown to lead to less diastereoselective reactions in the asymmetric Schmidt report.[85] On

the contrary, high regiochemical control was obtained from the reactions containing methyl or phenyl substitution at the 3 position. An instructive pair of examples is shown in Figures 1.17 and 1.18. Here again, the regiochemical outcomes of these reactions are governed by the combination of three principles outlined above.

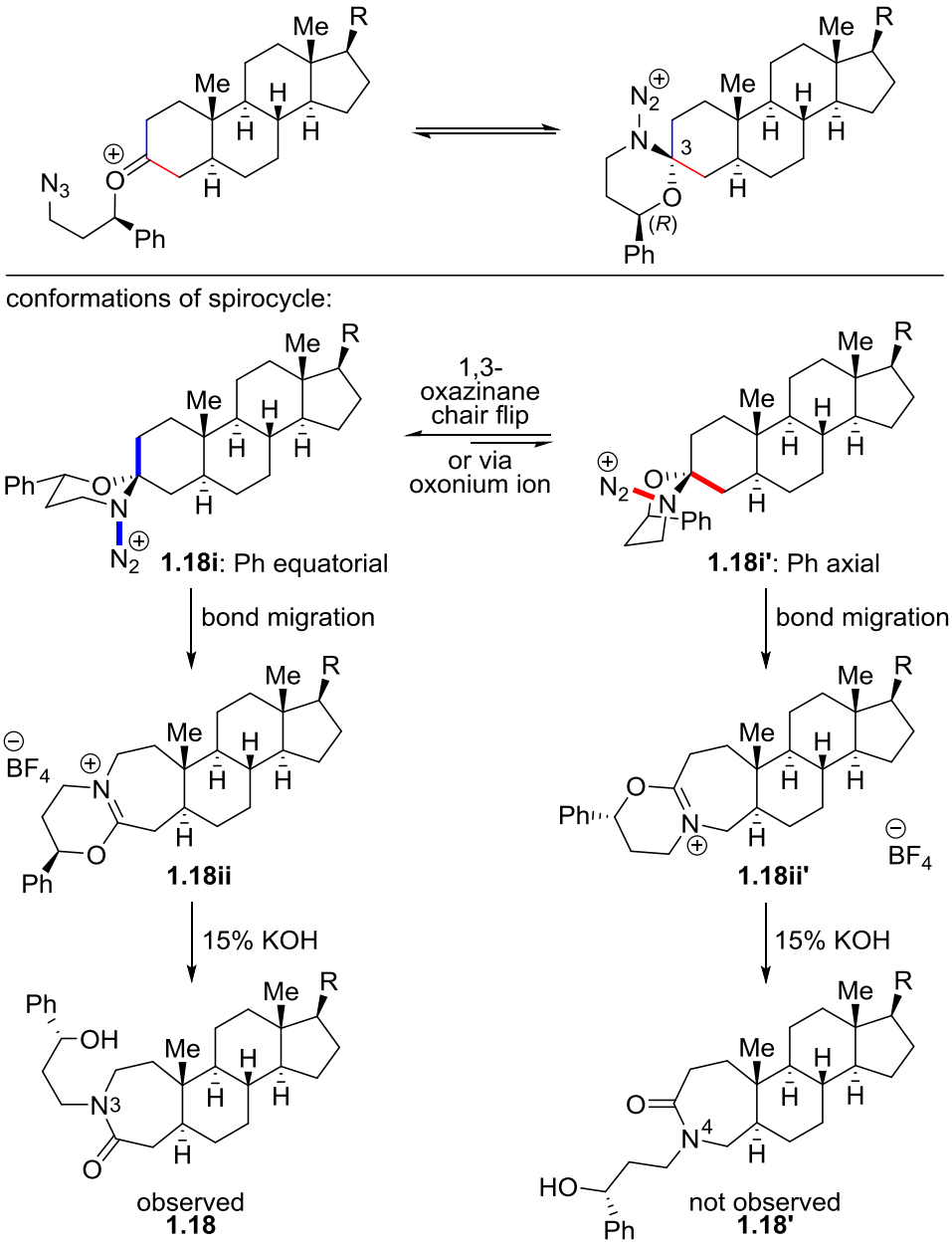

Figure 1.15. Mechanistic rationale for the ring expansion reaction of a 3-oxosteroid with (*R*)-3-azido-1-phenylpropanol (*R*)-**1.2**. In this example, β/equatorial attack by the azide is preferred and the conformation of the newly formed 1,3-oxazinane ring (**i**) is anchored by the 1-phenyl

substituent. This leads to migration of the C-2 carbon (blue bond) and following hydrolysis of iminium **1.18ii** affords isomer **1.18**. Differentiation between C-2 and C-4 migration is shown by the blue and red bonds, respectively, and key antiperiplanar relationship between the migrating group and the N_2^+ leaving group is indicated by bold bonds.

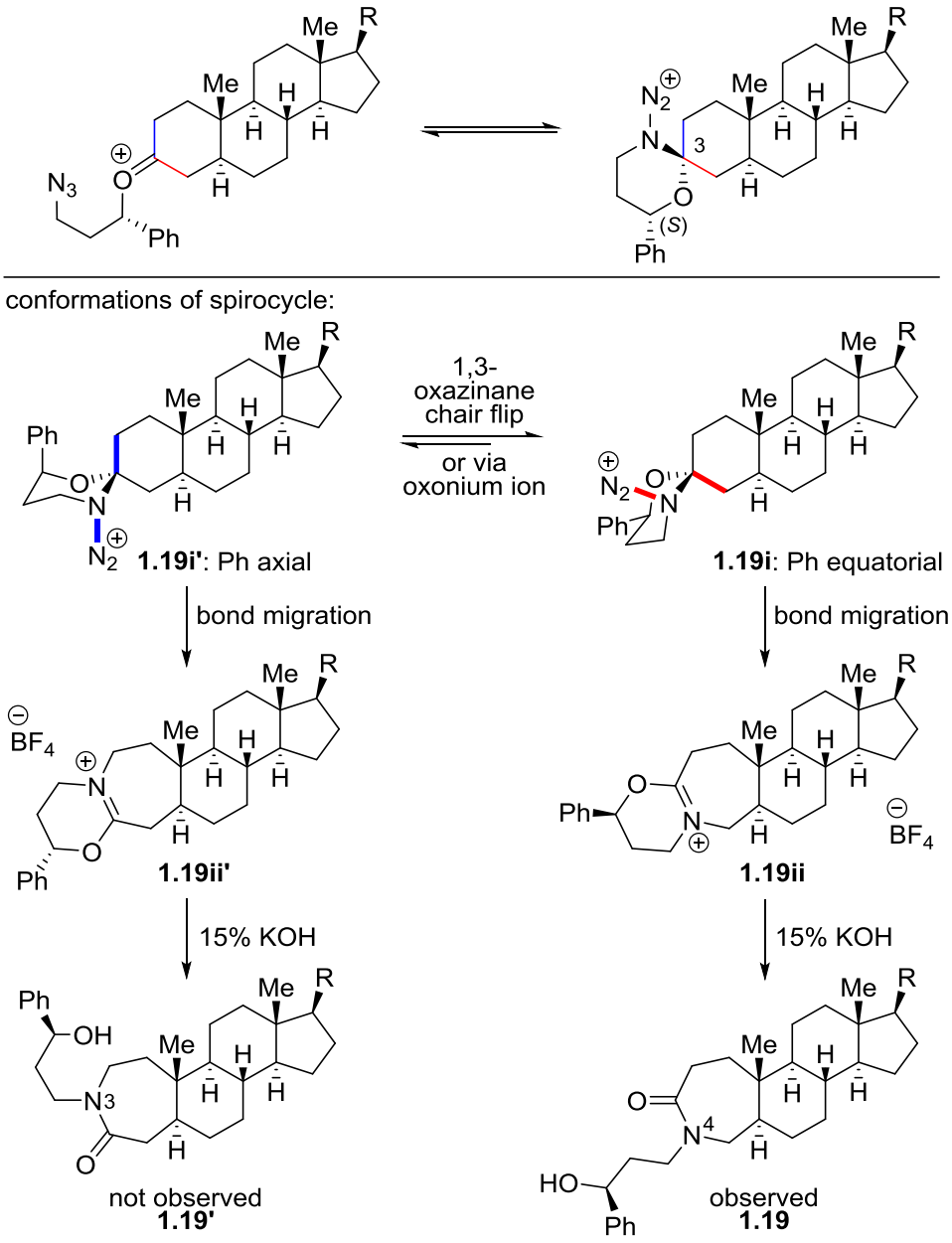

Figure 1.16. Mechanistic rationale for the ring expansion reaction of a 3-oxosteroid with (*S*)-3-azido-1-phenylpropanol (*S*)-**1.2**. In this example, β/equatorial attack by the azide is preferred and the conformation of the newly formed 1,3-oxazinane ring (**i**) is anchored by the 1-phenyl substituent. This leads to migration of the C-4 carbon (red bond) and following hydrolysis of iminium **1.19ii** affords isomer **1.19**. Differentiation between C-2 and C-4 migration is shown by

the blue and red bonds, respectively, and key antiperiplanar relationship between the migrating group and the N_2^+ leaving group is indicated by bold bonds.

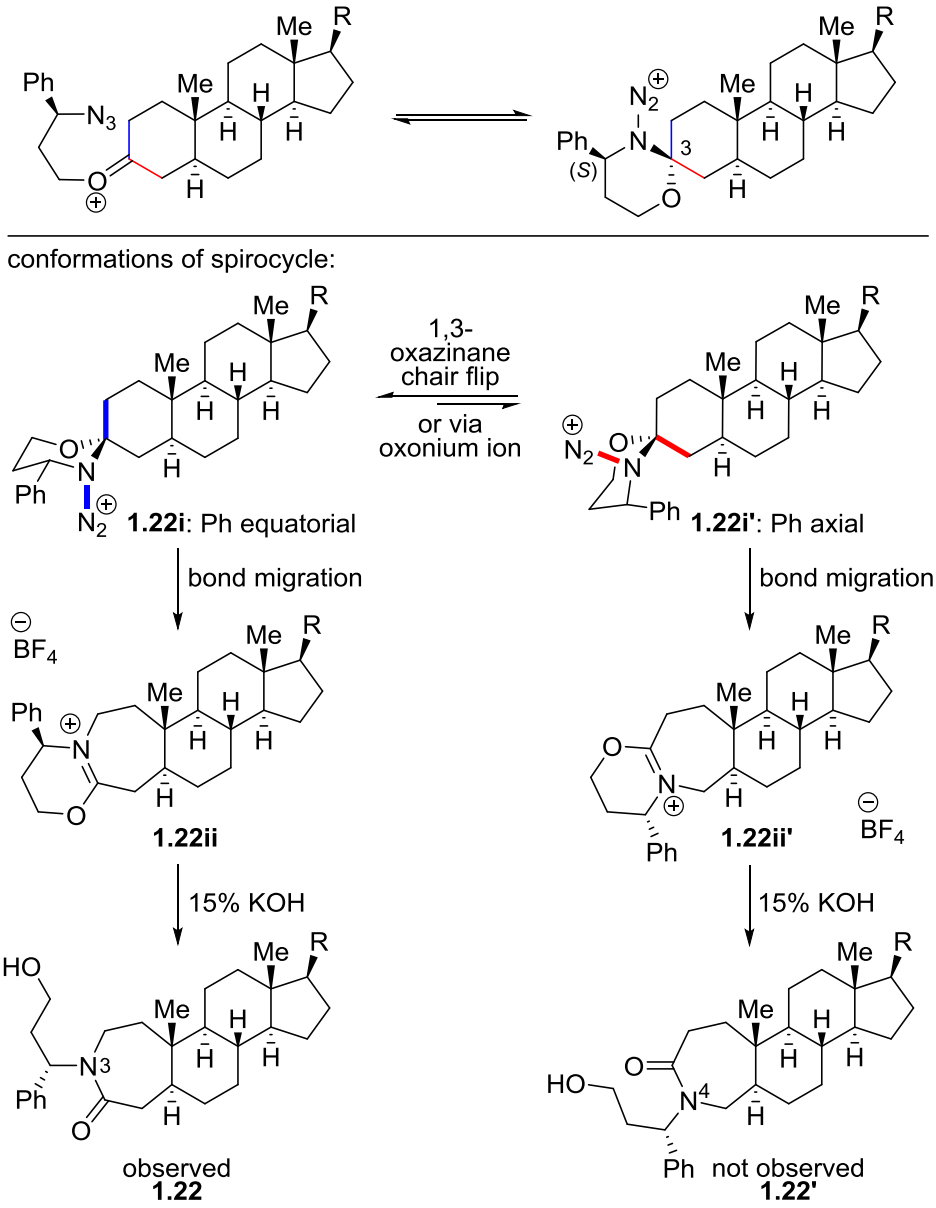

Figure 1.17. Mechanistic rationale for the ring expansion reaction of a 3-oxosteroid with (*S*)-3-azido-3-phenylpropanol (*S*)-**1.4**. In this example, β/equatorial attack by the azide is preferred and the conformation of the newly formed 1,3-oxazinane ring (**i**) is anchored by the 3-phenyl substituent. This leads to migration of the C-2 carbon (blue bond) and following hydrolysis of the iminium **1.22ii** affords isomer **1.22**. Differentiation between C-2 and C-4 migration is shown by the blue and red bonds, respectively, and key antiperiplanar relationship between the migrating group and the N_2^+ leaving group is indicated by bold bonds.

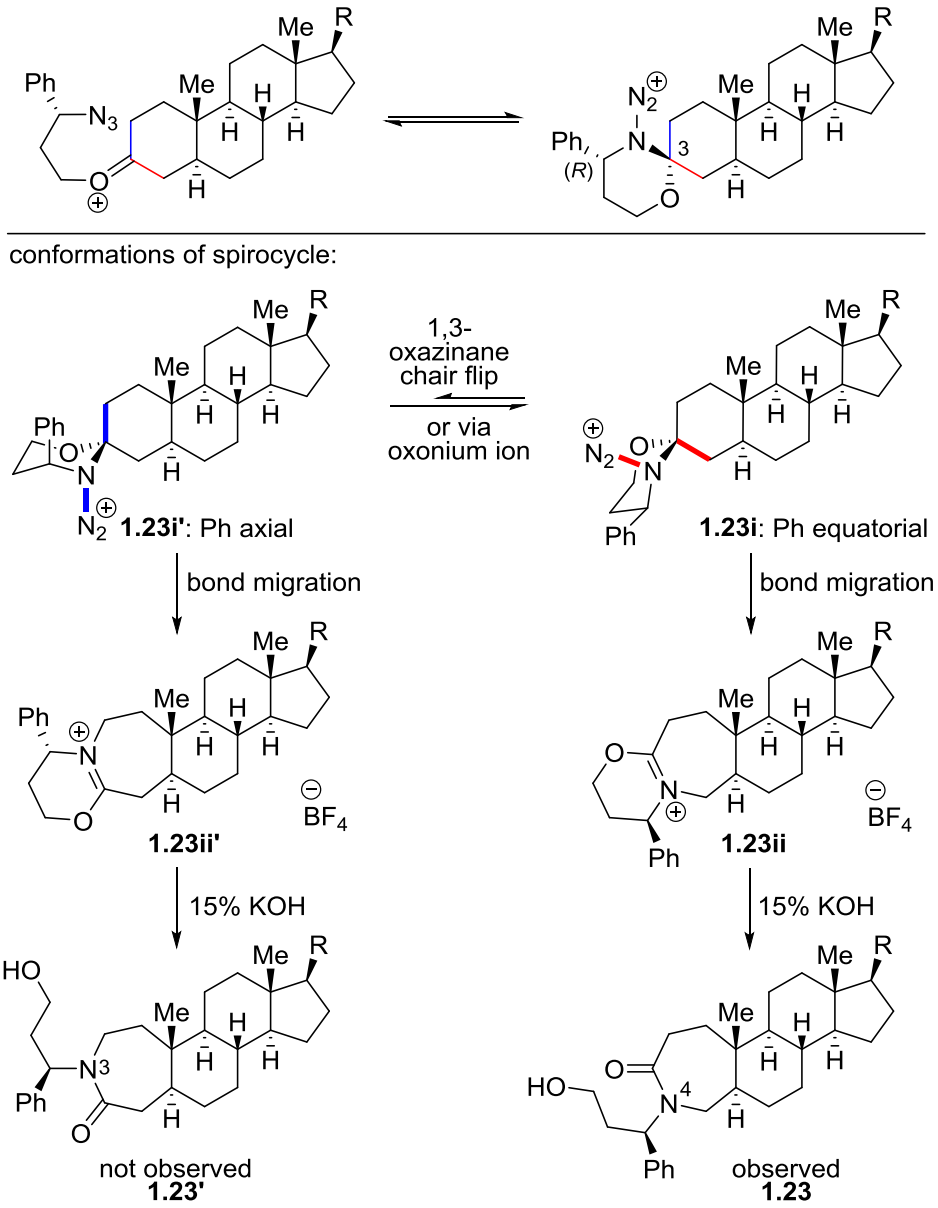

Figure 1.18. Mechanistic rationale for the ring expansion reaction of a 3-oxosteroid with (*R*)-3-azido-3-phenylpropanol (*R*)-**1.4**. In this example, β/equatorial attack by the azide is preferred and the conformation of the newly formed 1,3-oxazinane ring (**i**) is anchored by the 3-phenyl substituent. This leads to migration of the C-4 carbon (red bond) and following hydrolysis of iminium **1.23ii** affords isomer **1.23**. Differentiation between C-2 and C-4 migration is shown by the blue and red bonds, respectively, and key antiperiplanar relationship between the migrating group and the N_2^+ leaving group is indicated by bold bonds.

To expand the library, similar reactions to 3-cholestone **1.13** were carried out with substrates 5α-DHT **1.14** and 5β-DHT **1.15**. Overall yields for these reaction sequences were

excellent throughout (see Table 1.1). An additional opportunity was explored with 5α-DHT **1.14**, in which reactions were carried with a pair of enantioenriched *p*-bromophenyl azide reagents (entries 14 and 15). These analogs were synthesized because the bromo-functionality is a suitable handle for downstream cross-coupling activities.

An enlightening result during the library expansion was that the nitrogen insertion selectivities changed when the stereocontrolled ring expansion reactions were carried out with *cis*-AB steroid, 5β-DHT **1.15** (entries 22–25). When comparing C-5 epimeric steroids, 5α-DHT **1.14** and 5β-DHT **1.15**, opposite nitrogen insertion selectivities were observed. As shown in Scheme 1.10 for example, the same chiral reagent (*S*)-**1.2** reverses the overall directionality of the nitrogen insertion process and results in opposite regioisomeric lactams **1.28** (4-aza) and **1.38** (3-aza). This ensues because for *trans*-AB ring substrates equatorial attack is β, whereas for substrates containing a *cis*-AB ring fusion, equatorial attack is α. A general mechanistic outline for the *cis*-fusion outcome affording analogs **1.38** and **1.39** are shown in Figures 1.19 and 1.20, respectively. In this regard, facial selectivities in azide addition onto the oxonium species changes the absolute stereochemistry of the newly formed spirocycle stereogenic center, which in turn may lead to opposite regiochemical outcomes.

Scheme 1.10. Dependence of migration outcome on C-5 stereochemistry.

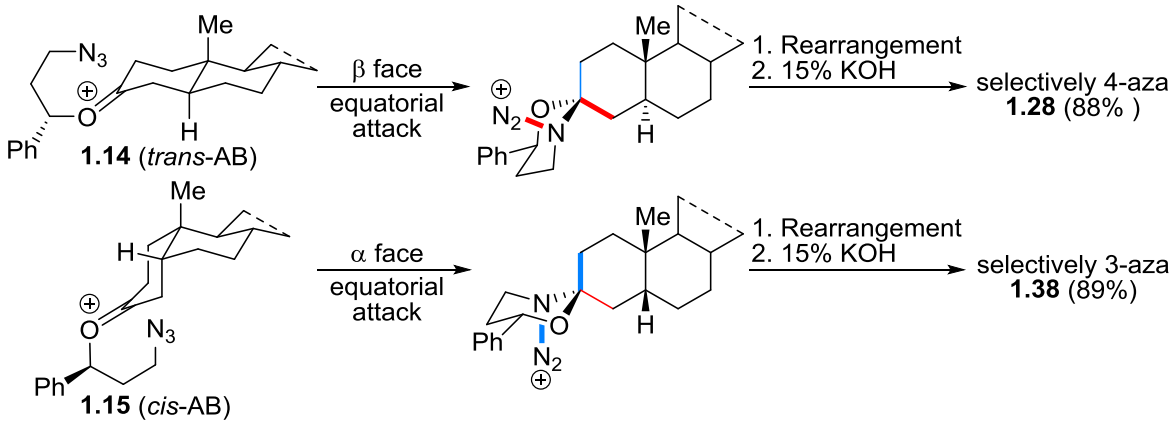

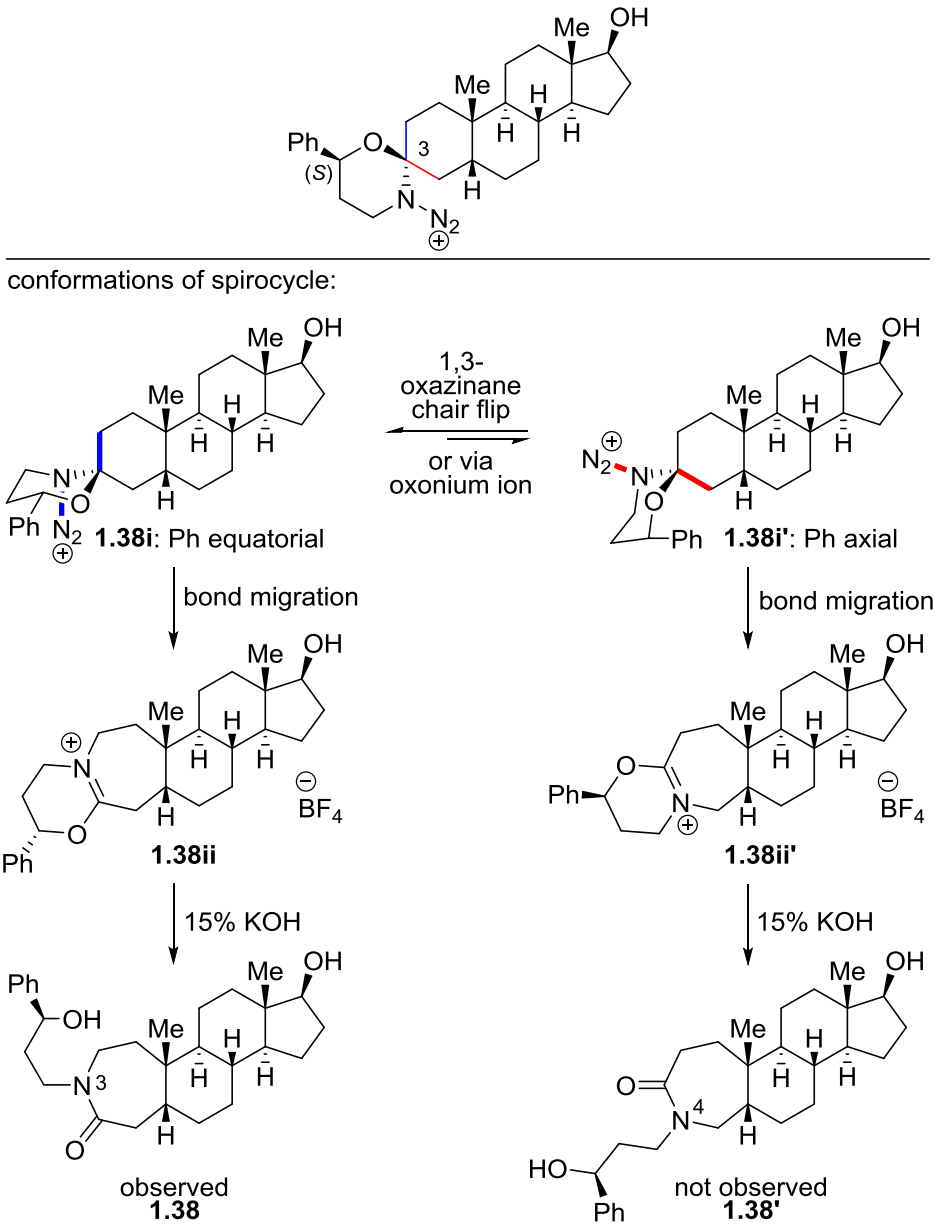

Figure 1.19. Mechanistic rationale for the ring expansion reaction of 5β-DHT **1.15** with (*S*)-3-azido-1-phenylpropanol (*S*)-**1.2**. In this example, α/equatorial attack by the azide is preferred and the conformation of the newly formed 1,3-oxazinane ring (**i**) is anchored by the 1-phenyl substituent. This leads to migration of the C-2 carbon (blue bond) and following hydrolysis of iminium **1.38ii** affords isomer **1.38**. Differentiation between C-2 and C-4 migration is shown by the blue and red bonds, respectively, and key antiperiplanar relationship between the migrating group and the N_2^+ leaving group is indicated by bold bonds.

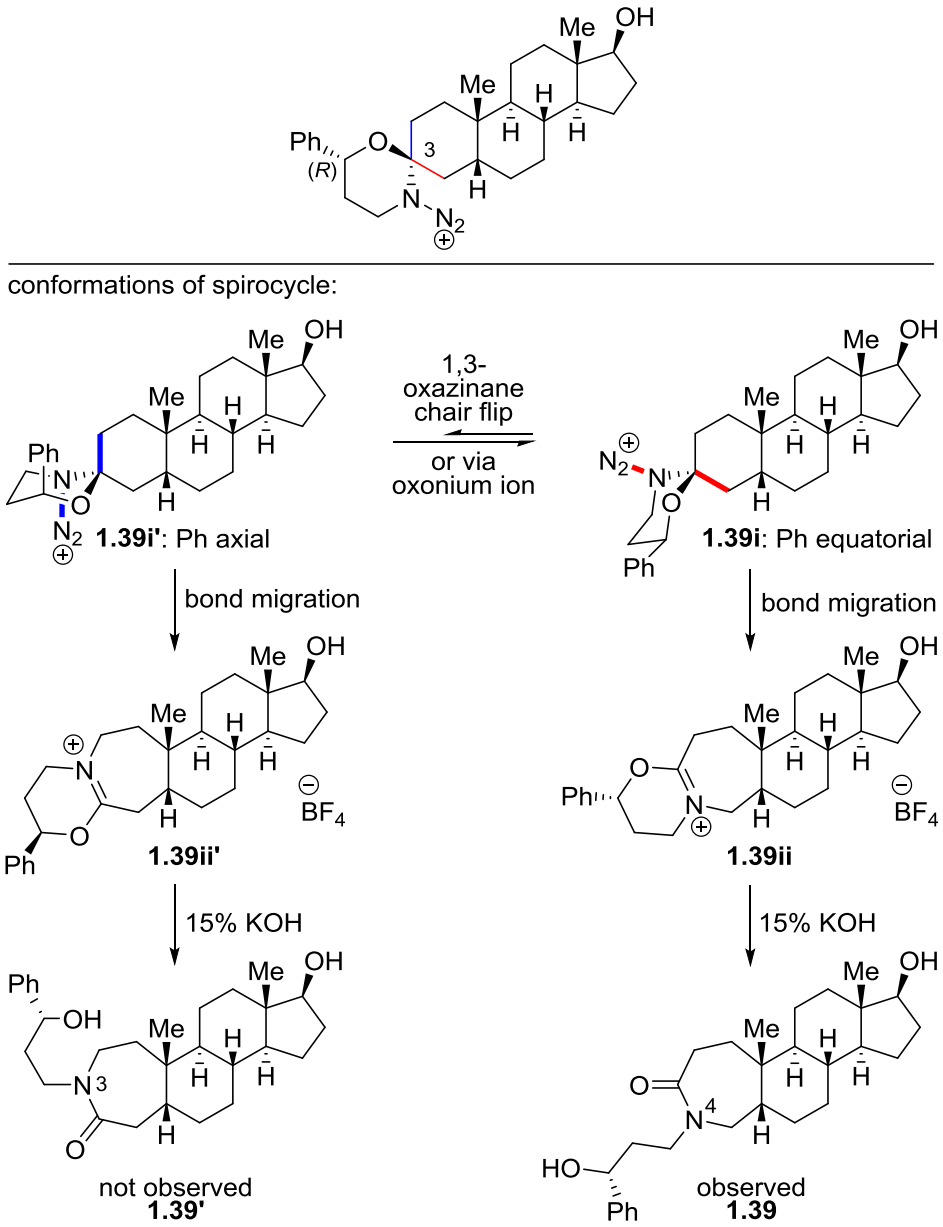

Figure 1.20. Mechanistic rationale for the ring expansion reaction of 5β-DHT **1.15** with (*R*)-3-azido-1-phenylpropanol (*R*)-**1.2**. In this example, α/equatorial attack by the azide is preferred and the conformation of the newly formed 1,3-oxazinane ring (**i**) is anchored by the 1-phenyl substituent. This leads to migration of the C-4 carbon (red bond) and following hydrolysis of iminium **1.39ii** affords isomer **1.39**. Differentiation between C-2 and C-4 migration is shown by the blue and red bonds, respectively, and key antiperiplanar relationship between the migrating group and the N_2^+ leaving group is indicated by bold bonds.

Generally, product selectivity was excellent in the reaction sequences between 3-oxosteroids with enantioenriched azidopropanol derivatives. In this part of our study alone, a

total of 22 isomerically pure azasteroid analogs were synthesized in ≥20 milligrams and ≥90% purity.

1.3.3 A Study on the Use of 1,2-Hydroxyalkyl Azides to Effect Ring Expansion on 3-Oxosteroids, Determination of Constitutional Isomerism Control, and Rationalization of Mechanism

In this study, readily available 5α-DHT **1.14** and 5β-DHT **1.15** were reacted with hydroxyalkyl azides **1.7**–**1.9** (Table 1.2). Not surprisingly (see below), the product outcome of these reaction sequences with azidoethanol derivatives afforded poorer regiochemistry ratios compared to that of the azidopropanol derivatives (Table 1.2, entries 1–3). For entries 1–3, ca. 40:60 ratios were observed, and regioisomers were difficult to purify chromatographically for spectroscopically pure lactams. However, in the remaining entries, the isomeric mixtures were separated in moderate yields and allowed trivial characterization of the major isomers. Isolation of major regioisomers in moderate yields suggest to poor isomeric mixtures and less selective reactions as compared to that of the azidopropanol reagents. Although these reactions were somewhat less selective than the azidopropanol reagents, the reactions with enantioenriched azidoethanol derivatives still provided isomerically pure 3-azasteroid and 4-azasteroid analogs **1.42**–**1.51** for the library collection.

In regards to the mechanism, the relationship between the migrating and leaving groups are less certain due to the presence of a five-membered ring requisite intermediate (i.e., uncertainty in assuming antiperiplanar angles for migration). Arguably from these results, a key source of regiochemical control is the minimization of steric interactions between the phenyl group of the side-chain and the migrating carbon of the steroid A-ring. In comparison to the

three-carbon azide reagents, the drop in selectivity associated with the two-carbon azide reagents is consistent with the requisite formation of five-membered ring conformers. Our reasoning is consistent with the data in Table 1.2.

Table 1.2. Reaction of 3-oxosteroid **1.13**–**1.14** with 1,2-hydroxyalkyl azides **1.7**–**1.9**.[a]

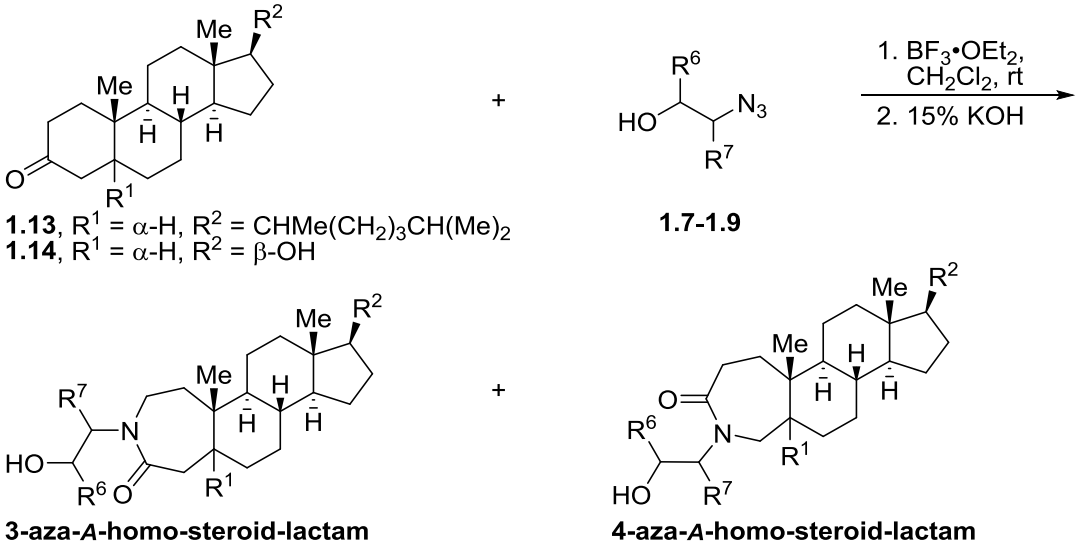

entry	steroid	azide	R^6	R^7	3-aza:4-aza ratio[b]	product(s)		isolated yield (%)
						3-aza	4-aza	
1	**1.13**	**1.7**	H	H	37:63[c]	**1.42** + **1.43**		95[d]
2	**1.13**	(*S*)-**1.8**	(*S*)-Ph	H	46:54	**1.44** + **1.45**		93[d]
3	**1.13**	(*R*)-**1.8**	(*R*)-Ph	H	33:67[c]	**1.46** + **1.47**		88[d,e]
4	**1.13**	(*S*)-**1.9**	H	(*S*)-CH_2Ph	ND	-	**1.48**	81[f,g]
5	**1.13**	(*R*)-**1.9**	H	(*R*)-CH_2Ph	ND	**1.49**	-	65[f,h]
6	**1.14**	(*S*)-**1.9**	H	(*S*)-CH_2Ph	ND	-	**1.50**	76[f,i]
7	**1.14**	(*R*)-**1.9**	H	(*R*)-CH_2Ph	ND	**1.51**	-	65[f]

[a]See Section 1.7.2 for reaction protocol. [b]Ratio of 3-aza- and 4-aza-*A*-homo-steroid lactam was determined by ^1H NMR of the final product. [c]Mixture of regioisomers observed by ^1H NMR of the crude reaction mixture, unless otherwise noted. [d]Isolated yield of a mixture of regioisomers. [e]Isomeric mixture was separated to give 26% isolated yield of **1.46** and 46% isolated yield of **1.47**. [f]Isolated yield of the major regioisomer. [g]Isolated 12% yield (<10.0 mg) of the minor regioisomer, however was not further characterized. [h]Isolated 22% yield (<17.0 mg) of minor regioisomer, however was not further characterized. [i]Minor regioisomer observed in the final product. ND = Not Determined.

Two of the analogs synthesized, **1.48** and **1.49**, provided crystals that were analyzed by X-ray crystallography to confirm regiochemistry, which permitted correlation with NMR

spectroscopic data for regiochemistry assignments (Figures 1.21 and 1.22). The X-ray crystal structures for these analogs are provided in the Cambridge Crystallography Deposit Center (CCDC).

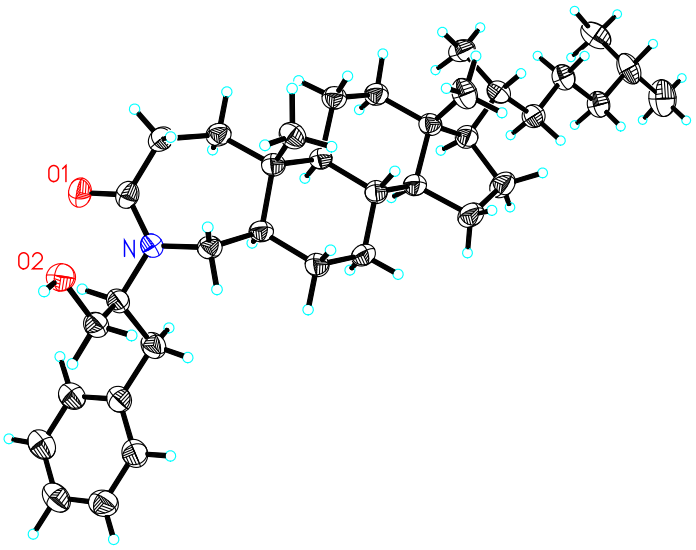

Figure 1.21. X-ray crystal structure for analog **1.48** (CCDC 1583534).

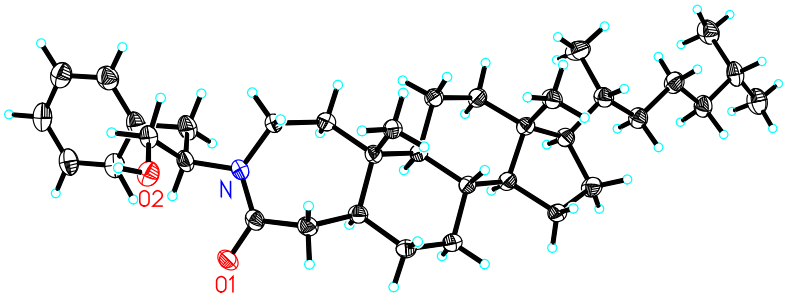

Figure 1.22. X-ray crystal structure for analog **1.49** (CCDC 1583534).

1.3.4 Functionalization of A-Ring Iminium Ions with Various Nucleophiles

The intermediacy of iminium ethers as primary rearrangement products facilitates the utility of this reaction in library development. This intermediate permitted a direct route to scaffold diversification by reaction with various nucleophiles. Conveniently, prior purification of iminium ether intermediates for functionalization was not necessary in these protocols. Using a

one-pot, three component reaction protocol, functionalized 3-aza- and 4-azasteroid analogs were prepared (Table 1.3). Specifically, readily available 5α-DHT **1.14** and 5β-DHT **1.15** substrates were reacted with hydroxyalkyl azides (*S*)- and (*R*)-**1.2**, as well as, (*S*)- and (*R*)-**1.4**, resulting in the regioselective formation of iminium ethers that were subsequently functionalized by treatment with four nucleophiles: sodium sulfide (Na_2S), the reducing agents sodium borohydride ($NaBH_4$) or hydrogen gas with Pd/C, NaN_3, and 4-methylthiophenoxide. As described in the introduction, iminium ethers are known to react with a variety of nucleophiles at two possible carbon sites: path *a* via the formal sp^2 iminium carbon and path *b* via the sp^3 carbon adjacent to the oxygen atom. In this series, nucleophiles proceeding through path *a* afforded thioamides **1.52**–**1.57** (via treatment with Na_2S) and amines **1.58**–**1.59** (via treatment with $NaBH_4$). Reduction of the iminium ion to access amines was accomplished under very mild conditions compared to those typically employed for amide bond conversion to amines (e.g., refluxing LAH).

Conversely, reduction of the iminium ion using hydrogenation conditions proceeded through path *b*, which resulted in a benzylic reduction and removed the regiodirecting stereocenter making this a 'traceless' process (Table 1.3, analogs **1.60**–**1.61**). Typically, nucleophiles associated with path *b* undergo S_N2-type reactions. In this series, azide-containing **1.62**–**1.67** and sulfide-containing **1.68**–**1.73** *N*-alkylated lactams were synthesized in moderate yields (compound collection is shown in Table 1.3). Moreover, we inferred inversion of stereochemistry of the analogs containing a phenyl substituent at the sp^3 carbon adjacent to the oxygen atom when the corresponding iminium intermediate reacted with azide and benzothiolate nucleophiles via path *b* (noted in the footnotes of Table 1.3 as well). It is also worth noting that

configuration of the side-chain hydroxyl is retained for analogs that proceed to react via path *a* (based on ^{18}O-labeling studies reported in the literature as discussed in the introduction).[84, 104]

Table 1.3. Three-component reactions for the synthesis of functionalized 3-azasteroids and 4-azasteroids.[a]

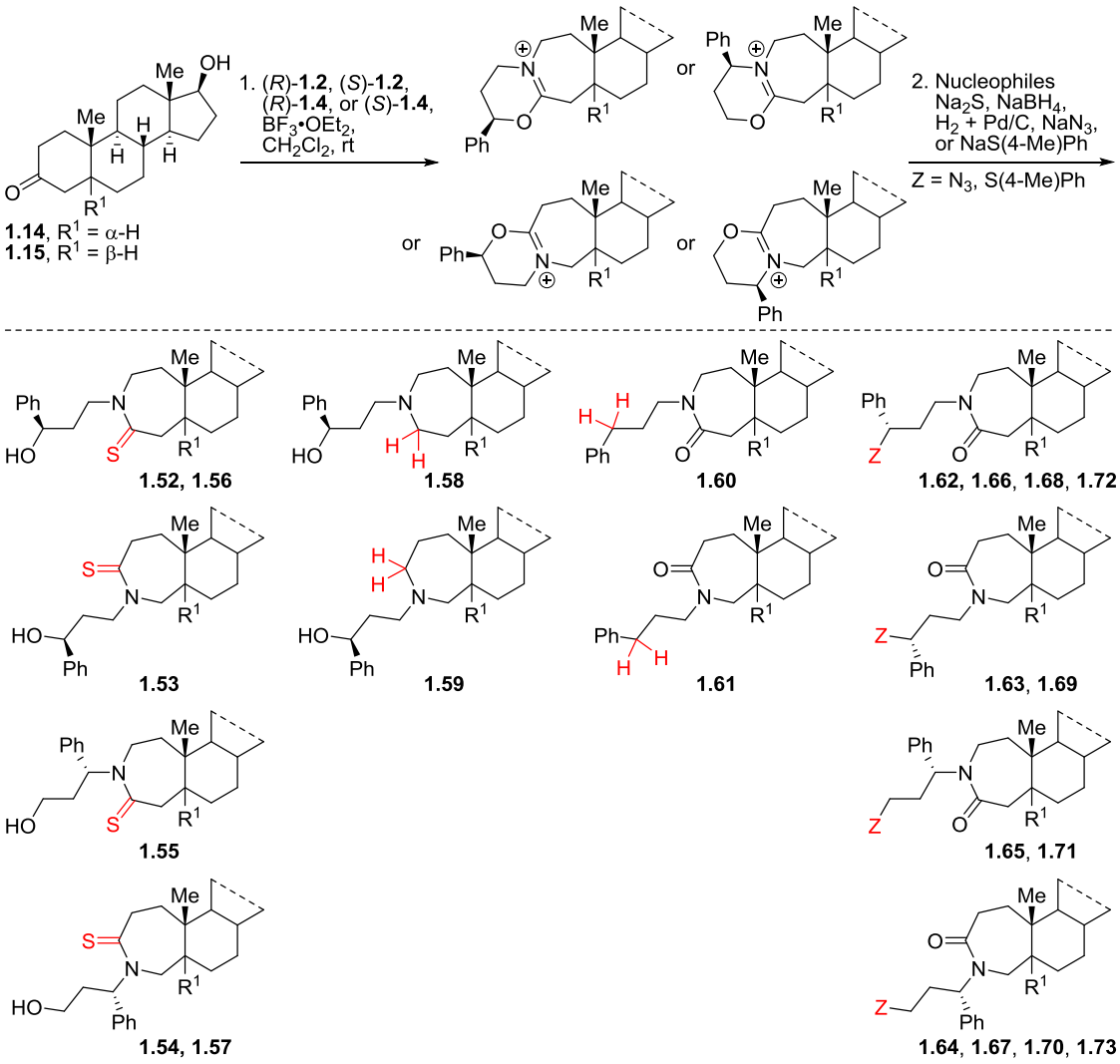

entry	steroid	azide	isolated yield (%)				
			S	H		Z	
						N_3	(4-Me)PhS[b]
1	**1.14**	(*R*)-**1.2**	85, **1.52**	87, **1.58**[c,d]	92, **1.60**[e]	56, **1.62**[f]	66, **1.68**[f]
2	**1.14**	(*S*)-**1.2**	45, **1.53**	50, **1.59**[c,g]	93, **1.61**[e]	73, **1.63**[f]	67, **1.69**[f]
3	**1.14**	(*R*)-**1.4**	59, **1.54**	-		65, **1.64**	83, **1.70**
4	**1.14**	(*S*)-**1.4**	80, **1.55**	-		60, **1.65**	65, **1.71**
5	**1.15**	(*S*)-**1.2**	62, **1.56**	-		82, **1.66**[f]	56, **1.72**[f]
6	**1.15**	(*S*)-**1.4**	78, **1.57**	-		84, **1.67**	76, **1.73**

[a]See Section 1.7.2 for reaction protocols. [b]0.66 M stock solution of sodium 4-methyl thiophenoxide was prepared immediately prior to use by adding sodium (1.0 equiv) to a solution of 4-methylbenzenethiol (1.1 equiv) in anhydrous DMF (15.0 mL) at 0 ˚C and stirring at room temperature overnight. [c]$NaBH_4$, MeOH. [d]51% isolated yield of **1.58** was also obtained from LAH reduction of **1.29**. [e]Hydrogenation using 10% Pd/C, EtOH. [f]Inversion of stereochemistry. [g]58% isolated yield of **1.59** was also obtained from LAH of **1.28**.

Finally, to further incorporate structural diversity, derivatives lacking the stereochemical information that was used to effect the specific ring-expansion reactions were synthesized (Scheme 1.11). If necessary, the "parent" lactams of the A-ring steroid are suitable precursors for downstream diversification. Removal of the regiodirecting stereocenter was carried out by two straightforward synthetic sequences: (1) hydrogenation to remove the benzylic hydroxyl group and (2) oxidation of the benzylic hydroxyl group to ketone functionality. As shown in Scheme 1.11a, 3-azasteroid derivatives **1.18** and **1.29** were converted to analogs **1.74**–**1.76** lacking stereochemical information in the *N*-side chain; in a similar manner, 4-azasteroid derivatives **1.77**–**1.79** were synthesized (Scheme 1.11b). Particularly in Scheme 1.12, oxidation of the side chain-benzylic hydroxyl group followed by elimination with sodium hydride (NaH) base afforded "parent" constitutional isomers. 3-Cholestone and 5α-DHT ketone derivatives **1.75**–**1.76** were converted to 3-azasteroid "parent" lactams **1.80**–**1.81** in high yields (Scheme 1.12a). Accordingly, using similar transformations 4-azasteroid derivatives were converted to its "parent" structure **1.82**–**1.83** (Scheme 1.12b).

Scheme 1.11. Stereoconvergence. (a) Stereoconvergence of 3-azasteroid analogs. (b) Stereoconvergence of 4-azasteroid analogs.

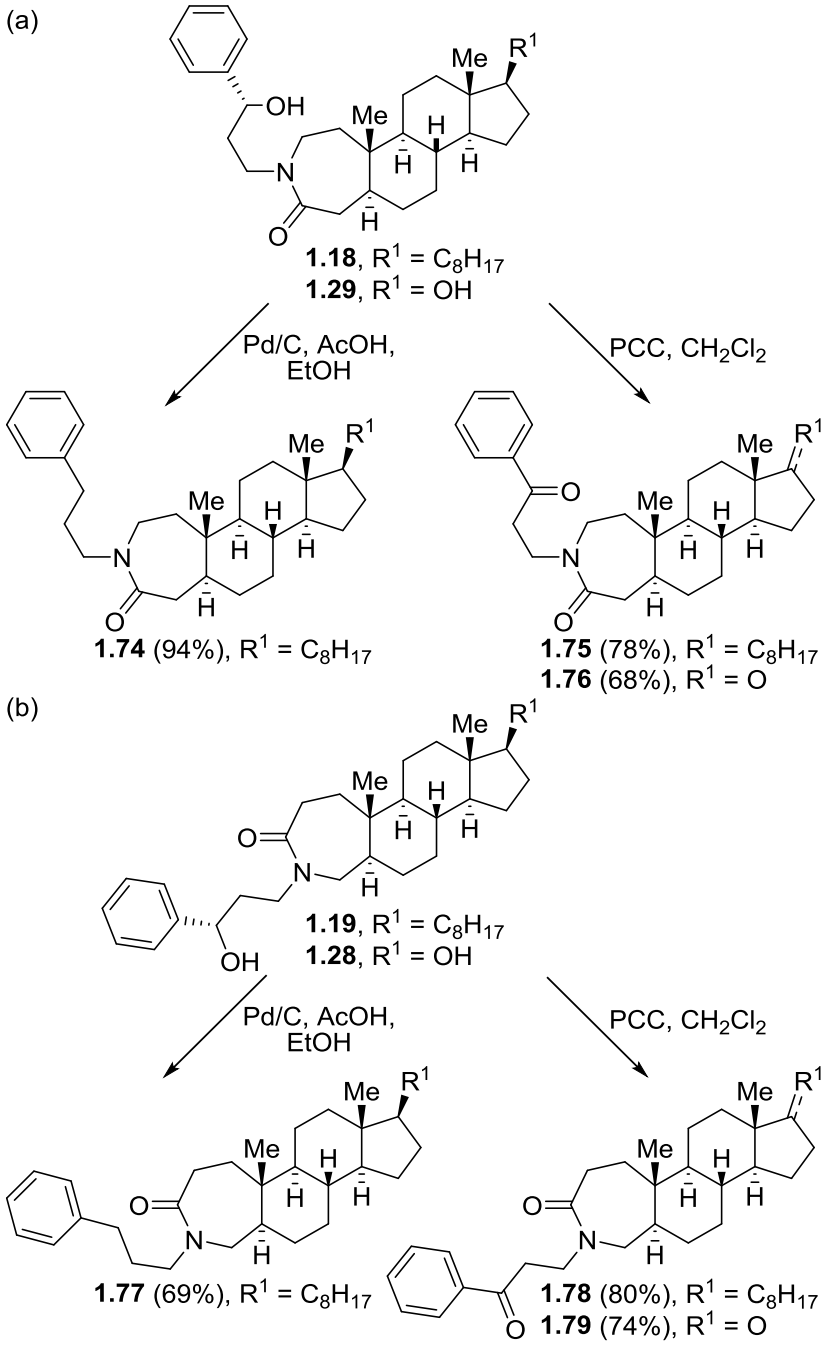

Scheme 1.12. Synthesis of the 'parent' NH A-ring lactams. (a) Synthesis of the 'parent' 3-azsteroid A-ring lactam. (b) Synthesis of the 'parent' 4-azsteroid A-ring lactam.

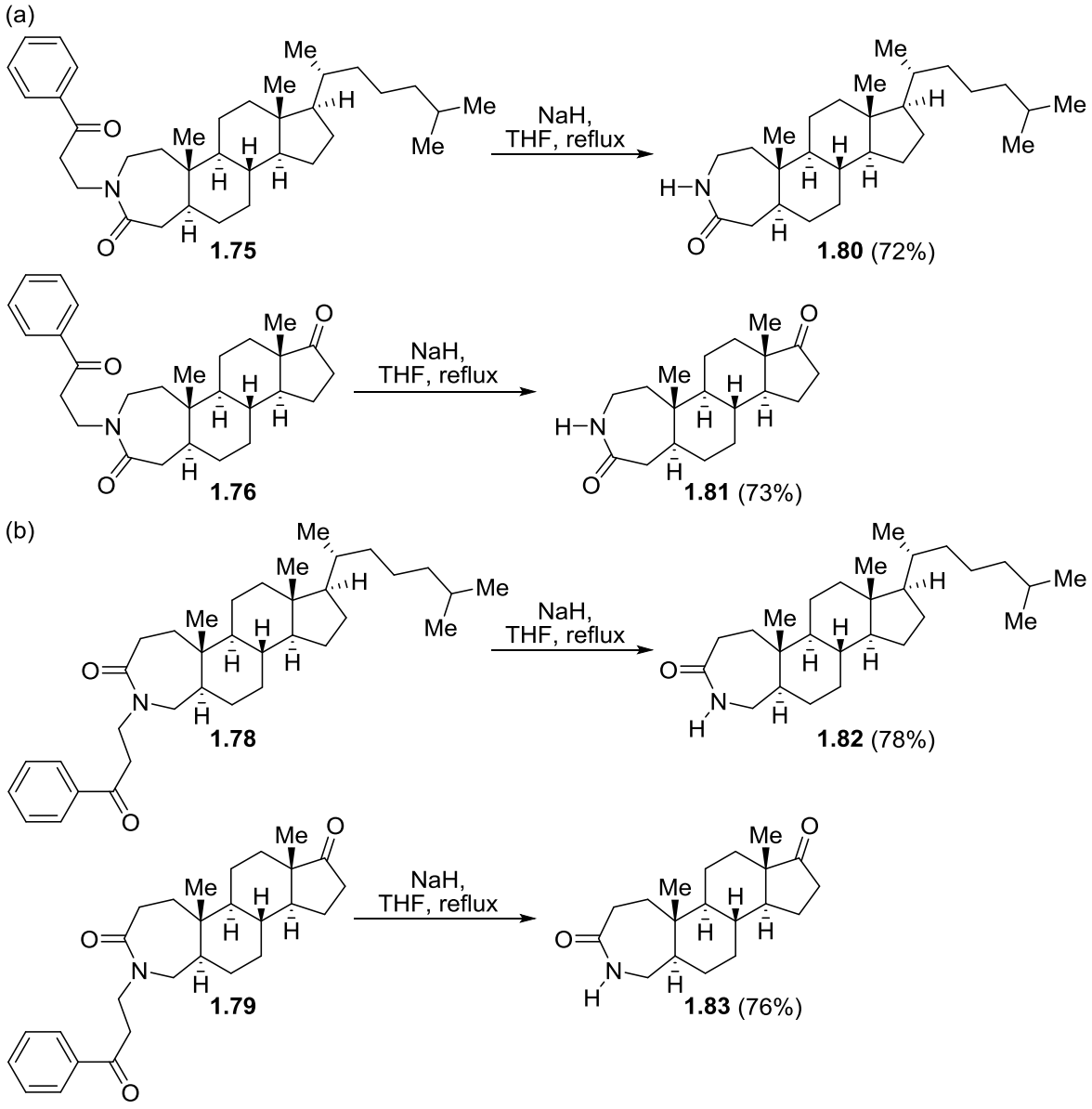

1.4 D-Ring Modifications

1.4.1 Beckmann Rearrangement of 17-Oxosteroids

The Beckmann rearrangement for ring expansion chemistry is analogous to the Schmidt reaction, and, so similarly, is a useful tool to introduce a nitrogen heteroatom into a carbocyclic

framework through the modification of a ketone.[70, 105] Although the Beckmann rearrangement of 17-oxosteroid has been known since 1956,[94] the analog was synthesized to demonstrate the Beckmann reaction as a complementary method; more importantly, to compare mechanistically and spectroscopically the regioisomeric outcome with that of the Schmidt reaction of hydroxyalkyl azide. In this work, the stereospecific isomerization of 17-oxime-steroid to give 17-lactam-steroid warrants discussion because the regiochemical outcome of the Beckmann reaction is complementary to that of the Schmidt reaction of azidopropanols.

The Beckmann rearrangement requires two synthetic steps. As shown in Scheme 1.13, oximes were prepared from starting ketone, *trans*-androsterone **1.84** and acetate-protected *trans*-androsterone **1.85**. Then, rearrangement of 17-oxime-steroids **1.86**–**1.87** was carried out by treatment with thionyl chloride ($SOCl_2$) in anhydrous tetrahydrofuran (THF). Unfortunately, the conversion to desired lactams **1.88**–**1.89** proceeded in low yields. A continual challenge for carrying out the Beckmann reaction is the requirement of harsh conditions. For example, we used 10.0 equiv excess of $SOCl_2$ to prepare the lactam products. Despite using excess acid, only one isomer of the rearranged product **1.88**–**1.89** was observed. Generally, the Beckmann rearrangement is stereospecific and the observed regiochemical outcome is consequential of the preferential formation of the (*E*)-oxime. Theoretically two constitutional (*E*)- and (*Z*)-oximes may occur, however biased by the steroid structure, formation of the sterically less hindered (*E*)-17-oxime is favorable (Figure 1.23). In contrast, the formation of (*Z*)-17-oxime is encumbered by syn-pentane-like interactions and is very unlikely. As a result, rearrangement proceeds exclusively through migration of the C-13 antiperiplanar to the activated OH leaving group affording the lactam **1.88**. Alternatively, one could rationalize the isolation of the exclusive

regioisomer as confirmation to the assignment of the (*E*)-17-oxime **1.86** as the sole oxime isomer.

Scheme 1.13. The Beckmann reaction of 17-oxosteroids **1.84**–**1.85**.

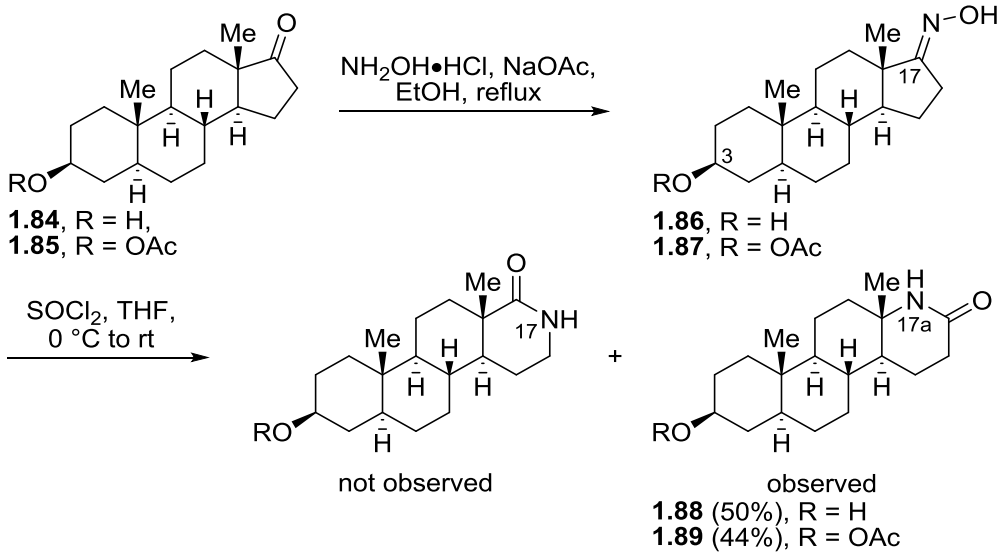

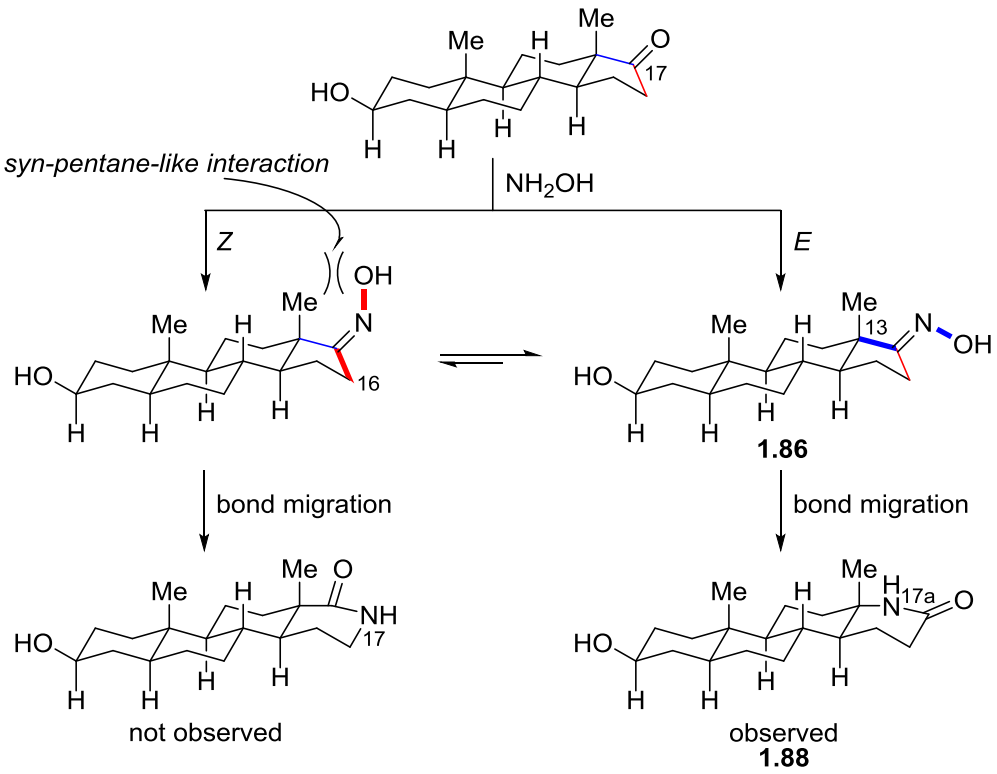

Figure 1.23. Proposed mechanism for the Beckmann reaction of *trans*-androsterone **1.84**. The Beckmann rearrangement has been established and shown[70] to occur through selective reaction of the sterically least hindered (*E*)-oxime isomer **1.86** and migration of the *trans*-antiperiplanar bond as depicted in bold blue.

Although the Beckmann rearrangement gave a clean conversion to one regioisomer, a continual restriction of this ring expansion chemistry is the lack of flexibility in providing access to either isomers selectively at will. Therefore, in order to find synthetic routes for selective preparation of all constitutional isomers other types of chemistry must be explored.

1.4.2 Intramolecular Schmidt Reaction of 17-Oxosteroids

The intramolecular Schmidt reaction was used to add to this library collection. First introduced in 1991 by Milligan and Aubé, the tethered alkyl azide reacts with ketone under acidic conditions in an intramolecular fashion to prepare a fused lactam.[106] Since its discovery,

the method has been extensively studied and usually leads to the fused lactam isomer. Here, a recently improved protocol of the intramolecular Schmidt reaction was applied to the structurally complex 17-oxosteroids, *trans*-androsterone **1.84** and estrone **1.90**.[107]

As shown in Scheme 1.14, the 3-hydroxyl group of *trans*-androsterone **1.84** was protected using *tert*-butyldimethylsilyl chloride (TBSCl) affording **1.91** prior to synthesis of the tethered alkyl azide. The C-16 alkylation of the 17-oxosteroidal substrates was carried out by deprotonation with lithium di-isopropyl amide (LDA) conditions followed by addition of 1-chloro-3-iodopropane to provide chloro-alkyl substituted tethers. The α stereochemistry at the C-16 position of **1.92** was determined by 1D-NOE NMR experiments, in which the C-16 β-hydrogen was found to be close to the C-13 methyl substituent. The chloro-alkyl tether derivative **1.92** was converted to azide-alkyl tether **1.93** by treatment with NaN_3. With **1.93** in hand, conversion to fused lactam **1.94** proceeded smoothly in good yields using 1.5 equiv of titanium tetrachloride ($TiCl_4$) in HFIP; excess acid facilitated the intramolecular Schmidt reaction and the removal of 3-hydroxyl-TBS protecting group. On the other hand, with an azide-alkyl estrone substrate **1.97**, the reaction only required 50 mol% of $TiCl_4$ to directly afford the corresponding fused lactam **1.98** in 69% yield. The following methoxy-deprotection of **1.98** with boron tribromide (BBr_3) reagent gave the 3-phenol-17-fused-lactam analog **1.99**.[108] Finally, it is worth noting that in both examples the intramolecular Schmidt reaction was exclusively selective for the fused lactam over the bridge lactam isomer; the fused lactam proceeds via formation of the most stable ring fusion (Figure 1.24). Although the intramolecular Schmidt reaction forced migration of C-16 over C-13 (compared to the Beckmann reaction), the attachment of an azidopropane side chain onto a steroid is a limited solution for late-stage diversification and

regiodivergent strategies. In these experiments, three analogs of the interesting pentacyclic lactams were synthesized and incorporated in the library collection.

Scheme 1.14. The intramolecular Schmidt reaction of *trans*-Androsterone **1.84**.

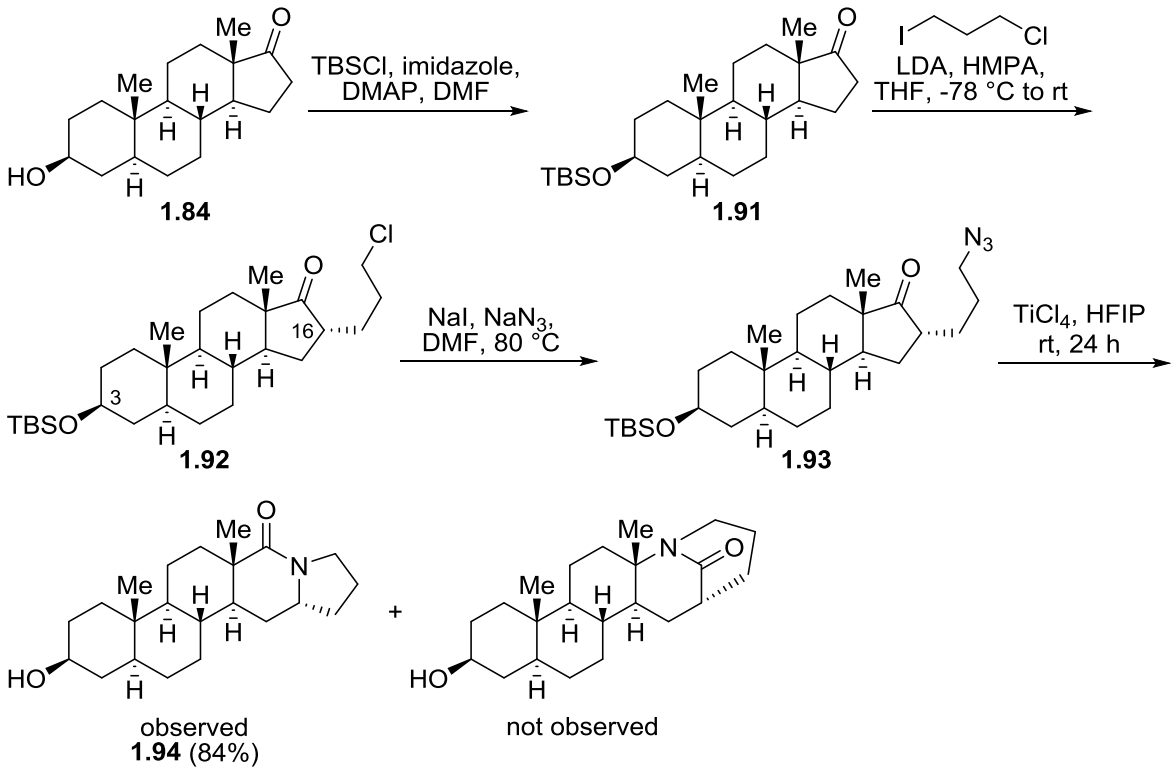

Scheme 1.15. The intramolecular Schmidt reaction of estrone **1.90**.

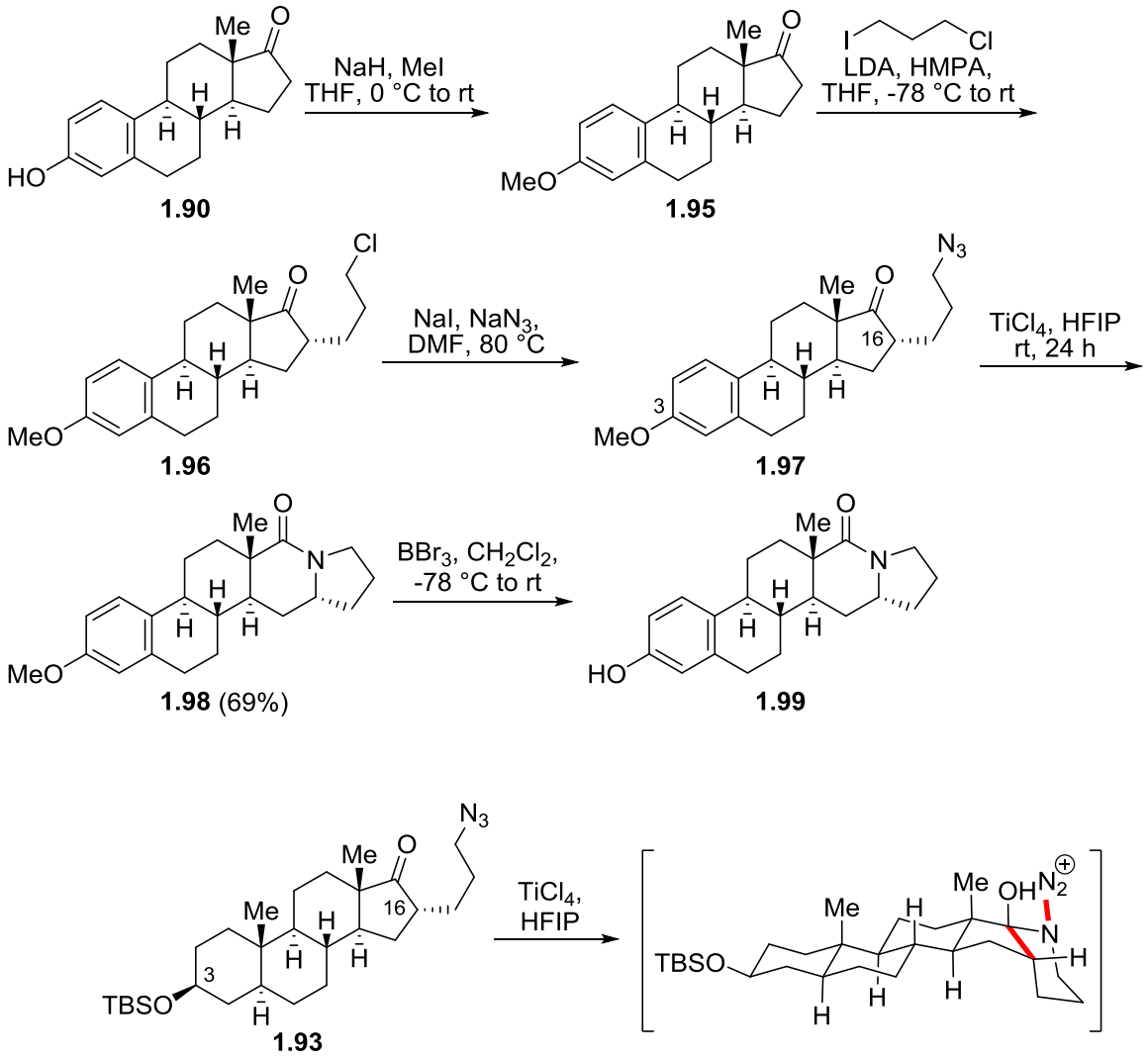

Figure 1.24. Proposed mechanism for the intramolecular Schmidt reaction of *trans*-androsterone **1.84**. The intramolecular Schmidt reaction of a tethered azido ketone entails formation of the most stable ring fusion upon azide addition to the $TiCl_4$-activated ketone and subsequent migration of a C–C bond antiperiplanar to the N_2^+ leaving group. In these reactions, the leaving group generally occupies an equatorial position and migration of the ring fusion carbon ensues. Under special conditions, axial N_2^+ is possible, leading to bridged adducts, but these cases are rare.[109] In the case shown, α-addition to C-17 is proposed because the *cis* bicyclic ring systems are generally preferred over the *trans* version, but the same outcome would be predicted from either direction of attack.

1.4.3 A Study on the Use of 1,3-Hydroxyalkyl Azides to Effect Ring Expansion on 17-Oxosteroids, Determination of Constitutional Isomerism Control, and Rationalization of Mechanism

To address the problem of D-ring regiochemical divergence, the Schmidt reaction of hydroxyalkyl azide (i.e., stereoelectronically controlled ring expansion) was employed to influence the *N*-side chain installation. In this study, readily available 17-oxosteroids **1.84** and **1.90** were reacted with hydroxyalkyl azides **1.1**–**1.6**. However, prior to the study, optimization studies of the reaction condition was carried out. Due to the relatively hindered nature of the D-ring neopentyl carbonyl, a survey of reaction conditions was explored. The reaction between *trans*-androsterone **1.84** and 3-azidopropanol **1.1** was optimized and these conditions are shown in Table 1.4. Generally, this Schmidt reaction variant requires 2.0–5.0 equiv of BF_3•OEt_2 in CH_2Cl_2 to execute efficient lactam synthesis from simple cyclic ketones. Unfortunately, under these conditions starting material remained unconsumed even after 24 hours and with increased acid loading to 7.0 equiv (entries 1–3). To address this poor reactivity, a recently improved protocol in hexafluoroisopropanol ($(CF_3)_2CHOH$ or HFIP) was adopted (the details of this methodology development are discussed in Chapter 2).[110]

Improved results were obtained by carrying out the reaction in HFIP. In surveying some protic acids in HFIP (entries 4–6), trifluoromethanesulfonic acid (CF_3SO_3H or TfOH) gave a complete conversion from starting material **1.84** to lactam **1.100** within 24 h and afforded 94% yield of exclusively one regioisomer (**1.100** isomer observed while **1.100'** isomer not observed). From this optimization study, a significant improvement in the minimization of acid equivalence resulted from using HFIP as a solvent media. However, a minimal promoter stoichiometry of 1.0 equiv is necessary to facilitate counterion stabilization of the iminium ether intermediate. To

complete this study, the use of TfOH for this reaction was compared in another fluorinated alcohol solvent trifluoroethanol (CF_3CH_2OH or TFE) and the traditional solvent CH_2Cl_2 (entries 7 and 8). These results failed to give complete conversions from starting material to lactam, which further affirmed the use of HFIP as optimal.

Table 1.4. Optimization of conditions for the reaction between *trans*-androsterone **1.84** and 3-azidopropanol **1.1**.[a]

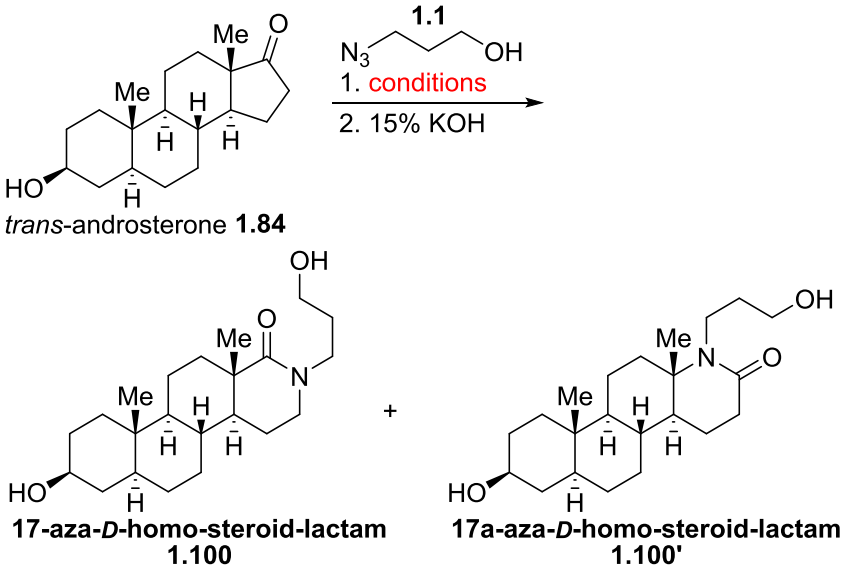

entry	azidopropanol 1.1 (equiv)	catalyst	catalyst (equiv)	solvent	conversion 1.100:1.84[b,c]	isolated yield (%)[d]
1	3.0	$BF_3•OEt_2$	2.0	CH_2Cl_2	21:79	16
2	3.0	$BF_3•OEt_2$	5.0[e]	CH_2Cl_2	82:18	80
3	2.0	$BF_3•OEt_2$	7.0[e]	CH_2Cl_2	89:11	85
4	2.0	$BF_3•OEt_2$	1.1	$(CF_3)_2CHOH$	78:22	72
5	2.0	H_2SO_4	0.55[f]	$(CF_3)_2CHOH$	86:14	78
6	2.0	CF_3SO_3H	1.1	$(CF_3)_2CHOH$	>98:2[g]	94
7	2.0	CF_3SO_3H	1.1	CF_3CH_2OH	61:39	61
8	2.0	CF_3SO_3H	1.1	CH_2Cl_2	16:84	10

[a]See Section 1.7.4 for reaction protocols. [b]Only regioisomer **1.100** was observed by ^{1}H NMR of the crude reaction mixture. [c]Product conversion was determined by ^{1}H NMR of the crude reaction mixture. [d]Isolated yields of regioisomer **1.100**. [e]Catalyst was added at 0 °C. [f]Generates 1.1 equiv of proton catalyst. [g]Complete conversion of *trans*-androsterone **1.84** to **1.100** was observed by ^{1}H NMR of the crude reaction mixture.

Surprisingly, over the course of this study exclusively one constitutional isomer (**1.100**) was observed by crude ^{1}H NMR. The structure of this isomer was confirmed by X-ray crystal analysis (Figure 1.25). This result warrants further explanation as the constitutional isomer is opposite to that of the Beckmann outcome (C-16 versus C-13 migration).

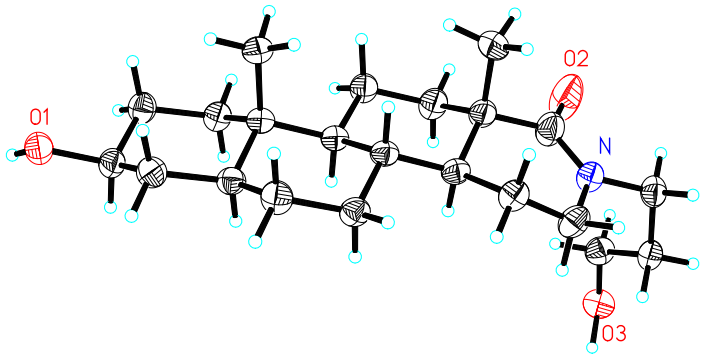

Figure 1.25. X-ray crystal structure of analog **1.100** (CCDC 1583536).

The intermolecular Schmidt reaction between 17-oxosteroid and achiral 3-azidopropanol is mechanistically intriguing. To explain this outcome, rationalization of key intermediates and transition structures formed in this ring expansion process is pertinent. The regiochemistry of this reaction may arise from a combination of two stereochemical and conformational considerations, neither of which is obvious based on precedent. The two factors include: (1) α versus β attack onto the C-17 oxonium ion and (2) the formation of 1,3-oxazinane ring conformers and favorable chair conformations. All possible transformations are assumed to involve antiperiplanar carbon migration to an axial N_2^+ leaving group. As shown in Figure 1.26, the newly formed 1,3-oxazinane ring can exist in two chair conformations **1.100i** and **1.100i'**. Upon azide addition, the spirocyclic center is attached to C-16 and C-13 of the steroid. The former C-16 is ethyl-like (medium substituent, M), and the latter C-13 is fully substituted, therefore *tert*-butyl-like (large substituent, L). Accordingly, C-13 should occupy an equatorial position in preference to the

smaller C-16 methylene group as shown in the figure (boxed). Stereoelectronically enforced migration of C-16 occurs through the preferred oxazinane conformer to afford the corresponding iminium **1.100ii**. Subsequent base treatment of **1.100ii** led to the observed product **1.100**, which was experimentally the exclusive product of the reaction. The matter of α versus β attack is less obvious in this example because, in either case, there is a stable chair conformation that would lead to the observed regiochemistry. However, this issue clearer in examples with substituents on the 3-azidopropanol reagents.

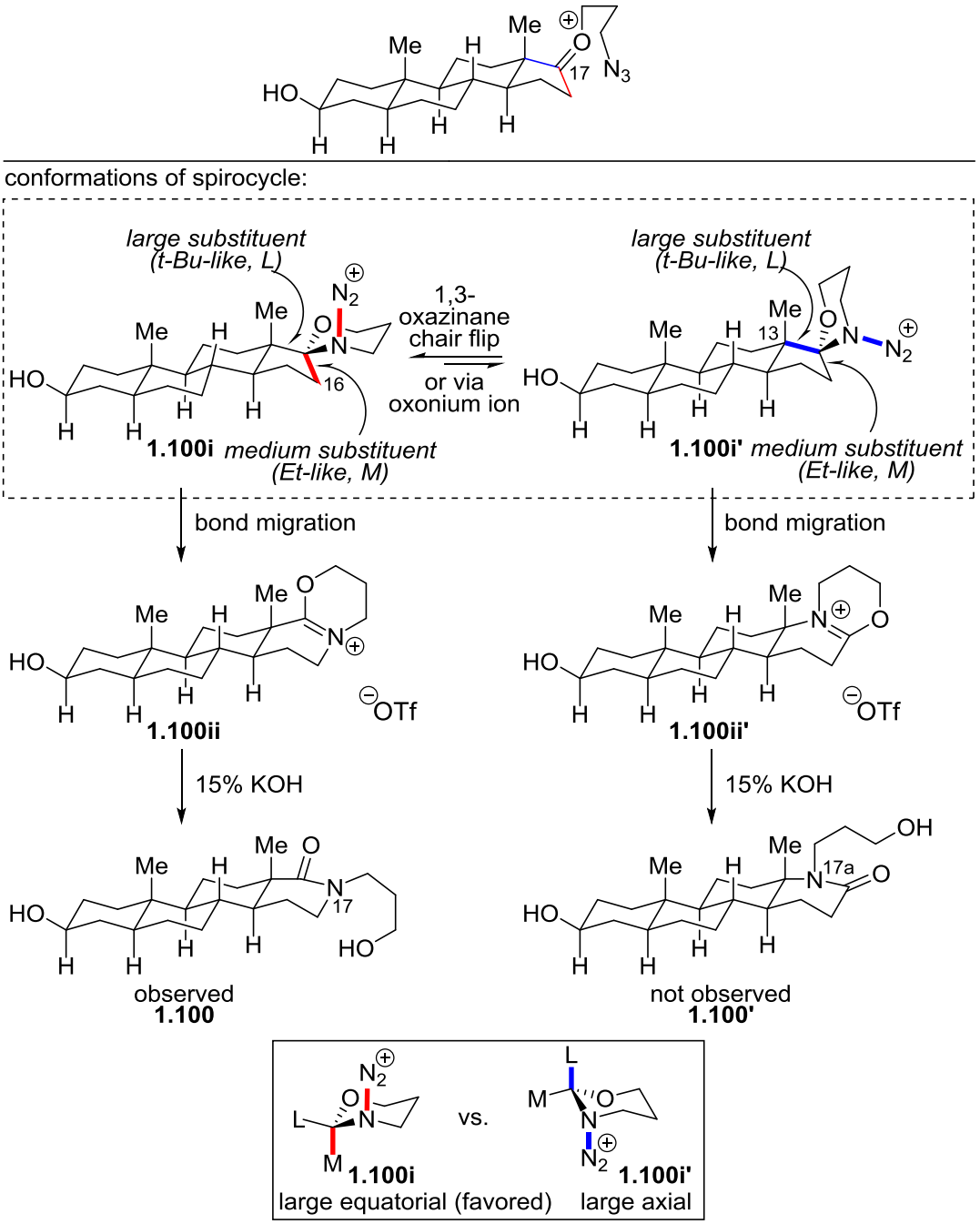

Figure 1.26. Proposed mechanism for the Schmidt reaction between *trans*-androsterone **1.84** and azidopropanol **1.1**. Differentiation between the large substituent (C-13, blue bond) and medium substituent (C-16, red bond) is denoted as L and M, respectively.

Despite the apparently high substrate bias of the 17-oxosteroids with 3-azidopropanol **1.1** as indicated by the results in Figure 1.26, it was proved possible to completely divert the reaction

outcome using chiral azides as reactants. In Table 1.5, readily available 17-oxosteroidal substrates were reacted with chiral hydroxyalkyl azides **1.3** and **1.5**. When **1.84** was reacted with (*S*)-**1.3**, a mixture of regioisomers **1.101** and **1.102** were observed by ^{1}H NMR of the crude reaction mixture, whereas when the substrate was treated with (*R*)-**1.3** exclusive migration of C-16 was observed (analog **1.103**, which represented a similar outcome to that observed with using achiral **1.1**). An instructive pair is the reaction of **1.84** with (*S*)- and (*R*)-**1.5**, because the experiments showed an intrinsic preference of the chiral 3-methyl hydroxyalkyl azides over the steroid substrate. Remarkably, the opposite migration occurred when the reaction was carried out using (*S*)-**1.5**, in which the chiral reagent forcibly led to the C-13 migration result over the natural substrate preference for C-16 migration affording the regio-diverted analog **1.104**. On the contrary, rearrangement with reagent (*R*)-**1.5** gave the natural substrate preference and the product outcome (analog **1.105**) was similar to that of the achiral **1.1**. Mechanistic considerations of the chiral reagent **1.5**-controlled ring expansions of **1.84** are shown in Figures 1.27 and 1.28. Here, discussion on the topic of α versus β attack is more fitting. In Figure 1.29, the depicted chair conformations reveal that there are variable stable chair conformations that would lead to the observed stereochemistry associated with an azide reactant. However, the literature is silent on the facial preference of intramolecular spirocycle formation in cases like these (as opposed to intermolecular organometallic additions, which prefer α attack away from the C-18 methyl group).[111] In retrospect, β attack seems more likely with respect to the heterocycle conformers because both the steroid and methyl substituents would satisfy more favorably when both are occupying the equatorial positions.

Moreover, C-16 migration was observed when (*R*)-3-azidobutanol (*R*)-**1.5** was the reactant in the reaction (Figure 1.28); whereas, the opposite regiochemistry (C-13 migration) was

observed when (*S*)-3-azidobutanol (*S*)-**1.5** was used as the azide reactant (Figure 1.27). The proposed β-attack of azide at C-17 oxonium is uniformly consistent because this mechanism clearly proceeds via the favorable formation of the more stable 1,3-oxazinane conformations (i.e., methyl substituents occupying equatorial positions in the ring conformer).

Table 1.5. Reactions of 17-oxosteroids **1.84**, **1.90**, and **1.95** with 1,3-hydroxyalkyl azides **1.1**, **1.3**, and **1.5**.[a]

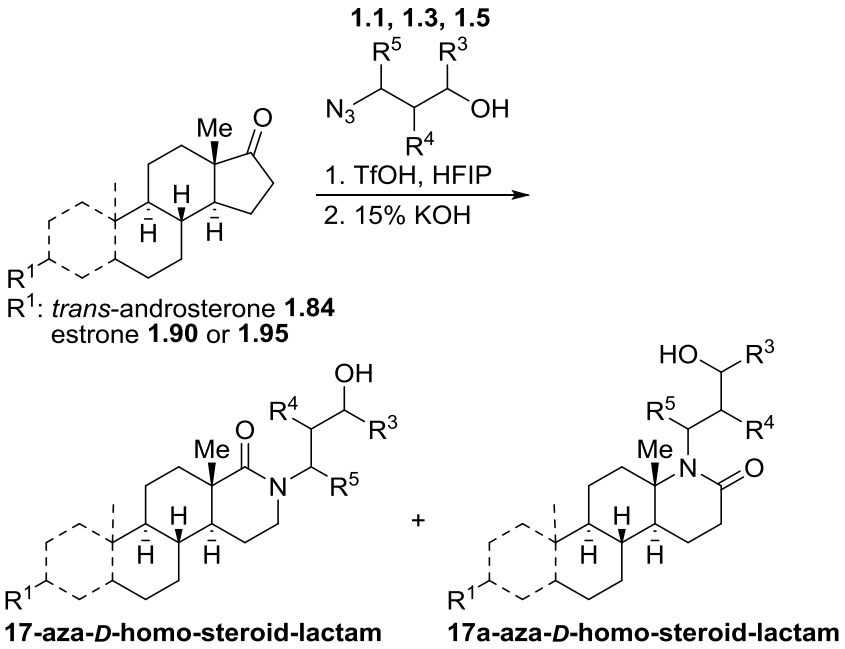

entry	steroid	azide	R^4	R^5	17-aza: 17a-aza ratio[b,c]	product(s)		isolated yield (%)[d]
						17-aza	17a-aza	
1	**1.84**	**1.1**	H	H	>95:5	**1.100**	-	94
2	**1.84**	(*S*)-**1.3**	(*S*)-Me	H	56:44[e]	**1.101** + **1.102**		53:35[f]
3	**1.84**	(*R*)-**1.3**	(*R*)-Me	H	>95:5	**1.103**	-	93
4	**1.84**	(*S*)-**1.5**	H	(*S*)-Me	5:>95	-	**1.104**	69
5	**1.84**	(*R*)-**1.5**	H	(*R*)-Me	>95:5	**1.105**	-	92
6	**1.90**	**1.1**	H	H	ND	**1.106**	-	91
7	**1.90**	(*S*)-**1.3**	(*S*)-Me	H	60:40[g]	**1.107** + **1.108**		52:34[f]
8	**1.90**	(*R*)-**1.3**	(*R*)-Me	H	ND	**1.109**	-	85
9	**1.90**	(*S*)-**1.5**	H	(*S*)-Me	ND		**1.110**	68
10	**1.90**	(*R*)-**1.5**	H	(*R*)-Me	ND	**1.111**	-	86
11	**1.95**	**1.1**	H	H	ND	**1.112**	-	93

[a]See Section 1.7.4 for reaction protocols. [b]Ratio of 17-aza- and 17a-aza-*D*-homo-steroid lactam was determined by ^{1}H NMR of the crude reaction mixture. [c]Only one 17-aza-regioisomer was observed by ^{1}H NMR of the crude reaction mixture, unless otherwise noted. [d]Isolated yields of only the major

regioisomer, unless otherwise noted. [e]Mixture of regioisomers observed by ^{1}H NMR of the crude reaction mixture. [f]Isolated yields of individual regioisomers. [g]Ratio determined by analytical HPLC of the crude reaction mixture. ND = Not determined; R^3 = H in all cases.

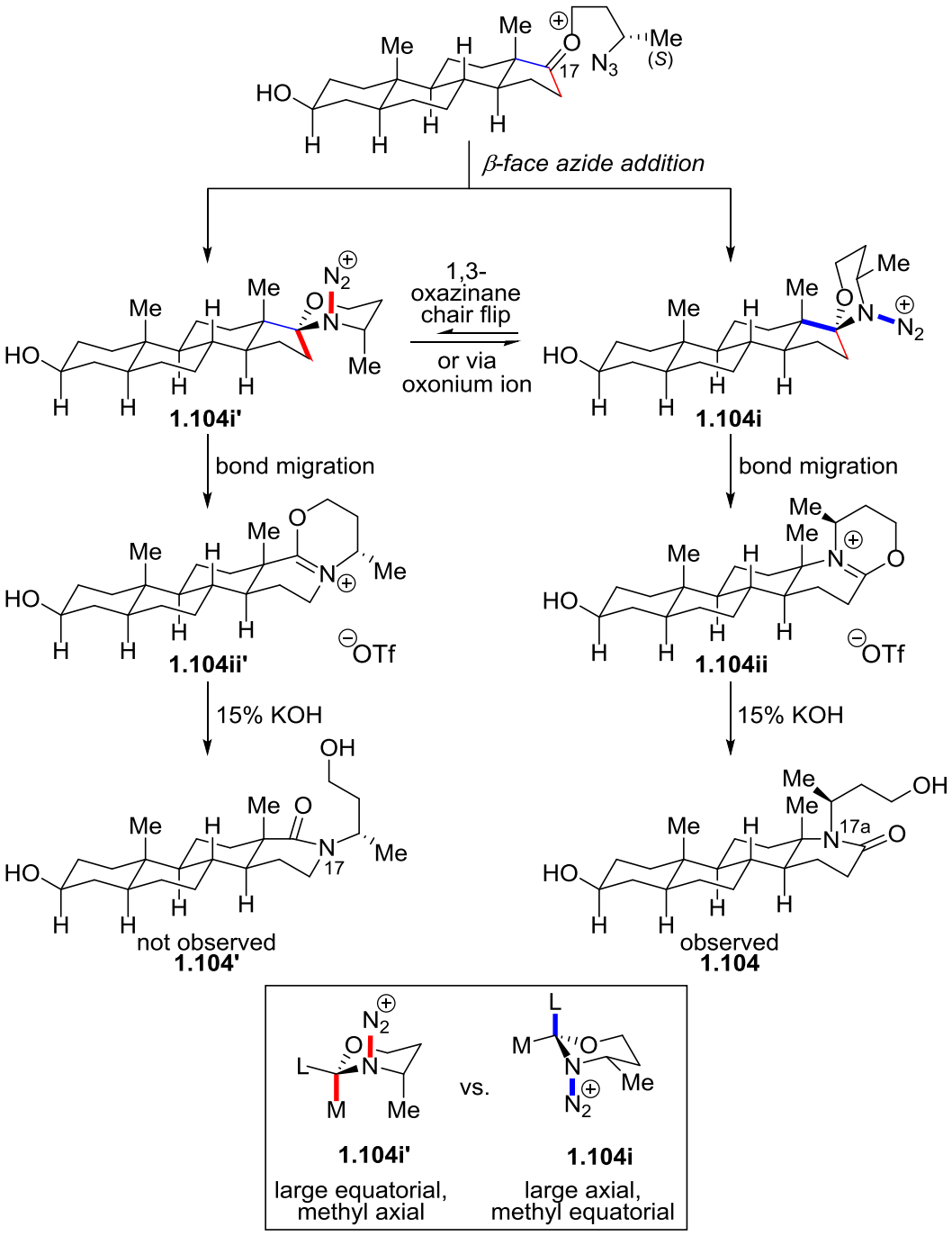

Figure 1.27. Proposed mechanism for the regioselectivity of *trans*-androsterone **1.84** with (*S*)-3-azidobutanol (*S*)-**1.5**. In this example, it was experimentally shown to lead to the isomer resulting from migration of C-13 (red bond). Together, these facts support the assignment of β attack onto

the C-17 oxonium ion as shown. Differentiation between the large substituent (C-13, blue bond) and medium substituent (C-16, red bond) is denoted as L and M, respectively.

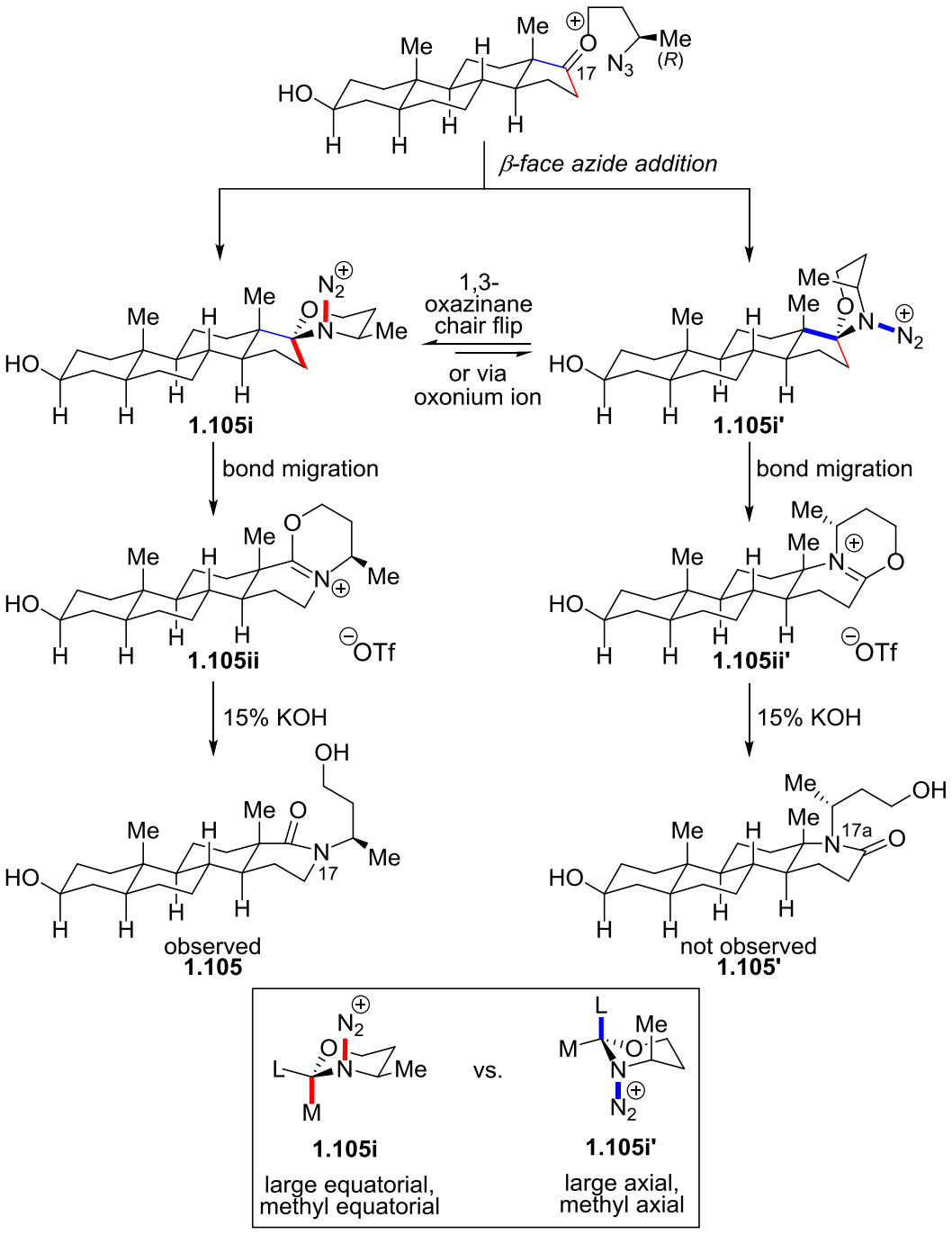

Figure 1.28. Proposed mechanism for the regioselectivity of *trans*-androsterone **1.84** with (*R)*-3-azidobutanol (*R*)-**1.5**. In this example, the (*R*)-methyl group and the placement of the large C-13 into an equatorial substituent clearly favor the 1,3-oxazinane **1.105i** conformation as shown, and experimentally observed was the isomer resulting from the migration of C-16. Together, these facts support the assignment of β attack onto the C-17 oxonium ion as shown. Differentiation

between the large substituent (C-13, blue bond) and medium substituent (C-16, red bond) is denoted as L and M, respectively.

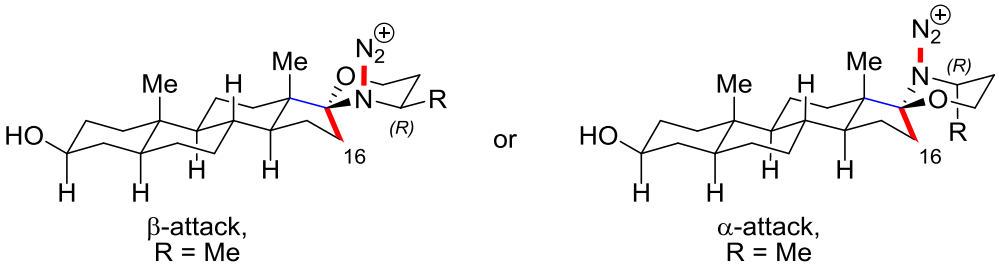

Figure 1.29. Possible ring conformations leadings to C-16 migration. In each case depicted, there is a stable chair conformation that would lead to the observed regiochemistry.

To further expand the library collection, similar reactions of the *trans*-androsterone series were carried out with the estrone substrates **1.90** and **1.95**. The crude regiochemistry of these reactions were difficult to examine due to the solubility of estrone derivatives in dimethylsulfoxide (DMSO) and not chloroform ($CDCl_3$). However, these additional reactions provided 7 new estrone-lactam derivatives for the collection and the regiochemical outcomes were analogously selective to that of the *trans*-androsterone **1.84** substrate discussed (Table 1.5).

1.4.4 A Study on the Use of 1,2-Hydroxyalkyl Azides to Effect Ring Expansion on 17-Oxosteroids, Determination of Constitutional Isomerism Control, and Rationalization of Mechanism

In this study, readily available 17-oxosteroid substrates were reacted with azidoethanol derivatives **1.7**–**1.11** (Table 1.4). These additional opportunities for isomer control were briefly examined. Not surprisingly, these reaction sequences with azidoethanol derivatives afforded poorer regiochemical control compared to those of the azidopropanol derivatives. Unfortunately, the crude regioisomer ratio for these reactions were difficult to discern, but isolation of major regioisomers in moderate yields clearly suggest to poor isomeric mixtures and less selective

reactions compared to that of the azidopropanol reagents. Despite this, these experiments still provided 15 isomerically pure 17- and 17a-azasteroid **1.113**–**1.114** for the library collection.

With respect to the mechanism, the ability of a five-membered ring intermediate to assume an antiperiplanar relationship between the migrating and leaving groups are less certain. Arguably from these results, a key source of regiochemical control is the minimization of steric interactions between the alkyl or phenyl group of the side-chain and the migrating carbon of the steroid D-ring. In comparison to the three-carbon azide reagents, the drop in selectivity associated with the two-carbon azide reagents is consistent with the requisite formation of five-membered ring conformers. Our reasoning is consistent with the data in Table 1.6.

Table 1.6. Reactions of 17-oxosteroids **1.84** and **1.90** with 1,2-hydroxyalkyl azides **1.7** and **1.9**–**1.11**.[a]

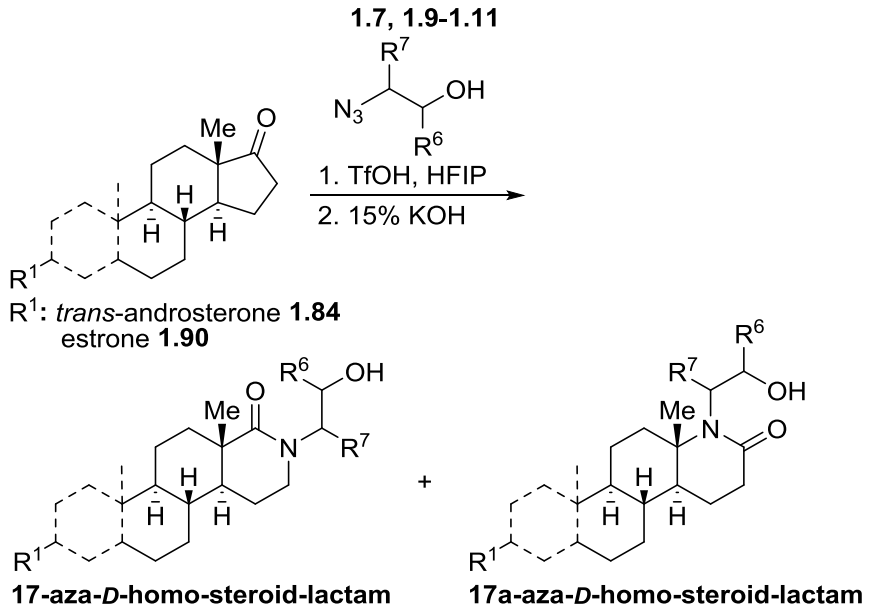

entry	steroid	azide	R^7	17-aza:17a-aza ratio[b]	product(s)		isolated yield (%)
					17-aza	17a-aza	
1	**1.84**	**1.7**	H	30:70[c]	**1.113** + **1.114**		96[d]
2	**1.84**	(*S*)-**1.9**	(*S*)-CH_2Ph	ND	-	**1.115**	89
3	**1.84**	(*R*)-**1.9**	(*R*)-CH_2Ph	ND	**1.116**	-	82[e]
4	**1.84**	(*S*)-**1.10**	(*S*)-Ph	ND	-	**1.117**	77
5	**1.84**	(*R*)-**1.10**	(*R*)-Ph	ND	**1.118**	-	51
6	**1.84**	(*S*)-**1.11**	(*S*)-CH_2CHMe_2	ND	-	**1.119**	86
7	**1.84**	(*R*)-**1.11**	(*R*)-CH_2CHMe_2	ND	**1.120**	-	83[e]
8	**1.90**	**1.7**	H	30:70[f]	**1.121** + **1.122**		94[g]
9	**1.90**	(*S*)-**1.9**	(*S*)-CH_2Ph	ND	-	**1.123**	91
10	**1.90**	(*R*)-**1.9**	(*R*)-CH_2Ph	ND	**1.124**	-	72[e]
11	**1.90**	(*S*)-**1.10**	(*S*)-Ph	ND	-	**1.125**	51
12	**1.90**	(*R*)-**1.10**	(*R*)-Ph	ND	**1.126**	-	56[e]
13	**1.90**	(*S*)-**1.11**	(*S*)-CH_2CHMe_2	ND	-	**1.127**	86
14	**1.90**	(*R*)-**1.11**	(*R*)-CH_2CHMe_2	ND	**1.128**	-	68

[a]See Section 1.7.4 for reaction protocols. [b]Ratio of 17-aza- and 17a-aza-*D*-homo-steroid lactam was determined by ^{1}H NMR of the crude reaction mixture, unless otherwise noted. [c]Ratio determined by ^{1}H NMR of final compound. [d]Isolated yield of a mixture of regioisomers. [e]Minor regioisomer was observed in ^{1}H NMR of final compound. [f]Ratio determined by analytical HPLC of crude reaction mixture. [g]Isomeric mixture was separated to give 27% isolated yield of **1.121** and 52% isolated yield of **1.122**. ND = Not determined; R^6 = H in all cases.

1.4.5 Functionalization of D-Ring Iminium Ions with Various Nucleophiles

The intermediacy of an iminium ether as a primary rearrangement product permit their versatility for diversification using experimentally straightforward chemistry. In the above examples, iminium ethers were hydrolyzed to the corresponding *N*-alkyl lactams, however, as mentioned previously iminium ethers are known to react with a variety of nucleophiles. Thus, a small library of diverse 17-aza-D-homo-steroids were prepared using a one-pot three component protocol (Table 1.7). Specifically, commercially available *trans*-androsterone **1.84** and estrone **1.90** were reacted with achiral 3-azidopropanol **1.1**, which resulted in regioselective iminiums that were subsequently functioned by treatment with four types of nucleophiles: Na_2S, the reducing agents $NaBH_4$ or sodium borodeuteride ($NaBD_4$), NaN_3, and 4-subsituted thiophenoxides. Through path *a* thioamides, **1.129** *trans*-androsterone-derived and **1.138** estrone-derived, were synthesized in moderate yields. Interestingly, path *a* reduction of D-ring with either $NaBH_4$ or $NaBD_4$ stereoselectively led to previously unobserved 1,3-oxazinanes **1.130**–**1.131** and **1.139**–**1.140**, *trans*-androsterone and estrone-derived, respectively. The unusual heterocyclic structure of **1.130** was confirmed by X-ray crystallography and shown in Figure 1.30. Reduction of the D-iminium to access the 1,3-oxazinane structure was accomplished under very mild conditions. In past attempts using simpler iminium ether substrates, conditions led to fully reduced tertiary amines due to the double addition of the hydride nucleophile. However, due to the bulky steroid framework only one addition of the hydride/deuteride species occurred despite using heat or excess amounts of reducing agent over an extended period of time.

Conversely, nucleophiles that proceed with path *b* typically undergo S_N2-type reactions and onto afford *N*-alkylated lactams. In this way, azide and sulfide *N*-alkylated lactams, **1.132**–**1.137** and **1.138**–**1.144**, were synthesized in moderate yields from 17-oxosteroid substrates. With

primary azide handles, analogs **1.132** and **1.141** were subjected to copper-promoted 1,3-dipolar Huisgen azide-alkyne cycloaddition reactions for the preparation of triazoles. Using standard click chemistry, four additional analogs were prepared with substituted acetylenes as shown in Scheme 1.16.

Table 1.7. Three-component reactions for the synthesis of functionalized 17-aza-*D*-homo-steroids **1.129**–**1.144**.[a]

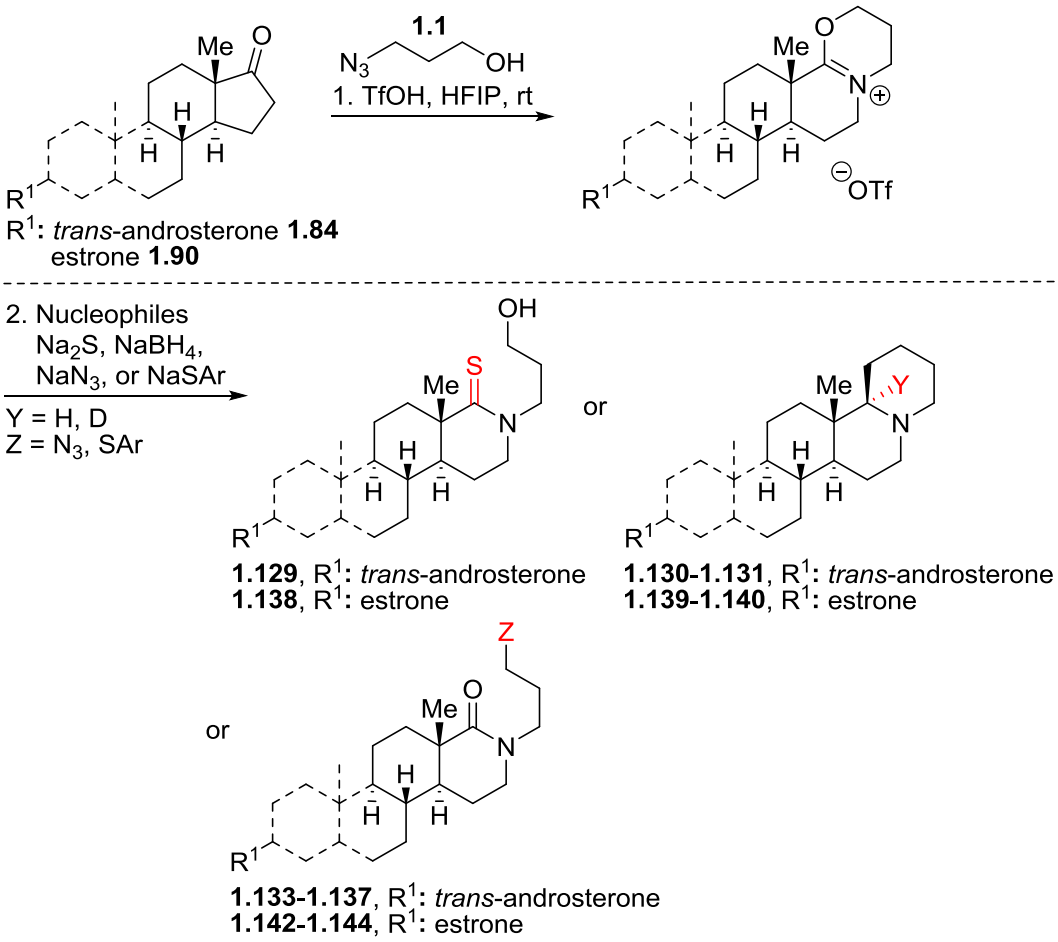

entry	steroid	nucleophile	S, Y or Z	product	isolated yield (%)
1	**1.84**	Na_2S	S	**1.129**	52
2	**1.84**	$NaBH_4$	H	**1.130**	85
3	**1.84**	$NaBD_4$	D	**1.131**	64
4	**1.84**	NaN_3	N_3	**1.132**	86
5	**1.84**	NaSAr	SC_6H_5 [b-c]	**1.133**	71
6	**1.84**	NaSAr	$S(4\text{-Me})C_6H_4$ [b-c]	**1.134**	76
7	**1.84**	NaSAr	$S(4\text{-OMe})C_6H_4$ [b,d]	**1.135**	65
8	**1.84**	NaSAr	$S(4\text{-Cl})C_6H_4$ [b,e]	**1.136**	69
9	**1.84**	NaSAr	$S(4\text{-Br})C_6H_4$ [b,f]	**1.137**	61
10	**1.90**	Na_2S	S	**1.138**	51
11	**1.90**	$NaBH_4$	H	**1.139**	83
12	**1.90**	$NaBH_4$	D	**1.140**	82
13	**1.90**	NaN_3	N_3	**1.141**	82
14	**1.90**	NaSAr	SC_6H_5 [b-c]	**1.142**	62
15	**1.90**	NaSAr	$S(4\text{-Me})C_6H_4$ [b-c]	**1.143**	60
16	**1.90**	NaSAr	$S(4\text{-OMe})C_6H_4$ [b,d]	**1.144**	63

[a]See Section 1.7.4 for reaction protocols. [b]Stock solutions of sodium thiophenoxides were prepared immediately prior to use by adding sodium (1.0 equiv) to a solution of thiophenols (1.1 equiv) in

anhydrous DMF (15.0 mL) at 0 ˚C and stirring at room temperature overnight. [c]0.66 M stock solution. [d]0.67 M stock solution. [e]0.70 M stock solution. [f]0.56 M stock solution.

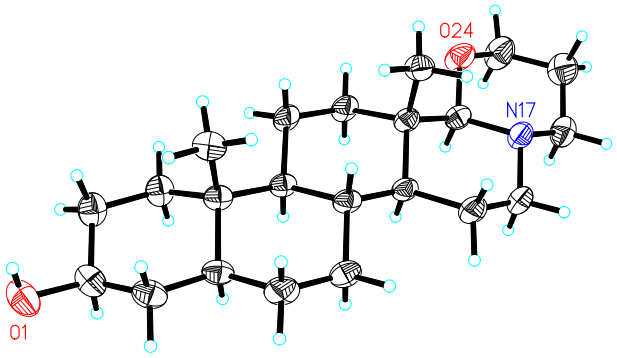

Figure 1.30. X-ray crystal structure of analog **1.130 (**CCDC 1583518).

Scheme 1.16. 1,3-Dipolar Huisgen azide-alkyne cycloaddition reactions for the preparation of triazole analogs.

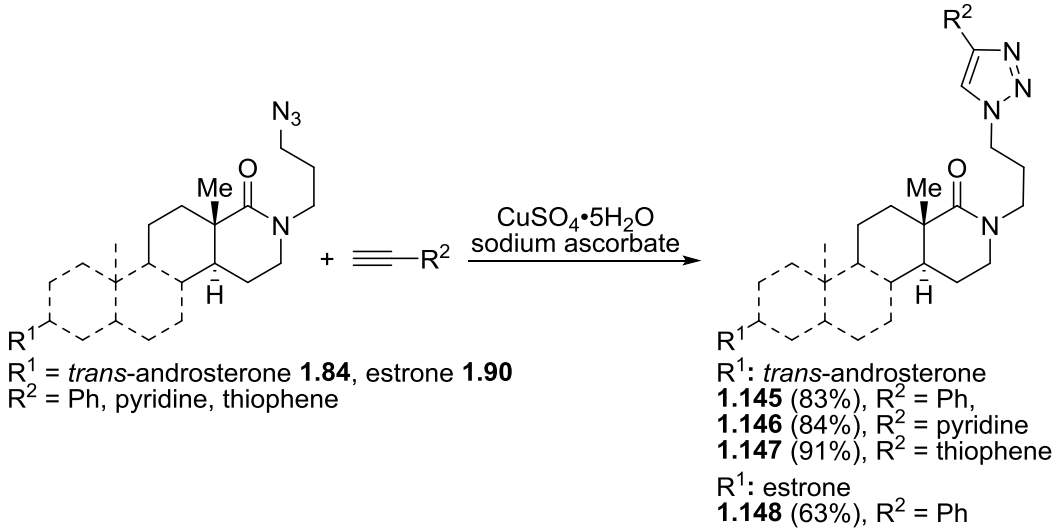

Finally, D-ring analogs that lacked the stereochemical information used to effect the specific ring-expansion reactions were synthesized. As shown in Scheme 1.17, the "parent" NH lactams of the D-ring steroid were prepared from dissolving metal reduction, in which these conditions facilitated cleavage at the benzylic site of the side chains. The establishment of pure

"parent" regioisomers further assured the opposing structural features by NMR spectroscopy as well as validated the effect of stereoelectronically controlled ring expansion sequence.

Scheme 1.17. Synthesis of the 'parent' NH D-ring lactams.

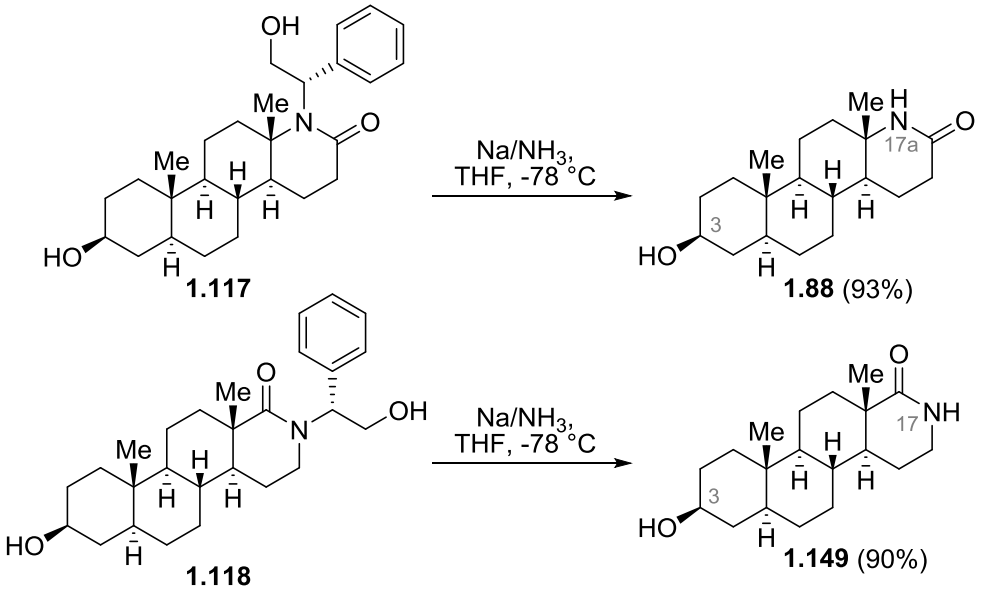

1.5 Conclusions and Future Directions

To summarize, we have demonstrated predictable and selective installation of nitrogen into the steroid backbone at four separate positions using stereoelectronically controlled ring expansion reactions. We have shown that judicious use of the appropriate azide reagent permits regioselective installation of the nitrogen substituent. Achiral and chiral enantioenriched hydroxyalkyl azides directed nitrogen insertion in cases where (1) there was minimal migration preference (i.e., 3-oxosteroids; C-3 and C-4 were isoelectronic) or, in contrast, (2) there was substantial substrate bias for a given regiochemistry (i.e., 17-oxosteroids, C-13 and C-16 were not isoelectronic). This work on A- and D-ring late-stage modification featured regiodivergent rearrangement, specifically demonstrated the concept of using chiral reagents to effect

regiocontrol in chiral natural products. Moreover, by combining the feature of regiochemical control with the versatility of iminium ethers as ambident electrophilic intermediates, a collection of functionalized analogs was prepared. In sum, 114 isomerically pure analogs with spatial and functional diversity were synthesized in >20 milligrams and >90% purity for this library collection. This work on reagent-controlled ring expansion should help enhance rationalization of the placement of new functional groups onto a natural product backbone and application towards library development and diversification programs.

Future Directions

Originally, we had aimed to describe a global approach of steroid ring-expansion chemistry that incorporated B- and C-ring nitrogenous modifications. Ring-expansion chemistry of these steroidal rings are quite rare, therefore represents a unique opportunity to explore the effect of reagent-controlled ring expansion in these chiral contexts and produce new steroid-like analogs for the library collection. Unfortunately, carrying out any general nitrogen ring-expansion chemistry at either B- or C-ring is very challenging for a number of reasons.

The first challenge is accessing ketone-starting materials. The synthesis of B- and C-ring ketones require multiple synthetic steps, which necessitates large-scale chemistry and tedious protecting-group manipulations. For example in Scheme 1.18, the preparation of 6-oxosteroid and 7-oxosteroid can be visualized through concomitant hydroboration and DMP oxidation, or allylic oxidation and enone reduction. Despite having potential access to B-ring oxosteroids, the spectroscopic identification of regiochemistry is more accurately represented by comparison both types of nitrogen insertion processes, the Beckmann and Schmidt reactions (in fact, may require substantial optimization to obtain high-yielding reactions).

Scheme 1.18. Synthesis of B-ring oxosteroids. (a) Synthesis of 6-oxosteroid. (b) Synthesis of benzyl-protected 6-oxosteroid. (c) Synthesis of 7-oxosteroid.

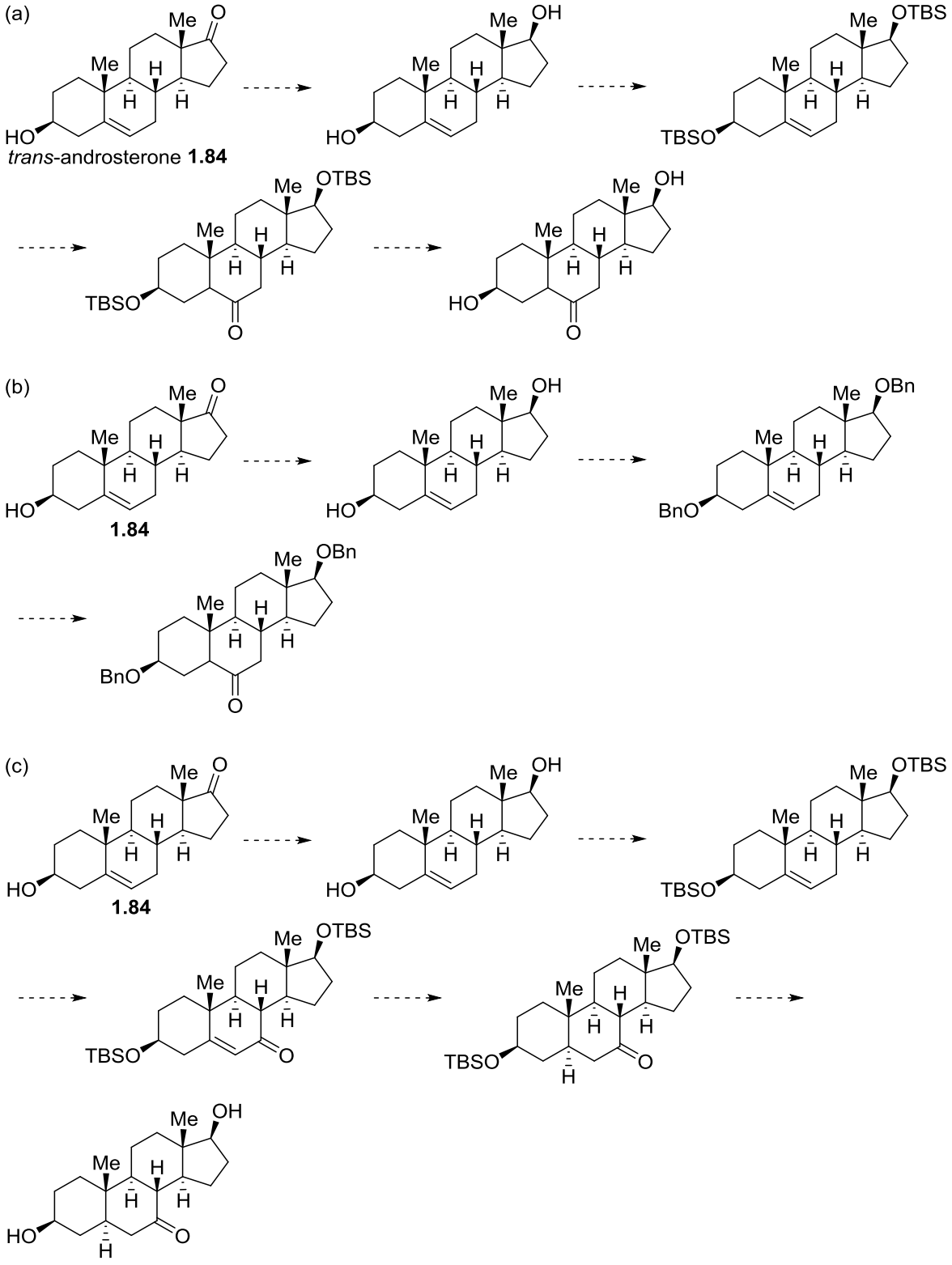

We had envisioned the synthesis of C-ring oxosteroids from readily available steroid materials: hydrocortisone, estrone, and cholic acid (Scheme 1.19). Similarly, to access C-ring ketones the preparation would require installing/changing the hydroxylation/oxidation states of the starting material via a series of protecting-group manipulations. We found this tedious route not promising because, based on literature readings, the reactivity of functionalities in those positions are quite poor. As a result, a shorter route to obtain carbonyl functionalities in the B- and C-ring system might be more promising and amendable towards ring-expansion chemistry and library development. This proposal is depicted in Figure 1.31; upon optimization of ozonolysis protocols on steroid substrates, this would result in two carbonyl handles on each individual steroid for experimentation. Seemingly, the carbonyls at these positions are less hindered, which suggests that these sites may be more reactive to ring-expansion studies. However, one would have to address the obvious issue of chemoselectivity, which could be interesting to study in concurrent with ring-expansion chemistry. Altogether, a strategic redesign is necessary to develop an approach for regiodivergent B- and C-ring nitrogenous modifications. In this aspect, other natural products such as gibberellic acid and stevioside may also be worthy evaluation. Perhaps a strategic redesign that permits a global application of the Schmidt reaction towards various chiral settings is more worthwhile and impactful.

Scheme 1.19. Potential routes for accessing C-ring oxosteroids.

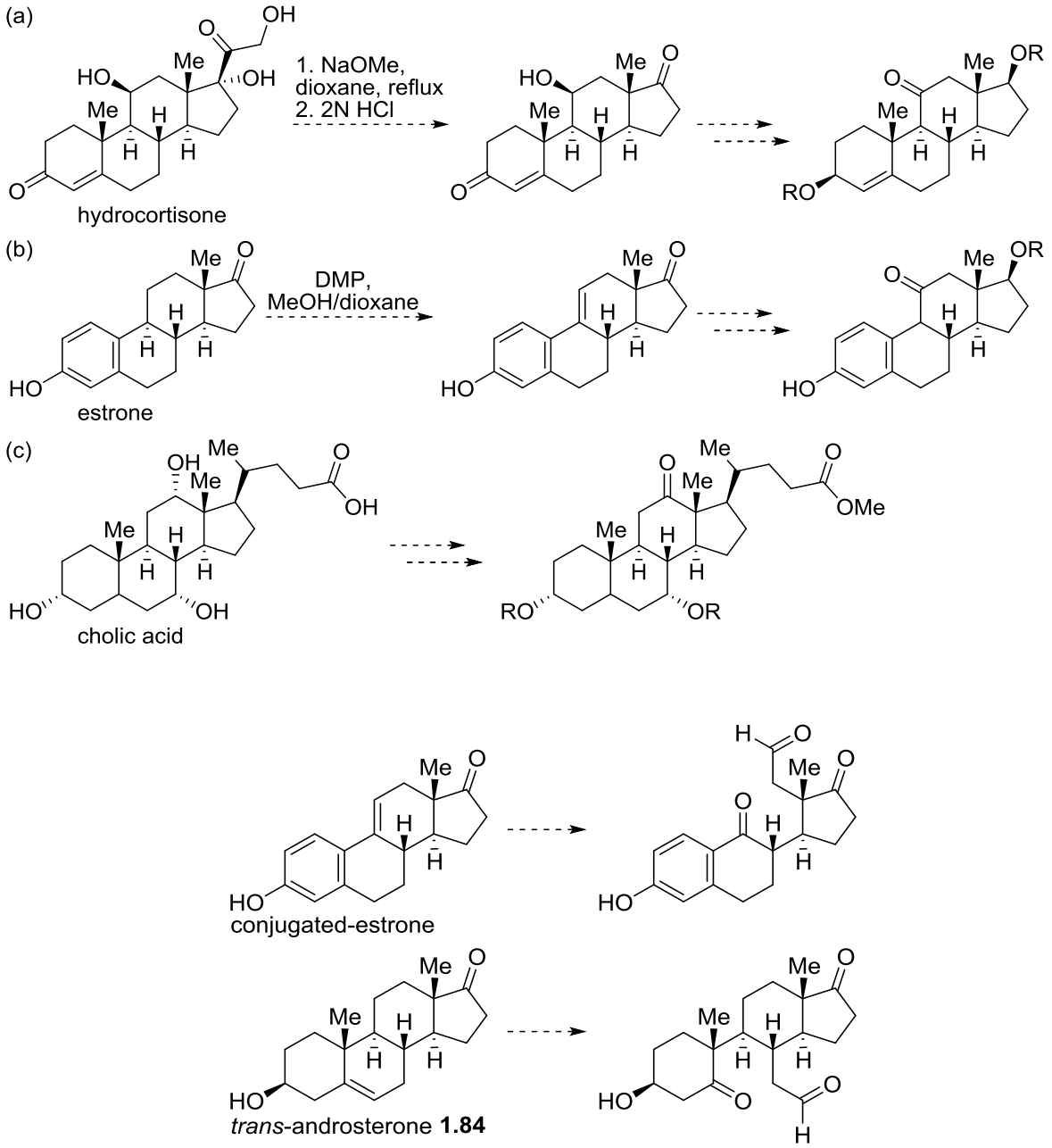

Figure 1.31. Redesign of B-ring and C-ring carbonyls for late-stage functionalization.

1.6 Experimental Section

1.6.1 General Information

Caution: Although we have not experienced any untoward events with the compounds mentioned in this thesis, azides and their precursors are known explosive hazards and should be used with appropriate safety precautions. Minimally, careful control of temperature and scale should be exercised. We do not recommend distillation of reaction mixtures that may contain residues of azide sources.

Reactions were performed under inert atmosphere (argon or nitrogen). Reactions were carried out in either flame-dried round bottom flasks or glass sample vials (TFE-lined cap). All chemicals were purchased from commercial sources and used without further purification. New containers of $BF_3 \bullet OEt_2$, TfOH, and HFIP were used. Anhydrous CH_2Cl_2, MeOH, DMF and THF were purchased from Sigma-Aldrich and used as received. Thin-layer chromatography (TLC) was performed using commercial glass-backed silica plates (250 μM) with an organic binder. Visualization was accomplished with UV light, Seebach's stain, or aqueous $KMnO_4$ stain, and heating. Purification was carried out by an automated flash chromatography/medium-pressure liquid chromatography (MPLC) system using normal phase silica gel flash columns (4, 12, 24, 40, or 80 g).

The infrared (IR) spectra were acquired as thin films using a universal ATR sampling accessory either on a PerkinElmer Spectrum One FT-IR spectrometer, Thermo Scientific Nicolet iS5 FT-IR spectrometer, or Bruker Alpha FT-IR spectrometer; the absorption frequencies are reported in cm^{-1}. All nuclear magnetic resonance spectra were recorded on a Varian 400 MHz, Varian 500 MHz with a dual carbon/proton cryoprobe, or Bruker 600 MHz with a dual carbon/proton cryoprobe instrument. NMR samples were recorded in deuterated chloroform ($CDCl_3$) or deuterated dimethylsulfoxide (DMSO-d_6). Chemical shifts are reported in parts per million (ppm) and referenced to the centerline of solvent ($CDCl_3$: δ 7.26 ppm for ^1H NMR and

77.16 ppm for ^{13}C NMR; DMSO-d_6 δ 2.50 ppm for ^{1}H NMR and 39.52 ppm for ^{13}C NMR). Coupling constants are given in hertz (Hz). HRMS data were collected using two instruments. (1) Time-of-flight mass spectrometer (TOF) with an electrospray ion source (ESI). (2) Thermo LTQ Fourier transform ion cyclotron resonance (FT-ICR, 7T) with a heated electrospray ion source (HESI), electrospray ion source (ESI), atmospheric-pressure chemical ionization source (APCI), or atmospheric-pressure photoionization (APPI). Purity data were collected using two instruments. (1) Waters Acquity H-class UPLC-PDA detector coupled to the Thermo LTQ Fourier transform ion cyclotron resonance mass spectrometer (FT-ICR, 7T) with a heated electrospray ion source (HESI). Samples were run on analytical Acquity UPLC BEH 2.1 × 50 mm, 1.7 μm, C18 column, and analytical Acquity UPLC HSS T3, 2.1 × 50 mm, 3.18 μm, C18 column, at 40 ˚C with mobile phases A (H_2O + 0.1% formic acid) and B (MeCN + 0.1% formic acid). (2) Agilent 6110 Series LCMS with a UV detector and a single quadrupole mass spectrometer. Samples were run on an analytical Agilent Eclipse Plus 4.6 × 50 mm, 1.8 μm, C18 column at room temperature with mobile phases A (H_2O + 0.1% acetic acid) and B (MeOH + 0.1% acetic acid). Melting points were determined in open capillary tubes using OptiMelt, an automated melting point apparatus, and were uncorrected. Compounds that appear in the experimental section, but were not discussed in the body of this chapter are given the prefix **S** (supplemental).

General Experimental Procedures for Azasteroid Library Production

General procedure A for the preparation of 1.16–1.51. To a solution of steroidal ketone **1.13**–**1.15** (0.124–0.302 mmol, 1.0 equiv) and hydroxyalkyl azide **1.1**–**1.6** (0.242–0.593 mmol, 2.0 equiv) in anhydrous CH_2Cl_2 (0.4 M) in a nitrogen-flushed, two-dram vial at 0 ˚C was

added BF_3•OEt_2 (5.0 equiv) dropwise. The vial was capped, and the reaction mixture was stirred at room temperature for 16 h. The solvent was removed under nitrogen, and the residual iminium was treated with an aqueous solution of 15% KOH (3.0 mL) and THF (0.5 mL). The biphasic mixture was stirred vigorously at room temperature for 24 h. The reaction mixture was diluted with CH_2Cl_2 (50 mL), dried over Na_2SO_4, filtered, and concentrated. Purification of analogs was carried out by an automated MPLC system on normal phase silica gel flash columns.

General procedure B for the preparation of 1.52–1.73. *Step 1—Formation of iminium ether intermediate of **1.14** or **1.15**:* In either a flame-dried, nitrogen-flushed, two-dram vial or 5 mL-microwave vial was added BF_3•OEt_2 (62.0–124 μL, 0.500–1.00 mmol, 5.0 equiv) dropwise to a solution of 5α-dihydrotestosterone **1.14** (29.0–60.0 mg, 0.100–0.207 mmol, 1.0 equiv) or 5β-dihydrotestosterone **1.15** (43.9–58.9 mg, 0.151–0.203 mmol, 1.0 equiv) and hydroxyalkyl azides (*R*)-**1.2** (44.5–72.7 mg, 0.250–0.410 mmol, 2.0 equiv), (*S*)-**1.2** (36.8–73.5 mg, 0.299–0.415 mmol, 2.0 equiv), (*S*)-**1.4** (44.3–74.0 mg, 0.250–0.418 mmol, 2.0 equiv), or (*R*)-**1.4** (44.5–73.4 mg, 0.250–0.414 mmol, 2.0 equiv) in anhydrous CH_2Cl_2 (0.4 M) at 0 ˚C. The vial was capped, and the reaction mixture was stirred at room temperature for 16 h. The solvent was removed under nitrogen, and the residual iminium was dried under vacuum before the addition of nucleophile.

Step 2— Addition of nucleophiles.

*2.1. Synthesis of **1.52–1.57** via nucleophilic addition of sulfide:* Na_2S (65.2–79.8 mg, 0.835–1.02 mmol, 4.1–5.0 equiv) was added to a solution of iminium ether in anhydrous DMF (5.0 mL). The reaction mixture was stirred at 65 ˚C for 24 h. The reaction mixture was diluted

with CH_2Cl_2 (20 mL), and was washed with a saturated solution of NH_4Cl (3 × 5 mL), brine (5 mL), dried over Na_2SO_4, filtered, and concentrated. Purification of analogs were carried out by an automated MPLC system on normal phase silica columns.

*2.2. Synthesis of **1.58** and **1.59** via nucleophilic addition of hydride:* To a solution of iminium residue in anhydrous MeOH (2.0 mL) at 0 ˚C was added $NaBH_4$ (30.0 mg, 0.799 mmol, 4.0 equiv) cautiously. The reaction mixture was stirred at room temperature for overnight. The reaction mixture was partitioned between saturated solution of $NaHCO_3$ (5 mL) and CH_2Cl_2 (20 mL). The organic layer was separated, dried over Na_2SO_4, filtered, and concentrated. Purification of analogs was carried out by an automated MPLC system on normal phase silica gel flash columns.

*2.3. Synthesis of **1.60** and **1.61** via nucleophilic addition of hydride:* 10% Pd/C (10.6–21.0 mg, 0.100-0.197 mmol, 1.0 equiv) was added to a solution of iminium ether in anhydrous EtOH (2.0–4.0 mL). The reaction was stirred under an atmosphere of hydrogen for 24 h. Purification of analogs was carried out by an automated MPLC system on normal phase silica gel flash columns.

*2.4. Synthesis of **1.62**–**1.67** via nucleophilic addition of azide:* NaN_3 (51.0–52.0 mg, 0.785–0.802 mmol, 4.0 equiv) was added to a solution of iminium ether in anhydrous DMF (2.0 mL). The reaction mixture was stirred at 70 ˚C for 24 h. The reaction mixture was partitioned between EtOAc (40 mL) and H_2O (20 mL). The organic layer was washed with H_2O (2 × 5 mL), brine (5 mL), dried over Na_2SO_4, filtered, and concentrated. Purification of analogs were carried out by an automated MPLC system on normal phase silica gel columns.

*2.5. Synthesis of **1.68**–**1.73** via nucleophilic addition of 4-methylbenzenethiolate:* Sodium 4-methylbenzenethiolate (0.66 M in DMF, 0.60–1.00 mL, 0.375–0.660 mmol, 3.0–4.0 equiv)

was added to a solution of iminium ether in anhydrous DMF (2.0 mL). The reaction mixture was stirred at 75 ˚C for 24 h. The reaction mixture was partitioned between EtOAc (40 mL) and H_2O (15 mL). The organic layer was washed with a saturated solution of $NaHCO_3$ (3 × 5 mL), brine (5 mL), dried over Na_2SO_4, filtered, and concentrated to afford crude residue. Purification of analogs were carried out by an automated MPLC system on normal phase silica gel columns.

General procedure C for the PCC oxidation of 1.18–1.19 and 1.28–1.29. To a slurry solution of **1.18–1.19** or **1.28–1.29** (53.0–93.0 mg, 0.099–0.212 mmol) in anhydrous CH_2Cl_2 (6.0–10.0 mL) and Celite at 0 ˚C was added PCC (43.0–190.0 mg, 0.200–0.880 mmol, 2.0–4.0 equiv). The brown reaction mixture was allowed to room temperature over 30 min and stirred overnight. The reaction mixture was diluted with CH_2Cl_2, filtered over Celite and concentrated. Purification of analogs was carried out by an automated MPLC system on normal phase silica gel flash columns.

General procedure D for the optimization of 1.100. To a solution of *trans*-androsterone **1.84** (0.150 mmol, 1.0 equiv) and 3-azidopropanol **1.1** (0.300–0.450 mmol, 2.0–3.0 equiv) in solvent (0.38 mL, 0.4 M) in a nitrogen-flushed, two-dram vial at room temperature (unless otherwise noted) was added acid catalyst (0.0825–1.05 mmol, 0.55–7.0 equiv) dropwise. The vial was capped, and the reaction mixture was stirred at room temperature for 24 h. The solvent was removed under nitrogen, and an aqueous solution of 15% KOH (3.0 mL) was added to the iminium residue. The reaction mixture was vigorously stirred at room temperature for 24 h. The reaction mixture was diluted with CH_2Cl_2 (50 mL), dried over anhydrous Na_2SO_4,

filtered, and concentrated. Purification was carried out by an automated MPLC system using a 4 g normal phase silica gel flash column with gradient elution from 0–5% MeOH/CH_2Cl_2.

General procedure E for the preparation of 1.100–1.105 and 1.113–1.120. To a solution of *trans*-androsterone **1.84** (0.125–0.153 mmol, 1.0 equiv) and hydroxyalkyl azide **1.1**, **1.3**, **1.5**, **1.7**, or **1.9**–**1.11** (0.250–0.302 mmol, 2.0 equiv) in HFIP (0.38 mL, 0.4 M) at room temperature or in anhydrous CH_2Cl_2 (0.50 mL, 0.3 M) at 0 ˚C in a nitrogen-flushed, two-dram vial was added TfOH (14.5–26.5 µL, 0.165–0.300 mmol, 1.1–2.0 equiv) or BF_3•OEt_2 (130 µL, 1.05 mmol, 7.0 equiv) dropwise. The vial was capped, and the reaction mixture was stirred at room temperature for 24 h. The solvent was removed under nitrogen, and the residual iminium was treated with an aqueous solution of 15% KOH (3.0 mL) and THF (0.5 mL). The biphasic mixture was stirred vigorously at room temperature for 24 h. The reaction mixture was diluted with CH_2Cl_2 (50 mL), dried over Na_2SO_4, filtered, and concentrated. Purification of analogs was carried out by an automated MPLC system on normal phase silica gel flash columns.

General procedure F for the preparation of 1.106–1.112 and 1.121–1.128. To a solution of estrone **1.90** (0.149–0.200 mmol, 1.0 equiv) and hydroxyalkyl azide **1.1**, **1.3**, **1.5**, **1.7**, or **1.9**–**1.11** (0.294–0.400 mmol, 2.0 equiv) in HFIP (0.38 mL, 0.4 M) at room temperature or in anhydrous CH_2Cl_2 (0.50 mL, 0.3 M) at 0 ˚C in a nitrogen-flushed, two-dram vial was added TfOH (14.5–26.5 µL, 0.165–0.300 mmol, 1.1–2.0 equiv) or BF_3•OEt_2 (130 µL, 1.05 mmol, 7.0 equiv) dropwise. The vial was capped, and the reaction mixture was stirred at room temperature for 24 h. The solvent was removed under nitrogen, and the residual iminium was treated with an aqueous solution of 15% KOH (3.0 mL) and THF (0.5 mL). The biphasic mixture was stirred

vigorously at room temperature for 24 h. The reaction mixture was diluted with a saturated solution of NH_4Cl, and extracted into CH_2Cl_2 (3 × 15 mL). The combined organic layers were washed with brine, dried over Na_2SO_4, filtered, and concentrated. Purification of analogs was carried out by an automated MPLC system on normal phase silica gel flash columns.

General procedure G for the preparation of 1.129–1.144. *Step 1: Formation of iminium ether intermediate of **1.84** or **1.90**:* To a solution of *trans*-androsterone **1.84** (43.6–145.0 mg, 0.150–0.500 mmol, 1.0 equiv) or estrone **1.90** (40.6–81.0 mg, 0.150–0.300 mmol, 1.0 equiv) and 3-azidopropanol **1.1** (30.1–101 mg, 0.300–1.00 mmol, 2.0 equiv) in HFIP (0.4 M) in either a flame-dried, nitrogen-flushed two-dram vial, 20 mL–scintillation vial, or 5 mL-microwave vial was added TfOH (14.5–48.5 μL, 0.165–0.550 mmol, 1.1 equiv) dropwise. The vial was capped, and the reaction mixture was stirred at room temperature for 24 h. The solvent was removed under nitrogen, and the residual iminium was dried under vacuum before the addition of nucleophile.

Step 2: Addition of nucleophiles.

*2.1. Synthesis of **1.129** and **1.138** via nucleophilic addition of sulfide:* Na_2S (195–234 mg, 2.50–3.00 mmol, 10.0 equiv) was added to a solution of iminium ether in anhydrous THF (5.0 mL). The reaction mixture was stirred at 65 ˚C for 24 h. The reaction mixture was diluted with Et_2O (20 mL), and was washed with a saturated solution of NH_4Cl (3 × 5 mL), brine (5 mL), dried over Na_2SO_4, filtered, and concentrated. Purification of analogs were carried out by an automated MPLC system on normal phase silica columns.

*2.2. Synthesis of **1.130**–**1.131** and **1.139**–**1.140** via nucleophilic addition of hydride:* To a solution of iminium residue in anhydrous MeOH (2.0 mL) at 0 ˚C was added $NaBH_4$ (151 mg,

0.400 mmol, 2.0 equiv) or $NaBD_4$ (167 mg, 0.400 mmol, 2.0 equiv) cautiously. The reaction mixture was stirred at room temperature for 3 h. The reaction mixture was partitioned between saturated solution of $NaHCO_3$ (5 mL) and CH_2Cl_2 (20 mL). The organic layer was separated, dried over Na_2SO_4, filtered, and concentrated. Purification of analogs was carried out by an automated MPLC system on normal phase silica gel flash columns.

*2.3. Synthesis of **1.132** and **1.141** via nucleophilic addition of azide:* NaN_3 (39.0–130 mg, 0.600–2.00 mmol, 4.0 equiv) was added to a solution of iminium ether in anhydrous DMF (2.0–5.0 mL). The reaction mixture was stirred at 70 ˚C for 24 h. The reaction mixture was partitioned between Et_2O (40 mL) and H_2O (20 mL). The organic layer was washed with H_2O (2 × 5 mL), brine (5 mL), dried over Na_2SO_4, filtered, and concentrated. Purification of analogs was carried out by an automated MPLC system on normal phase silica gel flash columns.

*2.4. Synthesis of **1.133**–**1.137** and **1.142**–**1.144** via nucleophilic addition of para-substituted benzenethiolates:* Sodium thiobenzolate (0.56–0.70 M in DMF, 0.54–0.67 mL, 2.5 equiv) was added to a solution of iminium ether in anhydrous DMF (2.0 mL). The reaction mixture was stirred at 75 ˚C for 24 h. The reaction mixture was partitioned between EtOAc (40 mL) and H_2O (15 mL). The organic layer was washed with a saturated solution of $NaHCO_3$ (3 × 5 mL), brine (5 mL), dried over Na_2SO_4, filtered, and concentrated. Purification of analogs was carried out by an automated MPLC system on normal phase silica gel flash columns.

General procedure H for the preparation of 1.145–1.148. A mixture of steroidal azides **1.132** or **1.141** (0.180–0.200 mmol, 1.0 equiv), substituted-acetylene (0.207–0.400 mmol, 1.0–2.0 equiv), copper sulfate pentahydrate (0.200–0.400 mmol, 1.0–2.0 equiv), and sodium L-ascorbate (0.400–0.800 mmol, 2.0–4.0 equiv) were dissolved in $^tBuOH/H_2O$ (1:1, 4.0 mL) at

room temperature and stirred overnight. The reaction mixture was diluted with CH_2Cl_2 (25 mL), and the organic layer was washed with aqueous NH_4OH (3 x 5 mL), brine (5 mL), dried over Na_2SO_4, filtered, and concentrated. Purification of analogs was carried out by an automated MPLC system on normal phase silica gel flash columns.

1.6.2 Experimental Section for 1.2

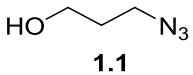

1.1

3-Azidopropanol, 1.1.[78] 3-Azidopropanol **1.1** was prepared following a previously published procedure. Characterization data were consistent with reported data.

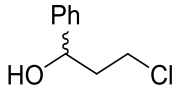

S1.1

(±)-3-Chloro-1-phenylpropanol, S1.1[112] (±)-3-Chloro-1-phenylpropanol **S1.2** was prepared following a previously published procedure. Characterization data were consistent with reported data.

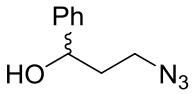

(±)-**1.2**

(±)-3-Azido-1-phenylpropanol, (±)-1.2. Following a literature procedure[85], (±)-3-azido-1-phenylpropanol (±)-**1.2** was prepared as described. A mixture of (±)-3-chloro-1-phenylpropanol **S1.1** (681 mg, 3.99 mmol), NaN_3 (780 mg, 12.0 mmol, 3.0 equiv), NaI (899 mg, 6.00 mmol, 1.5 equiv) in anhydrous DMF (40.0 mL) was stirred for 24 h at 80 ˚C. The reaction mixture was partitioned between Et_2O and water. The organic layer was washed with brine, dried

over anhydrous Na_2SO_4, filtered, and concentrated under a stream of nitrogen. The crude oil was purified by an automated MPLC system using a 24 g normal phase silica column with gradient elution of 0–15% EtOAc/hexanes. Concentration of solvents under nitrogen afforded racemic product as a colorless oil (619 mg, 3.50 mmol, 88% yield). R_f = 0.25 (10% EtOAc/hexanes); IR (neat) 3378, 2089 cm^{-1}; ^1H NMR (400 MHz, $CDCl_3$) δ 7.40–7.28 (m, 5H), 4.85 (m, 1H), 3.54–3.36 (m, 2H), 2.09–1.91 (m, 3H); ^{13}C NMR (101 MHz, $CDCl_3$) δ 144.0, 128.8, 128.1, 125.9, 72.0, 48.5, 38.0. HRMS (TOF, ESI) *m/z*: $[M - N_2 + H]^+$ calcd for $C_9H_{12}NO$ 150.0913, found 150.0898. HPLC: Chiralcel OD-H, Daicel Chemical Industries, Ltd.; 2–40% *i*-PrOH/hexanes over 60 min; flow rate 1.0 mL/min; UV 220 nm; (*S*) t_R = 10.29 min, (*R*) t_R = 11.03 min.

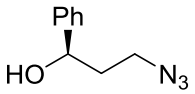

(*R*)-**1.2**

(*R*)-3-Azido-1-phenylpropanol, (*R*)-1.2.[85] (*R*)-3-Azido-1-phenylpropanol (*R*)-**1.2** was prepared following a previously published procedure. Characterization data were consistent with reported data.

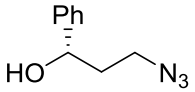

(*S*)-**1.2**

(*S*)-3-Azido-1-phenylpropanol, (*S*)-1.2. Following a literature procedure[85], (*S*)-3-azido-1-phenylpropanol (*S*)-**1.2** was prepared as described. A mixture of (*S*)-3-chloro-1-phenylpropanol (859 mg, 5.03 mmol), NaN_3 (975 mg, 15.0 mmol, 3.0 equiv), NaI (1.12 g, 7.50 mmol, 1.5 equiv) in anhydrous DMF (45.0 mL) was stirred for 24 h at 80 ˚C. The reaction mixture was partitioned between Et_2O and water. The organic layer was washed with brine, dried over anhydrous Na_2SO_4, filtered, and concentrated under a stream of nitrogen. The crude oil was

purified by an automated MPLC system using a 24 g normal phase silica column with gradient elution of 0–15% EtOAc/hexanes. Concentration of solvents under nitrogen afforded product as a colorless oil (797 mg, 4.50 mmol, 89% yield) in ≥99.5% ee as determined by analytical HPLC. R_f = 0.25 (10% EtOAc/hexanes); IR (neat) 3373, 2092 cm^{-1}; $[\alpha]_D^{23}$ = –35.9 (*c* 1.09, $CHCl_3$); ^1H NMR (400 MHz, $CDCl_3$) δ 7.40–7.28 (m, 5H), 4.84 (dd, *J* = 8.4, 4.7, 1H), 3.54–3.36 (m, 2H), 2.09–1.91 (m, 3H); ^{13}C NMR (101 MHz, $CDCl_3$) δ 144.0, 128.8, 128.1, 125.9, 72.0, 48.5, 38.0. HRMS (TOF, ESI) *m/z*: $[M - N_2 + H]^+$ calcd for 150.0913, found 150.0895. HPLC: Chiralcel OD-H, Daicel Chemical Industries, Ltd.; 2–40% *i*-PrOH/hexanes over 60 min; flow rate 1.0 mL/min; UV 220 nm; (*S*) t_R = 10.29 min, (*R*) t_R = 11.03 min.

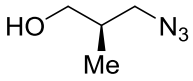

(*R*)-**1.3**

(*R*)-3-Azido-2-methylpropanol, (*R*)-1.3.[85] (*R*)-3-Azido-2-methylpropanol (*R*)-**1.3** was prepared following a previously published procedure at an elevated temperature of 45 ˚C for 24 h. Characterization data were consistent with reported data.

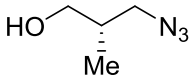

(*S*)-**1.3**

(*S*)-3-Azido-2-methylpropanol, (*S*)-1.3. Following a literature procedure, (*S*)-3-azido-2-methylpropanol (*S*)-**1.3** was prepared as described. A mixture of (*R*)-3-bromo-2-methylpropanol (310 µL, 2.96 mmol) and NaN_3 (975 mg, 15.0 mmol, 5.0 equiv) in anhydrous DMF (8.0 mL) was stirred for 24 h at 45 ˚C. The reaction mixture was partitioned between Et_2O and H_2O. The organic layer was washed with H_2O, brine, dried over anhydrous Na_2SO_4, filtered, and concentrated under a stream of nitrogen. The crude oil was purified by an automated MPLC

system using a 24 g normal phase silica column with gradient elution of 0–25% EtOAc/hexanes. Concentration of solvents under nitrogen afforded product as a colorless oil (315 mg, 2.74 mmol, 91% yield). R_f = 0.30 (25% EtOAc/hexanes); IR (neat) 3341, 2092 cm^{-1}; $[\alpha]_D^{23}$ = –5.98 (*c* 1.00, $CHCl_3$); ^1H NMR (400 MHz, $CDCl_3$) δ 3.58 (m, 2H), 3.35 (m, 2H), 1.93 (m, 1H), 1.65 (s, 1H), 0.97 (d, *J* = 6.9, 3H); ^{13}C NMR (101 MHz, $CDCl_3$) δ 65.5, 54.8, 36.0, 14.6. HRMS (TOF, ESI) *m/z*: $[2M - H]^-$ calcd for $C_8H_{17}N_6O_2$ 229.1418, found 229.1414.

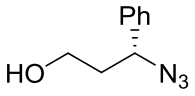

(*R*)-**1.4**

(*R*)-3-Azido-3-phenylpropanol, (*R*)-1.4.[85] (*R*)-3-Azido-3-phenylpropanol (*R*)-**1.4** was prepared following a previously published procedure, in which DPPA and DIAD were used instead of HN_3 and DEAD, respectively. Characterization data were consistent with reported data.

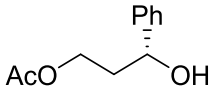

S1.2

(*R*)-3-Hydroxy-3-phenylpropyl acetate, S1.2. Following a literature procedure[85], (*R*)-3-hydroxy-3-phenylpropyl acetate **S1.2** was prepared as described. A mixture of (*R*)-3-chloro-1-phenylpropanol (1.03 g, 6.02 mmol), NaOAc (1.48 g, 18.0 mmol, 3.0 equiv) and NaI (1.08 mg, 7.20 mmol, 1.2 equiv) was heated at 130 ˚C in anhydrous DMF (60.0 mL) for 24 h. The reaction was cooled, and partitioned between Et_2O and water. The organic layer was washed with brine, dried over anhydrous Na_2SO_4, filtered, and concentrated under a stream of nitrogen. The crude oil was purified by an automated MPLC system using a 24 g normal phase silica column with gradient elution of 0–15% EtOAc/hexanes. Concentration of solvents under nitrogen afforded

product as a colorless oil (758 mg, 3.90 mmol, 65% yield). R_f = 0.30 (20% EtOAc/hexanes); IR (neat) 3424, 1728 cm^{-1}; $[\alpha]_D^{20}$ = +22.3 (*c* 1.03, $CHCl_3$); ^1H NMR (400 MHz, $CDCl_3$) δ 7.36 (m, 4H), 7.29 (m, 1H), 4.80 (m, 1H), 4.33 (m, 1H), 4.13 (m, 1H), 2.20 (m, 1H), 2.14–1.95 (m, 5H); ^{13}C NMR (101 MHz, $CDCl_3$) δ 171.4, 144.0, 128.7, 127.9, 125.9, 71.4, 61.7, 38.1, 21.1. HRMS (FT-ICR, ESI) *m/z*: $[M + Na]^+$ calcd for $C_{11}H_{14}NaO_3$ 217.0835, found 217.0832.

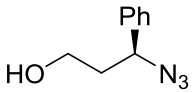

(*S*)-**1.4**

(*S*)-3-Azido-3-phenylpropanol, (*S*)-1.4. Following a literature procedure[85], (*S*)-3-azido-3-phenylpropan-1-ol (*S*)-**1.4** was prepared as described. A solution of (*R*)-3-hydroxy-3-phenylpropyl acetate **S1.2** (1.07 g, 5.50 mmol) dissolved in anhydrous THF (55.0 mL) was cooled to 0 ˚C. PPh_3 (2.17 g, 8.26 mmol, 1.5 equiv), DPPA (2.00 mL, 9.35 mmol, 1.7 equiv), and DIAD (1.6 mL, 8.25 mmol, 1.5 equiv) were added sequentially. The reaction mixture was warmed to room temperature and stirred for 18 h. The reaction mixture was partitioned between Et_2O and H_2O. The organic layer was washed with H_2O, brine, dried over anhydrous Na_2SO_4, filtered, and concentrated under a stream of nitrogen. The crude oil was purified by an automated MPLC system using a 24 g normal phase silica column with gradient elution of 0–20% EtOAc/hexanes. Concentration of solvents under nitrogen afforded a colorless impure oil (R_f = 0.73, 20% EtOAc/hexanes). The impure oil was directly hydrolyzed with K_2CO_3 (1.14 g, 8.25 mmol, 1.5 equiv) in anhydrous MeOH (45.0 mL) at room temperature for 24 h. MeOH was removed under a stream of nitrogen, and the crude residue was purified by an automated MPLC system using a 24 g normal phase silica column with gradient elution of 0–20% EtOAc/hexanes. Concentration of solvents under nitrogen afforded product as a colorless oil (815 mg, 4.56 mmol, 83% yield) in 97.0% ee (98.5:1.5 er) as determined by analytical HPLC. R_f = 0.30 (20%

EtOAc/hexanes); IR (neat) 3335, 2094 cm^{-1}; $[\alpha]_D^{23}$ = –168.4 (*c* 1.02, $CHCl_3$); ^1H NMR (400 MHz, $CDCl_3$) δ 7.43–7.26 (m, 5H), 4.71 (dd, *J* = 8.8, 5.8 Hz, 1H), 3.82–3.67 (m, 2H), 2.11–1.92 (m, 2H); ^{13}C NMR (101 MHz, $CDCl_3$) δ 139.4, 129.1, 128.6, 127.0, 63.6, 59.8, 38.9. HRMS (TOF, ESI) *m/z*: $[M - N_2 + H]^+$ calcd for $C_9H_{12}NO$ 150.0913, found 150.0900. HPLC: Chiralcel OD-H, Daicel Chemical Industries, Ltd.; 2–40% *i*-PrOH/hexanes over 60 min; flow rate 1.0 mL/min; UV 220 nm; (*R*) t_R = 11.29 min, (*S*) t_R = 12.77 min.

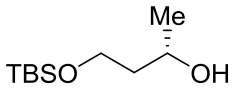

S1.3

(*S*)-4-((*tert*-Butyldimethylsilyl)oxy)butan-2-ol, S1.3. Following a literature procedure[113], (*S*)-4-((*tert*-butyldimethylsilyl)oxy)butan-2-ol **S1.3** was prepared as described. Imidazole (1.36 g, 20.0 mmol, 2.0 equiv) and DMAP (31.0 mg, 25.0 mmol, 2.5 equiv) were added to (*S*)-1,3-butandiol (900 µL, 10.0 mmol) in anhydrous DMF (25.0 mL, 0.4 M). The mixture was cooled to 0 ˚C and TBDMSCl (1.66 g, 11.0 mmol, 1.1 equiv) in anhydrous CH_2Cl_2 (12.0 mL) was added. The solution was stirred at 0 ˚C for 2 h and then stirred at room temperature overnight. The reaction mixture was diluted with H_2O and extracted with Et_2O (4 x 20 mL). The combined organic layers were dried over anhydrous Na_2SO_4, filtered, and concentrated under a stream of nitrogen. The crude oil was purified by an automated MPLC system using a 24 g normal phase silica column with gradient elution of 0–10% EtOAc/hexanes. Concentration of solvents under nitrogen afforded product as a colorless oil (1.82 g, 8.89 mmol, 89% yield). R_f = 0.32 (10% EtOAc/hexanes); IR (neat) 3388 cm^{-1}; $[\alpha]_D^{22}$ = –4.31 (*c* 1.02, $CHCl_3$); ^1H NMR (400 MHz, $CDCl_3$) δ 4.03 (m, 1H), 3.89 (m, 1H), 3.81 (m, 1H), 1.65 (m, 2H), 1.19 (d, *J* = 6.24 Hz, 3H), 0.90 (s, 9H), 0.081 (s, 6H); ^{13}C NMR (101 MHz, $CDCl_3$) δ 68.5, 62.9,

40.1, 26.0, 23.5, 18.3, -5.38, -5.43. HRMS (FT-ICR, ESI) *m/z*: $[M + Na]^+$ calcd for $C_{10}H_{24}NaO_2Si$ 227.1438, found 227.1434.

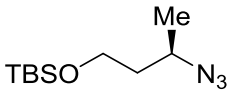

S1.4

(*R*)-(3-Azidobutoxy)(*tert*-butyl)dimethylsilane, S1.4. Following a literature procedure[85], (*R*)-(3-azidobutoxy)(*tert*-butyl)dimethylsilane **S1.4** was prepared as described. A solution of (*S*)-4-((*tert*-butyldimethylsilyl)oxy)butan-2-ol **S1.3** (1.02 g, 5.00 mmol) in anhydrous THF (50.0 mL) was cooled to 0 ˚C. PPh_3 (1.57 g, 6.00 mmol, 1.2 equiv), DPPA (1.60 mL, 7.42 mmol, 1.48 equiv), and DIAD (1.20 mL, 6.09 mmol, 1.2 equiv) were added sequentially. The reaction mixture was warmed to room temperature and stirred for 18 h. The reaction mixture was partitioned between Et_2O and H_2O. The organic layer was washed with H_2O, brine, dried over anhydrous Na_2SO_4, filtered, and concentrated under nitrogen atmosphere. The crude oil was purified by an automated MPLC system using a 24 g normal phase silica column with gradient elution of 100% hexanes. Concentration of solvents under nitrogen afforded product as a colorless oil (857 mg, 3.74 mmol, 75% yield). R_f = 0.75 (10% EtOAc/hexanes); IR (neat) 2098 cm^{-1}; $[\alpha]_D^{23}$ = –55.8 (*c* 1.00, $CHCl_3$); ^1H NMR (400 MHz, $CDCl_3$) δ 3.68 (m, 3H), 1.66 (m, 2H), 1.28 (d, *J* = 6.60 Hz, 3H), 0.90 (s, 9H), 0.062 (s, 3H), 0.057 (s, 3H); ^{13}C NMR (101 MHz, $CDCl_3$) δ 59.7, 54.9, 39.2, 26.1, 19.8, 18.4, -5.26. HRMS (TOF, ESI) *m/z*: $[M – N_2 + H]^+$ calcd for $C_{10}H_{24}NOSi$ 202.1622, found 202.1636.

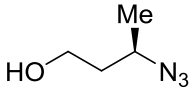

(*R*)-**1.5**

(*R*)-3-Azidobutanol, (*R*)-1.5. Following a literature procedure[85], (*R*)-3-azidobutanol (*R*)-**1.5** was prepared as described. A solution of (*R*)-(3-azidobutoxy)(*tert*-butyl)dimethylsilane **S1.4** (573 mg, 2.50 mmol) in anhydrous THF (50.0 mL) was treated with TBAF (1.0 M in THF, 2.75 mL, 2.75 mmol, 1.1 equiv). After stirring at room temperature for 30 min, the reaction was partitioned between Et_2O and H_2O. The organic layer was washed with a saturated solution of NH_4Cl, brine, dried over anhydrous Na_2SO_4, filtered, and concentrated under a stream of nitrogen. The crude oil was purified by an automated MPLC system using a 12 g normal phase silica column with gradient elution of 0–45% EtOAc/hexanes. Concentration of solvents under nitrogen afforded product as a colorless oil (234 mg, 2.03 mmol, 81% yield). R_f = 0.33 (25% EtOAc/hexanes); IR (neat) 3341, 2094 cm^{-1}; $[\alpha]_D^{23}$ = –107.3 (*c* 1.00, $CHCl_3$); ^1H NMR (400 MHz, $CDCl_3$) δ 3.81–3.68 (m, 3H), 1.72 (m, 2H), 1.32 (d, *J* = 6.56, 3H); ^{13}C NMR (101 MHz, $CDCl_3$) δ 60.0, 55.5, 38.7, 19.7. HRMS (TOF, ESI) *m/z*: $[2M - H]^-$ calcd for $C_8H_{17}N_6O_2$ 229.1418, found 229.1446.

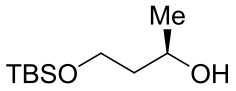

S1.5

(*R*)-4-((*tert*-Butyldimethylsilyl)oxy)butan-2-ol, S1.5.[113] (*R*)-4-((*tert*-Butyldimethylsilyl)'oxy butan-2-ol **S1.5** was prepared following a previously published procedure. Characterization data were consistent with reported data.

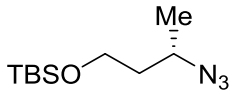

S1.6

(*S*)-(3-Azidobutoxy)(*tert*-butyl)dimethylsilane, S1.6. Following a literature procedure[85], (*S*)-(3-azidobutoxy)(*tert*-butyl)dimethylsilane **S1.6** was prepared as described. A solution of (*R*)-

4-((*tert*-butyldimethylsilyl)oxy)butan-2-ol **S1.5** (1.02 g, 5.00 mmol) in anhydrous THF (50.0 mL) was cooled to 0 ˚C. PPh_3 (1.57 g, 6.00 mmol, 1.2 equiv), DPPA (1.60 mL, 7.42 mmol, 1.48 equiv), and DIAD (1.20 mL, 6.09 mmol, 1.21 equiv) were added sequentially. The reaction mixture was warmed to room temperature and stirred for 18 h. The reaction mixture was partitioned between Et_2O and H_2O. The organic layer was washed with H_2O, brine, dried over anhydrous Na_2SO_4, filtered, and concentrated under a stream of nitrogen. The crude oil was purified by an automated MPLC system using a 24 g normal phase silica column with gradient elution of 100% hexanes. Concentration of solvents under nitrogen afforded product as a colorless oil (897 mg, 3.91 mmol, 78% yield). R_f = 0.75 (10% EtOAc/hexanes); IR (neat) 2098 cm^{-1}; $[\alpha]_D^{23}$ = +58.1 (*c* 1.02, $CHCl_3$); ^1H NMR (400 MHz, $CDCl_3$) δ 3.69 (m, 3H), 1.66 (m, 2H), 1.28 (d, *J* = 6.56, 3H), 0.90 (s, 9H), 0.062 (s, 3H), 0.057 (s, 3H); ^{13}C NMR (101 MHz, $CDCl_3$) δ 59.7, 55.0, 39.3, 26.0, 19.8, 18.4, -5.27. HRMS (TOF, ESI) *m/z*: $[M - N_2 + H]^+$ calcd for $C_{10}H_{24}NOSi$ 202.1622, found 202.1597.

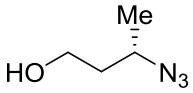

(*S*)-**1.5**

(*S*)-3-Azidobutanol, (*S*)-1.5. Following a literature procedure[85], (*S*)-3-azidobutanol (*S*)-**1.5** was prepared as described. A solution of (*S*)-(3-azidobutoxy)(*tert*-butyl)dimethylsilane **S1.6** (520 mg, 2.27 mmol) in anhydrous THF (45.0 mL) was treated with TBAF (1.0 M in THF, 2.50 mL, 2.50 mmol, 1.1 equiv). After stirring at room temperature for 30 min, the reaction was partitioned between Et_2O and H_2O. The organic layer was washed with a saturated solution of NH_4Cl, brine, dried over anhydrous Na_2SO_4, filtered, and concentrated under a stream of nitrogen. The crude oil was purified by an automated MPLC system using a 12 g normal phase silica column with gradient elution of 0–45% EtOAc/hexanes. Concentration of solvents under

nitrogen afforded product as a colorless oil (178 mg, 1.55 mmol, 68% yield). R_f = 0.32 (25% EtOAc/hexanes); IR (neat) 3341, 2094 cm^{-1}; $[\alpha]_D^{23}$ = +91.7 (*c* 1.00, $CHCl_3$); ^1H NMR (400 MHz, $CDCl_3$) δ 3.81–3.74 (m, 3H), 1.71 (m, 2H), 1.32 (d, *J* = 6.56 Hz, 3H); ^{13}C NMR (101 MHz, $CDCl_3$) δ 60.0, 55.5, 38.8, 19.7. HRMS (ESI) *m/z* calcd for $C_4H_{10}N_3O$ $[M + H]^+$ 116.0824, found 116.0485.

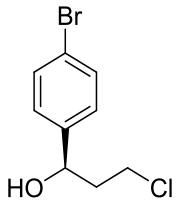

S1.7

(*R*)-1-(4-Bromophenyl)-3-chloropropanol, S1.7. Following a literature procedure[99], (*R*)-1-(4-bromophenyl)-3-chloropropanol **S1.7** was prepared as described. A flame-dried, three-neck 25 mL round bottom equipped with a thermocouple was charged with (*R*)-(+)-2-methyl-CBS-oxazaborolidine solution (1.0 M in toluene, 900 μL, 0.900 mmol, 0.15 equiv). Borane *N,N*-diethylaniline complex (1.60 mL, 9.00 mmol, 1.5 equiv), and was heated to 30 ˚C. 4′-Bromo-3-chloropropiophenone (1.48 g, 6.00 mmol) in anhydrous toluene (4.0 mL) was added dropwise to the reaction mixture using a syringe pump (0.07 mL/min) over 60 min. After ketone addition, the reaction mixture was stirred for an additional 1 h at 30 ˚C. The reaction mixture was allowed to 25 ˚C, and carefully quenched with MeOH (3.0 mL), followed by addition of 1.0 N HCl (5.0 mL) and stirred for 15–20 min. The aqueous layer was extracted with Et_2O (4 x 10 mL). The combined organic layers were washed with 1.0 N HCl (2 x 10 mL), H_2O, brine, dried over anhydrous Na_2SO_4, filtered, and concentrated. The crude oil was purified by an automated MPLC system using a 24 g normal phase silica column with gradient elution of 0–10% EtOAc/hexanes. Concentration of solvents under nitrogen afforded product as a colorless oil

(1.25 g, 5.02 mmol, 84% yield) in 92.2% ee (96.1:3.9 er) as determined by analytical HPLC. R_f = 0.30 (10% EtOAc/hexanes); IR (neat) 3366 cm^{-1}; $[\alpha]_D^{23}$ = +7.25 (*c* 1.00, $CHCl_3$); ^1H NMR (400 MHz, $CDCl_3$) δ 7.50 (m, 2H), 7.25 (m, 2H), 4.94 (m, 1H), 3.74 (m, 1H), 3.55 (m, 1H), 2.20 (m, 1H), 2.05 (m, 1H), 1.95 (br s, 1H); ^{13}C NMR (101 MHz, $CDCl_3$) δ 142.8, 131.9, 127.6, 121.8, 70.8, 41.6, 41.5. HRMS (TOF, ESI) *m/z*: $[M + HCOO]^-$ calcd for $C_{10}H_{11}BrClO_3$ 292.9580, found 292.9571. HPLC: Chiralcel OJ-H, Daicel Chemical Industries, Ltd.; 2–40% *i*-PrOH/hexanes over 60 min; flow rate 1.0 mL/min; UV 220 nm; *(S)* t_R = 11.57 min, (*R*) t_R = 12.89 min.

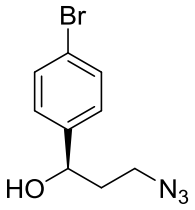

(*R*)-**1.6**

(*R*)-3-Azido-1-(4-bromophenyl)propanol, (*R*)-1.6. Following a literature procedure[85], (*R*)-3-azido-1-(4-bromophenyl)propanol (*R*)-**1.6** was prepared as described. A mixture of (*R*)-1-(4-bromophenyl)-3-chloropropanol **S1.7** (999 mg, 4.00 mmol), NaN_3 (780 mg, 12.0 mmol, 3.0 equiv), NaI (899 mg, 6.00 mmol, 1.5 equiv) in anhydrous DMF (40.0 mL) was stirred for 24 h at 80 ˚C. The reaction mixture was partitioned between Et_2O and H_2O. The organic layer was washed brine, dried over anhydrous Na_2SO_4, filtered, and concentrated under a stream of nitrogen. The crude oil was purified by an automated MPLC system using a 24 g normal phase silica column with gradient elution of 0–20% EtOAc/hexanes. Concentration of solvents under nitrogen afforded product as a colorless oil (902 mg, 3.52 mmol, 88% yield) in 92.7% ee (96.4:3.6 er) as determined by analytical HPLC. R_f = 0.20 (10% EtOAc/hexanes); IR (neat) 3386, 2092 cm^{-1}; $[\alpha]_D^{20}$ = +18.3 (*c* 1.00, $CHCl_3$); ^1H NMR (400 MHz, $CDCl_3$) δ 7.49 (m, 2H), 7.24 (m, 2H), 4.82 (dd, *J* = 8.5, 4.5, 1H), 3.52 (m, 1H), 3.38 (m, 1H), 2.09 (br s, 1H), 2.06–1.84

(m, 2H); ^{13}C NMR (101 MHz, $CDCl_3$) δ 143.0, 131.9, 127.6, 121.8, 76.8, 48.4, 38.0. HRMS (FT-ICR, APPI) *m/z*: $[M - N_2 + H]^+$ calcd for $C_9H_{11}BrNO$ 228.0019, found 228.0019. HPLC: Chiralpak IA, Daicel Chemical Industries, Ltd.; 8% EtOH/hexanes over 60 min; flow rate 1.0 mL/min; UV 220 nm; (*S*) t_R = 11.56 min, (*R*) t_R = 13.74 min.

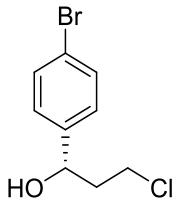

S1.8

(*S*)-1-(4-Bromophenyl)-3-chloropropanol, S1.8. Following a literature procedure[99], (*S*)-1-(4-bromophenyl)-3-chloropropanol **S1.8** was prepared as described. A flame-dried, three-neck 25 mL round bottom equipped with a thermocouple was charged with (*R*)-(+)-2-methyl-CBS-oxazaborolidine solution (1.0 M in toluene, 900 μL, 0.900 mmol, 0.15 equiv). Borane *N,N*-diethylaniline complex (1.60 mL, 9.00 mmol, 1.5 equiv), and was heated to 30 ˚C. 4′-Bromo-3-chloropropiophenone (1.48 g, 6.00 mmol) in anhydrous toluene (4.0 mL) was added dropwise to the reaction mixture using a syringe pump (0.07 mL/min) over 60 min. After ketone addition, the reaction mixture was stirred for an additional 1 h at 30 ˚C. The reaction mixture was allowed to 25 ˚C, and carefully quenched with MeOH (3.0 mL), followed by addition of 1.0 N HCl (5.0 mL) and stirred for 15–20 min. The aqueous layer was extracted with Et_2O (4 x 10 mL). The combined organic layers were washed with 1.0 N HCl (2 x 10 mL), H_2O, brine, dried over anhydrous Na_2SO_4, filtered, and concentrated. The crude oil was purified by an automated MPLC system using a 24 g normal phase silica column with gradient elution of 0–10% EtOAc/hexanes. Concentration of solvents under nitrogen afforded product as a colorless oil (1.20 g, 4.80 mmol, 80% yield) in 93.8% ee (96.9:3.1 er) as determined by analytical HPLC. R_f =

0.30 (10% EtOAc/hexanes); IR (neat) 3366 cm^{-1}; $[\alpha]_D^{23}$ = –6.00 (*c* 1.00, $CHCl_3$). Characterization data were consistent with reported data.[114] HPLC: Chiralcel OJ-H, Daicel Chemical Industries, Ltd.; 2–40% *i*-PrOH/hexanes over 60 min; flow rate 1.0 mL/min; UV 220 nm; (*S*) t_R = 11.57 min, (*R*) t_R = 12.89 min.

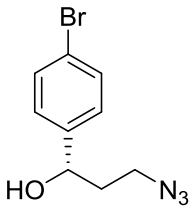

(*S*)-**1.6**

(*S*)-3-Azido-1-(4-bromophenyl)propanol, (*S*)-1.6. Following a literature procedure[85], (*S*)-3-azido-1-(4-bromophenyl)propanol (*S*)-**1.6** was prepared as described. A mixture of (*S*)-1-(4-bromophenyl)-3-chloropropanol **S1.8** (1.04 g, 4.16 mmol), NaN_3 (780 mg, 12.5 mmol, 3.0 equiv), NaI (890 mg, 6.24 mmol, 1.5 equiv) in anhydrous DMF (40.0 mL) was stirred for 24 h at 80 ˚C. The reaction mixture was partitioned between Et_2O and H_2O. The organic layer was washed with brine, dried over anhydrous Na_2SO_4, filtered, and concentrated under a stream of nitrogen. The crude oil was purified by an automated MPLC system using a 24 g normal phase silica column with gradient elution of 0–20% EtOAc/hexanes. Concentration of solvents under nitrogen afforded product as a colorless oil (1.01 g, 3.97 mmol, 95% yield) in 93.2% ee (96.6:3.4 er) as determined by analytical HPLC. R_f = 0.20 (10% EtOAc/hexanes); IR (neat) 3385, 2092 cm^{-1}; $[\alpha]_D^{20}$ = –18.1 (*c* 1.00, $CHCl_3$); ^{1}H NMR (400 MHz, $CDCl_3$) δ 7.49 (m, 2H), 7.24 (m, 2H), 4.81 (dd, *J* = 8.4, 4.5 Hz, 1H), 3.51 (m, 1H), 3.38 (m, 1H), 2.14 (br s, 1H), 2.05–1.83 (m, 2H); ^{13}C NMR (101 MHz, $CDCl_3$) δ 142.9, 131.9, 127.6, 121.8, 71.4, 48.4, 38.0. HRMS (FT-ICR, APPI) *m/z*: $[M - N_2 + H]^+$ calcd for $C_9H_{11}BrNO$ 228.0019, found 228.0019. HPLC: Chiralpak

IA, Daicel Chemical Industries, Ltd.; 8% EtOH/hexanes over 60 min; flow rate 1.0 mL/min; UV 220 nm; (*S*) t_R = 11.56 min, (*R*) t_R = 13.74 min.

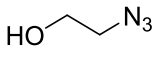

1.7

2-Azidoethanol, 1.7.[78] 2-Azidoethanol **1.7** was prepared following a previously published procedure. Characterization data were consistent with reported data.

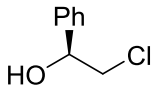

S1.9

(*S*)-2-Chloro-1-phenylethanol, S1.9. Following a literature procedure[99], (*S*)-2-chloro-1-phenylethanol **S1.9** was prepared as described. A flame-dried, three-neck 25 mL round bottom equipped with a thermocouple was charged with (*S*)-(+)-2-methyl-CBS-oxazaborolidine solution (1.0 M in toluene, 1.65 mL, 1.65 mmol, 0.1 equiv). Borane *N,N*-diethylaniline complex (3.0 mL, 1.01 mmol, 1.01 equiv), and was heated to 32 ˚C. 2-Chloroacetophenone (2.55 g, 16.5 mmol) in anhydrous toluene (6.0 mL) was added dropwise to the reaction mixture using a syringe pump (0.10 mL/min) over 90 min. After ketone addition, the reaction mixture was stirred for an additional 1 h at 32 ˚C. The reaction mixture was allowed to 25 ˚C, and carefully quenched with MeOH (5.0 mL), followed by addition of 1.0 N HCl (10.0 mL) and stirred for 15–20 min. The aqueous layer was extracted with Et_2O (4 x 15 mL). The combined organic layers were washed with 1.0 N HCl (2 x 10 mL), H_2O, brine, dried over anhydrous Na_2SO_4, filtered, and concentrated. The crude oil was purified by an automated MPLC system using a 24 g normal phase silica column with gradient elution of 0–5% EtOAc/hexanes. Concentration of solvents under nitrogen afforded product as a colorless oil (2.09 g, 13.3 mmol, 81% yield) in 97.8% ee

(98.9:1.1 er) as determined by analytical HPLC. R_f = 0.40 (10% EtOAc/hexanes); IR (neat) 3379 cm^{-1}; $[\alpha]_D^{22}$ = +57.3 (*c* 1.00, $CHCl_3$). Characterization data were consistent with reported data.[115] HPLC: Chiralcel OD-H, Daicel Chemical Industries, Ltd.; 2–40% *i*-PrOH/hexanes over 60 min; flow rate 1.0 mL/min; UV 220 nm; (*S*) t_R = 9.75 min, (*R*) t_R = 10.83 min.

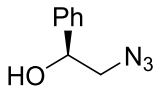

(*S*)-**1.8**

(*S*)-2-Azido-1-phenylethanol, (*S*)-1.8. Following a literature procedure[85], (*S*)-2-azido-1-phenylethanol (*S*)-**1.8** was prepared as described. A mixture of (*S*)-2-chloro-1-phenylethanol **S1.9** (313 mg, 2.00 mmol), NaN_3 (520 mg, 8.00 mmol, 4.0 equiv), and NaI (599 g, 4.00 mmol, 2.0 equiv) in anhydrous DMF (20.0 mL) was stirred for 30 h at 85 ˚C. The reaction mixture was partitioned between Et_2O and H_2O. The organic layer was washed with brine, dried over anhydrous Na_2SO_4, filtered, and concentrated under a stream of nitrogen. The crude oil was purified by an automated MPLC system using a 24 g normal phase silica column with gradient elution of 0–10% EtOAc/hexanes. Concentration of solvents under nitrogen afforded product as a colorless oil (292 mg, 1.79 mmol, 90% yield) in ≥99.5% ee as determined by analytical HPLC. R_f = 0.25 (10% EtOAc/hexanes); IR (neat) 3396, 2096 cm^{-1}; $[\alpha]_D^{22}$ = +87.9 (*c* 1.03, $CHCl_3$); ^1H NMR (400 MHz, $CDCl_3$) δ 7.45–7.29 (m, 5H), 4.89 (m, 1H), 3.47 (m, 2H), 2.32 (d, *J* = 3.2 Hz, 1H); ^{13}C NMR (101 MHz, $CDCl_3$) δ 140.7, 128.9, 128.6, 126.1, 73.6, 58.3. HRMS (TOF, ESI) *m/z*: $[M - N_2 + H]^+$ calcd for $C_8H_{10}NO$ 136.0757, found 136.0719. HPLC: Chiralcel OJ-H, Daicel Chemical Industries, Ltd.; 2% *i*-PrOH/hexanes over 60 min; flow rate 1.0 mL/min; UV 220 nm; (*R*) t_R = 24.41 min, (*S*) t_R = 29.05 min.

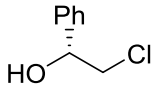

S1.10

(*R*)-2-Chloro-1-phenylethanol, S1.10. Following a literature procedure[99], (*R*)-2-chloro-1-phenylethanol **S1.10** was prepared as described. A flame-dried, three-neck 25 mL round bottom equipped with a thermocouple was charged with (*R*)-(+)-2-methyl-CBS-oxazaborolidine solution (1.0 M in toluene, 1.65 mL, 1.65 mmol, 0.1 equiv). Borane *N,N*-diethylaniline complex (3.0 mL, 1.01 mmol, 1.01 equiv), and was heated to 32 ˚C. 2-Chloroacetophenone (2.55 g, 16.5 mmol) in anhydrous toluene (6.0 mL) was added dropwise to the reaction mixture using a syringe pump (0.10 mL/min) over 90 min. After ketone addition, the reaction mixture was stirred for an additional 1 h at 32 ˚C. The reaction mixture was allowed to 25 ˚C, and carefully quenched with MeOH (5.0 mL), followed by addition of 1.0 N HCl (10.0 mL) and stirred for 15–20 min. The aqueous layer was extracted with Et_2O (4 x 15 mL). The combined organic layers were washed with 1.0 N HCl (2 x 10 mL), H_2O, brine, dried over anhydrous Na_2SO_4, filtered, and concentrated. The crude oil was purified by an automated MPLC system using a 24 g normal phase silica column with gradient elution of 0–5% EtOAc/hexanes. Concentration of solvents under nitrogen afforded product as a colorless oil (2.12 g, 13.5 mmol, 82% yield) in 96.0% ee (49:1 er) as determined by analytical HPLC. R_f = 0.40 (10% EtOAc/hexanes); IR (neat) 3383 cm^{-1}; $[\alpha]_D^{22}$ = –53.3 (*c* 1.00, $CHCl_3$). Characterization data were consistent with reported data.[114] HPLC: Chiralcel OD-H*,* Daicel Chemical Industries, Ltd.; 2–40% *i*-PrOH/hexanes over 60 min; flow rate 1.0 mL/min; UV 220 nm; (*S*) t_R = 9.75 min, (*R*) t_R = 10.83 min.

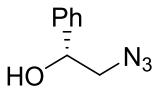

(*R*)-**1.8**

(*R*)-2-Azido-1-phenylethanol, (*R*)-1.8. Following a literature procedure[85], (*R*)-2-azido-1-phenylethanol (*R*)-**1.8** was prepared as described. A mixture of (*R*)-2-chloro-1-phenylethanol **S1.11** (472 mg, 3.01 mmol), NaN_3 (683 mg, 10.5 mmol, 3.5 equiv), and NaI (899 mg, 6.00 mmol, 2.0 equiv) in anhydrous DMF (30.0 mL) was stirred for 24 h at 85 ˚C. The reaction mixture was partitioned between Et_2O and H_2O. The organic layer was washed with brine, dried over anhydrous Na_2SO_4, filtered, and concentrated under a stream of nitrogen. The crude oil was purified by an automated MPLC system using a 24 g normal phase silica column with gradient elution of 0–10% EtOAc/hexanes. Concentration of solvents under nitrogen afforded product as a colorless oil (406 mg, 2.49 mmol, 83% yield) in ≥99.5% ee as determined by analytical HPLC. R_f = 0.25 (10% EtOAc/hexanes); IR (neat) 3392, 2097 cm^{-1}; $[\alpha]_D^{22}$ = –87.4 (*c* 1.02, $CHCl_3$); ^1H NMR (400 MHz, $CDCl_3$) δ 7.43–7.29 (m, 5H), 4.89 (m, 1H), 3.48 (m, 2H), 2.31 (br s, 1H); ^{13}C NMR (101 MHz, $CDCl_3$) δ 140.7, 128.9, 128.5, 126.1, 73.6, 58.3. HRMS (TOF, ESI) *m/z*: $[M - N_2 + H]^+$ calcd for $C_8H_{10}NO$ 136.0757, found 136.0747. HPLC: Chiralcel OJ-H, Daicel Chemical Industries, Ltd.; 2% *i*-PrOH/hexanes over 60 min; flow rate 1.0 mL/min; UV 220 nm; (*R*) t_R = 24.41 min, (*S*) t_R = 29.05 min.

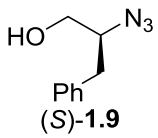

(*S*)-**1.9**

(*S*)-2-Azido-3-phenylpropanol, (*S*)-1.9.[100] (*S*)-2-Azido-3-phenylpropanol (*S*)-**1.9** was prepared following a previously published procedure. Characterization data were consistent with reported data.

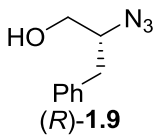

(*R*)-**1.9**

(*R*)-2-Azido-3-phenylpropanol, (*R*)-1.9.[100] (*R*)-2-Azido-3-phenylpropanol (*R*)-**1.9** was prepared following a previously published procedure. Characterization data were consistent with reported data.

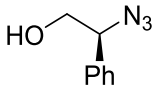

(*S*)-**1.10**

(*S*)-2-Azido-2-phenylethanol, (*S*)-1.10. Following the literature procedure[100, 116], (*S*)-2-azido-2-phenylethanol (*S*)-**1.10** was obtained as a yellow oil (376 mg, 2.31 mmol, 58% yield) in 94.9% ee (39:1 er) as determined by analytical HPLC. Purification was carried out by an automated MPLC system using a 24 g normal phase silica column with gradient elution of 0–10% EtOAc/hexanes. R_f = 0.22 (10% EtOAc/hexanes); IR (neat) 3356, 2094 cm^{-1}; $[\alpha]_D^{22}$ = +199.4 (*c* 0.98, $CHCl_3$); ^1H NMR (400 MHz, $CDCl_3$) δ 7.43–7.32 (m, 5H), 4.68 (dd, *J* = 7.1, 5.7 Hz, 1H), 3.80–3.72 (m, 2H); ^{13}C NMR (101 MHz, $CDCl_3$) δ 136.4, 129.1, 128.9, 127.3, 68.0, 66.7. HRMS (TOF, ESI) *m/z*: $[M - N_2 + H]^+$ calcd for $C_8H_{10}NO$ 136.0757, found 136.0749. HPLC: Chiralpak IA, Daicel Chemical Industries, Ltd.; 2–30% EtOH/hexanes over 60 min; flow rate 1.0 mL/min; UV 220 nm; (*S*) t_R = 13.38 min, (*R*) t_R = 15.38 min.

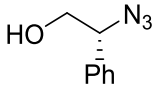

(*R*)-**1.10**

(*R*)-2-Azido-2-phenylethanol, (*R*)-1.10.[117] (*R*)-2-Azido-2-phenylethanol (*R*)-**1.10** was prepared following a previously published procedure. Characterization data were consistent with reported data.

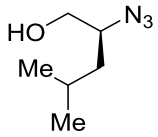

(*S*)-**1.11**

(*S*)-2-Azido-4-methylpentanol, (*S*)-1.11.[100] (*S*)-2-Azido-4-methylpentanol (*S*)-**1.11** was prepared following a previously published procedure. Characterization data were consistent with reported data.

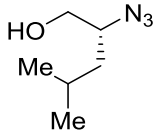

(*R*)-**1.11**

(*R*)-2-Azido-4-methylpentanol, (*R*)-1.11. Following the literature procedure[100, 116], (*R*)-2-azido-4-methylpentanol (*R*)-**1.11** was obtained as a yellow oil (363 mg, 2.56 mmol, 63% yield). Purification was carried out by an automated MPLC system using a 24 g normal phase silica column with gradient elution of 0–15% EtOAc/hexanes. R_f = 0.42 (10% EtOAc/hexanes); IR (neat) 3356, 2101 cm^{-1}; $[\alpha]_D^{22}$ = +5.0 (*c* 1.00, $CHCl_3$); ^1H NMR (400 MHz, $CDCl_3$) δ 3.73–3.67 (m, 1H), 3.57–3.50 (m, 2H), 1.83–1.73 (m, 1H), 1.49–1.42 (m, 1H), 1.32–1.25 (m, 1H), 0.96 (dd, *J* = 6.6, 0.8 Hz, 6H); ^{13}C NMR (101 MHz, $CDCl_3$) δ 65.8, 62.7, 39.6, 25.1, 23.1, 22.2. HRMS (TOF, ESI) *m/z*: $[M - N_2 + H]^+$ calcd for $C_8H_{10}NO$ 116.1070, found 116.1035.

1.6.3 Experimental Section for 1.3

Experimental section for 1.3.1

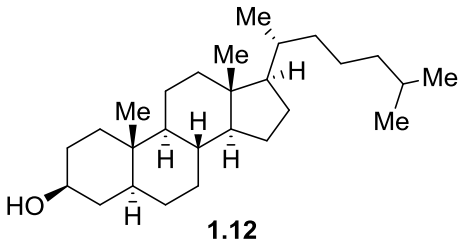

1.12

5α-Cholestan-3-ol, 1.12.[118] To a solution of cholesterol (2.03 g, 5.25 mmol) in anhydrous EtOH (55.0 mL, 0.1 M) was added 10% Pd/C (220 mg, 2.07 mmol, 0.40 equiv) under argon. The reaction mixture was degassed and charged with hydrogen. The reaction mixture was stirred under balloon-pressure hydrogen overnight. The reaction mixture was filtered over Celite and concentrated. Purification was carried out by an automated MPLC system using a 40 g normal phase silica column with gradient elution from 0–10% EtOAc/hexanes to afford **S1** as a white amorphous solid (1.86 g, 4.79 mmol, 91% yield). Characterization data were consistent with reported data.

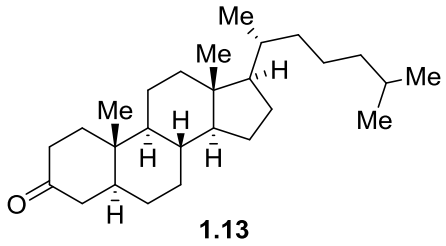

1.13

5α-Cholestan-3-one, 1.13.[119] To a solution of **1.12** (1.57 g, 4.04 mmol) in anhydrous CH_2Cl_2 (50.0 mL) was added Celite and PCC (1.31 g, 6.07 mmol, 1.5 equiv) at 0 ˚C. The reaction mixture was allowed to room temperature and stirred overnight. The reaction mixture was filtered through a short pad of Celite and concentrated. Purification was carried out by an automated MPLC system using a 40 g normal phase silica column with gradient elution from 0–10% EtOAc/hexanes to afford **1.13** as a white amorphous solid (1.45 g, 3.75 mmol, 93% yield). Characterization data were consistent with reported data; mp 129–130 ˚C.

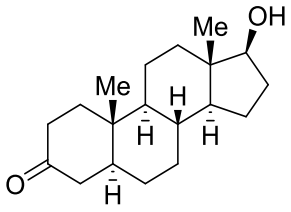

1.14

5α-Dihydrotestosterone, 1.14.[120] Following a literature procedure[121], 5α-Dihydrotestosterone **1.14** was prepared as described. To a solution of testosterone (570 mg, 1.98 mmol) in anhydrous THF (6.0 mL) was condensed liquid NH_3 (~30 mL) at –78 ˚C. To the cooled solution was added pieces of lithium wire (83.0 mg, 12.0 mmol, 6.0 equiv). The blue solution was stirred at –78 ˚C for 20 min, and was allowed to –35 ˚C and stirred for an additional 2 h. The reaction mixture was quenched by adding solid NH_4Cl slowly (until the disappearance of blue). The resulting mixture was diluted with H_2O and EtOAc. The organic layer was washed with brine, dried over anhydrous Na_2SO_4, filtered, and concentrated. Purification was carried out by an automated MPLC system using a 24 g normal phase silica column with gradient elution from 0–30% EtOAc/hexanes to afford **1.14** as a white amorphous solid (331 mg, 1.14 mmol, 58% yield). Characterization data were consistent with reported data; mp 179–181 ˚C.

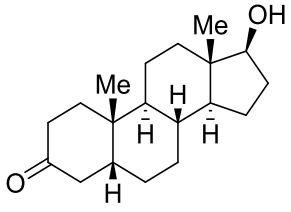

1.15

5β-Dihydrotestosterone, 1.15.[122] To a solution of testosterone (2.30 g, 8.00 mmol) in anhydrous THF (80.0 mL, 0.1 M) was added 10% Pd/C (341 mg, 3.20 mmol, 0.40 equiv) under argon. The reaction mixture was degassed and charged with hydrogen. The reaction mixture was stirred under balloon-pressure hydrogen overnight. The reaction mixture was filtered over Celite

and concentrated. Purification was carried out by an automated MPLC system using an 80 g normal phase silica column with gradient elution from 0–20% EtOAc/hexanes to afford **1.15** as a colorless amorphous solid (1.51 g, 5.20 mmol, 65% yield) and **2** as a white amorphous solid (414 mg, 1.43 mmol, 18% yield). Characterization data were consistent with reported data.

Experimental section for 1.3.2

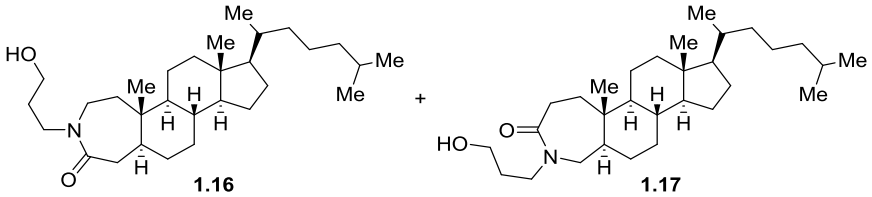

5α-Cholestane-derived A-Ring Lactams, 1.16 and 1.17. Following the general procedure A, 3-azidopropanol **1.1** (30.5 mg, 0.301 mmol, 2.0 equiv) was reacted with 5α-cholestan-3-one **1.13** (58.0 mg, 0.150 mmol) to give an inseparable mixture (38:62) of regioisomers **1.16** and **1.17** as a white amorphous solid (63.4 mg, 0.138 mmol, 92% yield). Purification was carried out by an automated MPLC system using a 4 g normal phase silica column with gradient elution from 0–5% MeOH/CH_2Cl_2. R_f = 0.43 (5% MeOH/CH_2Cl_2); IR (neat) 3318, 1625 cm^{-1}; key ^1H NMR (600 MHz, $CDCl_3$) δ 3.67–3.61 (m, 2H), 2.96 (ddd, *J* = 15.7, 6.5, 1.8 Hz, 1H), 2.79 (dd, *J* = 14.3, 10.6 Hz, 1H), 2.65 (t, *J* = 13.1 Hz, 1H), 2.34 (dd, *J* = 14.5, 7.6 Hz, 1H), 2.00–1.93 (m, 2H), 1.91–1.77 (m, 3H); ^{13}C NMR (151 MHz, $CDCl_3$) δ 177.3, 177.2, 58.10, 58.06, 56.5, 56.3, 54.2, 54.0, 52.0, 48.9, 45.4, 44.8, 44.5, 44.0, 42.44, 42.40, 41.0, 40.04, 40.01, 39.98, 39.6, 38.5, 38.3, 36.3, 35.9, 35.1, 34.9, 32.12, 32.06, 31.9, 31.0, 30.32, 30.28, 28.5, 28.4, 28.1, 24.3, 24.0, 22.9, 22.7, 21.4, 21.1, 18.77, 18.75, 12.21, 12.15. **Note**: Missing carbon signals due to signal overlap of regioisomers. HRMS (FT-ICR, ESI) *m/z*: $[M + H]^+$ calcd for $C_{30}H_{54}NO_2$ 460.4149, found 460.4149.

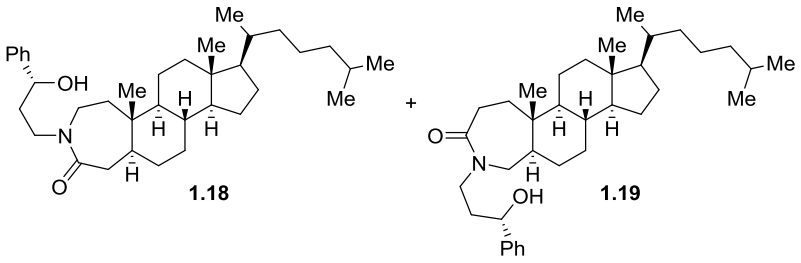

5α-Cholestane-derived A-Ring Lactams, 1.18 and 1.19. Following the general procedure A, (±)-3-azido-1-phenylpropanol **(±)-1.2** (44.3 mg, 0.250 mmol, 2.0 equiv) was reacted with 5α-cholestan-3-one **1.13** (48.3 mg, 0.125 mmol) to give a 50:50 mixture of regioisomers **1.18** and **1.19** as a white amorphous solid (61.4 mg, 0.115 mmol, 92% yield). Purification was carried out by an automated MPLC system using a 12 g normal phase column 0–5% MeOH/CH_2Cl_2. The mixture was intentionally not separated by column chromatography. R_f = 0.40 (5% MeOH/CH_2Cl_2); IR (neat) 3376, 1617 cm^{-1}; key ^1H NMR (400 MHz, $CDCl_3$) δ 4.67–4.62 (m, 2H), 4.15–4.03 (m, 2H), 3.73–3.63 (m, 2H), 3.15–3.07 (m, 2H), 3.01 (m, 1H), 2.71 (dd, *J* = 14.2, 10.4 Hz, 1H), 2.61–2.52 (m, 2H, contains d, 2.54, *J* = 15.6 Hz, 1H), 2.40–2.35 (m, 1H); ^{13}C NMR (101 MHz, $CDCl_3$) δ 177.21, 177.1, 144.3, 144.26, 128.47, 128.43, 127.2, 127.1, 125.7, 127.6, 70.0, 56.5, 56.4, 56.32, 56.30, 54.5, 54.3, 52.5, 49.6, 45.9, 45.7, 44.2, 42.5, 42.4, 41.2, 40.11, 40.05, 39.9, 39.65, 36.63, 38.5, 38.4, 38.1, 37.9, 36.3, 36.1, 35.9, 35.1, 34.9, 32.21, 32.17, 32.0, 31.0, 28.5, 28.3, 28.1, 24.29, 24.25, 23.9, 22.9, 22.7, 21.4, 21.1, 18.79, 18.76, 12.2, 12.1. **Note**: Missing carbon signals due to signal overlap of regioisomers. HRMS (FT-ICR, ESI) *m/z*: $[M + H]^+$ calcd for $C_{36}H_{58}NO_2$ 536.4462, found 536.4467.

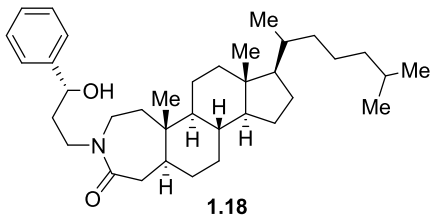

5α-Cholestane-derived A-Ring Lactam, 1.18. Following the general procedure A, (*R*)-3-azido-1-phenylpropanol (*R*)-**1.2** (44.5 mg, 0.251 mmol, 2.0 equiv) was reacted with 5α-cholestan-3-one **1.13** (48.4 mg, 0.125 mmol) to give **1.18** as a white amorphous solid (59.5 mg, 0.111 mmol, 89% yield). Purification was carried out by an automated MPLC system using a 12 g normal phase silica column 0–40% EtOAc/hexanes. R_f = 0.54 (50% EtOAc/hexanes); mp 178–182 ˚C; IR (neat) 3373, 1613 cm^{-1}; ^1H NMR (400 MHz, $CDCl_3$) δ 7.39–7.33 (m, 4H), 7.31–7.25 (m, 1H), 4.65 (dd, *J* = 9.8, 3.2 Hz, 1H), 4.07 (ddd, *J* = 14.6, 10.6, 4.2 Hz, 1H), 3.66 (dd, *J* = 15.7, 11.8 Hz, 1H), 3.12 (dt, *J* = 14.2, 4.6 Hz, 1H), 3.01 (dd, *J* = 15.6, 6.2 Hz, 1H), 2.71 (dd, *J* = 14.1, 10.4 Hz, 1H), 2.00–1.77 (complex, 4H, contains d, *J* = 14.2 Hz, 1H), 1.69–1.65 (m, 1H), 1.59–0.93 (complex, 24H), 0.94–0.85 (complex, 12H, contains s, 0.91, 3H; s, 0.89, 3H; d, 0.87, *J* = 1.8 Hz, 3H; d, 0.85, *J* = 1.9 Hz, 3H), 0.75–0.65 (m, 4H, contains s, 3H); ^{13}C NMR (101 MHz, $CDCl_3$) δ 177.2, 144.3, 128.4 (2C), 127.2, 125.7 (2C), 70.1, 56.5, 56.3, 54.5, 45.9 45.7, 44.2, 42.4, 41.8, 40.1, 40.07, 39.6, 38.5, 37.9, 36.3, 35.9, 34.9, 32.0, 31.0, 28.3, 28.1, 24.3, 24.0, 22.9, 22.7, 21.4, 18.9, 12.2, 12.1. HRMS (FT-ICR, ESI) *m/z*: $[M + H]^+$ calcd for $C_{36}H_{58}NO_2$ 536.4462, found 536.4463.

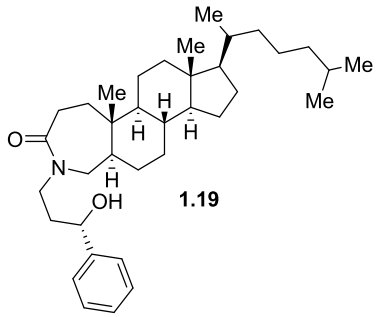

1.19

5α-Cholestane-derived A-Ring Lactam, 1.19. Following the general procedure A, (*S*)-3-azido-1-phenylpropanol (*S*)-**1.2** (86.6 mg, 0.500 mmol, 2.0 equiv) was reacted with 5α-cholestan-3-one **1.13** (96.6 mg, 0.250 mmol) to give **1.19** as a white amorphous solid (118 mg,

0.220 mmol, 88% yield). Purification was carried out by an automated MPLC system using a 12 g normal phase silica column 0–40% EtOAc/hexanes. R_f = 0.42 (50% EtOAc/hexanes); mp 194–199 ˚C; IR (neat) 3378, 1619 cm^{-1}; ^1H NMR (400 MHz, $CDCl_3$) δ 7.37–7.33 (m, 4H) 7.26 (m, 1H), 4.64 (dd, *J* = 9.8, 3.2 Hz, 1H), 4.10 (ddd, *J* = 14.6, 10.7, 4.3 Hz, 1H), 3.70 (dd, *J* = 15.5, 8.5 Hz, 1H), 3.11 (dt, *J* = 14.1, 4.5 Hz, 1H), 2.61–2.52 (m, 2H, contains d, 2.54, *J* = 15.5 Hz, 1H), 2.39 (m, 1H), 2.04–1.72 (complex, 6H), 1.61–1.47 (complex, 3H), 1.39–0.94 (complex, 19H), 0.91–0.85 (complex, 12H, contains s, 0.91, 3H; s, 0.89, 3H; d, 0.87, *J* = 1.9 Hz, 3H; d, 0.85, *J* = 1.9 Hz, 3H), 0.74–0.65 (m, 4H, contains s, 0.65, 3H); ^{13}C NMR (101 MHz, $CDCl_3$) δ 177.1, 144.4, 128.5 (2C), 127.1, 125.6 (2C), 70.1, 56.5, 56.3, 54.3, 52.5, 49.6, 45.9, 42.5, 40.0, 39.7, 38.4, 38.1, 36.3, 36.2, 35.9, 35.2, 32.2, 28.5, 28.3, 28.1, 24.3, 24.0, 22.9, 22.7, 21.1, 18.8, 12.2. **Note**: Missing two carbon signals due to signal overlap of methyl groups. HRMS (FT-ICR, HESI) *m/z*: $[M + H]^+$ calcd for $C_{36}H_{58}NO_2$ 536.4462, found 536.4449.

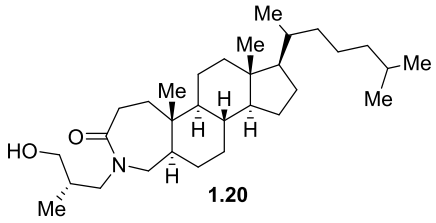

1.20

5α-Cholestane-derived A-Ring Lactam, 1.20. Following the general procedure A, (*S*)-3-azido-2-methylpropanol (*S*)-**1.3** (34.7 mg, 0.300 mmol, 2.0 equiv) was reacted with 5α-cholestan-3-one **1.13** (58.0 mg, 0.150 mmol) to give **1.20** as a white amorphous solid (59.5 mg, 0.126 mmol, 84% yield). Purification was carried out twice by an automated MPLC system first using a 12 g normal phase silica column with gradient elution from 0–40% EtOAc/Et_2O, and second using a 4 g column normal phase silica column with gradient elution from 0–5% MeOH/CH_2Cl_2. R_f = 0.35 (2% MeOH/CH_2Cl_2); mp 186–187 ˚C; IR (neat) 3417, 1623 cm^{-1}; ^1H NMR (400 MHz, $CDCl_3$) δ 3.68 (dd, *J* = 13.9, 10.1 Hz, 1H), 3.58 (m, 1H), 3.41 (dd, *J* = 11.9, 3.1

Hz, 1H), 3.28 (dd, *J* = 11.8, 3.7 Hz, 1H), 2.84 (dd, *J* = 13.9, 4.4 Hz, 1H), 2.64 (t, *J* = 14.0 Hz, 1H), 2.45 (d, *J* = 15.3 Hz, 1H), 2.33 (m, 1H), 1.95 (m, 1H), 1.88–1.65 (complex, 4H), 1.57–1.42 (m, 3H), 1.37–0.90 (complex, 22H, contains d, 0.95, *J* = 6.9 Hz, 3H), 0.88–0.80 (complex, 12H, contains d, 0.85, *J* = 1.9 Hz, 3H; d, 0.83, *J* = 1.9 Hz, 3H), 0.69 (m, 1H), 0.62 (s, 3H); ^{13}C NMR (101 MHz, $CDCl_3$) δ 177.2, 63.2, 56.5, 56.3, 54.0, 52.2, 50.9, 48.4, 42.5, 40.0, 39.6, 38.3, 36.3, 35.9, 35.8, 35.1, 34.3, 32.1, 31.9, 28.6, 28.3, 28.1, 24.3, 23.9, 22.9, 22.7, 21.1, 18.7, 15.2, 12.3, 12.1. HRMS (FT-ICR, ESI) *m/z*: $[M + H]^+$ calcd for $C_{31}H_{56}NO_2$ 474.4306, found 474.4305.

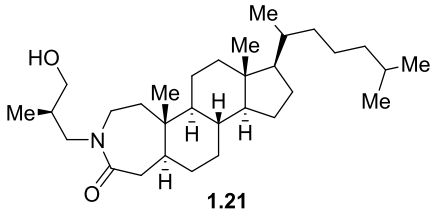

1.21

5α-Cholestane-derived A-Ring Lactam, 1.21. Following the general procedure A, (*R*)-3-azido-2-methylpropanol (*R*)-**1.3** (34.4 mg, 0.300 mmol, 2.0 equiv) was reacted with 5α-cholestan-3-one **1.13** (58.1 mg, 0.150 mmol) to give **1.21** as a white amorphous solid (50.2 mg, 0.106 mmol, 71%). Purification was carried out by an automated MPLC system using a 12 g normal phase silica with gradient elution from 0–5% MeOH/CH_2Cl_2. R_f = 0.27 (2% MeOH/CH_2Cl_2 run twice); mp 160–162 ˚C; IR (neat) 3347, 1616 cm^{-1}; ^{1}H NMR (400 MHz, $CDCl_3$) δ 3.67 (dd, *J* = 13.9, 10.2 Hz, 1H), 3.57 (dd, *J* = 15.5, 11.7 Hz, 1H), 3.43 (dd, *J* = 11.8, 3.1 Hz, 1H), 3.30 (dd, *J* = 11.9, 3.6 Hz, 1H), 2.95 (m, 1H), 2.85–2.76 (m, 2H), 1.99–1.92 (m, 2H, contains d, 1.94, *J* = 14.4 Hz, 1H), 1.85–1.61 (complex, 4H), 1.58–0.92 (complex, 25H, contains d, 0.96, *J* = 6.9 Hz, 3H), 0.90–0.84 (complex, 12H, contains t, 0.88, *J* = 3.3 Hz, 6H; d, 0.85, *J* = 2.0 Hz, 3H; d, 0.84, *J* = 1.9 Hz, 3H), 0.70 (m, 1H), 0.63 (s, 3H); ^{13}C NMR (101 MHz, $CDCl_3$) δ 177.2, 63.2, 56.5, 56.4, 54.3, 50.5, 45.5, 43.8, 42.4, 40.4, 40.08, 40.05, 39.6, 38.5, 36.2, 35.9,

34.9, 34.2, 32.1, 31.0, 28.3, 28.1, 24.2, 23.9, 22.9, 22.7, 21.4, 18.8, 15.3, 12.2, 12.1. HRMS (FT-ICR, ESI) *m/z*: $[M + H]^+$ calcd for $C_{31}H_{56}NO_2$ 474.4306, found 474.4306.

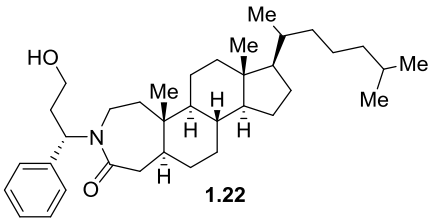

1.22

5α-Cholestane-derived A-Ring Lactam, 1.22. Following the general procedure A, (*S*)-3-azido-3-phenylpropanol (*S*)-**1.4** (44.2 mg, 0.249 mmol, 2.0 equiv) was reacted with 5α-cholestan-3-one **1.13** (48.4 mg, 0.125 mmol) to give **1.22** as a cream-colored amorphous solid (59.1 mg, 0.110 mmol, 88% yield). Purification was carried out by an automated MPLC system using a 12 g normal phase silica column with gradient elution from 0–50% EtOAc/hexanes. R_f = 0.39 (50% EtOAc/hexanes); mp 149–152 ˚C; IR (neat) 3416, 1618 cm^{-1}; ^1H NMR (400 MHz, $CDCl_3$) δ 7.36–7.24 (m, 5H), 5.88 (dd, *J* = 12.4, 3.3 Hz, 1H), 3.70 (m, 1H), 3.40 (m, 1H), 3.18 (dd, *J* = 15.3, 11.6 Hz, 1H), 2.82 (m, 2H), 2.13–2.02 (m, 2H, contains d, 2.06, *J* = 14.9 Hz, 1H), 1.95–1.74 (m, 3H), 1.66–1.43 (m, 5H), 1.37–0.87 (complex, 18H), 0.84 (dd, *J* = 6.5, 2.2 Hz, 9H), 0.77 (s, 3H), 0.57 (s, 3H), 0.47 (m, 1H), 0.38 (m, 1H); ^{13}C NMR (101 MHz, $CDCl_3$) δ 177.5, 139.1, 128.63 (2C), 128.55 (2C), 127.9, 58.5, 56.38, 56.32, 54.2, 52.5, 43.6, 42.3, 40.6, 40.4, 40.0, 39.6, 39.2, 38.1, 36.2, 35.8, 34.8, 32.0, 31.0. 28.3, 28.1, 24.2, 23.9, 22.9, 22.6, 21.1, 18.7, 12.0 (2C). HRMS (FT-ICR, ESI) *m/z*: $[M + H]^+$ calcd for $C_{36}H_{58}NO_2$ 536.4462, found 536.4466.

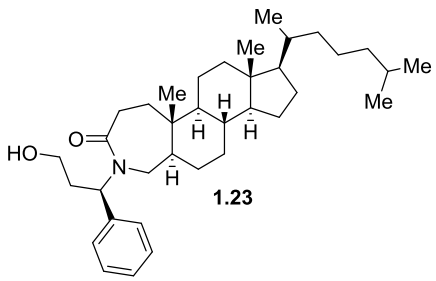

1.23

5α-Cholestane-derived A-Ring Lactam, 1.23. Following the general procedure A, (*R*)-3-azido-3-phenylpropanol (*R*)-**1.4** (44.3 mg, 0.250 mmol) was reacted with 5α-cholestan-3-one **1.13** (48.3 mg, 0.125 mmol) to give **1.23** as a white amorphous solid (58.4 mg, 0.109 mmol, 87% yield). Purification was carried out by an automated MPLC system using a 12 g normal phase silica column with gradient elution from 0–50% EtOAc/hexanes. R_f = 0.43 (50% EtOAc/hexanes); mp 187–189 ˚C; IR (neat) 3409, 1620 cm^{-1}; ^1H NMR (400 MHz, $CDCl_3$) δ 7.37–7.28 (m, 5H), 5.92 (dd, *J* = 12.5, 3.1 Hz, 1H), 3.72 (m, 1H), 3.42 (td, *J* = 11.7, 2.8 Hz, 1H), 3.18 (dd, *J* = 15.2, 9.0 Hz, 1H), 2.69 (t, *J* = 14.0 Hz, 1H), 2.47 (dd, *J* = 15.0, 7.4 Hz, 1H), 2.35 (d, *J* = 15.3 Hz, 1H), 2.09 (m, 1H), 1.95–1.83 (m, 3H), 1.79–1.71 (m, 1H), 1.53–0.82 (complex, 29 H), 0.77 (s, 3H), 0.58 (s, 3H), 0.52–0.43 (m, 2H), 0.34–0.23 (m, 2H); ^{13}C NMR (126 MHz, $CDCl_3$) δ 177.2, 139.1, 129.0 (2C), 128.5 (2C), 128.1, 58.5, 56.4 (2C), 54.0, 52.8, 48.8, 45.4, 42.4, 40.0, 39.6, 38.0, 36.3, 36.1, 35.9, 35.1, 32.6, 32.3, 31.6, 28.3, 28.1, 27.4, 24.2, 23.9, 22.9, 22.7, 21.0, 18.8, 12.10, 12.06. HRMS (FT-ICR, HESI) *m/z*: $[M + H]^+$ calcd for $C_{36}H_{58}NO_2$ 536.4462, found 436.4456.

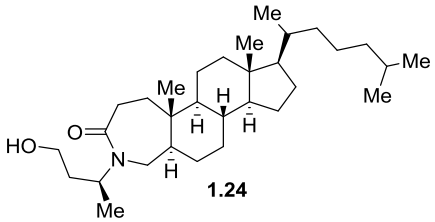

1.24

5α-Cholestane-derived A-Ring Lactam, 1.24. Following the general procedure A, (*S*)-3-azidobutanol (*S*)-**1.5** (28.5 mg, 0.248 mmol, 2.0 equiv) was reacted with 5α-cholestan-3-one **1.13** (48.6 mg, 0.126 mmol) to give **1.24** as a white amorphous (52.8 mg, 0.111 mmol, 88% yield). Purification was carried out by an automated MPLC system using a 12 g normal phase silica column with gradient elution from 0–5% MeOH/CH_2Cl_2. R_f = 0.37 (5% MeOH/CH_2Cl_2); mp 145–149 ˚C; IR (neat) 3338, 1620 cm^{-1}; ^1H NMR (400 MHz, $CDCl_3$) δ 4.78 (m, 1H), 3.51

(ddd, J = 12.1, 5.1, 2.5 Hz, 1H), 3.29–3.21 (m, 2H), 2.68 (t, J = 14.1 Hz, 1H), 2.50–2.40 (m, 2H, contains d, J = 2.48, 15.6 Hz, 1H), 1.98 (m, 1H), 1.91–1.77 (m, 2H), 1.74–1.44 (complex, 5H), 1.38–0.81 (complex, 35H), 0.70 (m, 1H), 0.64 (s, 3H); ^{13}C NMR (101 MHz, $CDCl_3$) δ 177.5, 58.6, 56.5, 56.3, 54.1, 49.9, 45.6, 44.4, 42.5. 40.0, 39.7, 38.4, 36.8, 36.3, 35.93, 35.92, 35.2, 32.5, 32.0, 28.4, 28.2, 27.6, 24.3, 24.0, 23.0, 22.7, 21.1, 18.9, 18.8, 12.3, 12.2. HRMS (FT-ICR, ESI) *m/z*: $[M + H]^+$ calcd for $C_{31}H_{56}NO_2$ 474.4306, found 474.4313.

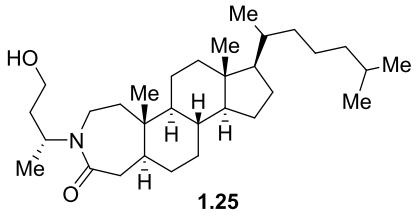

1.25

5α-Cholestane-derived A-Ring Lactam, A5. Following the general procedure A, (*R*)-3-azidobutanol (*R*)-**1.5** (29.5 mg, 0.256 mmol, 2.0 equiv) was reacted with 5α-cholestan-3-one **1.13** (48.9 mg, 0.126 mmol) to give **1.25** as a white amorphous solid (54.7 mg, 0.115 mmol, 92% yield). Purification was carried out by an automated MPLC system using a 12 g normal phase silica with gradient elution from 0–5% MeOH/CH_2Cl_2. R_f = 0.43 (5% MeOH/CH_2Cl_2); mp 142–146 ˚C; IR (neat) 3403, 1620 cm^{-1}; ^{1}H NMR (400 MHz, $CDCl_3$) δ 4.76 (m, 1H), 3.52 (ddd, J = 12.0, 5.0, 2.5 Hz, 1H), 3.30–3.20 (m, 2H), 2.98 (m, 1H), 2.82 (dd, J = 15.0, 10.8 Hz, 1H), 2.04 (d, J = 15.0 Hz, 1H), 1.97 (m, 1H), 1.87–1.77 (m, 2H), 1.73–1.64 (m, 2H), 1.59–0.85 (complex, 38H), 0.74–0.67 (m, 1H), 0.65 (s, 3H); ^{13}C NMR (101 MHz, $CDCl_3$) δ 177.7, 58.6, 56.5, 56.4, 54.4, 45.6, 43.8, 42.4, 42.0, 40.3, 40.1, 39.6, 38.5, 38.1, 36.6, 36.3, 35.9, 34.9, 32.1, 31.0, 28.4, 28.2, 24.3, 24.0, 23.0, 22.7, 21.4, 18.9, 18.8, 12.3, 12.2. HRMS (FT-ICR, ESI) *m/z*: $[M + H]^+$ calcd for $C_{31}H_{56}NO_2$ 474.4306, found 474.4309.

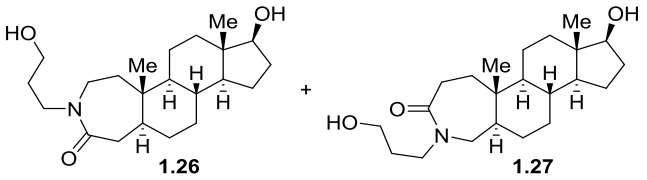

17β-Hydroxy-5α-androstane-derived A-Ring Lactams, 1.26 and 1.27. Following the general procedure A, 3-azidopropanol **1.1** (30.6 mg, 0.303 mmol, 2.0 equiv) was reacted with 5α-DHT **1.14** (43.6 mg, 0.150 mmol) to give a 40:60 mixture of regioisomers **1.26** and **1.27** as a white amorphous solid (51.6 mg, 0.142 mmol, 95% yield, UPLC/HRMS purity: ≥99.5%). Purification was carried out by an automated MPLC system using a 12 g normal phase silica column with gradient elution from 0–5% MeOH/CH_2Cl_2. R_f = 0.27 (5% MeOH/CH_2Cl_2); IR (neat) 3325, 1618, 1603 cm^{-1}; key ^1H NMR (400 MHz, $CDCl_3$) δ 2.91 (ddd, *J* = 15.6, 6.5, 1.8 Hz, 1H), 2.73 (dd, *J* = 14.2, 10.4 Hz, 1H), 2.59 (t, *J* = 13.0 Hz, 1H), 2.44 (d, *J* = 15.4 Hz, 1H), 2.29 (dd, *J* = 14.9, 6.9 Hz, 1H), 2.04–1.93 (m, 2H), 1.91–1.72 (m, 4H, contains d, *J* = 14.3 Hz, 1H); ^{13}C NMR (126 MHz, $CDCl_3$) δ 177.2, 177.1, 81.90, 81.86, 77.4, 77.2, 76.9, 58.11, 58.06, 54.4, 54.1, 52.0, 51.02, 51.01, 48.9, 45.3, 44.8, 44.5, 44.0, 42.9, 42.8, 41.1, 40.0, 38.6, 38.4, 36.8, 36.7, 36.0, 35.1, 34.9, 32.1, 31.6, 31.5, 30.9, 30.7, 30.6, 30.32, 30.29, 28.4, 23.4, 21.0, 20.7, 12.24, 12.19, 11.25, 11.23. **Note**: Missing carbon signals due to signal overlap of regioisomers. HRMS (FT-ICR, HESI) *m/z*: $[M + H]^+$ calcd for $C_{22}H_{38}NO_3$ 364.2846, found 364.2840.

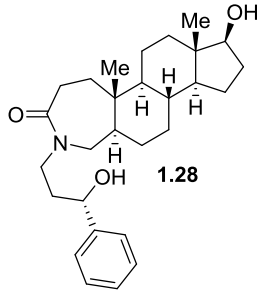

17β-Hydroxy-5α-androstane-derived A-Ring Lactam, 1.28. Following the general procedure A, (*S*)-3-azido-1-phenylpropanol (*S*)-**1.2** (44.3 mg, 0.250 mmol, 2.0 equiv) was reacted with 5α-DHT **1.14** (36.1 mg, 0.124 mmol) to give **1.28** as a cream-colored amorphous (48.1 mg, 0.109 mmol, 88% yield, UPLC/HRMS purity: ≥99.5%). Purification was carried out by an automated MPLC system using a 12 g normal phase silica column with gradient elution from 0–5% MeOH/CH_2Cl_2. R_f = 0.35 (5% MeOH/CH_2Cl_2); mp 155–157 ˚C; IR (neat) 3321, 1622 cm^{-1}; ^1H NMR (400 MHz, $CDCl_3$) δ 7.37–7.32 (m, 4H), 7.26 (m, 1H), 4.63 (dd, *J* = 9.8, 3.2 Hz, 1H), 4.09 (ddd, *J* = 14.6, 10.6, 4.3 Hz, 1H), 3.69 (m, 1H), 3.64 (t, *J* = 8.6 Hz, 1H), 3.11 (dt, *J* = 14.2, 4.5 Hz, 1H), 2.61–2.52 (m, 2H, contains d, 2.54, *J* = 15.6 Hz, 1H), 2.11–2.02 (m, 1H), 1.95–1.72 (complex, 5H), 1.68–1.55 (complex, 2H), 1.48–1.19 (complex, 9H), 1.06 (m, 1H), 0.98–0.84 (complex, 5H, contains s, 0.92, 3H), 0.75–0.68 (complex, 4H, contains s, 0.74, 3H); ^{13}C NMR (101 MHz, $CDCl_3$) δ 177.1, 144.3, 128.5 (2C), 127.2, 125.6 (2C), 81.9, 70.0, 54.4, 52.4, 51.1, 49.6, 45.9, 42.9, 38.5, 38.0, 36.7, 36.2, 35.2, 32.1, 31.8, 30.6, 28.4, 23.5, 20.7, 12.2, 11.3. HRMS (FT-ICR, HESI) *m/z*: $[M + H]^+$ calcd for $C_{28}H_{42}NO_3$ 440.3159, found 440.3167.

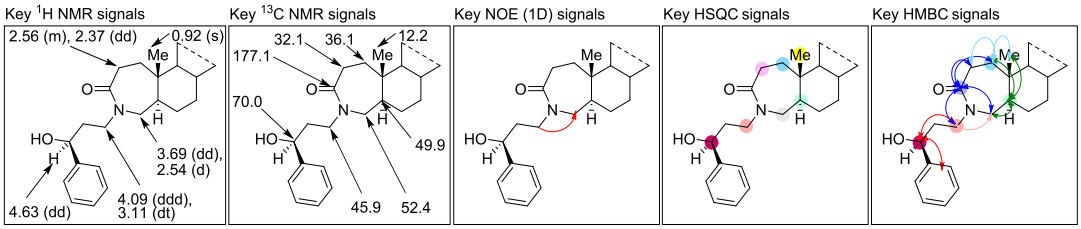

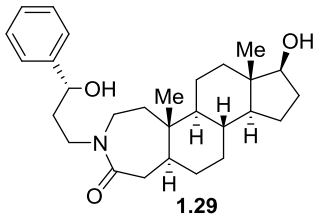

1.29

17β-Hydroxy-5α-androstane-derived A-Ring Lactam, 1.29. Following the general procedure A, (*R*)-3-azido-1-phenylpropanol (*R*)-**1.2** (44.1 mg, 0.250 mmol, 2.0 equiv) was reacted with 5α-DHT **1.14** (36.2 mg, 0.125 mmol) to give **1.29** as a cream-colored amorphous solid (46.0 mg, 0.105 mmol, 84% yield, UPLC/HRMS purity: 95.7%). Purification was carried out by an automated MPLC system using a 12 g normal phase silica column with gradient elution from 0–5% MeOH/CH_2Cl_2. R_f = 0.33 (5% MeOH/CH_2Cl_2); mp 155–157 ˚C; IR (neat) 3348, 1622 cm^{-1}; ^1H NMR (400 MHz, $CDCl_3$) δ 7.39–7.36 (m, 4H), 7.26 (m, 1H), 4.65 (dd, *J* = 9.9, 3.5 Hz, 1H), 4.06 (ddd, *J* = 14.6, 10.5, 4.4 Hz, 1H), 3.69–3.61 (m, 2H), 3.12 (dt, *J* = 14.5, 4.7 Hz, 1H), 3.02 (m, 1H), 2.72 (dd, *J* = 14.1, 10.3 Hz, 1H), 2.11–1.78 (complex, 6H, contains d, 1.98, *J* = 1.9 Hz, 1H), 1.70–1.65 (m, 1H), 1.62–1.54 (m, 2H), 1.51–1.15 (complex, 8H), 1.06 (m, 1H), 0.98–0.85 (complex, 5H, contains s, 0.90, 3H), 0.73–0.68 (complex, 4H, contains s, 0.73, 3H); ^{13}C NMR (126 MHz, $CDCl_3$) δ 177.1, 144.2, 128.4 (2C), 127.2, 125.7 (2C), 81.9, 70.0, 54.5, 51.0, 45.8, 45.7, 44.2, 42.8, 41.9, 40.0, 38.6, 37.8, 36.8, 34.9, 31.6, 30.9, 30.7, 23.4, 21.0, 12.1, 11.2. HRMS (FT-ICR, HESI) *m/z*: $[M + H]^+$ calcd for $C_{28}H_{42}NO_3$ 440.3159, found 440.3162.

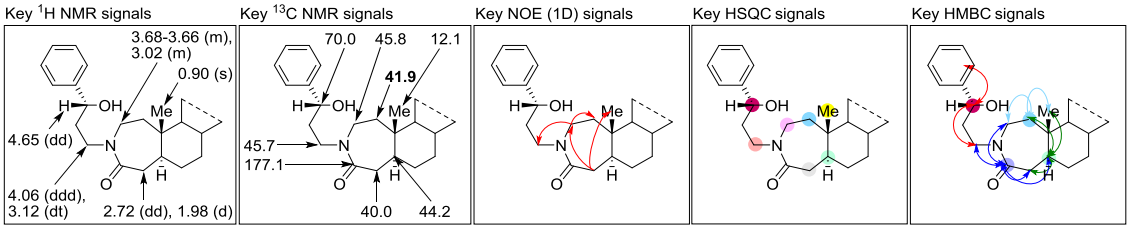

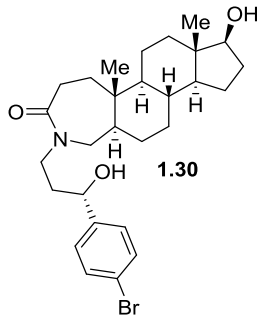

1.30

17β-Hydroxy-5α-androstane-derived A-Ring Lactam, 1.30. Following the general procedure A, (*S*)-3-azido-1-(4-bromophenyl)propanol (*S*)-**1.6** (65.8 mg, 0.257 mmol, 2.0 equiv) was reacted with 5α-DHT **1.14** (35.9 mg. 0.124 mmol) to give **1.30** as a white amorphous solid (54.9 mg, 0.106 mol, 86% yield, UPLC/HRMS purity: ≥99.5%). Purification was carried out by an automated MPLC system using a 12 g normal phase silica column with gradient elution from 0–2% MeOH/CH_2Cl_2. R_f = 0.38 (4% MeOH/CH_2Cl_2); mp 195–199 ˚C; IR (neat) 3334, 1615, 1598 cm^{-1}; ^1H NMR (400 MHz, $CDCl_3$) δ 7.47 (d, *J* = 8.4 Hz, 2H), 7.23 (d, *J* = 8.3 Hz, 2H), 4.58 (dd, *J* = 9.9, 3.1 Hz, 1H), 4.10 (dd, *J* = 14.6, 10.9, 3.9 Hz, 1H), 3.71 (m, 1H), 3.64 (t, *J* = 8.6 Hz, 1H), 3.08 (dt, *J* = 14.3, 4.4 Hz, 1H), 2.62–2.52 (m, 2H), 2.38 (m, 1H), 2.07 (m, 1H), 2.00–1.55 (complex, 6H), 1.49–1.20 (complex, 9H), 1.06 (m, 1H), 0.99–0.83 (m, 5H, contains s, 0.91, 3H), 0.74–0.67 (m, 4H, contains s, 0.74, 3H); ^{13}C NMR (101 MHz, $CDCl_3$) δ 177.2, 143.3, 131.5 (2C), 127.4 (2C), 120.9, 81.9, 69.4, 54.5, 52.5, 51.1, 49.8, 45.8, 42.9, 38.5, 38.0, 36.7, 36.2, 35.2, 32.1, 31.8, 30.6, 28.4, 23.5, 20.8, 12.2, 11.3. HRMS (FT-ICR, HESI) *m/z*: $[M + H]^+$ calcd for $C_{28}H_{41}NO_3$ 518.2264, found 518.2254.

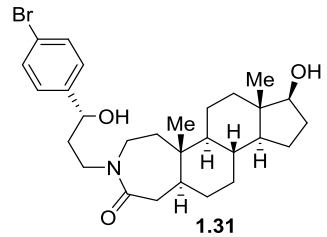

1.31

17β-Hydroxy-5α-androstane-derived A-Ring Lactam, 1.31. Following the general procedure A, (*R*)-3-azido-1-(4-bromophenyl)propanol (*R*)-**1.6** (64.1 mg, 0.250 mmol, 2.0 equiv) was reacted with 5α-DHT **1.14** (36.5 mg, 0.126 mmol) to give **1.31** as a white amorphous solid (53.9 mg, 0.104 mol, 83% yield, UPLC/HRMS purity: ≥99.5%). Purification was carried by an automated MPLC system using a 12 g normal phase silica column with gradient elution from 0–2% MeOH/CH_2Cl_2. R_f = 0.43 (4% MeOH/CH_2Cl_2); mp 213–217 ˚C; IR (neat) 3348, 1621 cm^{-1}; ^1H NMR (400 MHz, $CDCl_3$) δ 7.46 (m, 2H), 7.25 (m, 2H), 4.59 (dd, *J* = 10.0, 3.2, 1H), 4.06 (ddd, *J* = 14.6, 10.8, 4.0 Hz, 1H), 3.72–3.62 (m, 2H), 3.10 (dt, *J* = 14.2, 4.6 Hz, 1H), 3.02 (m, 1H), 2.73 (dd, *J* = 14.1, 10.4 Hz, 1H), 2.11–2.00 (m, 1H), 1.99 (d, *J* = 14.2 Hz, 1H), 1.94–1.55 (complex, 7H), 1.57–1.03 (complex, 9H), 0.98–0.83 (m, 5H, contains s, 0.93, 3H), 0.74–0.67 (m, 4H, contains s, 0.74, 3H); ^{13}C NMR (101 MHz, $CDCl_3$) δ 177.3, 143.3, 131.5 (2C), 127.5 (2C), 120.9, 81.9, 69.4, 54.6, 51.0, 46.0, 45.7, 44.2, 43.0, 41.9, 40.0, 38.6, 37.9, 36.8, 35.0, 31.6, 30.9, 30.7, 23.4, 21.0, 12.2, 11.2. HRMS (FT-ICR, HESI) *m/z*: $[M + H]^+$ calcd for $C_{28}H_{41}NO_3$ 518.2264, found 518.2319.

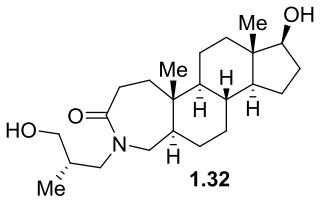

1.32

17β-Hydroxy-5α-androstane-derived A-Ring Lactam, 1.32. Following the general procedure A, (*S*)-3-azido-2-methylpropanol (*S*)-**1.3** (27.4 mg, 0.238 mmol, 2.0 equiv) 5α-DHT **1.14** (36.2 mg, 0.125 mmol) was reacted with to give **1.32** as an off-white amorphous solid (41.0 mg, 0.109 mol, 87% yield, UPLC/HRMS purity: ≥99.5%). Purification was carried out by an automated MPLC system using a 12 g normal phase silica column with gradient elution from 50–100% EtOAc/hexanes. R_f = 0.28 (4% MeOH/CH_2Cl_2); mp 196–200 ˚C; IR (neat) 3312, 1607

cm^{-1}; ^1H NMR (400 MHz, $CDCl_3$) δ 3.71 (dd, *J* = 14.0, 10.1, 1H), 3.65–3.58 (m, 2H), 3.43 (dd, *J* = 11.8, 3.1 Hz, 1H), 3.30 (dd, *J* = 11.8, 3.8 Hz, 1H), 2.86 (dd, *J* = 13.9, 4.4 Hz, 1H), 2.67 (t, *J* = 13.9 Hz, 1H), 2.50 (d, *J* = 15.3 Hz, 1H), 2.37 (dd, *J* = 14.8, 7.5 Hz, 1H), 2.05 (m, 1H), 1.88 (m, 1H), 1.81 (m, 1H), 1.75–1.18 (complex, 13H), 1.04 (m, 1H), 0.97 (d, *J* = 6.9 Hz, 3H), 0.85–0.86 (m, 4H, contains s, 0.91, 3H), 0.76–0.70 (m, 4H, contains s, 0.73, 3H); ^{13}C NMR (126 MHz, $CDCl_3$) δ 177.2, 81.9, 63.3, 54.2, 52.3, 51.1, 50.7, 48.4, 42.9, 38.5, 36.8, 35.9, 35.2, 34.3, 32.1, 31.5, 30.6, 28.5, 23.5, 20.7, 15.2, 12.4, 11.3. HRMS (FT-ICR, HESI) *m/z*: $[M + H]^+$ calcd for $C_{23}H_{40}NO_3$ 378.3003, found 378.2996.

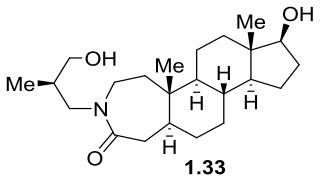

1.33

17β-Hydroxy-5α-androstane-derived A-Ring Lactam, 1.33. Following the general procedure A, (*R*)-3-azido-2-methylpropanol (*R*)-**1.3** (28.3 mg, 0.246 mmol, 2.0 equiv) was reacted with 5α-DHT **1.14** (36.4 mg, 0.125 mmol) to give **1.33** as a white crystalline solid (40.3 mg, 0.107 mol, 85% yield, UPLC/HRMS purity: ≥99.5%). Purification was carried by an automated MPLC system using a 12 g normal phase silica column with gradient elution from 0–6% MeOH/CH_2Cl_2. R_f = 0.47 (5% MeOH/CH_2Cl_2); mp 215–218 ˚C; IR (neat) 3354, 1617 cm^{-1}; ^1H NMR (400 MHz, $CDCl_3$) δ 3.71–3.65 (dd, *J* = 13.9, 10.1 Hz, 1H), 3.64–3.56 (m, 2H), 3.44 (dd, *J* = 11.8, 3.1 Hz, 1H), 3.31 (dd, *J* = 11.8, 3.8 Hz, 1H), 2.97 (m, 1H), 2.87–2.78 (m, 2H), 2.10–2.00 (m, 1H), 1.97 (d, *J* = 14.6 Hz, 1H), 1.83–1.18 (complex, 13H), 1.05 (m, 1H), 0.97 (d, *J* = 7.0 Hz, 3H), 0.94–0.82 (complex, 5H, contains s, 0.91, 3H), 0.77–0.70 (m, 4H, contains s, 0.73, 3H); ^{13}C NMR (151 MHz, $CDCl_3$) δ 177.3, 82.0, 63.3, 54.4, 51.1, 50.7, 45.6, 43.9, 42.9,

40.4, 40.0, 38.7, 36.9, 35.0, 34.3, 31.6, 30.9, 30.7, 23.5, 21.1, 15.3, 12.3, 11.2. HRMS (FT-ICR, HESI) *m/z*: $[M + H]^+$ for $C_{23}H_{40}NO_3$ 378.3003, found 378.2996.

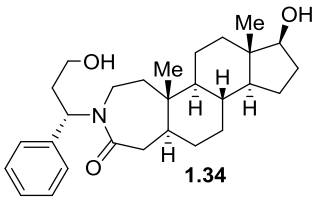

1.34

17β-Hydroxy-5α-androstane-derived A-Ring Lactam, 1.34. Following the general procedure A, (*S*)-3-azido-3-phenylpropanol (*S*)-**1.4** (44.1 mg, 0.249 mmol, 2.0 equiv) was reacted with 5α-DHT **1.14** (36.4 mg, 0.125 mmol) to give **1.34** as a cream-colored amorphous solid (48.6 mg, 0.111 mmol, 89% yield, UPLC/HRMS purity: ≥99.5%). Purification was carried out by an automated MPLC system using a 12 g normal phase silica column with gradient elution from 0–5% MeOH/CH_2Cl_2. R_f = 0.40 (5% MeOH/CH_2Cl_2); mp 197–202 ˚C; IR (neat) 3441, 3356, 1597 cm^{-1}; ^1H NMR (400 MHz, $CDCl_3$) δ 7.38–7.28 (m, 5H), 5.89 (dd, *J* = 12.4, 3.2 Hz, 1H), 3.72 (ddd, *J* = 12.1, 5.1, 2.5 Hz, 1H), 3.57 (t, *J* = 8.4 Hz, 1H), 3.40 (td, *J* = 11.7, 2.8 Hz, 1H), 3.20 (dd, *J* = 15.4, 11.7, 1H), 2.87–2.80 (m, 2H), 2.14–1.98 (m, 3H, contains d, 2.09, *J* = 14.8 Hz, 1H), 1.93 (m, 1H), 1.71–1.63 (m, 2H), 1.56–1.04 (complex, 10H), 0.97–0.80 (complex, 6H, contains s, 0.80, 3H), 0.67 (s, 3H), 0.49 (m, 1H), 0.40 (m, 1H); ^{13}C NMR (101 MHz, $CDCl_3$) δ 177.5, 139.1, 128.7 (2C), 128.6 (2C), 128.0, 81.9, 58.5, 54.3, 52.6, 50.9, 43.6, 42.8, 40.7, 40.4, 39.2, 38.3, 36.7, 34.9, 32.0, 31.6, 30.9, 30.7, 23.4, 20.8, 12.1, 11.1. HRMS (FT-ICR, HESI) *m/z*: $[M + H]^+$ calcd for $C_{28}H_{42}NO_3$ 440.3159, found 440.3164.

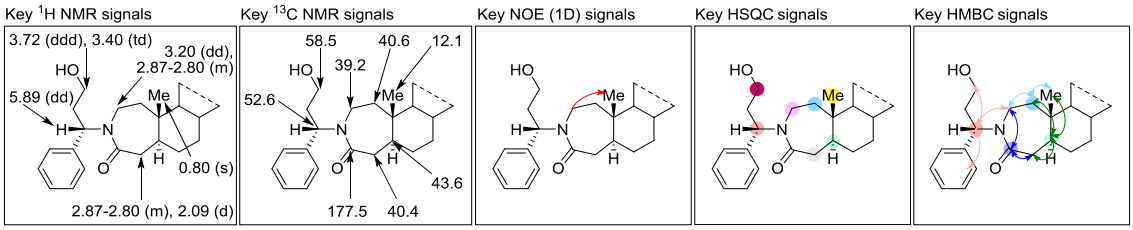

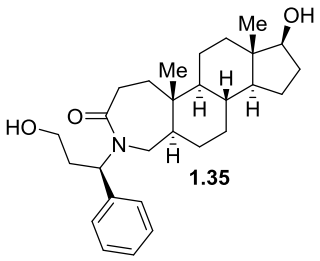

17β-Hydroxy-5α-androstane-derived A-Ring Lactam, 1.35. Following the general procedure A, (*R*)-3-azido-3-phenylpropanol (*R*)-**1.4** (44.4 mg, 0.251 mmol, 2.0 equiv) was reacted with 5α-DHT **1.14** (36.3 mg, 0.125 mmol) to give **1.35** as a cream-colored amorphous solid (49.5 mg, 0.113 mmol, 90% yield, UPLC/HRMS purity: ≥99.5%). Purification was carried by an automated MPLC system using a 12 g normal phase silica column with gradient elution from 0–4% MeOH/CH_2Cl_2. R_f = 0.40 (5% MeOH/CH_2Cl_2); mp 248–254 ˚C; IR (neat) 3344, 1613 cm^{-1}; ^1H NMR (400 MHz, $CDCl_3$) δ 7.37–7.28 (m, 5H), 5.92 (ddd, *J* = 12.0, 5.1, 2.5 Hz, 1H), 3.57 (t, *J* = 8.5 Hz, 1H), 3.42 (td, *J* = 11.7, 2.9 Hz, 1H), 3.19 (dd, *J* = 15.3, 9.0 Hz, 1H), 2.69 (m, 1H), 2.49 (m, 1H), 2.37 (d, *J* = 15.4 Hz, 1H), 2.12–1.84 (complex, 4H), 1.76 (m, 1H), 1.59–1.08 (complex, 8H), 1.03–0.74 (m, 7H, contains s, 0.78, 3H), 0.66 (s, 3H) 0.52–0.44 (m, 2H), 0.37–0.22 (m, 2H); ^{13}C NMR (101 MHz, $CDCl_3$) δ 177.2, 139.0, 129.0 (2C), 128.5 (2C), 128.1, 81.9, 58.5, 54.1, 52.8, 50.9, 48.8, 45.4, 42.8, 38.1, 36.7, 36.1, 35.1, 32.5, 32.2, 31.2, 30.6, 27.2, 23.4, 20.6, 12.1, 11.2. HRMS (FT-ICR, HESI) *m/z*: $[M + H]^+$ calcd for $C_{28}H_{42}NO_3$ 440.3159, found 440.3162.

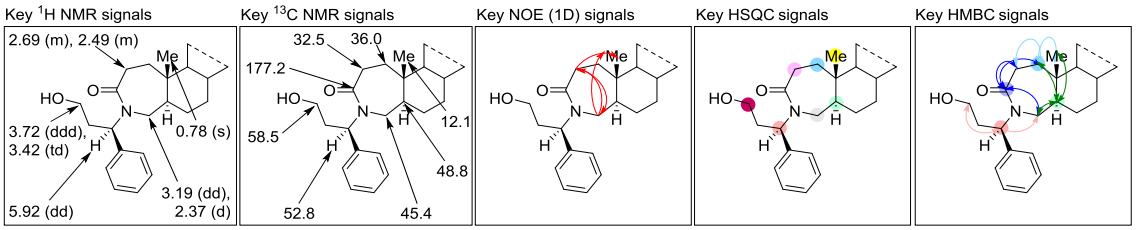

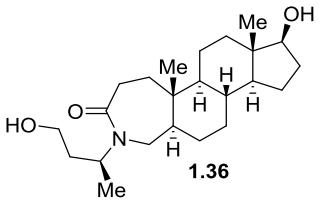

1.36

17β-Hydroxy-5α-androstane-derived A-Ring Lactam, 1.36. Following the general procedure A, (*S*)-3-azidobutanol (*S*)-**1.5** (29.5 mg, 0.256 mmol, 2.0 equiv) was reacted with 5α-DHT **1.14** (36.5 mg, 0.126 mmol) to give **1.36** as a white amorphous solid (40.3 mg, 0.107 mmol, 85% yield, UPLC/HRMS purity: 96.3%). Purification was carried out by an automated MPLC system using a 12 g normal phase silica column with gradient elution from 0–5% MeOH/CH_2Cl_2. R_f = 0.20 (80% EtOAc/hexanes); mp 217–219 ˚C; IR (neat) 3357, 1620 cm^{-1}; ^1H NMR (400 MHz, $CDCl_3$) δ 4.78 (m, 1H), 3.63 (t, *J* = 8.7 Hz, 1H), 3.51 (m, 1H), 3.29–3.22 (m, 2H), 2.69 (t, *J* = 14.2 Hz, 1H), 2.51–2.42 (m, 2 H, contains d, 2.49, *J* = 15.3 Hz, 1H), 2.49 (m, 1H), 1.89 (dd, *J* = 14.1, 7.5 Hz, 1H), 1.81 (dt, *J* = 12.3, 3.4 Hz, 1H), 1.75–1.53 (m, 4H), 1.48–1.12 (complex, 13H, contains d, 1.17, *J* = 8.1 Hz, 3H), 1.04 (m, 1H), 0.97–0.84 (m, 5H, contains s, 0.91, 3H), 0.75–0.68 (m, 4H, contains s, 0.73, 3H); ^{13}C NMR (101 MHz, $CDCl_3$) δ 177.4, 81.9, 58.6, 54.2, 51.1, 50.0, 45.6, 44.4, 42.9, 38.5, 36.7, 36.0, 35.5, 32.5, 31.6, 30.6, 27.5, 23.5, 20.7, 18.9, 12.3, 11.3. **Note**: Missing one carbon signal due to signal overlap. HRMS (FT-ICR, HESI) *m/z*: $[M + H]^+$ calcd for $C_{23}H_{40}NO_3$ 378.3003, found 378.2989.

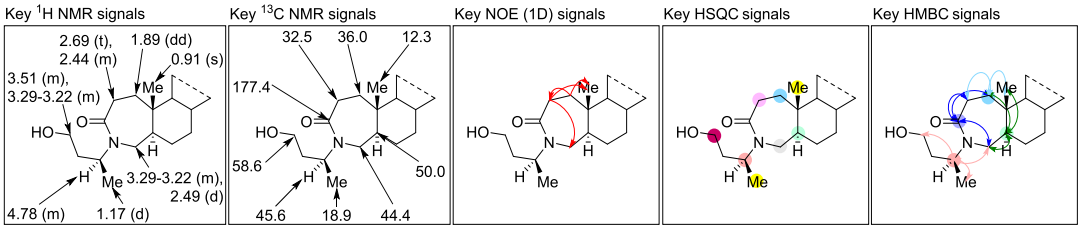

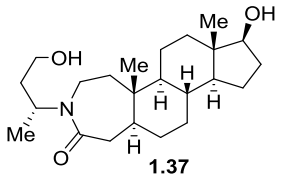

1.37

17β-Hydroxy-5α-androstane-derived A-Ring Lactam, 1.37. Following the general procedure A, (*R*)-3-azidobutanol (*R*)-**1.2** (27.9 mg, 0.242 mmol, 2.0 equiv) was reacted with 5α-DHT **1.14** (36.0 mg, 0.124 mmol) to give **1.37** as a white amorphous solid (39.7 mg, 0.105 mmol, 85% yield, UPLC/HRMS purity: 98.9%). Purification was carried out by an automated MPLC system using a 12 g normal phase silica column with gradient elution from 0–5% MeOH/CH_2Cl_2. R_f = 0.40 (5% MeOH/CH_2Cl_2); mp 179–184 ˚C; IR (neat) 3408, 3330, 1607 cm^{-1}; ^1H NMR (400 MHz, $CDCl_3$) δ 4.74 (m, 1H), 3.62 (t, *J* = 8.6 Hz, 1H), 3.52 (ddd, *J* = 12.0, 5.0, 2.5 Hz, 1H), 3.29–3.20 (m, 2H), 2.98 (m, 1H), 2.83 (dd, *J* = 15.0, 10.8 Hz, 1H), 2.10–2.01 (m, 2H, contains d, *J* = 15.0 Hz, 1H), 1.88–1.78 (m, 2H), 1.70–1.04 (complex, 17H, contains d, 1.18, *J* = 6.9 Hz, 1H), 0.96–0.83 (complex, 6H, contains s, 0.90, 3H), 0.75–0.68 (complex, 5H, contains s, 0.73, 3H); ^{13}C NMR (101 MHz, $CDCl_3$) δ 177.5, 81.9, 58.5, 54.5, 51.1, 45.5, 43.8, 42.9, 42.1, 40.4, 38.6, 38.0, 36.8, 36.6, 35.0, 31.7, 30.9, 30.7, 23.5, 21.0, 18.9, 12.3, 11.2. HRMS (FT-ICR, HESI) *m/z*: $[M + H]^+$ calcd for $C_{23}H_{40}NO_3$ 378.3003, found 378.2984.

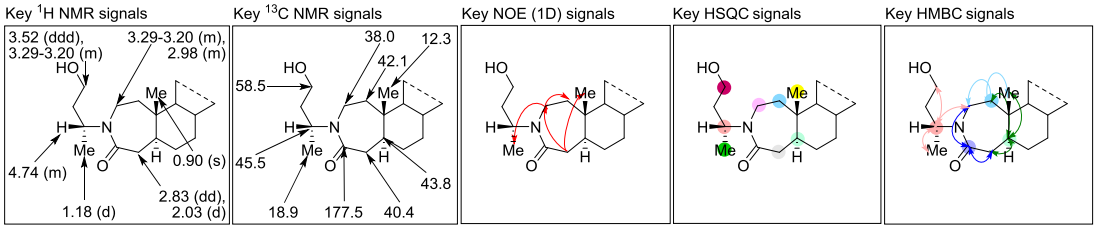

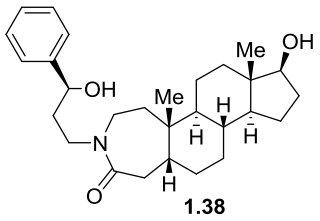

1.38

17β-Hydroxy-5β-androstane-derived A-Ring Lactam, 1.38. Following the general procedure A, (*S*)-3-azido-1-phenylpropanol (*S*)-**1.2** (105 mg, 0.593 mmol, 2.0 equiv) was reacted with 5β-DHT **1.15** (87.6 mg, 0.302 mmol) to give **1.38** a white amorphous solid (117 mg, 0.267 mmol, 89% yield, UPLC/HRMS purity: 97.6%). Purification was carried out by an automated MPLC system using a 12 g normal phase silica column with gradient elution from 0–2% MeOH/CH_2Cl_2. R_f = 0.35 (4% MeOH/CH_2Cl_2); mp 79–101 ˚C; IR (neat) 3374, 1616 cm^{-1}; ^1H NMR (400 MHz, $CDCl_3$) δ 7.38–7.30 (m, 4H), 7.25–7.22 (m, 1H), 4.63 (dd, *J* = 9.8, 3.2 Hz, 1H), 4.04 (ddd, *J* = 14.5, 10.5, 4.2 Hz, 1H), 3.66 (t, *J* = 8.5 Hz, 1H), 3.53 (dd, *J* = 15.4, 10.5 Hz, 1H), 3.15 (dt, *J* = 14.1, 4.7 Hz, 1H), 3.08–2.97 (m, 2H), 2.13–2.03 (m, 2H, contains d, *J* = 14.4 Hz, 1H), 1.99-1.75 (complex, 5H), 1.60 (m, 1H), 1.48–1.21 (complex, 10H), 1.15–1.01 (m, 5H, contains s, 1.01, 3H), 0.95–0.83 (m, 1H), 0.75 (s, 3H); ^{13}C NMR (151 MHz, $CDCl_3$) δ 176.8, 144.3, 128.5 (2C), 127.2, 125.7 (2C), 82.0, 70.2, 51.1, 45.9, 44.5, 43.2, 42.2, 41.0, 40.0, 39.3, 37.6, 37.1, 37.0, 36.0, 30.8, 29.9, 25.7, 24.2, 23.5, 21.0, 11.3. HRMS (FT-ICR, HESI) *m/z*: $[M + H]^+$ calcd for $C_{28}H_{42}NO_3$ 440.3159, found 440.3148.

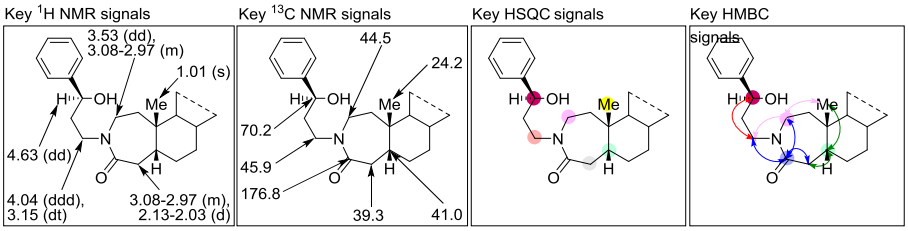

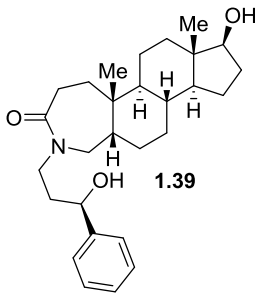

17β-Hydroxy-5β-androstane-derived A-Ring Lactam, 1.39. Following the general procedure A, (*R*)-3-azido-1-phenylpropanol (*R*)-**1.2** (44.3 mg, 0.250 mmol, 2.0 equiv) was reacted with 5β-DHT **1.15** (36.6 mg, 0.126 mmol) to give **1.39** as a white amorphous solid (45.9 mg, 0.104 mmol, 83% yield, UPLC/HRMS purity: ≥99.5%). Purification was carried out by an automated MPLC system using a 12 g normal phase silica column with gradient elution from 0–3.5% MeOH/CH_2Cl_2. R_f = 0.44 (5% MeOH/CH_2Cl_2); mp 79–101 ˚C; IR (neat) 3367, 1626 cm^{-1}; ^1H NMR (400 MHz, $CDCl_3$) δ 7.36–7.32 (m, 4H), 7.27–7.23 (m, 1H), 4.63 (dd, *J* = 9.6, 3.4 Hz, 1H), 4.10–4.01 (m, 2H), 3.66 (t, *J* = 8.5 Hz, 1H), 3.14 (dt, *J* = 14.1, 4.7 Hz, 1H), 2.74 (d, *J* = 15.4 Hz, 1H), 2.56 (dd, *J* = 15.0, 11.8 Hz, 1H), 2.29 (m, 1H), 2.07 (m, 1H), 1.95–1.79 (complex, 5H), 1.62–1.21 (complex, 11H), 1.18–1.09 (m, 1H), 1.06–0.99 (m, 4H, contains s, 1.02, 3H), 0.91–0.75 (m, 5H, contains s, 0.75, 3H); ^{13}C NMR (151 MHz, $CDCl_3$) δ177.2, 144.2, 128.5 (2C), 127.3, 125.7 (2C), 81.9, 70.3, 52.4, 51.0, 45.9, 45.6, 43.2, 37.9, 37.1, 37.0, 36.0, 34.4, 30.7, 28.8, 26.6, 24.3, 23.5, 20.7, 11.3. **Note**: Missing two carbon signals due to signal overlap. HRMS (FT-ICR, HESI) *m/z*: $[M + H]^+$ calcd for $C_{28}H_{42}NO_3$ 440.3159, found 440.3136.

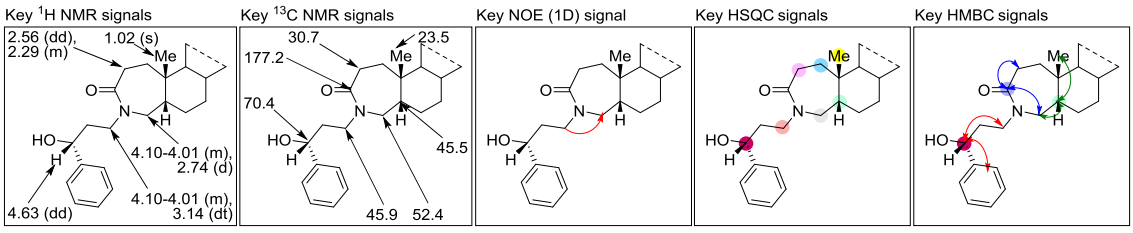

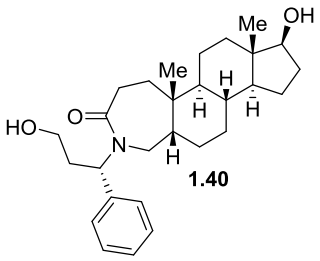

17β-Hydroxy-5β-androstane-derived A-Ring Lactam, 1.40. Following the general procedure A, (*S*)-3-azido-3-phenylpropanol (*S*)-**1.4** (44.0 mg, 0.248 mmol, 2.0 equiv) was reacted with 5β-DHT **1.15** (36.6 mg, 0.126 mmol) to give **1.40** as a white amorphous solid (48.1 mg, 0.109 mmol, 87% yield, UPLC/HRMS purity: 98.8%). Purification was carried out by an automated MPLC system using a 12 g normal phase silica column with gradient elution from 0–5% MeOH/CH_2Cl_2. R_f = 0.38 (5% MeOH/CH_2Cl_2); mp 223–227 ˚C; IR (neat) 3355, 1633 cm^{-1}; ^1H NMR (400 MHz, $CDCl_3$) δ 7.36–7.27 (m, 5H), 5.87 (dd, *J* = 12.2, 3.3 Hz, 1H), 3.73 (ddd, *J* = 12.1, 5.0, 2.6 Hz, 1H), 3.64–3.56 (m, 2H), 3.42 (td, *J* = 11.6, 2.9 Hz, 1H), 2.67 (dd, *J* = 15.3, 12.3 Hz, 1H), 2.57 (d, *J* = 15.2 Hz, 1H), 2.36 (dd, *J* = 15.4, 8.2 Hz, 1H), 2.11–1.79 (complex, 5H), 1.54–0.94 (complex, 13H), 0.79 (s, 3H), 0.69–0.53 (m, 5H, contains s, 0.69, 3H); ^{13}C NMR (151 MHz, $CDCl_3$) δ 177.5, 138.8, 128.6 (2C), 128.4 (2C), 127.9, 81.7, 58.2, 52.7, 50.8, 44.9, 44.4, 43.0, 41.1, 36.7, 35.6, 34.1, 31.8, 30.7, 30.4, 27.4, 26.2, 24.2, 23.2, 20.3, 11.0. **Note**: Missing one carbon signal due to signal overlap. HRMS (FT-ICR, HESI) *m/z*: $[M + H]^+$ calcd for $C_{28}H_{42}NO_3$ 440.3159, found 440.3178.

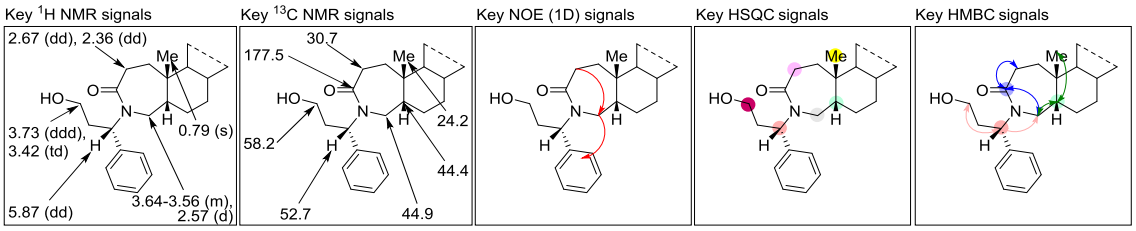

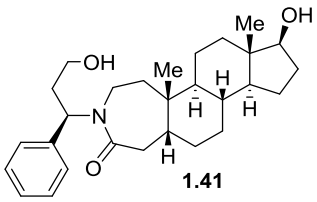

1.41

17β-Hydroxy-5β-androstane-derived A-Ring Lactam, 1.41. Following the general procedure A, (*R*)-3-azido-3-phenylpropanol (*R*)-**1.4** (43.8 mg, 0.247 mmol, 2.0 equiv) was reacted with 5β-DHT **1.15** (36.1 mg, 0.124 mmol) to give **1.41** as a white amorphous solid (49.1 mg, 0.112 mmol, 90% yield, UPLC/HRMS purity: 97.7%). Purification was carried out by an automated MPLC system using a 12 g normal phase silica column with gradient elution from 0–5% MeOH/CH_2Cl_2. R_f = 0.38 (5% MeOH/CH_2Cl_2); IR (neat) 3369, 1615 cm^{-1}; mp decomposed; ^1H NMR (400 MHz, $CDCl_3$) δ 7.37–7.26 (m, 5H), 5.97 (dd, *J* = 12.4, 3.3 Hz, 1H), 3.72 (ddd, *J* = 12.0, 5.1, 2.6 Hz, 1H), 3.63 (t, *J* = 8.5 Hz, 1H), 3.44 (td, *J* = 11.6, 2.9 Hz, 1H), 3.17 (dd, *J* = 15.5, 11.9 Hz, 1H), 3.03 (dd, *J* = 15.2, 8.0 Hz, 1H), 2.45 (br s, 1H), 2.27 (d, *J* = 15.4 Hz, 1H), 2.18–2.01 (m, 2H), 1.97–1.75 (m, 4H), 1.61–1.53 (m, 1H), 1.49–0.97 (complex, 12H), 0.94–0.77 (m, 5H, contains s, 0.82, 3H), 0.69 (s, 3H); ^{13}C NMR (151 MHz, $CDCl_3$) δ 176.7, 138.9, 128.7, 128.5, 127.9, 81.9, 58.6, 52.8, 51.0, 43.1, 42.7, 40.2, 39.6, 38.9, 38.2, 36.9, 36.7, 35.9, 31.9, 30.7, 29.7, 25.6, 23.4, 20.9, 11.3. **Note**: Missing one carbon signal due to signal overlap. HRMS (FT-ICR, HESI) *m/z*: $[M + H]^+$ for $C_{28}H_{42}NO_3$ 440.3159, found 440.3180.

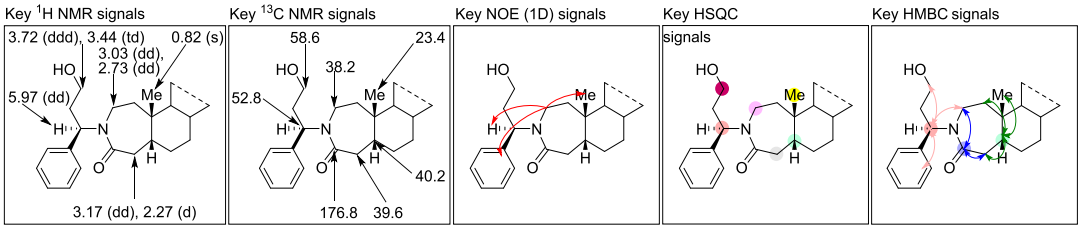

Experimental section for 1.3.3

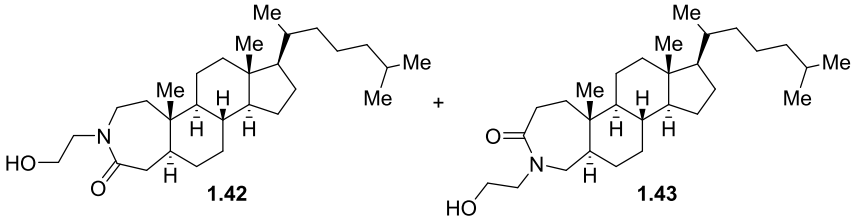

5α-Cholestane-derived A-Ring Lactams, 1.42 and 1.43. Following the general procedure A, 2-azidoethanol **1.7** (26.6 mg, 0.306 mmol, 2.0 equiv) was reacted with 5α-cholestan-3-one **1.13** (58.4 mg, 0.151 mmol) to give a 37:63 mixture of regioisomer **1.42** and **1.43** as a white amorphous solid (63.8 mg, 0.143 mmol, 95% yield). Purification was carried out by an automated MPLC system using a 4 g normal phase column with gradient elution from 0–5% MeOH/CH_2Cl_2. R_f = 0.30 (5% MeOH/CH_2Cl_2); IR (neat) 3391, 1623 cm^{-1}; key ^1H NMR (400 MHz, $CDCl_3$) δ 3.04 (ddd, *J* = 15.6, 6.4, 1.7 Hz, 1H), 2.79 (dd, *J* = 14.3, 10.8 Hz, 1H), 2.65 (t, *J* = 13.2 Hz, 1H), 2.58 (d, *J* = 15.5 Hz, 1H), 2.34 (ddd, *J* = 14.6, 7.7, 1.3 Hz, 1H); ^{13}C NMR (101 MHz, $CDCl_3$) δ 177.34, 177.26, 61.9, 56.5, 56.3, 54.1, 53.9, 53.1, 52.0, 51.8, 48.7, 46.6, 43.7, 42.40, 42.37, 41.0, 40.2, 40.02, 40.00, 39.6, 38.4, 38.2, 36.2, 35.9, 35.8, 35.1, 34.8, 32.3, 32.1, 31.9, 31.0, 28.4, 28.3, 28.1, 24.2, 23.9, 22.9, 22.6, 21.3, 21.1, 18.7, 12.2, 12.12, 12.09. **Note**: Missing carbon signals due to signal overlap of regioisomers. HRMS (FT-ICR, ESI) *m/z*: $[M + Na]^+$ calcd for $C_{29}H_{51}NNaO_2$ 468.3812, found 468.3824.

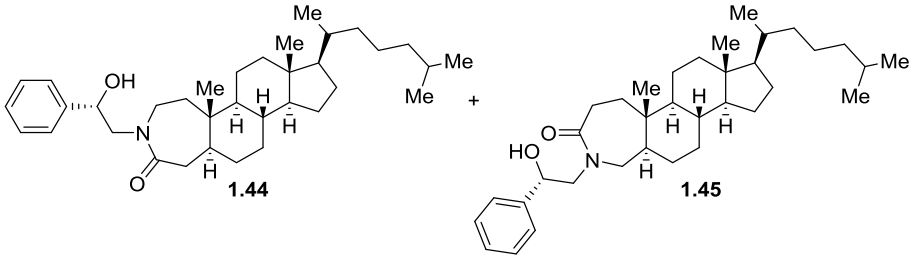

5α-Cholestane-derived A-Ring Lactams, 1.44 and 1.45. Following the general procedure A, (*S*)-2-azido-1-phenylethanol (*S*)-**1.8** (41.0 mg, 0.251 mmol, 2.0 equiv) was reacted with 5α-cholestan-3-one **1.13** (48.3 mg, 0.125 mmol) to give a 46:54 mixture of regioisomer **1.44** and **1.45** as a white amorphous solid (60.4 mg, 0.116 mmol, 93% yield). Purification was carried out by an automated MPLC system using a 12 g normal phase column with gradient elution from 0–5% MeOH/CH_2Cl_2. R_f = 0.47 (4% MeOH/CH_2Cl_2); IR (neat) 3303, 1615 cm^{-1}; key ^1H NMR (400 MHz, $CDCl_3$) δ 7.40–7.32 (m, 8H), 7.30–7.26 (m, 2H), 5.10 (d, *J* = 4.8 Hz, 1H), 4.99–4.93 (m, 2H), 4.55 (d, *J* = 4.3 Hz, 1H), 3.78–3.71 (m, 2H), 3.68–3.55 (m, 3H), 3.45 (dd, *J* = 15.8, 11.8 Hz, 1H), 2.80–2.68 (m, 2H), 2.61 (t, *J* = 13.8 Hz, 1H), 2.38–2.34 (m, 1H), 2.31 (d, *J* = 14.9 Hz, 1H), 1.98–1.94 (m, 3H); ^{13}C NMR (101 MHz, $CDCl_3$) δ 178.8, 178.5, 142.7, 142.6, 128.6 (2C), 128.5 (2C), 127.62, 127.60, 126.0 (2C), 125.9 (2C), 74.5, 74.2, 59.8, 58.4, 56.6, 56.5, 56.4, 54.8, 54.1, 53.8, 47.9, 47.6, 43.6, 42.5, 42.4, 40.9, 40.10, 40.07, 40.03, 39.7, 38.4, 38.0, 36.3, 35.91, 35.90, 35.6, 35.0, 34.9, 32.2, 32.1, 31.6, 31.0, 28.34, 28.31, 28.1, 24.3, 23.96, 23.95, 23.0, 22.7, 21.3, 21.1, 18.8, 12.15, 12.13. **Note**: Missing one carbon signal due to signal overlap. HRMS (FT-ICR, ESI) *m/z*: $[M + H]^+$ calcd for $C_{35}H_{56}NO_2$ 522.4306, found 522.4306.

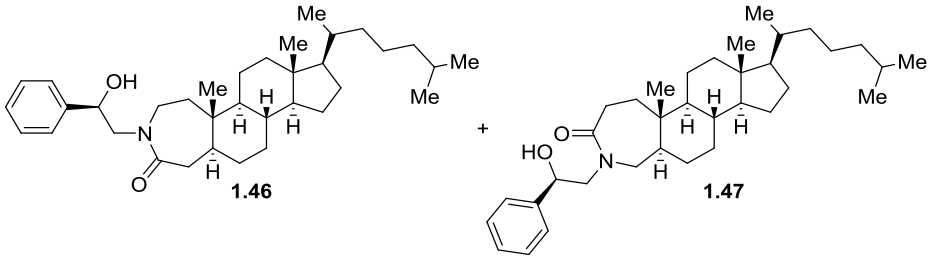

5α-Cholestane-derived A-Ring Lactams, 1.46 and 1.47. Following the general procedure A, (*R*)-2-azido-1-phenylethanol (*R*)-**1.5** (41.0 mg, 0.251 mmol, 2.0 equiv) was reacted with 5α-cholestan-3-one **1.13** (49.0 mg, 0.127 mmol) to give a 33:67 mixture of regioisomer **1.46** and **1.47** as a white amorphous solid (58.1 mg, 0.111 mmol, 88% yield). Purification was carried

out by an automated MPLC system using a 12 g normal phase column with gradient elution from 0–5% MeOH/CH_2Cl_2. The mixture of isomers was separated by using a 12 g normal phase column with 0–50% EtOAc/hexanes to give **1.47** as a white amorphous solid (32.2 mg, 0.0617 mmol, 49% yield) as the major regioisomer and **1.46** as a white amorphous solid (17.0 mg, 0.0326 mmol, 26% yield) as the minor regioisomer. **1.47**: R_f = 0.25 (50% EtOAc/hexanes); mp 210–213 ˚C; IR (neat) 3346, 1611 cm^{-1}; ^1H NMR (400 MHz, $CDCl_3$) δ 7.39–7.33 (m, 4H), 7.31–7.25 (m, 1H), 4.93 (m, 1H), 4.32 (d, *J* = 4.3 Hz, 1H), 3.64 (m, 2H), 3.54 (m, 1H), 2.62 (t, *J* = 13.4 Hz, 1H), 2.39–2.29 (m, 2H, contains d, 2.31, *J* = 15.7 Hz, 1H), 1.96 (m, 1H), 1.89–1.77 (m, 2H), 1.69–1.62 (m, 2H), 1.58–1.46 (m, 3H), 1.38–0.91 (complex, 17H), 0.90–0.83 (complex, 12H, contains d, 0.89, *J* = 6.5 Hz, 3H; d, 0.87, *J* = 1.9 Hz, 3H; d, 0.85, *J* = 1.9 Hz, 3H; s, 0.83, 3H), 0.71–0.65 (m, 1H), 0.63 (s, 3H); ^{13}C NMR (101 MHz, $CDCl_3$) δ 178.3, 142.5, 128.6 (2C), 127.3, 126.0 (2C), 74.3, 58.8, 56.5, 56.4, 54.5, 53.9, 48.6, 42.5, 40.0, 39.7, 38.2, 36.3, 35.9, 35.7, 35.1, 32.2, 31.8, 28.6, 28.3, 28.2, 24.3, 24.0, 23.0, 22.7, 21.1, 18.8, 12.2. **Note**: Missing one carbon signal due to signal overlap. HRMS (FT-ICR, ESI) *m/z*: $[M + H]^+$ calcd for $C_{35}H_{56}NO_2$ 522.4306, found 522.4310. **1.46**: R_f = 0.36 (50% EtOAc/hexanes); mp 162–165 ˚C; IR (neat) 3358, 1621 cm^{-1}; ^1H NMR (400 MHz, $CDCl_3$) δ 7.40–7.33 (m, 4H), 7.28–7.24 (m, 1H), 4.92 (m, 1H), 4.83 (m, 1H), 3.73–3.62 (m, 2H), 3.55 (dd, *J* = 14.3, 2.6 Hz, 1H), 2.85 (m, 1H), 2.76 (m, 1H), 1.97–1.92 (m, 2H, contains d, 1.94, *J* = 14.6 Hz, 1H), 1.86–1.77 (m, 1H), 1.65 (m, 1H), 1.56–0.93 (complex, 21H), 0.89–0.82 (complex, 12H, contains d, 0.89, *J* = 6.4 Hz, 3H; d, 0.87, *J* = 2.0 Hz, 3H; d, 0.85, *J* = 2.0 Hz, 3H; 0.82, s, 3H) 0.72–0.66 (m, 1H), 0.62 (s, 3H), 0.61–0.54 (m, 1H); ^{13}C NMR (101 MHz, $CDCl_3$) δ 178.6, 142.7, 128.6 (2C), 127.6, 126.0 (2C), 74.2, 59.2, 56.6, 56.4, 54.1, 48.0, 43.4, 42.4, 40.1, 39.9, 39.7, 38.3, 36.3, 35.9, 34.8, 32.1, 31.0, 29.8, 28.4,

28.1, 24.3, 24.0, 22.9, 22.7, 21.3 18.8, 12.19, 12.12. HRMS (FT-ICR, ESI) *m/z*: $[M + H]^+$ calcd for $C_{35}H_{56}NO_2$ 522.4306, found 522.4308.

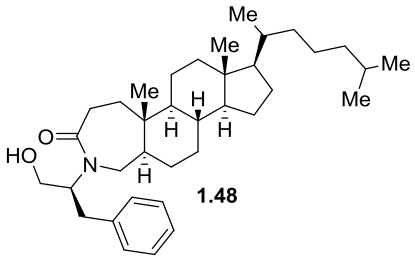

5α-Cholestane-derived A-Ring Lactam, 1.48. Following the general procedure A, (*S*)-2-azido-3-phenylpropanol (*S*)-**1.9** (53.4 mg, 0.301 mmol, 2.0 equiv) was reacted with 5α-cholestan-3-one **1.13** (58.1 mg, 0.150 mmol) to give **1.48** as a white amorphous solid (65.1 mg, 0.121 mmol, 81% yield) as the major regioisomers, in addition an uncharacterized, impure minor product was obtained (10.0 mg, 0.019 mmol, 12% yield). Purification was carried out by an automated MPLC system using a 12 g normal phase column with gradient elution from 0–5% MeOH/CH_2Cl_2. R_f = 0.23 (2% MeOH/CH_2Cl_2); mp 203–204 ˚C; IR (neat) 3415, 1618 cm^{-1}; ^1H NMR (400 MHz, $CDCl_3$) δ 7.31–7.26 (m, 2H), 7.24–7.20 (m, 3H), 4.64 (br s, 1H), 3.74 (dd, *J* = 11.6, 3.6 Hz, 1H), 3.64 (dd, *J* = 11.6, 7.7 Hz, 1H), 3.34 (dd, *J* = 15.6, 9.2 Hz, 1H), 2.89 (m, 2H), 2.61 (t, *J* = 13.8 Hz, 1H), 2.44 (d, *J* = 15.6 Hz, 1H), 2.33 (dd, *J* = 15.0, 7.2 Hz, 1H), 1.93 (m, 1H), 1.85–1.74 (m, 4H), 1.37–0.94 (complex, 20H), 0.91–0.81 (complex, 9H, contains s, 0.89, 3H; d, 0.87, *J* = 2.1 Hz, 3H; d, 0.85, *J* = 1.9 Hz, 3H), 0.79 (s, 3H), 0.74–0.67 (m, 1H), 0.61 (s, 3H), 0.42 (m, 1H); ^{13}C NMR (126 MHz, $CDCl_3$) δ 177.6, 138.2, 128.8 (2C), 128.6 (2C), 126.6, 64.1, 56.4, 56.3, 53.8, 48.4, 42.4, 39.9, 39.6, 37.9, 36.2, 35.9, 35.7, 35.03, 34.99, 33.0, 31.7, 28.3, 28.2, 28.1, 24.2, 23.9, 23.0, 21.0, 18.7, 12.13, 12.12. **Note**: Missing three carbon signals due to signal overlap. X-ray crystal structure of this analog is provided in the CCDC (CCDC 1583535). HRMS (FT-ICR, HESI) *m/z*: $[M + H]^+$ calcd for $C_{36}H_{58}NO_2$ 536.4462, found 536.4489.

Table 1.8. Selected crystallographic and refinement parameters for **1.48**.

compound	**1.48**
CCDC deposition number	1583535
empirical formula	$C_{36}H_{57}NO_2$
formula weight	535.82
temperature	100(2) K
wavelength	1.54178 Å
crystal system	orthorhombic
space group	P 21 21 21
unit cell dimensions	a = 7.1041(9) Å, α = 90°
	b = 8.9377(11) Å, β = 90°
	c = 50.231(6) Å, γ = 90°
Z	4
volume	3189.4(7) $Å^3$
density	1.116 Mg/m^3
absorption coefficient	0.509 μ mm^{-1}
F(000)	1184
crystal size	0.200 × 0.120 × 0.020 mm^3
Theta range for data collection	3.519 to 67.727°
index ranges	-8<=h<=8, -10<=k<=6, -56<=l<=57
reflections collected	14336
independent reflections	5254 [R(int) = 0.0413]
completeness to theta = 66.000°	96.1%
absorption correction	multi-scan
max. and min. transmission	1.000 and 0.762
refinement method	full-matrix least-squares on F^2
data/restraints/parameters	5254/0/580
Goodness-of-fit F^2	1.124
final R indices [I>2sigma(I)]	R1 = 0.0512, wR2 = 0.1349
R indices (all data)	R1 = 0.0543, wR2 = 0.1368
absolute structure parameter	-0.09(18)
largest diff. peak and hole	0.169 and -0.246 $e.Å^{-3}$

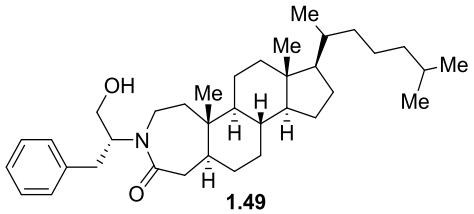

1.49

5α-Cholestane-derived A-Ring Lactam, 1.49. Following the general procedure A, (*R*)-2-azido-3-phenylpropanol (*R*)-**1.9** (53.5 mg, 0.302 mmol, 2.0 equiv) was reacted with 5α-cholestan-3-one **1.13** (57.9 mg, 0.150 mmol) to give **1.49** as a white amorphous solid (52.4 mg,

0.0978 mmol, 65% yield) as the major regioisomers; an uncharacterized, impure minor product was also obtained in this case (17.8 mg, 0.033 mmol, 22% yield). Purification was carried out by an automated MPLC system using a 12 g normal phase column with gradient elution from 0–100% EtOAc/Ether. The major isomer was subjected to a second purification using a 4 g normal phase column with gradient elution from 0–5% MeOH/CH_2Cl_2. R_f = 0.29 (25% EtOAc/Ether); mp 191–194 ˚C; IR (neat) 3415, 1620 cm^{-1}; ^1H NMR (400 MHz, $CDCl_3$) δ 7.31–7.26 (m, 2H), 7.23–7.18 (m, 3H), 4.38 (br s, 1H), 3.71 (m, 2H), 3.31 (dd, *J* = 15.7, 11.7 Hz, 1H), 2.99–2.73 (m, 3H), 2.75 (m, 1H), 1.95–1.89 (m, 2H, contains d, 1.91, *J* = 14.3 Hz, 1H), 1.80 (m, 1H), 1.65–1.46 (m, 4H), 1.42–0.93 (complex, 19H), 0.89–0.83 (complex, 11H, contains d, 0.88, *J* = 6.4 Hz, 3H; 0.86, d, *J* = 2.0 Hz, 3H; 0.85, d, *J* = 2.0 Hz, 3H), 0.79 (s, 3H), 0.61 (s, 3H), 0.50 (m, 1H); ^{13}C NMR (126 MHz, $CDCl_3$) δ 177.7, 138.5, 129.1 (2C), 128.6 (2C), 126.5, 64.0, 56.4, 56.3, 54.2, 43.6, 42.4, 41.2, 40.9, 40.0, 39.6, 38.2, 36.2, 35.9, 35.0, 34.8, 32.1, 31.0, 28.3, 28.1, 24.2, 23.9, 22.9, 22.7, 21.3, 18.7, 12.2, 12.1. **Note**: Missing two carbon signals due to signal overlap. X-ray crystal structure of this analog is provided in the CCDC (CCDC 1583534). HRMS (FT-ICR, ESI) *m/z*: $[M + H]^+$ calcd for $C_{36}H_{58}NO_2$ 536.4462, found 536.4471.

Table 1.9. Selected crystallographic and refinement parameters for **1.49**.

compound	**1.49**
CCDC deposition number	1583534
empirical formula	$C_{36}H_{57}NO_2$
formula weight	535.82
temperature	100(2) K
Wavelength Å	1.54178
crystal system	orthorhombic
space group	P 21 21 21
unit cell dimensions	a = 6.9681(10) Å, α = 90°
	b = 8.9956(12) Å, β = 90°
	c = 50.221(7) Å, γ = 90°
Z	4
volume	3148.0(7) $Å^3$
density	1.131 Mg/m^3

absorption coefficient	0.515 μ mm^{-1}
F(000)	1184
crystal size	0.450 × 0.180 × 0.020 mm^3
Theta range for data collection	3.520 to 67.956°
index ranges	-8<=h<=8, -10<=k<=7, -58<=l<=58
reflections collected	20015
independent reflections	5136 [R(int) = 0.0435]
completeness to theta = 66.000°	96.1%
absorption correction	multi-scan
max. and min. transmission	1.000 and 0.836
refinement method	full-matrix least-squares on F^2
data/restraints/parameters	5136/0/578
Goodness-of-fit F^2	1.235
final R indices [I>2sigma(I)]	R1 = 0.0491, wR2 = 0.1160
R indices (all data)	R1 = 0.0535, wR2 = 0.1180
absolute structure parameter	-0.03(9)
largest diff. peak and hole	0.184 and -0.196 e.Å^{-3}

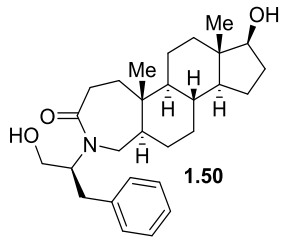

1.50

17β-Hydroxy-5α-androstane-derived A-Ring Lactam, 1.50. Following the general procedure A, (*S*)-2-azido-3-phenylpropanol (*S*)-**1.9** (45.8 mg, 0.458 mmol, 2.0 equiv) was reacted with 5α-DHT **1.14** (36.5 mg, 0.126 mmol) to give **1.50** as a white amorphous solid (42.0 mg, 0.096 mmol, 76% yield, LCMS purity: 96.0%) containing a slight impurity of minor regioisomer. Purification was carried out by an automated MPLC system using a 12 g normal phase silica column with gradient elution from 0–4% MeOH/CH_2Cl_2. R_f = 0.28 (4% MeOH/CH_2Cl_2); mp 157–159 ˚C; IR (neat) 3390, 1621 cm^{-1}; ^{1}H NMR (400 MHz, $CDCl_3$) δ 7.32–7.27 (m, 2H), 7.24–7.19 (m, 2H), 4.68 (br s, 1H), 3.74 (dd, *J* = 11.6, 3.6 Hz, 1H), 3.67–3.58 (m, 2H), 3.39 (dd, *J* = 15.6, 9.3 Hz, 1H), 2.992.82 (m, 2H), 2.66 (t, *J* = 13.9 Hz, 1H), 2.49–2.39 (m, 2H), 2.26 (m, 2H), 2.09–1.99 (m, 1H), 1.82–1.74 (m, 2H), 1.64–1.50 (m, 3H), 1.46–

1.36 (m, 1H), 1.32–0.95 (complex, 7H), 0.89–0.76 (m, 4H, contains s, 0.81, 3H), 0.76–0.65 (m, 4H, contains s, 0.69, 3H), 0.42 (m, 1H); ^{13}C NMR (151 MHz, $CDCl_3$) δ 178.0, 138.0, 128.8, 128.7, 126.7, 81.9, 64.1, 54.0, 51.0, 48.4, 42.9, 38.1, 36.7, 35.7, 35.0, 34.9, 32.6, 31.3, 30.6, 28.1, 23.4, 20.6, 12.2, 11.2. **Note**: Missing carbon two carbon signals due to signal overlap. HRMS (FT-ICR, HESI) *m/z*: $[M + H]^+$ calcd for $C_{28}H_{42}NO_3$ 440.3159, found 440.3154.

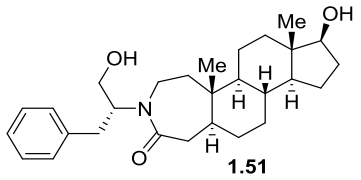

1.51

17β-Hydroxy-5α-androstane-derived A-Ring Lactam, 1.51. Following the general procedure A, (*R*)-2-azido-3-phenylpropanol (*R*)-**1.9** (44.7 mg, 0.252 mmol, 2.0 equiv) was reacted with 5α-DHT **1.14** (35.9 mg, 0.124 mmol) to give **1.51** as a white amorphous solid (35.1 mg, 0.080 mmol, 65% yield, LCMS purity: 97.3%). Purification was carried out by an automated MPLC system using a 12 g normal phase silica column with gradient elution from 0–4% MeOH/CH_2Cl_2 over 50 min. R_f = 0.32 (4% MeOH/CH_2Cl_2); IR (neat) 3375, 1619 cm^{-1}; mp 172–174 ˚C; ^{1}H NMR (400 MHz, $CDCl_3$) δ 7.32–7.26 (m, 2H), 7.24–7.19 (m, 3H), 3.78–3.68 (m, 2H), 3.61 (t, *J* = 8.5 Hz, 1H), 3.34 (dd, *J* = 15.9, 11.8 Hz, 1H), 3.02–2.85 (m, 3H), 2.81–2.75 (m, 1H), 2.09–1.99 (m, 4H), 1.77 (dt, *J* = 12.5, 3.4 Hz, 1H), 1.68–1.52 (m, 3H), 1.48–1.14 (complex, 7H), 1.02–0.79 (complex, 7H, contains s, 0.82, 3H), 0.70 (s, 3H), 0.53 (m, 1H); ^{13}C NMR (101 MHz, $CDCl_3$) δ 177.8, 138.5, 129.1 (2C), 128.7 (2C), 126.6, 81.9, 64.3, 54.4, 51.0, 43.7, 42.8, 41.3, 40.8, 38.4, 36.8, 35.0, 34.9, 31.6, 30.8, 30.7, 23.4, 20.9, 12.2, 11.2. **Note**: Missing two carbon signals due to signal overlap. HRMS (FT-ICR, HESI) *m/z*: $[M + H]^+$ calcd for $C_{28}H_{42}NO_3$ 440.3159, found 440.3151.

Experimental section for 1.3.4

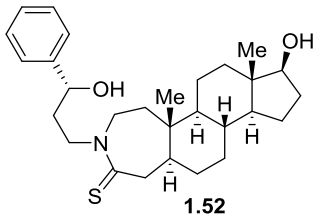

1.52

17β-Hydroxy-5α-androstane-derived A-Ring Thioamide, 1.52. Following the general procedure B, (*R*)-3-azido-1-phenylpropanol (*R*)-**1.2** (72.1 mg, 0.407 mmol, 2.0 equiv) was reacted with 5α-DHT **1.14** (58.3 mg, 0.201 mmol) to give **1.52** as an off-white solid (77.3 mg, 0.170 mmol, 85% yield, UPLC/HRMS purity: 98.9%). Purification was carried out by an automated MPLC system using a 12 g normal phase silica column with gradient elution from 0–45% EtOAc/hexanes. R_f = 0.38 (50% EtOAc/hexanes); mp 236–239 ˚C; IR (neat) 3331, 1529 cm^{-1}; ^1H NMR (400 MHz, $CDCl_3$) δ 7.39–7.33 (m, 4H), 7.29–7.27 (m, 1H), 4.73 (m, 1H), 4.68 (m, 1H), 3.91 (dd, *J* = 15.3, 11.9 Hz, 1H), 3.75 (m, 2H), 3.63 (t, *J* = 8.6 Hz, 1H), 3.36 (m, 1H), 3.10 (dd, *J* = 14.1, 9.7 Hz, 1H), 2.79 (d, *J* = 14.1 Hz, 1H), 2.21–1.78 (m, 3H), 1.88 (dd, *J* = 14.5, 6.4 Hz, 1H), 1.81 (dt, *J* = 12.4, 3.4 Hz, 1H), 1.69 (m, 1H), 1.63–1.17 (complex, 10 H), 1.05 (m, 1H), 0.99 (m, 4H, contains s, 0.91, 3H), 0.74–0.67 (m, 4H, contains s, 0.73, 3H); ^{13}C NMR (151 MHz, $CDCl_3$) δ 206.2, 143.9, 128.6 (2C), 127.6, 125.7 (2C), 81.9, 70.4, 54.6, 54.0, 51.0, 50.0, 49.8, 45.6, 42.9, 40.6, 38.4, 36.9, 36.8, 34.9, 31.6, 30.7, 23.4, 21.0, 12.6, 11.2. **Note**: Missing one carbon signal due to signal overlap. HRMS (FT-ICR, HESI) *m/z*: $[M + H]^+$ calcd for $C_{28}H_{42}NO_2S$ $[M + H]^+$ 456.2931, found 456.2921.

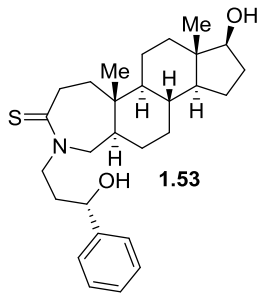

1.53

17β-Hydroxy-5α-androstane-derived A-Ring Thioamide, 1.53. Following the general procedure B, (*S*)-3-azido-1-phenylpropanol (*S*)-**1.2** (71.2 mg, 0.402 mmol, 2.0 equiv) was reacted with 5α-DHT **1.14** (58.6 mg, 0.202 mmol) to give **1.53** as a white amorphous solid (41.2 mg, 0.090 mmol, 45% yield, UPLC/HRMS purity: 97.6%). Purification was carried out by an automated MPLC system using a using 12 g normal phase silica column with gradient elution from 0–40% EtOAc/hexanes. R_f = 0.42 (50% EtOAc/hexanes); mp 229–233 ˚C; IR (neat) 3428, 3302, 1520 cm^{-}1; ^{1}H NMR (400 MHz, $CDCl_3$) δ 7.36 (m, 4H), 7.28 (m, 1H), 4.80 (ddd, *J* = 13.4, 10.1, 4.9 Hz, 1H), 4.73 (m, 1H), 3.96 (m, 2H), 3.70–3.62 (m, 2H), 3.21 (dd, *J* = 14.2, 7.1 Hz, 1H), 2.97 (t, *J* = 13.3 Hz, 1H), 2.88 (d, *J* = 15.1 Hz, 1H), 2.11–2.02 (m, 4H), 1.84–1.72 (m, 2H), 1.66–1.55 (m, 2H), 1.50–1.19 (complex, 7H), 1.05 (m, 1H), 0.97–0.84 (m, 5H, contains s, 0.92, 3H), 0.76–0.69 (m, 4H, contains s, 0.74, 3H); ^{13}C NMR (151 MHz, $CDCl_3$) δ 206.2, 143.9, 128.6 (2C), 127.4, 125.5 (2C), 81.8, 70.1, 56.1, 54.4, 54.1, 51.0, 48.3, 42.9, 42.2, 38.2, 37.4, 37.3, 36.6, 35.1, 31.6, 30.6, 28.2, 23.4, 20.6, 12.6, 11.3. HRMS (FT-ICR, HESI) *m/z*: $[M + H]^+$ calcd for $C_{28}H_{42}NO_2S$ 456.2931, found 456.2921.

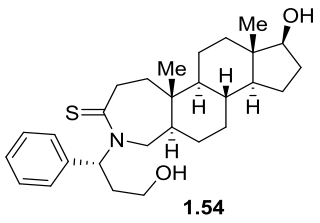

1.54

17β-Hydroxy-5α-androstane-derived A-Ring Thioamide, 1.54. Following the general procedure B, (*R*)-3-azido-3-phenylpropanol (*R*)-**1.4** (73.4 mg, 0.414 mmol, 2.0 equiv) was reacted with 5α-DHT **1.14** (58.9 mg, 0.203 mmol) to give **1.54** as a pale yellow amorphous solid (54.5 mg, 0.120 mmol, 59% yield, UPLC/HRMS purity: ≥99.5%). Purification was carried out using 12 g silica column with gradient elution from 0–50% EtOAc/hexanes. R_f = 0.34 (50% EtOAc/hexanes); IR (neat) 3410, 3310, 1495, 1451 cm^{-1}; mp 243–245 ˚C; ^1H NMR (400 MHz, $CDCl_3$) δ 7.43–7.31 (m, 5H), 7.14 (dd, J = 12.0, 3.2 Hz, 1H), 3.74 (m, 1H), 3.60–3.45 (m, 3H), 3.36 (dd, J = 14.8, 7.8 Hz, 1H), 3.01 (m, 1H), 2.72 (dd, J = 14.9 Hz, 1H), 2.18 (m, 1H), 2.11–1.96 (m, 2H), 1.88 (m, 1H), 1.75 (dt, J = 12.3, 3.4 Hz, 1H), 1.56–1.07 (complex, 9H), 1.00–0.73 (complex, 6H, contains s, 0.78, 3H), 0.63 (s, 3H), 0.40 (m, 3H), 0.18 (m, 1H); ^{13}C NMR (151 MHz, $CDCl_3$) δ 206.4, 138.1, 128.8 (2C), 128.7, 128.6 (2C), 81.9, 61.1, 58.1, 54.2, 50.8, 49.6, 47.9, 42.8, 42.3, 37.8, 37.2, 36.6, 35.0, 32.5, 31.1, 30.5, 27.1, 23.3, 20.5, 12.4, 11.2. HRMS (FT-ICR, HESI) *m/z*: $[M + H]^+$ calcd for $C_{28}H_{42}NO_2S$ 456.2931, found 456.2920.

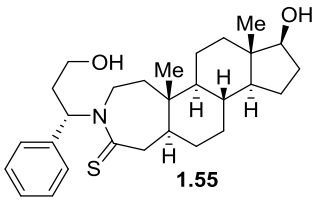

1.55

17β-Hydroxy-5α-androstane-derived A-Ring Thioamide, 1.55. Following the general procedure B, (*S*)-3-azido-3-phenylpropanol (*S*)-**1.4** (74.0 mg, 0.418 mmol, 2.1 equiv) was reacted with 5α-DHT **1.14** (58.8 mg, 0.202 mmol) to give **1.55** as an off-white amorphous solid (73.6 mg, 0.162 mmol, 80% yield, UPLC/HRMS purity: 90.3%). Purification was carried out by an automated MPLC system using a using 12 g normal phase silica column with gradient elution from 0–50% EtOAc/hexanes. R_f = 0.32 (50% EtOAc/hexanes); mp 249–251 ˚C; IR (neat) 3338, 1488, 1454 cm^{-1}; ^1H NMR (400 MHz, $CDCl_3$) δ 7.41–7.31 (m, 5H), 7.12 (dd, *J* = 12.0, 3.3 Hz,

1H), 3.79–3.71 (m, 1H), 3.57 (m, 1H), 3.52–3.44 (m, 3H), 3.25–3.12 (m, 2H), 2.96 (d, J = 14.6 Hz, 1H), 2.24–2.16 (m, 1H), 2.12–1.99 (m, 2H), 1.69–1.63 (m, 2H), 1.60–1.52 (m, 2H), 1.44–1.02 (complex, 9H), 0.96–0.81 (m, 3H), 0.81 (s, 3H), 0.66 (s, 3H), 0.41 (m, 1H), 0.21 (m, 1H); ^{13}C NMR (151 MHz, $CDCl_3$) δ 207.0, 138.0, 128.9 (2C), 128.6, 128.3 (2C), 81.9, 61.0, 58.1, 54.2, 50.8, 49.9, 44.9, 43.7, 42.8, 39.7, 38.0, 36.6, 34.8, 32.3, 31.5, 30.8, 30.7, 23.4, 20.7, 12.5, 11.1. HRMS (FT-ICR, HESI) *m/z*: $[M + H]^+$ calcd for $C_{28}H_{42}NO_2S$ $[M + H]^+$ 456.2931, found 456.2929.

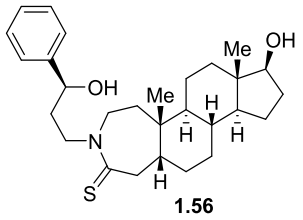

1.56

17β-Hydroxy-5β-androstane-derived A-Ring Thioamide, 1.56. Following the general procedure B, (*S*)-3-azido-1-phenylpropanol (*S*)-**1.2** (73.5 mg, 0.415 mmol, 2.1 equiv) was reacted with 5β-DHT **1.15** (58.9 mg, 0.203 mmol) to give **1.56** as a pale yellow foam solid (57.7 mg, 0.127 mmol, 62% yield, UPLC/HRMS purity: 98.0%). Purification was carried out using 12 g silica column with gradient elution from 0–50% EtOAc/hexanes. R_f = 0.33 (50% EtOAc/hexanes); IR (neat) 3425, 3312, 1495, 1451 cm^{-1}; ^{1}H NMR (400 MHz, $CDCl_3$) δ 7.38–7.32 (m, 4H), 7.29–7.25 (m, 1H), 4.75–4.64 (m, 2H), 3.85 (m, 2H), 3.74 (m, 1H), 3.65 (m, 1H), 3.46 (dd, J = 13.8, 11.2 Hz, 1H), 3.26 (dd, J= 15.2, 7.0 Hz, 1H), 2.92 (d, J = 13.8 Hz, 1H), 2.16–1.89 (complex, 4H), 1.85 (m, 1H), 1.77 (m, 1H), 1.64–1.02 (complex, 11H), 1.00 (s, 3H), 0.86 (m, 2H), 0.75 (s, 3H); ^{13}C NMR (151 MHz, $CDCl_3$) δ 206.2, 143.9, 128.6 (2C), 127.5, 125.7 (2C), 82.0, 70.3, 53.9, 51.1, 49.2, 48.6, 43.2, 42.8, 41.6 (br), 38.4, 37.1, 37.0, 36.9, 35.9, 30.8, 30.2, 25.7, 24.8 (br), 23.5, 21.0, 11.3. **Note**: Two broad carbon signals were consistently

observed amongst *cis*-AB analogs. HRMS (FT-ICR, HESI) *m/z*: $[M + H]^+$ calcd for $C_{28}H_{42}NO_2S$ 456.2931, found 456.2920.

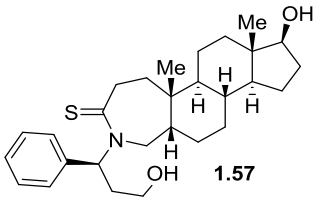

1.57

17β-Hydroxy-5β-androstane-derived A-Ring Thioamide, 1.57. Following the general procedure B, (*S*)-3-azido-3-phenylpropanol (*S*)-**1.4** (72.0 mg, 0.406 mmol, 2.0 equiv) was reacted with 5β-DHT **1.15** (58.2 mg, 0.200 mmol) to give **1.57** as a pale-yellow amorphous solid (71.6 mg, 0.156 mmol, 78% yield, UPLC/HRMS purity: ≥99.5%). Purification was carried out using 12 g silica column with gradient elution from 0–40% EtOAc/hexanes. R_f = 0.28 (50% EtOAc/hexanes); mp 226 ˚C (decomposed); IR (neat) 3366, 1501, 1446 cm^{-1}; ^1H NMR (400 MHz, $CDCl_3$) δ 7.41–7.31 (m, 5H), 7.08 (dd, *J* = 10.7, 4.4 Hz, 1H), 3.85 (dd, *J* = 14.8, 10.2 Hz, 1H), 3.74 (m, 1H), 3.61 (m, 2H), 3.50 (m, 1H), 3.21 (dd, *J* = 15.1, 8.3 Hz, 1H), 2.98 (dd, *J* = 15.0, 11.8 Hz, 1H), 2.92 (d, *J* = 14.8 Hz, 1H), 2.21–1.99 (m, 3H), 1.93 (dd, *J* = 15.1, 8.4 Hz, 1H), 1.03 (m, 1H), 1.55–0.83 (complex, 11H), 0.74 (s, 3H), 0.72–0.57 (m, 2H), 0.69 (s, 3H), 0.39 (m, 1H); ^{13}C NMR (151 MHz, $CDCl_3$) δ 207.0, 138.2, 128.8 (2C), 128.7, 128.4 (2C), 81.9, 61.2, 58.3, 51.0, 49.5, 44.0, 43.2, 41.5, 40.9, 36.9, 36.6, 35.8, 34.9, 32.4, 30.6, 27.5, 26.3, 24.4, 23.4, 20.6, 11.2. **Note**: Two broad carbon signals were consistently observed amongst *cis*-AB analogs. HRMS (FT-ICR, HESI) *m/z*: $[M + H]^+$ calcd for $C_{28}H_{42}NO_2S$ $[M + H]^+$ 456.2931, found 456.2924.

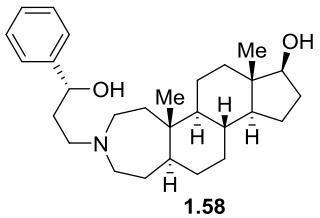

1.58

17β-Hydroxy-5α-androstane-derived A-Ring Amine, 1.58. Method 1: Following the general procedure B, (*R*)-3-azido-1-phenylpropanol (*R*)-**1.2** (72.7 mg, 0.410 mmol, 2.0 equiv) was reacted with 5α-DHT **1.14** (58.0 mg, 0.200 mmol) to give **1.58** as pale yellow sticky solid (73.6 mg, 0.173 mmol, 87% yield, UPLC/HRMS purity: ≥99.5%). Purification was carried out by an automated MPLC system using a 12 g normal phase silica column using MeOH/CH_2Cl_2. R_f = 0.15 (4% MeOH/CH_2Cl_2). HRMS (FT-ICR, HESI) *m/z*: $[M + H]^+$ calcd for $C_{28}H_{44}NO_2$ $[M + H]^+$ 426.3367, found 426.3356. Method 2: **1.29** (110.0 mg, 0.250 mmol) was added to a stirring suspension of LAH (1M THF, 0.500 mL, 0.500 mmol, 2.0 equiv) in anhydrous THF (14 mL) at 0 ˚C. The reaction mixture was allowed to room temperature, stirred for 4 h and then refluxed for 24 h. The reaction mixture was allowed to room temperature and quenched with a saturated aqueous solution of sodium potassium tartarate (5 mL). The biphasic mixture was stirred overnight. The biphasic mixture was diluted CH_2Cl_2 (50 mL). The organic layer was washed with aqueous solution of sodium potassium tartarate (2 × 5 mL), brine (5 mL), dried over Na_2SO_4, filtered, and concentrated. Purification was carried out by an automated MPLC system using a 12 g normal phase silica column using MeOH/CH_2Cl_2 to give **1.58** as white foam solid (53.9 mg, 0.127 mmol, 51% yield, UPLC/HRMS purity: ≥99.5%). mp decomposed; IR (neat) 3357, 2918, 2846, 1449 cm^{-1}; ^1H NMR (400 MHz, $CDCl_3$) δ 7.36 (m, 4H), 7.23 (m, 1H), 4.99 (dd, *J* = 7.9, 3.2 Hz, 1H), 3.61 (t, *J* = 8.6 Hz, 1H), 2.91 (m, 1H), 2.76 (m, 3H), 2.56 (m, 2H), 2.05 (m, 1H), 1.90 (m, 1H) 1.79 (m, 2H), 1.66–1.51 (complex, 4H), 1.03 (m, 1H), 0.90 (m, 2H), 0.83 (s, 3H), 0.76–0.73 (complex, 4H, contains s, 0.73, 3H); ^{13}C NMR (151 MHz, $CDCl_3$) δ 145.2,

128.3 (2C), 127.0, 125.7 (2C), 82.1, 75.5, 58.3, 54.7, 54.0, 51.3, 50.7, 46.2, 42.9, 38.5, 37.0, 35.3, 34.1, 31.7, 31.0, 30.7, 29.9, 23.6, 21.5, 13.3, 11.3. **Note**: Missing one carbon signal due to signal overlap. HRMS (FT-ICR, HESI) *m/z*: $[M + H]^+$ calcd for $C_{28}H_{44}NO_2$ $[M + H]^+$ 426.3367, found 426.3357.

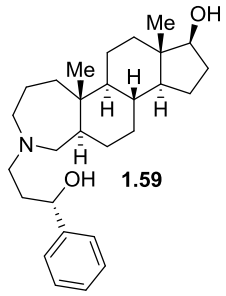

17β-Hydroxy-5α-androstane-derived A-Ring Amine, 1.59. Method 1: Following the general procedure B, (*S*)-3-azido-1-phenylpropanol (*S*)-**1.2** (71.1 mg, 0.401 mmol, 2.0 equiv) was reacted with 5α-DHT **1.14** (58.9 mg, 0.203 mmol) to give **1.59** as pale yellow sticky solid (43.1 mg, 0.101 mmol, 50% yield, UPLC/HRMS purity: ≥99.5%). Purification was carried out by an automated MPLC system using a 12 g normal phase silica column using MeOH/CH_2Cl_2. R_f = 0.15 (4% MeOH/CH_2Cl_2). HRMS (FT-ICR, HESI) *m/z*: $[M + H]^+$ calcd for $C_{28}H_{44}NO_2$ $[M + H]^+$ 426.3367, found 426.3357. Method 2: **1.28** (97.0 mg, 0.221 mmol) was added to a stirring suspension of LAH (1M THF, 0.43 mL, 0.430 mmol, 2.0 equiv) in anhydrous THF (10 mL) at 0 ˚C. The reaction mixture was allowed to room temperature, stirred for 4 h and then refluxed for 24 h. The reaction mixture was allowed to room temperature and quenched with a saturated aqueous solution of sodium potassium tartarate (5 mL). The biphasic mixture was stirred overnight. The biphasic mixture was diluted CH_2Cl_2 (50 mL). The organic layer was washed with aqueous solution of sodium potassium tartarate (2 × 5 mL), brine (5 mL), dried over Na_2SO_4, filtered, and concentrated. Purification was carried out by an automated MPLC system using a 12 g normal phase silica column using MeOH/CH_2Cl_2 to give **1.59** as white foam solid

(54.7 mg, 0.129 mmol, 58% yield, UPLC/HRMS purity: ≥99.5%). mp decomposed; IR (neat) 3337, 2920, 2848, 1448 cm^{-1}; ^1H NMR (400 MHz, $CDCl_3$) δ 7.36 (m, 4H), 7.23 (m, 1H), 4.95 (dd, *J* = 6.9, 4.7 Hz, 1H), 3.63 (t, *J* = 8.5 Hz, 1H), 2.86–2.61 (complex, 5H), 2.35 (d, *J* = 13.6 Hz, 1H), 2.05 (m, 1H), 1.83–1.18 (complex, 17H), 1.04 (m, 1H), 0.98–0.82 (complex, 5H, contains s, 0.82, 3H), 0.76–0.67 (complex, 4H, contains s, 0.73, 3H); ^{13}C NMR (101 MHz, $CDCl_3$) δ 145.4, 128.3 (2C), 126.9, 125.7 (2C), 82.1, 75.7, 58.3, 57.5, 55.3, 53.5, 51.3, 45.7, 43.0, 40.0, 38.3, 37.1, 35.4, 34.6, 31.7, 30.8, 28.9, 23.5, 22.0, 21.4, 14.0, 11.3. HRMS (FT-ICR, HESI) *m/z*: $[M + H]^+$ calcd for $C_{28}H_{44}NO_2$ $[M + H]^+$ 426.3367, found 426.3356.

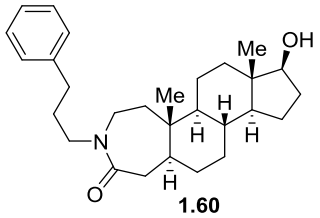

1.60

17β-Hydroxy-5α-androstane-derived A-Ring Lactam 1.60. Following the general procedure B, (*R*)-3-azido-1-phenylpropanol (*R*)-**1.2** (70.5 mg, 0.398 mmol, 1.9 equiv) was reacted with 5α-DHT **1.14** (60.0 mg, 0.207 mmol) to give **1.60** as white foam solid (80.9 mg, 0.191 mmol, 92% yield, UPLC/HRMS purity: ≥99.5%). Purification was carried out by an automated MPLC system using a 12 g normal phase silica column with gradient elution from 0–3% MeOH/CH_2Cl_2. R_f = 0.38 (4% MeOH/CH_2Cl_2); mp decomposed; IR (neat) 3214, 1626 cm^{-1}; ^1H NMR (400 MHz, $CDCl_3$) δ 7.29 (m, 2H), 7.18 (m, 3H), 3.59 (m, 2H), 3.48–3.31 (m, 2H), 2.95 (dd, *J* = 15.5, 6.3 Hz, 1H), 2.74 (dd, *J* = 14.3, 10.1 Hz, 1H), 2.62 (td, *J* = 7.4, 2.5 Hz, 2H), 2.04 (m, 1H), 1.93 (d, *J* = 14.3 Hz, 1H), 1.96–1.77 (m, 4H), 1.68–1.56 (complex, 4H), 1.48–1.14 (complex, 6H), 1.03 (m, 1H), 0.95–0.83 (complex, 6H, contains s, 0.88, 3H), 0.73–0.66 (complex, 4H, contains s, 0.73, 3H); ^{13}C NMR (101 MHz, $CDCl_3$) δ 175.4, 141.9, 128.52 (2C), 128.46 (2C), 126.0, 82.0, 54.5, 51.1, 47.9, 44.9, 43.9, 42.9, 41.6, 40.5, 38.5, 36.8, 35.0, 33.4,

31.7, 30.9, 30.7, 30.1, 23.5, 21.0, 12.2, 11.2. HRMS (FT-ICR, HESI) *m/z*: $[M + H]^+$ calcd for $C_{28}H_{42}NO_2$ $[M + H]^+$ 424.3210, found 424.3203.

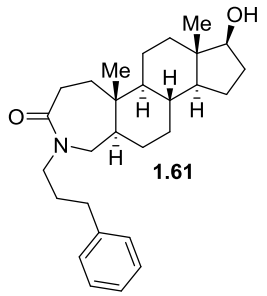

17β-Hydroxy-5α-androstane-derived A-Ring Lactam, 1.61. Following the general procedure B, (*S*)-3-azido-1-phenylpropanol (*S*)-**1.2** (36.8 mg, 0.208 mmol, 2.1 equiv) was reacted with 5α-DHT **1.14** (29.0 mg, 0.100 mmol) to give **1.61** as white foam solid (39.6 mg, 0.093 mmol, 93% yield, UPLC/HRMS purity: ≥99.5%). Purification was carried out by an automated MPLC system using a 12 g normal phase silica column with gradient elution from 0–3% MeOH/CH_2Cl_2. R_f = 0.38 (4% MeOH/CH_2Cl_2); mp decomposed; IR (neat) 3212, 1621 cm^{-1}; ^1H NMR (400 MHz, $CDCl_3$) δ 7.34 (m, 2H), 7.25 (m, 3H), 3.67 (m, 2H), 3.47 (m, 2H), 2.68 (m, 3H), 2.55 (d, *J* = 15.5 Hz, 1H), 2.39 (m, 1H), 2.11 (m, 1H), 1.97–1.83 (complex, 4H), 1.79–1.59 (complex, 4H), 1.10 (m, 1H), 1.02–0.90 (complex, 5H, contains s, 0.95, 3H), 0.83–0.72 (complex, contains s, 0.79, 3H); ^{13}C NMR (101 MHz, $CDCl_3$) δ 175.3, 141.9, 128.5 (2C), 128.4 (2C), 126.0, 81.9, 54.2, 51.5, 51.1, 49.1, 48.0, 42.8, 38.3, 36.8, 36.0, 35.2, 33.4, 32.5, 31.5, 30.6, 30.3, 28.4, 23.4, 20.7, 12.2, 11.2. HRMS (FT-ICR, HESI) *m/z*: $[M + H]^+$ calcd for $C_{28}H_{42}NO_2$ $[M + H]^+$ 424.3210, found 424.3202.

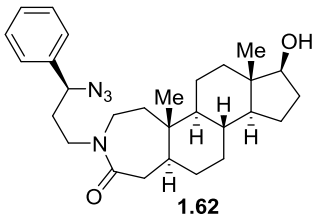

17β-Hydroxy-5α-androstane-derived A-Ring Lactam, 1.62. Following the general procedure B, (*R*)-3-azido-1-phenylpropanol (*R*)-**1.2** (71.6 mg, 0.404 mmol, 2.0 equiv) was reacted with 5α-DHT **1.14** (57.7 mg, 0.199 mmol) to give **1.62** as a yellow amorphous solid (52.0 mg, 0.112 mmol, 56% yield, UPLC/HRMS purity: 97.9%). Purification was carried out by an automated MPLC system using a 12 g normal phase silica column with gradient elution from 0–50% EtOAc/hexanes. R_f = 0.32 (50% EtOAc/hexanes); mp 160–163 ˚C; IR (neat) 3378, 2093, 1624 cm^{-1}; ^1H NMR (400 MHz, $CDCl_3$) δ 7.40–7.30 (m, 5H), 4.46 (t, *J* = 7.2 Hz, 1H), 3.62 (t, *J* = 8.5 Hz, 1H), 3.56–3.45 (m, 2H), 3.32 (m ,1H), 2.92 (m, 1H), 2.67 (dd, *J* = 14.3, 10.3 Hz, 1H), 2.05 (m, 1H), 1.97 (q, *J* = 7.3 Hz, 2H), 1.91 (d, *J* = 8.96 Hz, 1H), 1.82–1.77 (m, 2H), 1.69–1.63 (m, 1H), 1.62–1.16 (complex, 10H), 1.05 (m, 1H), 0.96–0.83 (m, 5H, contains s, 3H), 0.74–0.68 (m, 4H, contains s, 3H); ^{13}C NMR (101 MHz, $CDCl_3$) δ 175.6, 139.3, 129.0 (2C), 128.6, 127.0 (2C), 82.0, 64.4, 54.4, 51.1, 45.7, 45.2, 43.8, 42.9, 41.3, 40.3, 38.5, 36.8, 35.0, 34.7, 31.7, 30.9, 30.7, 23.5, 21.0, 12.2, 11.2. HRMS (FT-ICR, HESI) *m/z*: $[M + H]^+$ calcd for $C_{28}H_{41}N_4O_2$ 465.3224, found 465.3212.

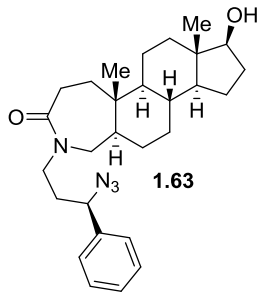

1.63

17β-Hydroxy-5α-androstane-derived A-Ring Lactam, 1.63. Following the general procedure B, (*S*)-3-azido-1-phenylpropanol (*S*)-**1.2** (71.0 mg, 0.401 mmol, 2.0 equiv) was reacted with 5α-DHT **1.14** (58.3 mg, 0.201 mmol) to give **1.63** as a yellow amorphous solid (67.9 mg, 0.146 mmol, 73% yield, UPLC/HRMS purity: ≥99.5%). Purification was carried out by an automated MPLC system using a using 12 g normal phase silica column with gradient

elution from 0–80% EtOAc/hexanes. R_f = 0.34 (50% EtOAc/hexanes); mp 148–150 ˚C; IR (neat) 3353, 2094, 1624 cm^{-1}; ^1H NMR (400 MHz, $CDCl_3$) δ 7.39–7.28 (m, 5H), 4.44 (t, *J* = 7.1 Hz, 1H), 3.61 (t, *J* = 8.5 Hz, 1H), 3.57–3.50 (m, 2H), 3.26 (dt, *J* = 13.7, 7.0 Hz, 1H), 2.51 (m, 1H), 2.44 (d, *J* = 15.4 Hz, 1H), 2.29 (m, 1H), 2.03 (m, 1H), 1.95 (q, *J* = 7.3 Hz, 2H), 1.87–1.67 (complex, 4H), 1.64–1.52 (m, 2H), 1.47–1.17 (complex, 7H), 1.03 (m, 1H), 0.96–0.87 (m, 2H), 0.85 (s, 3H), 0.72–0.66 (complex, 4H, contains s, 3H); ^{13}C NMR (101 MHz, $CDCl_3$) δ 175.4, 139.2, 129.0 (2C), 128.5, 127.0 (2C), 81.8, 64.3, 54.1, 51.8, 51.0, 49.0, 45.9, 42.8, 38.2, 36.7, 35.9, 35.1, 34.6, 32.3, 31.4, 30.5, 28.4, 23.4, 20.7, 12.2, 11.2. HRMS (FT-ICR, HESI) *m/z*: $[M + H]^+$ calcd for $C_{28}H_{41}N_4O_2$ 465.3224, found 465.3223.

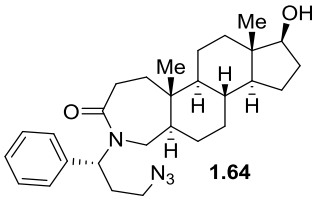

1.64

17β-Hydroxy-5α-androstane-derived A-Ring Lactam, 1.64. Following the general procedure B, (*R*)-3-azido-3-phenylpropanol (*R*)-**1.4** (71.6 mg, 0.404 mmol, 2.0 equiv) was reacted with 5α-DHT **1.14** (58.0 mg, 0.200 mmol) to give **1.64** as an orange amorphous solid (60.5 mg, 0.130 mmol, 65% yield, UPLC/HRMS purity: 94.4%). Purification was carried out by an automated MPLC system using a 12 g silica column with gradient elution from 0–60% EtOAc/hexanes. R_f = 0.28 (50% EtOAc/hexanes); mp 228–235 ˚C; IR (neat) 3275, 2091, 1611 cm^{-1}; ^1H NMR (400 MHz, $CDCl_3$) δ 7.34–7.28 (m, 5H), 5.93 (t, *J* = 7.7 Hz, 1H), 3.56 (t, *J* = 8.5 Hz, 1H), 3.42–3.25 (m, 3H), 2.64 (m, 1H), 2.49–2.42 (m, 2H, contains d, 1.57, *J* = 15.2 Hz, 1H), 2.14 (q, *J* = 7.5 Hz, 2H), 2.00 (m, 1H), 1.83 (m, 1H), 1.75 (m, 1H), 1.57–1.32 (m, 4H), 1.21–1.08 (m, 4H), 1.02–0.91 (m, 2H), 0.81–0.73 (m, 4H), 0.66 (s, 3H), 0.56 (m, 1H), 0.39 (m, 1H), 0.34–0.20 (m, 2H); ^{13}C NMR (101 MHz, $CDCl_3$) δ 175.6, 139.2, 128.7 (2C), 128.3 (2C), 128.1, 81.9,

54.1, 53.2, 50.9, 49.1, 48.7, 45.2, 42.8, 38.1, 36.7, 36.1, 35.1, 32.6, 31.2, 30.6, 29.5, 27.6, 23.4, 20.6, 12.1, 11.2. HRMS (FT-ICR, HESI) *m/z*: $[M + H]^+$ calcd for $C_{28}H_{41}N_4O_2$ 465.3224, found 465.3217.

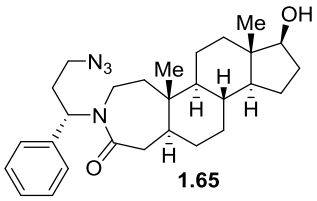

1.65

17β-Hydroxy-5α-androstane-derived A-Ring Lactam, 1.65. Following the general procedure B, (*S*)-3-azido-3-phenylpropanol (*S*)-**1.4** (71.1 mg, 0.401 mmol, 2.0 equiv) was reacted with 5α-DHT **1.14** (57.0 mg, 0.196 mmol) to give **1.65** as a pale yellow crystalline solid (54.6 mg, 0.118 mmol, 60% yield, LCMS purity: ≥99.5%). Purification was carried out by an automated MPLC system using a 12 g normal phase silica column with gradient elution from 0–50% EtOAc/hexanes. R_f = 0.32 (50% EtOAc/hexanes); mp decomposed; IR (neat) 3394, 2096, 1624 cm^{-1}; ^1H NMR (400 MHz, $CDCl_3$) δ 7.38–7.28 (m, 5H), 5.88 (dd, *J* = 8.9, 6.6 Hz, 1H), 3.57 (t, *J* = 8.6 Hz, 1H), 3.42–3.25 (m, 3H), 2.96 (m, 1H), 2.78 (m, 1H), 2.63 (m, 1H), 2.20–2.12 (m, 2H), 2.09–1.98 (m, 2H), 1.71–1.05 (complex, 11H), 0.96–0.80 (complex, 6H, contains s, 0.81, 3H), 0.67 (s, 3H), 0.44 (m, 1H), 0.30 (m, 1H); ^{13}C NMR (101 MHz, $CDCl_3$) δ 175.9, 139.1, 128.9 (2C), 128.1 (2C), 128.0, 82.0, 54.2, 53.4, 50.9, 49.1, 43.6, 42.8, 40.9, 40.5, 39.1, 38.2, 36.7, 34.9, 31.5, 30.9, 30.7, 29.4, 23.4, 20.8, 12.1, 11.2. HRMS (FT-ICR, HESI) *m/z*: $[M + H]^+$ calcd for $C_{28}H_{41}N_4O_2$ 465.3224, found 465.3215.

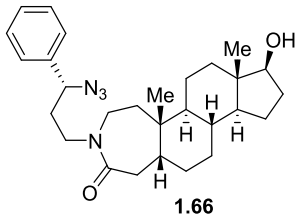

1.66

17β-Hydroxy-5β-androstane-derived A-Ring Lactam, 1.66. Following the general procedure B, (*S*)-3-azido-1-phenylpropanol (*S*)-**1.2** (69.9 mg, 0.394 mmol, 2.0 equiv) was reacted with 5β-DHT **1.15** (58.2 mg, 0.200 mmol) to give **1.66** as a cream-colored amorphous solid (76.1 mg, 0.164 mmol, 82% yield, UPLC/HRMS purity: 98.8%). Purification was carried out by an automated MPLC system using a 12 g normal phase silica column with gradient elution from 0–50% EtOAc/hexanes. R_f = 0.25 (50% EtOAc/hexanes); mp 137–142 ˚C; IR (neat) 3393, 2094, 1628 cm^{-1}; ^1H NMR (400 MHz, $CDCl_3$) δ 7.41–7.30 (m, 5H), 4.45 (t, *J* = 7.2 Hz, 1H), 3.65 (t, *J* = 8.6 Hz, 1H), 3.62–3.55 (m, 1H), 3.37 (dd, *J* = 15.2, 10.2 Hz, 1H), 3.26 (m, 1H), 3.02–2.92 (m, 2H), 2.12–2.03 (m, 2H, contains d, 2.06, *J* = 14.7 Hz, 1H), 1.97 (q, *J* = 7.3 Hz, 2H), 1.92–1.82 (m, 2H), 1.73 (m, 1H), 1.63–1.58 (m, 1H), 1.47–1.20 (complex, 10H), 1.13–0.96 (m, 5H, contains s, 0.98, 3H), 0.92–0.82 (m, 1H), 0.74 (s, 3H); ^{13}C NMR (101 MHz, $CDCl_3$) δ 175.0, 139.4, 129.0 (2C), 128.5, 127.0 (2C), 82.0, 64.4, 51.0, 45.9, 44.0, 43.2 (br), 42.6, 40.6, 39.7, 39.6, 37.0, 36.9, 36.0, 34.5, 30.8, 29.9, 25.7, 23.8 (br), 23.5, 21.0, 11.3. **Note**: Two broad carbon signals were consistently observed amongst *cis*-AB analogs. HRMS (FT-ICR, HESI) *m/z*: $[M + H]^+$ calcd for $C_{28}H_{41}N_4O_2$ 465.3224, found 465.3254.

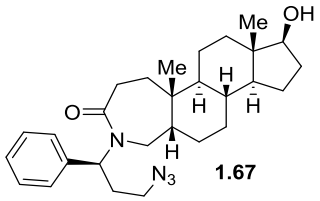

1.67

17β-Hydroxy-5β-androstane-derived A-Ring Lactam, 1.67. Following the general procedure B, (*S*)-3-azido-3-phenylpropanol (*S*)-**1.4** (69.7 mg, 0.393 mmol, 2.0 equiv) was reacted with 5β-DHT **1.15** (58.2 mg, 0.200 mmol) to give **1.67** as an orange amorphous solid (77.9 mg, 0.168 mmol, 84% yield, UPLC/HRMS purity: ≥99.5%). Purification was carried out by an automated MPLC system using a 12 g normal phase silica column with gradient elution

from 0–40% EtOAc/hexanes. R_f = 0.22 (50% EtOAc/hexanes); mp 174–178 ˚C; IR (neat) 3396, 2095, 1628 cm^{-1}; ^1H NMR (400 MHz, $CDCl_3$) δ 7.35–7.27 (m, 5H), 5.88 (m, 1H), 3.70 (dd, *J* = 15.3, 10.1 Hz, 1H), 3.63 (t, *J* = 8.5 Hz, 1H), 3.41 (m, 1H), 3.29 (m, 1H), 2.68–2.58 (m, 2H), 2.32 (dd, *J* = 14.9, 8.5 Hz, 1H), 2.21–2.11 (m, 2H), 2.04 (m, 1H), 1.88–1.79 (m, 2H), 1.56–0.93 (complex, 13H), 0.85–0.79 (m, 4H, contains s, 0.77, 3H), 0.69 (s, 3H), 0.53 (m, 1H); ^{13}C NMR (101 MHz, $CDCl_3$) δ 175.8, 139.1, 128.7 (2C), 128.2 (2C), 128.1, 81.9, 53.6, 51.0, 49.1, 45.1, 44.7, 43.2, 41.4 (br), 36.94, 36.97, 35.9, 34.2, 31.1, 30.7, 29.5, 27.9, 26.4, 24.1 (br), 23.4, 20.6, 11.2. **Note**: Two broad carbon signals were consistently observed amongst *cis*-AB analogs. HRMS (FT-ICR, HESI) *m/z*: $[M + H]^+$ calcd for $C_{28}H_{41}N_4O_2$ 465.3224, found 465.3213.

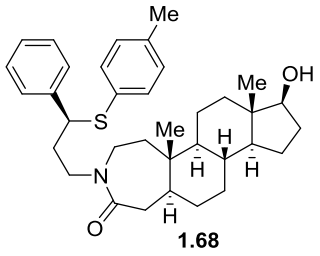

1.68

17β-Hydroxy-5α-androstane-derived A-Ring Lactam, 1.68. Following the general procedure B, (*R*)-3-azido-1-phenylpropanol (*R*)-**1.2** (44.5 mg, 0.250 mmol, 2.0 equiv) was reacted with 5α-DHT **1.14** (36.3 mg, 0.125 mmol) to give **1.68** as a yellow crystalline solid (45.2 mg, 0.0828 mmol, 66% yield, UPLC/HRMS purity: 97.0%). Purification was carried out by an automated MPLC system using a 12 g normal phase silica column with gradient elution from 0–60% EtOAc/hexanes. R_f = 0.30 (50% EtOAc/hexanes); mp 182–186 ˚C; IR (neat) 3395, 1632 cm^{-1}; ^1H NMR (400 MHz, $CDCl_3$) δ 7.27–7.17 (m, 5H), 7.12 (m, 2H), 6.99 (m, 2H), 4.05 (t, *J* = 7.4 Hz, 1H), 3.62 (t, *J* = 8.6 Hz, 1H), 3.44–3.28 (m, 3H), 2.83 (m, 1H), 2.58 (dd, *J* = 14.2, 10.4 Hz, 1H), 2.28 (s, 3H), 2.13 (q, *J* = 7.3 Hz, 2H), 2.04 (m, 1H), 1.85 (d, *J* = 14.3 Hz, 1H), 1.82–1.71 (m, 2H), 1.67–0.98 (complex, 11H), 0.94–0.80 (m, 5H, contains s, 0.83, 3H), 0.72 (s, 3H),

0.69–0.62 (m, 1H); ^{13}C NMR (126 MHz, $CDCl_3$) δ 175.4, 141.8, 137.6, 133.3 (2C), 130.8, 129.6 (2C), 128.5 (2C), 127.9 (2C), 127.3, 82.0, 54.3, 51.8, 51.0, 46.6, 45.0, 43.8, 42.8, 41.4, 40.4, 38.4, 36.8, 34.9, 34.3, 31.6, 30.9, 30.7, 23.4, 21.3, 21.0, 12.1, 11.2. HRMS (FT-ICR, HESI) *m/z*: $[M + H]^+$ calcd for $C_{35}H_{48}NO_2S$ $[M + H]^+$ 546.3400, found 546.3420.

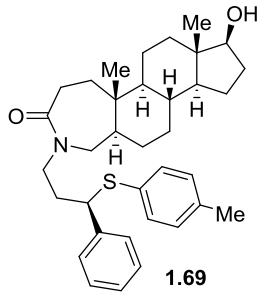

1.69

17β-Hydroxy-5α-androstane-derived A-Ring Lactam, 1.69. Following the general procedure B, (*S*)-3-azido-1-phenylpropanol (*S*)-**1.2** (53.4 mg, 0.301 mmol, 2.0 equiv) was reacted with 5α-DHT **1.14** (45.7 mg, 0.157 mmol) to give **1.69** as a yellow amorphous solid (57.3 mg, 0.105 mmol, 67% yield, UPLC/HRMS purity: 94.2%). Purification was carried out by an automated MPLC system using a using 12 g normal phase silica column with gradient elution from 0–40% EtOAc/hexanes. R_f = 0.22 (50% EtOAc/hexanes); mp 149–153 ˚C; IR (neat) 3390, 1632 cm^{-1}; ^{1}H NMR (400 MHz, $CDCl_3$) δ 7.26–7.16 (m, 5H), 7.11 (m, 2H), 7.00 (m, 2H), 4.04 (t, *J* = 7.2 Hz, 1H), 4.62 (t, *J* = 8.6 Hz, 1H), 3.46–3.52 (m, 3H), 2.46–2.35 (m, 2H), 2.28–2.22 (m, 4H, contains s, 2.28, 3H), 2.15-2.00 (m, 3H, contains q, 2.12, *J* = 7.3 Hz, 2H), 1.84–1.77 (m, 2H), 1.70–1.53 (complex, 5H), 1.47–1.16 (complex, 10H), 1.06–0.98 (m, 1H), 0.95–0.82 (m, 4H, contains s, 3H, 0.83), 0.72 (s, 3H), 0.66 (m, 1H); ^{13}C NMR (101 MHz, $CDCl_3$) δ 175.4, 141.8, 137.7, 133.4 (2C), 130.6, 129.6 (2C), 128.5 (2C), 127.9 (2C), 127.3, 81.9, 54.1, 51.7, 51.1, 49.0, 46.9, 42.9, 38.3, 36.8, 35.9, 35.2, 34.3, 32.3, 31.4, 30.6, 28.4, 23.5, 21.3, 20.7, 12.2, 11.2. **Note**: Missing one carbon signal due to signal overlap. HRMS (FT-ICR, HESI) *m/z*: $[M + H]^+$ calcd for $C_{35}H_{48}NO_2S$ 546.3400, found 546.3394.

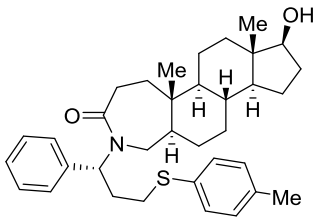

1.70

17β-Hydroxy-5α-androstane-derived A-Ring Lactam, 1.70. Following the general procedure B, (*R*)-3-azido-3-phenylpropanol (*R*)-**1.4** (44.5 mg, 0.250 mmol, 2.0 equiv) was reacted with 5α-DHT **1.14** (36.3 mg, 0.125 mmol) to give **1.70** as a cream-colored amorphous solid (57.0 mg, 0.104 mmol, 83% yield, UPLC/HRMS purity: 97.5%). Purification was carried out using 12 g silica column with gradient elution from 0–50% EtOAc/hexanes. R_f = 0.27 (50% EtOAc/hexanes); IR (neat) 3400, 1625 cm^{-1}; mp decomposed; ^1H NMR (400 MHz, $CDCl_3$) δ 7.30–7.21 (m, 7H), 7.07–7.05 (m, 2H), 5.89 (dd, *J* = 9.3, 6.1 Hz, 1H), 3.53 (t, *J* = 8.5 Hz, 1H), 3.19 (dd, *J* = 15.5, 8.9 Hz, 1H), 2.93–2.86 (m, 1H), 2.78–2.71 (m, 1H), 2.59 (t, *J* = 13.6 Hz, 1H), 2.42–2.37 (m, 1H), 2.28 (s, 3H), 2.19–2.05 (m, 2H), 1.98–1.93 (m, 1H), 1.79 (m, 1H), 1.71 (m, 1H), 1.53–1.05 (complex, 8H), 0.97–0.85 (m, 2H), 0.78–0.69 (m, 4H, contains s, 0.74, 3H), 0.62 (s, 3H), 0.52 (m, 1H), 0.34 (m, 1H), 0.23 (m, 2H); ^{13}C NMR (101 MHz, $CDCl_3$) δ 175.4, 139.6, 136.5, 132.5, 130.5, 129.9, 128.6, 128.4, 127.9, 81.9, 54.9, 54.1, 50.9, 48.7, 45.1, 42.8, 38.0, 36.7, 36.2, 35.1, 32.7, 31.5, 31.2, 30.6, 30.2, 27.6, 23.4, 21.1, 20.6, 12.1, 11.1. HRMS (FT-ICR, HESI) *m/z*: $[M + H]^+$ calcd for $C_{35}H_{48}NO_2S$ 546.3400, found 546.3396.

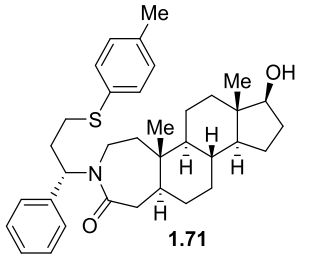

1.71

17β-Hydroxy-5α-androstane-derived A-Ring Lactam, 1.71. Following the general procedure B, (*S*)-3-azido-3-phenylpropanol (*S*)-**1.4** (44.2 mg, 0.249 mmol, 2.0 equiv) was reacted with 5α-DHT **1.14** (36.3 mg, 0.125 mmol) to give **1.71** as a white amorphous solid (44.3 mg, 0.081 mmol, 65% yield, UPLC/HRMS purity: 97.2%). Purification was carried out by an automated MPLC system using a using 12 g normal phase silica column with gradient elution from 0–40% EtOAc/hexanes. R_f = 0.53 (50% EtOAc/hexanes); mp 181–183 ˚C; IR (neat) 3313, 1613 cm^{-1}; ^1H NMR (400 MHz, $CDCl_3$) δ 7.34–7.24 (m, 7H), 7.10–7.08 (m, 2H), 5.87 (dd, *J* = 9.6, 5.9 Hz, 1H), 3.56 (t, *J* = 8.6 Hz, 1H), 3.23 (dd, *J* = 15.6, 11.5 Hz, 1H), 2.96–2.87 (m, 2H), 2.81–2.73 (m, 2H), 2.31 (s, 3H), 2.24–2.10 (m, 2H), 2.07–1.98 (m, 2H, contains d, 2.04, *J* = 14.3 Hz, 1H), 1.70–1.04 (complex, 13H), 0.95–0.76 (m, 5H, contains s, 0.79, 3H), 0.67 (s, 3H), 0.41 (m, 1H), 0.27 (m, 1H); ^{13}C NMR (101 MHz, $CDCl_3$) δ 175.7, 139.6, 136.5, 132.5, 130.5 (2C), 129.8 (2C), 128.6 (2C), 128.2 (2C), 127.8, 81.9, 55.0, 54.2, 50.9, 43.6, 42.8, 40.9, 40.6, 38.9, 38.2, 36.7, 34.9, 31.58, 31.55, 30.9, 30.7, 30.2, 23.4, 21.1, 20.8, 12.1, 11.1. HRMS (FT-ICR, HESI) *m/z*: $[M + H]^+$ calcd for $C_{35}H_{48}NO_2S$ $[M + H]^+$ 546.3400, found 546.3396.

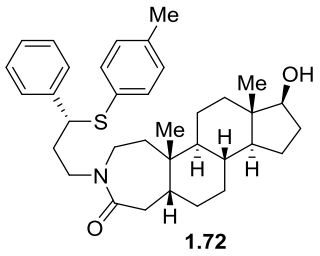

1.72

17β-Hydroxy-5β-androstane-derived A-Ring Lactam, 1.72. Following the general procedure B, (*S*)-3-azido-1-phenylpropanol (*S*)-**1.2** (53.0 mg, 0.299 mmol, 2.0 equiv) was reacted with 5β-DHT **1.15** (43.9 mg, 0.151 mmol) to give **1.72** as a white crystalline solid (46.1 mg, 0.084 mmol, 56% yield, UPLC/HRMS purity: 98.6%). Purification was carried out using 12 g silica column with gradient elution from 0–40% EtOAc/hexanes. R_f = 0.33 (50%

EtOAc/hexanes); IR (neat) 3380, 1621 cm^{-1}; mp 142–147 ˚C; ^1H NMR (400 MHz, $CDCl_3$) δ 7.26–7.17 (m, 5H), 7.13 (m, 2H), 7.00 (m, 2H), 4.04 (t, *J* = 7.2 Hz, 1H), 3.65 (t, *J* = 8.5 Hz, 1H), 3.46–3.29 (m, 2H), 3.23 (dd, *J* = 10.4, 15.2 Hz, 1H), 2.90–2.81 (m, 2H), 2.28 (s, 3H), 2.18–2.04 (m, 3H), 1.99 (d, *J* = 14.6 Hz, 1H), 1.89–1.75 (m, 3H), 1.68–1.54 (m, 2H), 1.47–0.94 (complex, 11H), 0.94 (s, 3H), 0.91–0.78 (m, 1H), 0.73 (s, 3H); ^{13}C NMR (101 MHz, $CDCl_3$) δ 175.0, 141.8, 137.8, 133.6 (2C), 130.7, 129.6 (2C), 128.5 (2C), 127.9 (2C), 127.3, 82.0, 52.0, 51.1, 47.0, 43.8, 43.2, 42.3 (br), 40.5, 39.6, 39.5, 37.0, 36.9, 35.9, 34.0, 30.8, 29.8, 25.7, 23.8 (br), 23.5, 21.3, 21.0, 11.3. **Note**: Two broad carbon signals were consistently observed amongst *cis*-AB analogs. HRMS (FT-ICR, HESI) *m/z*: $[M + H]^+$ calcd for $C_{35}H_{48}NO_2S$ 546.3400, found 546.3394.

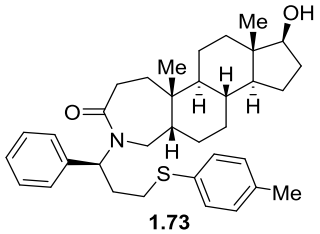

1.73

17β-Hydroxy-5β-androstane-derived A-Ring Lactam, 1.73. Following the general procedure B, (*S*)-3-azido-3-phenylpropanol (*S*)-**1.4** (51.0 mg, 0.288 mmol, 2.0 equiv) was reacted with 5β-DHT **1.15** (46.6 mg, 0.160 mmol) to give **1.73** as a white crystalline solid (66.8 mg, 0.122 mmol, 76% yield, UPLC/HRMS: 99.0%). Purification was carried out using 12 g silica column with gradient elution from 0–40% EtOAc/hexanes. R_f = 0.20 (40% EtOAc/hexanes); mp 212–215 ˚C; IR (neat) 3406, 1628 cm^{-1}; ^1H NMR (400 MHz, $CDCl_3$) δ 7.32–7.23 (m, 7H), 7.09 (m, 2H), 5.89 (m, 1H), 3.67–3.61 (m, 2H), 2.94 (m, 1H), 2.79 (m, 1H), 2.64–2.57 (m, 2H), 2.42–2.31 (m, 4H contains s, 2.31, 3H), 2.24–2.12 (m, 2H), 2.05 (m, 1H), 1.87–1.79 (m, 3H), 1.57–0.95 (complex, 11H), 0.88–0.74 (m, 4H, contains s, 0.76, 3H), 0.70–

0.60 (4H, contains s, 0.70, 3H), 0.49 (m, 1H); ^{13}C NMR (101 MHz, $CDCl_3$) δ 175.8, 139.4, 136.4, 132.4, 130.4 (2C), 129.9 (2C), 128.6 (2C), 128.2 (2C), 128.0, 82.0, 55.3, 51.1, 45.0, 44.6, 43.2, 41.5 (br), 37.0, 36.9, 35.9, 34.1, 31.4, 30.9, 30.7, 30.1, 27.9, 26.4, 24.0 (br), 23.5, 21.2, 20.6, 11.2. **Note**: Two broad carbon signals were consistently observed amongst *cis*-AB analogs. HRMS (FT-ICR, HESI) *m/z*: $[M + H]^+$ calcd for $C_{35}H_{48}NO_2S$ 546.3400, found 546.3414.

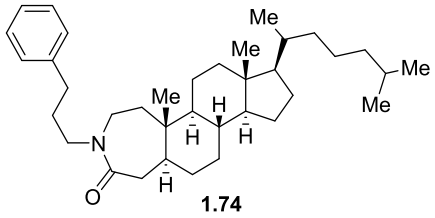

1.74

5α-Cholestane-derived A-Ring Lactam, 1.74. A solution of **1.18** (53.6 mg, 0.100 mmol), 10% Pd/C (42.6 mg, 0.400 mmol, 4.0 equiv), and acetic acid (2.0 mL) in anhydrous EtOH (15.0 mL) was placed under hydrogen atmosphere (40 psi) via a shaker-Parr hydrogenation apparatus over 24 h. The solution was filtered over Celite and concentrated. The crude residue was purified by an automated MPLC system using a 12 g normal phase silica column with gradient elution from 0–60% EtOAc/hexanes. Concentration of solvents afforded product **1.74** as white amorphous solid (48.6 mg, 0.0935 mmol, 94% yield). R_f = 0.68 (50% EtOAc/hexanes); mp 146–147 ˚C; IR (neat) 1624 cm^{-1}; ^{1}H NMR (400 MHz, $CDCl_3$) δ 7.31–7.27 (m. 2H), 7.20–7.16 (m, 3H), 3.58 (dd, *J* = 11.7, 15.6 Hz, 1H), 3.46–3.33 (m, 2H), 2.95 (dd, *J* = 15.4, 6.2 Hz, 1H), 2.74 (dd, *J* = 14.2, 10.3 Hz, 1H), 2.62 (m, 2H), 1.98–1.91 (m, 2H, contains d, *J* = 14.3 Hz, 1H), 1.87–1.75 (m, 3H), 1.67–1.63 (m, 2H), 1.59–0.92 (complex, 22H), 0.89–0.84 (complex, 12H), 0.71–0.64 (m, 4H, contains s, 0.64, 3H); ^{13}C NMR (101 MHz, $CDCl_3$) δ 175.5, 142.0 128.52 (2C), 128.46 (2C), 126.0, 56.5. 56.4, 54.3, 47.9, 45.0, 43.8, 42.5, 41.5, 40.5, 40.1, 39.7, 38.4, 36.3, 35.9, 34.9, 33.5, 32.1, 31.1, 30.1, 28.4, 28.1, 24.3, 23.9, 22.9, 22.7, 21.4, 18.8,

12.18, 12.16. HRMS (FT-ICR, ESI) *m/z*: $[M + H]^+$ calcd for $C_{36}H_{57}NO$ 520.4513, found 520.4523.

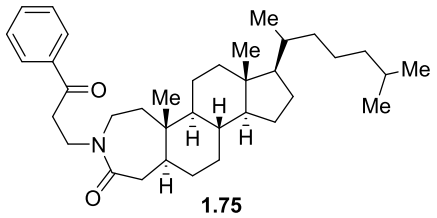

1.75

5α-Cholestane-derived A-Ring Lactam, 1.75. Following the general procedure C, **1.18** (530 mg, 0.099 mmol) was oxidized to give product **1.75** as a white amorphous solid (41.2 mg, 0.077 mmol, 78% yield). Purification was carried out by an automated MPLC system using a 12 g normal phase silica column with gradient elution from 0–25% EtOAc/hexanes. R_f = 0.63 (50% EtOAc/hexanes); mp 209–214 ˚C; IR (neat) 1683, 1642 cm^{-1}; ^1H NMR (400 MHz, $CDCl_3$) δ 7.98 (m, 2H), 7.56 (m, 1H), 7.47 (m, 2H), 3.79 (dt, *J* = 13.4, 6.7 Hz, 1H), 3.72–3.61 (m, 2H), 3.26 (m, 2H), 3.19 (m, 1H), 2.74 (dd, *J* = 14.2, 10.2 Hz, 1H), 1.98–1.93 (m, 1H), 1.90 (d, *J* = 14.3 Hz, 1H), 1.85–1.76 (m, 2H), 1.66–0.91 (complex, 23H), 0.83–0.90 (complex, 12H), 0.68–0.61 (m, 4H, contains s, 0.64, 3H); ^{13}C NMR (101 MHz, $CDCl_3$) δ 199.4, 175.9, 136.9, 133.4, 128.8 (2C), 128.4 (2C), 56.5, 56.4, 54.3, 46.7, 45.4, 43.7, 42.5, 41.4, 40.5, 40.1, 39.7, 38.4, 37.8, 36.3, 35.9, 34.9, 32.1, 31.1, 28.4, 28.1, 24.3, 24.0, 23.9, 22.9, 22.7, 21.4, 18.8, 12.2. HRMS (FT-ICR, ESI) *m/z*: $[M + H]^+$ calcd for $C_{36}H_{56}NO_2$ 534.4306, found 534.4313.

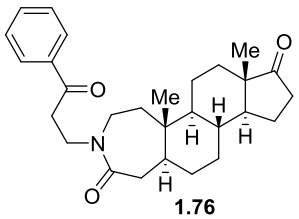

1.76

17β-Hydroxy-5α-androstane-derived A-Ring Lactam, 1.76. Following the general procedure C, **1.29** (75.0 mg, 0.170 mmol) was oxidized to give **1.76** as a white amorphous solid

(50 mg, 0.115 mmol, 68% yield, UPLC/HRMS purity: ≥99.5%). Purification was carried out by an automated MPLC system using a 12 g normal phase silica column with gradient elution from 0–2% MeOH/CH_2Cl_2. Concentration of solvents afforded a slightly impure azasteroid, which was subjected to a second purification on a 4 g normal phase silica column with gradient elution 0–80% EtOAc/hexanes. R_f = 0.20 (50% EtOAc/hexanes); mp 209–212 ˚C; IR (neat) 1726, 1673, 1645, 1628 cm^{-1}; ^1H NMR (400 MHz, $CDCl_3$) δ 7.97 (m, 2H), 7.56 (m, 1H), 7.46 (m, 2H), 3.82–3.62 (m, 3H), 3.31–3.20 (m, 3H), 2.75 (dd, *J* = 14.3, 9.9 Hz, 1H), 2.43 (m, 1H), 2.06 (m, 1H), 1.96–1.89 (m, 2H, contains d, *J* = 14.4 Hz, 1H), 1.82–1.75 (m, 3H), 1.68–1.63 (m, 1H), 1.53–1.14 (complex, 9H), 1.04–0.91 (m, 1H), 0.89 (s, 3H), 0.84 (s, 3H), 0.71 (m, 1H); ^{13}C NMR (101 MHz, $CDCl_3$) δ 221.1, 199.3, 175.7, 136.8, 133.5, 128.8 (2C), 128.3 (2C), 54.3, 51.4, 47.6, 46.6, 45.3, 43.7, 41.4, 40.3, 38.6, 37.8, 36.0 34.5, 31.6, 30.9, 30.7, 21.8, 20.7, 13.9, 12.2. HRMS (FT-ICR, HESI) *m/z*: $[M + H]^+$ calcd for $C_{28}H_{38}NO_3$ $[M + H]^+$ 436.2846, found 436.2823.

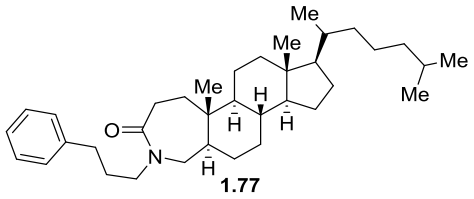

1.77

5α-Cholestane-derived A-Ring Lactam, 1.77. A solution of **1.19** (53.6 mg, 0.100 mmol), 10% Pd/C (21.3 mg, 0.200 mmol, 2.00 equiv), and acetic acid (200 μL) in anhydrous EtOH (15.0 mL) was placed under hydrogen atmosphere (40 psi) via a shaker-Parr hydrogenation apparatus over 24 h. The solution was filtered over Celite and concentrated. The crude residue was purified by purified by an automated MPLC system using a 12 g normal phase silica column with gradient elution from 0–60% EtOAc/hexanes. Concentration of solvents afforded product **1.77** as white amorphous solid (36.0 mg, 0.0692 mmol, 69% yield). R_f = 0.75 (50% EtOAc/hexanes); mp 155–157 ˚C; IR (neat) 1624 cm^{-1}; ^1H NMR (400 MHz, $CDCl_3$) δ

7.31–7.27 (m, 2H), 7.20–7.16 (m, 3H), 3.60 (dd, *J* = 15.4, 8.5 Hz, 1H), 3.40 (m, 2H), 2.66–2.56 (m, 3H), 2.48 (d, *J* = 15.4 Hz, 1H), 2.34 (dd, *J* = 14.4, 7.5 Hz, 1H), 1.97 (m, 1H), 1.88–1.43 (complex, 8H), 1.34–0.93 (complex, 19H), 0.92–0.85 (complex, 12H), 0.71–0.64 (m, 4H, contains s, 0.64, 3H); ^{13}C NMR (101 MHz, $CDCl_3$) δ 175.4, 142.0, 128.53 (2C), 128.45 (2C), 126.0, 56.5, 56.4, 54.1, 51.6, 49.1, 48.0, 42.5, 40.1, 39.7, 38.2. 36.3, 36.0, 35.9, 35.2, 33.5, 32.6, 32.0, 30.1, 28.6, 28.4, 28.2, 24.3, 24.0, 22.9, 22.7, 21.1, 18.8, 12.2, 12.16. HRMS (FT-ICR, ESI) *m/z*: $[M + H]^+$ calcd for $C_{36}H_{57}NO$ 520.4513, found 520.4513.

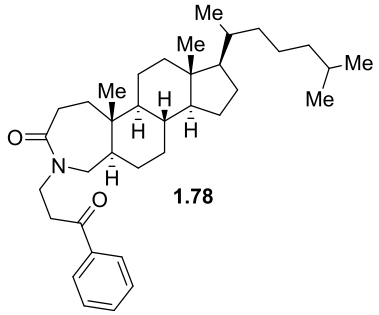

1.78

5α-Cholestane-derived A-Ring Lactam, 1.78. Following the general procedure C, **1.19** (536 mg, 0.100 mmol) was oxidized to give **1.78** as a white amorphous solid (426 mg, 0.080 mmol, 80% yield). Purification was carried out by an automated MPLC system using a 12 g normal phase silica column with gradient elution from 0–25% EtOAc/hexanes. R_f = 0.25 (25% EtOAc/hexanes); mp 177–179 ˚C; IR (neat) 1678, 1641 cm^{-1}; ^{1}H NMR (500 MHz, $CDCl_3$) δ 7.98 (m, 2H), 7.56 (m, 1H), 7.47 (m, 2H), 3.82 (dt, *J* = 13.5, 6.7 Hz, 1H), 3.78–3.60 (m, 2H), 3.25 (m, 2H), 2.75 (d, *J* = 15.4 Hz, 1H), 2.59 (t, *J* = 13.1 Hz, 1H), 2.30 (dd, *J* = 13.9, 7.2 Hz, 1H), 1.95 (dt, *J* = 12.6, 3.4 Hz, 1H), 1.86–1.76 (m, 2H), 1.69–1.64 (m, 3H), 1.56–1.47 (m, 3H), 1.43–0.77 (complex, 29H), 0.64–0.59 (m, 4H, contains s, 0.63, 3H); ^{13}C NMR (126 MHz, $CDCl_3$) δ 199.3, 175.9, 136.8, 133.4, 128.8 (2C), 128.3 (2C), 56.5, 56.3, 54.0, 53.2, 49.1, 45.4, 42.4, 40.0, 39.6, 38.2, 37.8, 36.3, 35.9, 35.8, 35.1, 32.5, 31.9, 28.4, 28.1, 24.3, 24.0, 23.0, 22.7,

21.1, 18.8, 12.2, 12.1. **Note**: Missing one carbon signal due to signal overlap. HRMS (FT-ICR, HESI) *m/z*: $[M + H]^+$ calcd for $C_{36}H_{57}NO_2$ 534.4306, found 534.4307.

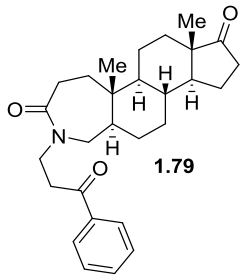

1.79

17β-Hydroxy-5α-androstane-derived A-Ring Lactam, 1.79. Following the general procedure C, **1.28** (93.0 mg, 0.212 mmol) was oxidized to give **1.79** as a white amorphous solid (68.6 mg, 0.157 mmol, 74% yield, UPLC/HRMS purity: 96.1%). Purification was carried out by an automated MPLC system using a 12 g normal phase silica column with gradient elution from 0–2% MeOH/CH_2Cl_2. Concentration of solvents afforded a slightly impure azasteroid, which was subjected to a second purification on a 4 g normal phase silica column with gradient elution 0–80% EtOAc/hexanes. R_f = 0.20 (50% EtOAc/hexanes); mp 217–221 ˚C; IR (neat) 1723, 1676, 1644 cm^{-1}; ^1H NMR (400 MHz, $CDCl_3$) δ 7.98 (m, 2H), 7.57 (m, 1H), 7.47 (m, 2H), 3.82 (dt, *J* = 13.3, 6.6 Hz, 1H), 3.73–3.65 (m, 2H), 3.33–3.20 (m, 2H), 2.81 (d, *J* = 15.5 Hz, 1H), 2.60 (m, 1H), 2.43 (dd, *J* = 19.9, 8.3 Hz, 1H), 2.33 (dd, *J* = 14.4, 7.7 Hz, 1H), 2.10–2.01 (m, 1H), 1.94–1.75 (complex, 4H), 1.72–1.67 (m, 1H), 1.54–1.43 (complex, 3H), 1.38–1.16 (complex, 6H), 0.97–0.89 (m, 4H, contains s, 0.89, 3H), 0.84 (s, 3H), 0.69 (1H); ^{13}C NMR (101 MHz, $CDCl_3$) δ 221.0, 199.2, 175.7, 136.9, 133.5, 128.8 (2C), 128.3 (2C), 54.1, 53.2, 51.4, 49.1, 47.6, 45.4, 38.4, 37.9, 36.0, 35.8, 34.7, 32.4, 31.6, 30.7, 28.0, 21.9, 20.4, 13.9, 12.3. HRMS (FT-ICR, HESI) *m/z*: $[M + H]^+$ calcd for $C_{28}H_{38}NO_3$ 436.2846, found 436.2851.

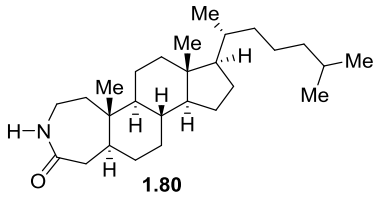

1.80

5α-Cholestane-derived A-Ring Lactam, 1.80. A solution of **1.75** (54.3 mg, 0.102 mmol) and sodium hydride (60% dispersion in mineral oil, 20.0 mg, 0.814 mmol, 4.8 equiv) in anhydrous THF (8.0 mL) was heated at 65 ˚C for 2 h. The reaction was cooled to room temperature and quenched with a saturated solution of NH_4Cl (5 mL). The reaction mixture was diluted with CH_2Cl_2 (20 mL) and washed with saturated solution of NH_4Cl (2 x 5 mL), H_2O (5 mL) and brine (5 mL). The combined organic layer was dried over anhydrous Na_2SO_4 filtered, and concentrated. The crude residue was purified by an automated MPLC system using a 12 g normal phase silica column with gradient elution from 0–5% MeOH/CH_2Cl_2. Concentration of solvents afforded product **1.80** as white amorphous solid (29.2 mg, 0.073 mmol, 72% yield). R_f = 0.23 (2% MeOH/CH_2Cl_2); mp 287–290 ˚C (decomposed); IR (neat) 3315, 3193, 1676, 1628 cm^{-1}; ^1H NMR (400 MHz, $CDCl_3$) δ 5.77 (br s, 1H), 3.39 (m, 1H), 2.98 (m, 1H), 2.75 (dd, *J* = 14.3, 11.0 Hz, 1H), 1.97 (dt, *J* = 12.6, 3.4 Hz, 1H), 1.88–1.77 (m, 3H), 1.66 (m, 1H), 1.57–0.94 (complex, 20H), 0.93–0.85 (complex, 14H), 0.74 (m, 1H), 0.65 (s, 3H); ^{13}C NMR (101 MHz, $CDCl_3$) δ 178.6, 56.5, 56.3, 54.2, 43.4, 42.4, 42.2, 40.1, 39.74, 39.65, 39.0, 38.1, 36.3, 35.9, 34.8, 32.2, 31.2, 28.4, 28.2, 24.3, 24.0, 23.0, 22.7, 21.4, 18.8, 12.16, 12.11. HRMS (FT-ICR, ESI) *m/z*: $[M + H]^+$ calcd for $C_{27}H_{48}NO$ 402.3730, found 402.3734.

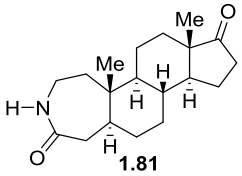

1.81

17β-Hydroxy-5α-androstane-derived A-Ring Lactam, 1.81. A solution of **1.76** (87.0 mg, 0.200 mmol) and sodium hydride (60% dispersion in mineral oil, 38.0 mg, 1.60 mmol, 4.8 equiv) in anhydrous THF (8.0 mL) was heated at 65 ˚C for 2 h. The reaction was cooled to room temperature and quenched with a saturated solution of NH_4Cl (5 mL). The reaction mixture was diluted with CH_2Cl_2 (20 mL) and washed with saturated solution of NH_4Cl (2 x 5 mL), H_2O (5 mL) and brine (5 mL). The combined organic layer was dried over anhydrous Na_2SO_4 filtered, and concentrated. The crude residue was purified by an automated MPLC system using a 12 g normal phase silica column with gradient elution from 0–5% MeOH/CH_2Cl_2. Concentration of solvents afforded product **1.76** as white amorphous solid (44.0 mg, 0.145 mmol, 73% yield, UPLC/HRMS purity: ≥99.5%). R_f = 0.25 (3% MeOH/CH_2Cl_2); mp 283–285 ˚C; IR (neat) 3303, 3219, 1736, 1668 cm^{-1}. ^1H NMR (400 MHz, $CDCl_3$) δ 5.77 (br s, 1H), 3.40 (ddd, *J* = 15.9, 11.8, 4.4 Hz, 1H), 3.00 (m, 1H), 2.77 (dd, *J* = 14.3, 11.0 Hz, 1H), 2.44 (dd, *J* = 19.4, 8.8 Hz, 1H), 2.08 (m, 1H), 1.97–1.78 (complex, 4H), 1.70 (m, 1H), 1.60–1.22 (complex, 10H), 1.03 (m, 1H), 0.94 (s, 3H), 0.89–0.78 (complex, 5H, contains s, 0.86, 3H); ^{13}C NMR (151 MHz, $CDCl_3$) δ 221.0, 178.3, 54.3, 51.5, 47.6, 43.4, 42.2, 39.7, 39.2, 38.0, 36.0, 34.4, 31.7, 31.0, 30.8, 21.9, 20.7, 13.9, 12.1. HRMS (FT-ICR, HESI) *m/z*: $[M + H]^+$ calcd for $C_{19}H_{20}NO_2$ 304.2271, found 304.2267.

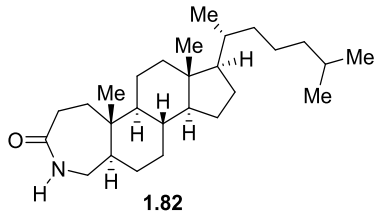

1.82

5α-Cholestane-derived A-Ring Lactam, 1.82. A solution of **1.78** (88.6 mg, 0.166 mmol) and sodium hydride (60% dispersion in mineral oil, 35.0 mg, 0.879 mmol, 5.3 equiv) in anhydrous THF (14.0 mL) was heated at 65 ˚C for 2 h. The reaction was cooled to room temperature and quenched with a saturated solution of NH_4Cl (5 mL). The reaction mixture was

diluted with CH_2Cl_2 (20 mL) and washed with saturated solution of NH_4Cl (2 x 5 mL), H_2O (5 mL) and brine (5 mL). The combined organic layer was dried over anhydrous Na_2SO_4 filtered, and concentrated. The crude residue was purified by an automated MPLC system using a 12 g normal phase silica column with gradient elution from 0–5% MeOH/CH_2Cl_2. Concentration of solvents afforded product **1.82** as white amorphous solid (51.7 mg, 0.129 mmol, 78% yield). R_f = 0.28 (3% MeOH/CH_2Cl_2); mp 301–304 ˚C (decomposed); IR (neat) 3190, 1672, 1627 cm^{-1}; ^1H NMR (400 MHz, $CDCl_3$) δ 5.60 (br s, 1H), 3.37 (m, 1H), 2.63–2.50 (m, 2H), 2.25 (m, 1H), 1.98 (m, 1H), 1.92–1.77 (m, 2H), 1.69 (m, 1H), 1.60–1.48 (m, 3H), 1.38–0.93 (complex, 18H), 0.90–0.85 (complex, 13H), 0.73 (m, 1H), 0.65 (s, 3H); ^{13}C NMR (101 MHz, $CDCl_3$) δ 178.7, 56.6, 56.4, 53.9, 49.8, 44.7, 42.5, 40.1, 39.7, 38.8, 36.3, 35.9, 35.4, 35.2, 31.9, 31.5, 28.4, 28.2, 27.9, 24.3, 24.0, 23.0, 22.7, 21.2, 18.8, 12.20, 12.18. HRMS (FT-ICR, ESI) *m/z*: $[M + H]^+$ calcd for $C_{27}H_{48}NO$ 402.3730, found 402.3732.

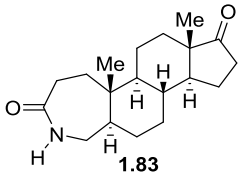

1.83

17β-Hydroxy-5α-androstane-derived A-Ring Lactam, 1.83. A solution of **1.79** (87.0 mg, 0.200 mmol) and sodium hydride (60% dispersion in mineral oil, 38.0 mg, 1.60 mmol, 4.8 equiv) in anhydrous THF (8.0 mL) was heated at 65 ˚C for 2 h. The reaction was cooled to room temperature and quenched with a saturated solution of NH_4Cl (5 mL). The reaction mixture was diluted with CH_2Cl_2 (20 mL) and washed with saturated solution of NH_4Cl (2 x 5 mL), H_2O (5 mL) and brine (5 mL). The combined organic layer was dried over anhydrous Na_2SO_4 filtered, and concentrated. The crude residue was purified by an automated MPLC system using a 12 g normal phase silica column with gradient elution from 0–4% MeOH/CH_2Cl_2. Concentration of

solvents afforded product **1.83** as white amorphous solid (46.7 mg, 0.153 mmol, 76% yield, UPLC/HRMS purity: ≥99.5%). R_f = 0.25 (4% MeOH/CH_2Cl_2); mp decomposed; IR (neat) 3202, 3091, 1732, 1647 cm^{-1}. ^1H NMR (400 MHz, $CDCl_3$) δ 6.02 (br s, 1H), 3.39 (m, 1H), 2.60 (m, 2H), 2.44 (dd, *J* = 19.2, 8.9 Hz, 1H), 2.27 (m, 1H), 2.07 (m, 1H), 1.96–1.21 (complex, 16H), 1.00–0.79 (complex, 5H, contains s, 0.94, 3H; s, 0.86, 3H); ^{13}C NMR (151 MHz, $CDCl_3$) δ 220.9, 178.5, 54.0, 51.5, 49.8, 47.6, 44.6, 39.0, 36.0, 35.4, 34.8, 31.7, 31.4, 30.7, 27.6, 21.9, 20.4, 13.9, 12.2. HRMS (FT-ICR, HESI) *m/z*: $[M + H]^+$ calcd for $C_{19}H_{30}NO_2$ 304.2271, found 304.2270.

1.6.4 Experimental Section for 1.4

Experimental section for 1.4.1

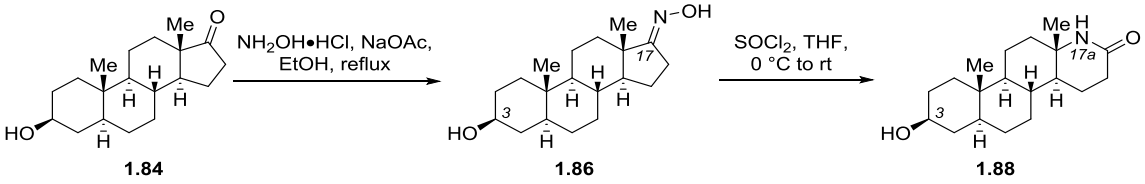

1.84 **1.86** **1.88**

Synthesis of 1.88

Intermediate **1.86** was prepared following a previously published procedure[94, 123]. Characterization data were consistent with reported data.[124] UPLC/HRMS purity: ≥99.5%.

3β-Hydroxy-5α-androstane-derived D-Ring Lactam, 1.88.[125] Following the literature procedure[44], to a solution of **1.86** (106 mg, 0.349 mmol) in anhydrous THF (7.0 mL, 0.05 M) at 0 ˚C was added $SOCl_2$ (0.25 mL, 10.0 equiv). The reaction mixture was stirred for 2 h at 0 ˚C, and stirred at room temperature overnight. The reaction mixture was terminated with a saturated aqueous solution of $NaHCO_3$ (20 mL) and H_2O (15 mL). The aqueous layer was extracted with

CH_2Cl_2, and the combined organic layers were washed with a solution of saturated $NaHCO_3$, H_2O, brine, dried over Na_2SO_4, filtered, and concentrated. Purification was carried out by an automated MPLC system using a 12 g normal phase silica column with gradient elution of 0–5% MeOH/CH_2Cl_2. Concentration of appropriate fractions afforded product as a cream-colored amorphous solid (53.0 mg, 0.174 mmol, 50% yield, UPLC/HRMS purity: ≥99.5%). R_f = 0.19 (3% MeOH/CH_2Cl_2); mp 286–294 ˚C (decomposed); IR (neat) 3155, 3038, 1654 cm^{-1}; ^1H NMR (400 MHz, $CDCl_3$) δ 6.18 (s, 1H), 3.59 (m, 1H), 2.50–2.29 (m, 2H), 2.24 (br s, 1H), 1.95–1.76 (m, 3H), 1.73–1.63 (m, 3H), 1.59 (m, 1H), 1.50–1.16 (complex, 9H), 1.17–1.07 (complex, 4H, contains s, 1.14, 3H), 1.02–0.80 (complex, 3H), 0.79 (s, 3H); ^{13}C NMR (101 MHz, $CDCl_3$) δ 172.2, 71.2, 54.79, 53.82, 47.8, 44.4, 40.2, 38.0, 36.9, 35.9, 35.7, 31.5, 30.9, 30.6, 28.5, 22.3, 21.3, 19.9, 12.4. HRMS (FT-ICR, HESI) *m/z*: $[M + H]^+$ calcd for $C_{19}H_{32}NO_2$ 306.2428, found 306.2424.

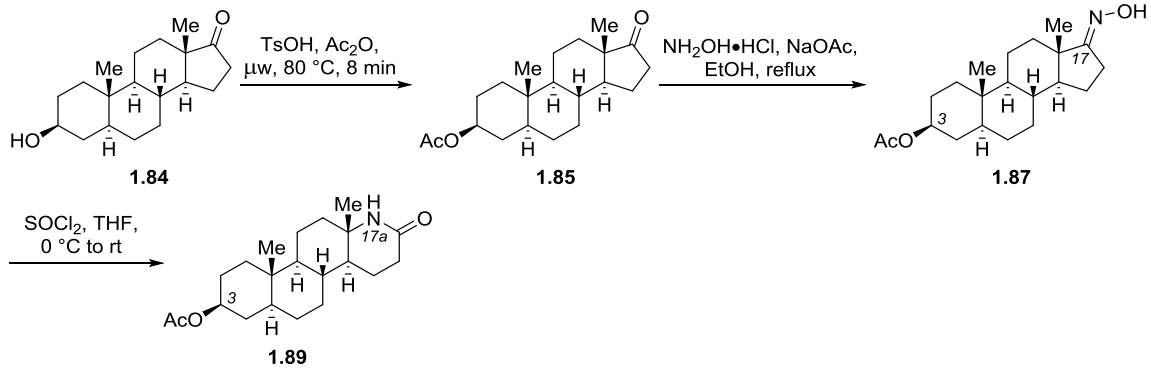

1.84 **1.85** **1.87** **1.89**

Synthesis of 1.89

Intermediate **1.85** was prepared and characterization data were consistent with reported data.[126]

3β-Acetoxy-5α-hydroxyandrostan-17-one Oxime, 1.87. Intermediate **1.87** was prepared following a previously published procedure[94, 123] as described. To a solution of **1.85** (598 mg, 1.80 mmol), NH_2OH•HCl (500 mg, 7.20 mmol, 4.0 equiv), NaOAc (591 mg, 7.20 mmol, 4.0 equiv) in anhydrous EtOH (9.0 mL, 0.2 M) was refluxed for 6 h. EtOH was removed under a stream of nitrogen, and the residual crude was dissolved in H_2O (40 mL). The aqueous layer was extracted with Et_2O (3 x 15 mL), filtered, and concentrated. Purification was carried by an automated MPLC system using a 24 g normal phase silica column with gradient elution of 0–30% EtOAc/hexanes. Concentration of fractions afforded product as a white amorphous solid (548 mg, 1.58 mmol, 88% yield, UPLC/HRMS purity: ≥99.5%). R_f = 0.44 (30% EtOAc/hexanes); mp 186–188 ˚C; IR (neat) 3456, 1714 cm^{-1}; ^1H NMR (400 MHz, $CDCl_3$) δ 4.68 (m, 1H), 2.62–2.45 (m, 2H), 2.03–1.99 (complex, 4H, contains s, 2.02, 3H), 1.86–1.80 (m, 3H), 1.76–1.71 (m, 2H), 1.67–1.59 (m, 2H), 1.55–1.15 (complex, 9H), 1.09–0.91 (complex, 5H, contains s, 0.93, 3H), 0.84 (s, 3H), 0.76–0.70 (m, 1H); ^{13}C NMR (101 MHz, $CDCl_3$) δ 173.9, 170.8, 73.7, 54.3, 54.0, 44.7, 36.8, 35.8, 34.9, 34.1, 33.9, 31.5, 28.4, 27.6, 26.1, 23.1, 21.6, 20.8, 17.1, 12.3. **Note**: Missing one carbon signal due to signal overlap. HRMS (FT-ICR, HESI) *m/z*: $[M + H]^+$ calcd for $C_{21}H_{34}NO_3$ 348.2533, found 348.2528.

3β-Hydroxy-5α-androstane-derived D-Ring Lactam, 1.89. Following a literature procedure[44], to a solution of **1.87** (139 mg, 0.400 mmol) in anhydrous THF (5.0 mL) at 0 ˚C was added $SOCl_2$ (0.29 mL, 10.0 equiv). The reaction mixture was stirred for 2 h at 0 ˚C, and stirred at room temperature overnight. The reaction mixture was terminated with saturated aqueous solution of $NaHCO_3$ (20 mL) and H_2O (15 mL). The aqueous layer was extracted with CH_2Cl_2, and the combined organic layers were washed with a solution of saturated $NaHCO_3$, H_2O, brine,

dried over Na_2SO_4, filtered, and concentrated. Purification was carried out by an automated MPLC system using a 12 g normal phase silica column with gradient elution of 0–2% MeOH/CH_2Cl_2. Concentration of fractions afforded product as a cream-colored amorphous solid (60.9 mg, 0.175 mmol, 44% yield, UPLC/HRMS purity: 98.0%). R_f = 0.25 (2% MeOH/CH_2Cl_2); mp decomposed; IR (neat) 3186, 3055, 1731, 1673 cm^{-1}; ^1H NMR (400 MHz, $CDCl_3$) δ 5.91 (br s, 1), 4.69 (m, 1H), 2.50–2.30 (m, 2H), 2.02 (s, 3H), 1.96–1.61 (complex, 7H), 1.55–1.17 (complex, 10H), 1.15 (s, 3H), 1.04 (m, 1H), 0.96–0.79 (complex, 5H, contains s, 0.81, 3H); ^{13}C NMR (101 MHz, $CDCl_3$) δ 172.0, 170.8, 73.5, 54.70 53.7, 47.7, 44.3, 40.2, 36.6, 35.9, 35.7, 33.9, 30.8, 30.7, 28.4, 27.5, 22.4, 21.6, 21.3, 19.9, 12.3. HRMS (FT-ICR, HESI) *m/z*: $[M + H]^+$ calcd for $C_{21}H_{34}NO_3$ 348.2533, found 348.2532.

Experimental section for 1.4.2

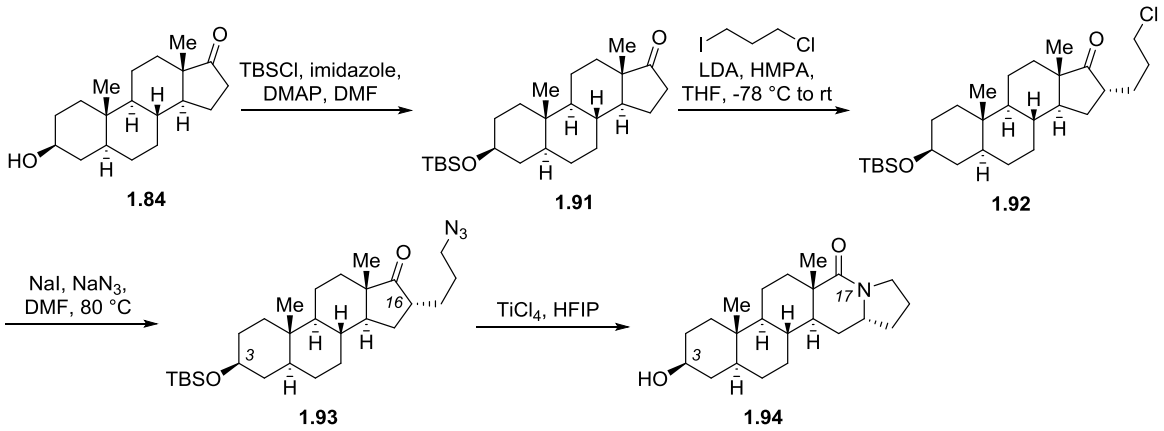

1.84 **1.91** **1.92** **1.93** **1.94**

Synthesis of 1.94

Intermediate 3β-(*tert*-butyldimethylsilyl)oxy)-epiandrosterone **1.91** was prepared following a previously published procedure.[127-128] Characterization data were consistent with reported data (mp 162–164 °C).[124, 127]

3β-((*tert*-Butyldimethylsilyl)oxy)-16α-(3′-chloropropyl)-5α-androstan-17-one, 1.92. Following a literature procedure[107], **1.92** was prepared as described: To a cooled 1.0 M LDA solution (260 μL, 1.82 mmol, 1.2 equiv) in anhydrous THF (15.0 mL, 0.1 M) at –78 ˚C was added **1.91** (609 mg, 1.51 mmol) cautiously. The reaction mixture was allowed to –10 ˚C and stirred for 1 h. To the pale yellow solution, HMPA (1.10 mL, 6.32 mmol, 4.2 equiv) was added followed by 1-chloro-3-iodopropane (240 μL, 2.24 mmol, 1.5 equiv). The pale yellow solution was stirred at –10 ˚C for 1 h, warmed to room temperature, and stirred overnight. The reaction mixture was quenched with a solution of saturated NH_4Cl (40 mL) and H_2O (20 mL). The aqueous layer was extracted with Et_2O (3 × 30 mL). The combined organic layer was washed with brine (15 mL), dried over Na_2SO_4, filtered, and concentrated. Purification was carried out by an automated MPLC system using a 24 g normal phase silica column with gradient elution of 0–40% CH_2Cl_2/hexanes. Fractions containing mixtures of **1.91** and **1.92** were subjected to a second automated purification using the same gradient. Concentration of fractions afforded product as a white amorphous solid (578 mg, 1.20 mmol, 80% yield). R_f = 0.80 (100% CH_2Cl_2); R_f = 0.58 (30% CH_2Cl_2/hexanes); IR (neat) 1736 cm^{-1}; ^1H NMR (400 MHz, $CDCl_3$) δ 3.58–3.48 (m, 3H), 2.42 (m, 1H), 1.93–1.16 (complex, 18H), 1.08 (m, 1H), 0.99–0.77 (complex, 19H, contains s, 0.89, 3H; s, 0.88, 9H; s, 0.82, 3H), 0.66 (m, 1H), 0.05 (s, 6H); ^{13}C NMR (101 MHz, $CDCl_3$) δ 222.1, 72.1, 54.7, 49.5, 48.7, 45.2, 45.0, 44.2, 38.8, 37.3, 35.9, 35.2, 32.0, 31.9, 31.3, 31.0, 28.8, 28.6, 28.0, 26.1 (3C), 20.5, 18.4, 14.7, 12.5, -4.4 (2C). HRMS (FT-ICR, APCI) *m/z*: $[M + H]^+$ calcd for $C_{22}H_{50}ClO_2Si$ 481.3263, found 481.3259.

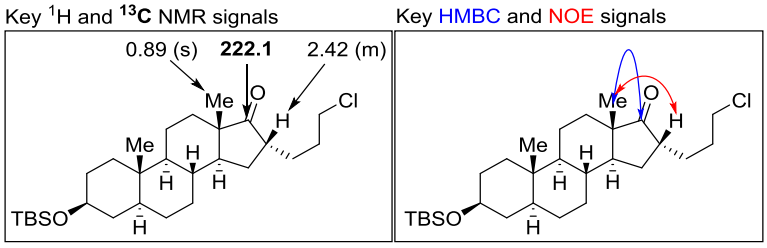

16α-(3′-Azidopropyl)-3β-((*tert*-butyldimethylsilyl)oxy)-5α-androstan-17-one, 1.93. Following a literature procedure[107], **1.93** was prepared as described. A mixture of **1.92** (482 mg, 1.00 mmol), NaI (300 mg, 2.00 mmol, 2.0 equiv), NaN_3 (195 mg, 3.00 mmol, 3.0 equiv) in anhydrous DMF (10.0 mL, 1.0 M) was stirred at 80 ˚C overnight. The reaction mixture was quenched with H_2O (50 mL). The aqueous layer was extracted with Et_2O (3 × 30 mL). The combined organic layer was washed with H_2O (3 × 15 mL), brine (15 mL), dried over Na_2SO_4, filtered, and concentrated. Purification was carried out by an automated MPLC system using a 24 g normal phase silica column with gradient elution of 0–6% EtOAc/hexanes. Concentration of fractions afforded product as a white amorphous solid (433 mg, 0.887 mmol, 89% yield) containing a minor unidentified impurity. The intermediate was used in the next step without further purification. R_f = 0.36 (4% EtOAc/hexanes); mp 82–86 ˚C; IR (neat) 2092, 1733 cm^{-1}; ^{1}H NMR (400 MHz, $CDCl_3$) δ 3.54 (m, 1H), 3.33–3.20 (m, 2H), 2.41 (m, 1H), 1.82–1.16 (complex, 18H), 1.08 (m, 1H), 0.99–0.87 (complex, 16H, contains s, 0.89, 3H; s, 0.88, 9H), 0.82 (s, 3H), 0.66 (m, 1H), 0.05 (s, 6H); ^{13}C NMR (101 MHz, $CDCl_3$) δ 222.0, 72.1, 54.7, 51.5, 49.5, 48.6, 45.2, 44.4, 38.7, 37.3, 35.8, 35.2, 32.0, 31.9, 31.0, 28.6, 28.5, 27.9, 27.6, 26.1 (3C), 20.5, 18.4, 14.7, 12.5, -4.397, -4.405. HRMS (FT-ICR, APCI) *m/z*: $[M - N_2 + H]^+$ calcd for $C_{22}H_{50}N_3O_2Si$ 460.3605, found 460.3600.

3β-Hydroxy-5α-androstane-derived D-Ring Lactam, 1.94. Following a literature procedure[107], **1.94** was prepared as described. To a solution of **1.93** (48.5 mg, 0.099 mmol) in HFIP (0.5 mL) at 0 ˚C under nitrogen atmosphere was added $TiCl_4$ (1.0 M in CH_2Cl_2, 149 μL, 0.149 mmol, 1.5 equiv). The vial was capped, and the reaction mixture was stirred at room temperature for 24 h. The reaction mixture was concentrated under a stream of nitrogen. The residue was diluted with CH_2Cl_2, washed with a solution of saturated NH_4Cl (2 × 5 mL), solution of saturated $NaHCO_3$ (5 mL), brine (5 mL), dried over Na_2SO_4, filtered, and concentrated. Purification was carried out by an automated MPLC system using a 12 g normal phase silica column with gradient elution of 0–4% MeOH/CH_2Cl_2. Concentration of fractions afforded product as a white amorphous solid (28.7 mg, 0.083 mmol, 84% yield, UPLC/HRMS purity: 96.5%). R_f = 0.25 (2% MeOH/CH_2Cl_2); mp 199–209 ˚C; IR (neat) 3393, 1621 cm^{-1}; ^1H NMR (400 MHz, $CDCl_3$) δ 3.63–3.51 (m, 3H), 3.37 (m, 1H), 2.12–2.01 (m, 2H), 1.93–1.54 (complex, 9H), 1.51–1.16 (complex, 9H), 1.12–0.93 (complex, 5H, contains s, 1.03, 3H), 0.90–0.79 (complex, 4H, contains s, 0.79, 3H), 0.65 (m, 1H); ^{13}C NMR (101 MHz, $CDCl_3$) δ 176.3, 71.4, 53.9, 53.2, 44.7, 44.3, 43.3, 40.3, 38.1, 37.2, 36.9, 35.6, 35.5, 33.9, 31.6, 31.2, 28.7, 28.5, 22.1, 20.2, 15.3, 12.4. HRMS (FT-ICR, HESI) *m/z*: $[M + H]^+$ calcd for $C_{22}H_{36}NO_2$ 346.2741, found 346.2737.

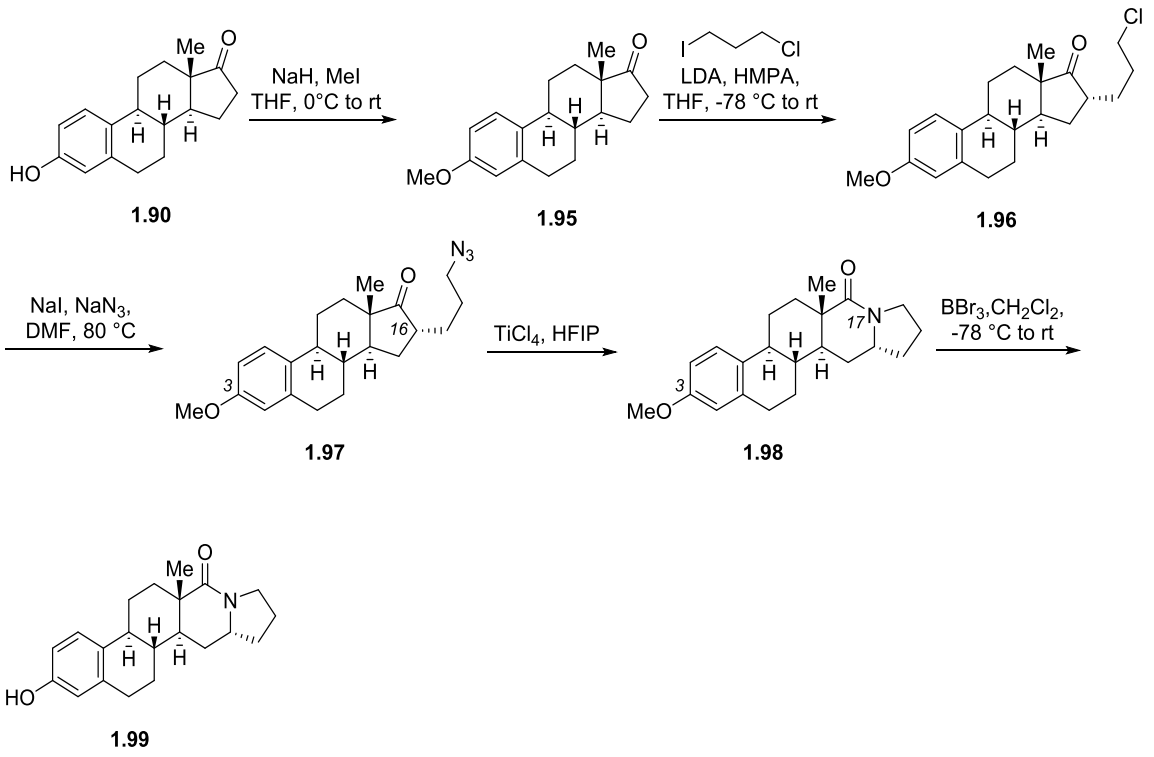

1.90 **1.95** **1.96**

1.97 **1.98**

1.99

Synthesis of 1.99

Intermediate **1.95** was prepared following a previously published procedure.[129] Characterization data were consistent with reported data (mp 168–173 ˚C).[129-130]

16α-(3′-Chloropropyl)-3-methoxy-estrone, 1.96. Following a literature procedure, **1.96** was prepared as described. To a cooled 1.0 M LDA solution (260 µL, 1.82 mmol, 1.2 equiv) in anhydrous THF (20.0 mL) at –78 ˚C was added mestrone **1.95** (425 mg, 1.50 mmol) cautiously. The reaction mixture was allowed to –10 ˚C and stirred for 1 h. To the pale yellow solution, HMPA (1.10 mL, 6.32 mmol, 4.2 equiv) was added followed by 1-chloro-3-iodopropane (240 µL, 2.24 mmol, 1.5 equiv). The pale yellow solution was stirred at –10 ˚C for 1 h, warmed to room temperature, and stirred overnight. The reaction mixture was quenched with a solution of saturated NH_4Cl (40 mL) and H_2O (20 mL). The aqueous layer was extracted with Et_2O (3 × 30

mL). The combined organic layer was washed with brine (15 mL), dried over Na_2SO_4, filtered, and concentrated. Purification was carried out by an automated MPLC system using a 24 g normal phase silica column with gradient elution of 0–10% Et_2O/hexanes. Fractions containing mixtures of **1.95** and **1.96** were subjected to a second automated purification using the same gradient. Concentration of appropriate fractions afforded desired product as a yellow oil/solid (426 mg, 1.17 mmol, 78% yield) containing a minor unidentified impurity. The intermediate was used in the next step without further purification. R_f = 0.40 (10% EtOAc/hexanes); IR (neat) 1730 cm^{-1}; ^1H NMR (400 MHz, $CDCl_3$) δ 7.20 (m, 1H), 6.73 (dd, *J* = 8.6, 2.8 Hz, 1H), 6.65 (d, *J* = 2.8 Hz, 1H), 3.78 (s, 3H), 3.61–3.46 (m, 2H), 2.92–2.89 (m, 2H), 2.49 (m, 1H), 2.39 (m, 1H), 2.25 (m, 1H), 2.01–1.82 (complex, 5H), 1.79–1.71 (m, 1H), 1.66–1.38 (complex, 7H), 0.95 (s, 3H). ^{13}C NMR (101 MHz, $CDCl_3$) δ 221.6, 157.7, 137.9, 132.1, 126.5, 114.0, 111.7, 55.4, 48.8, 48.4, 44.9, 44.3, 44.1, 38.5, 31.8, 31.4, 30.0, 28.8, 27.8, 26.6, 26.0, 14.8. HRMS (FT-ICR, APCI) *m/z*: $[M + H]^+$ $C_{22}H_{30}ClO_2$ calcd for $[M + H]^+$ 361.1929, found 361.1929.

16α-(3′-Azidopropyl)-3-methoxy-estrone, 1.97. Following a literature procedure[107], **1.97** was prepared as described. A mixture of **1.96** (419 mg, 1.16 mmol), NaI (348 mg, 2.32 mmol, 2.0 equiv), NaN_3 (226 mg, 3.48 mmol, 3.0 equiv) in anhydrous DMF (12.0 mL, 1.0 M) was stirred at 80 ˚C overnight. The reaction mixture was quenched with H_2O (50 mL). The aqueous layer was extracted with Et_2O (3 × 30 mL). The combined organic layer was washed with H_2O (3 × 15 mL), brine (15 mL), dried over Na_2SO_4, filtered, and concentrated. Purification was carried out by an automated MPLC system using a 24 g normal phase silica column with gradient elution of 0–10% EtOAc/hexanes. Concentration of fractions afforded desired product as a white oil (391 mg, 1.06 mmol, 92% yield) containing a minor unidentified impurity. The

intermediate was used in the next step without further purification. R_f = 0.29 (10% EtOAc/hexanes); IR (neat) 2091, 1733 cm^{-1}; ^1H NMR (400 MHz, $CDCl_3$) δ 7.20 (d, *J* = 8.6 Hz, 1H), 6.72 (dd, *J* = 8.6, 2.8 Hz, 1H), 6.65 (d, *J* = 2.7 Hz, 1H), 3.78 (s, 3H), 3.36–3.24 (m, 2H), 2.92–2.89 (m, 2H), 2.49 (m, 1H), 2.39 (m, 1H), 2.25 (m, 1H), 2.02–1.32 (complex, 13H), 0.95 (s, 3H). ^{13}C NMR (101 MHz, $CDCl_3$) δ 221.6, 157.7, 137.9, 132.1, 126.5, 114.0, 111.7, 55.4, 51.5, 48.8, 48.4, 44.5, 44.1, 38.5, 31.8, 29.8, 28.5, 27.72, 27.68, 26.6, 26.0, 14.7. HRMS (FT-ICR, HESI) *m/z*: $[M - N_2 + H]^+$ calcd for $C_{22}H_{30}N_3O_2$ 340.2271, found 340.2267.

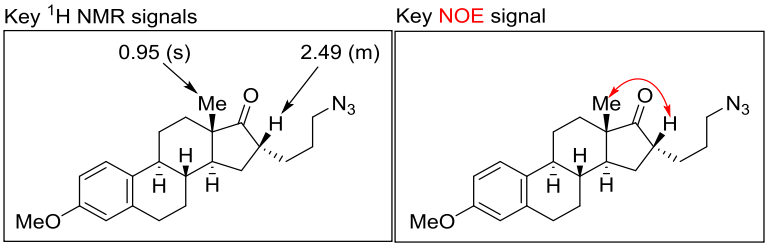

3-Methoxy-1,3,5-estratriene-derived D-Ring Lactam, 1.98. Following a literature procedure[107], **1.98** was prepared as described. To a solution of **1.97** (95.7 mg, 0.260 mmol) in HFIP (2.0 mL) at 0 ˚C under nitrogen atmosphere was added $TiCl_4$ (1.0 M in CH_2Cl_2, 130 µL, 0.130 mmol, 0.5 equiv). The vial was capped, and the reaction mixture was stirred at room temperature for 24 h. The reaction mixture was concentrated under nitrogen. The residue was diluted with CH_2Cl_2, washed with a solution of saturated NH_4Cl (2 × 8 mL), solution of saturated $NaHCO_3$ (8 mL), brine (8 mL), dried over Na_2SO_4, filtered, and concentrated. Purification was carried out by an automated MPLC system using a 12 g normal phase silica column with gradient elution of 0–70% EtOAc/hexanes. Concentration of fractions afforded product as a white amorphous solid (61.3 mg, 0.181 mmol, 69% yield, UPLC/HRMS purity: 97.7%). R_f = 0.25 (50% EtOAc/hexanes); mp 144–149 ˚C; IR (neat) 1612 cm^{-1}; ^1H NMR (400 MHz, $CDCl_3$) δ 7.24 (d, *J* = 8.7 Hz, 1H), 6.73 (dd, *J* = 8.6, 2.8 Hz, 1H), 6.62 (d, *J* = 2.7 Hz, 1H), 3.78 (s, 3H),

3.61 (m, 2H), 3.41 (m, 1H), 2.85 (m, 2H), 2.37 (m, 1H), 2.27–2.11 (m, 2H), 2.05–1.89 (m, 3H), 1.81–1.68 (m, 3H), 1.58–1.24 (complex, 6H), 1.08 (s, 3H); ^{13}C NMR (101 MHz, $CDCl_3$) δ 176.3, 157.7, 137.7, 132.4, 126.6, 113.7, 111.8, 55.4, 54.0, 44.9, 42.7, 42.0, 40.7, 40.4, 35.6, 33.9, 30.2, 28.4, 26.6, 26.0, 22.2, 15.2. HRMS (FT-ICR, HESI) *m/z*: $[M + H]^+$ calcd for $C_{22}H_{30}NO_2$ 340.2271, found 340.2269.

3-Hydroxy-1,3,5-estratriene-derived D-Ring Lactam, 1.99. To a solution of **1.98** (51.5 mg, 0.152 mmol) in anhydrous CH_2Cl_2 (5.0 mL) at –78 ˚C was added BBr_3 (1.0 M in CH_2Cl_2, 1.20 mL, 1.20 mmol, 8.0 equiv). The reaction mixture was stirred at –78 ˚C for 1 h, warmed to room temperature over 4 h, and continued stirring at room temperature for 1 h (pinkish-orange suspension). The reaction mixture was quenched with two drops of water and MeOH (2 mL). The solvent was removed under nitrogen, the residue was redissolved in MeOH, and loaded on silica gel for purification. Purification was carried out by an automated MPLC system using a 12 g normal phase silica column with gradient elution of 0–3% MeOH/CH_2Cl_2. Concentration of fractions afforded **1.99** as a white amorphous solid (38.1 mg, 0.117 mmol, 77% yield, UPLC/HRMS purity: ≥99.5%). R_f = 0.20 (2% MeOH/CH_2Cl_2); mp 283–300 ˚C (decomposed); IR (neat) 3303, 1621, 1606 cm^{-1}; ^{1}H NMR (600 MHz, DMSO-d_6) δ 8.99 (s, 1H), 7.07 (d, J = 8.5 Hz, 1H), 6.51 (d, J = 9.4 Hz, 1H), 6.43 (m, 1H), 3.59 (m, 1H), 3.40 (m, 1H), 3.20 (m, 1H), 2.70 (m, 2H), 2.27 (m, 1H), 2.09 (m, 2H), 1.93 (m, 3H), 1.81 (m, 1H), 1.67 (m, 2H), 1.56–1.37 (m, 2H), 1.29–1.18 (m, 4H), 0.98 (s, 3H); ^{13}C NMR (151 MHz, DMSO-d_6) δ 174.6, 155.0, 137.0, 130.1, 126.1, 114.6, 112.8, 53.1, 44.1, 42.1, 41.3, 40.0934, 40.0933, 34.8, 33.9, 29.4, 27.5, 25.9, 25.6, 21.5, 14.9. HRMS (FT-ICR, HESI) *m/z*: $[M + H]^+$ calcd for $C_{21}H_{28}NO_2$ 326.2115, found 326.2111.

Experimental section for 1.4.3

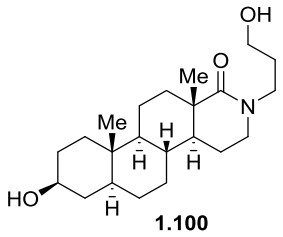

1.100

3β-Hydroxy-5α-androstane-derived D-Ring Lactam, 1.100. Following the general procedure E, 3-azidopropanol **1.1 (**30.3 mg, 0.300 mmol, 2.0 equiv) was reacted with *trans*-androsterone **1.84** (43.6 mg, 0.150 mmol) to give **1.100** as a white amorphous solid (51.0 mg, 0.141 mmol, 94% yield, UPLC/HRMS purity: ≥99.5%). Purification was carried out by an automated MPLC system using a 12 g normal phase silica column with gradient elution from 0–5% MeOH/CH_2Cl_2. R_f = 0.35 (5% MeOH/CH_2Cl_2); mp 177–181 ˚C; IR (neat) 3237, 1625 cm^{-1}; ^1H NMR (400 MHz, $CDCl_3$) δ 3.69–3.55 (m, 2H), 3.49–3.39 (m, 2H), 3.32–3.17 (m, 3H), 2.60 (br s, 2H), 2.19 (m, 1H), 1.94 (m, 1H), 1.89–1.22 (complex, 17H), 1.13–1.06 (m, 4H, contains s, 1.12, 3H), 1.00–0.93 (m, 1H), 0.91–0.62 (m, 1H), 0.80 (s, 3H), 0.68 (m, 1H); ^{13}C NMR (101 MHz, $CDCl_3$) δ 178.3, 71.3, 57.9, 53.4, 47.1, 45.9, 44.4, 43.0, 41.3, 38.1, 36.8, 35.7, 34.8, 34.6, 31.6, 31.0, 29.3, 28.6, 21.0, 20.3, 18.6, 12.4. **Note**: X-ray crystal structure of this analog is provided in the CCDC (CCDC 1583536). HRMS (FT-ICR, HESI) *m/z*: $[M + H]^+$ calcd for $C_{22}H_{38}NO_3$ 364.2846, found 364.2840.

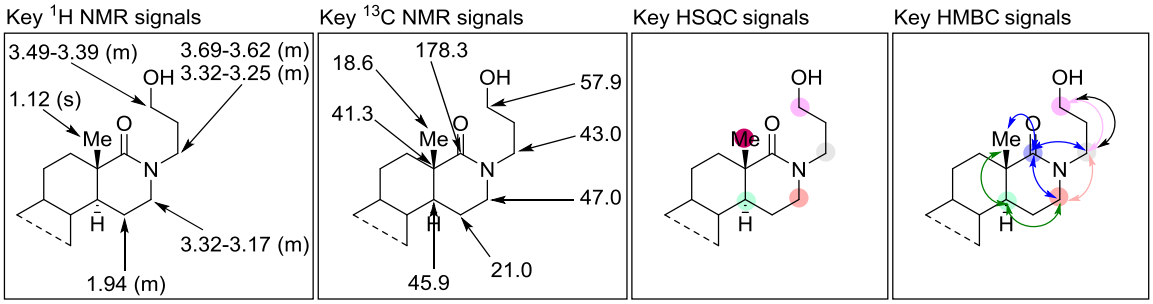

Table 1.10. Selected crystallographic and refinement parameters for **1.100**.

compound	**1.100**
CCDC deposition number	1583536
empirical formula	$C_{22}H_{37}NO_3$
formula weight	363.53
temperature	100(2) K
wavelength Å	1.54178 Å
crystal system	orthorhombic
space group	P 2(1)2(1)2(1)
unit cell dimensions	a = 6.8941(7) Å, α = 90°
	b = 11.1491(12) Å, β = 90°
	c = 25.762(3) Å, γ = 90°
Z	4
volume	1980.1(4) $Å^3$
density	1.219 Mg/m^3
absorption coefficient	0.624 μ mm^{-1}
F(000)	800
crystal size	0.08 × 0.07 × 0.06 mm^3
Theta range for data collection	4.32 to 68.53°
index ranges	-8<=h<=8, -12<=k<=13, -25<=l<=31
reflections collected	12012
independent reflections	3476 [R(int) = 0.0278]
completeness to theta = 66.000°	99.7%
absorption correction	multi-scan
max. and min. transmission	1.000 and 0.875
refinement method	full-matrix least-squares on F^2
data/restraints/parameters	3476/0/384
Goodness-of-fit F^2	1.047
final R indices [I>2sigma(I)]	R1 = 0.0324, wR2 = 0.0823
R indices (all data)	R1 = 0.0347, wR2 = 0.0840
absolute structure parameter	0.1(2)
extinction coefficient	0.0032(3)
largest diff. peak and hole	0.159 and -0.172 $e.Å^{-3}$

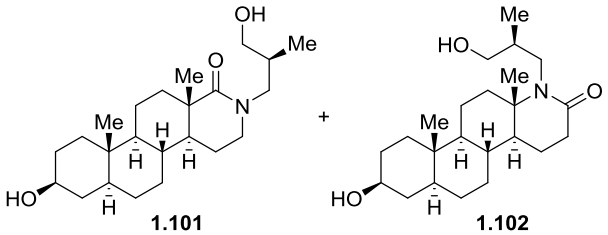

3β-Hydroxy-5α-androstane-derived D-Ring Lactams, 1.101 and 1.102. Following the general procedure E, (*S*)-3-azido-2-methylpropanol (*S*)-**1.3** (34.6 mg, 0.300 mmol, 2.0 equiv) was reacted with *trans*-androsterone **1.84** (43.7 mg, 0.151 mmol) to give **1.101** as a white

amorphous solid to afford a separable mixture of two regioisomeric lactams **1.101** (30.3 mg, 0.0803 mmol, 53% yield, UPLC/HRMS purity: 98.7%) and **1.102** (19.9 mg, 0.053 mmol, 35%, UPLC/HRMS purity: ≥99.5%). A 56:44 regioisomeric ratio was observed by ^{1}H NMR of crude reaction mixture. Purification was carried out by an automated MPLC system using a 12 g normal phase silica column with gradient elution from 0–20% EtOAc/Ether. Concentration of fractions afforded slightly impure **1.101** and **1.102**. A second purification of separated regioisomers using a 4 g column with gradient elution from 0–5% MeOH/DCM afforded pure regioisomers. **1.101**: R_f = 0.26 (50% EtOAc/Ether); IR (neat) 3440, 3283, 1632 cm^{-1}; mp 174–177 ˚C; ^{1}H NMR (400 MHz, $CDCl_3$) δ 3.65–3.53 (m, 2H), 3.35 (dd, *J* = 11.9, 3.3 Hz, 1H), 3.27 (m, 3H), 2.90 (dd, *J* = 13.9, 4.3 Hz), 2.16 (m, 1H), 1.93–1.51 (complex, 7H), 1.43–1.19 (complex. 9H), 1.10–1.03 (m, 4H, contains s, 1.10, 3H), 0.98–0.80 (m, 5H, contains d, *J* = 7.0 Hz, 3H), 0.78 (s, 3H), 0.66 (m, 1H); ^{13}C NMR (400 MHz, $CDCl_3$) δ 178.3, 71.2, 63.1, 53.3, 49.7, 48.6, 46.2, 44.4, 41.4, 38.0, 36.8, 35.7, 34.85, 34.79, 33.7, 31.5, 30.9, 28.6, 21.0, 20.3, 18.5, 15.3, 12.3. HRMS (FT-ICR, HESI) *m/z*: $[M + H]^+$ calcd for $C_{23}H_{40}NO_3$ 378.3003, found 378.2991. **1.102**: R_f = 0.11 (50% EtOAc/Ether); IR (neat) 3443, 3309, 1603 cm^{-1}; mp 196–198 ˚C; ^{1}H NMR (126 MHz, $CDCl_3$) δ 3.83 (dd, *J* = 14.8, 11.4 Hz, 1H), 3.58 (tt, *J* = 11.0, 4.8 Hz, 1H), 3.48–3.44 (m, 1H), 3.33 (dd, *J* = 11.9, 2.9 Hz, 1H) 3.03 (dd, *J* = 14.7, 4.6 Hz, 1H), 2.58–2.42 (m, 2H), 1.95 (m, 1H), 1.89 (m, 1H), 1.83–1.70 (complex, 4H), 1.58 (m, 1H), 1.52 (td, *J* = 12.8, 3.9 Hz, 1H), 1.41–1.18 (complex, 8H), 1.17 (s, 3H), 1.14–1.04 (m, 1H), 1.00–0.94 (m, 4H, contains d, *J* = 6.9 Hz, 3H), 0.91–0.80 (m, 1H), 0.76–0.71 (m, 4H, contains s, 0.76, 3H); ^{13}C NMR (126 MHz, $CDCl_3$) δ 172.3, 71.1, 62.7, 59.1, 52.7, 48.4, 44.2, 42.7, 37.9, 37.8, 37.5, 36.8, 36.1, 35.5, 31.4, 30.8, 30.2, 28.5, 21.8, 21.6, 20.1, 15.6, 12.2. HRMS (FT-ICR, HESI) *m/z*: $[M + H]^+$ calcd for $C_{23}H_{40}NO_3$ 378.3003, found 378.2986.

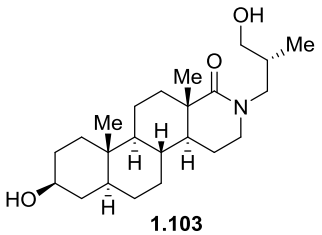

1.103

3β-Hydroxy-5α-androstane-derived D-Ring Lactam, 1.103. Following the general procedure E, (*R*)-3-azido-2-methylpropanol (*R*)-**1.3** (34.8 mg, 0.302 mmol, 2.0 equiv) was reacted with *trans*-androsterone **1.84** (43.9 mg, 0.151 mmol) to give **1.103** as a white amorphous solid (53.2 mg, 0.141 mmol, 93% yield, UPLC/HRMS purity: ≥99.5%). Purification was carried out by an automated MPLC system using a 12 g normal phase silica column with gradient elution from 0–5% MeOH/CH_2Cl_2. R_f = 0.33 (5% MeOH/CH_2Cl_2); mp 168–171 ˚C; IR (neat) 3380, 1614 cm^{-1}; ^1H NMR (400 MHz, $CDCl_3$) δ 3.89 (dd, *J* = 13.8, 11.0 Hz, 1H), 3.58 (tt, *J* = 10.7, 4.8 Hz, 1H), 3.41–3.27 (m, 3H), 3.18 (m, 1H), 2.77 (br s, 2H), 2.53 (dd, *J* = 13.9, 4.3 Hz, 1H), 2.18 (m, 1H), 1.93 (m, 1H), 1.88–1.18 (complex, 15H), 1.11–1.05 (m, 4H, contains s, 1.11, 3H), 1.00–0.96 (m, 4H, contains d, *J* = 7.0 Hz, 3H), 0.94–0.80 (m, 1H), 0.79 (s, 3H), 0.67 (m, 1H); ^{13}C NMR (101 MHz, $CDCl_3$) δ 178.2, 71.1, 63.1, 53.3, 49.1, 47.7, 45.5, 44.4, 41.3, 38.0, 36.8, 35.6, 34.7, 34.4, 33.5, 31.4, 30.9, 28.8, 21.0, 30.2, 18.5, 15.4, 12.3. HRMS (FT-ICR, HESI) *m/z*: $[M + H]^+$ calcd for $C_{23}H_{41}NO_3$ 378.3008 found 378.2995.

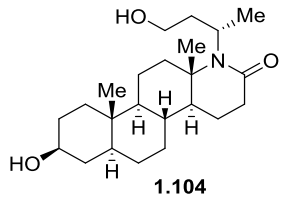

1.104

3β-Hydroxy-5α-androstane-derived D-Ring Lactam, 1.104. Following the general procedure E, (*S*)-3-azidobutanol (*S*)-**1.5** (34.6 mg, 0.300 mmol 2.0 equiv) was reacted with *trans*-androsterone **1.84** (43.6 mg, 0.150 mmol) to give **1.104** as a white amorphous solid (38.8 mg,

0.103 mmol, 69% yield, UPLC/HRMS purity: 97.2%). Purification was carried out by an automated MPLC system using a 12 g normal phase silica column with gradient elution from 0–5% MeOH/CH_2Cl_2. R_f = 0.26 (5% MeOH/CH_2Cl_2); IR (neat) 3352, 1612, 1594 cm^{-1}; mp 242–245 °C; ^1H NMR (400 MHz, $CDCl_3$) δ 3.73–3.67 (m, 2H), 3.64–3.56 (m, 2H), 2.52 (dd, *J* = 18.3, 6.5 Hz, 1H), 2.41–2.32 (m, 1H), 2.28–2.16 (m, 4H), 2.06–1.98 (m, 1H), 1.93–1.68 (complex, 4H), 1.59 (m, 1H), 1.46–1.20 (complex, 12H, contains d, *J* = 6.6 Hz, 3H), 1.18 (s, 3H), 1.14–1.06 (m, 1H), 1.02–0.83 (m, 2H), 0.78–0.71 (m, 4H, contains s, 0.78, 3H); ^{13}C NMR (101 MHz, $CDCl_3$) δ 171.6, 71.2, 61.9, 60.3, 53.1, 49.6, 48.0, 44.3, 38.5, 37.9, 37.6, 36.8, 36.2, 35.6, 33.3, 31.4, 31.0, 28.6, 21.9, 19.1, 18.9, 18.4, 12.3. HRMS (FT-ICR, HESI) *m/z*: $[M + H]^+$ calcd for $C_{23}H_{40}NO_3$ 378.3003 found 378.2995.

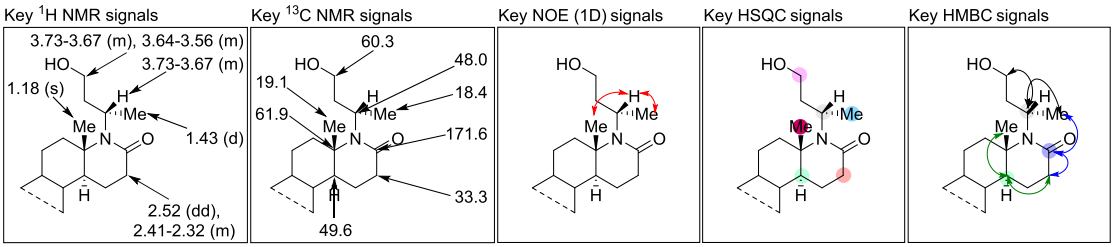

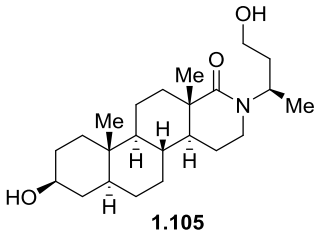

1.105

3β-Hydroxy-5α-androstane-derived D-Ring Lactam, 1.105. Following the general procedure E, (*R*)-3-azidobutanol (*R*)-**1.5** (34.4 mg, 0.299 mmol, 2.0 equiv) was reacted with *trans*-androsterone **1.84** (44.4 mg, 0.153 mmol) to give **1.105** as a white amorphous solid (52.9 mg, 0.140 mmol, 92% yield, UPLC/HRMS purity: 97.4%). Purification was carried out by an automated MPLC system using a 12 g normal phase silica column with gradient elution from 0–

4% MeOH/CH_2Cl_2. R_f = 0.31 (5% MeOH/CH_2Cl_2); mp 214–217 ˚C; IR (neat) 3380, 3291, 1596 cm^{-1}; ^1H NMR (400 MHz, $CDCl_3$) δ 4.87 (m, 1H), 3.59 (tt, *J* = 10.7, 4.8, 1H), 3.51 (ddd, *J* = 12.1, 5.0, 2.4 Hz, 1H), 3.27 (td, *J* = 11.8, 2.6, 1H), 3.19–3.03 (m, 2H), 2.59 (br s, 2H), 2.19 (m, 1H), 1.96 (m, 1H), 1.89–1.22 (complex, 16H), 1.18 (dd, *J* = 7.1 Hz, 3H), 1.13–1.05 (m, 1H), 0.97 (m, 1H), 0.91–0.82 (m, 1H), 0.80 (s, 3H), 0.68 (m, 1H); ^{13}C NMR (101 MHz, $CDCl_3$) δ 178.4, 71.3, 58.6, 53.5, 45.6, 44.5, 44.3, 41.9, 40.2, 38.1, 36.8, 36.2, 35.7, 34.7, 34.6, 31.6, 31.0, 28.6, 20.6, 20.3, 18.8, 18.4, 12.4. HRMS (FT-ICR, HESI) *m/z*: $[M + H]^+$ calcd for $C_{23}H_{40}NO_3$ 378.3003 found 378.2995.

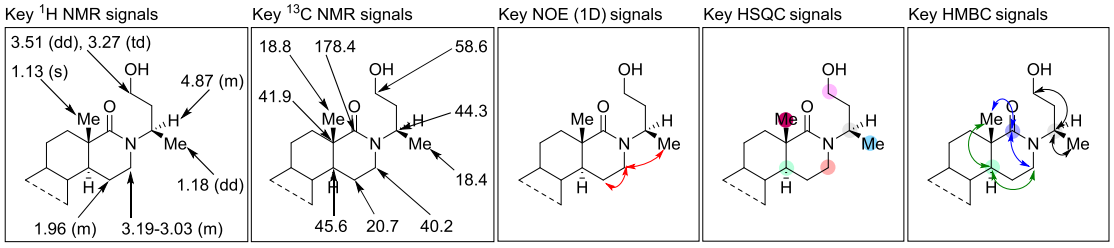

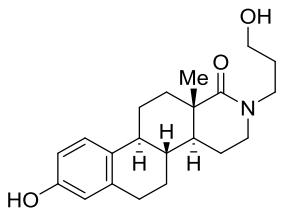

1.106

3-Hydroxy-1,3,5-estratriene-derived D-Ring Lactam, 1.106. Following the general procedure F, 3-azidopropanol **1.1** (30.5 mg, 0.302 mmol, 2.0 equiv) was reacted with estrone **1.90** (40.6 mg, 0.150 mmol) to give **1.106** as a white amorphous solid (46.7 mg, 0.136 mmol, 91% yield, UPLC/HRMS purity: ≥99.5%). Purification was carried out by an automated MPLC system using a 4 g normal phase silica column with gradient elution from 0–5% MeOH/CH_2Cl_2. R_f = 0.35 (5% MeOH/CH_2Cl_2); mp 228–235 ˚C; IR (neat) 3124, 1599 cm^{-1}; ^1H NMR (400 MHz, DMSO-d_6) δ 9.00 (s, 1H), 7.06 (d, *J* = 8.4 Hz, 1H), 6.51 (dd, *J* = 8.4, 2.6, 1H), 6.44 (d, *J* = 2.6

Hz, 1H), 3.39–3.22 (complex, 8H), 3.20–3.13 (m, 1H), 2.72 (m, 2H), 2.28 (m, 1H), 2.11 (m, 2H), 1.99 (m, 1H), 1.63–1.15 (complex, 6H), 1.02 (s, 3H); ^{13}C NMR (126 MHz, DMSO-d_6) δ 175.2, 155.0, 137.0, 130.2, 125.9, 114.6, 112.8, 58.3, 46.3, 43.9, 43.4, 42.3, 40.4, 38.1, 34.4, 29.8, 29.3, 25.7, 25.5, 20.4, 17.9. HRMS (FT-ICR, HESI) *m/z*: $[M + H]^+$ calcd for $C_{21}H_{30}NO_3$ 344.2220, found 344.2214.

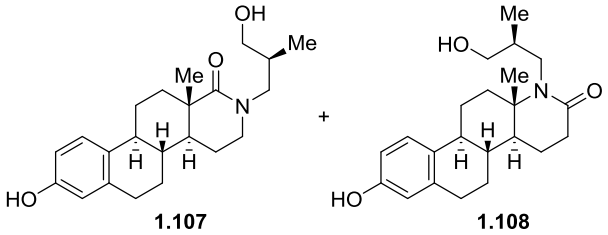

3-Hydroxy-1,3,5-estratriene-derived D-Ring Lactams, 1.107 and 1.108. Following the general procedure F, (*S*)-3-azido-2-methylpropanol (*S*)-**1.3** (46.0 mg, 0.400 mmol, 2.0 equiv) was reacted with estrone **1.90** (54.0 mg, 0.200 mmol) to afford a separable mixture of two regioisomeric lactams **1.107** (37.1 mg, 0.104 mmol, 52% yield, UPLC/HRMS purity: ≥99.5%) and **1.108** (24.2 mg, 0.068 mmol, 34% yield, UPLC/HRMS purity: ≥99.5%). A 60:40 regioisomeric ratio was observed by analytical HPLC of crude reaction mixture: Chiralpak IA, Daicel Chemical Industries, Ltd.; 0–30% EtOH/hexanes over 60 min; flow rate 1.0 mL/min; UV 220 nm; **1.107** = 40.48 min, **1.108** = 48.09 min. Purification was carried out by an automated MPLC system using a 12 g normal phase silica column with gradient elution from 0–80% EtOAc/hexanes. **1.107**: R_f = 0.48 (80% EtOAc/hexanes); mp 189–200 ˚C; IR (neat) 3197, 1615, 1602 cm^{-1}; ^{1}H NMR (400 MHz, DMSO-d_6) δ 9.00 (s, 1H), 7.06 (d, *J* = 8.4 Hz, 1H), 6.51 (dd, *J* = 8.4, 2.6 Hz, 1H), 6.44 (d, J = 2.5 Hz, 1H) 4.42 (t, *J* = 5.5 Hz, 1H), 3.37–3.19 (complex, 6H), 3.00 (dd, *J* = 13.2, 7.3 Hz, 1H), 2.72 (m, 2H), 2.27 (m, 1H), 2.17–2.08 (m, 2H), 1.98 (m, 1H), 1.88 (m, 1H), 1.65–1.15 (complex, 6H), 1.03 (s, 3H), 0.79 (dd, *J* = 6.8 Hz, 3H); ^{13}C NMR (126 MHz,

DMSO-d_6) δ 175.6, 155.0, 137.0, 130.2, 126.0, 114.7, 112.8, 63.7, 48.9, 46.9, 43.9, 42.3, 40.6, 38.2, 34.5, 33.6, 29.4, 25.8, 25.6, 20.5, 18.1, 14.9. HRMS (FT-ICR, HESI) *m/z* calcd for $C_{22}H_{32}NO_3$ $[M + H]^+$ 358.2377, found 358.2372. **1.108**: R_f = 0.29 (80% EtOAc/hexanes); mp 255–268 ˚C; IR (neat) 3135, 1569 cm^{-1}; ^1H NMR (400 MHz, DMSO-d_6) δ 9.02 (s, 1H), 7.06 (d, *J* = 8.4 Hz, 1H), 6.52 (dd, *J* = 8.4, 2.6 Hz, 1H), 6.45 (d, *J* = 2.6 Hz, 1H), 4.43 (t, *J* = 5.5 Hz, 1H), 3.38 (dd, *J* = 14.0, 8.0 Hz, 1H), 3.28–3.16 (m, 3H), 2.72 (m, 2H), 2.40–2.33 (m, 3H), 2.26 (m, 1H), 2.16 (m, 1H), 2.04–1.92 (m, 2H), 1.84 (h, *J* = 6.9, 6.2 Hz, 1H), 1.65 (m, 1H), 1.55–1.36 (m, 2H), 1.29–1.15 (m, 3H), 1.12 (s, 3H), 0.79 (d, *J* = 6.8 Hz, 3H); ^{13}C NMR (126 MHz, DMSO-d_6) δ 170.4, 155.1, 137.0, 129.9, 126.0, 114.6, 112.8, 64.3, 59.5, 46.7, 42.9, 41.8, 40.1, 37.5, 37.0, 31.0, 29.4, 26.6, 25.8, 19.5, 19.2, 15.3. HRMS (FT-ICR, HESI) *m/z*: $[M + H]^+$ calcd for $C_{22}H_{33}NO_3$ 358.2377, found 358.2370.

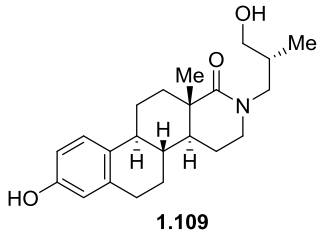

1.109

3-Hydroxy-1,3,5-estratriene-derived D-Ring Lactam, 1.109. Following the general procedure F, (*R*)-3-azido-2-methylpropanol (*R*)-**1.3** (34.5 mg, 0.300 mmol, 2.0 equiv) was reacted with estrone **1.90** (40.6 mg, 0.150 mmol) to give **1.109** as a white amorphous solid (45.8 mg, 0.128 mmol, 85% yield, UPLC/HRMS purity: 96.4%). Purification was carried out by an automated MPLC system using a 12 g normal phase silica column with gradient elution from 0–50% EtOAc/hexanes. R_f = 0.15 (50% EtOAc/hexanes); mp 219–222 ˚C; IR (neat) 3514, 1602 cm^{-1}; ^1H NMR (400 MHz, DMSO-d_6) δ 9.00 (s, 1H), 7.06 (d, *J* = 8.4 Hz, 1H), 6.51 (dd, *J* = 8.4, 2.6 Hz, 1H), 6.44 (d, 2.6 Hz, 1H), 4.37 (m, 1H), 3.36–3.16 (complex, 5H), 2.95 (dd, *J* = 13.3, 7.2

Hz, 1H), 2.72 (m, 2H), 2.28 (m, 1H), 2.17–2.09 (m, 2H), 1.99 (m, 2H), 1.88 (h, J = 6.8 Hz, 1H), 1.61–1.15 (complex, 6H), 3.02 (s, 3H), 0.81 (d, J = 6.8 Hz, 3H); ^{13}C NMR (151 MHz, DMSO-d_6) δ 175.7, 155.0, 137.0, 130.2, 126.0, 114.7, 112.8, 63.8, 49.0, 46.9, 43.8, 42.3, 40.6, 38.1, 34.5, 33.5, 29.4, 25.8, 25.6, 20.4, 18.1, 14.9. HRMS (FT-ICR, HESI) *m/z*: $[M + H]^+$ calcd for $C_{22}H_{32}NO_3$ 358.2377, found 358.2371.

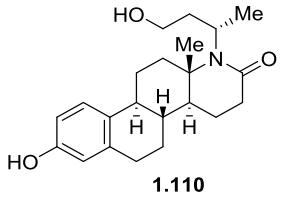

1.110

3-Hydroxy-1,3,5-estratriene-derived D-Ring Lactam, 1.110. Following the general procedure F, (*S*)-3-azidobutanol (*S*)-**1.5** (34.6 mg, 0.300 mmol, 2.0 equiv) was reacted with estrone **1.90** (40.5 mg, 0.150 mmol) to give **1.110** as an off-white amorphous solid (36.7 mg, 0.103 mmol, 68% yield, UPLC/HRMS purity: 96.1%). Purification was carried out by an automated MPLC system using a 12 g normal phase silica column with gradient elution from 0–6% MeOH/CH_2Cl_2. R_f = 0.13 (4% MeOH/CH_2Cl_2); mp 248–255 ˚C; IR (neat) 3328, 3114, 1620 cm^{-1}; ^{1}H NMR (600 MHz, DMSO-d_6) δ 8.96 (s, 1H), 7.05 (d, J = 8.6 Hz, 1H), 6.52 (dd, J = 8.5, 2.6 Hz, 1H), 6.45 (d, J = 2.6 Hz, 1H), 4.33 (t, J = 5.0 Hz, 1H), 3.62 (m, 1H), 3.45–3.34 (m, 2H), 2.73 (m, 2H), 2.39–2.19 (complex, 5H), 2.12–2.02 (m, 2H), 1.86 (m, 2H), 1.55 (m, 1H), 1.44–1.33 (m, 2H), 1.30 (d, J = 6.5 Hz, 3H), 1.27–1.20 (m, 3H), 1.15 (s, 3H); ^{13}C NMR (151 MHz, DMSO-d_6) δ 168.8, 155.0, 136.9, 129.9, 125.8, 114.5, 112.8, 60.6, 58.5, 47.7, 46.6, 42.0, 39.3, 38.4, 36.9, 33.0, 29.2, 26.9, 25.9, 18.61, 18.56, 18.1. HRMS (FT-ICR, HESI) *m/z*: $[M + H]^+$ calcd for $C_{22}H_{32}NO_3$ 358.2377, found 358.2370.

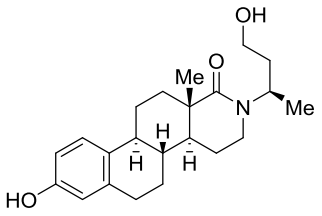

1.111

3-Hydroxy-1,3,5-estratriene-derived D-Ring Lactam, 1.111. Following the general procedure F, (*R*)-3-azidobutanol (*R*)-**1.5** (33.8 mg, 0.294 mmol, 2.0 equiv) was reacted with estrone **1.90** (40.4 mg, 0.149 mmol) to give **1.111** as a white amorphous solid (46.2 mg, 0.129 mmol, 86% yield, UPLC/HRMS purity: 97.9%). Purification was carried out by an automated MPLC system using a 12 g normal phase silica column with gradient elution from 0–4% MeOH/CH_2Cl_2. R_f = 0.38 (5% MeOH/CH_2Cl_2); mp 246–242 ˚C; IR (neat) 3160, 1585 cm^{-1}; ^1H NMR (600 MHz, DMSO-d_6) δ 8.95 (s, 1H), 7.05 (d, *J* = 8.5 Hz, 1H), 6.52 (dd, *J* = 8.4, 2.6 Hz, 1H), 6.44 (d, *J* = 2.6 Hz, 1H), 4.57 (m, 1H), 4.27 (t, *J* = 5.4 Hz, 1H), 3.30 (m, 1H), 3.21–3.10 (m, 2H), 2.73 (m, 1H), 2.27 (m, 1H), 2.16–1.98 (complex, 4H), 1.64 (m, 1H), 1.55–1.41 (complex, 4H), 1.34–1.15 (complex, 3H), 1.06 (d, *J* = 6.9 Hz, 3H), 1.02 (s, 3H); ^{13}C NMR (151 MHz, DMSO-d_6) δ 175.2, 154.9, 136.9, 130.2, 125.8, 114.6, 112.7, 58.1, 44.8, 43.6, 42.2, 40.8, 38.1, 36.1, 34.5, 29.2, 25.7, 25.5, 20.3, 18.0, 17.3. **Note**: Missing one carbon signal due to signal overlap. HRMS (FT-ICR, HESI) *m/z*: $[M + H]^+$ calcd for $C_{22}H_{32}NO_3$ 358.2377, found 358.2371.

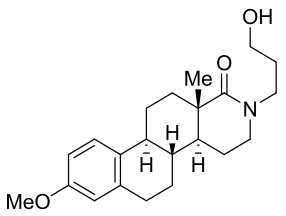

1.112

3-Methoxy-1,3,5-estratriene-derived D-Ring Lactam, 1.112. Following the general procedure F, 3-azidopropanol **1.1** (30.6 mg, 0.303 mmol 2.0 equiv) was reacted with estrone 3-

methyl ether **1.95** (42.7 mg, 0.150 mmol) to give **1.112** as an off-white amorphous solid (50.0 mg, 0.140 mmol, 93% yield, UPLC/HRMS purity: 97.8%). Purification was carried out by an automated MPLC system using a 12 g normal phase silica column with gradient elution from 0–5% MeOH/CH_2Cl_2. R_f = 0.35 (5% MeOH/CH_2Cl_2); mp 142–145 ˚C; IR (neat) 3354, 1601 cm^{-1}; ^1H NMR (400 MHz, $CDCl_3$) δ 7.22 (d, *J* = 8.6 Hz, 1H), 6.73 (dd, *J* = 8.6, 2.8 Hz, 1H), 6.63 (d, *J* = 2.6 Hz, 1H), 4.20 (br s, 1H), 3.77 (s, 3H), 3.68 (ddd, *J* = 14.0, 8.2, 4.6 Hz, 1H), 3.52–3.41 (m, 2H), 3.89–3.25 (m, 3H), 2.87 (m, 2H), 2.41–2.32 (m, 2H), 2.30–2.21 (m, 1H), 2.06 (m, 2H), 1.79–1.21 (complex, 8H), 1.16 (s, 3H); ^{13}C NMR (101 MHz, $CDCl_3$) δ 178.2, 157.8, 137.6, 132.3, 126.4, 113.7, 111.8, 58.0, 55.3, 47.0, 44.7, 43.0, 42.9, 41.4, 38.5, 34.6, 30.0, 29.4, 26.4, 25.9, 21.0, 18.5. HRMS (FT-ICR, HESI) *m/z*: $[M + H]^+$ calcd for $C_{22}H_{32}NO_3$ 358.2377, found 358.2371.

Experimental section for 1.4.4

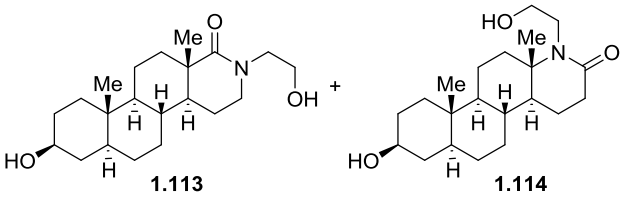

3β-Hydroxy-5α-androstane-derived D-Ring Lactams, 1.113 and 1.114. Following the general procedure E, azidoethanol **1.7** (26.1 mg, 0.300 mmol, 2.0 equiv) was reacted with *trans*-androsterone **1.84** (43.6 mg, 0.150 mmol) to give an inseparable mixture (30:70) of regioisomers **1.113** and **1.114** as a white amorphous solid (50.4 mg, 0.144 mmol, 96% yield, UPLC/HRMS purity: ≥99.5%). Purification was carried out by an automated MPLC system using a 12 g normal phase silica column with gradient elution from 0–5% MeOH/CH_2Cl_2. R_f = 0.26 (5% MeOH/CH_2Cl_2); IR (neat) 3328, 1600 cm^{-1}; key ^1H NMR (400 MHz, $CDCl_3$) δ 4.46 (br s, 1H), 3.86 (m, 1H), 3.77 (m, 2H), 3.65–3.56 (complex, 4H), 3.37 (m, 1H), 3.26 (m, 1H), 2.52 (m, 1H),

2.44 (m, 1H); ^{13}C NMR (151 MHz, $CDCl_3$) δ 179.5, 173.7, 71.3, 71.2, 65.0, 62.2, 60.5, 53.4, 53.0, 51.4, 48.8, 48.7, 45.7, 44.9, 44.4, 44.3, 41.3, 38.2, 38.1, 38.0, 36.9, 36.3, 35.7, 35.6, 34.8, 34.5, 31.7, 31.6, 31.5, 31.0, 30.9, 28.6, 28.5, 21.6, 21.2, 20.3, 19.3, 19.0, 18.5, 12.4, 12.3. **Note**: Missing one carbon signal due to signal overlap of regioisomers. HRMS (FT-ICR, HESI) *m/z*: $[M + H]^+$ calcd for $C_{21}H_{36}NO_3$ 350.2690, found 350.2683.

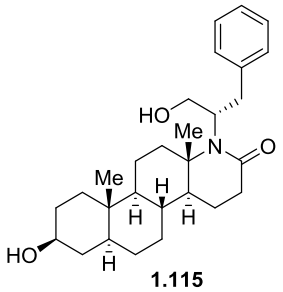

1.115

3β-Hydroxy-5α-androstane-derived D-Ring Lactam, 1.115. Following the general procedure E, (*S*)-2-azido-3-phenylpropanol (*S*)-**1.9** (53.2 mg, 0.300 mmol, 2.0 equiv) was reacted with *trans*-androsterone **1.84** (43.6 mg, 0.150 mmol) to give **1.115** as a white amorphous solid (58.9 mg, 0.134 mmol, 89% yield, UPLC/HRMS purity: 96.9%). Purification was carried out by an automated MPLC system using a 12 g normal phase silica column with gradient elution from 50–100% EtOAc/hexanes. R_f = 0.26 (80% EtOAc/hexanes); mp 236–240 ˚C; IR (neat) 3332, 1596 cm^{-1}; ^{1}H NMR (400 MHz, $CDCl_3$) δ 7.31–7.18 (m, 5H), 3.76–3.68 (m, 2H), 3.63–3.49 (m, 3H), 2.99 (m, 1H), 2.56 (m, 1H), 2.42 (ddd, *J* = 18.6, 10.2, 8.0 Hz, 1H), 1.98 (m, 1H), 1.92–1.79 (m, 3H), 1.71–1.65 (m, 2H), 1.61–1.56 (m, 1H), 1.44–1.03 (complex, 13H), 1.00–0.80 (m, 4H, contains s, 0.88, 3H), 0.76–0.68 (m, 4H, contains s, 0.74, 3H); ^{13}C NMR (101 MHz, $CDCl_3$) δ 173.3, 140.0, 129.7 (2C), 128.6 (2C), 126.6, 71.2, 65.6, 62.0, 59.7, 53.0, 49.8, 44.3, 37.9, 37.8, 36.8, 36.2, 35.6, 34.6, 33.1, 31.4, 31.1, 28.5, 21.7, 18.8, 18.3, 12.2. HRMS (FT-ICR, HESI) *m/z*: $[M + H]^+$ calcd for $C_{28}H_{42}NO_3$ 440.3159, found 440.3137.

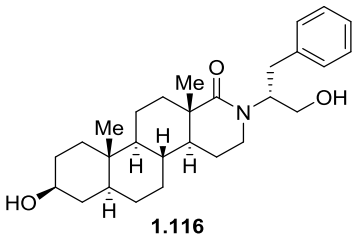

1.116

3β-Hydroxy-5α-androstane-derived-derived D-Ring Lactam, 1.116. Following the general procedure E, (*R*)-2-azido-3-phenylpropanol (*R*)-**1.9** (53.2 mg, 0.300 mmol, 2.0 equiv) was reacted with *trans*-androsterone **1.84** (43.7 mg, 0.150 mmol) to give **1.116** as a white amorphous solid (54.0 mg, 0.123 mmol, 82% yield, UPLC/HRMS purity: 97.2%) containing a minor uncharacterized regioisomer (regioisomer ratio 89:11). Purification was carried out by an automated MPLC system using a 12 g normal phase silica column with gradient elution from 0–5% MeOH/CH_2Cl_2 over 40 min. R_f = 0.30 (80% EtOAc/hexanes); mp 109–118 ˚C; IR (neat) 3426, 3280, 1603 cm^{-1}; key ^1H NMR (400 MHz, $CDCl_3$) δ 7.31–7.24 (m, 2H), 7.22–7.18 (m, 3H), 4.06 (m, 1H), 3.95 (m, 1H), 3.83–3.71 (m, 2H), 3.61–3.53 (m, 2H), 3.13–3.05 (m, 2H), 2.96–2.89 (m, 2H), 2.12 (m, 1H); ^{13}C NMR (101 MHz, $CDCl_3$) δ 178.8, 138.7, 129.2 (2C), 128.5 (2C), 126.5, 71.3, 64.1, 53.3, 46.9, 45.1, 44.4, 41.7, 38.1, 36.8, 35.7, 34.79, 34.78, 33.9, 31.6, 30.9, 29.8, 28.6, 21.2, 20.3, 18.1, 12.3. **Note**: Characterization above only denotes peaks of the major regioisomer. HRMS (FT-ICR, HESI) *m/z*: $[M + H]^+$ calcd for $C_{28}H_{42}NO_3$ 440.3159, 440.3139.

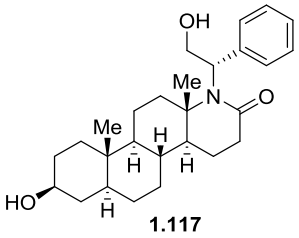

1.117

3β-Hydroxy-5α-androstane-derived D-Ring Lactam, 1.117. Following the general procedure E, (*S*)-2-azido-2-phenylethanol (*S*)-**1.10** (40.8 mg, 0.250 mmol, 2.0 equiv) was reacted with *trans*-androsterone **1.84** (36.3 mg, 0.125 mmol) to give **1.117** as a white amorphous solid (40.8 mg, 0.0959 mmol, 77% yield, UPLC/HRMS purity: 97.8%). Purification was carried out by an automated MPLC system using a 12 g normal phase silica column with gradient elution from 50–100% EtOAc/hexanes. R_f = 0.38 (5% MeOH/CH_2Cl_2); mp 212–217 ˚C; IR (neat) 3352, 3235, 1608 cm^{-1}; ^1H NMR (400 MHz, $CDCl_3$) δ 7.33–7.28 (m, 4H), 7.24–7.19 (m, 1H), 4.75 (m, 1H), 4.41 (dd, *J* = 11.9, 5.3 Hz, 1H), 4.03 (dd, *J* = 11.9, 2.4 Hz, 1H), 3.60 (m, 1H), 2.62 (ddd, *J* = 18.8, 7.3, 1.6 Hz, 1H), 2.48 (ddd, *J* = 18.8, 10.5, 8.4 Hz, 1H), 2.16 (m, 1H), 1.99–1.91 (m, 2H), 1.83–1.68 (m, 4H), 1.62–1.19 (complex, 11H), 1.15 (s, 3H), 1.12–0.88 (m, 3H), 0.82–0.76 (m, 4H, contains s, 0.77, 3H); ^{13}C NMR (101 MHz, $CDCl_3$) δ 173.0, 138.3, 128.4 (2C), 127.2 (2C), 126.7, 71.1, 66.1, 62.2, 59.7, 53.0, 49.9, 44.3, 38.4, 37.9, 36.9, 36.4, 35.6, 32.9, 31.4, 31.1, 28.5, 22.0, 19.3, 19.1, 12.3. HRMS (FT-ICR, HESI) *m/z*: $[M + H]^+$ calcd for $C_{27}H_{39}NO_3$ 426.3003, found 426.2983.

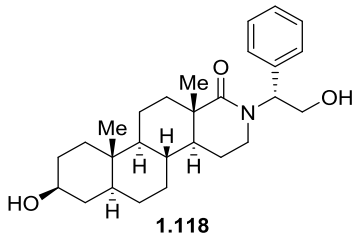

1.118

3β-Hydroxy-5α-androstane-derived D-Ring Lactam, 1.118. Following the general procedure E, (*R*)-2-azido-2-phenylethanol (*R*)-**1.10** (40.8 mg, 0.250 mmol, 2.0 equiv) was reacted with *trans*-androsterone **1.84** (36.2 mg, 0.125 mmol) to give **1.118** as a yellow amorphous solid (27.0 mg, 0.0634 mmol, 51% yield, UPLC/HRMS purity: 98.9%). Purification was carried out by an automated MPLC system using a 12 g normal phase silica column with

gradient elution from 50–100% EtOAc/hexanes. R_f = 0.36 (4% MeOH/CH_2Cl_2); IR (neat) 3364, 1601 cm^{-1}; mp 212–214 ˚C; ^1H NMR (400 MHz, $CDCl_3$) δ 7.35–7.19 (m, 5H), 5.66 (t, *J* = 7.1 Hz, 1H), 4.10 (d, *J* = 7.1 Hz, 2H), 3.57 (m, 1H), 3.21 (ddd, *J* = 12.4, 7.3, 2.0 Hz, 1H), 2.82 (ddd, *J* = 12.4, 10.6, 7.1 Hz, 1H), 2.21 (m, 1H), 1.87–1.18 (complex, 17H), 1.15 (s, 3H), 1.10–0.91 (m, 2H), 0.85–0.74 (m, 4H, contains s, 0.78, 3H), 0.67 (m, 1H); ^{13}C NMR (126 MHz, $CDCl_3$) δ 179.0, 137.0, 128.7 (2C), 128.0 (2C), 127.8, 71.2, 62.1, 59.0, 53.2, 45.1, 44.4, 42.9, 41.9, 38.0, 36.8, 35.6, 34.91, 34.86, 31.4, 30.8, 28.5, 21.0, 20.3, 18.3, 12.3. HRMS (FT-ICR, HESI) *m/z*: [M + H]$^+$ calcd for $C_{27}H_{40}NO_3$ 426.3003, found 426.2985.

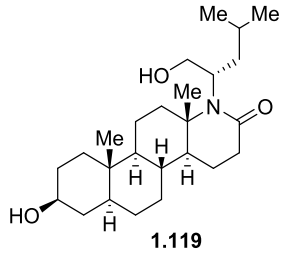

1.119

3β-Hydroxy-5α-androstane-derived D-Ring Lactam, 1.119. Following the general procedure E, (*S*)-2-azido-4-methylpentanol (*S*)-**1.11** (43.2 mg, 0.302 mmol, 2.0 equiv) was reacted with *trans*-androsterone **1.84** (43.9 mg, 0.151 mmol) to give **1.119** as a white amorphous solid (52.6 mg, 0.130 mmol, 86% yield, UPLC/HRMS purity: ≥99.5%). Purification was carried out by an automated MPLC system using a 12 g normal phase silica column with gradient elution from 0–80% EtOAc/hexanes. R_f = 0.33 (80% EtOAc/hexanes); mp 164–168 ˚C; IR (neat) 3317, 1604 cm^{-1}; ^1H NMR (400 MHz, $CDCl_3$) δ 5.68 (d, *J* = 9.3 Hz, 1H), 3.82 (m, 1H), 3.67–3.56 (m, 2H), 3.51 (m, 1H), 2.64 (ddd, *J* = 13.6, 11.1, 4.0 Hz, 1H), 2.50 (ddd, *J* = 18.6, 7.0, 1.5 Hz, 1H), 2.37 (ddd, *J* = 18.8, 11.0, 8.1 Hz, 1H), 2.10 (dt, *J* = 12.3, 3.6 Hz, 1H), 1.93–1.06 (complex, 20H, contains s, 1.18, 3H), 1.02–0.84 (complex, 10H, contains dd, 0.94, *J* = 6.6, 1.3 Hz, 6H), 0.79–0.71 (complex, 4H, contains s, 0.78, 3H); ^{13}C NMR (101 MHz, $CDCl_3$) δ 172.8,

71.1, 64.9, 61.9, 55.1, 53.0, 49.7, 44.3, 37.9, 37.5, 36.8, 36.0, 35.6, 33.0, 31.4, 31.0, 25.5, 24.1, 21.9, 21.8, 18.9, 18.8, 12.3. **Note**: Missing two carbons signal due to signal overlap. HRMS (FT-ICR, HESI) *m/z*: $[M + H]^+$ calcd for $C_{25}H_{44}NO_3$ 406.3316, found 406.3296.

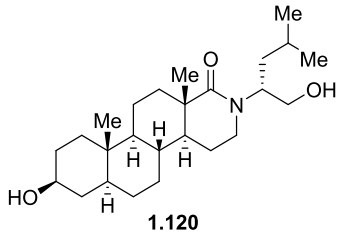

1.120

3β-Hydroxy-5α-androstane-derived D-Ring Lactam, 1.120. Following the general procedure E, (*R*)-2-azido-4-methylpentanol (*R*)-**1.11** (43.2 mg, 0.302 mmol, 2.0 equiv) was reacted with trans-androsterone **1.84** (43.9 mg, 0.151 mmol) to give **1.11** as a white amorphous solid (51.0 mg, 0.126 mmol, 83% yield, UPLC/HRMS purity: 92.4%). Purification was carried out by an automated MPLC system using a 12 g normal phase silica column with gradient elution from 0–5% MeOH/CH_2Cl_2 over 50 min. R_f = 0.27 (5% MeOH/CH_2Cl_2); IR (neat) 3364, 1611 cm^{-1}; mp 97–115 °C; key ^1H NMR (400 MHz, $CDCl_3$) δ 4.30 (m, 1H), 3.67 (dd, *J* = 11.5, 3.8 Hz, 1H), 3.64–3.55 (m, 2H), 2.16 (m, 1H), 1.95 (m, 1H); ^{13}C NMR (101 MHz, $CDCl_3$) δ 179.0, 71.3, 64.1, 55.8, 53.4, 45.4, 44.5, 43.3, 41.8, 38.1, 36.9, 35.7, 34.97, 34.95, 31.6, 31.0, 28.6, 25.1, 23.3, 22.5, 21.2, 20.4, 18.2, 12.4. **Note**: Missing one carbon signal due to signal overlap; characterization above only denotes peaks of the major regioisomer. HRMS (FT-ICR, HESI) *m/z*: $[M + H]^+$ calcd for $C_{25}H_{45}NO_3$ 406.3316, found 406.3298.

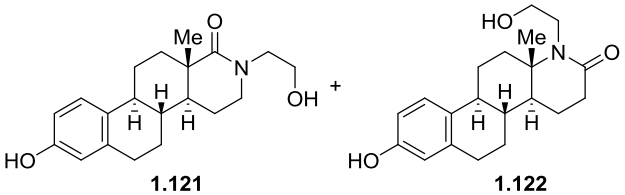

1.121 **1.122**

3-Hydroxy-1,3,5-estratriene-derived D-Ring Lactams, 1.121 and 1.122. Following the general procedure F, 2-azidoethanol **1.7** (26.1 mg, 0.300 mmol, 2.0 equiv) was reacted with estrone **1.95** (40.6 mg, 0.150 mmol) to give a mixture of **1.121**:**1.122** as an off-white amorphous solid (46.3 mg, 0.141 mmol, 94% yield). Purification was carried out by an automated MPLC system using a 12 g normal phase silica column with gradient elution from 0–5% MeOH/CH_2Cl_2. A 30:70 regioisomeric ratio was observed by analytical HPLC of crude reaction mixture: Chiralpak IB, Daicel Chemical Industries, Ltd.; 0–30% EtOH/hexanes over 60 min; flow rate 1.0 mL/min; UV 220 nm; **1.121** = 28.03 min, **1.122** = 34.55 min. The mixture was subjected to a second purification using Chiralpak IB prep HPLC with gradient elution from 0–5% EtOH/hexanes over 60 min to give **1.121** (36.1 mg, 0.110 mmol, 27% yield, UPLC/HRMS purity: 98.1%) as a white amorphous solid and **1.122** (68.9 mg, 0.209 mmol, 52% yield, UPLC/HRMS purity: 99.0%) as a white amorphous solid. **1.121** + **1.122** mixture: R_f = 0.38 (5% MeOH/CH_2Cl_2); IR (neat) 3334, 1596, 1567 cm^{-1}. **1.121**: mp decomposed; IR (neat) 3479, 3309, 1595 cm^{-1}; ^1H NMR (400 MHz, DMSO-d_6) δ 9.03 (s, 1H), 7.06 (d, J = 8.5 Hz, 1H), 6.51 (dd, J = 8.4, 2.7 Hz, 1H), 6.44 (d, J = 2.6 Hz, 1H), 4.64 (m, 1H), 3.49–3.16 (complex, 5H), 2.72 (m, 2H), 2.28 (m, 1H), 2.17–2.07 (m, 2H), 1.97 (m, 2H), 1.60–1.14 (complex, 7H), 1.02 (s, 3H); ^{13}C NMR (126 MHz, DMSO-d_6) δ 175.2, 155.1, 137.0, 130.2, 126.0, 114.7, 112.8, 58.6, 49.2, 47.7, 43.8, 42.4, 40.5, 38.1, 34.5, 29.4, 25.8, 25.6, 20.5, 18.1. HRMS (FT-ICR, HESI) *m/z*: $[M + H]^+$ calcd for $C_{20}H_{28}NO_3$ 330.2064, found 330.2059. **1.122**: mp 259–262 ˚C; IR (neat) 3332, 1566 cm^{-1}; ^1H NMR (400 MHz, DMSO-d_6) δ 9.02 (s, 1H), 7.06 (d, J = 8.5 Hz, 1H), 6.52 (dd, J = 8.4, 2.6 Hz, 1H), 6.44 (d, J = 2.6 Hz, 1H), 4.67 (t, J = 5.4 Hz, 1H), 3.58–3.45 (m, 2H), 3.33 (m, 1H), 3.13 (m, 1H), 2.72 (m, 2H), 2.41–2.15 (complex, 5H), 2.03 (m, 1H), 1.92 (m, 1H), 1.59 (m, 1H), 1.49–1.35 (m, 2H), 1.30–1.19 (m, 3H), 1.11 (s, 3H); ^{13}C NMR (126 MHz, DMSO-d_6) δ 169.7, 155.1,

137.0, 129.9, 126.1, 114.6, 112.9, 60.0, 59.2, 46.9, 43.4, 42.0, 39.6, 37.4, 31.3, 29.4, 26.7, 25.8, 18.9, 18.6. HRMS (FT-ICR, HESI) *m/z*: $[M + H]^+$ calcd for $C_{20}H_{28}NO_3$ 330.2064, found 330.2059.

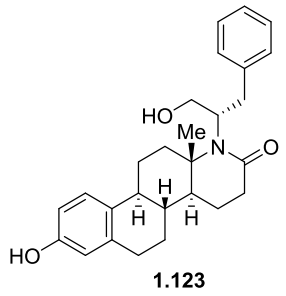

1.123

3-Hydroxy-1,3,5-estratriene-derived D-Ring Lactam, 1.123. Following the general procedure F, (*S*)-2-azido-3-phenylpropanol (*S*)-**1.9** (53.2 mg, 0.300 mmol, 2.0 equiv) was reacted with estrone **1.90** (40.6 mg, 0.150 mmol) to give **1.123** as a white amorphous solid (57.3 mg, 0.137 mmol, 91% yield, UPLC/HRMS purity: 96.8%). Purification was carried out by an automated MPLC system using a 12 g normal phase silica column with gradient elution from 0–80% EtOAc/hexanes. R_f = 0.21 (50% EtOAc/hexanes); mp 246–253 ˚C; IR (neat) 3247, 1602 cm^{-1}; ^1H NMR (400 MHz, DMSO-d_6) δ 9.01 (s, 1H), 7.27 (m, 2H), 7.17 (3H), 7.01 (d, *J* = 8.5 Hz, 1H), 6.50 (dd, *J* = 8.4, 2.6 Hz, 1H), 6.42 (d, *J* = 2.6 Hz, 1H), 4.98 (m, 1H), 3.72 (m, 2H), 3.50 (m, 1H), 3.27 (m, 1H), 3.09 (dd, *J* = 13.2, 5.9 Hz, 1H), 2.67 (m, 2H), 2.43–2.24 (m, 3H), 2.16 (m, 1H), 2.07 (m, 1H), 1.97 (m, 1H), 1.83 (m, 1H), 1.61 (m, 1H), 1.39 (m, 1H), 1.26–1.04 (m, 4H), 0.47 (s, 3H); ^{13}C NMR (126 MHz, DMSO-d_6) δ 170.6, 155.1, 140.5, 137.0, 129.8, 129.5 (2C), 128.2 (2C), 126.1, 126.0, 114.6, 112.8, 63.4, 60.4, 59.7, 47.6, 42.0, 39.6, 37.1, 34.4, 32.7, 29.3, 26.7, 25.9, 18.5, 17.6. HRMS (FT-ICR, HESI) *m/z*: $[M + H]^+$ calcd for $C_{27}H_{34}NO_3$ 420.2533, found 420.2525.

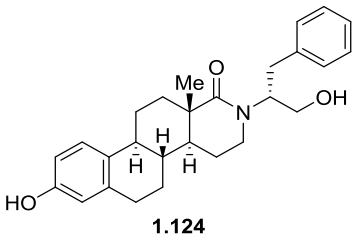

1.124

3-Hydroxy-1,3,5-estratriene-derived D-Ring Lactam, 1.124. Following the general procedure F, (*R*)-2-azido-3-phenylpropanol (*R*)-**1.9** (53.2 mg, 0.300 mmol, 2.0 equiv) was reacted with estrone **1.95** (41.2 mg, 0.152 mmol) to give **1.124** as a white crystalline solid (45.6 mg, 0.109 mmol, 72% yield, UPLC/HRMS purity: 98.5%) containing a minor uncharacterized regioisomer. Purification was carried out by an automated MPLC system using a 12 g normal phase silica column with gradient elution from 0–5% MeOH/CH_2Cl_2. R_f = 0.40 (5% MeOH/CH_2Cl_2); IR (neat) 3298, 1609 cm^{-1}; mp 115–134 ˚C; ^1H NMR (400 MHz, DMSO-d_6) δ 9.00 (s, 1H), 7.25 (m, 2H), 7.18 (m, 3H), 7.03 (d, J = 8.5 Hz, 1H), 6.50 (dd, J = 8.4, 2.6 Hz, 1H), 6.42 (d, J = 2.7 Hz, 1H), 4.73 (m, 1H), 3.57 (m, 1H), 3.48 (m, 1H), 3.14 (m, 2H), 2.82 (m, 2H), 2.69 (m, 3H), 2.21 (m, 1H), 2.00–1.86 (m, 3H), 1.40–1.03 (complex, 7H), 0.94 (s, 3H); ^{13}C NMR (151 MHz, DMSO-d_6) δ 175.6, 155.0, 138.9, 137.0, 130.2, 128.9 (2C), 128.0 (2C), 125.93, 125.90, 114.6, 112.8, 61.0, 43.1, 42.4, 40.7, 38.2, 34.7, 33.7, 29.3, 25.8, 25.5, 20.4, 17.5. **Note**: Missing two carbon signals due to signal overlap; characterization above only denote peaks of the major regioisomer. HRMS (FT-ICR, HESI) *m/z*: $[M + H]^+$ calcd for $C_{27}H_{34}NO_3$ 420.2533, found 420.2527.

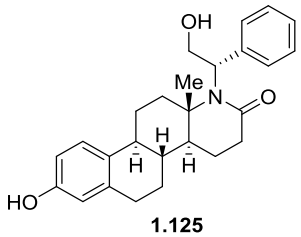

1.125

3-Hydroxy-1,3,5-estratriene-derived D-Ring Lactam, 1.125. Following the general procedure F, (*S*)-2-azido-2-phenylethanol (*S*)-**1.10** (64.6 mg, 0.396 mmol, 2.0 equiv was reacted with estrone **1.90** (54.5 mg, 0.201 mmol) to give **1.125** as a white amorphous solid (41.5 mg, 0.102 mmol, 51% yield, UPLC/HRMS purity: ≥99.5%). Purification was carried out by an automated MPLC system using a 12 g normal phase silica column with gradient elution from 0–2% MeOH/CH_2Cl_2. R_f = 0.23 (2% MeOH/CH_2Cl_2); mp 254–259 ˚C; IR (neat) 3233, 1734 cm^{-1}; ^1H NMR (400 MHz, $CDCl_3$) δ 9.02 (s, 1H), 7.36 (d, *J* = 7.7 Hz, 2H), 7.25 (m, 2H), 7.15 (m, 1H), 7.07 (d, *J* = 8.5 Hz, 1H), 6.53 (dd, *J* = 8.4, 2.7 Hz, 1H), 6.45 (d, *J* = 2.6 Hz, 1H), 5.02 (t, *J* = 5.4 Hz, 1H), 4.16 (m, 1H), 4.03 (m, 1H), 2.74 (m, 1H), 2.43–2.27 (m, 5H), 2.07–2.05 (m, 1H), 1.99–1.92 (m, 1H), 1.78 (m, 1H), 1.60–1.44 (m, 2H), 1.33–1.21 (m, 4H), 1.14 (s, 3H); ^{13}C NMR (101 MHz, $CDCl_3$) δ 170.1, 155.1, 141.0, 137.0, 129.9, 127.5, 127.2, 126.0, 125.7, 114.6, 112.8, 65.4, 64.9, 61.1, 59.2, 47.8, 42.0, 37.5, 32.5, 29.3, 27.0, 26.0, 19.2, 18.6, 15.1. **Note**: Missing one carbon signal due to signal overlap. HRMS (FT-ICR, HESI) *m/z*: $[M + H]^+$ calcd for $C_{26}H_{32}NO_3$ 406.2377, found 406.2370.

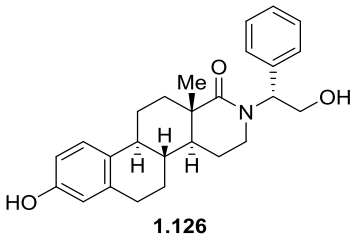

1.126

3-Hydroxy-1,3,5-estratriene-derived D-Ring Lactam, 1.126. Following the general procedure F, (*R*)-2-azido-2-phenylethanol (*R*)-**1.10** (41.7 mg, 0.256 mmol, 2.0 equiv) was reacted with estrone **1.90** (34.5 mg, 0.128 mmol) to give **1.126** as a yellow solid/oil (29.1 mg, 0.072 mmol, 56% yield, UPLC/HRMS purity: ≥99.5%) containing a minor uncharacterized regioisomer. Purification was carried out by an automated MPLC system using a 12 g normal

phase silica column with gradient elution from 0–2% MeOH/CH_2Cl_2. R_f = 0.17 (2% MeOH/CH_2Cl_2, run twice); IR (neat) 3414, 3344, 1591 cm^{-1}; ^1H NMR (400 MHz, DMSO-d_6) δ 8.99 (s, 1H), 7.34 (m, 2H), 7.26 (m, 3H), 7.05 (d, J = 8.5 Hz, 1H), 6.51 (dd, J = 8.4, 2.6 Hz, 1H), 6.43 (d, J = 2.6 Hz, 1H), 5.63 (t, J = 7.3 Hz, 1H), 4.87 (t, J = 5.5 Hz, 1H), 3.92 (m, 1H), 3.83 (m, 1H), 2.84 (m, 1H), 2.70 (m, 2H), 2.28 (m, 1H), 2.13 (m, 1H), 1.93 (m, 1H), 1.58–1.11 (complex, 8H), 1.08 (s, 3H); ^{13}C NMR (101 MHz, DMSO-d_6) δ 175.8, 155.0, 138.5, 137.0, 130.2, 128.3 (2C), 127.7 (2C), 126.9, 125.9, 114.6, 112.8, 59.7, 56.4, 43.3, 42.1, 41.1, 40.9, 38.4, 34.8, 29.3, 25.7, 25.6, 20.4, 17.8. **Note**: Characterization above only denotes peaks of the major regioisomer. HRMS (FT-ICR, HESI) *m/z*: $[M + H]^+$ calcd for $C_{26}H_{32}NO_3$ 406.2377, found 406.2376.

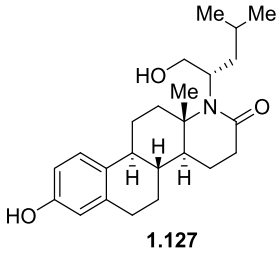

1.127

3-Hydroxy-1,3,5-estratriene-derived D-Ring Lactam, 1.127. Following the general procedure F, (*S*)-2-azido-4-methylpentanol (*S*)-**1.11** (43.0 mg, 0.300 mmol, 2.0 equiv) was reacted with estrone **1.90** (0.0411 mg, 0.152 mmol to give **1.127** as a white amorphous solid (50.6 mg, 0.131 mmol, 86% yield, UPLC/HRMS purity: ≥99.5%). Purification was carried out by an automated MPLC system using a 12 g normal phase silica column with gradient elution from 0–80% EtOAc/hexanes. R_f = 0.25 (50% EtOAc/hexanes); mp 233–236 ˚C; IR (neat) 3152, 1598, 1571 cm^{-1}; ^1H NMR (400 MHz, DMSO-d_6) δ 9.02 (s, 1H), 7.06 (d, J = 8.4 Hz, 1H), 6.52 (dd, J = 8.4, 2.6 Hz, 1H), 6.44 (d, J = 2.6 Hz, 1H), 4.96 (dd, J = 6.7, 4.4 Hz, 1H), 3.75 (m, 1H), 3.56 (m, 1H), 3.42 (m, 1H), 2.73 (m, 2H), 2.40–2.15 (complex, 6H), 2.03 (m, 1H), 1.88 (m, 1H),

1.64 (m, 2H), 1.48–1.15 (complex 9H, contains s, 1.15, 3H), 0.90 (dd, J = 18.9, 6.5 Hz, 6H); ^{13}C NMR (126 MHz, DMSO-d_6) δ 170.2, 155.1, 136.9, 129.9, 125.9, 114.6, 112.8, 63.7, 60.7, 54.9, 47.5, 41.9, 39.5, 37.3, 32.5, 29.3, 26.9, 25.9, 25.4, 23.7, 22.3, 18.9, 18.5. **Note**: Missing one carbon signals due to signal overlap. HRMS (FT-ICR, HESI) *m/z*: $[M + H]^+$ calcd for $C_{24}H_{36}NO_3$ 386.2690, found 386.2683.

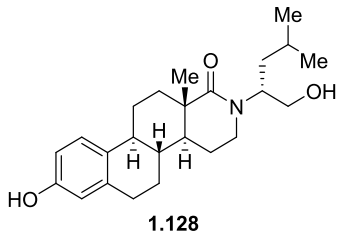

1.128

3-Hydroxy-1,3,5-estratriene-derived D-Ring Lactam, 1.128. Following the general procedure F, (*R*)-2-azido-4-methylpentanol (*R*)-**1.1** (43.4 mg, 0.303 mmol, 2.0 equiv) was reacted with estrone **1.90** (41.6 mg, 0.153 mmol) to give **1.128** as a white crystalline solid (40.2 mg, 0.104 mmol, 68% yield, UPLC/HRMS purity: 98.8%). Purification was carried out by an automated MPLC system using a 12 g normal phase silica column with gradient elution from 0–5% MeOH/CH_2Cl_2. R_f = 0.17 (5% MeOH/CH_2Cl_2); IR (neat) 3247, 1601 cm^{-1}; mp 117–142 ˚C; ^{1}H NMR (400 MHz, $CDCl_3$) δ 9.00 (s, 1H), 7.05 (d, J = 8.5 Hz, 1H), 6.51 (dd, J = 8.5, 2.5 Hz, 1H), 6.44 (d, J = 2.6 Hz, 1H), 4.58 (t, J = 5.6 Hz, 1H), 4.48 (m, 1H), 3.42–3.24 (m, 3H), 3.09 (m, 1H), 2.72 (m, 2H), 2.29–2.25 (m, 1H), 2.17–2.08 (m, 2H), 2.00–1.97 (m, 2H), 1.56–1.45 (complex, 9H), 1.02 (s, 3H), 0.87 (dd, J = 8.5, 6.3 Hz, 6H); ^{13}C NMR (151 MHz, $CDCl_3$) δ 175.6, 155.0, 137.0, 130.3, 125.9, 114.6, 112.8, 61.8, 43.6, 42.3, 40.9, 38.4, 36.2, 34.9, 29.4, 25.7, 25.6, 24.4, 23.5, 21.9, 20.5, 17.8. **Note**: Missing two carbon signals due to signal overlap. HRMS (FT-ICR, HESI) *m/z*: $[M + H]^+$ calcd for $C_{24}H_{36}NO_3$ 386.2690, found 386.2684.

Experimental section for 1.4.5

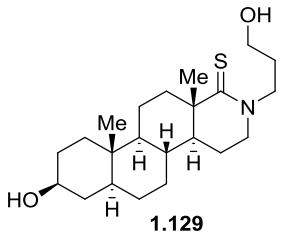

1.129

3β-Hydroxy-5α-androstane-derived D-Ring Thioamide, 1.129. Following the general procedure G, **1.129** was prepared as a white amorphous solid (49.1 mg, 0.129 mmol, 52% yield, UPLC/HRMS purity: 98.6%). Purification was carried out by an automated MPLC system using a 12 g normal phase silica column with gradient elution from 0–1.5% MeOH/CH_2Cl_2. R_f = 0.33 (5% MeOH/CH_2Cl_2); mp 212–216 ˚C; IR (neat) 3241, 1519 cm^{-1}; ^1H NMR (400 MHz, $CDCl_3$) δ 4.46 (dt, *J* = 13.3, 6.6 Hz, 1H), 3.88 (dt, *J* = 13.4, 5.9 Hz, 1H), 3.62–3.47 (m, 3H), 3.44–3.31 (m, 2H), 2.74 (m, 1H), 2.05 (m, 1H), 1.90–1.53 (complex, 7H), 1.46–1.22 (complex, 9H), 1.18 (s, 3H), 1.09 (m, 1H), 0.97 (m, 1H), 0.85 (m, 1H), 0.79 (s, 3H), 0.65 (m, 1H); ^{13}C NMR (101 MHz, $CDCl_3$) δ 211.7, 71.3, 58.1, 53.0, 51.7, 50.6, 46.4, 44.6, 44.4, 39.7, 38.0, 36.8, 36.0, 35.6, 31.6, 31.0, 29.6, 28.6, 21.3, 21.2, 12.3. **Note**: Missing one carbon signal due to signal overlap. HRMS (FT-ICR, HESI) *m/z*: $[M + H]^+$ calcd for $C_{22}H_{38}NO_2S$ 380.2618, found 380.2612.

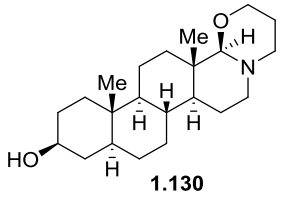

1.130

3β-Hydroxy-5α-androstane-derived D-Ring Oxazinane, 1.130. Following the general procedure G, **1.130** was prepared as a white amorphous solid (59.4 mg, 0.171 mmol, 85% yield, LCMS Purity: ≥99.5%). Purification was carried out by an automated MPLC system using a 12 g normal phase silica column with gradient elution from 0–10% MeOH (0.5% NH_4OH)/CH_2Cl_2. R_f = 0.25 (5% MeOH (0.5% NH_4OH)/CH_2Cl_2); mp 178–184 ˚C; IR (neat) 3350, 2929, 2848 cm^{-1};

^{1}H NMR (400 MHz, $CDCl_3$) δ 4.00 (m, 1H), 3.58 (m, 1H), 3.38 (m, 1H), 2.96–2.81 (m, 3H), 2.11–1.94 (m, 3H), 1.83–1.71 (m, 4H), 1.61–1.18 (complex, 11H), 1.10–1.01 (m, 1H), 0.99–0.88 (m, 5H, contains s, 0.95, 3H), 0.83–0.72 (m, 5H, contains s, 0.78, 3H), 0.65 (m, 1H); ^{13}C NMR (101 MHz, $CDCl_3$) δ 102.3, 71.4, 67.9, 54.8, 54.6, 53.9, 49.4, 44.6, 38.3, 37.9, 37.0, 35.9, 35.7, 34.5, 31.6, 31.0, 28.7, 25.9, 23.7, 20.2, 13.6, 12.4. HRMS (FT-ICR, HESI) *m/z*: $[M + H]^+$ calcd for $C_{22}H_{38}NO_2$ 348.2897, found 348.2890. **Note**: X-ray crystal structure of this analog is provided in the CCDC (CCDC 1583518).

Table 1.11. Selected crystallographic and refinement parameters for **1.130**.

compound	**1.130**
CCDC deposition number	1583518
empirical formula	$C_{22}H_{41}NO_4$
formula weight	383.56
temperature	200(2) K
wavelength Å	1.54178 Å
crystal system	orthorhombic
space group	P $2_12_12_1$
unit cell dimensions	a = 7.4276(3) Å, α = 90°
	b = 10.1060(12) Å, β = 90°
	c = 28.7302(12) Å, γ = 90°
Z	4
volume	2156.58(15) Å^3
density	1.219 Mg/m^3
absorption coefficient	0.629 μ mm^{-1}
F(000)	848
crystal size	0.150 × 0.150 × 0.020 mm^3
Theta range for data collection	3.076 to 69.815°
index ranges	-8<=h<=8, -10<=k<=12, -32<=l<=33
reflections collected	18686
independent reflections	3675 [R(int) = 0.0545]
completeness to theta = 66.000°	98.4%
absorption correction	multi-scan
max. and min. transmission	1.000 and 0.718
refinement method	full-matrix least-squares on F^2
data/restraints/parameters	3675/0/408
Goodness-of-fit F^2	1.028
final R indices [I>2sigma(I)]	R1 = 0.0385, wR2 = 0.1012
R indices (all data)	R1 = 0.0418, wR2 = 0.1031
absolute structure parameter	0.12(12)
largest diff. peak and hole	0.197 and -0.160 e.Å^{-3}

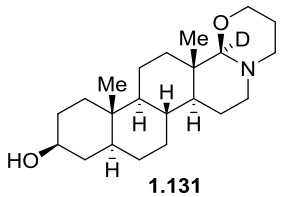

1.131

3β-Hydroxy-5α-androstane-derived D-Ring Oxazinane, 1.131. Following the general procedure G, **1.131** was prepared as a white amorphous solid (45.0 mg, 0.128 mmol, 64% yield, LCMS Purity: ≥99.5%). Purification was carried out by an automated MPLC system using a 12 g normal phase silica column with gradient elution from 0–10% MeOH (0.5% NH_4OH)/CH_2Cl_2. R_f = 0.25 (5% MeOH (0.5% NH_4OH)/CH_2Cl_2); mp 178–184 ˚C; IR (neat) 3519, 3243, 2930, 2847 cm^{-1}; ^1H NMR (400 MHz, $CDCl_3$) δ 4.01 (m, 1H), 3.58 (m, 1H), 3.38 (m, 1H), 2.96–2.82 (m, 2H), 2.13–1.95 (m, 3H), 1.83–1.71 (m, 3H), 1.58–1.18 (complex, 12H), 1.10–1.03 (m, 1H), 0.99–0.91 (m, 5H, contains s, 0.96, 3H), 0.84–0.72 (m, 5H, contains s, 0.78, 3H), 0.65 (m, 1H); ^{13}C NMR (101 MHz, $CDCl_3$) δ 71.4, 67.5, 54.7, 54.5, 53.8, 49.3, 44.5, 38.2, 38.0, 36.9, 35.83, 35.80, 35.7, 34.4, 31.6, 31.0, 28.7, 25.6, 23.4, 20.1, 13.4, 12.4. HRMS (FT-ICR, HESI) *m/z*: $[M + H]^+$ calcd for $C_{22}H_{37}DNO_2$ 349.2960, found 349.2952.

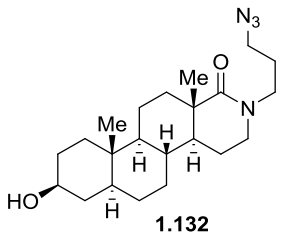

1.132

3β-Hydroxy-5α-androstane-derived D-Ring Lactam, 1.132. Following the general procedure G, **1.132** was prepared as an off-white amorphous solid (166 mg, 0.429 mmol, 86% yield, UPLC/HRMS purity: ≥99.5%). Purification was carried out by an automated MPLC system using a 12 g normal phase silica column with gradient elution from 0–75%

EtOAc/hexanes. R_f = 0.25 (50% EtOAc/hexanes); mp 135–139 ˚C; IR (neat) 3469, 3330, 2092, 1607 cm^{-1}; ^1H NMR (400 MHz, $CDCl_3$) δ 3.59 (m, 1H), 3.49 (m, 1H), 3.35–3.18 (complex, 5H), 2.18 (m, 1H), 1.95–1.72 (complex, 6H), 1.66–1.49 (m, 3H), 1.45–1.19 (complex, 9H), 1.13–1.05 (m, 4H, contains s, 1.09, 3H), 0.97 (m, 1H), 0.91–0.82 (m, 1H), 0.80 (s, 3H); ^{13}C NMR (101 MHz, $CDCl_3$) δ 176.8, 71.3, 53.4, 49.5, 47.6, 46.0, 44.9, 44.5, 41.2, 38.1, 36.9, 35.7, 34.9, 34.6, 31.9, 31.0, 28.6, 36.7, 21.2, 20.3. 18.4, 12.4. HRMS (FT-ICR, HESI) *m/z*: $[M + H]^+$ calcd for $C_{22}H_{37}N_4O_2$ 389.2911, found 389.2904.

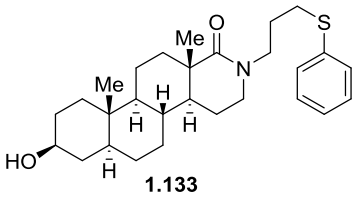

1.133

3β-Hydroxy-5α-androstane-derived D-Ring Lactam, 1.133. Following the general procedure G, **1.133** was prepared as a white amorphous solid (48.7 mg, 0.107 mmol, 71% yield, UPLC/HRMS purity: 98.6%). Purification was carried out by an automated MPLC system using a 12 g normal phase silica column with gradient elution from 0–50% EtOAc/hexanes. R_f = 0.48 (50% EtOAc/hexanes); mp 133–136 ˚C; IR (neat) 3367, 1617 cm^{-1}; ^1H NMR (400 MHz, $CDCl_3$) δ 7.36–7.25 (m, 4H), 7.17 (m, 1H), 3.63–3.48 (m, 2H), 3.30–3.15 (m, 3H), 2.29–2.86 (m, 2H), 2.18 (m, 1H), 1.92–1.21 (complex, 18H), 1.12–1.05 (m, 4H, contains s, 1.08, 3H), 1.00–0.91 (m, 1H), 0.89–0.80 (m, 1H), 0.79 (s, 3H) 0.66 (m, 1H); ^{13}C NMR (101 MHz, $CDCl_3$) δ 176.7, 136.6, 129.3 (2C), 129.0 (2C), 126.1, 71.3, 53.4, 47.3, 46.2, 46.0, 44.5, 41.2, 38.1, 36.9, 35.7, 34.9, 34.6, 31.6, 31.3, 31.0, 28.6, 27.0, 21.2, 20.3, 18.4, 12.4. HRMS (FT-ICR, HESI) *m/z*: $[M + H]^+$ calcd for $C_{28}H_{42}NO_2S$ 456.2931, found 456.2923.

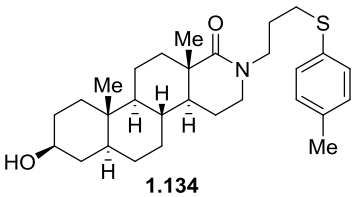

1.134

3β-Hydroxy-5α-androstane-derived D-Ring Lactam, 1.134. Following the general procedure G, **1.134** was prepared as a white amorphous solid (53.1 mg, 0.113 mmol, 76% yield, UPLC/HRMS purity: 99.0%). Purification was carried out by an automated MPLC system using a 12 g normal phase silica column with gradient elution from 0–60% EtOAc/hexanes. R_f = 0.24 (50% EtOAc/hexanes); mp 171–175 ˚C; IR (neat) 3413, 1614 cm^{-1}; ^1H NMR (400 MHz, $CDCl_3$) δ 7.24 (m, 3H), 7.09 (m, 2H), 3.59 (m, 1H), 3.51 (m, 1H), 3.29–3.14 (m, 3H), 2.85 (m, 2H), 2.31 (s, 3H), 2.17 (m, 1H), 1.92–1.21 (complex, 18H), 1.12–1.05 (m, 4H, contains s, 1.07, 3H), 1.02–0.93 (m, 1H), 0.89–0.82 (m, 1H), 0.79 (s, 3H), 0.66 (m, 1H); ^{13}C NMR (101 MHz, $CDCl_3$) δ 176.7, 136.3, 132.7, 130.2 (2C), 129.8 (2C), 71.3, 53.4, 47.3, 46.2, 45.9, 44.5, 41.2, 38.1, 36.9, 35.7, 34.9, 34.6, 32.0, 31.6, 31.0, 28.6, 27.0, 21.2, 21.1, 20.3, 18.5, 12.4. HRMS (FT-ICR, HESI) *m/z*: $[M + H]^+$ calcd for $C_{29}H_{44}NO_2S$ 470.3087, found 470.3078.

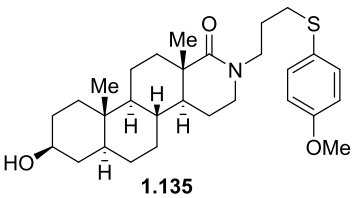

1.135

3β-Hydroxy-5α-androstane-derived D-Ring Lactam, 1.135. Following the general procedure G, **1.135** was prepared as a white amorphous solid (47.4 mg, 0.0976 mmol, 65% yield, UPLC/HRMS purity: 98.5%). Purification was carried out by an automated MPLC system using a 12 g normal phase silica column with gradient elution from 0–55% EtOAc/hexanes. R_f = 0.27 (50% EtOAc/hexanes); mp 152–155 ˚C; IR (neat) 3402, 1612 cm^{-1}; ^1H NMR (400 MHz, $CDCl_3$)

δ 7.33 (m, 2H), 6.84 (m, 2H), 3.79 (s, 3H), 3.59 (m, 1H), 3.49 (m, 1H), 3.28–3.13 (m, 3H), 2.78 (m, 2H), 2.17 (m, 1H), 1.91–1.21 (complex, 18H), 1.12–1.04 (m, 4H, contains s, 1.07, 3H), 1.00–0.93 (m, 1H), 0.90–0.80 (m, 1H), 0.79 (s, 3H), 0.66 (m, 1H); ^{13}C NMR (101 MHz, $CDCl_3$) δ 176.6, 159.1, 133.3 (2C), 126.6, 114.7 (2C), 71.3, 55.5, 53.2, 47.3, 46.1, 45.9, 44.5, 41.2, 38.1, 36.8, 35.7, 34.8, 34.6, 33.5, 31.6, 31.0, 28.6, 27.0, 21.2, 20.3, 18.4, 12.3. HRMS (FT-ICR, HESI) *m/z*: $[M + H]^+$ calcd 486.3036, found 486.3028.

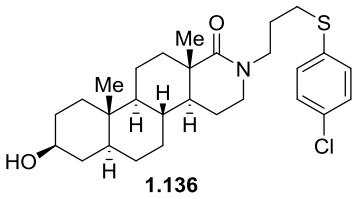

1.136

3β-Hydroxy-5α-androstane-derived D-Ring Lactam, 1.136. Following the general procedure G, **1.136** was prepared as a white amorphous solid (51.0 mg, 0.104 mmol, 69% yield, UPLC/HRMS purity: 96.6%). Purification was carried out by an automated MPLC system using a 12 g normal phase silica column with gradient elution from 0–65% EtOAc/hexanes. R_f = 0.28 (50% EtOAc/hexanes); mp 188–196 ˚C; IR (neat) 3393, 1613 cm^{-1}; ^{1}H NMR (400 MHz, $CDCl_3$) δ 7.24 (m, 4H), 3.63–3.48 (m, 2H), 3.29–3.15 (m, 3H), 2.89 (m, 2H), 2.17 (m, 1H), 1.92–1.21 (complex, 18H), 1.12–1.05 (m, 4H, contains s, 1.07, 3H), 0.96 (m, 1H), 0.89–0.80 (m, 1H), 0.79 (s, 3H), 0.66 (m, 1H); ^{13}C NMR (101 MHz, $CDCl_3$) δ 176.8, 135.1, 132.1, 130.7 (2C), 129.2 (2C), 71.3, 53.4, 47.3, 46.2, 45.9, 44.5, 41.2, 38.1, 36.9, 35.7, 34.8, 34.6, 31.5850, 31.5849, 31.0, 28.6, 26.9, 21.2, 20.3, 18.5, 12.4. HRMS (FT-ICR, HESI) *m/z*: $[M + H]^+$ calcd for $C_{28}H_{41}ClNO_2S$ 490.2541, found 490.2532.

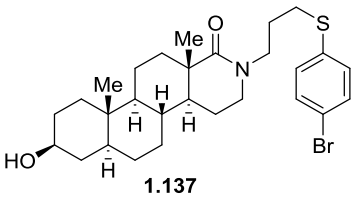

1.137

3β-Hydroxy-5α-androstane-derived D-Ring Lactam, 1.137. Following the general procedure G, **1.137** was prepared as a white amorphous solid (48.9 mg, 0.0913 mmol, 61% yield, UPLC/HRMS purity: 98.9%). Purification was carried out by an automated MPLC system using a 12 g normal phase silica column with gradient elution from 0–60% EtOAc/hexanes. R_f = 0.29 (50% EtOAc/hexanes); mp 196–199 ˚C; IR (neat) 3408, 1610 cm^{-1}; ^1H NMR (400 MHz, $CDCl_3$) δ 7.39 (m, 2H), 7.18 (m, 2H), 3.59 (m, 1H), 3.56–3.49 (m, 1H), 3.30–3.15 (m, 3H), 2.87 (m, 2H), 2.18 (m, 1H), 1.91–1.21 (complex, 18H), 1.13–1.05 (m, 4H, contains s, 1.08, 3H), 0.97 (m, 1H), 0.90–0.80 (m, 1H), 0.79 (s, 3H). 0.67 (m, 1H); ^{13}C NMR (101 MHz, $CDCl_3$) δ 176.8, 135.9, 132.1 (2C), 130.8 (2C), 119.9, 71.3, 53.4, 47.3, 46.2, 45.9, 44.5, 41.2, 38.1, 36.9, 35.7, 34.8, 34.6, 31.6, 31.4, 31.0, 28.6, 26.8, 21.2, 20.3, 18.5, 12.4. HRMS (FT-ICR, HESI) *m/z*: $[M + H]^+$ calcd for $C_{28}H_{41}BrNO_2S$ 534.2036, found 534.2028.

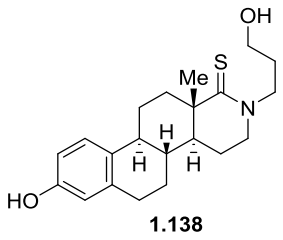

1.138

3-Hydroxy-1,3,5-estratriene-derived D-Ring Thioamide, 1.138. Following the general procedure G, **1.138** was prepared as a white amorphous solid (55.1 mg, 0.153 mmol, 51% yield, UPLC/HRMS purity: 92.0%). Purification was carried out by an automated MPLC system using a 12 g normal phase silica column with gradient elution from 0–1.5% MeOH/CH_2Cl_2. R_f = 0.40 (5% MeOH/CH_2Cl_2); mp 216–219 ˚C; IR (neat) 3227, 1531, 1501 cm^{-1}; ^1H NMR (400 MHz,

DMSO-d_6) δ 8.99 (s, 1H), 7.06 (d, J = 8.5 Hz, 1H), 6.52 (d, J = 8.5 Hz, 1H), 6.44 (s, 1H), 4.50 (m, 1H), 4.02 (m, 1H), 3.78 (m, 1H), 3.63 (m, 1H), 3.51 (m, 1H), 3.43 (m, 2H), 2.70 (m, 3H), 2.31 (m, 1H), 2.07 (m, 3H), 1.81 (m, 2H), 1.64–1.15 (complex, 6H), 1.08 (s, 3H); ^{13}C NMR (126 MHz, DMSO-d_6) δ 207.8, 155.0, 137.0, 130.2, 126.0, 114.7, 112.8, 58.5, 52.2, 50.6, 45.2, 42.3, 41.9, 39.3, 29.4, 28.2, 26.4, 25.8, 20.6, 20.4. **Note**: Missing one carbon signal due to signal overlap. HRMS (FT-ICR, HESI) *m/z*: $[M + H]^+$ calcd for $C_{21}H_{30}NO_2S$ 360.1992, found 360.1990.

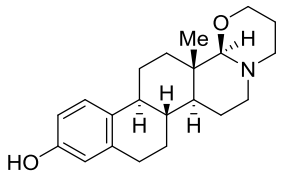

1.139

3-Hydroxy-1,3,5-estratriene-derived D-Ring Oxazinane, 1.139. Following the general procedure G, **1.139** was prepared as a white amorphous solid (54.2 mg, 0.166 mmol, 83% yield, LCMS purity: ≥99.5%). Purification was carried out by an automated MPLC system using a 12 g normal phase silica column with gradient elution from 0–8% MeOH (0.5% NH_4OH)/CH_2Cl_2. R_f = 0.20 (5% MeOH (0.5% NH_4OH)/CH_2Cl_2); mp 206–212 ˚C; IR (neat) 2936, 2851, 1609, 1509 cm^{-1}; ^{1}H NMR (400 MHz, DMSO-d_6) δ 8.97 (s, 1H), 7.03 (d, J = 8.6 Hz, 1H), 6.50 (dd, J = 8.4, 2.6 Hz, 1H), 6.42 (d, J = 2.6 Hz, 1H), 3.93 (m, 1H), 3.29 (m, 1H), 2.83–2.67 (m, 4H), 2.21 (m, 1H), 2.12 (m, 1H), 2.05–1.90 (m, 3H), 1.84–1.68 (m, 2H), 1.56 (m, 1H), 1.40 (m, 1H), 1.30–1.10 (complex, 6H), 1.03–0.96 (m, 1H), 0.89 (s, 3H); ^{13}C NMR (126 MHz, DMSO-d_6) δ 154.9, 137.0, 130.4, 125.9, 114.7, 112.8, 101.1, 66.5, 53.9, 53.6, 47.3, 42.8, 37.9, 37.7, 35.5, 29.4, 25.7, 25.6, 25.4, 23.0, 13.6. HRMS (FT-ICR, HESI) *m/z*: $[M + H]^+$ calcd for $C_{21}H_{30}NO_2$ 328.2271, found 328.2267.

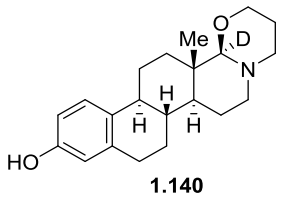

1.140

3-Hydroxy-1,3,5-estratriene-derived D-Ring Oxazinane, 1.140. Following the general procedure G, **1.140** was prepared as a white amorphous solid (53.9 mg, 0.164 mmol, 82% yield, LCMS purity: ≥99.5%). Purification was carried out by an automated MPLC system using a 12 g normal phase silica column with gradient elution from 0–10% MeOH (0.5% NH_4OH)/CH_2Cl_2. R_f = 0.20 (5% MeOH (0.5% NH_4OH)/CH_2Cl_2); mp 212–215 ˚C; IR (neat) 2936, 2855, 1610, 1505 cm^{-1}; ^1H NMR (400 MHz, DMSO-d_6) δ 8.97 (s, 1H), 7.03 (d, J = 8.3 Hz, 1H), 6.50 (dd, J = 8.4, 2.6 Hz, 1H), 6.42 (d, J = 2.6 Hz, 1H), 3.93 (m, 1H), 3.30 (m, 1H), 2.83 (m, 1H), 2.75–2.68 (m, 3H), 2.21 (m, 1H), 2.12 (m, 1H), 2.05–1.89 (m, 3H), 1.84–1.68 (m, 2H), 1.55 (m, 1H), 1.40 (m, 1H), 1.30–1.05 (complex, 5H), 1.02–0.96 (m, 1H), 0.89 (s, 3H); ^{13}C NMR (126 MHz, DMSO-d_6) δ 154.9, 137.0, 130.4, 125.9, 114.7, 112.8, 101.1, 66.5, 53.9, 53.6, 47.3, 42.8, 37.9, 37.6, 35.5, 29.4, 25.7, 25.6, 25.4, 23.0, 13.6. HRMS (FT-ICR, HESI) *m/z*: $[M + H]^+$ calcd for $C_{21}H_{29}DNO_2$ 329.2334, found 329.2329.

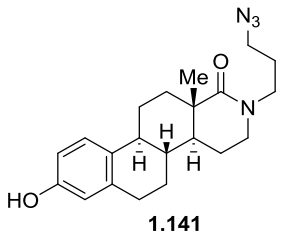

1.141

3-Hydroxy-1,3,5-estratriene-derived D-Ring Lactam, 1.141. Following the general procedure G, **1.141** was prepared as an off-white amorphous solid (45.2 mg, 0.123 mmol, 82% yield, UPLC/HRMS purity: 94.5%). Purification was carried out by an automated MPLC system using a 4 g normal phase silica column with gradient elution from 0–30% EtOAc/hexanes. R_f =

0.50 (50% EtOAc/hexanes); mp 204–210 ˚C; IR (neat) 3323, 2098, 1619, 1607 cm^{-1}; ^1H NMR (400 MHz, DMSO-d_6) δ 9.00 (s, 1H), 7.06 (d, J = 8.4 Hz, 1H), 6.51 (dd, J = 8.4, 2.7 Hz, 1H), 6.43 (d, J = 2.6 Hz, 1H), 3.40–3.14 (complex, 6H), 2.72 (m, 2H), 2.28 (m, 1H), 2.11 (m, 2H), 2.00 (m, 2H), 1.72 (p, J = 6.9 Hz, 2H), 1.61–1.11 (complex, 6H), 1.02 (s, 3H); ^{13}C NMR (101 MHz, DMSO-d_6) δ 175.1, 155.0, 137.0, 130.2, 125.8, 114.6, 112.8, 48.6, 46.3, 43.8, 43.7, 42.3, 40.5, 38.1, 34.4, 29.3, 25.9, 25.7, 25.5, 20.4, 17.9. HRMS (FT-ICR, HESI) *m/z*: $[M + H]^+$ calcd for $C_{21}H_{29}N_4O_2$ 369.2285, found 369.2283.

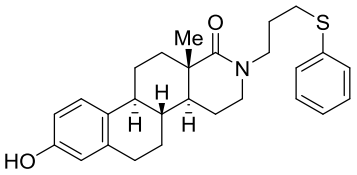

1.142

3-Hydroxy-1,3,5-estratriene-derived D-Ring Lactam, 1.142. Following the general procedure G, **1.142** was prepared as an off-white amorphous solid (40.6 mg, 0.0932 mmol, 62% yield, UPLC/HRMS purity: 97.8%). Purification was carried out by an automated MPLC system using a 12 g normal phase silica column with gradient elution from 0–60% EtOAc/hexanes. R_f = 0.63 (50% EtOAc/hexanes); mp 209–215 ˚C; IR (neat) 3053, 1560, 1585 cm^{-1}; ^1H NMR (400 MHz, DMSO-d_6) δ 9.01 (s, 1H), 7.32 (m, 4H), 7.19 (m, 1H), 7.05 (d, J = 8.5 Hz, 1H), 6.51 (dd, J = 8.4, 2.6 Hz, 1H), 6.44 (d, J = 2.6 Hz, 1H), 3.41 (m, 1H), 3.32–3.19 (m, 4H), 2.91 (m, 2H), 2.72 (m, 2H), 2.26 (m, 1H), 2.10 (m, 2H), 1.98 (m, 1H), 1.76 (p, J = 7.2 Hz, 2H), 1.57–1.14 (complex, 6H), 1.01 (s, 3H); ^{13}C NMR (126 MHz DMSO-d_6) δ 175.2, 155.0, 137.0, 136.3, 130.2, 129.1 (2C), 128.0 (2C), 126.0, 125.6, 114.7, 112.8, 46.5, 45.4, 43.8, 42.3, 40.5, 38.1, 34.4, 29.7, 29.4, 26.3, 25.8, 25.6, 20.4, 18.0. HRMS (FT-ICR, HESI) *m/z*: calcd for $C_{27}H_{34}NO_2S$ $[M + H]^+$ 436.2305, found 436.2301.

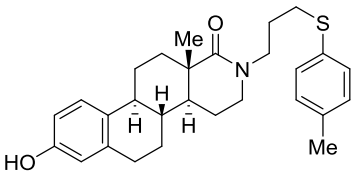

1.143

3-Hydroxy-1,3,5-estratriene-derived D-Ring Lactam, 1.143. Following the general procedure G, **1.143** was prepared as a white amorphous solid (40.2 mg, 0.0894 mmol, 60% yield, UPLC/HRMS purity: 99.0%). Purification was carried out by an automated MPLC system using a 12 g normal phase silica column with gradient elution from 0–50% EtOAc/hexanes. R_f = 0.50 (50% EtOAc/hexanes); mp 208–212 ˚C; IR (neat) 3282, 1602 cm^{-1}; ^1H NMR (400 MHz, DMSO-d_6) δ 9.00 (s, 1H), 7.22 (m, 2H), 7.13 (m, 2H), 7.05 (d, J = 8.4 Hz, 1H), 6.51 (dd, J = 8.4, 2.6 Hz, 1H), 6.44 (d, J = 2.6 Hz, 1H), 3.39 (m, 1H), 3.29–3.16 (m, 3H), 2.86 (m, 2H), 2.72 (m, 2H), 2.32–2.25 (m, 4H, contains s, 2.26, 3H), 2.10 (m, 2H), 1.97 (m, 2H), 1.72 (p, J = 7.2 Hz, 2H), 1.60–1.14 (complex, 6H), 1.00 (s, 3H); ^{13}C NMR (126 MHz, DMSO-d_6) δ 175.1, 155.0, 137.0, 135.3, 132.4, 130.2, 129.7 (2C), 128.9 (2C), 126.0, 114.7, 112.8, 46.4, 45.4, 43.8, 42.3, 40.5, 38.1, 34.4, 30.4, 29.4, 26.4, 25.8, 25.6, 20.5, 20.4, 18.0. HRMS (FT-ICR, HESI) *m/z*: $[M + H]^+$ calcd for $C_{28}H_{36}NO_2S$ 450.2461, found 450.2458.

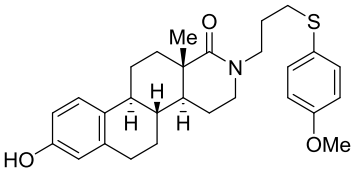

1.144

3-Hydroxy-1,3,5-estratriene-derived D-Ring Lactam, 1.144. Following the general procedure G, **1.144** was prepared as an off-white crystalline solid (44.0 mg, 0.0945 mmol, 63% yield, UPLC/HRMS purity: ≥99.5%). Purification was carried out by an automated MPLC system using a 12 g normal phase silica column with gradient elution from 0–80%

EtOAc/hexanes. R_f = 0.38 (50% EtOAc/hexanes); mp 206–209 ˚C; IR (neat) 3301, 1618, 1606 cm^{-1}; ^1H NMR (400 MHz, DMSO-d_6) δ 9.00 (s, 1H), 7.32 (m, 2H), 7.05 (d, J = 8.4 Hz, 1H), 6.91 (m, 2H), 6.51 (dd, J = 8.4, 2.6 Hz, 1H), 6.44 (d, J = 2.6 Hz, 1H), 3.74 (s, 3H), 3.37 (m, 1H), 3.29–3.16 (m, 3H), 2.78 (m, 2H), 2.72 (m, 2H), 2.27 (m, 1H), 2.11 (m, 2H), 1.98 (m, 2H), 1.69 (p, J = 7.2 Hz, 2H), 1.59–1.16 (complex, 6H), 1.00 (s, 3H); ^{13}C NMR (126 MHz, DMSO-d_6) δ 175.1, 158.3, 155.0, 137.0, 132.2 (2C), 130.2, 125.97 (2C), 125.91, 114.8, 114.7, 112.8, 55.2, 46.4, 45.3, 43.8, 42.3, 40.5, 38.1, 34.4, 32.0, 29.4, 26.4, 25.8, 25.6, 20.4, 18.0. HRMS (FT-ICR, HESI) *m/z*: $[M + H]^+$ calcd for $C_{28}H_{36}NO_3S$ 466.2410, found 466.2408.

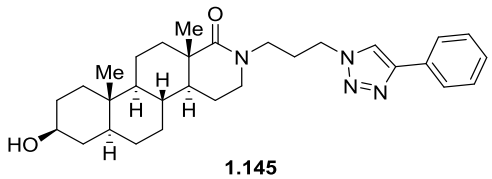

1.145

3β-Hydroxy-5α-androstane-derived D-Ring Lactam, 1.145. Following the general procedure H, **1.145** was prepared as a white amorphous solid (81.7 mg, 0.167 mmol, 83% yield, UPLC/HRMS purity: 98.9%). Purification was carried out by an automated MPLC system using a 12 g normal phase silica column with gradient elution from 0–5% MeOH/CH_2Cl_2. R_f = 0.25 (3% MeOH/CH_2Cl_2); mp 197–202 ˚C; IR (neat) 3400, 1619 cm^{-1}; ^1H NMR (400 MHz, $CDCl_3$) δ 7.93 (s, 1H), 7.84 (m, 2H), 7.41 (m, 2H), 7.32 (m, 1H), 4.40 (m, 2H), 3.58 (m, 1H), 3.42 (m, 2H), 3.30–3.15 (m, 2H), 2.36–2.13 (m, 3H), 1.87 (m, 1H), 1.69 (m, 2H), 1.72–1.10 (complex, 12H), 1.06–0.98 (m, 4H, contains s, 1.06, 3H), 2.93 (s, 3H) 0.50 (m, 1H); ^{13}C NMR (101 MHz, $CDCl_3$) δ 172.3, 147.7, 130.8, 128.9 (2C), 128.2, 125.9 (2C), 120.4, 71.3, 53.1, 48.5, 47.3, 45.6, 44.8, 44.3, 41.2, 38.1, 36.7, 35.6, 34.8, 34.5, 31.5, 30.9, 28.6, 27.7, 21.0, 20.2, 18.4, 12.3. HRMS (FT-ICR, HESI) *m/z*: $[M + H]^+$ calcd for $C_{30}H_{43}N_4O_2$ 491.3381, found 491.3372.

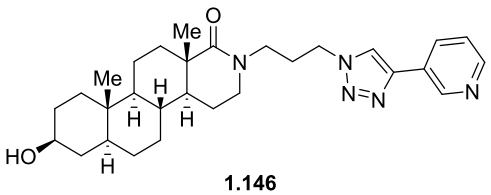

1.146

3β-Hydroxy-5α-androstane-derived D-Ring Lactam, 1.146. Following the general procedure H, **1.146** was prepared as a white amorphous solid (74.9 mg, 0.152 mmol, 84% yield, UPLC/HRMS purity: 97.9%). Purification was carried out by an automated MPLC system using a 12 g normal phase silica column with gradient elution from 0–5% MeOH/CH_2Cl_2. R_f = 0.16 (5% MeOH/CH_2Cl_2); mp 190–194 ˚C; IR (neat) 3353, 1640, 1609 cm^{-1}; ^1H NMR (400 MHz, $CDCl_3$) δ 9.04 (s, 1H), 8.57 (m, 1H), 8.19 (m, 1H), 8.08 (s, 1H), 7.36 (ddd, *J* = 7.9, 4.8, 0.8 Hz,) 4.42 (m, 2H), 3.59 (m, 1H), 3.50–3.17 (m, 4H), 2.34–2.12 (m, 3H), 1.91 (m, 1H), 1.83 (m, 1H), 1.71 (m, 2H), 1.62–1.15 (complex, 11H), 1.08–0.99 (m, 4H, contains s, 1.08, 3H), 0.95–0.79 (m, 2H), 0.77 (s, 3H), 0.54 (m, 1H); ^{13}C NMR (101 MHz, $CDCl_3$) δ 177.4, 149.3, 147.3, 144.6, 133.1, 127.0, 123.8, 120.9, 71.2, 53.2, 48.5, 47.3. 45.7, 44.6, 44.4, 41.3, 38.1, 36.8, 35.6, 34.8, 34.6, 31.5, 30.9, 28.6, 27.8, 21.1, 20.2, 18.5, 12.3. HRMS (FT-ICR, HESI) *m/z*: $[M + H]^+$ calcd for $C_{29}H_{42}N_5O_2$ 492.3333, found 492.3322.

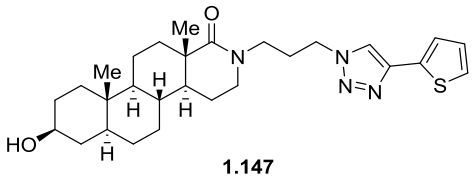

1.147

3β-Hydroxy-5α-androstane-derived D-Ring Lactam, 1.147. Following the general procedure H, **1.147** was prepared as a white foam/crystalline solid (81.5 mg, 0.164 mmol, 91% yield, UPLC/HRMS purity: 95.9%). Purification was carried out by an automated MPLC system using a 12 g normal phase silica column with gradient elution from 0–5% MeOH/CH_2Cl_2. R_f =

0.35 (5% MeOH/CH_2Cl_2); mp 140–144 ˚C; IR (neat) 3345, 1622 cm^{-1}; ^1H NMR (500 MHz, $CDCl_3$) δ 7.83 (s, 1H), 7.68 (m, 1H), 7.46 (m, 1H), 7.37 (m, 1H), 4.38 (m, 2H), 3.59 (tt, *J* = 10.7, 4.8 Hz, 1H), 3.41 (m, 2H), 3.28–3.15 (m, 2H), 2.28 (m, 1H), 2.16 (m, 2H), 1.88 (m, 1H), 1.82–1.67 (m, 3H), 1.60–1.18 (complex, 11H), 1.12 (m, 1H), 1.06–1.00 (m, 4H, contains s, 1.06, 3H), 0.91 (m, 1H), 0.85–0.78 (m, 1H), 0.76 (s, 3H), 0.50 (m, 1H); ^{13}C NMR (126 MHz, $CDCl_3$) δ 177.3 143.9, 132.0, 126.4, 126.0, 121.1, 120.2, 71.3, 53.0, 48.5, 47.3, 45.5, 44.8, 44.3, 41.1, 38.1, 36.7, 35.6, 34.7, 34.5, 31.5, 30.9, 28.6, 27.6, 21.0, 20.2, 18.4, 12.3. HRMS (FT-ICR, HESI) *m/z*: $[M + H]^+$ calcd for $C_{28}H_{41}N_4O_2S$ 497.2945, found 497.2936.

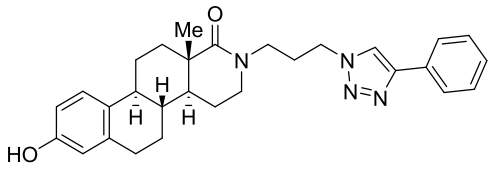

1.148

3-Hydroxy-1,3,5-estratriene-derived D-Ring Lactam, 1.148. Following the general procedure H, **1.148** was prepared as a white crystalline/amorphous solid (58.8 mg, 0.125 mmol, 63% yield, UPLC/HRMS purity: ≥99.5%). Purification was carried out by an automated MPLC system using a 12 g normal phase silica column with gradient elution from 30–85% EtOAc/hexanes. R_f = 0.30 (80% EtOAc/hexanes); mp 217–223 ˚C; IR (neat) 3363, 1593 cm^{-1}; ^1H NMR (400 MHz, DMSO-d_6) δ 9.00 (s, 1H), 8.60 (s, 1H), 7.84 (m, 2H), 7.44 (m, 2H), 7.32 (m, 1H), 7.04 (d, *J* = 8.5 Hz, 1H), 6.51 (dd, *J* = 8.4, 2.6 Hz, 1H), 6.44 (d, *J* = 2.6 Hz, 1H), 4.37 (t, *J* = 7.0 Hz, 1H), 3.39–3.35 (m, 2H), 3.29–3.21 (m, 2H), 2.71 (m, 2H), 2.25 (m, 1H), 2.16–2.06 (m, 5H), 1.98 (m, 2H), 1.59–1.17 (complex, 6H), 1.02 (s, 3H); ^{13}C NMR (126 MHz, DMSO-d_6) δ 175.4, 155.0, 146.3, 137.0, 130.4, 130.2, 128.9 (2C), 127.8, 126.0, 125.1 (2C), 121.4, 114.7, 112.8, 47.7, 46.3, 43.8, 43.7, 42.2, 40.5, 38.1, 34.3, 29.4, 27.2, 25.8, 25.6, 20.4, 18.0. HRMS (FT-ICR, HESI) *m/z*: $[M + H]^+$ calcd for $C_{29}H_{35}N_4O_2$ 471.2755, found 471.2752.

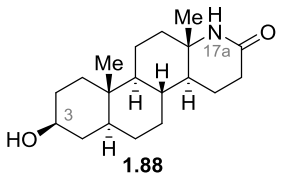

1.88

3β-Hydroxy-5α-androstane-derived D-Ring Lactam, 1.88. To a solution of **1.117** (85.0 mg, 0.200 mmol) in anhydrous THF (4.0 mL) was condensed liquid NH_3 (~15 mL) at –78 ˚C. To the cooled solution was added pieces of sodium metal until the solution turned blue. The blue solution was stirred at –78˚C for 2 h, and was quenched by adding solid NH_4Cl slowly (until the disappearance of blue). The resulting mixture was diluted with H_2O (20 mL) and EtOAc (30 mL). The organic layer was washed with brine, dried over anhydrous Na_2SO_4, filtered, and concentrated. Purification was carried out by an automated MPLC system using a 12 g normal phase silica column with gradient elution from 0–5% MeOH/CH_2Cl_2 to afford **1.88** as a white amorphous solid (56.8 mg, 0.186 mmol, 93% yield, UPLC/HRMS purity: ≥99.5%). Characterization data were consistent to **1.88** synthesized via the Beckmann rearrangement. HRMS (FT-ICR, HESI) *m/z*: $[M + H]^+$ calcd for $C_{19}H_{32}NO_2$ 306.2428, found 306.2423.

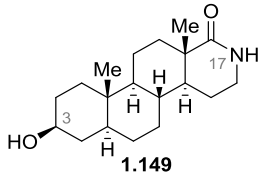

1.149

3β-Hydroxy-5α-androstane-derived D-Ring Lactam, 1.149. To a solution of **1.118** (57.2 mg, 0.134 mmol) in anhydrous THF (4.0 mL) was condensed liquid NH_3 (~15 mL) at –78 ˚C. To the cooled solution was added pieces of sodium metal until the solution turned blue. The blue solution was stirred at –78 ˚C for 2 h, and was quenched by adding solid NH_4Cl slowly (until the disappearance of blue). The resulting mixture was diluted with H_2O (20 mL) and EtOAc (30 mL). The organic layer was washed with brine, dried over anhydrous Na_2SO_4,

filtered, and concentrated. Purification was carried out by an automated MPLC system using a 12 g normal phase silica column with gradient elution from 0–5% MeOH/CH_2Cl_2 to afford **1.149** as a white amorphous solid (37.1 mg, 0.121 mmol, 90% yield, UPLC/HRMS purity: ≥99.5%). R_f = 0.26 (4% MeOH/CH_2Cl_2); IR (neat) 3378, 1646 cm^{-1}; mp 253–256 ˚C; ^1H NMR (400 MHz, $CDCl_3$) δ 5.52 (s, 1H), 3.59 (tt, *J* = 10.7, 4.8 Hz, 1H), 3.34 (m, 1H), 3.24 (m, 1H), 2.14 (m, 1H), 1.91–1.72 (m, 3H), 1.67–1.21 (complex, 12H), 1.14 (s, 3H), 1.12–1.05 (m, 1H), 1.00–0.83 (m, 2H), 0.80 (s, 3H), 0.69 (m, 1H); ^{13}C NMR (101 MHz, $CDCl_3$) δ 179.2, 71.3, 53.5, 46.0, 44.4, 41.6, 41.1, 38.1, 36.8, 35.8, 34.6, 34.0, 31.6, 31.2, 28.6, 20.5, 20.1, 18.4, 12.4. HRMS (FT-ICR, HESI) *m/z*: $[M + H]^+$ calcd for $C_{19}H_{32}NO_2$ 306.2428, found 306.2423.

1.7 References

1. Dandapani, S.; Rosse, G.; Southall, N.; Salvino, J. M.; Thomas, C. J. Selecting, Acquiring, and Using Small Molecule Libraries for High-Throughput Screening. *Current Protocols in Chemical Biology* **2012**, *4*, 177-191.

2. Swinney, D. C.; Anthony, J. How were New Medicines Discovered? *Nat. Rev. Drug Discov.* **2011**, *10*, 507-519.

3. Macarron, R.; Banks, M. N.; Bojanic, D.; Burns, D. J.; Cirovic, D. A.; Garyantes, T.; Green, D. V. S.; Hertzberg, R. P.; Janzen, W. P.; Paslay, J. W.; Schopfer, U.; Sittampalam, G. S. Impact of High-Throughput Screening in Biomedical Research. *Nat. Rev. Drug Discov.* **2011**, *10*, 188-195.

4. Heeres, J. T.; Hergenrother, P. J. High-Throughput Screening for Modulators of Protein-Protein Interactions: Use of Photonic Crystal Biosensors and Complementary Technologies. *Chem. Soc. Rev.* **2011**, *40*, 4398-4410.

5. Li, J. W. H.; Vederas, J. C. Drug Discovery and Natural Products: End of an Era or an Endless Frontier? *Science* **2009**, *325*, 161-165.

6. Schreiber, S. L. Target-Oriented and Diversity-Oriented Organic Synthesis in Drug Discovery. *Science* **2000**, *287*, 1964-1969.

7. Wetzel, S.; Bon, R. S.; Kumar, K.; Waldmann, H. Biology-Oriented Synthesis. *Angew. Chem. Int. Ed.* **2011**, *50*, 10800-10826.

8. McLeod, M. C.; Singh, G.; Plampin Iii, J. N.; Rane, D.; Wang, J. L.; Day, V. W.; Aubé, J. Probing Chemical Space with Alkaloid-Inspired Libraries. *Nat. Chem.* **2014**, *6*, 133-140.

9. Huigens III, R. W.; Morrison, K. C.; Hicklin, R. W.; Flood Jr, T. A.; Richter, M. F.; Hergenrother, P. J. A Ring-Distortion Strategy to Construct Stereochemically Complex and Structurally Diverse Compounds from Natural Products. *Nat. Chem.* **2013**, *5*, 195-202.

10. Merrifield, R. B. Solid Phase Peptide Synthesis. I. The Synthesis of a Tetrapeptide. *J. Am. Chem. Soc.* **1963**, *85*, 2149-2154.

11. Bunin, B. A.; Plunkett, M. J.; Ellman, J. A. The Combinatorial Synthesis and Chemical and Biological Evaluation of a 1,4-Benzodiazepine Library. *Proc. Natl. Acad. Sci. U.S.A.* **1994**, *91*, 4708-4712.

12. Nielsen, T. E.; Schreiber, S. L. Towards the Optimal Screening Collection: A Synthesis Strategy. *Angew. Chem. Int. Ed.* **2007**, *47*, 48-56.

13. O' Connor, C. J.; Beckmann, H. S. G.; Spring, D. R. Diversity-Oriented Synthesis: Producing Chemical Tools for Dissecting Biology. *Chem. Soc. Rev.* **2012**, *41*, 4444-4456.

14. Burke, M. D.; Schreiber, S. L. A Planning Strategy for Diversity-Oriented Synthesis. *Angew. Chem. Int. Ed.* **2003**, *43*, 46-58.

15. Morrison, K. C.; Hergenrother, P. J. Natural Products as Starting Points for the Synthesis of Complex and Diverse Compounds. *Nat. Prod. Rep.* **2014**, *31*, 6-14.

16. Švenda, J.; Sheremet, M.; Kremer, L.; Maier, L.; Bauer, J. O.; Strohmann, C.; Ziegler, S.; Kumar, K.; Waldmann, H. Biology-Oriented Synthesis of a Withanolide-Inspired Compound Collection Reveals Novel Modulators of Hedgehog Signaling. *Angew. Chem. Int. Ed.* **2015**, *54*, 5596-5602.

17. Maltais, R.; Tremblay, M. R.; Poirier, D. Solid-Phase Synthesis of Hydroxysteroid Derivatives Using the Diethylsilyloxy Linker. *J. Comb. Chem.* **2000**, *2*, 604-614.

18. Doi, T.; Hijikuro, I.; Takahashi, T. An Efficient Solid-Phase Synthesis of the Vitamin D3 System. *J. Am. Chem. Soc.* **1999**, *121*, 6749-6750.

19. Lednicer, D. *Steroid Chemistry at a Glance*. John Wiley & Sons, Ltd. : Hoboken, GB, 2010; Vol. 26, p 1-144.

20. Brueggemeier, R. W.; Li, P.-K.; Abraham, D. J., Fundamentals of Steroid Chemistry and Biochemistry. In *Burger's Medicinal Chemistry and Drug Discovery*, John Wiley & Sons, Inc.: 2003.

21. Pines, S. H. The Merck Bile Acid Cortisone Process: The Next-to-Last Word. *Org. Process Res. Dev.* **2004**, *8*, 708-724.

22. Marker, R. E. Sterols. CV. The Preparation of Testosterone and Related Compounds from Sarsasapogenin and Diosgenin. *J. Am. Chem. Soc.* **1940**, *62*, 2543-2547.

23. Renneberg, R. Biotech History: Mexico, the Father of the Pill and the Race for Cortisone. *Biotechnology Journal* **2008**, *3*, 449-451.

24. Djerassi, C. Steroid Research at Syntex: “The Pill” and Cortisone. *Steroids* **1992**, *57*, 631-641.

25. Hanson, J. R. Steroids: Partial Synthesis in Medicinal Chemistry. *Nat. Prod. Rep.* **2007**, *24*, 1342-1349.

26. Hanson, J. R. Steroids: Partial Synthesis in Medicinal Chemistry. *Nat. Prod. Rep.* **2010**, *27*, 887-899.

27. Ibrahim-Ouali, M.; Rocheblave, L. Recent Advances in Azasteroids Chemistry. *Steroids* **2008**, *73*, 375-407.

28. Singh, R.; Panda, G. An Overview of Synthetic Approaches for Heterocyclic Steroids. *Tetrahedron* **2013**, *69*, 2853-2884.

29. Frye, S. V. Discovery and Clinical Development of Dutasteride, a Potent Dual 5a-Reductase Inhibitor. *Curr. Top. Med. Chem.* **2006**, *6*, 405-421.

30. Logothetis, C. J.; Efstathiou, E.; Manuguid, F.; Kirkpatrick, P. Abiraterone Acetate. *Nat. Rev. Drug Discov.* **2011**, *10*, 573-574.

31. Mitchell, H. J.; Dankulich, W. P.; Hartman, G. D.; Prueksaritanont, T.; Schmidt, A.; Vogel, R. L.; Bai, C.; McElwee-Witmer, S.; Zhang, H. Z.; Chen, F.; Leu, C.-T.; Kimmel, D. B.; Ray, W. J.; Nantermet, P.; Gentile, M. A.; Duggan, M. E.; Meissner, R. S. Design, Synthesis, and Biological Evaluation of 16-Substituted 4-Azasteroids as Tissue-Selective Androgen Receptor Modulators (SARMs). *J. Med. Chem.* **2009**, *52*, 4578-4581.

32. Rasmusson, G. H.; Reynolds, G. F.; Steinberg, N. G.; Walton, E.; Patel, G. F.; Liang, T.; Cascieri, M. A.; Cheung, A. H.; Brooks, J. R.; Berman, C. Azasteroids: Structure-Activity Relationships for Inhibition of 5a-Reductase and of Androgen Receptor Binding. *J. Med. Chem.* **1986**, *29*, 2298-2315.

33. Tan, M. H. E.; Li, J.; Xu, H. E.; Melcher, K.; Yong, E.-l. Androgen Receptor: Structure, Role in Prostate Cancer and Drug Discovery. *Acta Pharmacologica Sinica* **2014**, *36*, 3.

34. Cabeza, M.; Sánchez-Márquez, A.; Garrido, M.; Silva, A.; Bratoeff, E. Recent Advances in Drug Design and Drug Discovery for Androgen-Dependent Diseases. *Curr. Med. Chem.* **2016**, *23*, 792-815.

35. Batchelor, K. W.; Frye, S. V.; Dorsey, G. F.; Mook, R. A. Androstenone Derivative. 1996.

36. Satyanarayana, K.; Srinivas, K.; Himabindu, V.; Reddy, G. M. A Scaleable Synthesis of Dutasteride: A Selective 5α-Reductase Inhibitor. *Org. Process Res. Dev.* **2007**, *11*, 842-845.

37. Potter, G. A.; Barrie, S. E.; Jarman, M.; Rowlands, M. G. Novel Steroidal Inhibitors of Human Cytochrome P45017a (a-Hydroxylase-C17,20-lyase): Potential Agents for the Treatment of Prostatic Cancer. *J. Med. Chem.* **1995**, *38*, 2463-2471.

38. DeVore, N. M.; Scott, E. E. Structures of Cytochrome P450 17A1 with Prostate Cancer Drugs Abiraterone and TOK-001. *Nature* **2012**, *482*, 116-119.

39. Shi, J.; Manolikakes, G.; Yeh, C.-H.; Guerrero, C. A.; Shenvi, R. A.; Shigehisa, H.; Baran, P. S. Scalable Synthesis of Cortistatin A and Related Structures. *J. Am. Chem. Soc.* **2011**, *133*, 8014-8027.

40. Salvador, J. A. R.; Carvalho, J. F. S.; Neves, M. A. C.; Silvestre, S. M.; Leitao, A. J.; Silva, M. M. C.; Sa e Melo, M. L. Anticancer Steroids: Linking Natural and Semi-Synthetic Compounds. *Nat. Prod. Rep.* **2013**, *30*, 324-374.

41. Bansal, R.; Acharya, P. C. Man-Made Cytotoxic Steroids: Exemplary Agents for Cancer Therapy. *Chem. Rev.* **2014**, *114*, 6986-7005.

42. Verma, A. K.; Lee, C. Y.; Habtemariam, S.; Harvey, A. L.; Jindal, D. P. Synthesis and Biological Activity of 17-Azasteroidal Neuromuscular-Blocking Agents. *Eur. J. Med. Chem.* **1994**, *29*, 331-338.

43. Covey, D. F.; Han, M.; Kumar, A. S.; de la Cruz, M. A. M.; Meadows, E. S.; Hu, Y.; Tonnies, A.; Nathan, D.; Coleman, M.; Benz, A.; Evers, A. S.; Zorumski, C. F.; Mennerick, S. Neurosteroid Analogues. 8. Structure−Activity Studies of N-Acylated 17a-Aza-D-homosteroid Analogues of the Anesthetic Steroids (3α,5α)- and (3α,5β)-3-Hydroxypregnan-20-one. *J. Med. Chem.* **2000**, *43*, 3201-3204.

44. Huang, Y.; Cui, J.; Zhong, Z.; Gan, C.; Zhang, W.; Song, H. Synthesis and cytotoxicity of 17a-aza-d-homo-androster-17-one derivatives. *Bioorganic Med. Chem. Lett.* **2011**, *21*, 3641-3643.

45. Cernak, T.; Dykstra, K. D.; Tyagarajan, S.; Vachal, P.; Krska, S. W. The Medicinal Chemist's Toolbox for Late Stage Functionalization of Drug-Like Molecules. *Chem. Soc. Rev.* **2016**, *45*, 546-576.

46. Karimov, R. R.; Sharma, A.; Hartwig, J. F. Late Stage Azidation of Complex Molecules. *ACS Central Science* **2016**, *2*, 715-724.

47. Shugrue, C. R.; Miller, S. J. Applications of Nonenzymatic Catalysts to the Alteration of Natural Products. *Chem. Rev.* **2017**, *117*, 11894-11951.

48. Breslow, R. Biomimetic Control of Chemical Selectivity. *Acc. Chem. Res.* **1980**, *13*, 170-177.

49. Barton, D. H. R.; Doller, D. The Selective Functionalization of Saturated Hydrocarbons: Gif Chemistry. *Acc. Chem. Res.* **1992**, *25*, 504-512.

50. Buchschacher, P.; Kalvoda, J.; Arigoni, D.; Jeger, O. Direct Introduction of a Nitrogen Function at C-18 in a Steroid. *J. Am. Chem. Soc.* **1958**, *80*, 2905-2906.

51. Reese, P. B. Remote Functionalization Reactions in Steroids. *Steroids* **2001**, *66*, 481-497.

52. Gutekunst, W. R.; Baran, P. S. C-H Functionalization Logic in Total Synthesis. *Chem. Soc. Rev.* **2011**, *40*, 1976-1991.

53. Corey, E. J.; Hertler, W. R. The Synthesis of Dihydroconessine. A Method for Functionalizing Steroid at C18. . *J. Am. Chem. Soc.* **1958**, *80*, 2903-2904.

54. Barton, D.; Beaton, J.; Geller, L.; Pechet, M. A New Photochemical Reaction. *J. Am. Chem. Soc.* **1961**, *83*, 4076-4083.

55. Breslow, R.; Zhang, X.; Huang, Y. Selective Catalytic Hydroxylation of a Steroid by an Artificial Cytochrome P-450 Enzyme. *J. Am. Chem. Soc.* **1997**, *119*, 4535-4536.

56. Grieco, P. A.; Stuk, T. L. Remote Oxidation of Unactivated Carbon-Hydrogen Bonds in Steroids via Oxometalloporphinates. *J. Am. Chem. Soc.* **1990**, *112*, 7799-7801.

57. Kaufman, M. D.; Grieco, P. A.; Bougie, D. W. Functionalization of Unactivated Carbon-Hydrogen Bonds in Steroids via (Salen)manganese(III) Complexes. *J. Am. Chem. Soc.* **1993**, *115*, 11648-11649.

58. Engle, K. M.; Mei, T.-S.; Wasa, M.; Yu, J.-Q. Weak Coordination as a Powerful Means for Developing Broadly Useful C–H Functionalization Reactions. *Acc. Chem. Res.* **2012**, *45*, 788-802.

59. Lyons, T. W.; Sanford, M. S. Palladium-Catalyzed Ligand-Directed C−H Functionalization Reactions. *Chem. Rev.* **2010**, *110*, 1147-1169.

60. Giuliano, M. W.; Miller, S. J. Site-Selective Reactions with Peptide-Based Catalysts. *Top. Curr. Chem.* **2016**, 157-201.

61. Brückl, T.; Baxter, R. D.; Ishihara, Y.; Baran, P. S. Innate and Guided C–H Functionalization Logic. *Acc. Chem. Res.* **2012**, *45*, 826-839.

62. Lewis, J. C.; Coelho, P. S.; Arnold, F. H. Enzymatic Functionalization of Carbon-Hydrogen Bonds. *Chem. Soc. Rev.* **2011**, *40*, 2003-2021.

63. Huang, X.; Bergsten, T. M.; Groves, J. T. Manganese-Catalyzed Late-Stage Aliphatic C–H Azidation. *J. Am. Chem. Soc.* **2015**, *137*, 5300-5303.

64. Shang, M.; Wang, M.-M.; Saint-Denis, T. G.; Li, M.-H.; Dai, H.-X.; Yu, J.-Q. Copper-Mediated Late-Stage Functionalization of Heterocycle-Containing Molecules. *Angew. Chem. Int. Ed.* **2017**, *56*, 5317-5321.

65. Phipps, R. J.; Gaunt, M. J. A Meta-Selective Copper-Catalyzed C–H Bond Arylation. *Science* **2009**, *323*, 1593-1597.

66. McNally, A.; Haffemayer, B.; Collins, B. S. L.; Gaunt, M. J. Palladium-catalysed C–H Activation of Aliphatic Amines to give Strained Nitrogen Heterocycles. *Nature* **2014**, *510*, 129.

67. Topczewski, J. J.; Cabrera, P. J.; Saper, N. I.; Sanford, M. S. Palladium-catalysed Transannular C–H Functionalization of Alicyclic Amines. *Nature* **2016**, *531*, 220.

68. Howell, J. M.; Feng, K.; Clark, J. R.; Trzepkowski, L. J.; White, M. C. Remote Oxidation of Aliphatic C–H Bonds in Nitrogen-Containing Molecules. *J. Am. Chem. Soc.* **2015**, *137*, 14590-14593.

69. Nanjo, T.; de Lucca, E. C.; White, M. C. Remote, Late-Stage Oxidation of Aliphatic C–H Bonds in Amide-Containing Molecules. *J. Am. Chem. Soc.* **2017**, *139*, 14586-14591.

70. Gawley, R. E., The Beckmann Reactions: Rearrangements, Elimination–Additions, Fragmentations, and Rearrangement–Cyclizations. In *Organic Reactions*, John Wiley & Sons, Inc.: 2004; Vol. 35, pp 1-420.

71. Wolff, H., The Schmidt Reaction. In *Organic Reactions*, John Wiley & Sons, Inc.: 1946; Vol. 3, pp 307-332.

72. Wrobleski, A.; Coombs, T. C.; Huh, C. W.; Li, S.-W.; Aubé, J., The Schmidt Reaction. In *Organic Reactions*, John Wiley & Sons, Inc.: 2012; Vol. 78, pp 1-320.

73. Briggs, L. H.; De Ath, G. C.; Ellis, S. R. Reactions of Hydrazoic Acid. *J. Chem. Soc.* **1942**, 61-63.

74. Smith, P. A. S. Schmidt Reaction: Experimental Conditions and Mechanism. *J. Am. Chem. Soc.* **1948**, *70*, 320-323.

75. Boyer, J. H.; Hamer, J. The Acid-catalyzed Reaction of Alkyl Azides Upon Carbonyl Compounds. *J. Am. Chem. Soc.* **1955**, *77*, 951-4.

76. Boyer, J. H.; Canter, F. C.; Hamer, J.; Putney, R. K. Acid-catalyzed Reactions of Aliphatic Azides. *J. Am. Chem. Soc.* **1956**, *78*, 325-7.

77. Boyer, J. H.; Morgan, L. R., Jr. Acid-catalyzed Reactions Between Carbonyl Compounds and Organic Azides. II. Aromatic Aldehydes. *J. Org. Chem.* **1959**, *24*, 561-2.

78. Badiang, J. G.; Aubé, J. One-Step Conversion of Aldehydes to Oxazolines and 5,6-Dihydro-4H-1,3-oxazines Using 1,2- and 1,3-Azido Alcohols. *J. Org. Chem.* **1996**, *61*, 2484-2487.

79. Gracias, V.; Milligan, G. L.; Aube, J. Efficient Nitrogen Ring-Expansion Process Facilitated by in situ Hemiketal Formation. An Asymmetric Schmidt Reaction. *J. Am. Chem. Soc.* **1995**, *117*, 8047-8048.

80. Gracias, V.; Milligan, G. L.; Aubé, J. Synthesis of Functionalized N-Alkyl Heterocycles from Ketones by a Sequential Ring Expansion/Nucleophilic Addition Process. *J. Org. Chem.* **1996**, *61*, 10-11.

81. Gracias, V.; Frank, K. E.; Milligan, G. L.; Aubé, J. Ring Expansion by in situ Tethering of Hydroxy Azides to Ketones: The Boyer Reaction. *Tetrahedron* **1997**, *53*, 16241-16252.

82. Forsee, J. E.; Aubé, J. Hydrolysis of Iminium Ethers Derived from the Reaction of Ketones with Hydroxy Azides: Synthesis of Macrocyclic Lactams and Lactones. *J. Org. Chem.* **1999**, *64*, 4381-4385.

83. Fenster, E.; Rayabarapu, D. K.; Zhang, M.; Mukherjee, S.; Hill, D.; Neuenswander, B.; Schoenen, F.; Hanson, P. R.; Aubé, J. Three-Component Synthesis of 1,4-Diazepin-5-ones and the Construction of γ-Turn-like Peptidomimetic Libraries. *J. Comb. Chem.* **2008**, *10*, 230-234.

84. Fenster, E.; Smith, B. T.; Gracias, V.; Milligan, G. L.; Aubé, J. Nucleophilic Addition to Iminium Ethers in the Preparation of Functionalized N-Alkyl Heterocycles. *J. Org. Chem.* **2008**, *73*, 201-205.

85. Sahasrabudhe, K.; Gracias, V.; Furness, K.; Smith, B. T.; Katz, C. E.; Reddy, D. S.; Aubé, J. Asymmetric Schmidt reaction of hydroxyalkyl azides with ketones. *J. Am. Chem. Soc.* **2003**, *125*, 7914-7922.

86. Hewlett, N. D.; Aubé, J.; Radkiewicz-Poutsma, J. L. Ab Initio Approach to Understanding the Stereoselectivity of Reactions between Hydroxyalkyl Azides and Ketones. *J. Org. Chem.* **2004**, *69*, 3439-3446.

87. Katz, C. E.; Aubé, J. Unusual Tethering Effects in the Schmidt Reaction of Hydroxyalkyl Azides with Ketones: Cation−π and Steric Stabilization of a Pseudoaxial Phenyl Group. *J. Am. Chem. Soc.* **2003**, *125*, 13948-13949.

88. Aube, J.; Hammond, M.; Gherardini, E.; Takusagawa, F. Syntheses and Rearrangements of Spirocyclic Oxaziridines Derived from Unsymmetrical Ketones. *J. Org. Chem.* **1991**, *56*, 499-508.

89. Aube, J. Oxaziridine Rearrangements in Asymmetric Synthesis. *Chem. Soc. Rev.* **1997**, *26*, 269-277.

90. Aubé, J.; Hammond, M. Directed Regiochemical Control in the Ring Expansion Reactions of a Substituted *trans*-Decalone. *Tetrahedron Lett.* **1990**, *31*, 2963-2966.

91. Brandes, B. D.; Jacobsen, E. N. Regioselective Ring Opening of Enantiomerically Enriched Epoxides via Catalysis with Chiral (Salen)Cr(III) Complexes. *Synlett* **2001**, *2001*, 1013-1015.

92. Romney, D. K.; Colvin, S. M.; Miller, S. J. Catalyst Control over Regio- and Enantioselectivity in Baeyer–Villiger Oxidations of Functionalized Ketones. *J. Am. Chem. Soc.* **2014**, *136*, 14019-14022.

93. Smith, B. T.; Gracias, V.; Aubé, J. Regiochemical Studies of the Ring Expansion Reactions of Hydroxy Azides with Cyclic Ketones. *J. Org. Chem.* **2000**, *65*, 3771-3774.

94. Regan, B. M.; Hayes, F. N. 17- and 17a-Aza-D-homosteroids. *J. Am. Chem. Soc.* **1956**, *78*, 639-643.

95. Covey, D. F.; Han, M.; Kumar, A. S.; de la Cruz, M. A. M.; Meadows, E. S.; Hu, Y.; Tonnies, A.; Nathan, D.; Coleman, M.; Benz, A.; Evers, A. S.; Zorumski, C. F.; Mennerick, S. Neurosteroid Analogues. Structure−activity Studies of *N*-Acylated 17a-Aza-D-homosteroid Analogues of the Anesthetic Steroids (3α,5α)- and (3α,5β)-3-Hydroxypregnan-20-one. *J. Med. Chem.* **2000**, *43*, 3201-3204.

96. Huang, L.-H.; Wang, Y.-G.; Xu, G.; Zhang, X.-H.; Zheng, Y.-F.; He, H.-L.; Fu, W.-Z.; Liu, H.-M. Novel 4-Azasteroidal *N*-Glycoside Analogues Bearing Sugar-like D Ring: Synthesis and Anticancer Activities. *Bioorg. Med. Chem. Lett.* **2011**, *21*, 6203-6205.

97. Doorenbos, N. J.; Singh, H. Preparation of Azasteroids from Cholestenone and Progesterone. *J. Pharm. Sci.* **1962**, *51*, 418-420.

98. Thomas, A. V.; Ghosh, A. K.; Sridhar, P. R., Diphenyl Phosphorazidate. In *Encyclopedia of Reagents for Organic Synthesis*, John Wiley & Sons, Ltd: 2001.

99. Salunkhe, A. M.; Burkhardt, E. R. Highly Enantioselective Reduction of Prochiral Ketones with *N*,*N*-Diethylaniline·borane (DEANB) in Oxazaborolidine-catalyzed Reductions. *Tetrahedron Lett.* **1997**, *38*, 1523-1526.

100. Ramanathan, S. K.; Keeler, J.; Lee, H.-L.; Reddy, D. S.; Lushington, G.; Aubé, J. Modular Synthesis of Cyclic Peptidomimetics Inspired by γ-Turns. *Org. Lett.* **2005**, *7*, 1059-1062.

101. Barton, D. H. R.; Robinson, C. H. The Stereospecificity of Carbanion Reduction Processes. *Journal of the Chemical Society* **1954**, 3045-3051.

102. Stork, G.; Darling, S. D. Stereochemistry of the Lithium-ammonia reduction of α,β-Unsaturated Ketones. *J. Am. Chem. Soc.* **1960**, *82*, 1512-1513.

103. Iwasaki, K.; Wan, K. K.; Oppedisano, A.; Crossley, S. W. M.; Shenvi, R. A. Simple, Chemoselective Hydrogenation with Thermodynamic Stereocontrol. *J. Am. Chem. Soc.* **2014**, *136*, 1300-1303.

104. Lucas, B. S.; Fisher, B.; McGee, L. R.; Olson, S. H.; Medina, J. C.; Cheung, E. An Expeditious Synthesis of the MDM2–p53 Inhibitor AM-8553. *J. Am. Chem. Soc.* **2012**, *134*, 12855-12860.

105. Holth, T. A. D.; Hutt, O. E.; Georg, G. I., Beckmann Rearrangements and Fragmentations in Organic Synthesis. In *Molecular Rearrangements in Organic Synthesis*, John Wiley & Sons, Inc: 2015; pp 111-150.

106. Aube, J.; Milligan, G. L. Intramolecular Schmidt Reaction of Alkyl Azides. *J. Am. Chem. Soc.* **1991**, *113*, 8965-8966.

107. Motiwala, H. F.; Fehl, C.; Li, S.-W.; Hirt, E.; Porubsky, P.; Aubé, J. Overcoming Product Inhibition in Catalysis of the Intramolecular Schmidt Reaction. *J. Am. Chem. Soc.* **2013**, *135*, 9000-9009.

108. Motiwala, F. H. I. Catalysis of Intra- and Intermolecular Schmidt Reactions. II. Copper-Catalyzed Oxaziridine-Mediated C–H Bond Oxidation. III. Synthesis and Cytotoxic Evaluation of Withalongolide A Analogues. University of Kansas, Lawrence, KS, 2014.

109. Gutierrez, O.; Aubé, J.; Tantillo, D. J. Mechanism of the Acid-Promoted Intramolecular Schmidt Reaction: Theoretical Assessment of the Importance of Lone Pair-Cation, Cation-π, and Steric Effects in Controlling Regioselectivity. *J. Org. Chem.* **2012**, *77*, 640-647.

110. Motiwala, H. F.; Charaschanya, M.; Day, V. W.; Aubé, J. Remodeling and Enhancing Schmidt Reaction Pathways in Hexafluoroisopropanol. *J. Org. Chem.* **2016**, *81*, 1593-1609.

111. Lu, H.-L.; Wu, Z.-W.; Song, S.-Y.; Liao, X.-D.; Zhu, Y.; Huang, Y.-S. An Improved Synthesis of Nomegestrol Acetate. *Org. Process Res. Dev.* **2014**, *18*, 431-436.

112. Park, J.-Y.; Kim, S.-W.; Lee, J.-K.; Im, W. B.; Jin, B. K.; Yoon, S.-H. Simplified Heterocyclic Analogues of Fluoxetine Inhibit Inducible Nitric Oxide Production in Lipopolysaccharide-Induced BV2 Cells. *Biol. Pharm. Bull.* **2011**, *34*, 538-544.

113. Werner, T.; Barrett, A. G. M. Simple Method for the Preparation of Esters from Grignard Reagents and Alkyl 1-Imidazolecarboxylates. *J. Org. Chem.* **2006**, *71*, 4302-4304.

114. De Angelis, S.; De Renzo, M.; Carlucci, C.; Degennaro, L.; Luisi, R. A Convenient Enantioselective CBS-Reduction of Arylketones in Flow-Microreactor Systems. *Org. Biomol. Chem.* **2016**, *14*, 4304-4311.

115. Touge, T.; Hakamata, T.; Nara, H.; Kobayashi, T.; Sayo, N.; Saito, T.; Kayaki, Y.; Ikariya, T. Oxo-Tethered Ruthenium(II) Complex as a Bifunctional Catalyst for Asymmetric Transfer Hydrogenation and H2 Hydrogenation. *J. Am. Chem. Soc.* **2011**, *133*, 14960-14963.

116. Klein, M.; Krainz, K.; Redwan, I. N.; Dinér, P.; Grøtli, M. Synthesis of Chiral 1,4-Disubstituted-1,2,3-Triazole Derivatives from Amino Acids. *Molecules* **2009**, *14*, 5124.

117. Chaudhry, P.; Schoenen, F.; Neuenswander, B.; Lushington, G. H.; Aubé, J. One-Step Synthesis of Oxazoline and Dihydrooxazine Libraries. *J. Comb. Chem.* **2007**, *9*, 473-476.

118. Mukherjee, S.; Maji, B.; Tlahuext-Aca, A.; Glorius, F. Visible-Light-Promoted Activation of Unactivated C(sp3)–H Bonds and Their Selective Trifluoromethylthiolation. *J. Am. Chem. Soc.* **2016**, *138*, 16200-16203.

119. Mo, F.; Lim, H. N.; Dong, G. Bifunctional Ligand-Assisted Catalytic Ketone α-Alkenylation with Internal Alkynes: Controlled Synthesis of Enones and Mechanistic Studies. *J. Am. Chem. Soc.* **2015**, *137*, 15518-15527.

120. Purushottamachar, P.; Njar, V. C. O. A New Simple and High-Yield Synthesis of 5α-Dihydrotestosterone (DHT), a Potent Androgen Receptor Agonist. *Steroids* **2012**, *77*, 1530-1534.

121. Schmidt, A. W.; Doert, T.; Goutal, S.; Gruner, M.; Mende, F.; Kurzchalia, T. V.; Knölker, H.-J. Regio- and Stereospecific Synthesis of Cholesterol Derivatives and their Hormonal Activity in Caenorhabditis Elegans. *Eur. J. Org. Chem.* **2006**, *2006*, 3687-3706.

122. Singh, C.; Hassam, M.; Verma, V. P.; Singh, A. S.; Naikade, N. K.; Puri, S. K.; Maulik, P. R.; Kant, R. Bile Acid-Based 1,2,4-Trioxanes: Synthesis and Antimalarial Assessment. *J. Med. Chem.* **2012**, *55*, 10662-10673.

123. Wang, C.; Wang, S.; Xu, Y.; Hu, Y.; Hu, H. Preparation of (5α,13α)-D-azasteroids as key precursors of a new family of potential GABAA receptor modulators. *Steroids* **2003**, *68*, 677-683.

124. Hamilton, N. M.; Dawson, M.; Fairweather, E. E.; Hamilton, N. S.; Hitchin, J. R.; James, D. I.; Jones, S. D.; Jordan, A. M.; Lyons, A. J.; Small, H. F.; Thomson, G. J.; Waddell, I. D.; Ogilvie, D. J. Novel Steroid Inhibitors of Glucose 6-Phosphate Dehydrogenase. *J. Med. Chem.* **2012**, *55*, 4431-4445.

125. Marcano, D.; De Méndez, J.; Ortiz, A. C.; Salinas, M. Carbon-13 Nuclear Magnetic Resonance Spectra of Some Heterocyclic D-Homoandrostanes. *Org. Mass Spectrom.* **1984**, *22*, 736-738.

126. Moriyama, K.; Nakamura, Y.; Togo, H. Oxidative Debenzylation of *N*-Benzyl Amides and O-Benzyl Ethers Using Alkali Metal Bromide. *Org. Lett.* **2014**, *16*, 3812-3815.

127. Czajkowska-Szczykowska, D.; Rodríguez-Molina, B.; Magaña-Vergara, N. E.; Santillan, R.; Morzycki, J. W.; Garcia-Garibay, M. A. Macrocyclic Molecular Rotors with Bridged Steroidal Frameworks. *J. Org. Chem.* **2012**, *77*, 9970-9978.

128. Hilton, P. J.; McKinnon, W.; Gravett, E. C.; Peron, J.-M. R.; Frampton, C. M.; Nicholls, M. G.; Lord, G. Selective Inhibition of the Cellular Sodium Pump by Emicymarin and 14ß Anhydroxy Bufadienolides. *Steroids* **2010**, *75*, 1137-1145.

129. Rodríguez-Molina, B.; Pérez-Estrada, S.; Garcia-Garibay, M. A. Amphidynamic Crystals of a Steroidal Bicyclo[2.2.2]octane Rotor: A High Symmetry Group That Rotates Faster than Smaller Methyl and Methoxy Groups. *J. Am. Chem. Soc.* **2013**, *135*, 10388-10395.

130. Smith, A. B.; Kürti, L.; Davulcu, A. H. A New Modular Indole Synthesis. Construction of the Highly Strained CDEF Parent Tetracycle of Nodulisporic Acids A and B. *Org. Lett.* **2006**, *8*, 2167-2170.

Chapter 2

New Variations of the Schmidt Reaction

2.1 Introduction

2.1.1 The Schmidt Reaction

The "Schmidt reaction" is a family of related transformations that involves the reaction of hydrazoic acid (HN_3; generally formed *in situ* from sodium azide (NaN_3)) or alkyl azides with an electrophile to prepare various types of nitrogen-inserted products.[1-2] In 1923, Karl F. Schmidt first reported the Schmidt reaction as a method for preparing amides from sulfuric acid (H_2SO_4)-promoted treatment of HN_3 with carbonyl reactants. Thus, the phrase "classical Schmidt reaction" is loosely defined as reactions that specifically combine HN_3 with ketones or aldehydes (Scheme 2.1). The mechanism of the classical Schmidt reaction is shown in Figure 2.1.[1-2] The initial nucleophilic attack of HN_3 onto the acid-activated ketone leads to the formation of an azidohydrin intermediate. At this point, the reaction may proceed via one of two routes to afford the corresponding amide. In path *a*, analogous to that of the Baeyer-Villiger reaction, direct rearrangement proceeds through concomitant migration of the antiperiplanar carbon and elimination of the nitrogen leaving group. Alternatively, as shown as path *b*, initial dehydration affords a diazoiminium species which subsequently rearranges to form an iminium ion (drawn in two resonance forms: iminocarbonium or nitrilium ion); the iminium ion becomes hydrated to give the final lactam product. Path *b* mechanism was originally proposed by Peter A. S. Smith in the 1940s and is related to that of the Beckmann rearrangement.[3] Mechanism *b* is commonly preferred for a several reasons: (1) the correlation of the migrating group size with antiperiplanar migration is resultant from the formation of the least sterically hindered diazoiminium ion (i.e., migratory aptitude), and (2) the synthesis of tetrazole byproducts indicates involvement of the iminium ion

intermediates. The reaction of such intermediates with a second nucleophilic azide produces a tetrazole (tetrazoles are more commonly seen when excess amounts of azide and ketone substrates are used).

Scheme 2.1. The classical Schmidt reaction.

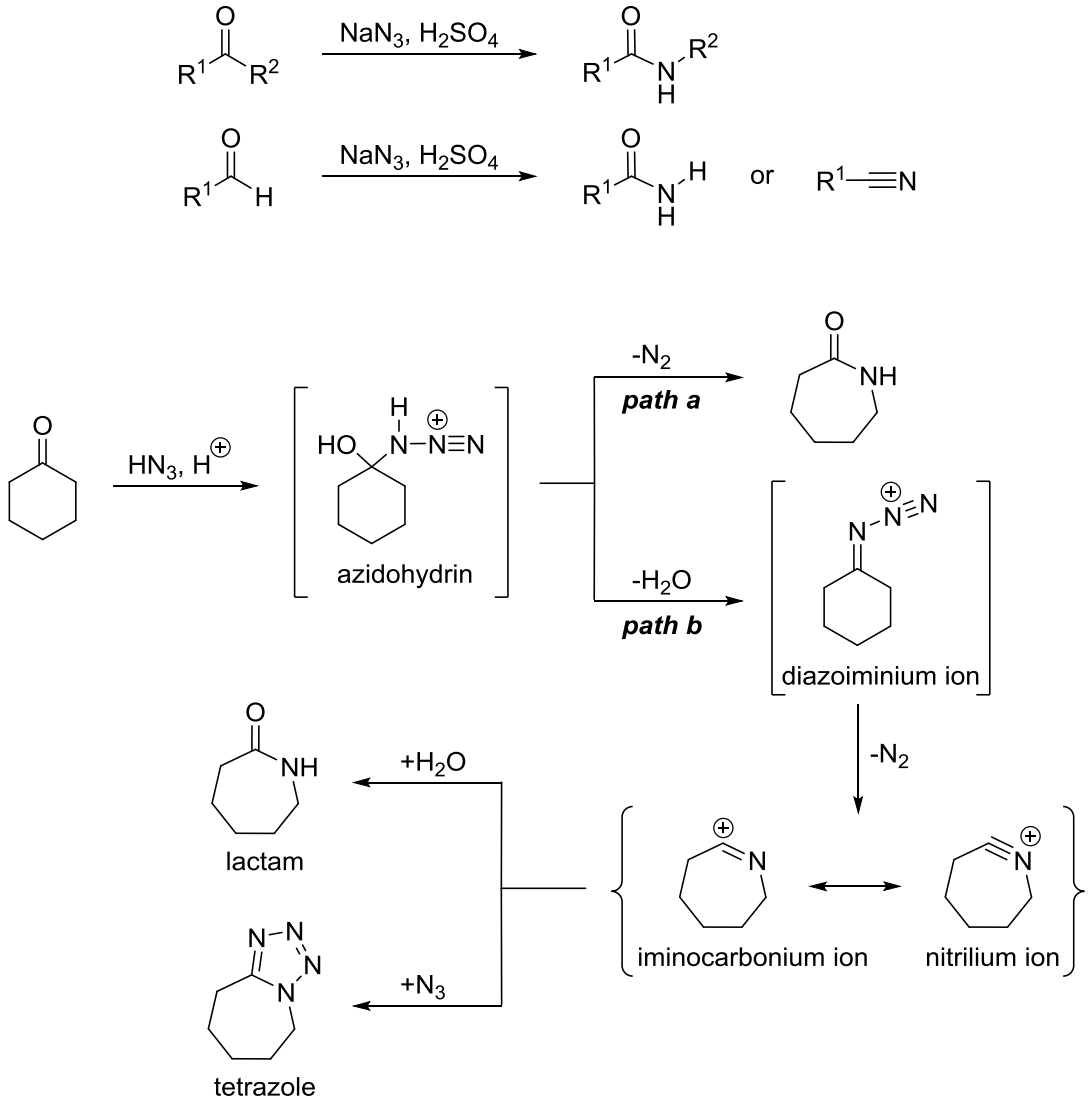

Figure 2.1. Mechanism of the Schmidt reaction between cyclohexanone and HN_3.

The Schmidt reaction is a useful transformation for the synthesis of nitrogenous compounds. Despite this broad utility, the reaction remains underutilized in the synthetic

community for a number of reasons. One practical limitation affecting nearly every version of the Schmidt reaction has been the requirement of using super-stoichiometric amounts of acid catalysts for high product conversions, which unfortunately renders the reaction unsuitable for acid-sensitive substrates, as well as restricting scalability. This issue is mainly attributed to the product being a strong Lewis basic amide, which sequesters catalyst deterring reaction progress and requiring use of excess acid. In 2013, a former research group member, Dr. Hashim F. Motiwala, discovered that a strong hydrogen-bond-donating solvent, hexafluoro-2-isopropanol (HFIP), promotes catalysis in the intramolecular Schmidt reaction and reduces the amount of acid equivalents necessary for mediating this reaction (Figure 2.2a).[4] Originally, this transformation was invented by Milligan and Aubé in 1991, and they used super-stoichiometric amounts (>3.0 equiv) of titanium (IV) chloride ($TiCl_4$) to facilitate high reaction conversions.[5] The recent report by Motiwala el al. is a significant advancement because the authors demonstrated that (1) HFIP aided in overcoming the complexation formed between the catalyst and product that typically inhibited catalyst turnover (Figure 2.2b), and (2) HFIP was key to high conversions using low loadings of HCl generated *in situ* from dissolving procatalysts, acetyl chloride (AcCl) or $TiCl_4$, in the solvent.

Another critical drawback of the classical Schmidt reaction is associated with the use of toxic and explosive HN_3, which in recent years have been replaced with azidotrimethylsilane ($TMSN_3$) as a more convenient azide source. Although, like any other azide source $TMSN_3$ requires safe handling, it is more stable and commercially available than HN_3, and avoids the need for *in situ* generation of the latter.[6] Altogether, we envisioned that the shortcomings of the Schmidt reaction could be circumvented by developing modern variants of these reaction types. Herein, we envisage starting this program with replacements of traditional solvents and azide sources with

HFIP and $TMSN_3$ that could aid in the development of milder and new variations of these reaction types. These alterations could entail (1) reducing the amounts of catalyst equivalents, (2) reducing reaction times, and (3) enhancing substrate scope.

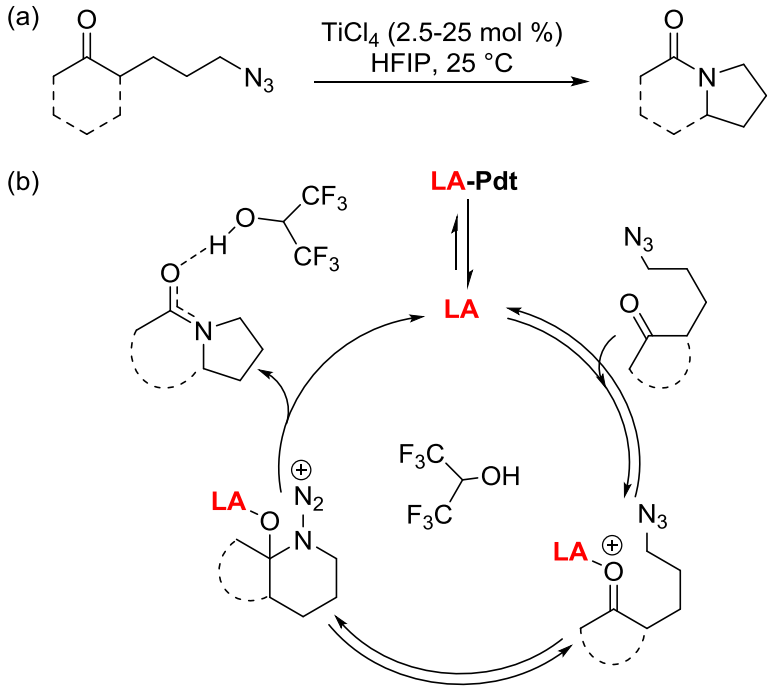

Figure 2.2. The intramolecular Schmidt reaction of azidoalkyl ketones mediated by HFIP. (a) The catalytic intramolecular Schmidt reaction of azidoalkyl ketones. (b) Proposed catalytic cycle using HFIP as solvent to overcome product inhibition of catalyst regeneration (adapted from Motiwala et al.[4]).

In this chapter, I focus on development of a new variation of the Schmidt reaction, specifically the "interrupted Schmidt" reaction. This work arose from initial collaborative efforts with Dr. Motiwala to determine whether other types of Schmidt reactions (other than the intramolecular Schmidt reaction) could benefit in yield and scope, or lead to changes in reactivity and reaction profile from being carried out in HFIP media (Scheme 2.2a).[7] One main conclusion from this collaborative study was that HFIP is indeed an attractive medium for carrying out

synthetic variants of the Schmidt reaction. Particularly, we learned that the reaction of ketone with $TMSN_3$ in HFIP led to a change in product profile where selectivity was observed for tetrazole over lactam as compared to those reactions carried out traditional solvents (discussion of this work in Section 2.2). Moreover, we believe that HFIP either stabilizes or renders more reactive the iminium ions (iminocarbonium or nitrilium ion) formed in the proposed step-wise rearrangement proceeding via path *b* mechanism. This work led to a hypothesis: HFIP may enable iminocarbonium or nitrilium ion reactivity with various nucleophiles and allow extension of the Schmidt reaction pathway towards the synthesis of new heterocycles (Scheme 2.2b). To test this hypothesis, I showed that it was possible to interrupt the classical Schmidt reaction between ketones and $TMSN_3$ in HFIP media using 1,3,5-trimethoxybenzene (1,3,5-TMB) as the nucleophile. This concept of diverting the classical Schmidt reaction from its normal pathway with an added reagent has been phrased the "interrupted Schmidt reaction". Traditionally, the iminium ions prepared through the Schmidt reaction have only been reacted with water leading to a lactam product and azide leading to a tetrazole product. We envisioned that intercepting the iminium ion with various nucleophiles could represent a modern variation of the Schmidt reaction.

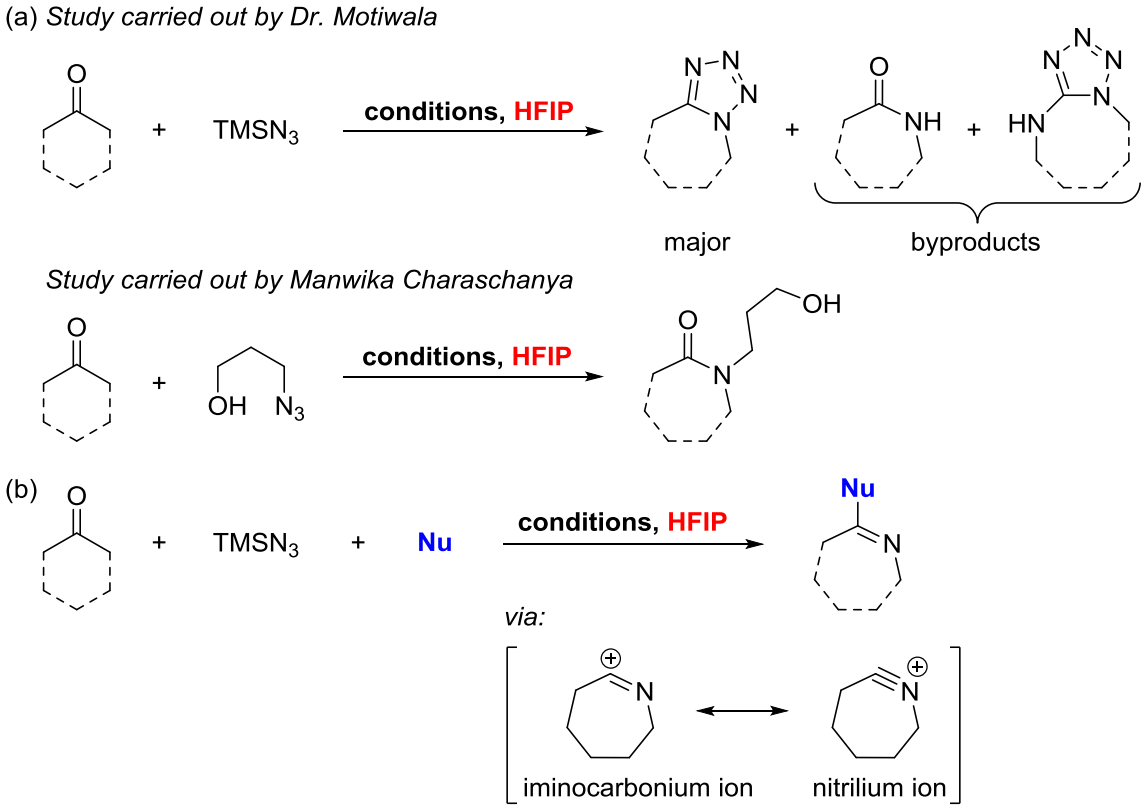

Scheme 2.2. Remodeling the Schmidt reaction pathways in HFIP. (a) Collaborative study about the effect of HFIP on the reaction of ketones with $TMSN_3$ and hydroxyalkyl azide. (b) Development of the "interrupted Schmidt reaction" concept.

2.1.2 Examples of "Interrupted Reactions"

Interrupted Beckmann and Schmidt reactions

Evidence for iminium intermediates generated via either the Beckmann or Schmidt reactions have been reported in the literature.[8] For example, nitrilium ions observed via the Beckmann rearrangement of oximes have been isolated and characterized as tosylate-imines or pyridine-imine cations by a number of researchers (Scheme 2.3).[9-12] Although examples other than the traditional hydrolysis to amide or lactam outcome exists, these representative examples from the early literature are typically products generated from nucleophiles that arise from the acid counterion (e.g., tosylate) or solvent (e.g., pyridine, methanol). In 1982, Yamamoto and coworkers

described a route to iminoethers, imino selenoethers, and imino nitriles from oxime sulfonates using organoaluminum reagents.[13] To my knowledge, this was the first example of methodology development that aimed to extend the nucleophile scope of the Beckmann rearrangement. In this work, organoaluminum reagents were applied to "attach" or capture the intermediate cation with various nucleophiles, particularly these reagents dually acted to promote the Beckmann rearrangement and trap the iminocarbocation (Scheme 2.4a).

In 1991, Schinzer and coworkers demonstrated the synthesis of heterocycles by carrying out tandem reactions of the Beckmann rearrangement and an intramolecular Sakurai reaction.[14-16] In this sequence, diisobutylaluminum hydride (DIBAH) first induces the rearrangement, giving a ring-expanded intermediate, which is then intramolecularly trapped by allylsilane as shown in Scheme 2.4b. Besides Schinzer's endeavor, there are relatively few examples of the interrupted Beckmann reaction with olefins and allylsilanes, and most of which are examples that were intramolecularly designed.[17-18]

Only a few interrupted Schmidt ring-expansion reactions are known. An early example was demonstrated in a report where the iminocarbocation was intercepted with trifluoroacetate or trichloroacetate counterions of the reagents used to promote the Schmidt reaction of flavonoids (Scheme 2.5a).[19] More recently Ghorai described the trapping of an azidocarbenium ion derived from an aldehyde precursor[20] (Scheme 2.5b) and Chiba reported accidental intramolecular trapping of the cationic intermediate with tosyl amine to afford dihydroimidazole[21] (Scheme 2.5c).

Scheme 2.3. Iminium intermediates observed in early Beckmann rearrangement literature. The scheme was adapted from Gawley.[8] (a) 2-Arylcyclohexanone oxime tosylate solvolyzed in pyridine. (b) Treatment of oxime with *p*-toluene sulfonyl chloride (TsCl) in pyridine. (c) Treatment of oxime tosylate in mild Lewis acid (e.g., silica, alumina) affords tosyl-caprolactam. (d) Cycloheptanone oxime tosylate solvolyzed in methanol affords the ring-expanded ether.

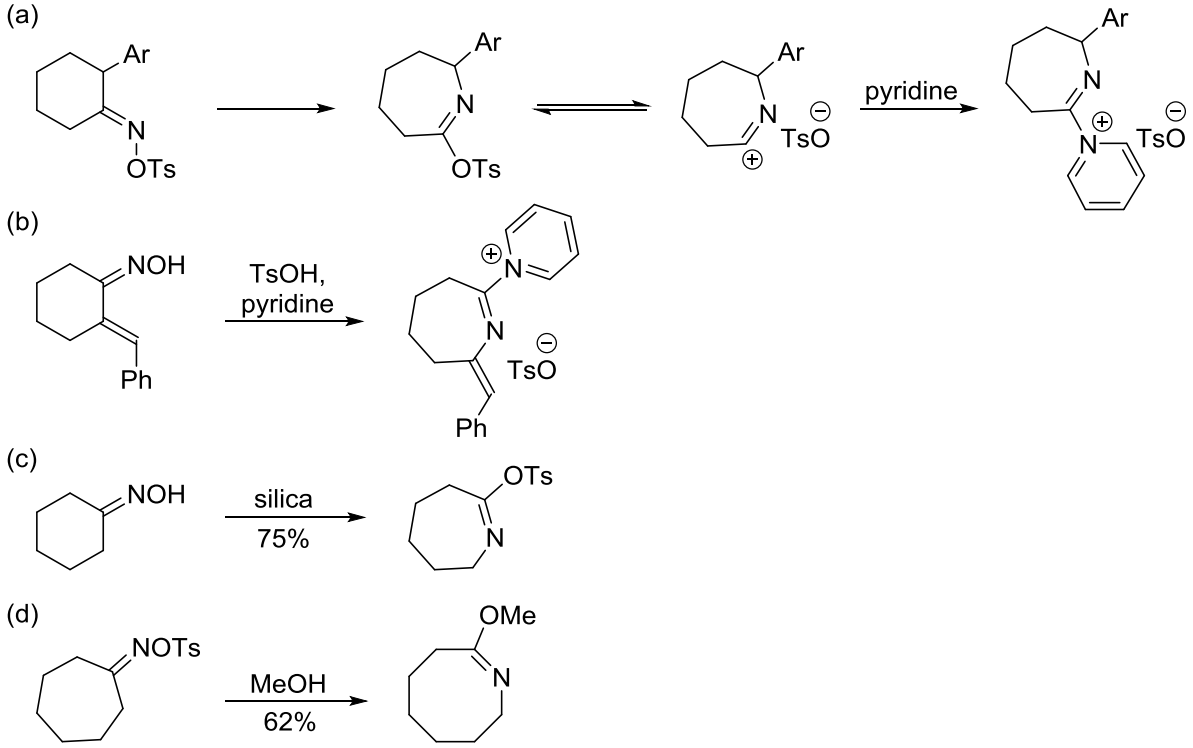

Scheme 2.4. Examples of the interrupted Beckmann reaction. (a) Yamamoto's organoaluminum-promoted Beckmann rearrangement. (b) Schinzer's tandem Beckmann-Sakurai reaction.

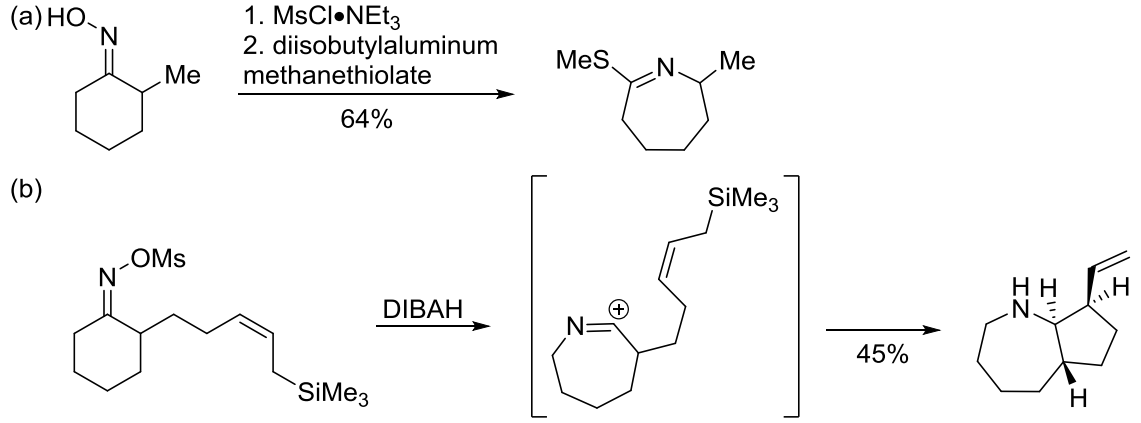

Scheme 2.5. Examples of the interrupted Schmidt reaction. (a) Synthesis of iminoesters. (b) Trapping of azidocarbenium ion with triethylsilane. (c) Trapping of nitrilium ion with tosyl amine.

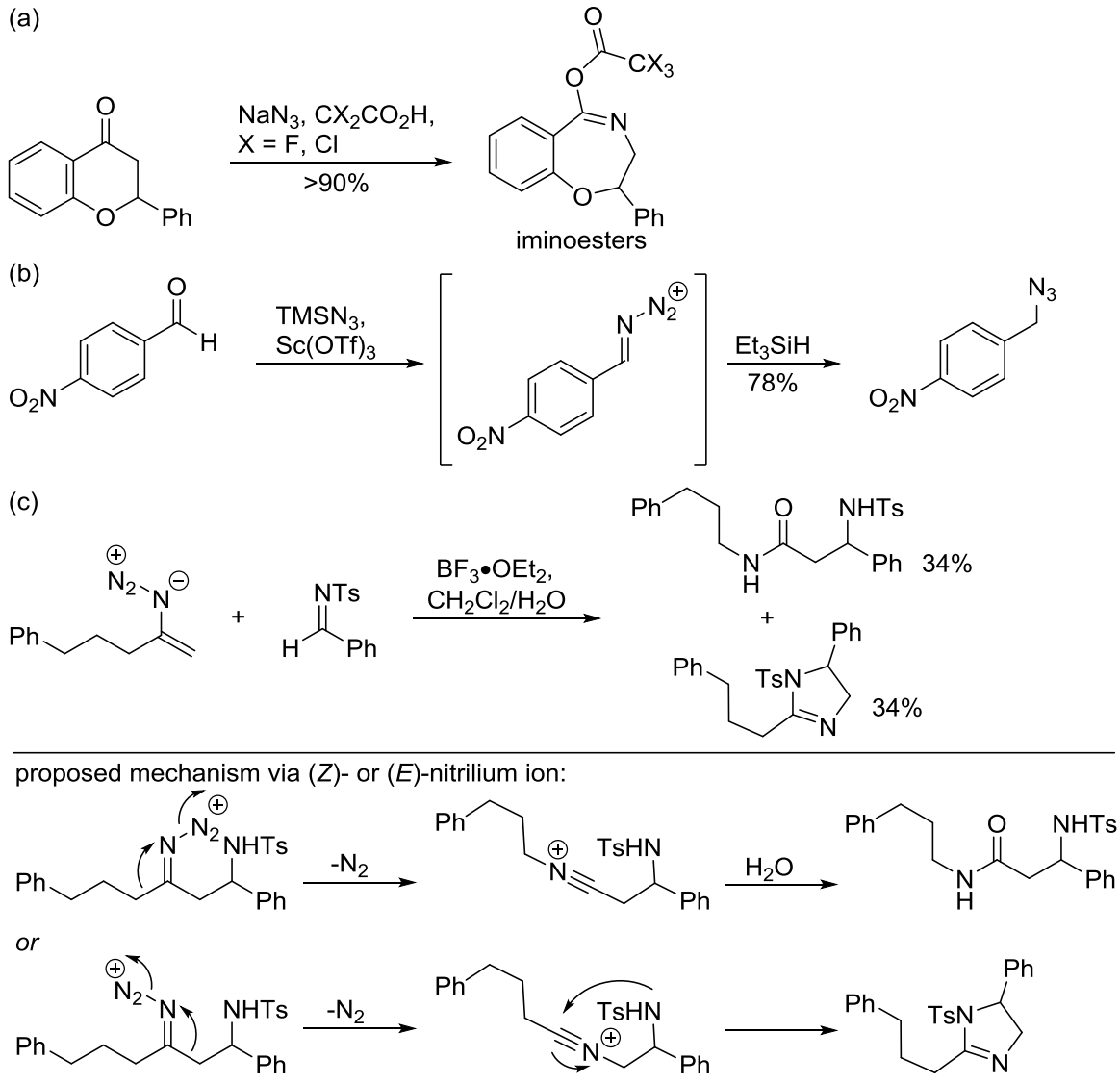

Interrupted Nazarov reaction

The Nazarov reaction is an intramolecular 4π-electrocyclic ring closure of a conjugated dienone (divinyl ketone) substrate into a cyclopentanone and is catalyzed by strong Lewis or Brønsted acids.[22-23] Conventionally, upon ring closure, the five-membered oxyallyl cation undergoes elimination through loss of β-hydrogen and enol tautomerization to form the

cyclopentanone product (Scheme 2.6a). Since its discovery, new methods have been developed to intercept the oxyallyl cation with various carbon- or heteroatom-based nucleophiles leading to a wide array of functionalized cyclopentanones.[22-23] For example, West and coworkers described examples using the thermal Nazarov cyclization to perform cationic cyclizations. In Scheme 2.6b, upon electrocyclic conrotatory closure, cation-olefin cyclization resulted in a stereoselective polycyclic product.[24] This seminal work and other reports by West inspired broad development of scope using various nucleophilic trapping groups with the oxyallyl cation intermediate, which included amongst other olefins, arenes, and heteroarenes nucleophiles (Scheme 2.6c).[22-23]

Scheme 2.6. Classical and modern variants of the Nazarov reaction. (a) The classical Nazarov reaction. (b) The first interrupted thermal Nazarov reaction developed by Fredrick G. West. (c) Representative examples of the interrupted Nazarov reaction with various trapping groups.

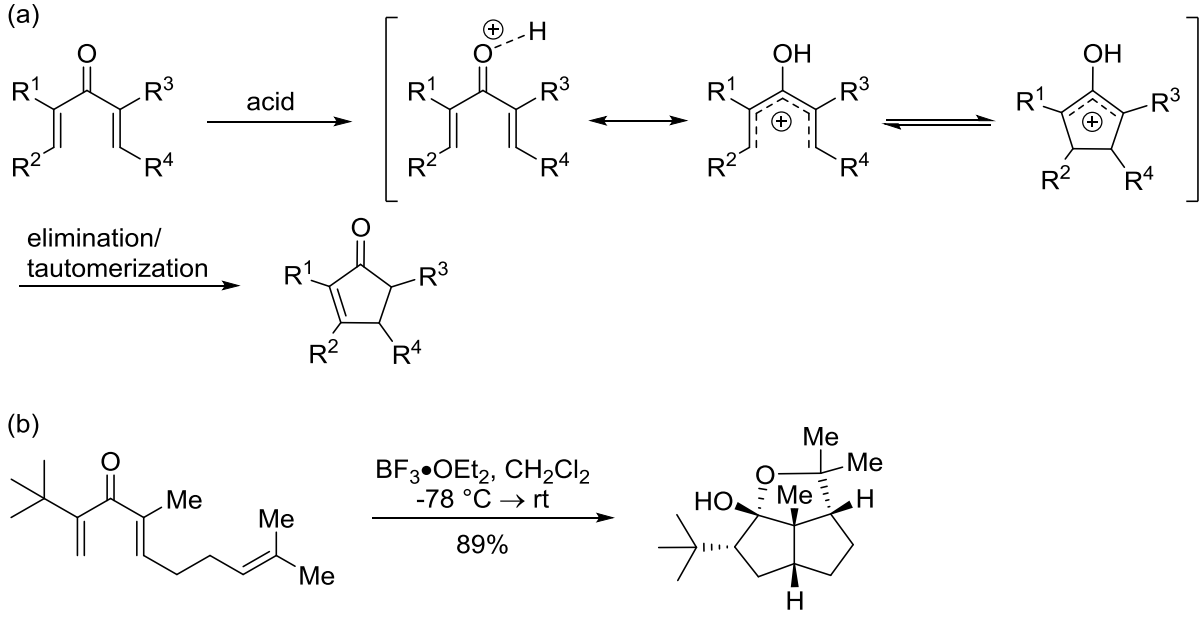

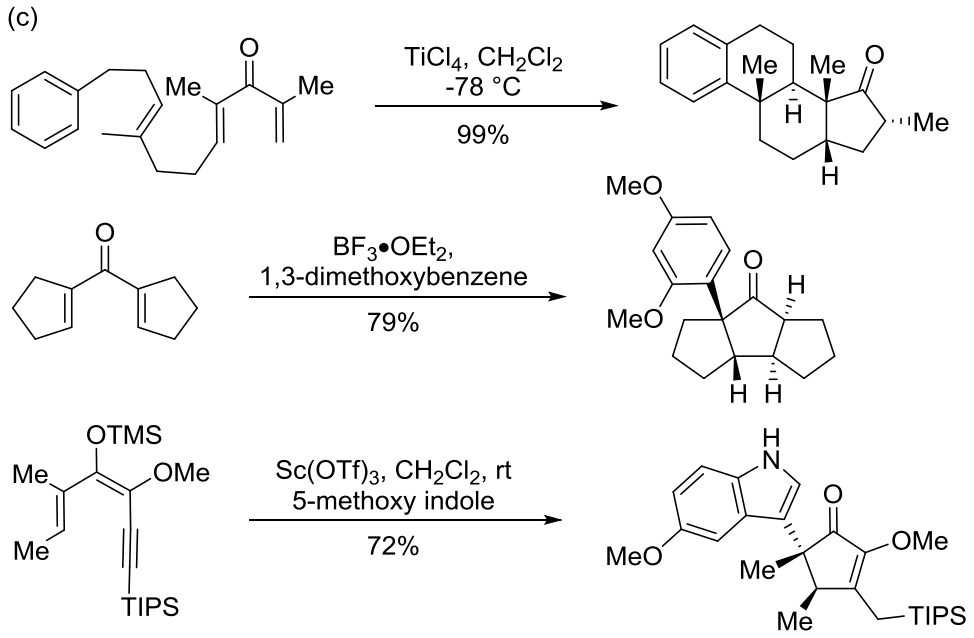

Interrupted Fischer-Indolization

Sporadic examples of the interrupted Fischer indolization reactions have been reported in the literature over the past 50 years.[25-27] Recently, Garg and coworkers developed a general approach to access the indoline scaffold shown in Scheme 2.7.[27-29] Here, the implementation of the interrupted Fischer indolization process led to the formation of two heterocyclic rings, three new bonds, and two new stereogenic centers. The authors used this methodology to prepare indoline scaffolds representative in general complex natural products.[27-29]

Scheme 2.7. An example of the interrupted Fischer-Indolization reaction.

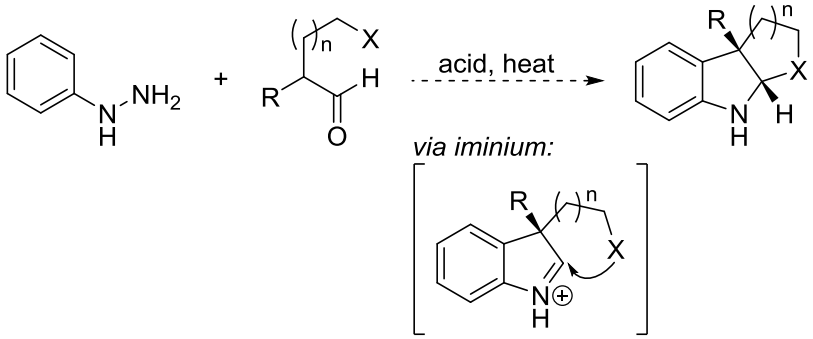

2.2 Enhancing and Remodeling the Schmidt Reaction Pathways in HFIP

2.2.1 The Reaction of Ketone with Azidotrimethylsilane in HFIP

In 2013, Dr. Motiwala reported that HFIP as a solvent improved the outcome of the intramolecular Schmidt reaction, particularly by aiding in overcoming catalyst sequestration by Lewis basic amide products.[4] The use of HFIP allowed catalyst turnover, and accordingly, permitted the use of low catalyst loadings, which led to better yields as compared to those in the original report ($TiCl_4$ in CH_2Cl_2).[5] With this new condition in hand, Dr. Motiwala and I investigated the effect of HFIP solvent on two other variants of the Schmidt reaction: the reaction of ketones with (1) $TMSN_3$ and (2) hydroxyalkyl azide (Scheme 2.2a above). Specifically, Dr. Motiwala examined the reactions of ketones with $TMSN_3$, while I studied those with hydroxyalkyl azide. The studies carried out in the following section were published in the *Journal of Organic Chemistry* in 2016.[7] We instituted this study with the straightforward goal of simply determining whether HFIP-modified conditions could lead to improvements in catalyst loading, yield, and scope. Unexpectedly, this study also led to alterations in the reaction profile and product outcome of the reaction of ketone with $TMSN_3$. In this section, I provided a brief overview to Dr. Motiwala's study because these experiments were critical towards to the design and development of the interrupted Schmidt reaction. Mainly, the change in reaction pathway along with the observation of certain side-products prompted a plausible hypothesis towards various diversions in reaction pathway from the classical Schmidt reaction pathway.

Generally, the classical Schmidt reaction of ketones with an azide (HN_3, NaN_3 or $TMSN_3$) yields amides or lactams as the major products, while tetrazoles are usually observed as the minor byproducts.[1-2] The formation of tetrazoles has received less attention employing the Schmidt methodology because excess amounts of azide are required for its synthesis, and the prevalence of

such heterocycles are highly dependent on the reaction conditions and ketone structures. To our surprise, Dr. Motiwala determined that the formation of tetrazoles was the preferred outcome in HFIP media during the reactions of ketones with $TMSN_3$ regardless of stoichiometry. Following optimization studies, triflic acid (TfOH) was identified as the optimal acid catalyst for the transformation of ketones to tetrazoles at room temperature. For example (Scheme 2.8), 4-phenylcyclohexanone **2.1** was reacted with 2.5 equiv of $TMSN_3$ to afford tetrazole **2.2** in high yield, while aminotetrazole **2.3** and lactam **2.4** were observed as minor byproducts (**2.3** resulting from two ring expansions). This protocol represents a significant advance over Nishiyama's report, which described the synthesis of tetrazoles using 10 mol% tin (II) chloride dihydrate ($SnCl_2 \bullet H_2O$) and 3.0 equiv of $TMSN_3$ under solvent-free conditions at an elevated temperature of 55 ˚C for 16 h.[30] A report by Yadav and coworker described the synthesis of only lactam products from ketones with 1.5 equiv of $TMSN_3$ using 1.0 equiv of iron (III) chloride ($FeCl_3$) in 1,2-dichloroethane (DCE) in moderate yields.[31] For comparison, Motiwala et al. carried out a similar reaction to Yadav and coworkers using $FeCl_3$ in HFIP, which gave a 60% isolated yield of tetrazole **2.2**.

Scheme 2.8. HFIP-modified reaction between 4-phenylcyclohexanone **2.1** and $TMSN_3$.

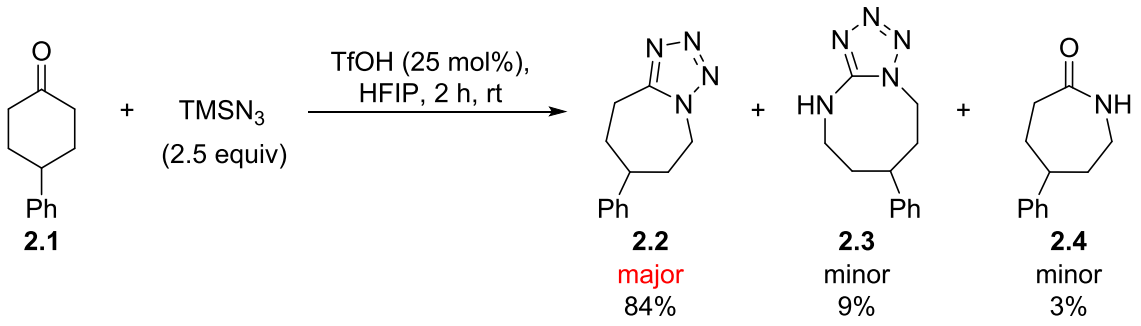

Overall, Dr. Motiwala obtained a range of tetrazoles in modest yields in this study.[7] This diversion of the reaction pathway to favor tetrazoles over lactams as the primary reaction product

suggests that the intermediate iminocarbonium or nitrilium ions are better stabilized or rendered more reactive in HFIP that in traditional reaction solvents. This possibility is consistent with the fact that HFIP is a highly polar and ionizing solvent.[32] Seemingly, the properties of HFIP allow persistent reactivity of carbocation with a second nucleophile azide, which also explains the increased amounts of the "double Schmidt" aminotetrazole byproducts. Interestingly, the formation of aminotetrazoles was consistently observed as minor byproducts throughout this investigation (Figure 2.3). Although substituted aminotetrazoles are known in the literature[33-36] and represent a unique heterocyclic scaffold, they are rarely observed and prepared from the Schmidt reaction.[2]

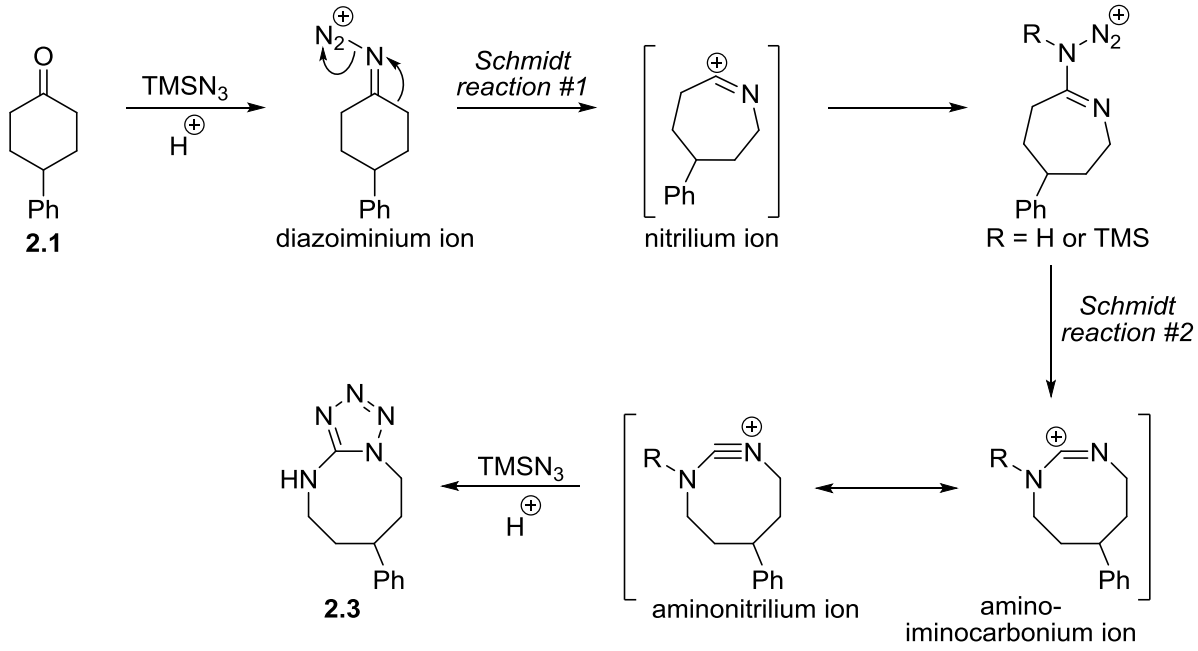

Figure 2.3. Proposed mechanism for aminotetrazole **2.3** formation. The figure was adapted from Motiwala et al.[7]

The product profile of the reaction of flavanone was mechanistically intriguing in so far as it afforded tetrazole in moderate yields along with three unusual minor products. These byproducts

(shown in Scheme 2.9) an iminoether, guanyl azide (a doubly ring expanded product), and aminobenzoxazole were obtained presumably through an intra- and intermolecular trapping of the nitrilium ion with either HFIP or azide. Iminoether arising from HFIP trapping of the nitrilium ion is related to the formation of iminoesters, which was previously documented as the major product upon treatment of flavanone with NaN_3 in trifluoroacetic acid (see Scheme 2.5a above).[19] The intramolecular trapping of the aminonitrilium or amino-iminocarbonium ion with azide nucleophile led to the formation of guanyl azide. In principle, this product should cyclize to afford the aminotetrazole, however this was not the case (transient stability of certain iminium intermediates has been noted for specific cases in old literature).[37] The formation of aminobenzoxazole is mechanistically fascinating, because it is formed after two sequential Schmidt reactions. Specifically following the second ring expansion, the oxygen atom interacts intramolecularly with the iminium intermediate, which subsequently becomes hydrated leading to the final aminobenzoxazole (Figure 2.4). The formation of aminobenzoxazole has been reported to arise from the Schmidt reaction of substituted flavanones with NaN_3.[38]

Scheme 2.9. Byproducts obtained from the reaction of flavanone with $TMSN_3$ in HFIP. The scheme was adapted from Motiwala et al.[7]

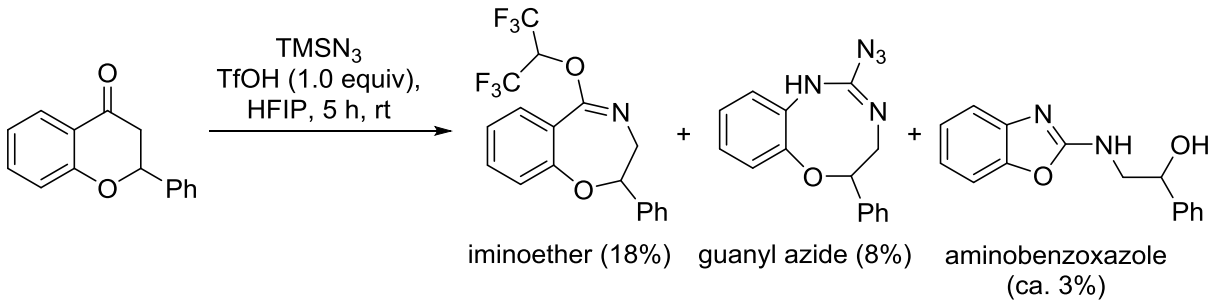

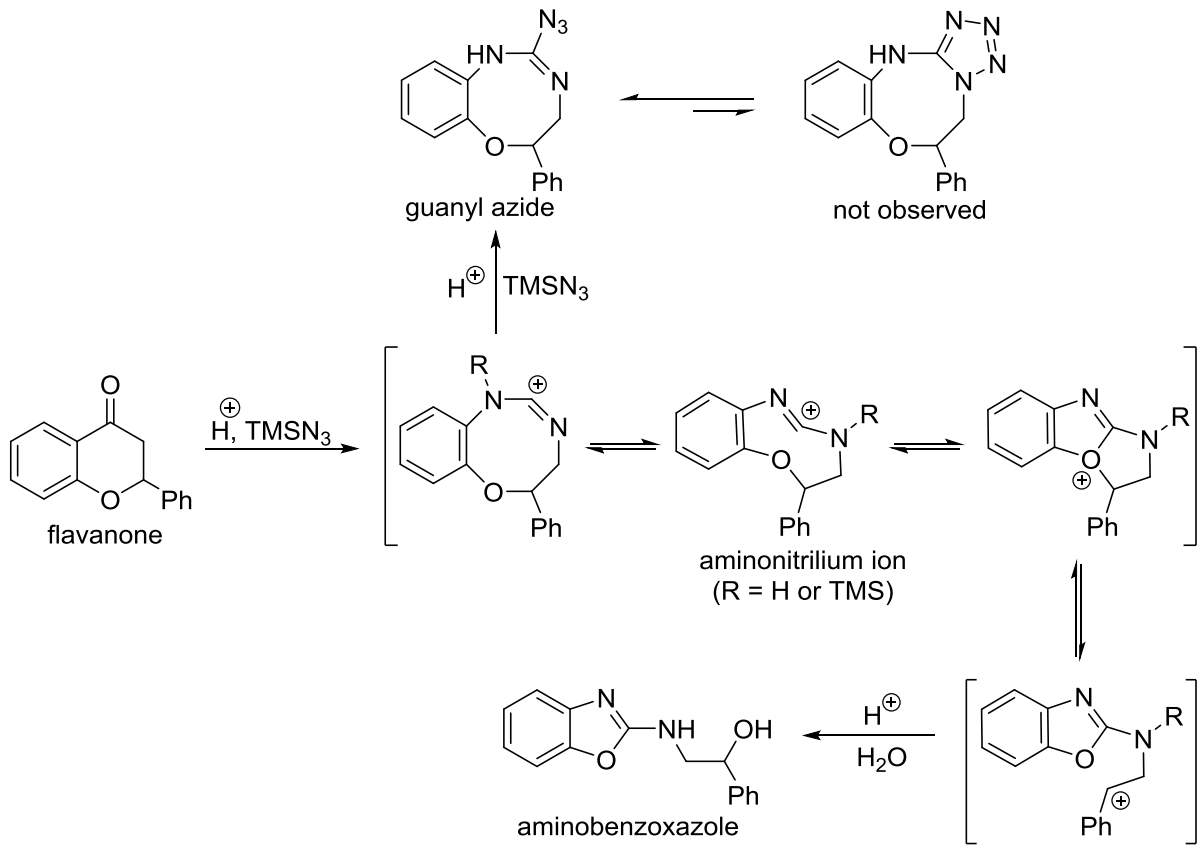

Figure 2.4. Proposed mechanism for guanyl azide and aminobenzoxazole formation. The figure was adapted from Motiwala et al.[7]

2.2.2 The Reaction of Ketone with 3-Azidopropanol in HFIP.

In this section, I describe work toward improving the Schmidt reaction of ketones with hydroxyalkyl azide **1.1** to prepare *N*-hydroxyalkyl lactams.[39-40] This variant was originally developed to overcome the poor reactivity and scoped associated with the $TiCl_4$-promoted intermolecular Schmidt reaction of alkyl azides (e.g., *n*-hexyl, benzyl azides) with ketones.[41-42] Since then, this reaction has been applied towards asymmetric ring expansion reactions and developments of screening collections as discussed in Chapter 1.

Originally, this version of the Schmidt reaction required 2.0–5.0 equiv of boron trifluoride diethyl etherate (BF_3•OEt_2) in dichloromethane (CH_2Cl_2) to achieve successful iminium ether

formation over extended reaction times.[39-40] However, in principle, only 1.0 equiv of the acid promoter should be sufficient to promote the reaction to completion as only 1.0 equiv of counterion should be necessary to stabilize the iminium ether intermediate. Thus, carrying out this transformation with minimally 1.0 equiv of acid promoter over a short time period would constitute as a significant and practical improvement to prepare the iminium ether intermediate.

We began optimization by comparing the standard BF_3•OEt_2-promoted reaction of 4-phenylcyclohexanone **2.1** with 3-azidopropanol **1.1** in the presence of CH_2Cl_2 or HFIP at room temperature (entries 1–3, Table 2.1). In this optimization study, the iminium ether intermediate was hydrolyzed with a saturated solution of sodium bicarbonate ($NaHCO_3$). Compared to CH_2Cl_2, the use of HFIP efficiently promoted the reaction in 6 h requiring just 1.1 equiv of BF_3•OEt_2 for good conversions (cf. entries 1 and 2 with entry 3). In previous reports,[39-40] other Lewis and protic acids could be used in place of BF_3•OEt_2; accordingly, expanding our screen to other acid sources (entries 4–7) revealed that 1.0 equiv of TfOH in HFIP was sufficient to afford a complete conversion from **2.1** to the corresponding iminium ether within a 1 h reaction time. Following hydrolysis and purification, *N*-hydroxyalkyl lactam **2.5** was isolated in 95% yield (entry 7).

Table 2.1. Optimization of conditions for the reaction of 4-phenylcyclohexanone **2.1** with 3-azidopropanol **1.1**.[a,b]

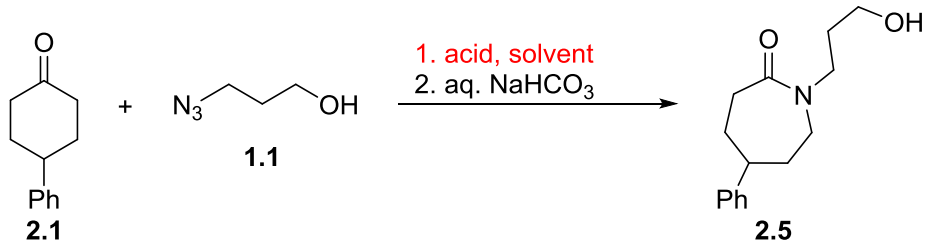

entry	1.1 equiv	catalyst	catalyst (equiv)	solvent	time (h)	^{1}H NMR ratio 2.5:2.1[c]	yield (%)[d]
1	2.0	BF_3•OEt_2	2.0	CH_2Cl_2	24	88:12	82[e]
2	1.5	BF_3•OEt_2	1.1	CH_2Cl_2	6	73:27	62
3	1.5	BF_3•OEt_2	1.1	HFIP	6	>98:2	92
4	1.5	H_2SO_4	0.55[f]	HFIP	6	71:29	62
5	1.5	$TiCl_4$	0.28[f]	HFIP	6	>97:3	89
6	1.5	CH_3COCl	1.1[f]	HFIP	6	>95:5	85
7	1.5	CF_3SO_3H	1.0	HFIP	1	>98:2[g]	95

[a]To a solution of 4-phenylcyclohexanone **2.1** (1.0 equiv) and 3-azidopropanol **1.1** in solvent (0.75 mL) at room temperature was added a catalyst and reaction mixture was allowed to stir for a specified time. Further hydrolysis with aqueous $NaHCO_3$ for 12–14 h followed by purification on a silica gel afforded product **2.5**. [b]Concentration of reaction mixture ca. 0.40 M. [c]^{1}H NMR ratio of crude reaction mixture. [d]Isolated yield. [e]The yield of 88% has been reported when the reaction was allowed to stirred for 48 h.[40] [f]Acetyl chloride is known to generate an equimolar amount of HCl upon dissolution in HFIP.[4] [g]Complete conversion of **2.1** to **2.5** was observed as determined by ^{1}H NMR of a crude reaction mixture.

Encouraged by these initial results, we subjected a selection of ketones to the optimized conditions (Table 2.2). Reaction of simple cyclohexanones afforded very high yields of *N*-hydroxyalkyl lactams in 1–6 h (entries 1–4). In entry 1, unsubstituted cyclohexanone **2.6** was converted to lactam **2.7** in an excellent yield in just 1 h; similarly in entry 2, a mixture of isomeric dimethylcyclohexanones **2.8** afforded the corresponding lactams **2.9** in 94% yield. Functionalized six-membered cyclic ketones such as tetrahydropyran-4-one **2.10** and 1-benzoyl-4-piperidone **2.12**, each having a functional group capable of catalyst deactivation, still underwent facile conversion to their corresponding lactams within 6 h in good yields (entries 3 and 4, respectively). Previously, seven- and eight-membered cyclic ketones had required relatively harsh conditions (5.0 equiv of BF_3•OEt_2 in refluxing CH_2Cl_2 for 72 h) to get either lactam or amino-lactone

depending on the base ($NaHCO_3$ or NaOH) used in the hydrolysis step.[43] Application of the HFIP-methodology to cycloheptanone **2.14** provided a moderate yield of the corresponding lactam **2.15** upon hydrolysis with NaOH (entry 5). The reaction of cyclooctanone **2.16** afforded the corresponding macrocyclic amino-lactone **2.17** exclusively, and in a higher yield than previously reported (entry 6).[43] The reaction of benzylic ketones provided lactams in excellent yield (entry 7 and 8); however, unsymmetrical β-tetralone **2.18** gave an isomeric mixture of lactams as ca. 2:1 ratio (entry 7). In the presence of HFIP, the reaction of isatin **2.23** proceeded for 6 h affording products with two different ring systems quinoxaline dione **2.24** and quinazoline dione **2.25** as a mixture in ca. 2:1 ratio in an overall 76% isolated yield.

Table 2.2. Synthesis of *N*-hydroxyalkyl lactams.

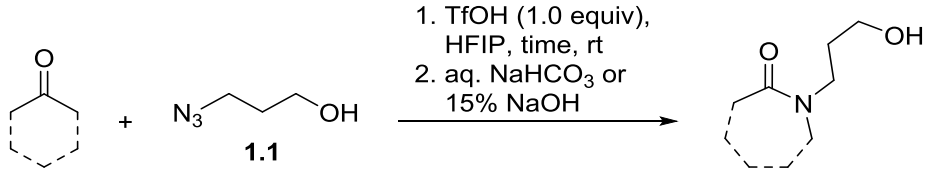

entry	ketone	time (h)	product	yield (%)[c]
1	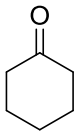 **2.6**	1	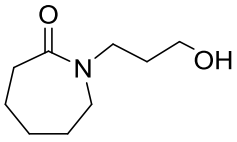 **2.7**	95
2	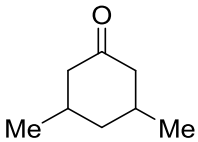 **2.8**[d]	1	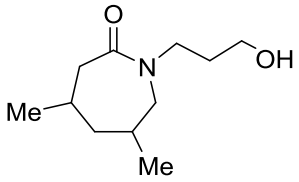 **2.9**[d]	94[e]

3	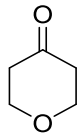 **2.10**	6	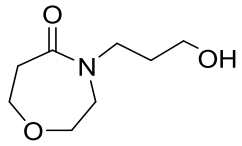 **2.11**	84
4	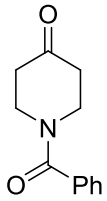 **2.12**	6	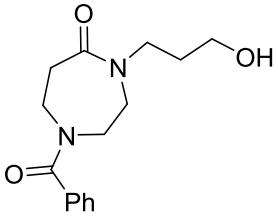 **2.13**	80
5	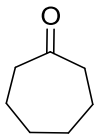 **2.14**	6	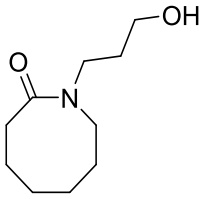 **2.15**	61[f]
6	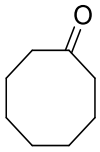 **2.16**	6	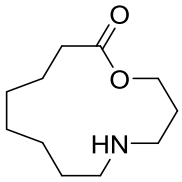 **2.17**	56
7	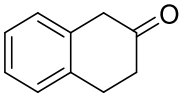 **2.18**	3	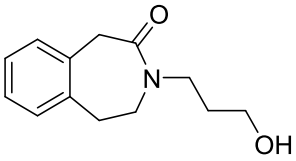 **2.19** 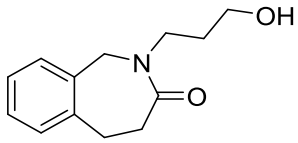 **2.20** **2.19**:**2.20** = 63:37[g]	94
8	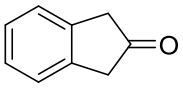 **2.21**	1	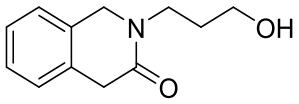 **2.22**	90

9	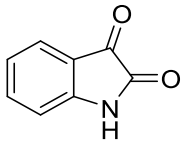	6	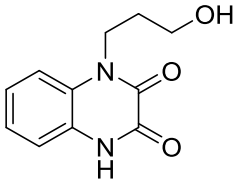	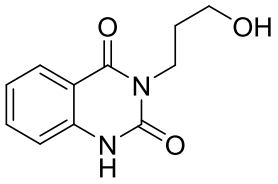	76
	2.23		**2.24**	**2.25**	
			2.24:**2.25** = 63:37[g]		
10	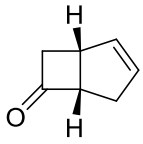	1	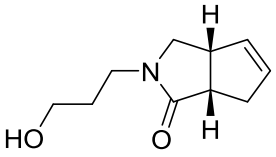	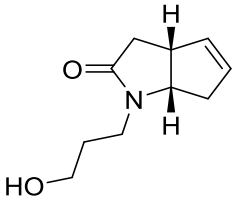	95
	2.26		**2.27**	**2.28**	
			2.27:**2.28** = 74:26[g]		
11	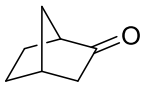	2	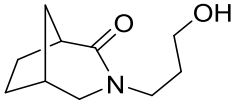	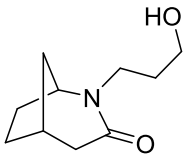	90
	2.29		**2.30**	**2.31**	
			2.30:**2.31** = 58:42[g]		
12	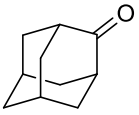	1	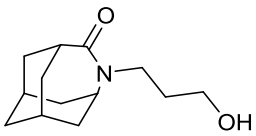		96
	2.32		**2.33**		
13	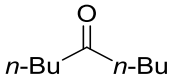	6	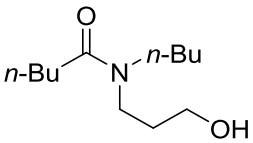	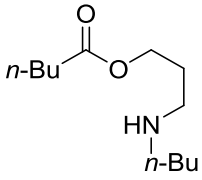	84[h,i]
	2.34		**2.35** (15%)[j]	**2.36** (69%)	

[a]To a solution of a ketone (1.0 equiv) and **1.1** (1.5 equiv) in HFIP (1.0 mL) at room temperature was added TfOH (1.0 equiv) and the reaction was allowed to stir at room temperature for the specified time (time indicated in the table refers to the time required for the formation of iminium ether). Further hydrolysis with aqueous $NaHCO_3$ or 15% NaOH for 12–24 h followed by purification on a silica gel afforded products (see the Experimental Section for details). [b]Concentration of ketone ca. 0.40 M. [c]Isolated yield. [d]Mixture of isomers (ca. 95% major isomer). [e]Corrected yield of major isomer from a mixture of isomers (see the Experimental Section for details). [f]Similar reaction of cycloheptanone with

1.5 equiv of TfOH provided **2.15** in 69% yield (see the Experimental Section for details). [g]Ratio of two inseparable isomers from a purified mixture as determined by ^{1}H NMR. [h]The reaction was carried out with 1.5 equiv of TfOH. [i]Combined yield of **2.35** and **2.36**. [j]Mixture of rotamers (ratio = 79:21).

The reaction with bicyclic ketones proceeded efficiently in 1–2 h to afford the corresponding lactams in excellent yields as a mixture of two regiochemical isomers (entries 10 and 11). 2-Adamantanone **2.32** also only required just 1 h to afford the tricyclic lactam **2.33** in 96% yield (entry 12). In the case of acyclic ketone **2.34**, 1.5 equiv of TfOH was required for successful iminium ether conversion, which upon hydrolysis with $NaHCO_3$ provided aminoester **2.36** as the major product in 69% yield and hydroxypropylamide **2.35** in 15% yield (entry 13).[43] Overall, good to excellent yields were obtained with only 1.0 equiv of TfOH in a relatively short time period, which is a practical advancement to original protocol published in 1995.

In this study, we demonstrated that HFIP aided dramatically towards reducing the amount of acid required to promote the initial iminium ether formation reaction between ketone and 3-azidopropanol. The key highlights of this improved protocol include the reduced use of acid equivalents and short reaction times. However, the methodology remains more robust and practical with cyclic ketones than acyclic ketones. Several other acyclic ketones (e.g., dicyclohexyl ketone, dibenzyl ketone) were also investigated during this time, however, pure products were difficult to isolate.

2.3 Method Development of the Interrupted Schmidt Reaction in HFIP

In this section, I described the development of a general protocol to effect an interruption of the classic Schmidt reaction in HFIP media, particularly to capture the cationic ring-expanded intermediate (nitrilium or iminocarbonium ion) with various nucleophiles in order extend the

synthetic utility of Schmidt transformations. In doing so, the methodology devised would provide access to new and diverse types of ring-expanded heterocycles, which may be of medicinal value.

2.3.1. Optimization of Reaction Conditions

The investigation of an interrupted Schmidt reaction began with identifying an acid catalyst in HFIP that would allow trapping of the cationic ring-expanded intermediate with an added electron-rich arene nucleophile, 1,3,5-trimethoxybenzene (1,3,5-TMB). While there is no precedence for carbon-based nucleophiles participating in the interrupted Schmidt reaction, minimal precedence is available on heteroatom-based nucleophiles as trapping reagents. For example, Chiba and coworkers have previously published an example on intramolecular trapping of nitrilium ion with tosylamine to observe dihydroimidazole in a moderate yield (see Scheme 2.5c above).[21] Comparablely, we have reported azide and HFIP as incidental trapping groups for this cationic intermediate in a flavanone substrate (see Scheme 2.9 above).[7] We sought to develop a more valuable protocol on a six-membered cyclic ketone substrate, which is a prime substrate for Schmidt ring-expansion chemistry. 4-Phenylcyclohexanone **2.1** was selected for this study as it also includes an inherent chromophore to aid in visualization. Furthermore, since the iminium ion intermediate is an electrophile, we figured that a carbon-based π-electron-rich nucleophile may prove suitable in preliminary development work. Accordingly, a recent disclosure on HFIP-promoted Friedel-Crafts reaction[44-45] using electron-rich arenes prompted the selection of 1,3,5-TMB as the trapping reagent. Thus, we carried out an acid screen on the conversion of 4-phenylcyclohexanone **2.1** to 1,3,5-TMB-trapped imine product **2.37** using $TMSN_3$ to facilitate nitrogen ring-expansion in HFIP media (Tables 2.3 and 2.4). In Tables 2.3 and 2.4, the reactions were carried out using a syringe pump, which permitted slow addition (over 6 h) a solution of

$TMSN_3$ (2.0 equiv) in HFIP (2.0 mL) into a solution of ketone **2.1**, acid catalyst (1.0 equiv), and 1,3,5-TMB (5.0 equiv) in HFIP (1.0 mL).

In Table 2.3, we examined 15 Lewis acids using 1.0 equiv of catalyst with HFIP as the solvent at room temperature. Of these, aluminum bromide ($AlBr_3$) gave a complete conversion from ketone **2.1** to desired imine product **2.37** by ^1H NMR quantification of reaction mixture using benzyl benzoate as the internal standard, whereas, aluminum chloride ($AlCl_3$), bismuth (III) triflate ($Bi(OTf)_3$), silicon tetrachloride ($SiCl_4$), and titanium tetrachloride ($TiCl_4$) gave moderate conversions. However, some of these reagents were not selected for further screening because they also promoted the conversion to either lactam **2.2** or tetrazole **2.4** byproducts. Additionally, the basic workup of reactions using $TiCl_4$ and $SiCl_4$ were tedious due to the presence of emulsions. Therefore, $AlCl_3$ and $AlBr_3$ were selected for further evaluation. Attempts to lower the catalyst loading of either aluminum reagents led to reduced yields and observations of minor amounts of tetrazole, however these reagents were still promising for further optimization studies.

Table 2.3. Lewis acid catalyst screen in HFIP.[a-d]

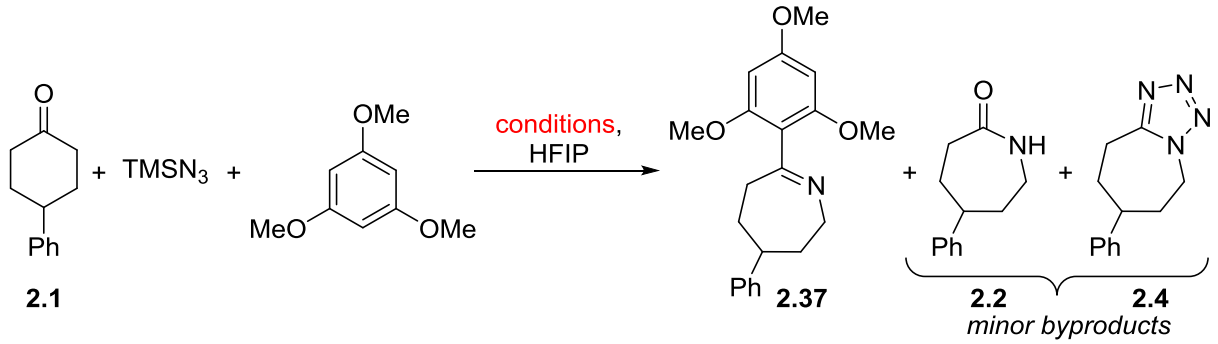

entry	catalyst	catalyst (equiv)	conversion (%)		
			2.37[b,c]	**2.1:2.37**[b,d]	**2.4**[b]
1	$AlCl_3$	1.00	74 (54)	ND	ND
2	$AlCl_3$	0.30[e]	29	52:29	5
3	$AlBr_3$	0.30[e]	20	77:20	2
4	$AlBr_3$	1.00	95 (83)	5:≥95[f]	ND
5	$Al(OTf)_3$	1.00	38	46:38	10
6	$MgCl_2$	1.00	NR	100:0[g]	NR
7	$InCl_3$	1.00	NR	100:0[g]	NR
8	$ZnBr_2$	1.00	NR	100:0[g]	NR
9	$In(OTf)_3$	1.00	75	19:75	9
10	$Bi(OTf)_3$	1.00	77	15:77	12
11	BF_3•OEt_2	1.00	46	47:46	4
12	$SiCl_4$[h]	1.00	75	ND	ND
13	$Sc(OTf)_3$	1.00	38	59:38	1
14	$FeCl_3$	1.00	ND (14)	ND	ND
15	$TiCl_4$[h]	1.00	68[i]	ND	ND
16	$TiCl_4$[h]	0.25[j]	37	40:37	ND
17	AgOTf	1.00	13	78:13	2
18	$Cu(OAc)_2$	0.20	NR	100:0[g]	NR
19	CuCl	0.20	NR	100:0[g]	NR
20	$AuCl_3$	0.20	ND	77:0	5

[a]See experimental section general procedure B for reaction protocol. [b]Product conversion was determined by ^{1}H NMR of the crude reaction mixture using benzyl benzoate as an internal standard. [c]Yield in parentheses represents isolated yield. [d]Conversion was determined using ^{1}H NMR of the crude reaction mixture. [e]Speculation on generation of an equimolar amount of HX (X = Cl, Br) upon dissolution in HFIP.[4] [f]Complete conversion of **2.1** to **2.37** was observed by ^{1}H NMR of the crude reaction mixture. [g]Catalyst was insoluble in HFIP. [h]1.0 M solution in CH_2Cl_2 was used. [i]15% conversion to **2.2** was observed by ^{1}H NMR of the crude reaction mixture using benzyl benzoate as an internal standard. [j]$TiCl_4$ is known to generate an equimolar amount of HCl upon dissolution in HFIP.[4] ND = Not determined; NR = No reaction.

We then examined the efficiency of protic acids in the presence of HFIP at room temperature to mediate the interrupted Schmidt reaction (Table 2.4). Particularly, upon treatment of 4-phenylcyclohexanone **2.1**, 1,3,5-TMB, and $TMSN_3$ in HFIP with 1.0 equiv of either TfOH or

TsOH acid gave ca. 60% of the desired product **2.37** along with minor amounts (>10%) of tetrazoles (entries 1 and 2). A similar reaction carried out using 2.0 equiv of TsOH did not prove more effective (entry 3). In contrast, attempts to carry out the reaction with other acids, particularly with reagents acetyl chloride (AcCl) or acetyl bromide (AcBr), which are known in the presence of HFIP[4] to *in situ* generate HCl or HBr, failed (entries 4–7). Perfluoro-*tert*-butyl alcohol (PFTB, p*K*a 5.4) is a highly acidic media similar to HFIP (p*K*a 9.3). As seen in entries 8 and 9, we examined the reaction only in fluorinated solvents, however without added acids neither resulted in any reaction.

Table 2.4. Bronsted acid catalyst screen in HFIP.[a-d]

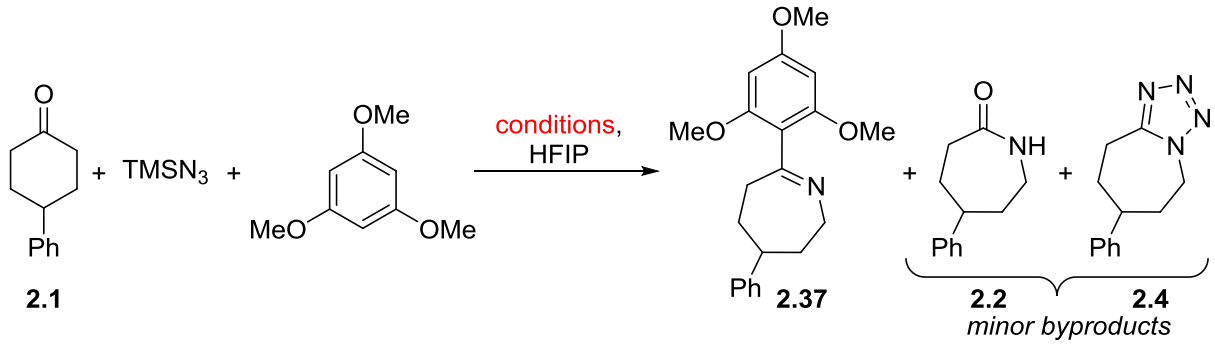

entry	catalyst	catalyst (equiv)	conversion (%)		
			2.37[b,c]	**2.1:2.37**[b,d]	**2.4**[b]
1	TfOH	1.00	60	17:60	7
2	TsOH	1.00	64[g]	17:64	6
3	TsOH	2.00	59[h]	0:59	4
4	TFA	1.00	9[i]	87:9	ND
5	TMSOTf	1.00	10	54:10	6
6	CH_3COCl[e]	1.00	ND (15)	72:0[j]	ND
7	CH_3COBr[f]	1.00	18	ND[k]:18	4
8	PFTB	1.00	NR	100:0	NR
9	HFIP	1.00	NR	100:0	NR

[a]See experimental section general procedure B for reaction protocol. [b]Product conversion was determined by ^{1}H NMR of the crude reaction mixture using benzyl benzoate as an internal standard. [c]Yield in parentheses represents isolated yield. [d]Conversion was determined using ^{1}H NMR of the crude reaction mixture. [e]Known to generate an equimolar amount of HCl upon dissolution in HFIP.[4] [f]Speculation on generation an equimolar amount of HBr upon dissolution in HFIP.[4] [g]15% conversion to **2.2** was observed by ^{1}H NMR of the crude reaction mixture using benzyl benzoate as an internal standard. [h]37% conversion to **2.2** was observed by ^{1}H NMR of the crude reaction mixture using benzyl benzoate as an internal standard. [i]9% **2.2** to lactam was observed by ^{1}H NMR of the crude reaction mixture using benzyl benzoate

as an internal standard. [j]**2.37** minimally observed by ^{1}H NMR of the crude reaction. [k]**2.1** observed by ^{1}H NMR of the crude reaction. ND, Not determined; NR, No reaction.

The preliminary acid screen of 22 reagents revealed that $AlBr_3$ and $AlCl_3$ catalysts were effective for the promotion of the interrupted Schmidt reaction of 1,3,5-TMB. In particular, the identification of $AlBr_3$ mediated a complete conversion over 6 h. We then explored the effects of time and stoichiometry in the interrupted Schmidt using $AlCl_3$ in presence of HFIP (Table 2.5). The reaction is critically dependent on the order of addition (cf entries 1 and 2). Without the slow addition of $TMSN_3$ solution, the conversion to desired **2.37** stalls and 38% of product was isolated after an extended reaction time of 24 h. In contrast, 6 h slow addition of $TMSN_3$ solution revealed 43% conversion to **2.37** by ^{1}H NMR quantification of reaction mixture using benzyl benzoate as the internal standard. Changing the time of slow addition from 2–7 h did not have an effect on the reaction outcome (entries 2–5). However, increasing the concentration of the reaction mixture aided in conversion to product (cf. entries 7 and 8). More significantly, increasing $AlCl_3$ catalyst loading to 2.0 equiv improved the conversion (cf. entries 2 and 10), although the reaction was still incomplete. Comparing entries 11 and 12, it is apparent that 2.0 equiv of $TMSN_3$ was necessary for high and complete conversions; following basic workup, 88% was observed by internal standard and 75% was isolated after normal phase column chromatography. These results were comforting because previous acid screens were carried out with 2.0 equiv of $TMSN_3$ (reaffirming this amount was also shown in entries 19–21).

Table 2.5. Optimization of conditions with $AlCl_3$ in HFIP.[a-c]

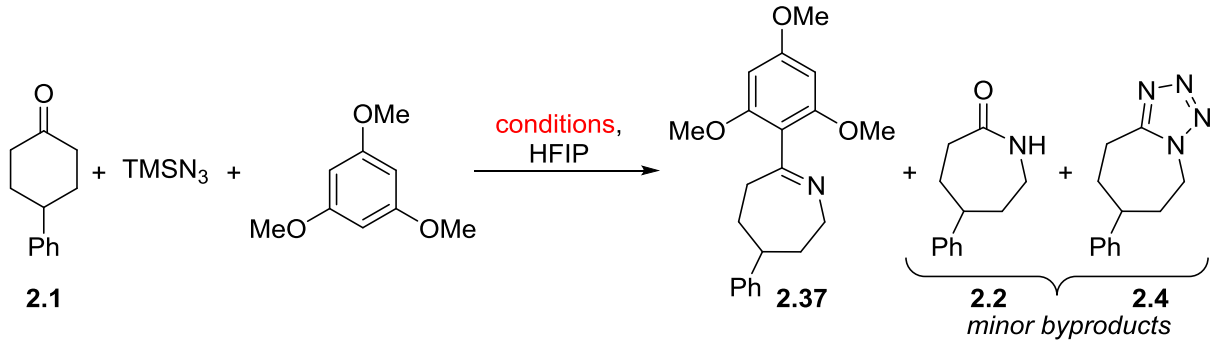

entry	catalyst (equiv)	$TMSN_3$ (equiv)	HFIP (mL)	slow addition (h)	conversion (%)	
					2.37[b,c]	**2.1:2.37**[d]
1	1.00	1.25	4.0	6[e,f]	(33)	ND
2	1.00	1.25	4.0	6	(43)	ND
3	1.00	1.25	4.0	2	(37)	ND
4	1.00	1.25	4.0	5	(44)	ND
5	1.00	1.25	4.0	7	(47)	ND
6[g]	1.20	1.25	4.0	6	68 (57)	ND
7	1.20	1.25	4.0	6	66 (52)	ND
8	1.20	1.25	3.0	6	71 (62)	21:71
9	1.50	1.25	3.0	6	71 (52)	19:71
10	2.00	1.25	3.0	6	76 (64)	13:87
11	2.00	1.50	3.0	6	79 (71)	11:89
12	2.00	2.00	3.0	6	88 (75)	5:≥95[h]
13	2.00	2.00	3.0	6[i]	87 (79)	5:≥95[h]
14	2.00	2.00	3.0	6[i,j]	83 (77)	5:≥95[h]
15[k]	2.00	2.00	3.0	6	85 (74)	5:≥95[h]
16[l]	2.00	2.00	3.0	6	64 (53)	9:≥91[h]
17	2.00	2.00	3.0	10	87 (75)	5:≥95[h]
18	2.00	2.00	3.0	2	80[m]	14:80
19	1.50	2.00	3.0	6	80 (66)	5:≥95[h]
20	1.20	2.00	3.0	6	74 (61)	15:85
21	1.00	2.00	3.0	6	74 (54)	ND
22	1.00	2.00	3.0	6[e]	31[n]	ND
23	2.00	2.00	3.0	6[e]	54[o]	20:54
24	2.00	-[p]	3.0	6[e]	-	66:3
25	2.00	-[p,q]	3.0	6[e]	-	52:5

[a]See experimental section general procedure C for reaction protocol. [b]Product conversion was determined by ^{1}H NMR of the crude reaction mixture using benzyl benzoate as an internal standard. [c]Yield in parentheses represents isolated yield. [d]Ratio was determined using ^{1}H NMR of the crude reaction mixture. [e]Dump and stir: slow addition was not carried out. [f]The reaction was allowed to stir further at room temperature for 24 h, which still only gave 38% of isolated product **2.37**. [g]The reaction was carried out without a nitrogen balloon. [h]Complete conversion of **2.1** to **2.37** was observed by ^{1}H NMR of the crude reaction mixture. [i]Following slow addition the reaction mixture was allowed to stir for an additional 15 h. [j]Basic work up with a saturated solution of $NaHCO_3$ was not carried; product isolated as iminium HCl salt **2.38**. [k]The reaction was carried out with 7.0 equiv of 1,3,5-trimethoxybenzene. [l]The reaction was carried out with 2.0 equiv of 1,3,5-trimethoxybenzene. [m]3% conversion to **2.4** was observed by ^{1}H NMR of the crude reaction mixture using benzyl benzoate as an internal standard. [n]9% conversion to **2.4**

was observed by ^{1}H NMR of the crude reaction mixture using benzyl benzoate as an internal standard. [o]23% conversion to **2.4** was observed by ^{1}H NMR of the crude reaction mixture using benzyl benzoate as an internal standard. [p]NaN_3 (2.0 equiv) was used instead of $TMSN_3$ solution. [q]TMSCl (1.0 equiv) was used as an additive. ND, Not determined.

Moreover, we determined that increasing the reaction time to overnight at room temperature following slow addition did not impact the isolation of **2.37** (cf. entries 12 and 13). Likewise, isolating the product in its HCl salt form **2.38** still afforded product in less than 80% yield (cf. entries 13 and 14). Conversely, the reaction with 7.0 equiv of 1,3,5-TMB, instead of 5.0 equiv, yielded similar conversions (cf. entries 12 and 15). In contrast, the reaction with 2.0 equiv of 1,3,5-TMB diminished conversions significantly (entry 16). Lastly, we demonstrated that replacing $TMSN_3$ with NaN_3, or attempting to generate *in situ* $TMSN_3$ via mixing NaN_3 with TMSCl were both detrimental reactions (entries 24 and 25).

Due to the requirement of excess $AlCl_3$ for complete reaction conversions, we examined $AlBr_3$ for the transformation. We speculated that if the TMB-trapped imine were isolated as the HCl salt form **2.38,** under these conditions $AlBr_3$ might generate HBr *in situ*, along with versions of $Al[OCH(CF_3)_2]_3$ or $Al[OCH(CF_3)_2]Br_2$. Evaluation of $AlBr_3$ revealed it indeed led to better reaction conversions and isolated yields, specifically Table 2.6 depicts these improvements in the isolation of desired product **2.39** as its HBr salt. We again reaffirmed that slow addition was necessary for complete conversion; entry 1 of Table 2.6 revealed 50% conversion to **2.39** when the reaction was set up as a standard "dump and stir". However, upon 6 h of slow addition of the azide-HFIP solution followed by additional stirring at room temperature overnight, normal phase chromatographic purification afforded TMB-imine HBr salt **2.39** in 92% yield. The product outcome was confirmed by X-ray crystal analysis and is shown in Figure 2.5. Lastly, as expected, changing or diluting HFIP solvent with a related fluorinated solvent trifluoroethanol (TFE, p*K*a 12.4), or a non-fluorinated solvent toluene was detrimental towards **2.39** formation.

Table 2.6. Optimization of conditions with $AlBr_3$ in HFIP.[a-c]

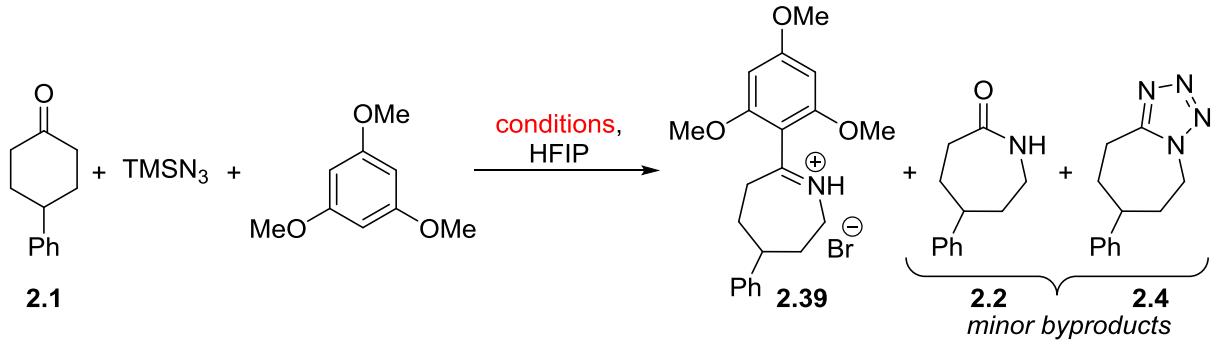

entry	catalyst (equiv)	$TMSN_3$ (equiv)	HFIP (mL)	slow addition (h)	conversion (%)	
					2.39[b,c]	**2.1:2.39**[d]
1	1.00	2.00	3.0	6[e]	50[f]	ND
2	1.00	2.00	3.0	6	95 (78)[g]	5:≥95[h]
3	1.00	2.00	3.0	6[i]	95 (87)[g]	5:≥95[h]
4	1.00	2.00	3.0	6[i]	≥100 (92)	5:≥95[h]
5	0.50	2.00	3.0	6[i]	63	ND
6	1.00	1.50	3.0	6[i]	93	5:≥95[g]
7	1.00	2.00	3.0	2	33[g]	ND[j]:33
8[k]	1.00	2.00	3.0	6[i]	47[l]	ND[j]:47
9	1.00	2.00	TFE (1):2.0	6	42[g]	21:42
10	1.00	2.00	Toluene (1):2.0	6	10[g]	90:10

[a]See experimental section general procedure D for reaction protocol. [b]Product conversion was determined by ^{1}H NMR of the crude reaction mixture using benzyl benzoate as an internal standard. [c]Yield in parentheses represents isolated yield. [d]Ratio was determined using ^{1}H NMR of the crude reaction mixture. [e]"Dump and stir"; slow addition was not carried out. [f]3% conversion to **2.4** was observed by ^{1}H NMR of the crude reaction mixture using benzyl benzoate as an internal standard. [g]Basic work up with a saturated solution of $NaHCO_3$ and brine was carried out; free imine **2.37** was isolated. [h]Complete conversion of **2.1** to **2.39** was observed by ^{1}H NMR of the crude reaction mixture. [i]After slow addition, the reaction mixture was allowed to stir for an additional 15 hours at rt. [j]**2.1** was observed by ^{1}H NMR of the crude reaction. [k]The reaction was carried out with 2.0 equiv of 1,3,5-trimethoxybenzene. [l]2% conversion to **2.4** was observed by ^{1}H NMR of the crude reaction mixture using benzyl benzoate as an internal standard.

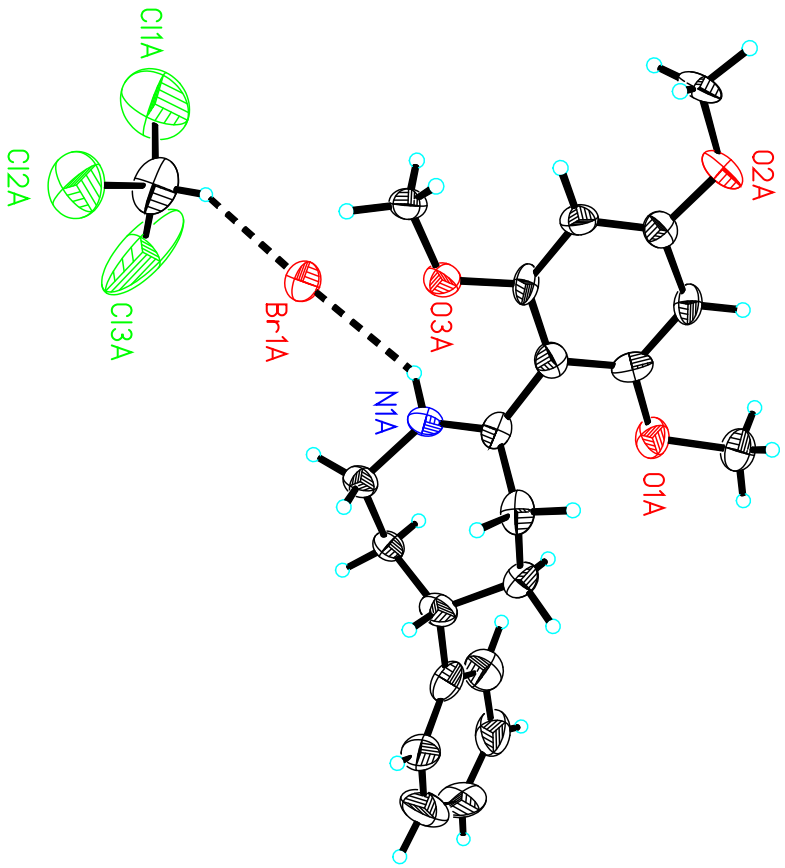

Figure 2.5. X-ray crystal structure of **2.39** (CCDC 1832152).

2.3.2 Ketone Scope and Functionalization

Having identified suitable reaction conditions that achieved a high conversion to imine **2.39**, we sought to establish the ketone scope of this interrupted Schmidt reaction. The above noted conditions proved acceptable for most cyclic and acyclic ketone substrates (Table 2.7). We began with cyclohexanone derivatives (entries 1–10) because these are generally the most facile substrates for nitrogen ring-expansion. Indeed, excellent results were obtained with unhindered 4-substituted cyclohexanone derivatives using the 6 h slow addition protocol at room temperature (entries 1–4). However, the transformation proved more robust with either extended room temperature stir or slight heating of the reaction mixture. For example, the reaction of 4-methylketone **2.40** to imine **2.41** proceeded in 80% isolated yield, however the yield improved to

87% when the reaction mixture was heated at 35 ˚C. The reaction of 2-substituted cyclohexanone proceeded but met some challenges; the reaction of 2-methylcyclohexanone **2.48** afforded desired imine **2.49** in 83% isolated yield when the reaction was performed at 35 ˚C, whereas the reaction of 2-*tert*-butylcyclohexanone **2.50** afforded only 11% isolated yield of product **2.51** under similar conditions. The difference in yields obtained from the reactions with 2-methyl or 2-*tert*-butylcyclohexanone exemplify the sensitivity of the reaction toward additional steric bulk near the reacting carbonyl. Moreover, the reaction of functionalized and sterically hindered cyclohexanones required extended time and slight heat to afford imines in moderate yields (entries 7–8). The reaction of enantiopure L-methanone **2.52** delivered at best 54% of imine **2.53**, however, minor amounts of previously reported tetrazole were also isolated during this reaction (entry 7). Functionalized six-membered cyclic ketones such as tetrahydropyran-4-one **2.10** proceeded to afford imine **2.54** in moderate yields (entry 8), whereas the reaction of 1-methylpiperidin-4-one **2.55** in the presence of $TMSN_3$ and trapping reagent 1,3,5-TMB did not yield any desired imine (entry 9 and Scheme 2.10). Instead, likely due to the presence of a functional group capable of catalyst deactivation, the ketone underwent an addition-elimination reaction with 1,3,5-TMB to afford **2.56**.

Table 2.7. Synthesis of 1,3,5-TMB imines.[a-c]

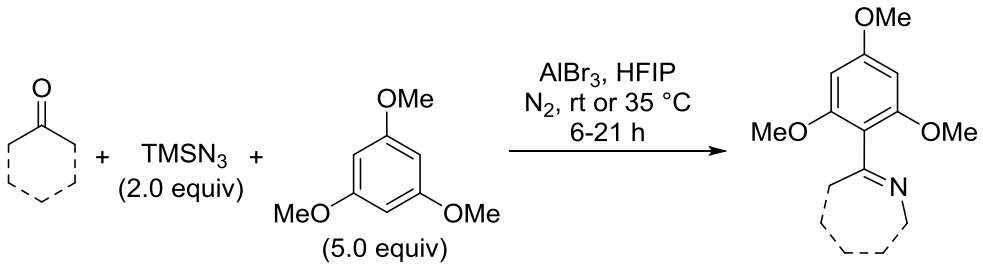

entry	ketone	product	yield (%)[b]

1	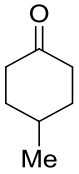	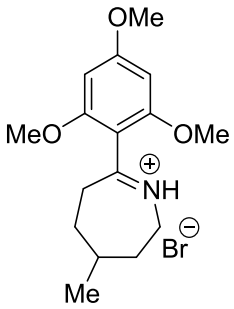	80[c] (87[d])
	2.40	**2.41**	
2	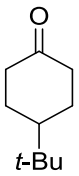	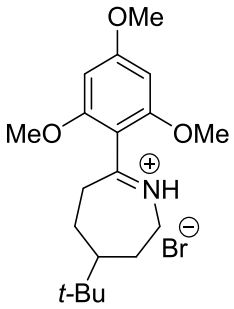	91[c]
	2.42	**2.43**	
3	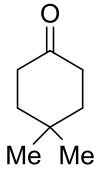	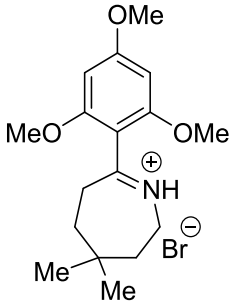	79 (83[d])[h]
	2.44	**2.45**	
4	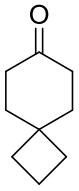	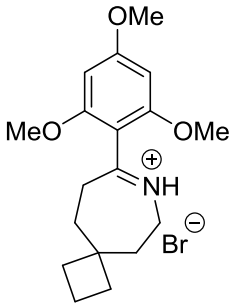	78[c]
	2.46	**2.47**	

5	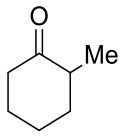	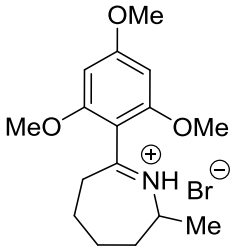	74 (83[d])
	2.48	**2.49**	
6	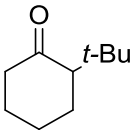	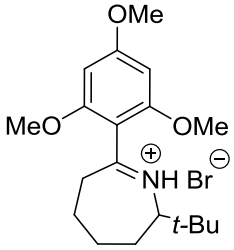	11[d]
	2.50	**2.51**	
7	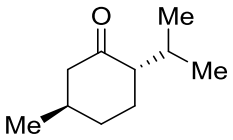	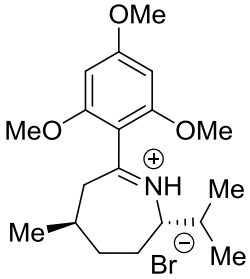	30[c,f] (54[d,f])
	2.52	**2.53**	
8	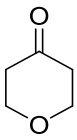	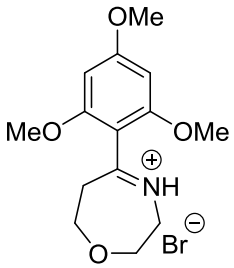	63[c]
	2.10	**2.54**	
9	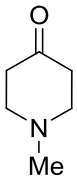	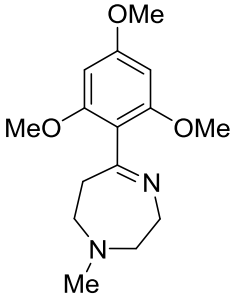	-
	2.55	*not observed* (see Scheme 2.10 for product **2.56**)	

10	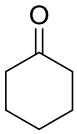	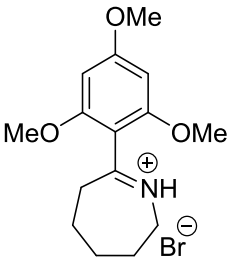	90
	2.6	**2.57**	
11	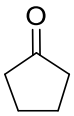	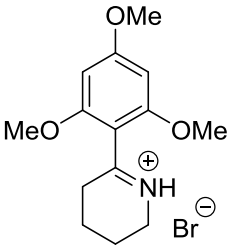	14 ($20^{c,e}$)
	2.58	**2.59**	
12	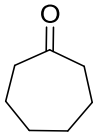	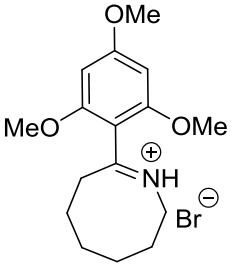	$50^{c,f}$ ($66^{d,f}$)
	2.14	**2.60**	
13	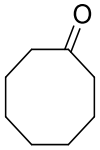	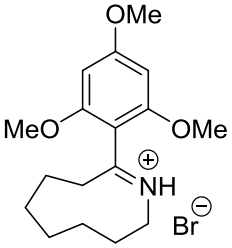	$30^{c,f}$ ($38^{d,f}$)
	2.16	**2.61**	
14	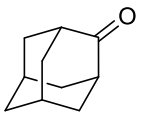	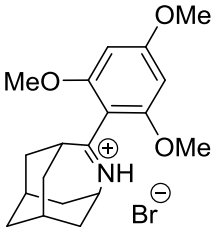	20 (26^{g})
	2.32	**2.62**	

15	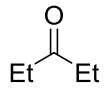	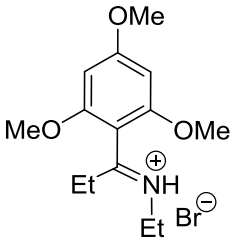	74[c] (88[d])
	2.63	**2.64**	
16	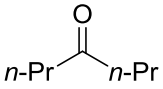	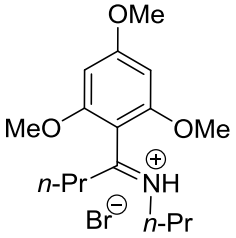	71 (89[d])
	2.65	**2.66**	
17	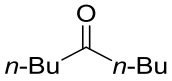	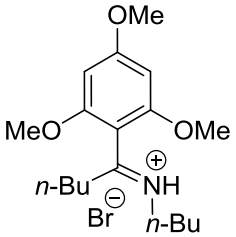	68[c] (81[d])
	2.34	**2.67**	
18	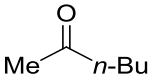	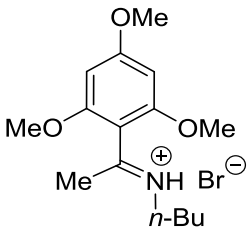 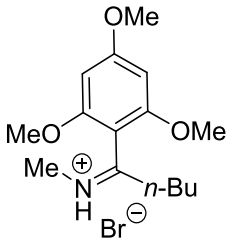	71 (78[d])
	2.68	**2.69** **2.70** **2.69:2.70** = 80:20 [i]	

[a]See experimental section general procedure E and F for reaction protocol. [b]Isolated yield after 6 h slow addition, unless otherwise noted. [c]Isolated yield following an additional 15 h stir of the reaction mixture at room temperature after the 6 h slow addition of azide solution. [d]Isolated yield following an additional 15 h stir of reaction mixture at 35 ˚C after the 6 h slow addition of azide solution at 35 ˚C. [e]Yield determined by ^{1}H NMR of the crude reaction mixture using benzyl benzoate as an internal standard. [f]Minor amounts (2–19%) of previously reported tetrazole were isolated. [g]Reaction was carried out over 18 h slow addition of azide solution. [h]**2.45** confirmed as HBr salt by elemental analysis. [i]Regiochemical isomers were inseparable from normal phase purification and ratio of mixture was determined by ^{1}H NMR.

Scheme 2.10. Reaction of 1-methylpiperidin-4-one **2.55** with 1,3,5-TMB.

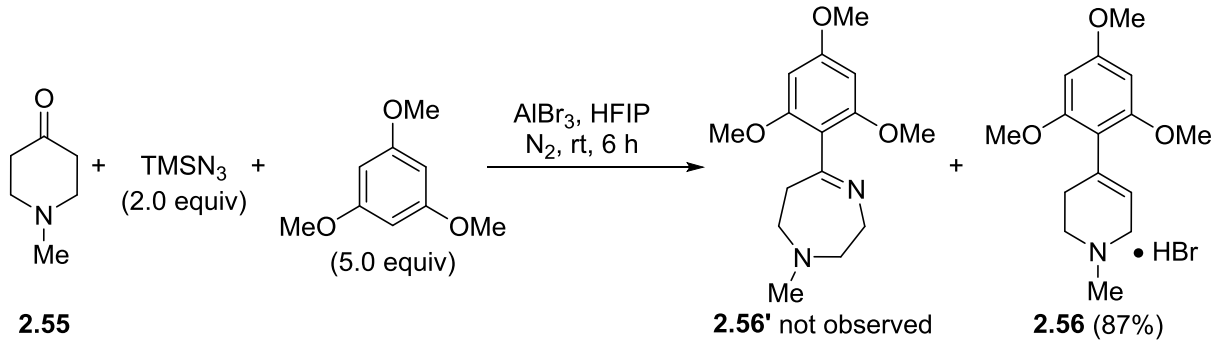

Reactions of smaller and medium-sized ketone rings faced expected challenges and afforded imines in poor to moderate yields (cf. entry 10 with entries 11–13). A poor yield was obtained with cyclopentanone **2.58**, in which 14% of imine **2.59** was isolated following normal phase column chromatography. We have been unable so far to obtain reasonable yields of the ring-expansion products from cyclopentanone derivatives; at most 20% was observed by ^{1}H NMR of the crude reaction mixture of the simple cyclopentanone substrate using an internal standard (along with unidentifiable peaks). Likewise, the reactions of cyclobutanone substrates were sluggish and failed to provide any quantifiable imine. Application of the present methodology to cycloheptanone **2.14** provided a reasonable yield of the corresponding imine **2.60**. In fact, we found that heating the reaction mixture at 35 ˚C improved the yield by 16% (50→66%). However, the reaction of cyclooctanone **2.16** afforded both the desired imine **2.61** and previously observed tetrazole[7] in poor yields (entry 13). We attributed the poor yields especially that of the cyclopentanone and cyclooctanone examples to the lack of ketone reactivity with the azide nucleophile and to ring strain associated with the formation of tetrahedral intermediates during the course of nitrogen insertion. In fact, cyclopentanones are not good reacting partners in the $TiCl_4$-promoted ring expansion with simple alkyl azides either.[41] Likewise, the reaction of 2-

adamantanone **2.32** proceeded sluggishly to the corresponding tricyclic imine **2.62** and resulted in 20% isolated yield (entry 14).

The interrupted Schmidt reaction of acyclic aliphatic ketones with the model 1,3,5-TMB trapping reagent proceeded smoothly to afford the corresponding imines in good yields (Table 2.7, entries 15–18). In some cases, these reactions were more facile when carried out 35 ˚C as opposed to room temperature and resulted in relatively high yields (68–89%). The reaction of unsymmetrical ketone **2.68** afforded 80:20 isomeric mixture of imine **2.69**, and reliably, with migratory preference for the electron-rich alkyl group. We investigated relatively few unsymmetrical ketones because regiochemical control is difficult to achieve with this variant of the Schmidt reaction. A range of benzylic and aromatic ketones were also investigated, i.e., specifically substrates α-tetralone, β-tetralone, flavanone, and indanone. However, these reactions were unsuccessful and failed to provide any quantifiable imine products. With respect to α-tetralone and flavanone, both substrates were non-reactive with $AlBr_3$ and led to recovery of starting material. The non-reactivity of flavanone was especially surprising because previous report with TfOH in HFIP furnished tetrazoles, as well as HFIP- and azide-trapped imine products.[7]

Upon successful synthesis of a range of 1,3,5-TMB-trapped imines, we sought to extend the scope of this methodology towards the preparation of related functionalities. We next examined the synthesis of enamide with a range of ketones and electrophiles (e.g., acetic anhydride as electrophile in Scheme 2.11). Enamides are versatile organic substrates that display balance in stability and reactivity, as well as are commonly present in medicinal compounds.[46-47] Interestingly, a direct conversion of ketones to substituted ring-expanded enamides is an unprecedented transformation in the literature. We realized this represented a straightforward

opportunity to incorporate functional diversity to our methodology, and accordingly devised a one-pot protocol to report a direct conversion of ketone to ring-expanded enamides. To do this, we utilized, either separately or in combination, 4-dimethylaminopyridine (DMAP) or triethylamine (TEA) bases to mediate the transformation with electrophiles. Figure 2.6 depicts the synthesis of seven acetyl-enamide derivatives **2.71**–**2.77** in good yields. We carried out this two-step transformation in one pot; fortuitously, the enamide proved easier to purify by normal phase chromatography (i.e., they appeared as a clean single spot as opposed to a streak on TLC). The synthesis of enamide derivatives **2.75** and **2.76** were obtained in higher yields as compared to their imine precursors **2.60** and **2.61**, respectively.

Scheme 2.11. Formation of enamide using acetic anhydride.

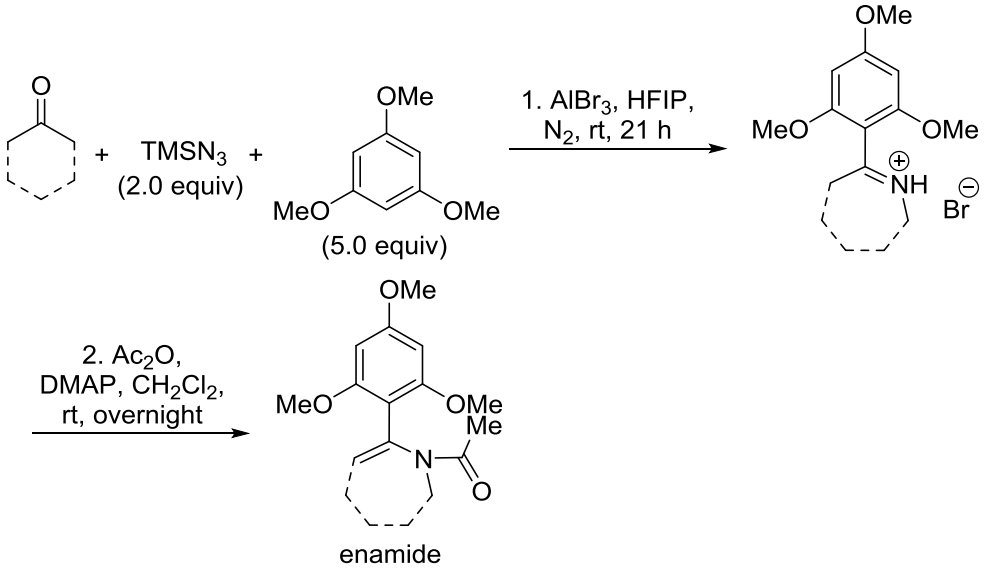

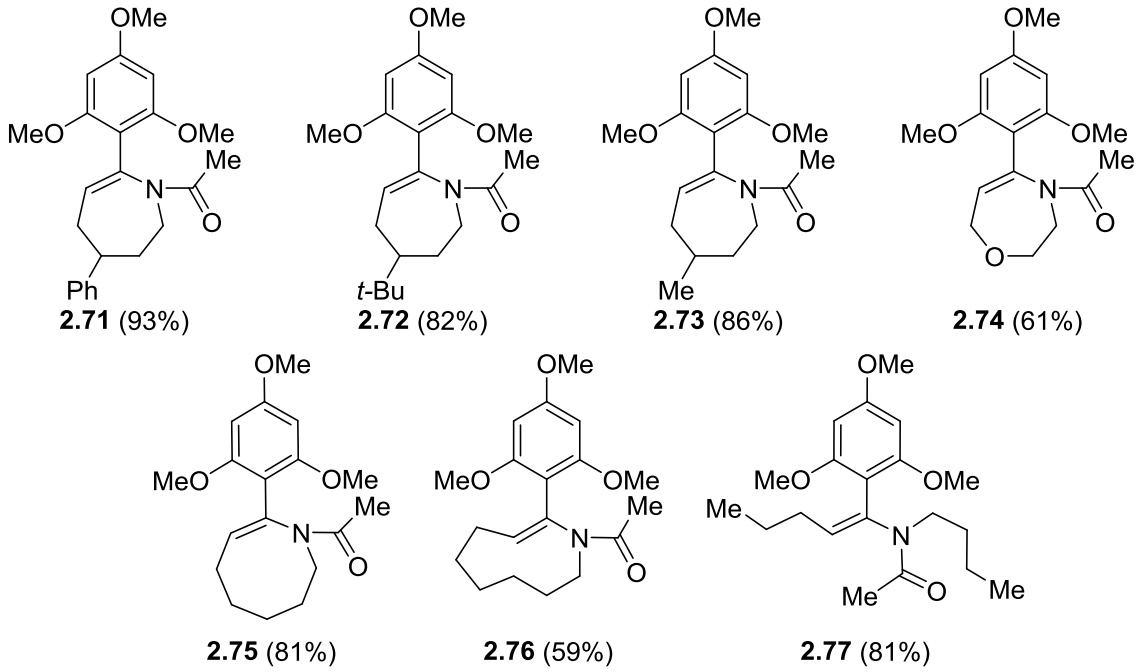

Figure 2.6. Synthesis of enamide derivatives using acetic anhydride. Yield in parentheses refer to the overall yield for the two sequential steps.

Given the success with acetic anhydride as the electrophile, we sought to apply the methodology towards application of other readily available electrophiles. As shown in Figure 2.7, we applied the developed route to synthesize a range of functionalized enamides. Here again, the reaction was mediated by DMAP and/or TEA base. Instead of acetic anhydride, the **2.1**-ketone derived imine substrates were reacted with additional electrophiles, including di-*tert*-butyl dicarbonate, 4-substituted acyl chlorides, tosyl chlorides, and 4-substituted phenyl isocyanates. The corresponding enamide derivatives **2.78**–**2.86** were synthesized in 29–77% yields. Even though the process of enamide formation is unoptimized, this current application demonstrated medicinal chemistry utility of the newly developed interrupted Schmidt reaction.

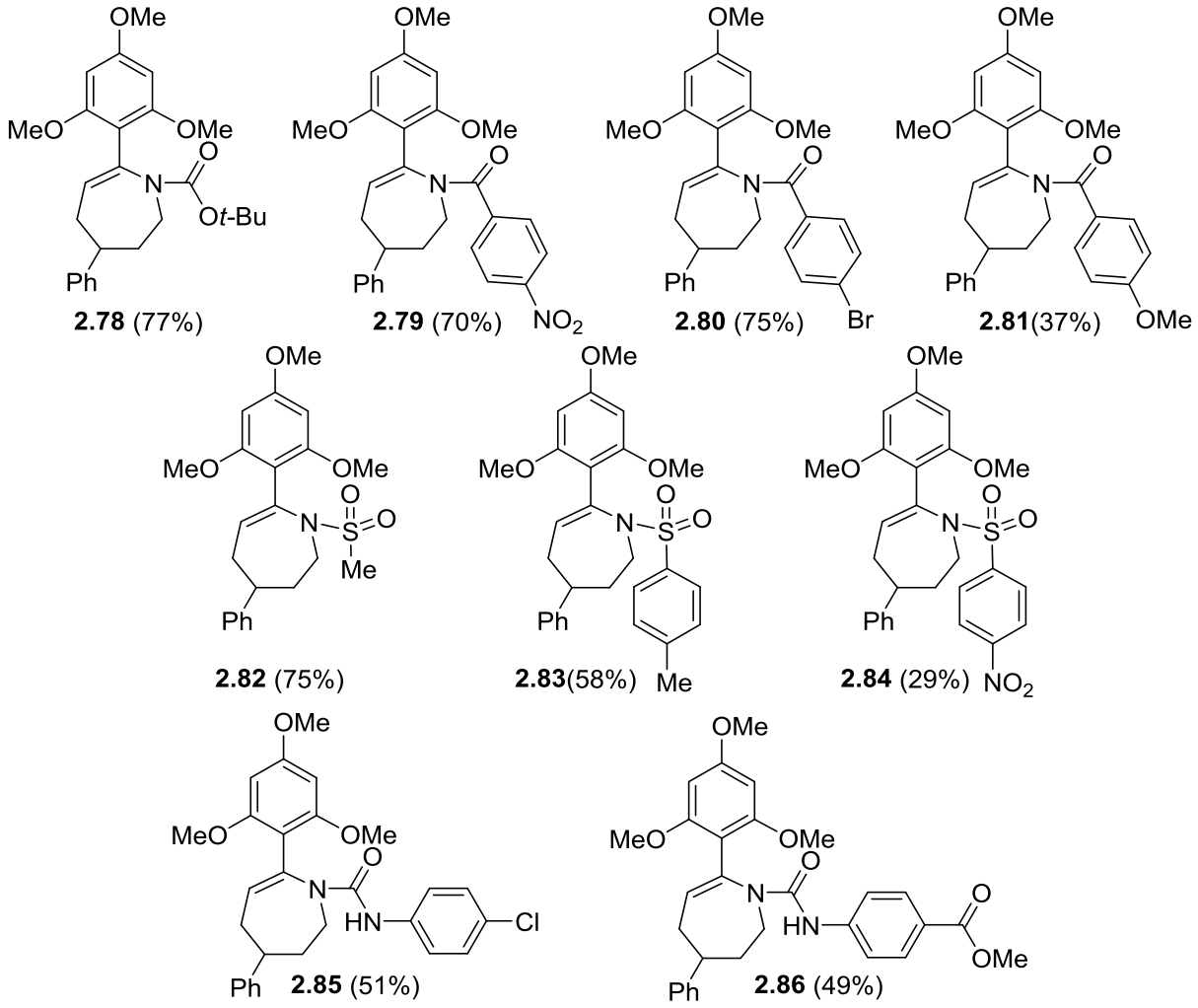

Figure 2.7. Synthesis of enamide derivatives using various electrophiles. Yield in parentheses refer to the overall yield for the two sequential steps.

Given the ease of preparing enamides, we sought to determine if the imine could also be reductively converted to amines, which would further advance the utility of this methodology. In order to devise a one-pot route towards amine preparation, we carried out a brief screen of reducing agents, which included sodium borohydride, triethysilane, and sodium triacetoxyborohydride. Of the reagents screened, only sodium borohydride ($NaBH_4$) gave clean and relatively high conversions to the amine **2.87** (Scheme 2.12). In fact, by using an achiral substrate, we achieved stereoselective conversion to amine **2.87** in high diastereoselectivity (dr 20:1). Using ^{1}H NMR, we

observed only one isomer and the stereochemistry of **2.87** was assigned as shown in Scheme 2.12. Stereochemical assignments were proposed based on large *J*-coupling values of the protons adjacent to the aromatic substitution. Additionally, in a one-pot fashion, the amine **2.87** was readily derivatized using acetic anhydride and di-*tert*-butyl dicarbonate to afford **2.88** and **2.89** in 76% yields, respectively.

Scheme 2.12. Synthesis of amine derivatives. Yield in parentheses refer to the overall yield for the two or three sequential steps.

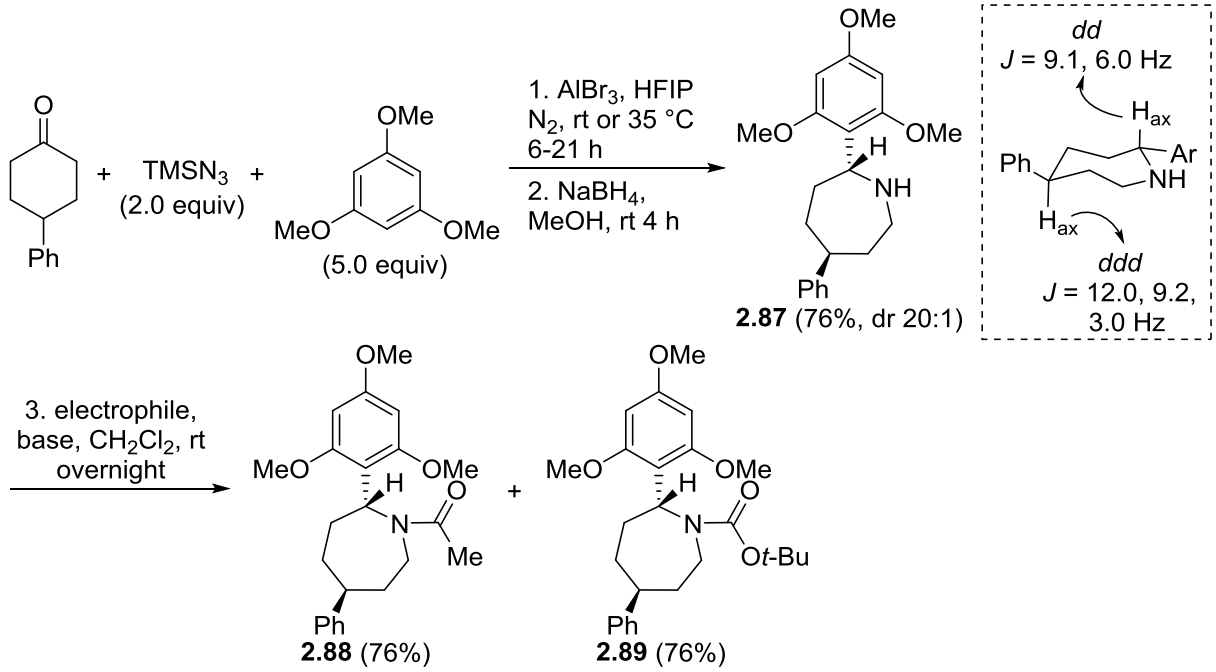

2.3.3 Nucleophile Scope and Mechanism Discussion

The most challenging endeavor associated with the development of the interrupted Schmidt reaction that we have encountered has been the extension of the current methodology towards various arene nucleophiles. For example, adapting the current methodology to closely related arenes like 1,2,3-trimethoxybenzene, 1,3-dimethoxybenzene, and anisole failed. These reactions do not produce quantifiable product outcomes, though in some cases product masses were

observed by UPLC. To address this, we examined a modification of the current methodology in which nucleophiles were added after the slow addition of azide solution. This methodology (Table 2.8) discloses preliminary investigations of protocols that include the addition of nucleophile in portions during or after slow addition (entries 1–5) or, alternatively, dual slow addition of nucleophile and azide using the syringe pumps (entry 6). Unfortunately, only moderate conversions (>80%) to desired imine **2.39** were observed. Despite this setback, the proposed method would be most impactful if it could accommodate other nucleophiles. Thus, we chose to carry out a preliminary screen of a limited set of reaction partners.

Table 2.8. Preliminary investigation of other protocols for the interrupted Schmidt reaction.

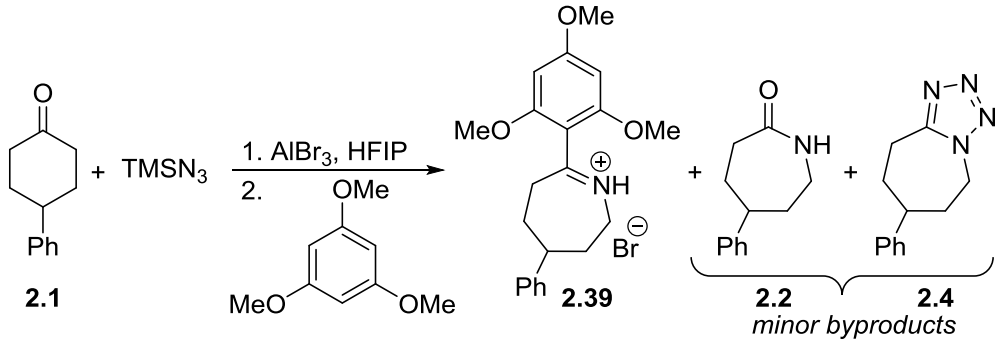

entry	catalyst (equiv)	$TMSN_3$[a] (equiv)	HFIP[b] (mL)	slow addition[c] (h)	1,3,5-TMB addition notes	conversion (%) 2.39:2.4[d]
1	1.00	2.00	3.0	6	5.0 equiv	64:4
2	1.50	2.00	3.0	6	5.0 equiv	55:11
3	1.00	2.00	3.0	6	5.0 equiv[e]	56:ND
4	1.00	2.00	3.5	6	1.0 equiv added after 3 h, then 4.0 equiv after 6 h[f]	71:ND
5	1.00	2.00	3.5	6	2.5 equiv added after 3 h, then 2.5 equiv after 6 h[f]	67:ND
6	1.00	2.00	4.0	6	5.0 equiv (+ HFIP 2.0 mL) added using syringe pump[g]	79:ND

[a]Azide added as a solution in HFIP (1.0 mL) using syringe pump (0.40 mL/h, 20 gauge needle). [b]Total volume of reaction mixture after slow addition. [c]1,3,5-TMB was added after 6 h slow addition and the reaction mixture was allowed to stir overnight (+15 h), unless otherwise noted. [d]Conversion to desired **2.39** and side-product **2.4** were observed by ^{1}H NMR of the crude reaction mixture using benzyl benzoate as an internal standard. [e]The reaction was heated at 40 °C after addition of 1,3,5-trimethoxybenzene. [f]Nucleophile added in portions during and after slow addition. [g]Nucleophile added at the same rate as the azide solution using a syringe pump (0.40 mL/h, 20 gauge needle). ND, Not determined.

The results of the nucleophile investigation are shown in Figure 2.8. So far, we successfully examined and reported examples for 1,3-dimethoxybenzene, indole derivatives, and pyrrole as nucleophile trapping agents added after the slow addition of $TMSN_3$ in HFIP (Figure 2.8a). A moderate amount of optimization was performed for these individual examples. For example, when 5.0 equiv of 1,3-dimethoxybenzene was added to the reactive species derived from 4-phenylcyclohexanone **2.1** and $TMSN_3$ 43% of the isomer **2.90** was isolated (the reaction was also carried using 10.0 equiv of 1,3-dimethoxybenzene, however similar conversions were obtained by crude ^1H NMR to that of the reaction with 5.0 equiv). Alternatively, we found that the reaction was slightly sensitive to the order of nucleophile addition for indoles **2.91**–**2.95**. As can be seen by comparing yields of **2.92**, **2.94** and **2.95**, higher amounts were isolated when the nucleophile was added in two portions (once at the 3 h time point of slow addition, and then again after 6 h slow addition). Although the synthesis of indole-derivatives proceeded in moderate yields, it appears that electron-rich or electron-poor indoles may function as effective nucleophiles for the interrupted Schmidt reaction. Pyrrole was also effective in trapping the Schmidt ring-expanded cation and resulted in the product **2.96**. Our preliminary examination into other nucleophiles including 1,2,3-TMB, anisole, triethylsilane, allylsilane, furan, benzofuran, and benzothiophene were unsuccessful (Figure 2.8b). In spite of this, the preliminary success with indole nucleophiles suggests that adaptation to other carbon-based nucleophiles and broad utility in synthesis may be likely.

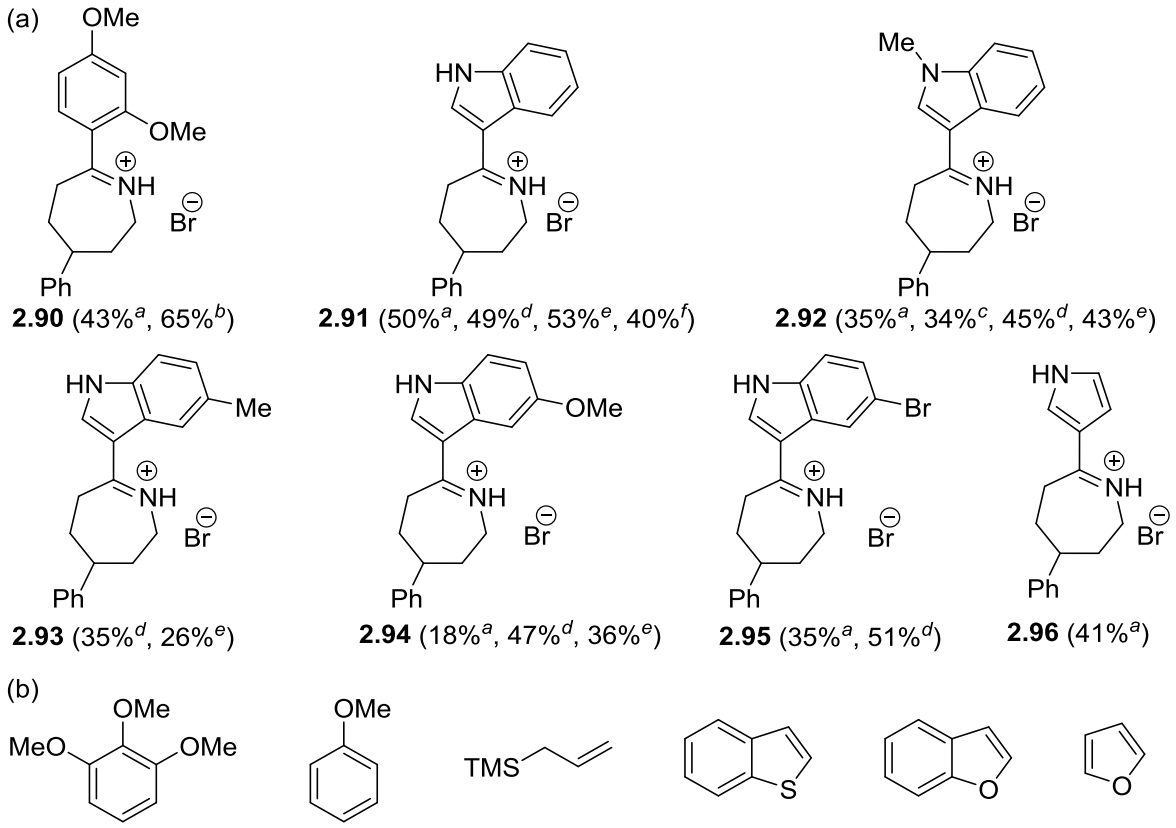

Figure 2.8. Preliminary screen of nucleophiles for the interrupted Schmidt reaction. (a) Successful examples. (b) Unsuccessful nucleophiles as trapping reagents. [a]After slow addition of azide-HFIP solution, ca. 5.0 equiv of nucleophile was added and the reaction mixture allowed to stir for an additional 15 h at room temperature. [b]After slow addition of azide-HFIP solution, ca. 10.0 equiv of nucleophile was added and conversion was determined by ^{1}H NMR of the crude reaction mixture using benzyl benzoate as an internal standard. [c]After slow addition of azide-HFIP solution, ca. 10.0 equiv of nucleophile was added and the reaction mixture allowed to stir for an additional 15 h at room temperature. [d]Nucleophile was added in portions during and after the slow addition of azide-HFIP solution. [e]Nucleophile and azide were added as HFIP solutions using syringe pumps.

A proposed mechanism for the interrupted Schmidt reaction is summarized in Figure 2.9. The mechanism begins with activation of the carbonyl by $AlBr_3$ and formation of an azidohydrin intermediate, which dehydrates to afford a diazonium ion species (Figure 2.9a). At this point, rearrangement gives an iminium ion intermediate, which may directly react with 1,3,5-TMB, forming the C–C bond and resulting in the final imine **2.39** (Figure 2.9b). Alternatively, the nitrilium ion could react with $AlBr_3$, *in situ* generated HBr, or solvent HFIP. This would lead to a

substituted intermediate (halo-iminium ion or HFIP-iminium ion) that might behave as the active species in the reaction with 1,3,5-TMB. In this scenario, stepwise addition of 1,3,5-TMB and elimination of X (Br, $OCH(CF_3)_2$) takes place to afford the product **2.39**. At the present time, we have not established which pathway is occurring, however subsequent work towards answering this question is proposed in the laboratory.

The thought-provoking question is why does the iminium ion persist long enough in solution to react with 1,3,5-TMB. In either mechanism, $AlBr_3$ or silyl byproducts contribute to sequestering the hydroxide ion, which may circumvent its addition to the nitrilium ion to generate lactam, and as described above, facilitate the formation of the proposed active species (X-iminium ion in Figure 2.9b). Lastly, the course of the aluminium reagent is unclear (Figure 2.9c). It is likely that $AlBr_3$ reacts with HFIP to generate *in situ* HBr (indicative through the isolation of products as HBr salts). The ionization process could be envisioned in many variations, although the role of such species during the course of the reaction remains unclear.

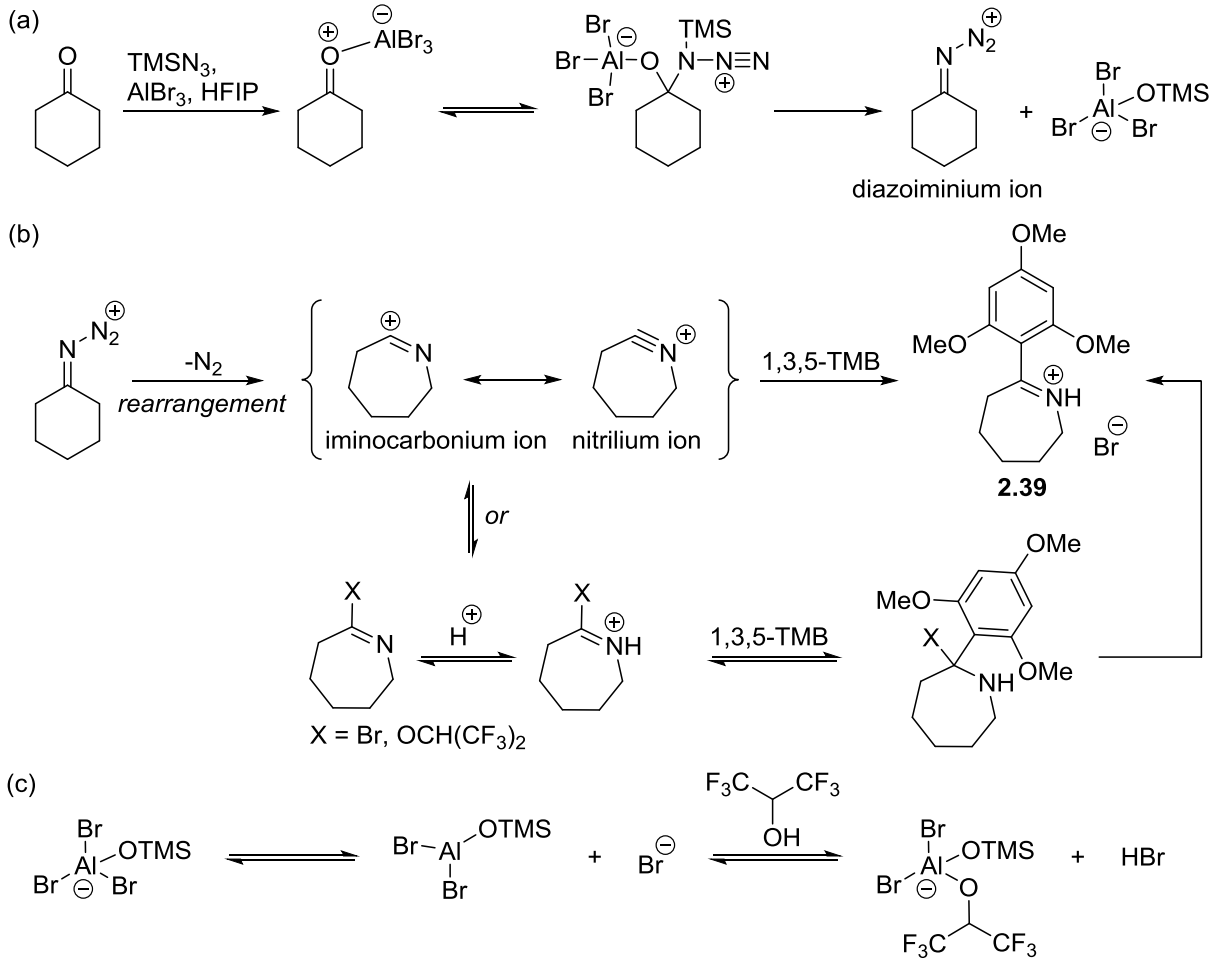

Figure 2.9. Proposed mechanism for the interrupted Schmidt reaction. (a) Formation of diazoiminum ion. (b) Formation of possible iminium ion intermediates. (c) Representative fates of aluminum reagent.

2.4 Conclusion and Future Directions

In summary, we have for the first time disclosed a general methodology to promote the interrupted Schmidt reaction concomitant with C–C bond formation. A promising synthetic strategy was established for intercepting the Schmidt reaction cationic intermediate using slow addition of $TMSN_3$ solution and $AlBr_3$ in the presence of HFIP. The ketone scope of the current methodology was extensively explored with 1,3,5-TMB and the preliminary nucleophile scope has been examined which identified indoles effective as trapping reagents as well. Additionally,

functional diversity was incorporated in this work by enabling the protocol towards the preparation of imine, enamide, and amine derivatives.

There is opportunity for further optimization towards substantial extension of carbon-based and heteroatom-based nucleophiles for the interrupted Schmidt reaction. Although further work to elucidate the mechanism of this reaction is important, the utility of the method for heterocycle synthesis has been demonstrated and should lead to other applications in organic and medicinal chemistry.

2.5 Experimental Section

2.5.1 Experimental Section for 2.2.2

General Information. ***Caution: Although we have not experienced any untoward events with the compounds mentioned in this thesis, azides and their precursors are known explosive hazards and should be used with appropriate safety precautions. Minimally, careful control of temperature and scale should be exercised. We do not recommend distillation of reaction mixtures that may contain residues of azide sources.***

Reactions were performed under inert atmosphere (argon or nitrogen) in glass sample vials with TFE-lined cap. All chemicals were purchased from commercial sources and used without further purification. New containers of $BF_3 \bullet OEt_2$, TfOH, and HFIP were used. Anhydrous was dried by passage through neutral alumina columns using a commercial solvent purification system prior to use. Thin-layer chromatography (TLC) was performed using commercial glass-backed silica plates (250 μM) with an organic binder. Preparative TLC was carried out using silica gel GF TLC plates (UV 254 nm, 1000 μM). Visualization was accomplished with UV light, Seebach's stain, or aqueous $KMnO_4$ stain, and heating. Purification was carried out by an automated flash

chromatography/medium-pressure liquid chromatography (MPLC) system using normal phase silica gel flash columns (4 or 12 g). The infrared (IR) spectra were acquired as thin films or solids using a universal ATR sampling accessory on a PerkinElmer Spectrum One FT-IR spectrometer; the absorption frequencies are reported in cm^{-1}. All nuclear magnetic resonance spectra were recorded on a Bruker 400 MHz, or 500 MHz with a dual carbon/proton cryoprobe. NMR samples were recorded in deuterated chloroform ($CDCl_3$) or deuterated dimethylsulfoxide (DMSO-d_6). Chemical shifts are reported in parts per million (ppm) and referenced to the center line of solvent ($CDCl_3$: δ 7.26 ppm for ^1H NMR and 77.16 ppm for ^{13}C NMR; DMSO-d_6 δ 2.50 ppm for ^1H NMR and 39.52 ppm for ^{13}C NMR). Coupling constants are given in Hertz (Hz). HRMS data were collected using a Time-of-flight mass spectrometer (TOF) with an electrospray ion source (ESI). Melting points were determined in open capillary tubes using OptiMelt, an automated melting point apparatus, and were uncorrected. Data for the known compounds prepared according to the methodology described in the section match with those reported in the literature.

General procedure A for the synthesis of *N*-hydroxyalkyl lactams. To a solution of ketone (0.400 mmol, 1.0 equiv) and 3-azidopropanol **1.1** (0.600 mmol, 1.5 equiv) in HFIP (1.0 mL) in a nitrogen-flushed two-dram vial was added TfOH (0.400–0.600 mmol, 1.0–1.5 equiv); immediate gas evolution was noted upon addition of acid for most substrates. The vial was capped and the reaction mixture was stirred at room temperature for 1–6 h. The solution was concentrated under nitrogen using a sample concentrator and dried under vacuum. The residual oil was diluted with CH_2Cl_2 and treated with either saturated $NaHCO_3$ solution (1.5 mL) or 1M NaOH solution (1.5 mL) at room temperature for 12–24 h. The reaction mixture was further diluted with CH_2Cl_2 (50 mL), dried over Na_2SO_4, filtered, and concentrated to afford a crude oil. Purification was

carried out either by elution with 10% MeOH/CH_2Cl_2 through a short bed of silica gel packed in a phase separator tabless, or by using a 4 g normal phase silica flash column on an automated MPLC system with a gradient elution from 0–25% MeOH/CH_2Cl_2. Concentration of appropriate fractions afforded products.

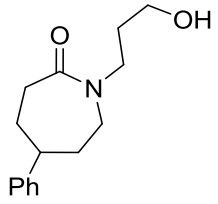

2.5

1-(3′-Hydroxypropyl)-5-phenylazepan-2-one, 2.5.[40] Prepared as described in the general procedure A. Colorless oil (70.5 mg, 0.285 mmol, 95% yield).

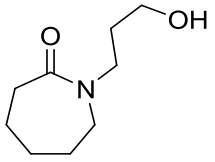

2.7

1-(3′-Hydroxypropyl)azepan-2-one, 2.7.[40] Following the general procedure A, to a solution of cyclohexanone **2.6** (39.3 mg, 0.400 mmol, 1.0 equiv) and 3-azidopropanol **1.1** (60.7 mg, 0.600 mmol, 1.5 equiv) in HFIP (1.0 mL) was added TfOH (35.0 μL, 0.395 mmol, 1.0 equiv). The reaction mixture was stirred at room temperature for 1 h. Subsequently, hydrolysis was carried out with saturated $NaHCO_3$ solution for 12 h. The crude oil obtained was eluted through a short bed of silica gel using 10% MeOH/CH_2Cl_2. Concentration of solvents afforded **2.7** as a colorless oil (64.8 mg, 0.378 mmol, 95% yield).

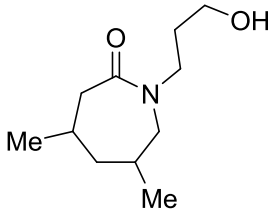

2.9

1-(3′-Hydroxypropyl)-4,6-dimethylazepan-2-one, 2.9. Following the general procedure A, to a solution of 3,5-dimethylcyclohexanone **2.8** (ca. 95% major isomer, 50.6 mg, 0.401 mmol, 1.0 equiv) and 3-azidopropanol **1.1** (60.4 mg, 0.597 mmol, 1.5 equiv) in HFIP (1.0 mL) was added TfOH (35.0 μL, 0.397 mmol, 1.0 equiv). The reaction mixture was stirred at room temperature for 1 h. Subsequently, hydrolysis was carried out by treatment with 1 M NaOH solution for 14 h. Purification was carried out on an automated MPLC system with gradient elution from 0–10% MeOH/CH_2Cl_2 to afford **2.9** as a colorless oil (76.8 mg, 0.385 mmol, 94% yield). R_f = 0.40 (5% MeOH/CH_2Cl_2); IR (neat) 3390, 1619 cm^{-1}; ^1H NMR (400 MHz, $CDCl_3$) δ 0.84 (m, 4H), 0.92 (m, 3H), 1.58 (m, 3H), 1.70 (m, 1H), 1.79 (m, 1H), 2.25 (m, 1H), 2.35–2.42 (dd, *J* = 13.6, 11.2 Hz, 1H), 2.84 (m, 1H), 3.20–3.26 (dd, *J* = 14.9, 10.1 Hz, 1H), 3.42 (m, 4H), 4.11 (s, 1H); ^{13}C NMR (100 MHz, $CDCl_3$) δ 21.0, 24.5, 30.1, 30.2, 34.0, 44.6, 44.9, 48.0, 56.3, 58.0, 175.9. HRMS (ESI) *m/z* calcd for $C_{11}H_{22}NO_2$ $[M + H]^+$ 200.1651, found 200.1656.

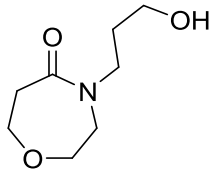

2.11

4-(3′-Hydroxypropyl)-1,4-oxazepan-5-one, 2.11. Following the general procedure A, to a solution of tetrahydro-4*H*-pyran-4-one **2.10** (37.0 μL, 0.401 mmol, 1.0 equiv) and 3-azidopropanol **1.1** (60.6 mg, 0.599 mmol, 1.5 equiv) in HFIP (1.0 mL) was added TfOH (35.0 μL,

0.397 mmol, 1.0 equiv). The reaction mixture was stirred at room temperature for 6 h. Subsequently, hydrolysis was carried out with saturated $NaHCO_3$ solution for 13 h. Purification was carried out on an automated MPLC system with gradient elution from 0–5% MeOH/CH_2Cl_2 to afford **2.11** as a colorless oil (58.5 mg, 0.338 mmol, 84% yield). R_f = 0.51 (5% MeOH/CH_2Cl_2); IR (neat) 3394, 1620 cm^{-1}; ^1H NMR (400 MHz, $CDCl_3$) δ 1.66 (m, 2H), 2.75 (m, 2H), 3.45 (m, 2H), 3.52 (m, 4H), 3.72 (m, 2H), 3.76 (m, 2H); ^{13}C NMR (100 MHz, $CDCl_3$) δ 30.3, 41.1, 45.3, 52.1, 58.2, 65.6, 70.4, 175.9. HRMS (ESI) *m/z* calcd for $C_8H_{16}NO_3$ $[M + H]^+$ 174.1130, found 174.1134.

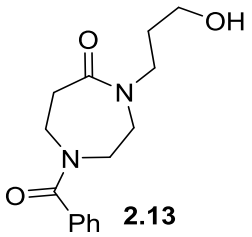

2.13

1-Benzoyl-4-(3′-hydroxypropyl)-1,4-diazepan-5-one, 2.13. Following the general procedure A, to a solution of 1-benzoyl-4-piperidone **2.12** (81.3 mg, 0.400 mmol, 1.0 equiv) and 3-azidopropanol **1.1** (60.4 mg, 0.597 mmol, 1.5 equiv) in HFIP (1.0 mL) was added TfOH (35.0 μL, 0.397 mmol, 1.0 equiv). The reaction mixture was stirred at room temperature for 6 h. Subsequently, hydrolysis was carried out with saturated $NaHCO_3$ solution for 12 h. Purification was carried out on an automated MPLC system with gradient elution from 0–10% MeOH/CH_2Cl_2 to afford **2.13** as a colorless oil (88.9 mg, 0.322 mmol, 80% yield). R_f = 0.20 (5% MeOH/CH_2Cl_2); IR (neat) 3408, 1618 cm^{-1}; ^1H NMR (400 MHz, $CDCl_3$) δ 1.67 (br s, 2H), 2.71 (br s, 2H), 3.51–3.84 (complex, 10H), 7.32–7.42 (complex, 5H); ^{13}C NMR (100 MHz, $CDCl_3$) δ 30.4, 39.0, 45.2, 45.4, 50.1, 50.7, 58.3, 127.0, 128.9, 130.2, 135.4, 171.3, 174.5. HRMS (ESI) *m/z* calcd for $C_{15}H_{21}N_2O_3$ $[M + H]^+$, 277.1552, found 277.1562.

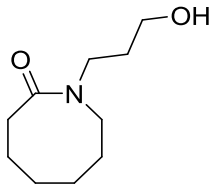

2.15

1-(3′-Hydroxypropyl)-1-azacyclooctan-2-one, 2.15.[48] Following the general procedure A, to a solution of cycloheptanone **2.14** (44.7 mg, 0.399 mmol, 1.0 equiv) and 3-azidopropanol **1.1** (60.8 mg, 0.601 mmol, 1.5 equiv) in HFIP (1.0 mL) was added TfOH (35.0 μL, 0.397, 1.0 equiv). The reaction mixture was stirred at room temperature for 6 h. Subsequently, hydrolysis was carried out with 1 M NaOH solution for 24 h. The crude oil obtained was eluted through a short bed of silica gel using 10% MeOH/DCM. Concentration of solvents afforded **2.15** as a yellow oil (45.2 mg, 0.244 mmol, 61% yield).

Similarly, the solution of cycloheptanone **2.14** (44.9 mg, 0.400 mmol, 1.0 equiv) and 3-azidopropanol **1.1** (60.7 mg, 0.600 mmol, 1.5 equiv) in HFIP (1.0 mL) was treated with TfOH (53.0 μL, 0.600 mmol, 1.5 equiv) for 6h. Subsequent hydrolysis and purification as described above afforded **2.15** as a yellow oil (51.0 mg, 0.275 mmol, 69% yield).

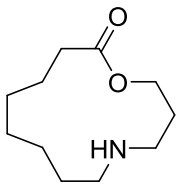

2.17

1-Oxa-5-azacyclotridecan-13-one, 2.17.[48] Following the general procedure A, to a solution of cyclooctanone **2.16** (50.8 mg, 0.403 mmol, 1.0 equiv) and 3-azidopropanol **1.1** (60.9 mg, 0.602 mmol, 1.5 equiv) in HFIP (1.0 mL) was added TfOH (35.0 μL, 0.397 mmol, 1.0 equiv). The reaction mixture was stirred at room temperature for 6 h. Subsequently, hydrolysis was carried

out with saturated $NaHCO_3$ solution for 12 h. Purification was carried out on an automated MPLC system with gradient elution from 0–25% MeOH/CH_2Cl_2 to afford **2.17** as an orange low melting solid (45.3 mg, 0.227 mmol, 56% yield).

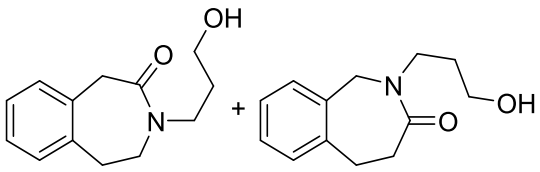

2.19 + 2.20

3-(3′-Hydroxypropyl)-4,5-dihydro-1*H*-benzo[*d*]azepin-2(3*H*)-one, 2.19 and 2-(3′-hydroxypropyl)-4,5-dihydro-1*H*-benzo[*c*]azepin-3(2*H*)-one, 2.20. Following the general procedure A, to a solution of β-tetralone (58.5 mg, 0.400 mmol, 1.0 equiv) **2.18** and 3-azidopropanol **1.1** (60.7 mg, 0.600 mmol, 1.5 equiv) in HFIP (1.0 mL) was added TfOH (35.0 μL, 0.397 mmol, 1.0 equiv). The reaction mixture was stirred at room temperature for 3 h. Subsequently, hydrolysis was carried out with saturated $NaHCO_3$ solution for 13 h. Purification was carried out on an automated MPLC system with gradient elution from 0–10% MeOH/CH_2Cl_2 to afford a mixture of lactams **2.19** and **2.20** as an orange oil (combined yield of **2.19** and **2.20**: 82.3 mg, 0.375 mmol, 94%; ratio of **2.19:2.20** = 63:37). **2.19** and **2.20**: R_f = 0.39 (5% MeOH/CH_2Cl_2); IR (neat) 3382, 1625 cm^{-1}; ^1H NMR (400 MHz, $CDCl_3$) δ 1.65 (m, 2H), 1.72 (m, 2H), 2.94 (m, 2H), 3.13 (m, 2H), 3.18 (t, *J* = 6.68 Hz, 2H), 3.35 (t, *J* = 5.52 Hz, 2H), 3.48 (t, *J* = 5.52 Hz, 2H), 3.57 (m, 2H), 3.61 (m, 2H), 3.72 (m, 2H), 3.92 (s, 2H), 4.49 (s, 2H), 7.04–7.25 (complex, 8H); ^{13}C NMR (100 MHz, $CDCl_3$) δ 28.8, 30.4, 30.5, 32.4, 33.5, 42.9, 43.6, 44.5, 46.9, 53.1, 58.0, 58.2, 126.2, 126.7, 127.3, 128.3 128.7, 130.4, 130.6, 131.0, 131.3, 134.3, 135.6, 137.4, 173.4, 175.0. Diagnostic peaks of **2.19**: ^1H NMR (400 MHz, $CDCl_3$) δ 1.72 (m, 2H), 3.13 (m, 2H), 3.48 (t, *J* = 5.52 Hz, 2H), 3.57 (m, 2H), 3.72 (m, 2H), 3.92 (s, 2H); ^{13}C NMR (100 MHz, $CDCl_3$)

δ 30.5, 32.4, 42.9, 43.6, 46.9, 58.2, 131.3, 135.6, 173.4. Diagnostic peaks of **2.20**: ^{1}H NMR (400 MHz, $CDCl_3$) δ 1.65 (m, 2H), 2.94 (m, 2H), 3.18 (m, J = 6.68 Hz, 2H), 3.35 (t, J = 5.52 Hz, 2H), 3.61 (m, 2H), 4.49 (s, 2H); ^{13}C NMR (100 MHz, $CDCl_3$) δ 28.8, 30.4, 33.5, 44.5, 53.1, 58.0, 175.0. HRMS (ESI) *m/z* calcd for $C_{13}H_{18}NO_2$ $[M + H]^+$ 220.1338, found 220.1346.

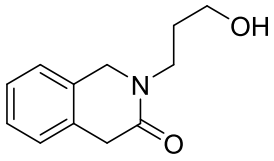

2.22

2-(3′-Hydroxypropyl)-1,2-dihydroisoquinolin-3(4*H*)-one, 2.22.[40] Following the procedure A, to a solution of 2-indanone **2.21** (39.7 mg, 0.300 mmol, 1.0 equiv) and 3-azidopropanol **1.1** (45.5 mg, 0.450 mmol, 1.5 equiv) in HFIP (0.75 mL) was added TfOH (27.0 μL, 0.306, 1.0 equiv). The reaction mixture was stirred at room temperature for 1 h. Subsequently, hydrolysis was carried out with saturated $NaHCO_3$ solution for 24 h. Purification was carried out on an automated MPLC system with gradient elution from 0–10% MeOH/CH_2Cl_2 to afford **2.22** as a brown oil (55.4 mg, 0.270 mmol, 90% yield).

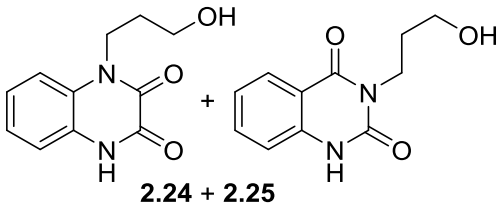

2.24 + 2.25

1-(3′-Hydroxypropyl)quinoxaline-2,3(1*H*,4*H*)-dione, 2.24 and 3-(3′-hydroxypropyl)quinazoline-2,4(1*H*, 3*H*)-dione, 2.25. Following the general procedure A, to a solution of isatin **2.23** (58.9 mg, 0.400 mmol, 1.0 equiv) and 3-azidopropanol **1.1** (60.7 mg, 0.600 mmol, 1.5 equiv) in HFIP (1.0 mL) was added TfOH (35.0 μL, 0.397 mmol, 1.0 equiv). The reaction mixture was stirred at room temperature for 6 h. Subsequently, hydrolysis was carried out

with saturated $NaHCO_3$ solution for 12 h. The precipitate was filtered, washed with water, and dried under vacuum to obtain a mixture of lactams **2.24** and **2.25** as a cream amorphous solid (combined yield of **2.24** and **2.25**: 67.2 mg, 0.305 mmol, 76% yield; ratio of **2.24:2.25** = 63:37. **2.24** and **2.25**: R_f = 0.21 and 0.48 (5% MeOH/CH_2Cl_2); IR (neat): 3410, 1673, 1601; ^{1}H NMR (400 Hz, DMSO-*d*) δ 1.72–1.77 (m, 4H), 3.47 (t, *J* = 6.40 Hz, 2H), 3.52 (t, *J* = 6.1 Hz, 2H), 3.94 (m, 2H), 4.14 (m, 2H), 7.19 (m, 5H), 7.39 (m, 1H), 7.63 (ddd, *J* = 8.4, 7.3, 1.5 Hz, 1H), 7.91 (dd, *J* =8.0, 1.5 Hz, 1H); ^{13}C NMR (100 MHz, DMSO-*d*) δ 30.8, 31.8, 38.8, 40.9, 59.2, 59.8, 114.7, 115.8, 116.0, 116.7, 123.4, 124.2, 124.4, 126.8, 127.2, 128.3, 135.8, 140.3, 151.1, 154.5, 156.0, 162.9. Diagnostic peaks of **2.24**: ^{1}H NMR (400 Hz, DMSO-d_6) δ 3.52 (t, *J* = 6.08 Hz, 2H), 4.14 (m, 2H), 7.39 (m, 1H); ^{13}C NMR (100 MHz, DMSO-d_6) δ 31.8, 40.9, 59.2, 126.8, 127.3, 154.5, 156.0. HRMS (ESI) *m/z* calcd for $C_{11}H_{13}N_2O_3$ $[M + H]^+$ 221.0926, found 221.0937. Diagnostic peaks of **2.25**: ^{1}H NMR (400 Hz, DMSO-d_6) 3.47 (t, *J* = 6.40 Hz, 2H), 3.94 (m, 2H), 7.63 (ddd, *J* = 8.4, 7.3, 1.5 Hz, 1H), 7.91 (dd, *J* = 8.0, 1.5 Hz, 1H); ^{13}C NMR (100 MHz, DMSO-d_6) δ 30.8, 38.8, 59.8, 114.7, 128.3, 135.8, 140.3, 151.1, 162.9. HRMS (ESI) *m/z* calcd for $C_{11}H_{13}N_2O_3$ $[M + H]^+$ 221.0926, found 221.0928.

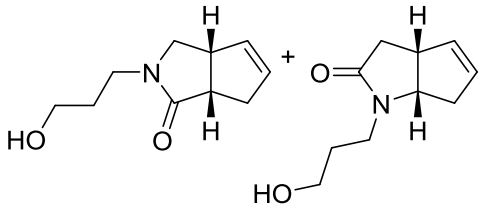

2.27 + 2.28

(3a*R,6a*S**)-2-(3′-Hydroxypropyl)-2,3,3a,4-tetrahydrocyclopenta[*c*]pyrrol-1(6a*H*)-one 2.27 and (3a*R**,6a*S**)-1-(3′-hydroxypropyl)-3,3a,6,6a-tetrahydrocyclopenta[*b*]pyrrol-2(1*H*)-one 2.28.** Following the general procedure A, to a solution of (±)-*cis*-bicyclo[3.2.0]hept-2-en-6-one **2.26** (42.0 μL, 0.398 mmol, 1.0 equiv) and 3-azidopropanol **1.1** (60.7 mg, 0.600 mmol,

1.5 equiv) in HFIP (1.0 mL) was added TfOH (35.0 μL, 0.397 mmol, 1.0 equiv). The reaction mixture was stirred at room temperature for 1 h. Subsequently, hydrolysis was carried out with saturated $NaHCO_3$ solution for 12 h. The crude oil obtained was eluted through a short bed of silica gel using 10% MeOH/CH_2Cl_2. Concentration of solvents afforded a mixture of lactams **2.27** and **2.28** as a brown oil (combined yield of **2.27** and **2.28**: 69.0 mg, 0.381 mmol, 95% yield; ratio of **2.27:2.28** = 74:26). **2.27** and **2.28**: R_f = 0.25 (5% MeOH/CH_2Cl_2); IR (neat) 1652, 3382 cm^{-1}; ^1H NMR (400 MHz, $CDCl_3$) δ 1.56–1.71 (complex, 4H), 2.28 (dd, *J* = 17.5, 2.9, 1H), 2.48 (m, 1H), 2.53 (m, 1H), 2.67–2.56 (complex, 2H), 2.69 (m, 1H), 2.74 (m, 1H), 3.09–3.17 (complex, 2H), 3.20 (m, 1H), 3.29 (m, 1H), 3.40–3.34 (complex, 3H), 3.52–3.42 (complex, 3H), 3.60 (m, 2H), 4.24 (td, *J* = 6.9, 1.8 Hz, 1H), 5.58 (m, 1H), 5.65 (m, 1H), 5.67 (m, 1H), 5.78 (m, 1H); ^{13}C NMR (100 MHz, $CDCl_3$) 29.4, 30.2, 35.8, 36.2, 37.3, 37.4, 38.8, 42.3, 42.5, 44.6, 51.9, 58.1, 58.5, 61.6, 128.7, 131.8, 132.0, 133.1, 175.5, 178.3. Diagnostic peaks of **2.27**: ^1H NMR (400 MHz, $CDCl_3$) δ 5.58 (m, 1H), 5.78 (m, 1H); ^{13}C NMR (100 MHz, $CDCl_3$) δ 29.4, 36.2, 38.8, 42.5, 44.6, 51.9, 58.1, 131.8, 132.0, 178.3. HRMS (ESI) *m/z* calcd for $C_{10}H_{16}NO_2$ $[M + H]^+$ 182.1181, found 182.1184. Diagnostic peaks of **2.28**: ^1H NMR (400 MHz, $CDCl_3$) δ 2.28 (dd, *J* = 17.5, 2.9, 1H), 2.48 (m, 1H), 2.53 (m, 1H), 2.74 (m, 1H), 3.20 (m, 1H), 4.24 (td, *J* = 6.9, 1.8 Hz, 1H), 5.65 (m, 1H), 5.67 (m, 1H); ^{13}C NMR (100 MHz, $CDCl_3$) δ 30.2, 35.8, 37.3, 37.4, 42.3, 58.5, 61.6, 128.7, 133.1, 175.5. HRMS (ESI) *m/z* calcd for $C_{10}H_{16}NO_2$ $[M + H]^+$ 182.1181, found 182.1180.

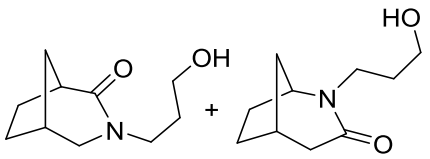

2.30 + 2.31

(1*R,5*S**)-3-(3′-Hydroxypropyl)-3-azabicyclo[3.2.1]octan-2-one, 2.30 and (1*R**,5*S**)-2-(3′-hydroxypropyl)-2-azabicyclo[3.2.1]octan-3-one, 2.31.** Following the general procedure A, to a solution of norcamphor **2.29** (44.9 mg, 0.408 mmol, 1.0 equiv) and 3-azidopropanol **1.1** (61.0, 0.603 mmol, 1.5 equiv) in HFIP (1.0 mL) was added TfOH (35.0 μL, 0.397 mmol, 1.0 equiv). The reaction mixture was stirred at room temperature for 2 h. Subsequently, hydrolysis was carried out with 1 M NaOH solution for 12 h. Purification was carried out on an automated MPLC system with gradient elution from 0–10% MeOH/CH_2Cl_2 to afford a mixture of lactams **2.30** and **2.31** as orange oil (combined yield of **2.30** and **2.31**: 67.1 mg, 0.366 mmol, 90% yield; ratio of **2.30:2.31** = 58:42). **2.30** and **2.31**: R_f = 0.32 (5% MeOH/CH_2Cl_2); IR (neat) 3380, 1616 cm^{-1}. ^1H NMR (400 MHz, $CDCl_3$) δ 1.49–1.81 (complex, 10 H), 1.82–1.97 (complex, 6H), 2.24 (m, 1H), 2.51 (m, 2H), 2.59 (m, 1H), 2.75 (br, s, 1H), 2.92 (m, 1H), 3.07 (m, 1H), 3.20 (m, 1H), 3.31 (dd, *J* = 11.4, 4.04 Hz, 1H), 3.36–3.43 (m, 1H), 3.45 (m, 1H), 3.50–3.64 (m, 2H), 3.81 (m, 1H); ^{13}C NMR (100 MHz, $CDCl_3$) δ 29.1, 29.21 (2C), 29.3, 30.2, 31.4, 32.6, 32.9, 33.5, 33.6, 36.6, 41.6, 42.1, 42.8, 43.5, 55.7, 58.1, 58.7, 170.8, 176.2. Diagnostic peaks of **2.30:** ^1H NMR (400 MHz, $CDCl_3$) δ 2.75 (br, s, 1H), 2.92 (m, 1H), 3.20 (m, 1H), 3.31 (dd, *J* = 11.4, 4.04 Hz, 1H); ^{13}C NMR (100 MHz, $CDCl_3$) δ 41.6, 43.5, 55.7, 176.2. Diagnostic peaks of **2:31**: ^1H NMR (400 MHz, $CDCl_3$) δ 2.24 (m, 1H), 2.59 (m, 1H), 3.07 (m, 1H), 3.81 (m, 1H); ^{13}C NMR (100 MHz, $CDCl_3$) δ 36.6, 42.1, 42.8, 58.7, 170.8. HRMS (ESI) *m/z* calcd for $C_{10}H_{18}NO_2$ $[M + H]^+$ 184.1138, found 184.1341.

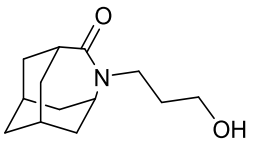

2.33

(1*R,3*R**,8*S**)-4-(3′-Hydroxypropyl)-4-azatricyclo[4.3.1.1^{3,8}]undecan-5-one, 2.33.** Following the general procedure A, to a solution of 2-adamantanone **2.32** (60.0 mg, 0.399 mmol, 1.0 equiv) and 3-azidopropanol **1.1** (60.7 mg, 0.600 mmol, 1.5 equiv) in HFIP (1.0 mL) was added TfOH (35.0 μL, 0.397 mmol, 1.0 equiv). The reaction mixture was stirred at room temperature for 1 h. Subsequently, hydrolysis was carried out with 1 M NaOH solution for 12 h. The crude oil obtained was eluted through a short bed of silica gel using 10% MeOH/CH_2Cl_2. Concentration of solvents afforded **2.33** as a yellow oil (85.6 mg, 0.383 mmol, 96% yield). R_f = 0.21 (5% MeOH/CH_2Cl_2); IR (neat) 3387, 1604 cm^{-1}; ^{1}H NMR (400 MHz, $CDCl_3$) δ 1.64 (m, 2H), 1.70–1.95 (complex, 10H), 2.05 (m, 2H), 2.86 (m, 1H), 3.33 (m, 1H), 3.51 (m, 4H), 4.26 (t, *J* = 7.16 Hz, 1H); ^{13}C NMR (100 MHz, $CDCl_3$) δ 26.4 (2C), 30.2, 31.3 (2C), 34.5, 35.7 (2C), 42.4, 45.4, 53.7, 58.1, 180.6. HRMS (ESI) *m/z* calcd for $C_{13}H_{22}NO_2$ $[M + H]^+$ 224.1651, found 224.1645.

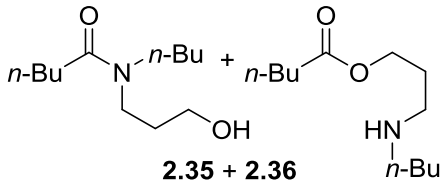

2.35 + 2.36

***N*-(3′-Hydroxypropyl)-*N*-butylpentanamide (mixture of rotamers) 2.35, and 3-Butylaminopropylpentanoate, 2.36.**[48] Following the general procedure A, to a solution of 5-nonanone **2.34** (57.5 mg, 0.404 mmol, 1.0 equiv) and 3-azidopropanol **1.1** (60.7 mg, 0.600 mmol, 1.5 equiv) in HFIP (1.0 mL) was added TfOH (35.0 μL, 0.397 mmol, 1.0 equiv). The reaction mixture was stirred at room temperature for 6 h, and was followed by hydrolysis with saturated $NaHCO_3$ solution for 24 h. Purification was carried out on an automated MPLC system with gradient elution from 0–25% MeOH/CH_2Cl_2 to afford **2.35** (mixture of rotamers) as a colorless oil

(13.1 mg, 0.0610 mmol, 15% yield; ratio of rotamers = 79:21) and **2.36** as a yellow oil (59.9 mg, 0.278 mmol, 69% yield).

2.5.2 Experimental Section for 2.3

Caution: Although we have not experienced any untoward events with the compounds mentioned in this paper, azides and their precursors are known explosive hazards and should be used with appropriate safety precautions. Minimally, careful control of temperature and scale should be exercised. We do not recommend distillation of reaction mixtures that may contain residues of azide sources. We recommend the use of blast shields for heated reactions.

Reactions were performed under inert atmosphere (argon or nitrogen). Reactions were carried out in flame-dried round bottom flasks. Slow addition reactions were carried out a Harvard Apparatus Pump 33, which features a dual infuse/withdraw pump system. All chemicals were purchased from commercial sources and used without further purification. New containers of acid catalysts and HFIP were used. HFIP was purchased from Oakwood Chemical. Anhydrous CH_2Cl_2, MeOH, and DMF were purchased from Sigma-Aldrich and used as received. Thin-layer chromatography (TLC) was performed using commercial glass-backed silica plates (250 μM) with an organic binder. Visualization was accomplished with UV light and an iodine chamber. Reaction was monitored on analytical Waters Acquity UPLC using C18 column, BEH 2.1 × 50 mm, 1.7 μm, at 30 ˚C with mobile phases A (H_2O + 0.1% formic acid) and B (MeCN + 0.1% formic acid). Purification was carried out by an automated flash chromatography/medium-pressure liquid chromatography (MPLC) system using normal phase silica gel flash columns (4 or 12 g) and reverse phase C18 columns (13 g, Gold 15.5 g, or Gold 50.0 g).

The infrared (IR) spectra were acquired as thin films or solids using a universal ATR sampling accessory on a Thermo Scientific Nicolet iS5 FT-IR spectrometer; the absorption frequencies are reported in cm^{-1}. All nuclear magnetic resonance spectra were recorded on a Varian 400 MHz, Varian 500 MHz with a dual carbon/proton cyroprobe, or Bruker 600 MHz with a dual carbon/proton cryoprobe instrument. NMR samples were recorded in deuterated chloroform ($CDCl_3$) or deuterated dimethylsulfoxide (DMSO-d_6). Chemical shifts are reported in parts per million (ppm) and referenced to the center line of solvent ($CDCl_3$: δ 7.26 ppm for ^1H NMR and 77.16 ppm for ^{13}C NMR; DMSO-d_6 δ 2.50 ppm for ^1H NMR and 39.52 ppm for ^{13}C NMR); coupling constants are given in Hertz (Hz). HRMS data were collected using Thermo LTQ Fourier transform ion cyclotron resonance (FT-ICR, 7T) with a heated electrospray ion source (HESI) or electrospray ion source (ESI). Purity data were collected using Waters Acquity H-class UPLC-PDA detector coupled to the Thermo LTQ Fourier transform ion cyclotron resonance mass spectrometer (FT-ICR, 7T) with a heated electrospray ion source (HESI). Samples were run on analytical Acquity UPLC BEH 2.1 × 50 mm, 1.7 μm, C18 column, and analytical Acquity UPLC HSS T3, 2.1 × 50 mm, 3.18 μm, C18 column, at 40 ˚C with mobile phases A (H_2O + 0.1% formic acid) and B (MeCN + 0.1% formic acid). Melting points were determined in open capillary tubes using OptiMelt, an automated melting point apparatus and are uncorrected. Elemental analysis was serviced by Atlantic Microlab, Inc. Data for the known tetrazoles prepared according to the methodology described in the section match with those reported in the literature.

General procedure B for catalyst screening. To a solution of 4-phenylcyclohexanone **2.1** (0.300 mmol, 1.0 equiv), 1,3,5-trimethoxybenzene (1.50 mmol, 5.0 equiv), and catalyst (0.060–0.300 mmol, 20–100 mol%) in HFIP (1.0 mL) in a flame-dried nitrogen-flushed 25 mL round

bottom flask was added a solution of $TMSN_3$ (80 μL, 0.600 mmol, 2.0 equiv) in HFIP (2.0 mL) using a syringe pump (0.40 mL/h, 14.00 mm diameter, and 20 gauge needle) over 6 h at room temperature. Following slow addition, the reaction mixture was stirred for an additional 20–30 min and concentrated under a stream of nitrogen. The residual crude was redissolved in CH_2Cl_2 (ca. 40 mL). The organic layer was washed with a saturated solution of $NaHCO_3$ (3 × 5 mL), brine (5 mL), dried over anhydrous Na_2SO_4, filtered, and concentrated. Conversion to product was determined by ^1H NMR of the crude reaction mixture using benzyl benzoate as an internal standard; alternatively, purification was carried out by an automated MPLC system using a 12 g normal phase silica column with gradient elution from 0–6% MeOH/CH_2Cl_2.

General procedure C for the Optimization of Reaction Conditions Using $AlCl_3$. To a solution of 4-phenylcyclohexanone **2.1** (0.300 mmol, 1.0 equiv), 1,3,5-trimethoxybenzene (0.600–2.10 mmol, 2.0–7.0 equiv), and $AlCl_3$ (0.300–0.600 mmol, 1.0–2.0 equiv) in HFIP (1.0–2.0 mL) in a flame-dried nitrogen-flushed 25 mL round bottom flask was added a solution of $TMSN_3$ (0.375–0.600 mmol, 1.25–2.0 equiv) in HFIP (2.0 mL) using a syringe pump (0.20–1.00 mL/h, 14.00 mm diameter, and 20 gauge needle) over 2–10 h at room temperature. Following slow addition, the reaction mixture was stirred for an additional 20–30 min or 15 h and concentrated under a stream of nitrogen. The residual crude was redissolved in CH_2Cl_2 (ca. 40 mL). The organic layer was washed with a saturated solution of $NaHCO_3$ (3 × 5 mL), brine (5 mL), dried over anhydrous Na_2SO_4, filtered, and concentrated, unless otherwise noted. Conversion to product was determined by ^1H NMR of the crude reaction mixture using benzyl benzoate as an internal standard; alternatively, purification was carried out by an automated MPLC system using a 12 g normal phase silica column with gradient elution from 0–5% MeOH/CH_2Cl_2.

General procedure D for the optimization of reaction conditions using $AlBr_3$. To a solution of 4-phenylcyclohexanone **2.1** (0.300 mmol, 1.0 equiv), 1,3,5-trimethoxybenzene (0.600–1.50 mmol, 2.0–5.0 equiv), and $AlBr_3$ (0.150–0.300 mmol, 0.5–1.0 equiv) in HFIP (1.0 mL) in a flame-dried nitrogen-flushed 25 mL round bottom flask was added a solution of $TMSN_3$ (0.400–0.600 mmol, 1.5–2.0 equiv) in HFIP (2.0 mL) using a syringe pump (0.20–0.40 mL/h, 14.00 mm diameter, and 20 gauge needle) over 2–6 h at room temperature. Following slow addition, the reaction mixture was stirred for an additional 20–30 min or 15 h and concentrated under a stream of nitrogen. The residual crude was redissolved in CH_2Cl_2 (ca. 40 mL), filtered to remove residual solids, and concentrated, unless otherwise noted. Conversion to product was determined by ^1H NMR of the crude reaction mixture using benzyl benzoate as an internal standard; alternatively, purification was carried out by an automated MPLC system using a 12 g normal phase silica column with MeOH/CH_2Cl_2 gradient elution or using a 15.5 g C18 reverse phase column with H_2O/MeCN gradient elution.

General procedure E for reactions carried out at room temperature using $AlBr_3$. To a solution of 4-phenylcyclohexanone **2.1** (0.300 mmol, 1.0 equiv), 1,3,5-trimethoxybenzene (1.50 mmol, 5.0 equiv), and $AlBr_3$ (0.300–0.480 mmol, 1.0–1.6 equiv) in HFIP (1.0–2.0 mL) in a flame-dried nitrogen-flushed 25 mL round bottom flask was added a solution of $TMSN_3$ (80.0 μL, 0.600 mmol, 2.0 equiv) in HFIP (2.0 mL) using a syringe pump (0.40 mL/h, 14.00 mm diameter, and 20 gauge needle) over 6 h at room temperature. Following slow addition, the reaction mixture was stirred for an additional 20–30 min or 15 h, and concentrated under a stream of nitrogen. The crude residue was redissolved in CH_2Cl_2 (ca. 40 mL), filtered to remove residual solids, and

concentrated. Conversion to product was determined by ^{1}H NMR of the crude reaction mixture using benzyl benzoate as an internal standard; alternatively, purification was carried out by an automated MPLC system using a 12 g normal phase silica column with MeOH/CH_2Cl_2 gradient elution or using a 15.5 g C18 reverse phase column with H_2O/MeCN gradient elution.

General procedure F for reactions carried out under heating at 35 °C using $AlBr_3$. To a solution of 4-phenylcyclohexanone **2.1** (0.300 mmol, 1.0 equiv), 1,3,5-trimethoxybenzene (1.50 mmol, 5.0 equiv) and $AlBr_3$ (0.300–0.337 mmol, 1.0–1.1 equiv) in HFIP (1.0 mL) in a flame-dried nitrogen-flushed 25 mL round bottom was added a solution of $TMSN_3$ (80.0 μL, 0.600 mmol, 2.0 equiv) in HFIP (2.0 mL) using a syringe pump (0.40 mL/h, 14.00 mm diameter, and 20 gauge needle) over 6 h at 35 °C. Following slow addition, the reaction mixture was stirred at 35 °C for an additional 15 h, allowed to room temperature, and concentrated under nitrogen. The crude residue was redissolved in CH_2Cl_2 (~40 mL), filtered to remove residual solids, and concentrated. Conversion to product was determined by ^{1}H NMR of the crude reaction mixture using benzyl benzoate as an internal standard; alternatively, purification was carried out by an automated MPLC system using a 12 g normal phase silica column with MeOH/CH_2Cl_2 gradient elution.

General procedure G for enamide formation. Following slow addition via general procedure E, the crude residue was redissolved in CH_2Cl_2 (~40 mL), filtered to remove residual solids, and concentrated under high vacuum. To the crude residue in anhydrous CH_2Cl_2 (3.0–4.0 mL) was added an electrophile (0.641–3.71 mmol, 2.2–13.0 equiv), DMAP (0.196–0.451 mmol, 0.65–1.5 equiv), and/or triethylamine (0.360–0.897 mmol, 1.2–3.0 equiv). The reaction mixture was stirred at room temperature for 24 h under argon atmosphere. Purification was carried out by

an automated MPLC system using a 12 g normal phase silica column with MeOH/CH_2Cl_2 gradient elution or a C18 reverse phase column with H_2O/MeCN gradient elution.

General procedure H for amine formation. Following slow addition via general procedure E, the crude residue was redissolved in CH_2Cl_2 (~40 mL), filtered to remove residual solid, and concentrated under high vacuum. To the crude residue in anhydrous MeOH (3.0 mL) at 0 °C was added sodium borohydride (15.0–23.0 mg, 0.397–0.608 mmol, 1.9–2.0 equiv). The reaction mixture was stirred at room temperature for 4 h under argon atmosphere. MeOH was removed under a stream of nitrogen. The residual crude was diluted with CH_2Cl_2 (35 mL), washed with H_2O (5 mL), saturated solution of $NaHCO_3$ (2 × 5 mL), brine (5 mL), dried over anhydrous Na_2SO_4, filtered, and concentrated. Purification was carried out by an automated MPLC system using a 12 g normal phase silica column with MeOH (0.5% NH_4OH)/CH_2Cl_2 gradient elution; alternatively, the crude residue was further functionalized using acetic anhydride or di-*tert*-butyl dicarbonate.

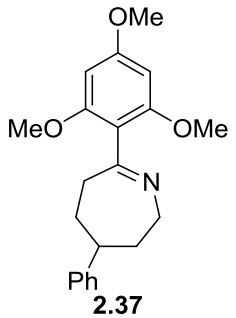

2.37

4-Phenyl-7-(2,4,6-trimethoxyphenyl)-3,4,5,6-tetrahydro-2*H*-azepine, 2.37. Following the general procedure B, $TMSN_3$ (80.0 μL, 0.603 mmol, 2.0 equiv) in HFIP (2.0 mL) was added using a syringe pump over 6 h to a solution of 4-phenylcyclohexanone **2.1** (52.2 mg, 0.300 mmol, 1.0 equiv), $AlCl_3$ (80.2 mg, 0.601 mmol, 2.0 equiv), and 1,3,5-trimethoxybenzene (252 mg, 1.50

mmol, 5.0 equiv) in HFIP (1.0 mL). Purification by an automated MPLC system on a 12 g normal phase silica column with gradient elution from 0–5.5% MeOH/CH_2Cl_2 afforded the **2.37** as a yellow oil (80.6 mg, 0.237 mmol, 79% yield). R_f = 0.25 (4% MeOH/CH_2Cl_2); IR (neat) 2931, 2840, 1650, 1605, 1586 cm^{-1}. ^1H NMR (400 MHz, $CDCl_3$) ^1H NMR (400 MHz, $CDCl_3$) δ 7.33–7.29 (m, 2H), 7.22–7.18 (m, 3H), 6.13 (s, 2H), 4.23 (ddd, *J* = 12.8, 6.5, 1.5 Hz, 1H), 3.81 (d, *J* = 5.3 Hz, 9H), 3.64 (m, 1H), 2.94–2.86 (m, 1H), 2.84–2.77 (m, 1H), 2.65–2.60 (m, 1H), 2.03–1.97 (m, 1H), 1.84–1.72 (m, 3H); ^{13}C NMR (101 MHz, $CDCl_3$) δ 172.7, 160.9, 158.0, 147.8, 128.5, 126.8, 126.2, 115.6, 90.7, 55.9, 55.4, 51.7, 49.7, 35.3, 33.7, 30.7. HRMS (FT-ICR, ESI) *m/z*: [M + H]$^+$ calcd for $C_{21}H_{26}NO_3$ 340.1907, found 340.1904.

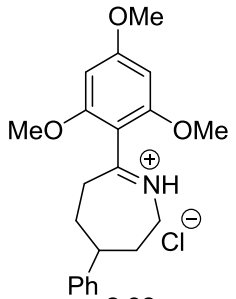

2.38

4-Phenyl-7-(2,4,6-trimethoxyphenyl)-3,4,5,6-tetrahydro-2*H*-azepinium Chloride, 2.38. Following the general procedure C, $TMSN_3$ (80.0 μL, 0.603 mmol, 2.0 equiv) in HFIP (2.0 mL) was added using a syringe pump over 6 h to a solution of 4-phenylcyclohexanone **2.1** (52.3 mg, 0.300 mmol, 1.0 equiv), $AlCl_3$ (80.2 mg, 0.601 mmol, 2.0 equiv), and 1,3,5-trimethoxybenzene (252 mg, 1.50 mmol, 5.0 equiv) in HFIP (1.0 mL). Following slow addition, the reaction mixture was stirred for an additional 15 h and concentrated under a stream of nitrogen. Purification by an automated MPLC system on a 12 g normal phase silica column with gradient elution from 0–5.5% MeOH/CH_2Cl_2 afforded the **2.38** as a yellow oil (87.3 mg, 0.232 mmol, 77% yield). R_f = 0.25 (4% MeOH/CH_2Cl_2); IR (neat) 3386, 2940, 2842, 1650, 1602 cm^{-1}. ^1H NMR (400

MHz, $CDCl_3$) δ 7.31 (m, 2H), 7.23 (m, 1H), 7.16 (m, 2H), 6.12 (s, 2H), 4.44 (m, 1H), 3.84 (d, *J* = 9.8 Hz, 9H), 3.72–3.65 (m, 1H), 3.07 (m, 1H), 2.97–2.82 (m, 2H), 2.12–2.06 (m, 1H), 2.02–1.97 (m, 1H), 1.91–1.76 (m, 2H); ^{13}C NMR (151 MHz, $CDCl_3$) δ 180.8, 165.2, 159.9, 145.7, 128.8, 126.8, 126.6, 106.3, 91.0, 56.2, 55.7, 48.8, 47.3, 35.5, 32.4, 29.7. HRMS (FT-ICR, ESI) *m/z*: [M – Cl]$^+$ calcd for $C_{21}H_{26}NO_3$ 340.1907, found 340.1903.

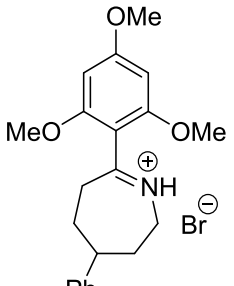

2.39

4-Phenyl-7-(2,4,6-trimethoxyphenyl)-3,4,5,6-tetrahydro-2*H*-azepinium Bromide, 2.39. Following the general procedure F, $TMSN_3$ in HFIP was added to a solution of 4-phenylcyclohexanone **2.1** (52.3 mg, 0.300 mmol, 1.0 equiv), $AlBr_3$ (80.0 mg, 0.300 mmol, 1.0 equiv), and 1,3,5-trimethoxybenzene (252 mg, 1.50 mmol, 5.0 equiv) in HFIP. Following slow addition, the reaction mixture was stirred for an additional 15 h and concentrated under a stream of nitrogen. Purification by an automated MPLC system on a 12 g normal phase silica column with gradient elution from 0–5% MeOH/CH_2Cl_2 afforded the **2.39** as a colorless amorphous solid (116 mg, 0.276 mmol, 92% yield). R_f = 0.25 (5% MeOH/CH_2Cl_2); mp decomposed; IR (neat) 3405, 2942, 2841, 1649, 1599, 1576 cm^{-1}. ^1H NMR (400 MHz, $CDCl_3$) ^1H NMR (400 MHz, $CDCl_3$) δ 13.5 (br s, 1H), 7.32 (m, 2H), 7.23 (m, 1H), 7.17 (m, 2H), 6.13 (s, 2H), 4.60 (dt, *J* = 13.2, 6.3 Hz, 1H), 3.88 (d, *J* = 14.7 Hz, 9H), 3.72 (m, 1H), 3.29 (dd, *J* = 14.5, 7.4 Hz, 1H), 3.00–2.86 (m, 2H), 2.18–2.06 (m, 2H), 1.97–1.79 (m, 2H); ^{13}C NMR (101 MHz, $CDCl_3$) δ 182.4, 166.4, 160.5, 145.4, 128.9, 127.1, 126.7, 104.5, 91.2, 56.6, 55.9, 48.5, 46.7, 35.7, 32.3, 29.7. **Note**: X-ray crystal

structure of this analog is provided in the CCDC (CCDC 1832152). HRMS (FT-ICR, ESI) *m/z*: $[M - Br]^+$ calcd for $C_{21}H_{26}NO_3$ 340.1907, found 340.1897.

Table 2.9. Selected crystallographic and refinement parameters for **2.39**.

compound	**2.39**
CCDC	1832152
empirical formula	$C_{22}H_{27}BrCl_3NO_3$
formula weight	539.70
temperature	200(2) K
wavelength	1.54178 Å
crystal system	monoclinic
space group	Pc
unit cell dimensions	a = 11.9047(5) Å, α = 90°
	b = 14.5768(5) Å, β = 101.780(2)°
	c = 29.1414(10) Å, γ = 90°
Z	8
volume	4950.5(3) $Å^3$
density	1.448 Mg/m^3
absorption coefficient	5.430 μ mm^{-1}
F(000)	2208
crystal size	0.105 × 0.045 × 0.025 mm^3
Theta range for data collection	1.548 to 69.844°
index ranges	-14<=h<=11, -17<=k<=16, -32<=l<=34
reflections collected	64216
independent reflections	12880 [R(int) = 0.0633]
completeness to theta = 66.000°	98.6%
absorption correction	multi-scan
max. and min. transmission	1.000 and 0.632
refinement method	full-matrix least-squares on F^2
data/restraints/parameters	12880/14/1084
Goodness-of-fit F^2	1.068
final R indices [I>2sigma(I)]	R1 = 0.0591, wR2 = 0.1525
R indices (all data)	R1 = 0.0670, wR2 = 0.1588
largest diff. peak and hole	1.080 and -1.131 $e.Å^{-3}$

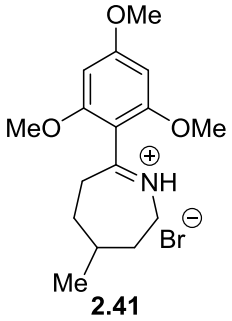

2.41

4-Methyl-7-(2,4,6-trimethoxyphenyl)-3,4,5,6-tetrahydro-2*H*-azepinium Bromide, 2.41. Following the general procedure F, $TMSN_3$ in HFIP was added to a solution of-methylcyclohexanone **2.40** (37.0 μL, 0.301 mmol, 1.0 equiv), $AlBr_3$ (82.1 mg, 0.308 mmol, 1.0 equiv), 1,3,5-trimethoxybenzene (252 mg, 1.50 mmol, 5.0 equiv) in HFIP. Following slow addition, the reaction mixture was stirred for an additional 15 h and concentrated under a stream of nitrogen. Purification by an automated MPLC system on a 12 g normal phase silica column with gradient elution from 0–5% MeOH/CH_2Cl_2 afforded **2.41** as an off-white amorphous solid (86.7 mg, 0.242 mmol, 80% yield). R_f = 0.17 (4% MeOH/CH_2Cl_2); mp 182–183 ˚C; IR (neat) 2952, 2870, 1637, 1601, 1576 cm^{-1}. ^1H NMR (400 MHz, $CDCl_3$) δ 13.3 (br s, 1H), 6.11 (s, 2H), 4.42 (m, 1H), 3.88 (s, 6H), 3.85 (s, 3H), 3.62 (m, 1H), 3.14 (m, 1H), 2.77 (m, 1H), 1.89 (m, 3H), 1.38 (m, 2H), 1.02 (d, J = 6.3 Hz, 3H); ^{13}C NMR (101 MHz, $CDCl_3$) δ 182.8, 166.2, 160.3 (2C), 104.6, 91.1 (2C), 56.5 (2C), 55.8, 46.4, 36.8, 35.01, 33.1, 29.7, 23.0. HRMS (FT-ICR, ESI) *m/z*: [M – Br]$^+$ calcd for $C_{16}H_{24}NO_3$ 278.1751, found 278.1746.

Alternatively following the general procedure F, $TMSN_3$ in HFIP was added to a solution of **2.40** (37.0 μL, 0.301 mmol, 1.0 equiv), $AlBr_3$ (87.4 mg, 0.328 mmol, 1.1 equiv), 1,3,5-trimethoxybenzene (252 mg, 1.50 mmol, 5.0 equiv) in HFIP. Purification by an automated MPLC system on a 12 g normal phase silica column with gradient elution from 0–5% MeOH/CH_2Cl_2

afforded **2.41** as an off-white crystalline solid (94.4 mg, 0.263 mmol, 87% yield). Characterization data was consistent with the above entry.

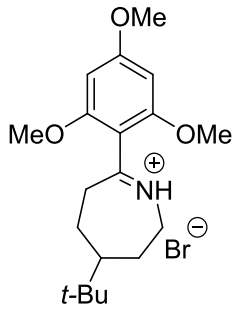

2.43

4-(*tert*-Butyl)-7-(2,4,6-trimethoxyphenyl)-3,4,5,6-tetrahydro-2*H*-azepinium Bromide, 2.43. Following the general procedure F, $TMSN_3$ in HFIP was added to a solution of 4-*tert*-butylcyclohexanone **2.42** (46.4 mg, 0.301 mmol, 1.0 equiv), $AlBr_3$ (82.7 mg, 0.310 mmol, 1.0 equiv), and 1,3,5-trimethoxybenzene (252 mg, 1.50 mmol, 5.0 equiv) in HFIP. Following slow addition, the reaction mixture was stirred for an additional 15 h and concentrated under a stream of nitrogen. Purification by an automated MPLC system on a 12 g normal phase silica column with gradient elution from 0–5% MeOH/CH_2Cl_2 afforded **2.43** as a colorless amorphous solid (109 mg, 0.272 mmol, 91% yield). R_f = 0.40 (5% MeOH/CH_2Cl_2); mp 168–172 ˚C; IR (neat) 2949, 2868, 1655, 1600, 1577 cm^{-1}. ^1H NMR (400 MHz, $CDCl_3$) δ 13.37 (br s, 1H), 6.12 (s, 2H), 4.51 (m, 1H), 3.89 (s, 6H), 3.86 (s, 3H), 3.55 (m, 1H), 3.21 (dd, *J* = 14.4, 7.6 Hz, 1H), 2.69 (m, 1H), 2.13–2.03 (m, 2H), 1.48–1.32 (m, 3H), 0.90 (s, 9H); ^{13}C NMR (101 MHz, $CDCl_3$) δ 182.7, 166.2, 160.4 (2C), 104.5, 91.1 (2C), 56.6 (2C), 55.9, 52.1, 46.9, 35.5, 33.6, 27.5 (3C), 26.6, 23.0. HRMS (FT-ICR, ESI) *m/z*: $[M - Br]^+$ calcd for $C_{19}H_{30}NO_3$ 320.2220, found 320.2214.

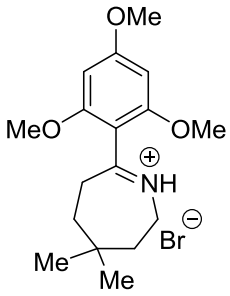

2.45

4,4-Dimethyl-7-(2,4,6-trimethoxyphenyl)-3,4,5,6-tetrahydro-2*H*-azepinium Bromide, 2.45. Following the general procedure E, $TMSN_3$ in HFIP was added to a solution of 4,4-dimethylcyclohexanone **2.44** (38.3 mg, 0.303 mmol, 1.0 equiv), $AlBr_3$ (80.3 mg, 0.301 mmol, 1.0 equiv), and 1,3,5-trimethoxybenzene (252 mg, 1.50 mmol, 4.9 equiv) in HFIP. Purification by an automated MPLC system on a 12 g normal phase silica column with gradient elution from 0–2% MeOH/CH_2Cl_2 afforded **2.45** as a white amorphous solid (88.8 mg, 0.239 mmol, 79% yield). R_f = 0.29 (5% MeOH/CH_2Cl_2); mp 181–184 ˚C; IR (neat) 2940, 2862, 2836, 1648, 1602, 1579 cm^{-1}. ^1H NMR (400 MHz, $CDCl_3$) δ 13.3 (br s, 1H), 6.12 (s, 2H), 4.00 (m, 2H), 3.90 (s, 6H), 3.86 (s, 3H), 2.92 (m, 2H), 1.60 (m, 4H), 1.07 (s, 6H); ^{13}C NMR (101 MHz, $CDCl_3$) δ 182.7, 166.2, 160.4 (2C), 104.6, 91.2 (2H), 56.8, 56.0 (2C), 43.3, 37.8, 34.4, 33.4, 31.7, 28.9 (2C). HRMS (FT-ICR, ESI) *m/z*: $[M - Br]^+$ calcd for $C_{17}H_{26}NO_3$ 292.1907, found 292.1902; Anal. calcd. for $C_{17}H_{26}BrNO_3$: C 54.84, H 7.04, N 3.76, Br 21.46, found C 54.72, H 7.09, N 3.77, Br 21.32.

Alternatively following the general procedure F, $TMSN_3$ in HFIP was added to a solution of **2.44** (37.4 mg, 0.296 mmol, 1.0 equiv), $AlBr_3$ (82.9 mg, 0.311 mmol, 1.1 equiv), and 1,3,5-trimethoxybenzene (252 mg, 1.50 mmol, 5.1 equiv) in HFIP. Purification by an automated MPLC system on a 12 g normal phase silica column with gradient elution from 0–2% MeOH/CH_2Cl_2 afforded **2.45** as a white amorphous solid (91.4 mg, 0.245 mmol, 83% yield). Characterization data was consistent with the above entry.

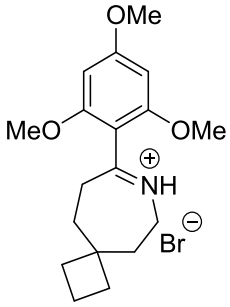

2.47

8-(2,4,6-Trimethoxyphenyl)-7-azaspiro[3.6]dec-7-en-7-ium Bromide, 2.47. Following the general procedure E, $TMSN_3$ in HFIP was added to a solution of spiro[3.5]nonan-7-one **2.46** (42.4 mg, 0.307 mmol, 1.0 equiv), $AlBr_3$ (88.0 mg, 0.330 mmol, 1.1 equiv), 1,3,5-trimethoxybenzene (251 mg, 1.49 mmol, 4.9 equiv) in HFIP. Following slow addition, the reaction mixture was stirred for an additional 15 h and concentrated under a stream of nitrogen. Purification by an automated MPLC system on a 12 g normal phase silica column with gradient elution from 0–5% MeOH/CH_2Cl_2 afforded **2.47** as a pale pink crystalline solid (91.9 mg, 0.239 mmol, 78% yield). R_f = 0.28 (4% MeOH/CH_2Cl_2); mp 183–185 ˚C; IR (neat) 2919, 2839, 1637, 1601, 1574 cm^{-1}. ^1H NMR (400 MHz, $CDCl_3$) δ 6.11 (s, 2H), 3.93 (m, 2H), 3.88 (s, 6H), 3.85 (s, 3H), 2.85 (m, 2H), 2.02–1.80 (complex, 10H); ^{13}C NMR (151 MHz, $CDCl_3$) δ 182.9, 166.1, 160.3 (2C), 104.6, 91.1 (2C), 56.5 (2C), 55.8, 43.2, 42.2, 36.8, 33.6, 32.4, 31.6, 14.3. **Note**: Missing one carbon signal due to signal overlap. HRMS (FT-ICR, ESI) *m/z*: $[M - Br]^+$ calcd for $C_{18}H_{26}NO_3$ 304.1907, found 304.1902.

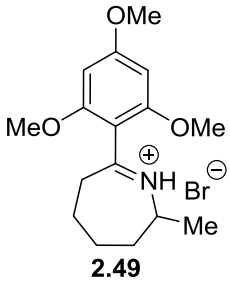

2.49

2-Methyl-7-(2,4,6-trimethoxyphenyl)-3,4,5,6-tetrahydro-2*H*-azepinium Bromide, 2.49. Following the general procedure E, $TMSN_3$ in HFIP was added to a solution of 2-methylcyclohexanone **2.48** (36.0 μL, 0.297 mmol, 1.0 equiv), $AlBr_3$ (83.1 mg, 0.312 mmol, 1.1 equiv), and 1,3,5-trimethoxybenzene (251 mg, 1.49 mmol, 5.0 equiv) in HFIP. Purification by an automated MPLC system on a 12 g normal phase silica column with gradient elution from 0–6% MeOH/CH_2Cl_2 afforded **2.49** as a pale yellow amorphous solid (78.9 mg, 0.220 mmol, 74% yield). Characterization data was consistent with the entry below.

Alternatively following the general procedure F, $TMSN_3$ in HFIP was added to a solution of **2.48** (36.0 μL, 0.297 mmol, 1.0 equiv), $AlBr_3$ (83.4 mg, 0.331 mmol, 1.1 equiv), and 1,3,5-trimethoxybenzene (251 mg, 1.49 mmol, 5.0 equiv) in HFIP. Purification by an automated MPLC system on a 12 g normal phase silica column with gradient elution from 0–6% MeOH/CH_2Cl_2 afforded **2.49** as a pale yellow amorphous solid (88.5 mg, 0.247 mmol, 83% yield, UPLC-HRMS purity: ≥99.5%). R_f = 0.19 (3% MeOH/CH_2Cl_2); mp 156–160 ˚C (decomposed); IR (neat) 2933, 2858, 1601, 1578 cm^{-1}. ^1H NMR (400 MHz, $CDCl_3$) δ 13.1 (br s, 1H), 6.10 (s, 2H), 4.32 (m, 1H), 3.87 (s, 6H), 3.84 (s, 3H), 3.04 (m, 1H), 2.90 (m, 1H), 2.03 (m, 1H), 1.88–1.76 (complex, 5H), 1.73 (d, J = 7.0 Hz, 3H); ^{13}C NMR (151 MHz, $CDCl_3$) δ 182.9, 166.0, 160.1 (2C), 104.8, 91.1 (2C), 56.7, 56.4 (2C), 55.7, 36.3, 32.7, 27.9, 21.8, 20.1. HRMS (FT-ICR, HESI) *m/z*: $[M - Br]^+$ calcd for $C_{16}H_{24}NO_3$ 278.1751, found 278.1746.

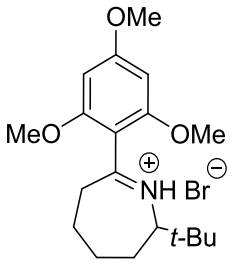

2.51

2-(*tert*-Butyl)-7-(2,4,6-trimethoxyphenyl)-3,4,5,6-tetrahydro-2*H*-azepinium Bromide, 2.51. Following the general procedure F, $TMSN_3$ in HFIP was added to a solution of 2-(*tert*-butyl)cyclohexanone **2.50** (45.9 mg, 0.298 mmol, 1.0 equiv), $AlBr_3$ (117 mg, 0.438 mmol, 1.5 equiv), and 1,3,5-trimethoxybenzene (252 mg, 1.50 mmol, 5.0 equiv) in HFIP. Purification by an automated MPLC system on a 12 g normal phase silica column with gradient elution from 0–9% MeOH/CH_2Cl_2 afforded **2.51** as a yellow oil (12.8 mg, 0.032 mmol, 11% yield). R_f = 0.15 (4% MeOH/CH_2Cl_2); IR (neat) 2938, 2861, 1601, 1579 cm^{-1}. ^1H NMR (400 MHz, $CDCl_3$) δ 6.11 (s, 2H), 3.84 (s, 9H), 3.66 (m, 1H), 2.98–2.90 (m, 2H), 2.07–1.88 (m, 3H), 1.82–1.67 (m, 2H), 1.47 (m, 1H), 1.18 (s, 9H); ^{13}C NMR (151 MHz, $CDCl_3$) δ 165.1, 160.1 (2C), 91.3 (2C), 70.9, 56.3 (2C), 55.8, 36.0, 34.6, 29.8, 28.9, 26.8 (2C), 26.7, 22.3. **Note**: Missing two imine peaks in ^{13}C NMR spectra. HRMS (FT-ICR, ESI) *m/z*: $[M - Br]^+$ calcd for $C_{19}H_{30}NO_3$ 320.2220, found 320.2216.

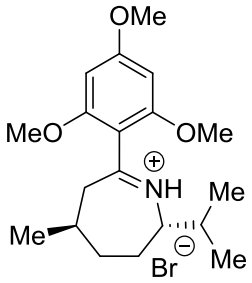

2.53

(2*S*,5*R*)-2-Isopropyl-5-methyl-7-(2,4,6-trimethoxyphenyl)-3,4,5,6-tetrahydro-2*H*-azepin-ium Bromide, 2.53. Following the general procedure E, $TMSN_3$ in HFIP was added to a solution of L-methanone **2.52** (52.0 μL, 0.301 mmol, 1.0 equiv), $AlBr_3$ (86.0 mg, 0.322 mmol, 1.1 equiv), and 1,3,5-trimethoxybenzene (252 mg, 1.50 mmol, 5.0 equiv) in HFIP. Purification by an automated MPLC system on a 12 g normal phase silica column with gradient elution from 0–3% MeOH/CH_2Cl_2 afforded **2.53** as an off-white amorphous solid (36.0 mg, 0.089 mmol, 30% yield)

and known tetrazole ((5*S*,8*R*)-5-isopropyl-8-methyl-6,7,8,9-tetrahydro-5*H*tetrazolo[1,5-*a*]azepine,[7] 1.40 mg, 0.007 mmol, 2% yield). R_f = 0.14 (4% MeOH/CH_2Cl_2); mp 146–150 ˚C; IR (neat) 2958, 2915, 2870, 1597, 1569 cm^{-1}; $[\alpha]_D^{22}$ = + 28.0 (c = 0.50, $CHCl_3$). ^1H NMR (400 MHz, $CDCl_3$) δ 12.7 (br s, 1H), 6.09 (s, 2H), 3.85 (s, 6H), 3.82 (s, 3H), 3.58 (m, 1H), 2.88 (d, *J* = 14.1 Hz, 1H), 2.75–2.64 (m, 2H), 2.04–1.91 (m, 3H), 1.64–1.41 (m, 2H), 1.15 (d, *J* = 6.6 Hz, 3H), 1.05 (dd, *J* = 6.7, 3.0 Hz, 6H); ^{13}C NMR (101 MHz, $CDCl_3$) δ 181.2, 166.2, 160.5 (2C), 104.7, 91.1 (2C), 67.4, 56.2, 55.8 (2C), 43.2, 37.8, 30.1, 28.3, 27.7, 23.6, 20.5, 19.4. HRMS (FT-ICR, ESI) *m/z*: $[M - Br]^+$ calcd for $C_{19}H_{30}NO_3$ 320.2220, found 320.2218.

Alternatively following the general procedure F, $TMSN_3$ in HFIP was added to a solution of **2.52** (52.0 µL, 0.301 mmol, 1.0 equiv), $AlBr_3$ (84.0 mg, 0.315 mmol, 1.1 equiv), and 1,3,5-trimethoxybenzene (252 mg, 1.50 mmol, 5.0 equiv) in HFIP. Purification by an automated MPLC system on a 12 g normal phase silica column with gradient elution from 0–5% MeOH/CH_2Cl_2 afforded **2.53** as an off-white amorphous solid (64.5 mg, 0.161 mmol, 54% yield) and known tetrazole[7] ((5*S*,8*R*)-5-isopropyl-8-methyl-6,7,8,9-tetrahydro-5*H*tetrazolo[1,5-*a*]azepine, 6.90 mg, 0.036 mmol, 12% yield). Characterization data was consistent with the above entry.

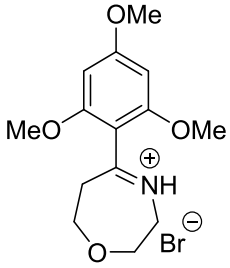

2.54

5-(2,4,6-Trimethoxyphenyl)-2,3,6,7-tetrahydro-1,4-oxazepin-4-ium Bromide, 2.54. Alternatively following the general procedure F, $TMSN_3$ in HFIP was added to a solution of tetrahydro-4H-pyran-4-one **2.10** (28.0 µL, 0.303 mmol, 1.0 equiv), $AlBr_3$ (124 mg, 0.464 mmol,

1.5 equiv), and 1,3,5-trimethoxybenzene (255 mg, 1.52 mmol, 5.0 equiv) in HFIP (2.0 mL). Following slow addition, the reaction mixture was stirred for an additional 15 h and concentrated under a stream of nitrogen. Purification by an automated MPLC system on a 12 g normal phase silica column with gradient elution from 0–4% MeOH/CH_2Cl_2 afforded **2.54** as a yellow amorphous solid (66.5 mg, 0.192 mmol, 63% yield). R_f = 0.36 (5% MeOH/CH_2Cl_2); mp 165–169 ˚C (decomposed); IR (neat) 2942, 2848, 1601, 1572 cm^{-1}. ^1H NMR (400 MHz, $CDCl_3$) δ 6.13 (s, 2H), 4.28 (m, 2H), 3.92–3.90 (m, 8H), 3.88–3.86 (m, 5H), 3.26 (m, 2H); ^{13}C NMR (101 MHz, $CDCl_3$) δ 182.5, 166.8, 160.5 (2C), 104.3, 91.2 (2C), 67.9, 64.8, 56.7 (2C), 55.9, 50.8, 40.9. HRMS (FT-ICR, ESI) *m/z*: $[M - Br]^+$ calcd for $C_{14}H_{20}NO_4$ 266.1387, found 266.1383.

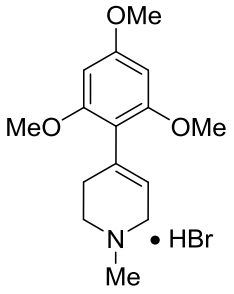

2.56

1-Methyl-4-(2,4,6-trimethoxyphenyl)-1,2,3,6-tetrahydropyridine Hydrobromide, 2.56. A solution of 1-methylpiperidin-4-one **2.55** (37.0 μL, 0.300 mmol, 1.0 equiv), 1,3,5-trimethoxybenzene (254 mg, 1.51 mmol, 5.0 equiv), and $AlBr_3$ (85.1 mg, 0.319 mmol, 1.1 equiv) in HFIP (1.5 mL) was stirred at room temperature for 6 h. HFIP was removed under a stream of nitrogen. The crude residue was redissolved in CH_2Cl_2 (ca. 40 mL), filtered to remove residual solids, and purified. Purification by an automated MPLC system on a 12 g normal phase silica column with gradient elution from 0–6% MeOH/CH_2Cl_2 afforded **2.56** as an off-white amorphous solid (90.1 mg, 0.262 mmol, 87% yield). R_f = 0.31 (4% MeOH/CH_2Cl_2); mp 221–223 ˚C; IR (neat) 2939, 2673, 1607, 1582 cm^{-1}. ^1H NMR (400 MHz, $CDCl_3$) δ 6.12 (s, 2H), 5.48 (m, 1H), 3.82–3.74

(complex, 10H, contains s, 3.82, 3H; s, 3.76, 6H), 3.36 (m, 2H), 2.92 (s, 3H), 2.63 (m, 2H); ^{13}C NMR (151 MHz, $CDCl_3$) δ 161.2, 158.2 (2C), 131.0, 117.5, 110.4, 90.7 (2C), 56.0 (2C), 55.5, 51.4, 49.9, 40.5, 24.1. **Note**: Missing one proton signal. HRMS (FT-ICR, ESI) *m/z*: $[M - Br]^+$ calcd for $C_{15}H_{22}NO_3$ 264.1594, found 264.1575. Anal. calcd. for $C_{15}H_{22}BrNO_3$: C 52.34, H 6.44, N 4.07, Br 23.21, found C 52.45, H 6.47, N 4.01, Br 23.07.

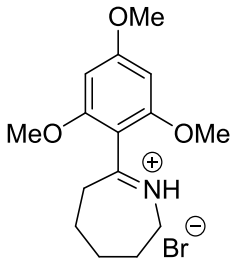

2.57

7-(2,4,6-Trimethoxyphenyl)-3,4,5,6-tetrahydro-2*H*-azepinium Bromide, 2.57. Following the general procedure E, $TMSN_3$ in HFIP was added to a solution of cyclohexanone **2.6** (31.0 μL, 0.299 mmol, 1.0 equiv), $AlBr_3$ (82.5 mg, 0.309 mmol, 1.0 equiv), and 1,3,5-trimethoxybenzene (252 mg, 1.50 mmol, 5.0 equiv) in HFIP. Purification by an automated MPLC system on a 15.5 g C18 reverse phase column with gradient elution from 0–100% MeCN/H_2O afforded **2.57** as a colorless amorphous solid (93.0 mg, 0.270 mmol, 90% yield). R_f = 0.25 (5% MeOH/CH_2Cl_2); mp 185–188 ˚C (decomposed); IR (neat) 2944, 2866, 1642, 1603, 1575 cm^{-1}. ^{1}H NMR (400 MHz, $CDCl_3$) δ 13.4 (br s, 1H), 6.11 (s, 2H), 4.05 (m, 2H), 3.89 (s, 6H), 3.85 (s, 3H), 2.98 (m, 2H), 1.94 (m, 2H), 1.82 (m, 4H); ^{13}C NMR (101 MHz, $CDCl_3$) δ 183.5, 166.1, 160.2 (2C), 104.8, 91.1 (2C), 56.5 (2C), 55.8, 47.9, 36.6, 30.4, 25.5, 22.1. HRMS (FT-ICR, ESI) *m/z*: $[M - Br]^+$ calcd for $C_{15}H_{22}NO_3$ 264.1594, found 264.1590.

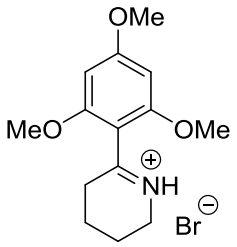

2.59

6-(2,4,6-Trimethoxyphenyl)-2,3,4,5-tetrahydropyridinium Bromide, 2.59. Following the general procedure E, $TMSN_3$ in HFIP was added to a solution of cyclopentanone **2.58** (27.0 µL, 0.305 mmol, 1.0 equiv), $AlBr_3$ (83.1 mg, 0.312 mmol, 1.0 equiv), 1,3,5-trimethoxybenzene (250 mg, 1.49 mmol, 4.9 equiv) in HFIP. Purification by an automated MPLC system on a 12 g normal phase silica column with gradient elution from 0–4% MeOH/CH_2Cl_2 afforded **2.59** as an orange oil (13.6 mg, 0.041 mmol, 14% yield). R_f = 0.22 (5% MeOH/CH_2Cl_2); IR (neat) 2936, 1603, 1581 cm^{-1}. ^1H NMR (400 MHz, $CDCl_3$) δ 6.10 (s, 2H), 3.91 (m, 2H), 3.85 (s, 6H), 3.83 (s, 3H), 2.93 (m, 2H), 1.91 (m, 4H); ^{13}C NMR (151 MHz, $CDCl_3$) δ 178.3, 165.5, 159.7 (2C), 103.6, 91.1 (2C), 56.5 (2C), 55.7, 45.0, 31.5, 19.9, 17.8. HRMS (FT-ICR, ESI) *m/z*: $[M - Br]^+$ calcd for $C_{14}H_{20}NO_3$ 250.1438, found 250.1433.

Alternatively following the general procedure E, $TMSN_3$ in HFIP was added to a solution of **2.58** (27.0 µL, 0.305 mmol, 1.0 equiv), $AlBr_3$ (80.5 mg, 0.302 mmol, 1.0 equiv), 1,3,5-trimethoxybenzene (252 mg, 1.50 mmol, 4.9 equiv) in HFIP. Following slow addition, the reaction mixture was stirred for an additional 15 h and concentrated under a stream of nitrogen. Conversion of 20% (19.6 mg, 0.059 mmol) to the **2.59** was determined by ^1H NMR of the crude reaction mixture using benzyl benzoate as an internal standard.

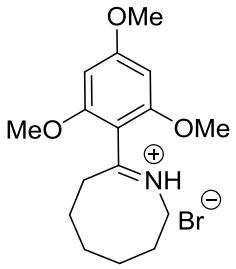

2.60

(*E*)-8-(2,4,6-Trimethoxyphenyl)-2,3,4,5,6,7-hexahydroazocinium Bromide, 2.60. Following the general procedure F, $TMSN_3$ in HFIP was added to a solution of cycloheptanone **2.14** (35.0 μL, 0.297 mmol, 1.0 equiv), $AlBr_3$ (83.5 mg, 0.313 mmol, 1.1 equiv), 1,3,5-trimethoxybenzene (252 mg, 1.50 mmol, 5.0 equiv) in HFIP. Following slow addition, the reaction mixture was stirred for an additional 15 h and concentrated under a stream of nitrogen. Purification by an automated MPLC system on a 12 g normal phase silica column with gradient elution from 0–5% MeOH/CH_2Cl_2 afforded **2.60** as a white amorphous solid (53.0 mg, 0.148 mmol, 50% yield) and known tetrazole (5,6,7,8,9,10-hexahydrotetrazolo[1,5-a]azocine,[7] 8.40 mg, 0.055 mmol, 19% yield). R_f = 0.21 (4% MeOH/CH_2Cl_2); mp 169–171 ˚C; IR (neat) 2924, 2630, 1671, 1606, 1584 cm^{-1}. ^1H NMR (400 MHz, $CDCl_3$) δ 6.13 (s, 2H), 3.98 (m, 2H), 3.89 (s, 6H), 3.85 (3H), 3.06 (m, 2H), 2.06 (m, 2H), 1.83 (m, 3H), 1.73–1.61 (m, 3H); ^{13}C NMR (151 MHz, $CDCl_3$) δ 182.4, 165.6, 159.8 (2C), 103.6, 91.3 (2C), 56.4 (2C), 55.8, 46.0, 32.7, 30.4, 29.5, 25.8, 24.2. HRMS (FT-ICR, ESI) *m/z*: $[M - Br]^+$ calcd for $C_{16}H_{24}NO_3$ 278.1751, found 278.1743.

Alternatively following the general procedure F, $TMSN_3$ in HFIP was added to a solution of **2.14** (35.0 μL, 0.297 mmol, 1.0 equiv), $AlBr_3$ (82.0 mg, 0.307 mmol, 1.1 equiv), and 1,3,5-trimethoxybenzene (252 mg, 1.50 mmol, 5.1 equiv) in HFIP. Purification by an automated MPLC system on a 12 g normal phase silica column with gradient elution from 0–5% MeOH/CH_2Cl_2 afforded **2.60** as a white amorphous solid (69.8 mg, 0.195 mmol, 66% yield) and known tetrazole

((5,6,7,8,9,10-hexahydrotetrazolo[1,5-a]azocine,[7] 8.30 mg, 0.055 mmol, 18% yield). Characterization data was consistent with the above entry.

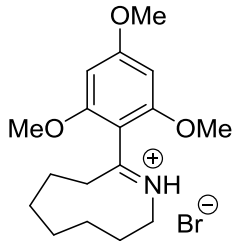

2.61

(*E*)-9-(2,4,6-Trimethoxyphenyl)-3,4,5,6,7,8-hexahydro-2*H*-azoninium Bromide, 2.61. Following the general procedure E, $TMSN_3$ in HFIP was added to a solution of cyclooctanone **2.16** (39.0 mg, 0.309 mmol, 1.0 equiv), $AlBr_3$ (93.0 mg, 0.349 mmol, 1.1 equiv), 1,3,5-trimethoxybenzene (251 mg, 1.49 mmol, 4.8 equiv) in HFIP. Following slow addition, the reaction mixture was stirred for an additional 15 h and concentrated under a stream of nitrogen. Purification by an automated MPLC system on a 12 g normal phase silica column with gradient elution from 0–6% MeOH/CH_2Cl_2 afforded **2.61** as yellow amorphous solid (34.6 mg, 0.094 mmol, 30% yield) and known tetrazole (6,7,8,9,10,11-hexahydro-5*H*-tetrazolo[1,5-*a*]azonine,[7] 5.30 mg, 0.032 mmol, 10% yield). R_f = 0.22 (4% MeOH/CH_2Cl_2); mp 151–154 ˚C; IR (neat) 2925, 2892, 2844, 1643, 1599, 1576 cm^{-1}. ^1H NMR (400 MHz, $CDCl_3$) δ 6.13 (s, 2H), 4.02 (m, 2H), 3.86 (s, 6H), 3.84 (s, 3H), 3.07 (m, 2H), 2.03 (m, 2H), 1.78–1.54 (m, 8H); ^{13}C NMR (151 MHz, $CDCl_3$) δ 181.3, 165.2, 159.6 (2C), 104.1, 91.3 (2C), 56.4 (2C), 55.7, 47.8, 33.1, 26.4, 26.0, 25.6, 23.7, 21.4. HRMS (FT-ICR, ESI) *m/z*: $[M - Br]^+$ calcd for $C_{17}H_{26}NO_3$ 292.1907, found 292.1902.

Alternatively following the general procedure F, $TMSN_3$ in HFIP was added to a solution of **2.16** (39.7 mg, 0.315 mmol, 1.0 equiv), $AlBr_3$ (83.3 mg, 0.312 mmol, 1.0 equiv), and 1,3,5-trimethoxybenzene (252 mg, 1.50 mmol, 4.7 equiv) in HFIP. Purification by an automated MPLC system on a 12 g normal phase silica column with gradient elution from 0–6% MeOH/CH_2Cl_2

afforded the **2.61** as a cream amorphous solid (44.2 mg, 0.119 mmol, 38% yield) and known tetrazole (6,7,8,9,10,11-hexahydro-5*H*-tetrazolo[1,5-*a*]azonine,[7] 5.30 mg, 0.032 mmol, 10% yield). Characterization data was consistent with the above entry.

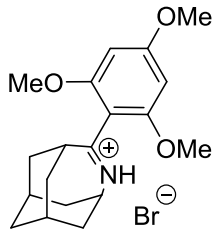

2.62

(1*R*,3*r*,6*s*,8*S*)-5-(2,4,6-Trimethoxyphenyl)-4-azatricyclo[4.3.1.13,8]undec-4-en-4-ium Bromide, 2.62. Following the general procedure E, $TMSN_3$ in HFIP was added to a solution of 2-adamantanone **2.32** (45.8 mg, 0.305 mmol, 1.0 equiv), $AlBr_3$ (82.3 mg, 0.309 mmol, 1.0 equiv), 1,3,5-trimethoxybenzene (254 mg, 1.51 mmol, 5.0 equiv) in HFIP. Purification by an automated MPLC system on a 12 g normal phase silica column with gradient elution from 0–5% MeOH/CH_2Cl_2 afforded **2.62** as a white amorphous solid (24.5 mg, 0.062 mmol, 20% yield). R_f = 0.36 (5% MeOH/CH_2Cl_2); IR (neat) 2930, 2653, 1662, 1606, 1576 cm^{-1}. ^1H NMR (600 MHz, $CDCl_3$) δ 13.6 (br s, 1H), 6.11 (s, 2H), 4.63 (m, 1H), 3.88 (s, 6H), 3.84 (s, 3H), 3.20 (m, 1H), 2.26 (m, 2H), 2.08–2.04 (m, 4H), 1.97 (m, 2H), 1.89–1.85 (m, 4H); ^{13}C NMR (151 MHz, $CDCl_3$) δ 186.9, 165.7, 159.7 (2C), 105.1, 91.1 (2C), 56.5 (2C), 55.8, 52.7, 40.4, 34.4, 32.3 (2C), 29.4 (2C), 27.1 (2C). HRMS (FT-ICR, ESI) *m/z*: $[M - Br]^+$ calcd for $C_{19}H_{26}NO_3$ 316.1907, found 316.1906.

Alternatively, to a solution of **2.32** (45.0 mg, 0.300 mmol, 1.0 equiv), $AlBr_3$ (91.8 mg, 0.344 mmol, 1.2 equiv), and 1,3,5-trimethoxybenzene (250 mg, 1.50 mmol, 5.0 equiv) in HFIP (1.0 mL) in a flame-dried nitrogen-flushed 25 mL round bottom was added a solution of $TMSN_3$ (0.600 mmol, 2.0 equiv) in HFIP (2.0 mL) using a syringe pump (0.15 mL/h, 14.00 mm diameter, and 20 gauge needle) over 18 h at room temperature. Following slow addition, the reaction mixture

was stirred for an additional 1 h and concentrated under nitrogen. The residual crude was redissolved in CH_2Cl_2 (ca. 40 mL), filtered, and concentrated. Purification by an automated MPLC system on a 12 g normal phase silica column with gradient elution from 0–7% MeOH/CH_2Cl_2 afforded **2.62** as a white amorphous solid (30.6 mg, 0.077 mmol, 26% yield). Characterization data was consistent with the above entry.

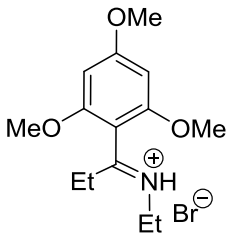

2.64

(*E*)-*N*-(1-(2,4,6-Trimethoxyphenyl)propylidene)ethanaminium Bromide, 2.64. Following the general procedure E, $TMSN_3$ in HFIP was added to a solution of pentan-3-one **2.63** (32.0 µL, 0.302 mmol, 1.0 equiv), $AlBr_3$ (100.6 mg, 0.377 mmol, 1.3 equiv), 1,3,5-trimethoxybenzene (252 mg, 1.50 mmol, 5.0 equiv) in HFIP. Following slow addition, the reaction mixture was stirred for an additional 15 h and concentrated under a stream of nitrogen. Purification by an automated MPLC system on a 12 g normal phase silica column with gradient elution from 0–5% MeOH/CH_2Cl_2 afforded **2.64** as a yellow sticky oil (74.5 mg, 0.224 mmol, 74% yield). R_f = 0.30 (3% MeOH/CH_2Cl_2); IR (neat) 3409, 2976, 2841, 2706, 1666, 1603, 1581 cm^{-1}. ^1H NMR (400 MHz, $CDCl_3$) δ 6.16 (s, 2H), 3.86 (s, 3H), 3.80 (s, 6H), 3.46 (q, J = 7.3 Hz, 2H), 3.19 (q, J = 7.6 Hz, 2H), 1.38 (t, J = 7.3 Hz, 3H), 1.09 (t, J = 7.6 Hz, 3H); ^{13}C NMR (151 MHz, $CDCl_3$) δ 186.2, 164.8, 157.6 (2C), 100.4, 90.9 (2C), 56.1 (2C), 55.9, 44.8, 31.8, 13.4, 10.7. HRMS (FT-ICR, HESI) *m/z*: $[M - Br]^+$ calcd for $C_{14}H_{22}NO_3$ 252.1594, found 252.1594.

Alternatively following the general procedure F, $TMSN_3$ in HFIP was added to a solution of pentan-3-one **2.63** (32.0 µL, 0.302 mmol, 1.0 equiv), $AlBr_3$ (82.0 mg, 0.307 mmol, 1.0 equiv),

1,3,5-trimethoxybenzene (251 mg, 1.49 mmol, 4.9 equiv) in HFIP. Purification by an automated MPLC system on a 12 g normal phase silica column with gradient elution from 0–5% MeOH/CH_2Cl_2 afforded **2.64** as a yellow sticky oil (87.9 mg, 0.265 mmol, 88% yield). Characterization data was consistent with the above entry.

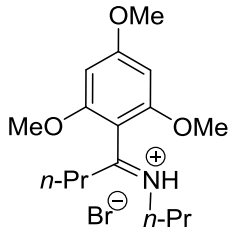

2.66

(*E*)-*N*-(1-(2,4,6-Trimethoxyphenyl)butylidene)propanaminium Bromide, 2.66. Following the general procedure E, $TMSN_3$ in HFIP was added to a solution of heptan-4-one **2.65** (42.0 μL, 0.300 mmol, 1.0 equiv), $AlBr_3$ (86.6 mg, 0.325 mmol, 1.1 equiv), 1,3,5-trimethoxybenzene (252 mg, 1.50 mmol, 5.0 equiv) in HFIP. Purification by an automated MPLC system on a 12 g normal phase silica column with gradient elution from 0–5% MeOH/CH_2Cl_2 afforded **2.66** as a yellow sticky oil (66.2 mg, 0.214 mmol, 71% yield, UPLC-HRMS purity: ≥95.5%). R_f = 0.25 (3% MeOH/CH_2Cl_2); IR (neat) 3424, 2966, 2700, 1665, 1606, 1582 cm^{-1}. ^1H NMR (400 MHz, $CDCl_3$) δ 6.16 (s, 2H), 3.87 (s, 3H), 3.81 (s, 6H), 3.37 (t, *J* = 7.4 Hz, 2H), 3.18 (t, *J* = 7.8 Hz, 2H), 1.89 (h, *J* = 7.4 Hz, 2H), 1.53 (h, *J* = 7.4 Hz, 2H), 0.96 (t, *J* = 7.4 Hz, 3H), 0.85 (t, *J* = 7.4 Hz, 3H); ^{13}C NMR (151 MHz, $CDCl_3$) δ 185.0, 164.8, 157.7 (2C), 101.0, 90.9 (2C), 56.1 (2C), 55.8, 51.5, 40.0, 21.4, 20.3, 13.8, 11.3. HRMS (FT-ICR, HESI) *m/z*: $[M - Br]^+$ calcd for $C_{16}H_{26}NO_3$ 280.1907, found 280.1907.

Alternatively following the general procedure F, $TMSN_3$ in HFIP was added to a solution of **2.65** (42.0 μL, 0.300 mmol, 1.0 equiv), $AlBr_3$ (82.9 mg, 0.311 mmol, 1.0 equiv), 1,3,5-trimethoxybenzene (252 mg, 1.50 mmol, 5.0 equiv) in HFIP. Purification by an automated MPLC

system on a 12 g normal phase silica column with gradient elution from 0–5% MeOH/CH_2Cl_2 afforded **2.66** as a yellow sticky oil (96.7 mg, 0.268 mmol, 89% yield). Characterization data was consistent with the above entry.

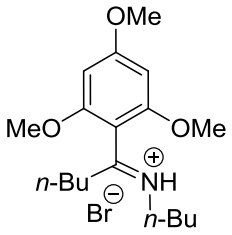

2.67

(*E*)-*N*-(1-(2,4,6-Trimethoxyphenyl)pentylidene)butan-1-aminium Bromide, 2.67. Following the general procedure E, $TMSN_3$ in HFIP was added to a solution of **2.34** (52.0 µL, 0.302 mmol, 1.0 equiv), $AlBr_3$ (87.4 mg, 0.328 mmol, 1.1 equiv), 1,3,5-trimethoxybenzene (252 mg, 1.50 mmol, 5.0 equiv) in HFIP. Following slow addition, the reaction mixture was stirred for an additional 15 h and concentrated under a stream of nitrogen. Purification by an automated MPLC system on a 12 g normal phase silica column with gradient elution from 0–5% MeOH/CH_2Cl_2 afforded **2.67** as a yellow sticky oil (79.5 mg, 0.205 mmol, 68% yield, UPLC-HRMS purity: ≥95.5%). R_f = 0.30 (4% MeOH/CH_2Cl_2); IR (neat) 2956, 2932, 2870, 2605, 1662, 1604, 1582 cm^{-1}. ^1H NMR (400 MHz, $CDCl_3$) δ 6.15 (s, 2H), 3.86 (s, 3H), 3.79 (s, 6H), 3.30 (t, *J* = 7.5 Hz, 2H), 3.00 (br s, 2H), 1.75 (p, *J* = 7.7 Hz, 2H), 1.48–1.21 (complex, 6H), 0.83 (dtd, *J* = 14.6, 7.3, 1.1 Hz, 6H); ^{13}C NMR (151 MHz, $CDCl_3$) δ 163.9, 157.5 (2C), 103.2, 90.7 (2C), 55.9 (2C), 55.7, 50.4, 38.8, 30.5, 28.6, 22.5, 20.1, 13.9, 13.6. **Note**: Missing imine carbonyl signal. HRMS (FT-ICR, ESI) *m/z*: $[M - Br]^+$ calcd for $C_{18}H_{30}NO_3$ 308.2220, found 308.2214.

Following the general procedure F, $TMSN_3$ in HFIP was added to a solution of **2.34** (52.0 µL, 0.302 mmol, 1.0 equiv), $AlBr_3$ (90.0 mg, 0.337 mmol, 1.1 equiv), 1,3,5-trimethoxybenzene (251 mg, 1.49 mmol, 4.9 equiv) in HFIP. Purification by an automated MPLC system on a 12 g

normal phase silica column with gradient elution from 0–5% MeOH/CH_2Cl_2 afforded **2.67** as a yellow sticky oil (95.4 mg, 0.246 mmol, 81% yield). Characterization data was consistent with the above entry.

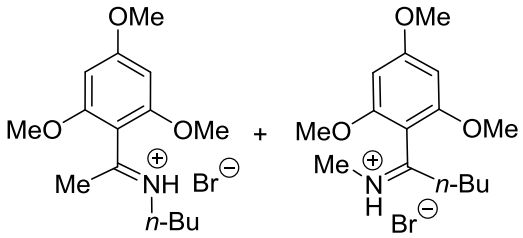

2.69 + **2.70**

(*E*)-*N*-(1-(2,4,6-Trimethoxyphenyl)ethylidene)butanaminium Bromide, 2.69 and (*Z*)-*N*-(1-(2,4,6-Trimethoxyphenyl)pentylidene)methanaminium Bromide 2.70. Following the general procedure E, $TMSN_3$ in HFIP was added to a solution of **2.68** (37.0 µL, 0.300 mmol, 1.0 equiv), $AlBr_3$ (88.5 mg, 0.332 mmol, 1.1 equiv), 1,3,5-trimethoxybenzene (252 mg, 1.50 mmol, 5.0 equiv) in HFIP. Purification by an automated MPLC system on a 12 g normal phase silica column with gradient elution from 0–5% MeOH/CH_2Cl_2 afforded the **2.69** and **2.70** as a yellow sticky oil (73.5 mg, 0.212 mmol, 71% yield) as a mixture of isomers (ratio 80:20). **2.69** and **2.70**: R_f = 0.29 (3% MeOH/CH_2Cl_2); IR (neat) 2933, 2841, 1667, 1603, 1580, 1455, 1413 cm^{-1}. Diagnostic peaks of **2.69**: ^1H NMR (400 MHz, $CDCl_3$) δ 6.15 (s, 2H), 3.86 (s, 3H), 3.80 (s, 6H), 3.36 (m, 2H), 2.75 (s, 3H), 1.80 (m, 2H), 1.29 (m, 2H), 0.82 (m, 3H); ^{13}C NMR (151 MHz, $CDCl_3$) δ 180.6, 164.6, 157.3 (2C), 102.6, 90.8 (2C), 56.1 (2C), 55.8, 49.9, 29.8, 25.7, 20.0, 13.5. Diagnostic peaks of **2.70**: ^1H NMR (400 MHz, $CDCl_3$) δ 6.16 (s, 2H), 3.86 (s, 3H), 3.81 (s, 6H), 3.12 (s, 3H), 3.08 (m, 2H), 1.46 (m, 2H), 1.34 (m, 2H), 0.93 (m, 3H); ^{13}C NMR (151 MHz, $CDCl_3$) δ 164.8, 157.9, 101.3, 90.9, 38.4, 35.7, 28.7, 22.4, 13.8. HRMS (FT-ICR, HESI) *m/z*: $[M - Br]^+$ calcd for $C_{15}H_{24}NO_3$ 266.1751, found 266.1746.

Alternatively following the general procedure F, $TMSN_3$ in HFIP was added to a solution of **2.68** (37.0 μL, 0.300 mmol, 1.0 equiv), $AlBr_3$ (89.9 mg, 0.337 mmol, 1.1 equiv), 1,3,5-trimethoxybenzene (253 mg, 1.50 mmol, 5.0 equiv) in HFIP. Purification by an automated MPLC system on a 12 g normal phase silica column with gradient elution from 0–5% MeOH/CH_2Cl_2 afforded **2.69** as a yellow sticky oil (80.9 mg, 0.234 mmol, 78% yield) as a mixture of isomers (ratio 80:20). Characterization data was consistent with the above entry.

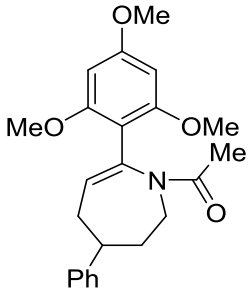

2.71

1-(4-Phenyl-7-(2,4,6-trimethoxyphenyl)-2,3,4,5-tetrahydro-1*H*-azepinyl)ethanone, 2.71. Following the general procedure E, $TMSN_3$ in HFIP was added to a solution of **2.1** (52.8 mg, 0.303 mmol, 1.0 equiv), $AlBr_3$ (83.8 mg, 0.314 mmol, 1.0 equiv), 1,3,5-trimethoxybenzene (253 mg, 1.50 mmol, 5.0 equiv) in HFIP. Then, following general procedure G to the crude residue in anhydrous CH_2Cl_2 (3.0 mL) was added acetic anhydride (0.20 mL, 2.12 mmol, 7.0 equiv) and DMAP (25.0 mg, 0.205 mmol, 0.66 equiv). Purification by an automated MPLC system on a 12 g normal phase silica column with gradient elution from 0–3% MeOH/CH_2Cl_2 afforded **2.71** as a white amorphous solid (108 mg, 0.283 mmol, 93% yield, UPLC-HRMS purity: 99.0%). R_f = 0.41 (3% MeOH/CH_2Cl_2); mp 106–109 ˚C; IR (neat) 2940, 1599, 1580 cm^{-1}. ^1H NMR (400 MHz, $CDCl_3$) δ 7.29 (m, 2H), 7.21 (m, 3H), 6.12 (s, 2H), 5.79 (dd, *J* = 8.7, 4.7 Hz, 1H), 4.48 (br s, 1H), 3.83 (s, 3H), 3.78 (s, 6H), 3.33 (br s, 1H), 2.71–2.57 (m, 2H), 2.38 (m, 1H), 2.05 (m, 2H), 1.79 (s, 3H); ^{13}C NMR (151 MHz, $CDCl_3$) δ 170.3, 161.0, 159.0 (2C), 147.6, 136.9, 128.9, 128.4 (2C),

126.7 (2C), 126.1, 109.5, 90.6 (2C), 55.7 (2C), 55.3, 46.3, 42.3, 37.7, 35.0, 21.6. HRMS (FT-ICR, HESI) *m/z*: $[M + H]^+$ calcd for $C_{23}H_{28}NO_4$ 382.2013, found 382.2011.

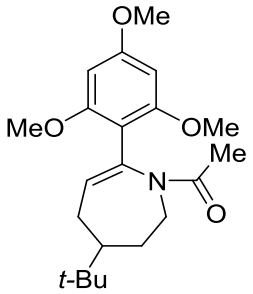

2.72

1-(4-(t*ert*-Butyl)-7-(2,4,6-trimethoxyphenyl)-2,3,4,5-tetrahydro-1*H*-azepinyl)ethanone, 2.72. Following the general procedure E, $TMSN_3$ in HFIP was added to a solution of **2.42** (46.2 mg, 0.300 mmol, 1.0 equiv), $AlBr_3$ (86.8 mg, 0.324 mmol, 1.1 equiv), 1,3,5-trimethoxybenzene (251 mg, 1.50 mmol, 5.0 equiv) in HFIP. Then, following general procedure G to the crude residue in anhydrous CH_2Cl_2 (3.0 mL) was added acetic anhydride (0.35 mL, 3.71 mmol, 12.0 equiv) and DMAP (38.0 mg, 0.311 mmol, 1.0 equiv). Purification by an automated MPLC system on a 12 g normal phase silica column with gradient elution from 0–3% MeOH/CH_2Cl_2 afforded **2.72** as a white amorphous solid (88.1 mg, 0.244 mmol, 82% yield, UPLC-HRMS purity: ≥95.5%). R_f = 0.48 (3% MeOH/CH_2Cl_2); mp 137–139 ˚C; IR (neat) 2944, 1636, 1602, 1579 cm^{-1}. ^1H NMR (400 MHz, $CDCl_3$) δ 6.10 (s, 2H), 5.71 (dd, *J* = 8.7, 5.3 Hz, 1H), 4.38 (br s, 1H), 3.82 (s, 3H), 3.76 (s, 6H), 3.23 (br s, 1H), 2.31 (m, 1H), 2.05–1.93 (m, 2H), 1.73 (s, 3H), 1.64–1.54 (m, 1H), 1.22 (m, 1H), 0.88 (s, 9H); ^{13}C NMR (151 MHz, $CDCl_3$) δ 170.2, 160.9, 159.2 (2C), 136.3, 130.0, 110.0, 90.7 (2C), 55.9 (2C), 55.4, 46.9, 45.6, 33.3, 30.6, 29.3, 27.6 (3C), 21.8. HRMS (FT-ICR, HESI) *m/z*: $[M + H]^+$ calcd for $C_{21}H_{32}NO_4$ 362.2326, found 362.2325.

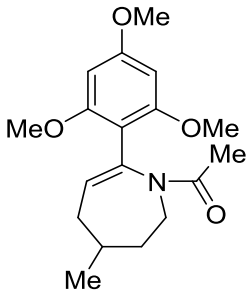

2.73

1-(4-Methyl-7-(2,4,6-trimethoxyphenyl)-2,3,4,5-tetrahydro-1*H*-azepinyl)ethanone, 2.73. Following the general procedure E, $TMSN_3$ in HFIP was added to a solution of **2.40** (37.0 μL, 0.301 mmol, 1.0 equiv), $AlBr_3$ (88.0 mg, 0.330 mmol, 1.1 equiv), 1,3,5-trimethoxybenzene (251 mg, 1.49 mmol, 5.0 equiv) in HFIP. Then, following general procedure G to the crude residue in anhydrous CH_2Cl_2 (3.0 mL) was added acetic anhydride (0.35 mL, 3.71 mmol, 12.3 equiv) and DMAP (44.0 mg, 0.360 mmol, 1.2 equiv). Purification by an automated MPLC system on a 12 g normal phase silica column with gradient elution from 0–3% MeOH/CH_2Cl_2 afforded **2.73** as a white amorphous solid (82.9 mg, 0.260 mmol, 86% yield, UPLC-HRMS purity: ≥95.0%). R_f = 0.32 (4% MeOH/CH_2Cl_2); IR (neat) 2943, 1626, 1602, 1578 cm^{-1}; mp 132–134 °C. ^1H NMR (400 MHz, $CDCl_3$) δ 6.10 (s, 2H), 5.67 (m, 1H), 4.19 (br s, 1H), 3.81 (s, 3H), 3.75 (s, 6H), 3.36 (br s, 1H), 2.16–2.04 (m, 2H), 1.87 (m, 1H), 1.73 (s, 3H), 1.67 (br s, 1H), 1.52 (m, 1H), 0.96 (d, J = 6.6 Hz, 3H); ^{13}C NMR (151 MHz, $CDCl_3$) δ 170.1, 160.9, 159.2 (2C), 136.6, 129.1, 110.2, 90.8 (2C), 55.9 (2C), 55.4, 45.9, 37.6, 35.7, 30.3, 22.7, 21.8. HRMS (FT-ICR, HESI) *m/z*: $[M + H]^+$ calcd for $C_{18}H_{26}NO_4$ 320.1856, found 320.1851.

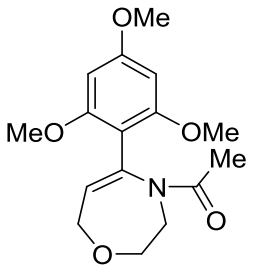

2.74

1-(5-(2,4,6-Trimethoxyphenyl)-2,3-dihydro-1,4-oxazepin-4(7*H*)-yl)ethan-1-one, 2.74. Following the general procedure E, $TMSN_3$ in HFIP was added to a solution of **2.10** (28.0 µL, 0.303 mmol, 1.0 equiv), $AlBr_3$ (128.0 mg, 0.480 mmol, 1.6 equiv), 1,3,5-trimethoxybenzene (253 mg, 1.50 mmol, 5.0 equiv) in HFIP. Then, following general procedure G to the crude residue in anhydrous CH_2Cl_2 (3.0 mL) was added acetic anhydride (0.35 mL, 3.70 mmol, 12.2 equiv) and DMAP (44.0 mg, 0.360 mmol, 1.2 equiv). Purification by an automated MPLC system on a 12 g normal phase silica column with gradient elution from 0–3% MeOH/CH_2Cl_2 afforded **2.74** as an off-white amorphous solid (63.8 mg, 0.184 mmol, 61% yield). R_f = 0.48 (3% MeOH/CH_2Cl_2); IR (neat) 2949, 2840, 1658, 1636, 1602, 1581 cm^{-1}; mp 158–160 ˚C. ^1H NMR (400 MHz, $CDCl_3$) δ 6.10 (d, *J* = 0.9 Hz, 2H), 5.76 (td, *J* = 6.2, 0.9 Hz, 1H), 4.18 (d, *J* = 6.2 Hz, 1H), 3.94 (br s, 2H), 3.84–3.82 (complex, 5H, contains d, *J* = 0.9 Hz, 3H), 3.76 (d, *J* = 0.9 Hz, 6H), 1.76 (d, *J* = 0.9 Hz, 3H); ^{13}C NMR (151 MHz, $CDCl_3$) δ 170.2, 161.5, 159.3 (2C), 139.7, 126.4, 109.1, 90.6 (2C), 71.5, 66.8, 55.9 (2C), 55.5, 48.0, 21.9. HRMS (FT-ICR, HESI) *m/z*: $[M + H]^+$ calcd for $C_{16}H_{22}NO_4$ 308.1492, found 308.1487.

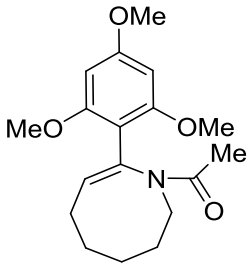

2.75

(*Z*)-1-(8-(2,4,6-Trimethoxyphenyl)-3,4,5,6-tetrahydroazocin-1(2*H*)-yl)ethanone, 2.75. Following the general procedure F, $TMSN_3$ in HFIP was added to a solution of **2.14** (35.0 μL, 0.296 mmol, 1.0 equiv), $AlBr_3$ (81.9 mg, 0.307 mmol, 1.0 equiv), 1,3,5-trimethoxybenzene (250 mg, 1.49 mmol, 5.0 equiv) in HFIP. Then, following general procedure G to the crude residue in anhydrous CH_2Cl_2 (3.0 mL) was added acetic anhydride (0.35 mL, 3.71 mmol, 12.0 equiv) and DMAP (44.0 mg, 0.360 mmol, 1.2 equiv). Purification by an automated MPLC system on a 12 g normal phase silica column with gradient elution from 0–3% MeOH/CH_2Cl_2 afforded **2.75** as a white sticky (low boiling) solid (76.9 mg, 0.241 mmol, 81% yield, UPLC-HRMS purity: ≥95.5%). R_f = 0.43 (3% MeOH/CH_2Cl_2); IR (neat) 2929, 2846, 1633, 1602, 1580 cm^{-1}. ^1H NMR (400 MHz, $CDCl_3$) δ 6.11 (s, 2H), 5.85 (m, 1H), 3.81 (s, 3H), 3.74 (s, 6H), 3.55 (m, 2H), 2.17 (m, 2H), 2.11 (s, 3H), 1.74–1.60 (complex, 6H); ^{13}C NMR (151 MHz, $CDCl_3$) δ 171.7, 161.0, 159.7 (2C), 135.0, 132.1, 108.7, 90.7 (2C), 55.6 (2C), 55.4, 47.5, 28.3, 27.5, 26.9, 26.3, 21.9. HRMS (FT-ICR, HESI) *m/z*: $[M + H]^+$ calcd for $C_{18}H_{26}NO_4$ 320.1856, found 320.1851.

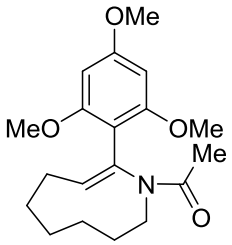

2.76

(*E*)-1-(9-(2,4,6-Trimethoxyphenyl)-2,3,4,5,6,7-hexahydro-1*H*-azoninyl)ethanone,

2.76. Following the general procedure F, $TMSN_3$ in HFIP was added to a solution of **2.16** (38.3 mg, 0.303 mmol, 1.0 equiv), $AlBr_3$ (88.2 mg, 0.331 mmol, 1.1 equiv), 1,3,5-trimethoxybenzene (252 mg, 1.50 mmol, 4.9 equiv) in HFIP. Then, following general procedure G to the crude residue in anhydrous CH_2Cl_2 (3.0 mL) was added acetic anhydride (0.35 mL, 3.70 mmol, 12.0 equiv) and DMAP (44.0 mg, 0.360 mmol, 1.2 equiv). Purification by an automated MPLC system on a 12 g normal phase silica column with gradient elution from 0–3% MeOH/CH_2Cl_2 afforded **2.76** as an off-white crystalline solid (59.8 mg, 0.179 mmol, 59% yield, UPLC-HRMS purity: ≥95.5%). R_f = 0.47 (3% MeOH/CH_2Cl_2); mp 133–135 ˚C; IR (neat) 2935, 2853, 1629, 1602, 1579 cm^{-1}. ^1H NMR (500 MHz, $CDCl_3$, 0 ˚C) δ 6.10 (s, 2H), 5.51 (t, J = 8.2 Hz, 1H), 3.82 (s, 3H), 3.74 (s, 6H), 3.68 (br m, 1H), 2.72 (br m, 1H), 2.52 (br m, 1H), 2.22 (s, 3H), 2.08 (br m, 2H), 1.61–1.32 (complex, 7H); ^{13}C NMR (151 MHz, $CDCl_3$) δ 172.1, 161.1, 159.9 (2C), 134.0, 132.4, 108.8, 90.7 (2C), 55.7 (2C), 55.5, 44.4, 26.4, 25.06, 25.02, 22.6, 21.6, 21.2. HRMS (FT-ICR, HESI) *m/z*: $[M + H]^+$ calcd for $C_{19}H_{28}NO_4$ 334.2013, found 334.2008.

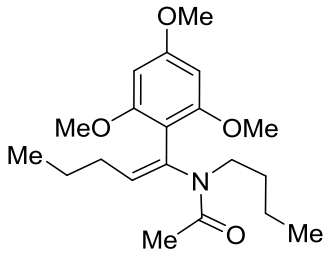

2.77

(*E*)-*N*-Butyl-*N*-(1-(2,4,6-Trimethoxyphenyl)pentenyl)acetamide, 2.77. Following the general procedure F, $TMSN_3$ in HFIP was added to a solution of **2.34** (50.0 µL, 0.290 mmol, 1.0 equiv), $AlBr_3$ (81.8 mg, 0.307 mmol, 1.1 equiv), 1,3,5-trimethoxybenzene (252 mg, 1.50 mmol, 5.2 equiv) in HFIP. Then, following general procedure G to the crude residue in anhydrous CH_2Cl_2 (3.0 mL) was added acetic anhydride (0.35 mL, 3.70 mmol, 13.0 equiv) and triethylamine (50.0 µL, 0.360 mmol, 1.2 equiv). Purification by an automated MPLC system on a 12 g normal phase silica column with gradient elution from 0–3% MeOH/CH_2Cl_2 afforded **2.77** as a colorless oil (82.2 mg, 0.235 mmol, 81% yield, UPLC-HRMS purity: ≥95.5%). R_f = 0.46 (3% MeOH/CH_2Cl_2); IR (neat) 2931, 2867, 1630, 1604, 1581 cm^{-1}. ^1H NMR (400 MHz, $CDCl_3$) δ 6.11 (s, 2H), 5.50 (t, *J* = 7.4 Hz, 1H), 3.83 (s, 3H), 3.74 (s, 6H), 3.13 (m, 2H), 2.29 (s, 3H), 1.84 (q, *J* = 7.4 Hz, 2H), 1.39 (m, 4H), 1.19 (m, 2H), 0.83 (dt, *J* = 9.6, 7.4 Hz, 6H); ^{13}C NMR (151 MHz, $CDCl_3$) δ 171.4, 161.7, 159.7 (2C), 132.9, 131.9, 105.6, 90.3 (2C), 55.48 (2C), 55.45, 44.5, 30.8, 29.6, 22.3, 22.1, 20.3, 14.05, 14.01. HRMS (FT-ICR, HESI) *m/z*: $[M + H]^+$ calcd for $C_{20}H_{32}NO_4$ 350.2326, found 350.2311.

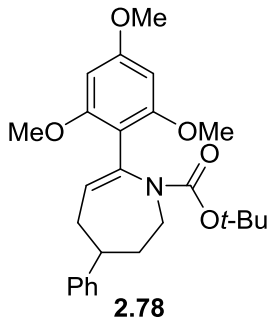

2.78

***tert*-Butyl-4-phenyl-7-(2,4,6-trimethoxyphenyl)-2,3,4,5-tetrahydro-1*H*-azepine-1-carboxylate, 2.78.** Following the general procedure E, $TMSN_3$ in HFIP was added to a solution of **2.1** (52.4 mg, 0.301 mmol, 1.0 equiv), $AlBr_3$ (85.5 mg, 0.321 mmol, 1.1 equiv), 1,3,5-trimethoxybenzene (253 mg, 1.50 mmol, 5.0 equiv) in HFIP. Then, following general procedure

G to the crude residue in anhydrous CH_2Cl_2 (3.0 mL) was added di-*tert*-butyl carbonate (0.21 mL, 0.910 mmol, 3.0 equiv) and DMAP (44.0 mg, 0.360 mmol, 1.2 equiv). Purification by an automated MPLC system on a 12 g normal phase silica column with gradient elution from 0–20% EtOAc/hexanes afforded **2.78** as a colorless oil (102 mg, 0.232 mmol, 77% yield, UPLC-HRMS purity: ≥95.5%). R_f = 0.49 (20% EtOAc/hexanes); IR (neat) 2936, 1682, 1651, 1602, 1584 cm^{-1}. ^1H NMR (400 MHz, $CDCl_3$) δ 7.34–7.20 (m, 5H), 6.15 (s, 2H), 5.62 (m, 1H), 4.34 (m, 1H), 3.86 (s, 3H), 3.80 (s, 6H), 3.36 (m, 1H), 2.74 (m, 2H), 2.43 (m, 1H), 2.05 (m, 2H), 1.17 (s, 9H); ^{13}C NMR (151 MHz, $CDCl_3$) δ 160.4, 159.1 (2C), 154.5, 148.1, 136.4, 128.5 (2C), 127.0 (2C), 126.1, 124.8, 111.4, 90.5, 79.6, 55.8 (2C), 55.5, 47.6, 42.1, 38.3, 35.1, 28.1 (3C). HRMS (FT-ICR, HESI) *m/z*: $[M + H]^+$ calcd for $C_{26}H_{34}NO_5$ 440.2431, found 440.2421.

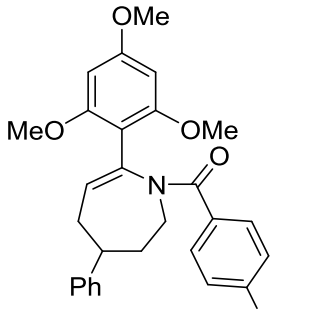

2.79

(4-Nitrophenyl)(4-phenyl-7-(2,4,6-trimethoxyphenyl)-2,3,4,5-tetrahydro-1*H*-azepin-1-yl)methanone, 2.79. Following the general procedure E, $TMSN_3$ in HFIP was added to a solution of **2.1** (52.5 mg, 0.301 mmol, 1.0 equiv), $AlBr_3$ (80.5 mg, 0.302 mmol, 1.0 equiv), 1,3,5-trimethoxybenzene (253 mg, 1.51 mmol, 5.0 equiv) in HFIP. Then, following general procedure G to the crude residue in anhydrous CH_2Cl_2 (4.0 mL) was added 4-nitrobenzoyl chloride (164 mg, 0.882 mmol, 2.9 equiv), DMAP (55.1 mg, 0.451 mmol, 1.5 equiv), and triethylamine (125 µL, 0.897 mmol, 3.0 equiv). Purification was carried out by an automated MPLC system on a 12 g normal phase silica column with gradient elution from 0–45% EtOAc/hexanes afforded **2.79** as a

yellow amorphous solid (103 mg, 0.210 mmol, 70% yield). R_f = 0.38 (30% EtOAc/hexanes); IR (neat) 2936, 2838, 1630, 1599, 1580 cm^{-1}; mp 200–202 ˚C. ^1H NMR (400 MHz, $CDCl_3$) δ 7.95 (m, 2H), 7.35 (m, 2H), 7.30–7.22 (m, 5H), 5.75–5.71 (complex, 3H, contains s, 5.75, 2H), 4.75 (br s, 1H), 3.71 (s, 3H), 3.55 (s, 6H), 2.85–2.75 (m, 3H), 2.60 (m, 1H), 2.25–2.09 (m, 2H); ^{13}C NMR (151 MHz, $CDCl_3$) δ 168.4, 161.3, 158.5 (2C), 147.6, 147.3, 143.3, 136.7, 128.7 (2C), 127.6 (2C), 127.2, 126.9 (2C), 126.4, 122.4 (2C), 109.8, 89.8 (2C), 55.5 (2C), 55.4, 46.8, 42.0, 38.1, 35.5. HRMS (FT-ICR, ESI) *m/z*: $[M + Na]^+$ calcd for $C_{28}H_{28}N_2O_6$ 511.1840, found 511.1839.

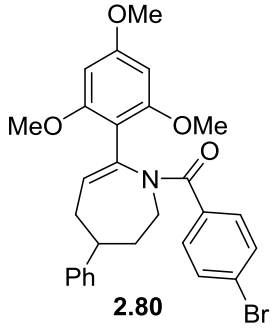

2.80

(4-Bromophenyl)(4-phenyl-7-(2,4,6-trimethoxyphenyl)-2,3,4,5-tetrahydro-1*H*-azepin-yl)methanone, 2.80. Following the general procedure E, $TMSN_3$ in HFIP was added to a solution of **2.1** (52.2 mg, 0.300 mmol, 1.0 equiv), $AlBr_3$ (90.8 mg, 0.340 mmol, 1.1 equiv), 1,3,5-trimethoxybenzene (251 mg, 1.49 mmol, 5.0 equiv) in HFIP. Then, following general procedure G to the crude residue in anhydrous CH_2Cl_2 (4.0 mL) was added 4-bromobenzoyl chloride (200 mg, 0.911 mmol, 3.0 equiv), DMAP (55.0 mg, 0.450 mmol, 1.5 equiv), and triethylamine (84.0 μL, 0.603 mmol, 2.0 equiv). Purification was carried out twice by an automated MPLC system on a 12 g normal phase silica column with gradient elution from 0–35% EtOAc/hexanes afforded **2.80** as a white foam (117 mg, 0.223 mmol, 75% yield). R_f = 0.23 (30% EtOAc/hexanes); IR (neat) 2936, 1630, 1602, 1586 cm^{-1}; mp (decomposed). ^1H NMR (400 MHz, $CDCl_3$) δ 7.31 (m, 4H), 7.22 (m, 3H), 7.00 (m, 2H), 5.80 (s, 2H), 5.67 (m, 1H), 4.74 (br s, 1H), 3.74 (s, 3H), 3.57 (s, 6H), 3.37

(br s, 1H), 2.79–2.72 (m, 2H), 2.55 (t, J = 10.9 Hz, 1H), 2.21–2.05 (m, 2H); ^{13}C NMR (151 MHz, $CDCl_3$) δ 169.8, 161.0, 158.6 (2C), 147.6, 137.5, 136.4, 130.3 (2C), 128.7 (2C), 128.4 (2C), 126.9 (2C), 126.3, 122.7, 110.1, 89.9, 55.6 (2C), 55.5, 46.7, 42.1, 38.6, 35.6. **Note**: Missing two carbon signal due to signals overlap. HRMS (FT-ICR, ESI) *m/z*: $[M + H]^+$ calcd for $C_{28}H_{29}NO_4$ 522.1274, found 522.1268.

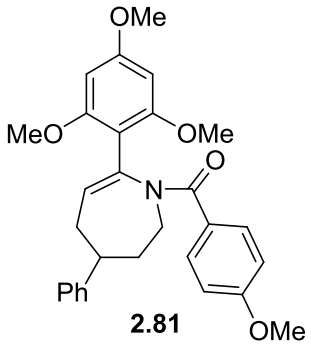

2.81

(4-Methoxyphenyl)(4-phenyl-7-(2,4,6-trimethoxyphenyl)-2,3,4,5-tetrahydro-1H-azepin-1-yl)methanone, 2.81. Following the general procedure E, $TMSN_3$ in HFIP was added to a solution of **2.1** (52.3 mg, 0.300 mmol, 1.0 equiv), $AlBr_3$ (81.6 mg, 0.306 mmol, 1.0 equiv), 1,3,5-trimethoxybenzene (253 mg, 1.50 mmol, 5.0 equiv) in HFIP. Then, following general procedure G to the crude residue in anhydrous CH_2Cl_2 (4.0 mL) was added 4-methoxybenzoyl chloride (41.0 μL, 0.303 mmol, 1.0 equiv) and DMAP (55.0 mg, 0.450 mmol, 1.5 equiv). Purification was carried out by an automated MPLC system on a 12 g normal phase silica column with gradient elution from 0–40% EtOAc/hexanes afforded **2.81** as a white amorphous solid (52.8 mg, 0.111 mmol, 37% yield). R_f = 0.20 (30% EtOAc/hexanes); IR (neat) 2935, 1603, 1582 cm^{-1}; mp 153–155 ˚C. ^{1}H NMR (400 MHz, $CDCl_3$) δ 7.32–7.24 (m, 4H), 7.20 (m, 1H), 7.13 (m, 2H), 6.60 (m, 2H), 5.78 (s, 2H), 5.66 (m, 1H), 4.78 (br s, 1H), 3.73 (s, 3H), 3.70 (s, 3H), 3.55 (s, 6H), 3.35 (br s, 1H), 2.78 (m, 2H), 2.54 (m, 1H), 2.09 (m, 2H); ^{13}C NMR (151 MHz, $CDCl_3$) δ 170.4, 160.6, 160.1, 158.6 (2C), 147.9, 138.2, 130.3, 128.7 (2C), 128.6 (2C), 127.0 (2C), 126.2, 125.7, 112.5 (2C), 110.4,

90.0 (2C), 55.6 (2C), 55.4 (2C), 46.7, 42.1, 38.7, 35.6. HRMS (FT-ICR, ESI) *m/z*: $[M + H]^+$ calcd for $C_{29}H_{32}NO_5$ 474.2275, found 474.2262.

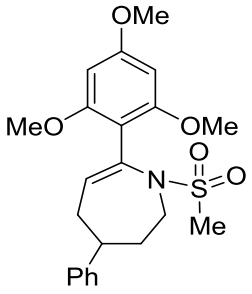

2.82

1-(Methylsulfonyl)-4-phenyl-7-(2,4,6-trimethoxyphenyl)-2,3,4,5-tetrahydro-1*H*-azepine, 2.82. Following the general procedure E, $TMSN_3$ in HFIP was added to a solution of **2.1** (52.4 mg, 0.301 mmol, 1.0 equiv), $AlBr_3$ (83.5 mg, 0.313 mmol, 1.0 equiv), 1,3,5-trimethoxybenzene (251 mg, 1.49 mmol, 5.0 equiv) in HFIP. Then, following general procedure G to the crude residue in anhydrous CH_2Cl_2 (4.0 mL) was added methanesulfonyl chloride (50.0 µL, 0.646 mmol, 2.2 equiv), DMAP (40.0 mg, 0.327 mmol, 1.1 equiv), and triethylamine (100 µL, 0.717 mmol, 2.4 equiv). Purification was carried out by an automated MPLC system on a 12 g normal phase silica column with gradient elution from 0–50% EtOAc/hexanes afforded **2.82** as a pale yellow amorphous solid (117 mg, 0.223 mmol, 75% yield, UPLC-HRMS purity: ≥95.5%). R_f = 0.55 (50% EtOAc/hexanes); IR (neat) 2938, 2839, 1601, 1582 cm^{-1}; mp 153–155 ˚C. ^1H NMR (400 MHz, $CDCl_3$) δ 7.32–7.28 (m, 2H), 7.25–7.18 (m, 3H), 6.13 (br s, 2H), 5.69 (dd, *J* = 8.8, 4.9 Hz, 1H), 3.95 (dt, *J* = 14.3, 3.9 Hz, 1H), 3.83 (br s, 9H), 3.45 (ddd, *J* = 14.0, 11.1, 2.5 Hz, 1H), 2.87 (m, 1H), 2.66 (m, 1H), 2.50 (s, 3H), 2.39 (m, 1H), 2.21–2.05 (m, 2H); ^{13}C NMR (151 MHz, $CDCl_3$) δ 161.4, 159.7 (2C), 147.7, 135.0, 128.7, 128.6 (2C), 126.9 (2C), 126.3, 108.3, 91.1, 90.6, 56.3, 55.8, 55.5, 49.9, 42.3, 40.1, 38.9, 35.0. HRMS (FT-ICR, ESI) *m/z*: $[M + H]^+$ calcd for $C_{22}H_{28}NO_5S$ 418.1683, found 418.1669.

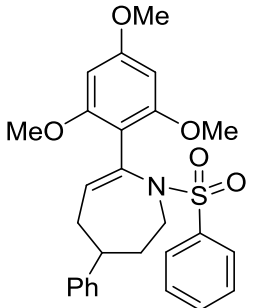

2.83

4-Phenyl-1-tosyl-7-(2,4,6-trimethoxyphenyl)-2,3,4,5-tetrahydro-1*H*-azepine, 2.83. Following the general procedure E, $TMSN_3$ in HFIP was added to a solution of **2.1** (52.6 mg, 0.302 mmol, 1.0 equiv), $AlBr_3$ (87.4 mg, 0.328 mmol, 1.1 equiv), 1,3,5-trimethoxybenzene (252 mg, 1.50 mmol, 5.0 equiv) in HFIP. Then, following general procedure G to the crude residue in anhydrous CH_2Cl_2 (4.0 mL) was added 4-toluenesulfonyl chloride (138 mg, 0.725 mmol, 2.4 equiv), DMAP (46.4 mg, 0.380 mmol, 1.3 equiv), and triethylamine (91.0 μL, 0.660 mmol, 2.2 equiv). Purification was carried out by an automated MPLC system on a 12 g normal phase silica column with gradient elution from 0–25% EtOAc/hexanes afforded **2.83** as a pale yellow solid (87.0 mg, 0.176 mmol, 58% yield). R_f = 0.30 (30% EtOAc/hexanes); IR (neat) 2938, 1602, 1584 cm^{-1}; mp 182–184 ˚C. ^1H NMR (400 MHz, $CDCl_3$) δ 7.33–7.26 (m, 4H), 7.23–7.19 (m, 3H), 7.08 (d, *J* = 7.9 Hz, 2H), 6.12 (br s, 1H), 5.77 (br s, 1H), 5.70 (dd, *J* = 8.8, 4.8 Hz, 1H), 4.11 (dt, *J* = 14.4, 3.9 Hz, 1H), 3.83 (s, 6H), 3.45 (m, 1H), 3.34 (br s, 3H), 2.76 (m, 1H), 2.64 (m, 1H), 2.38 (s, 3H), 2.33 (m, 1H), 2.27–2.17 (m, 1H), 2.07 (m, 1H); ^{13}C NMR (151 MHz, $CDCl_3$) δ 161.2, 159.6, 159.3, 147.8, 141.9, 138.7, 135.1, 128.9, 128.7 (2C), 128.6 (2C), 127.2 (2C), 126.9 (2C), 126.2, 108.7, 90.8, 90.1, 56.3, 55.5, 54.9, 50.3, 42.1, 39.8, 34.8, 21.5. HRMS (FT-ICR, ESI) *m/z*: $[M + H]^+$ calcd for $C_{28}H_{32}NO_5S$ 494.1996, found 494.1983.

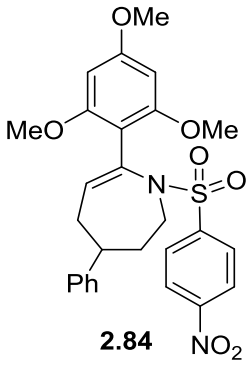

2.84

1-((4-Nitrophenyl)sulfonyl)-4-phenyl-7-(2,4,6-trimethoxyphenyl)-2,3,4,5-tetrahydro-1*H*-azepine, 2.84. Following the general procedure E, $TMSN_3$ in HFIP was added to a solution of **2.1** (51.5 mg, 0.296 mmol, 1.0 equiv), $AlBr_3$ (80.1 mg, 0.300 mmol, 1.0 equiv), 1,3,5-trimethoxybenzene (253 mg, 1.50 mmol, 5.1 equiv) in HFIP. Then, following general procedure G to the crude residue in anhydrous CH_2Cl_2 (4.0 mL) was added 4-nitrobenzenesulfonyl chloride (150 mg, 0.725 mmol, 2.3 equiv), DMAP (44.9 mg, 0.368 mmol, 1.2 equiv), and triethylamine (91.0 μL, 0.653 mmol, 2.2 equiv). Purification was carried out by an automated MPLC system on a 12 g normal phase silica column with gradient elution from 0–25% EtOAc/hexanes afforded **2.84** as a yellow amorphous solid (44.5 mg, 0.085 mmol, 29% yield). R_f = 0.60 (30% EtOAc/hexanes); IR (neat) 2928, 1603, 1583, 1524 cm^{-1}; mp 184–220 ˚C. ^1H NMR (400 MHz, $CDCl_3$) δ 8.06 (m, 2H), 7.47 (m, 2H), 7.31 (m, 2H), 7.34–7.19 (m, 3H), 6.12 (br s, 1H), 5.74 (dd, *J* = 8.8, 4.8 Hz, 1H), 5.62 (br s, 1H), 4.14 (dt, *J* = 14.3, 3.8 Hz, 1H), 3.80 (br s, 3H), 3.77 (s, 3H), 3.51 (m, 1H), 3.33 (br s, 3H), 2.82 (m, 1H), 2.67 (m, 1H), 2.40 (m, 1H), 2.28–2.18 (m, 1H), 2.12 (m, 1H); ^{13}C NMR (151 MHz, $CDCl_3$) δ 161.7, 159.8, 159.2, 149.2, 147.4, 147.1, 134.1, 130.0, 128.7 (2C), 128.1 (2C), 126.9 (2C), 126.4, 123.2, 107.9, 91.0, 89.4, 56.3, 55.5, 55.1, 50.9, 42.0, 40.2, 34.8. HRMS (FT-ICR, ESI) *m/z*: $[M + H]^+$ calcd for $C_{27}H_{29}N_2O_7S$ 525.1690, found 525.1698.

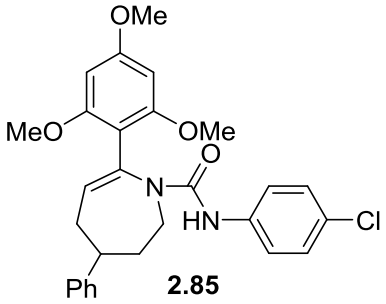

2.85

***N*-(4-Chlorophenyl)-4-phenyl-7-(2,4,6-trimethoxyphenyl)-2,3,4,5-tetrahydro-1*H*-azepine-1-carboxamide, 2.85.** Following the general procedure E, $TMSN_3$ in HFIP was added to a solution of **2.1** (52.0 mg, 0.298 mmol, 1.0 equiv), $AlBr_3$ (85.4 mg, 0.320 mmol, 1.1 equiv), 1,3,5-trimethoxybenzene (253 mg, 1.50 mmol, 5.1 equiv) in HFIP. Then, following general procedure G to the crude residue in anhydrous THF (4.0 mL) was added 4-chlorophenyl isocyanate (98.5 mg, 0.641 mmol, 2.2 equiv), DMAP (24.5 mg, 0.672 mmol, 0.67 equiv), and triethylamine (63.0 µL, 0.452 mmol, 1.5 equiv). Purification was carried out twice by an automated MPLC system; first using a 12 g normal phase silica column with gradient elution from 0–15% EtOAc/hexanes, and second using a 13 g C18 reverse phase column with 0–100% MeCN/H_2O gradient elution afford **2.85** a white amorphous solid (75.2 mg, 0.153 mmol, 51% yield). R_f = 0.31 (25% EtOAc/hexanes); IR (neat) 3360, 2940, 1667, 1603, 1591, 1521, 1491 cm^{-1}; mp decomposed. ^1H NMR (400 MHz, $CDCl_3$) δ 7.48 (s, 1H), 7.32–7.15 (m, 9H), 6.14 (br s, 2H), 5.84 (m, 1H), 4.49 (br s, 1H), 3.87 (s, 6H), 3.81 (s, 3H), 3.43 (br s, 1H), 2.69–2.63 (m, 2H), 2.42–2.37 (m, 1H), 2.13–2.06 (m, 2H); ^{13}C NMR (151 MHz, $CDCl_3$) δ 161.5, 158.9 (2C), 153.3, 147.8, 138.7, 131.9, 128.8 (2C), 128.6 (2C), 127.0, 126.9 (2C), 120.1 (2C), 109.5, 91.1 (2C), 56.1 (2C), 55.5, 46.0, 42.1, 38.6, 35.3. HRMS (FT-ICR, ESI) *m/z*: $[M + H]^+$ calcd for $C_{28}H_{30}ClN_2O_4$ 493.1889, found 493.1895.

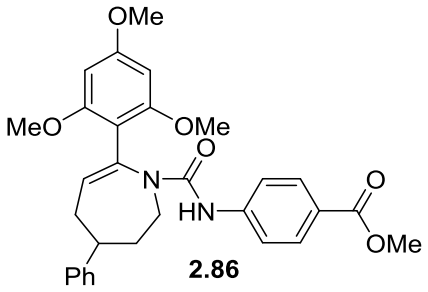

2.86

Methyl 4-(4-phenyl-7-(2,4,6-trimethoxyphenyl)-2,3,4,5-tetrahydro-1*H*-azepine-1-carboxamido)benzoate, 2.86. Following the general procedure E, $TMSN_3$ in HFIP was added to a solution of **2.1** (52.7 mg, 0.302 mmol, 1.0 equiv), $AlBr_3$ (87.2 mg, 0.327 mmol, 1.1 equiv), 1,3,5-trimethoxybenzene (252 mg, 1.50 mmol, 5.0 equiv) in HFIP. Then, following general procedure G to the crude residue in anhydrous THF (4.0 mL) was added methyl 4- isocyanatobenzoate (126 mg, 0.709 mmol, 2.3 equiv), DMAP (24.0 mg, 0.196 mmol, 0.65 equiv), and triethylamine (63.0 µL, 0.454 mmol, 1.5 equiv). Purification was carried out twice by an automated MPLC system; first using a 12 g normal phase silica column with gradient elution from 0–40% EtOAc/hexanes, and then using a 13 g C18 reverse phase column with 0–100% MeCN/H_2O gradient elution afforded **2.86** a white amorphous solid (77.2 mg, 0.149 mmol, 49% yield). R_f = 0.20 (20% EtOAc/hexanes); IR (neat) 3355, 2945, 1715, 1674, 1605, 1589, 1522 cm^{-1}; mp 105 ˚C decomposed. ^1H NMR (400 MHz, $CDCl_3$) δ 7.91 (m, 2H), 7.67 (s, 1H), 7.39 (m, 2H), 7.29 (m, 2H), 7.22 (m, 3H), 6.14 (s, 2H), 5.87 (m, 1H), 4.50 (br s, 1H), 3.89 (s, 6H), 3.86 (s, 3H), 3.80 (s, 3H), 3.45 (br s, 1H), 2.67 (m, 2H), 2.41 (m, 1H), 2.08 (m, 2H); ^{13}C NMR (151 MHz, $CDCl_3$) δ 167.1, 161.5, 158.8 (2C), 153.0, 147.7, 144.4, 134.9, 132.2, 130.8 (2C), 128.7 (2C), 126.9 (2C), 126.3, 123.4, 117.7 (2C), 109.3, 91.1 (2C), 56.1 (2C), 55.5, 51.9, 46.1, 42.1, 38.6, 35.3. HRMS (FT-ICR, ESI) *m/z*: $[M + H]^+$ calcd for $C_{30}H_{33}N_2O_6$ 517.2333, found 517.2327.

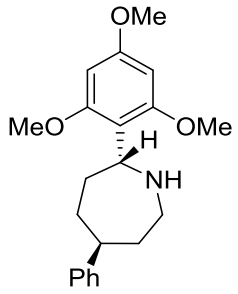

2.87

(2*R*,5*S*)-5-Phenyl-2-(2,4,6-trimethoxyphenyl)azepane, 2.87. Following the general procedure E, $TMSN_3$ in HFIP was added to a solution of **2.1** (52.3 mg, 0.300 mmol, 1.0 equiv), $AlBr_3$ (87.7 mg, 0.329 mmol, 1.1 equiv), 1,3,5-trimethoxybenzene (252 mg, 1.50 mmol, 5.0 equiv) in HFIP. Then, following the general procedure H to the crude residue in anhydrous MeOH (3.0 mL) was added sodium borohydride (23.0 mg, 0.608 mmol, 2.0 equiv). Purification by an automated MPLC system on a 12 g normal phase silica column with gradient elution from 0–12% MeOH (0.5% NH_4OH)/CH_2Cl_2) afforded **2.87** as a cream amorphous solid (78.2 mg, 0.229 mmol, 76% yield, dr 20:1). R_f = 0.49 (20% EtOAc/hexanes); IR (neat) 3372, 3027, 2996, 2921, 2837, 1598, 1585, 1117, 670 cm^{-1}; mp 123–126 ˚C. ^1H NMR (500 MHz, $CDCl_3$) δ 7.30 (m, 2H), 7.24 (m, 2H), 7.18 (m, 1H), 6.13 (s, 2H), 4.56 (dd, *J* = 9.1, 6.0 Hz, 1H), 3.83 (s, 6H), 3.79 (s, 3H), 3.38 (dt, *J* = 14.4, 3.6 Hz, 1H), 2.94 (ddd, *J* = 12.0, 9.2, 3.0 Hz, 1H), 2.80 (ddd, *J* = 14.6, 12.1, 2.7 Hz, 1H), 2.23–2.08 (m, 2H), 2.02–1.96 (m, 2H), 1.94–1.81 (m, 2H); ^{13}C NMR (151 MHz, $CDCl_3$) δ 159.9 (2C), 158.1, 149.6, 128.6 (2C), 126.7 (2C), 125.8, 115.1, 91.3 (2C), 55.9 (2C), 55.5, 54.0, 50.6, 45.0, 42.4, 34.4, 33.9. HRMS (FT-ICR, ESI) *m/z*: $[M + H]^+$ calcd for $C_{21}H_{28}NO_3$ 342.2064, found 342.2060.

Alternatively, following the general procedure H, to a solution of **2.39** (85.0 mg, 0.202 mmol, 1.0 equiv) in anhydrous MeOH (3.0 mL) was added sodium borohydride (15.0 mg, 0.397 mmol, 2.0 equiv). Purification by an automated MPLC system on a 12 g normal phase silica

column with gradient elution from 0–12% MeOH(0.5%NH_4OH)/CH_2Cl_2 afforded **2.87** as a cream amorphous solid (63.3 mg, 0.185 mmol, 92% yield). Characterization data was consistent with the above entry.

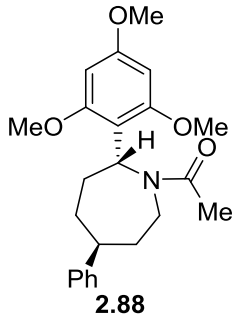

2.88

1-((2*R*,5*S*)-5-Phenyl-2-(2,4,6-trimethoxyphenyl)azepanyl)ethanone, 2.88. Following the general procedure E, $TMSN_3$ in HFIP was added to a solution of **2.1** (52.5 mg, 0.301 mmol, 1.0 equiv), $AlBr_3$ (81.1 mg, 0.304 mmol, 1.0 equiv), 1,3,5-trimethoxybenzene (251 mg, 1.49 mmol, 5.0 equiv) in HFIP. Then, following the general procedure H to the crude residue in anhydrous MeOH (3.0 mL) was added sodium borohydride (23.0 mg, 0.608 mmol, 2.0 equiv). Following reaction work-up, to a solution of crude residue in anhydrous CH_2Cl_2 (3.0 mL) was added di-*tert*-butyl carbonate (0.21 mL, 0.910 mmol, 3.0 equiv) and DMAP (7.40 mg, 0.061 mmol, 0.2 equiv). The reaction mixture was stirred at room temperature for 24 h under argon atmosphere. Purification by an automated MPLC system on a 12 g normal phase silica column with gradient elution from 0–3% MeOH/CH_2Cl_2 afforded **2.88** as a white sticky (low boiling) solid (87.7 mg, 0.229 mmol, 76% yield) as a mixture of rotamers (ratio = 76:24). R_f = 0.33 (2% MeOH/CH_2Cl_2); IR (neat) 2921, 2846, 1643, 1602, 1584 cm^{-1}. Diagnostic peaks of major rotamer: ^1H NMR (400 MHz, $CDCl_3$) δ 7.33–7.28 (m, 4H), 7.22–7.26 (m, 1H), 6.09 (s, 2H), 5.25 (dd, *J* = 12.2, 4.0 Hz, 1H), 4.42 (ddd, *J* = 14.6, 4.9, 3.7 Hz, 1H), 3.78 (s, 3H), 3.76 (s, 6H), 3.73–3.67 (m, 1H), 3.05 (m, 1H), 2.38–1.88 (complex, 8H, contains s, 1.93, 3H), 1.66 (m, 1H); ^{13}C NMR (101 MHz, $CDCl_3$) δ

171.8, 160.3 (2C), 158.3, 145.7, 128.5 (2C), 127.6 (2C), 125.9, 112.1, 91.0 (2C), 55.8 (2C), 55.4, 54.6, 39.1, 39.0, 33.3, 33.2, 28.8, 21.7. Diagnostic peaks of minor rotamer: ^{1}H NMR (400 MHz, $CDCl_3$) δ 6.09 (s, 2H), 5.74 (dd, *J* = 13.1, 3.8 Hz, 1H), 4.20 (ddd, *J* = 16.1, 11.3, 5.0 Hz, 1H), 3.80 (s, 3H), 2.75 (s, 6H), 2.08 (s, 3H); ^{13}C NMR (101 MHz, $CDCl_3$) δ 170.2, 159.7, 158.7, 145.8, 128.5, 127.5, 126.2, 113.6, 91.6, 56.1, 55.4, 51.9, 42.4, 34.4, 33.2, 28.3, 27.3, 22.3. HRMS (FT-ICR, ESI) *m/z*: $[M + H]^+$ calcd for $C_{23}H_{30}NO_4$ 384.2169, found 384.2177.

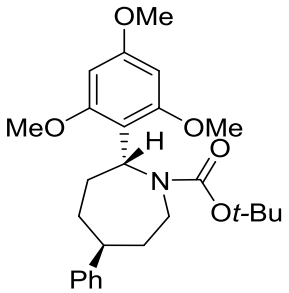

2.89

***tert*-Butyl (2*R*,5*S*)-5-Phenyl-2-(2,4,6-trimethoxyphenyl)azepane-1-carboxylate, 2.89.** Following the general procedure E, $TMSN_3$ in HFIP was added to a solution of **2.1** (52.6 mg, 0.302 mmol, 1.0 equiv), $AlBr_3$ (80.4 mg, 0.301 mmol, 1.0 equiv), 1,3,5-trimethoxybenzene (252 mg, 1.50 mmol, 5.0 equiv) in HFIP. Then, following the general procedure H to the crude residue in anhydrous MeOH (3.0 mL) was added sodium borohydride (22.0 mg, 0.582 mmol, 1.9 equiv). Following reaction work-up, to a solution of crude residue in anhydrous CH_2Cl_2 (3.0 mL) was added di-*tert*-butyl carbonate (0.17 mL, 0.730 mmol, 2.4 equiv) and DMAP (14.0 mg, 0.115 mmol, 0.4 equiv). The reaction mixture was stirred at room temperature for 24 h under argon atmosphere. Purification by an automated MPLC system on a 12 g normal phase silica column with gradient elution from 0–20% EtOAc/hexanes afforded **2.89** as a colorless sticky (low boiling) solid (101 mg, 0.302 mmol, 76% yield) as a mixture of rotamers (ratio = 79:21). R_f = 0.25 (15% EtOAc/hexanes); IR (neat) 2929, 1682, 1590, 1401 cm^{-1}. Diagnostic peaks of major rotamer: ^{1}H

NMR (400 MHz, $CDCl_3$) δ 7.32–7.27 (m, 4H), 7.18 (m, 1H), 6.07 (s, 2H), 5.34 (dd, *J* = 12.3, 3.6 Hz, 1H), 4.09 (m, 1H), 3.82–3.74 (complex, 10H, contains s, 3.79, 3H; s, 3.74, 6H), 3.06 (m, 1H), 2.27–1.90 (complex, 5H), 1.64 (m, 1H), 1.41 (s, 3H), 1.24 (s, 6H); ^{13}C NMR (151 MHz, $CDCl_3$) δ 159.5 (2C), 158.4, 156.4, 146.2, 128.4 (2C), 127.6 (2C), 125.8, 114.4, 90.7 (2C), 78.8, 55.7 (2C), 55.4, 52.9, 39.9, 39.5, 34.2, 33.2, 28.5 (3C), 28.1. Diagnostic peaks of minor rotamer: ^1H NMR (400 MHz, $CDCl_3$) δ 5.53 (m, 1H); ^{13}C NMR (101 MHz, $CDCl_3$) δ 158.7, 156.0, 146.5, 125.8, 114.0, 91.7, 78.6, 565.2, 52.6, 40.9, 39.4, 28.8, 28.2. HRMS (FT-ICR, ESI) *m/z*: $[M + Na]^+$ calcd for $C_{26}H_{35}NO_5$ 464.2407 found, 464.2389.

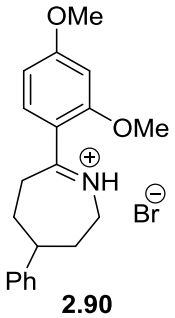

2.90

7-(2,4-Dimethoxyphenyl)-4-phenyl-3,4,5,6-tetrahydro-2*H*-azepinium Bromide, 2.90. To a solution of **2.1** (53.0 mg, 0.304 mmol, 1.0 equiv) and $AlBr_3$ (85.0 mg, 0.319 mmol, 1.1 equiv) in HFIP (1.0 mL) in a flame-dried nitrogen-flushed 25 mL round bottom was added a solution of $TMSN_3$ (80.0 μL, 0.603 mmol, 2.0 equiv) in HFIP (2.0 mL) using a syringe pump (0.40 mL/h, 14.00 mm diameter, and 20 gauge needle) over 6 h at room temperature. Following slow addition, 1,3-dimethoxybenzene (200 μL, 1.53 mmol, 5.2 equiv) was added and the reaction mixture was stirred for an additional 15 h. The reaction mixture was concentrated under nitrogen, the crude residue was redissolved in CH_2Cl_2 (~40 mL), filtered to remove residual solids, and concentrated. Conversion of 65% (76.8 mg, 0.197 mmol) to **2.89** was determined by ^1H NMR of the crude reaction mixture using benzyl benzoate as an internal standard. Purification by an automated

MPLC system using on a 12 g normal phase silica column with gradient elution from 0–7% MeOH/CH_2Cl_2 afforded **2.90** as a colorless sticky (low boiling) solid (50.9 mg, 0.130 mmol, 43% yield). R_f = 0.29 (4% MeOH/CH_2Cl_2); IR (neat) 2922, 1598 cm^{-1}. ^1H NMR (600 MHz, $CDCl_3$) δ 7.72 (d, *J* = 8.7 Hz, 1H), 7.31 (t, *J* = 7.6 Hz, 2H), 7.23 (t, *J* = 7.4 Hz, 1H), 7.17 (m, 2H), 6.61 (dd, *J* = 8.8, 2.3 Hz, 1H), 6.50 (d, *J* = 2.3 Hz, 1H), 4.54 (dd, *J* = 13.7, 5.9 Hz, 1H), 3.93 (s, 3H), 3.87 (s, 3H), 3.72 (m, 1H), 3.35 (dd, *J* = 14.4, 7.3 Hz, 1H), 2.97 (m, 1H), 2.87 (m, 1H), 2.17–2.07 (m, 2H), 1.85 (m, 1H), 1.74 (q, *J* = 12.5 Hz, 1H); ^{13}C NMR (151 MHz, $CDCl_3$) δ 181.8, 165.6, 160.7, 145.9, 132.9, 128.9 (2C), 126.9, 126.8 (2C), 117.5, 105.9, 99.1, 56.3, 56.0, 48.8, 48.4, 33.4, 32.9, 30.2. HRMS (FT-ICR, ESI) *m/z*: $[M - Br]^+$ calcd for $C_{20}H_{24}NO_2$ 310.1802, found 310.1800.

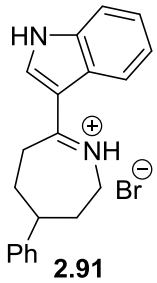

2.91

7-(1*H*-indol-3-yl)-4-phenyl-3,4,5,6-tetrahydro-2*H*-azepinium Bromide, 2.91. To a solution of **2.1** (52.5 mg, 0.301 mmol, 1.0 equiv) and $AlBr_3$ (82.8 mg, 0.310 mmol, 1.0 equiv) in HFIP (1.0 mL) in a flame-dried nitrogen-flushed 25 mL round bottom flask was added a solution of $TMSN_3$ (80.0 μL, 0.603 mmol, 2.0 equiv) in HFIP (2.0 mL) using a syringe pump (0.40 mL/h, 14.00 mm diameter, and 20 gauge needle) over 6 h at room temperature. Following 3 h slow addition, 1H-indole (90.0 mg, 0.768 mmol, 2.6 equiv) was added, and then after 6 h additional 1H-indole (90.0 mg, 0.768 mmol, 2.6 equiv) was added and the reaction mixture was stirred for an additional 15 h. The reaction mixture was concentrated under nitrogen, the crude residue was redissolved in CH_2Cl_2 (ca. 40 mL), filtered to remove residual solids, and concentrated. Purification carried out twice by an automated MPLC system using a 15.5 g C18 reverse phase

column with gradient elution from 0–100% MeCN/H_2O afforded **2.91** as a cream amorphous solid (58.6 mg, 0.159 mmol, 53% yield). RT = 1.80 (UPLC, MeOH(0.05% CH_2O_2)/H_2O); mp decomposed; IR (neat) 3024, 2912, 1603, 1580, 1433 cm^{-1}. ^1H NMR (600 MHz, $CDCl_3$) δ 8.34 (br s, 1H), 8.05 (s, 1H), 7.74 (d, *J* = 8.0 Hz, 1H), 7.33–7.23 (m, 6H), 7.16 (d, *J* = 7.6Hz, 1H), 4.48 (m, 1H), 3.71 (m, 1H), 2.97 (m, 1H), 2.84 (t, *J* = 13.3 Hz, 1H), 2.21 (m, 2H), 1.86 (q, *J* = 12.7 Hz, 1H), 1.65 (q, *J* = 12.9 Hz, 1H); ^{13}C NMR (151 MHz, $CDCl_3$) δ 177.4, 145.0, 137.8, 137.6, 129.0 (2C), 127.2, 126.7 (2C), 124.6, 124.0, 123.8, 120.8, 114.3, 109.4, 48.3, 45.8, 33.8, 32.1, 30.6. HRMS (FT-ICR, ESI) *m/z*: $[M - Br]^+$ calcd for $C_{20}H_{21}BrN_2$ 289.1699, found 289.1688.

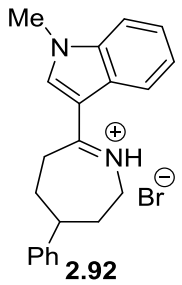

2.92

7-(1-Methyl-1*H*-indol-3-yl)-4-phenyl-3,4,5,6-tetrahydro-2*H*-azepin-1-ium bromide, 2.92. To a solution of **2.1** (52.6 mg, 0.302 mmol, 1.0 equiv) and $AlBr_3$ (83.3 mg, 0.312 mmol, 1.0 equiv) in HFIP (1.0 mL) in a flame-dried nitrogen-flushed 25 mL round bottom flask was added a solution of $TMSN_3$ (80.0 μL, 0.603 mmol, 2.0 equiv) in HFIP (2.0 mL) using a syringe pump (0.40 mL/h, 14.00 mm diameter, and 20 gauge needle) over 6 h at room temperature. Following 3 h slow addition, 1-methyl-1H-indole (100 μL, 0.801 mmol, 2.7 equiv) was added, and then after 6 h additional 1-methyl-1H-indole (100 μL, 0.801 mmol, 2.7 equiv) was added and the reaction mixture was stirred for an additional 15 h. The reaction mixture was concentrated under nitrogen, the crude residue was redissolved in CH_2Cl_2 (ca. 40 mL), filtered to remove residual solids, and concentrated. Purification carried out twice by an automated MPLC system using a 15.5 g C18 reverse phase column with gradient elution from 0–100% MeCN/H_2O afforded **2.92** as an orange

amorphous solid (51.7 mg, 0.135 mmol, 45% yield). RT = 1.87 (UPLC, MeOH(0.05% CH_2O_2)/H_2O); mp decomposed; IR (neat) 3022, 2932, 1605, 1579, 1531 cm^{-1}. ^1H NMR (400 MHz, $CDCl_3$) δ 12.6 (br s, 1H), 9.42 (s, 1H), 7.88 (d, *J* = 7.4 Hz, 1H), 7.47–7.44 (m, 1H), 7.42–7.37 (m, 2H), 7.34–7.30 (m, 2H), 7.24 (m, 1H), 7.18–7.15 (m, 2H), 4.42 (dt, *J* = 13.4, 6.3 Hz, 1H), 3.96 (s, 3H), 3.87 (dd, *J* = 14.6, 7.8 Hz, 1H), 3.75 (m, 1H), 3.03 (m, 2H), 2.36 (m, 1H), 2.18 (m, 1H), 1.97–1.78 (m, 2H); ^{13}C NMR (151 MHz, $CDCl_3$) δ 177.5, 145.0, 140.7, 138.5, 129.0 (2C), 127.3, 126.7 (2C), 125.9, 124.5, 124.4, 120.2, 111.7, 108.5, 48.6, 45.1, 34.7, 33.7, 31.6, 30.2. HRMS (FT-ICR, ESI) *m/z*: $[M - Br]^+$ calcd for $C_{21}H_{23}BrN_2$ 303.1856, found 303.1844. Anal. calcd. for $C_{21}H_{23}BrNO_2$: C 65.80, H 6.05, N 7.31, found C 66.12, H 6.07, N 7.15.

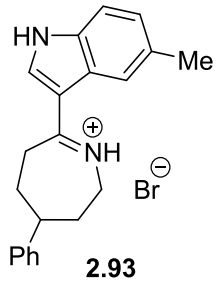

2.93

7-(5-Methyl-1*H*-indol-3-yl)-4-phenyl-3,4,5,6-tetrahydro-2*H*-azepinium Bromide, 2.93. To a solution of **2.1** (52.5 mg, 0.301 mmol, 1.0 equiv) and $AlBr_3$ (83.9 mg, 0.315 mmol, 1.1 equiv) in HFIP (1.0 mL) in a flame-dried nitrogen-flushed 25 mL round bottom flask was added a solution of $TMSN_3$ (80.0 μL, 0.600 mmol, 2.0 equiv) in HFIP (2.0 mL) using a syringe pump (0.40 mL/h, 14.00 mm diameter, and 20 gauge needle) over 6 h at room temperature. Following 3 h slow addition, 5-methyl-1H-indole (100 mg, 0.762 mmol, 2.5 equiv) was added, and then after 6 h additional 5-methyl-1H-indole (100 mg, 0.762 mmol, 2.5 equiv) was added and the reaction mixture was stirred for an additional 15 h. The reaction mixture was concentrated under nitrogen, the crude residue was redissolved in CH_2Cl_2 (~40 mL), filtered to remove residual aluminum, and concentrated. Purification was carried out twice by an automated MPLC system; first, using a 15.5

g C18 reverse phase column with gradient elution from 0–50% MeCN/H_2O, and then using a 12 g normal phase silica column with gradient elution from 0–8% MeOH/CH_2Cl_2 afforded **2.93** as a pale cream amorphous solid (40.2 mg, 0.105 mmol, 35% yield). RT = 1.88 (UPLC, MeOH(0.05% CH_2O_2)/H_2O); mp decomposed; IR (neat) 2918, 1603, 1586, 1516, 1434 cm^{-1}. ^1H NMR (400 MHz, $CDCl_3$) δ 8.37 (br s, 1H), 7.85 (s, 1H), 7.63 (d, *J* = 8.3 Hz, 1H), 7.33–7.29 (m, 2H), 7.26–7.21 (m, 2H), 7.16–7.10 (m, 3H), 4.44 (dd, *J* = 14.4, 5.6 Hz, 1H), 3.69 (m, 1H), 3.41 (m, 1H), 2.96 (m, 1H), 2.80 (m, 1H), 2.51 (m, 3H), 2.23–2.15 (m, 2H), 1.83 (q, *J* = 12.7 Hz, 1H), 1.61 (q, *J* = 12.8 Hz, 1H); ^{13}C NMR (151 MHz, $CDCl_3$) δ 177.2, 145.1, 137.5, 136.2, 133.9, 129.0 (2C), 127.2, 126.7 (2C), 126.1, 124.2, 120.6, 114.0, 109.0, 48.4, 45.6, 34.0, 31.9, 30.6, 21.9. HRMS (FT-ICR, ESI) *m/z*: $[M - Br]^+$ calcd for $C_{21}H_{23}BrN_2$ 303.1856, found 303.1850. Anal. calcd. for $C_{21}H_{22.95}Br_{0.95}N_2$: C 66.50, H 6.10, N 7.39, found C 66.51, H 6.49, N 7.03.

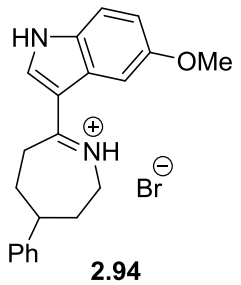

2.94

7-(5-Methoxy-1*H*-indol-3-yl)-4-phenyl-3,4,5,6-tetrahydro-2*H*-azepinium Bromide, 2.94. To a solution of **2.1** (52.5 mg, 0.301 mmol, 1.0 equiv) and $AlBr_3$ (83.7 mg, 0.314 mmol, 1.0 equiv) in HFIP (1.0 mL) in a flame-dried nitrogen-flushed 25 mL round bottom flask was added a solution of $TMSN_3$ (80.0 μL, 0.603 mmol, 2.0 equiv) in HFIP (2.0 mL) using a syringe pump (0.40 mL/h, 14.00 mm diameter, and 20 gauge needle) over 6 h at room temperature. Following 3 h slow addition, 5-methoxy-1H-indole (110 mg, 0.747 mmol, 2.5 equiv) was added, and then after 6 h additional 5-methyl-1H-indole (110 mg, 0.747 mmol, 2.5 equiv) was added and the reaction mixture was stirred for an additional 15 h. The reaction mixture was concentrated under nitrogen,

the crude residue was redissolved in CH_2Cl_2 (ca. 40 mL), filtered to remove residual aluminum, and concentrated. Purification was carried out twice by an automated MPLC system; first, using a 50.0 g C18 reverse phase column with gradient elution from 0–100% MeCN/H_2O, and then using a 12 g normal phase silica column with gradient elution from 0–8% MeOH/CH_2Cl_2 afforded **2.94** as a cream amorphous solid (57.0 mg, 0.143 mmol, 47% yield). RT = 1.73 (UPLC, MeOH(0.05% CH_2O_2)/H_2O); mp decomposed; IR (neat) 2918, 1604, 1516, 1486, 1440 cm^{-1}. ^1H NMR (400 MHz, $CDCl_3$) δ 7.82 (br s, 1H), 7.59 (s, 1H), 7.52 (d, *J* = 8.9 Hz, 1H), 7.34–7.31 (m, 2H), 7.28–7.22 (m, 4H), 6.90 (m, 1H), 4.59 (dd, *J* = 14.5, 5.5 Hz, 1H), 4.07 (s, 3H), 3.65 (m, 1H), 3.17 (m, 1H), 2.93 (m 1H), 2.78 (m, 1H), 2.19 (m, 2H), 1.87 (m, 1H), 1.63 (m, 1H); ^{13}C NMR (151 MHz, $CDCl_3$) δ 176.1, 157.2, 145.2, 137.7, 132.3, 129.0 (2C), 127.2, 126.8 (2C), 124.1, 115.2, 114.9, 109.3, 103.0, 56.7, 48.5, 45.9, 33.9, 32.6, 31.1. HRMS (FT-ICR, ESI) *m/z*: $[M - Br]^+$ calcd for $C_{21}H_{23}BrN_2O$ 319.1805, found 319.1797.

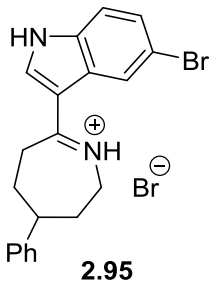

2.95

7-(5-Bromo-1*H*-indol-3-yl)-4-phenyl-3,4,5,6-tetrahydro-2*H*-azepinium Bromide, 2.95. To a solution of **2.1** (52.6 mg, 0.302 mmol, 1.0 equiv) and $AlBr_3$ (88.1 mg, 0.330 mmol, 1.1 equiv) in HFIP (1.0 mL) in a flame-dried nitrogen-flushed 25 mL round bottom flask was added a solution of $TMSN_3$ (80.0 μL, 0.600 mmol, 2.0 equiv) in HFIP (2.0 mL) using a syringe pump (0.40 mL/h, 14.00 mm diameter, and 20 gauge needle) over 6 h at room temperature. Following 3 h slow addition, 5-bromo-1H-indole (150 mg, 0.765 mmol, 2.5 equiv) was added, and then after 6 h additional 5-bromo-1H-indole (150 mg, 0.765 mmol, 2.5 equiv) was added and the reaction

mixture was stirred for an additional 15 h. The reaction mixture was concentrated under nitrogen, the crude residue was redissolved in CH_2Cl_2 (ca. 40 mL), filtered to remove residual aluminum, and concentrated. Purification by an automated MPLC system using a 15.5 g C18 reverse phase column with gradient elution from 0–100% MeCN/H_2O afforded **2.95** as a pale brown amorphous solid (69.5 mg, 0.155 mmol, 51% yield). RT = 1.92 (UPLC, MeOH (0.05% CH_2O_2)/H_2O); mp decomposed; IR (neat) 3082, 1611, 1518, 1451 cm^{-1}. ^1H NMR (400 MHz, $CDCl_3$) δ 12.6 (br s, 1H), 11.6 (br s, 1H), 8.56 (s, 1H), 8.09 (s, 1H), 7.57 (dd, *J* = 8.7 Hz, 1H), 7.30–7.25 (m, 3H), 7.23–7.18 (m, 1H), 7.12 (m, 2H), 4.45 (m, 1H), 3.82 (m, 1H), 3.49 (dd, *J* = 14.6, 7.5 Hz, 1H), 2.98 (m, 2H), 2.25 (m, 1H), 2.15 (m, 1H), 1.86 (q, *J* = 12.3, 1H), 1.67 (q, *J* = 12.6 Hz, 1H); ^{13}C NMR (151 MHz, $CDCl_3$) δ 177.7, 144.9, 137.8, 136.4, 129.0 (2C), 127.5, 127.2, 126.7 (2C), 125.6, 123.0, 117.5, 115.8, 108.8, 48.4, 46.0, 33.6, 32.3, 30.4. HRMS (FT-ICR, ESI) *m/z*: $[M - Br]^+$ calcd for $C_{20}H_{20}Br_2N_2$ 367.0804, found 367.0804.

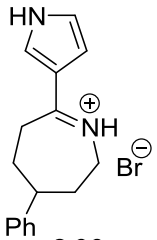

2.96

4-Phenyl-7-(1*H*-pyrrol-3-yl)-3,4,5,6-tetrahydro-2*H*-azepinium Bromide, 2.96. To a solution of **2.1** (52.3 mg, 0.300 mmol, 1.0 equiv) and $AlBr_3$ (82.4 mg, 0.309 mmol, 1.0 equiv) in HFIP (1.0 mL) in a flame-dried nitrogen-flushed 25 mL round bottom flask was added a solution of $TMSN_3$ (80.0 μL, 0.600 mmol, 2.0 equiv) in HFIP (2.0 mL) using a syringe pump (0.40 mL/h, 14.00 mm diameter, and 20 gauge needle) over 6 h at room temperature. Following slow addition, 1H-pyrrole (104 μL, 1.50 mmol, 5.0 equiv) was added and the reaction mixture was stirred for an additional 15 h. The reaction mixture was concentrated under nitrogen, the crude residue was

redissolved in CH_2Cl_2 (ca. 40 mL), filtered to remove residual solids, and concentrated. Purification by an automated MPLC system using a 15.5 g C18 reverse phase column with gradient elution from 0–100% MeCN/H_2O afforded **2.96** as a pale brown amorphous solid (39.1 mg, 0.122 mmol, 41% yield). RT = 1.55 (UPLC, MeOH (0.05% CH_2O_2)/H_2O); mp decomposed; IR (neat) 3142, 3080, 3007, 2926, 2869, 1626 cm^{-1}. ^1H NMR (400 MHz, $CDCl_3$) δ 13.0 (br s, 1H), 12.6 (br s, 1H), 7.53 (m, 1H), 7.34–7.31 (m, 2H), 7.27–7.20 (m, 2H), 7.15 (m, 2H), 6.45 (dt, *J* = 4.3, 2.2 Hz, 1H), 4.20–4.12 (m, 1H), 3.70 (ddd, *J* = 15.1, 11.4, 4.5 Hz, 1H), 3.40 (dd, *J* = 14.8 , 7.6 Hz, 1H), 2.95 (tt, *J* = 12.3, 3.6 Hz, 1H), 2.86 (dd, *J* = 14.6, 12.1 Hz, 1H), 2.27 (m, 1H), 2.17 (m, 1H), 1.87 (m, 1H), 1.70 (m, 1H); ^{13}C NMR (151 MHz, $CDCl_3$) δ 169.0, 144.9, 134.4, 129.1 (2C), 127.3, 126.7 (2C), 125.6, 124.5, 113.5, 48.5, 45.1, 33.9, 31.2, 30.3. HRMS (FT-ICR, ESI) *m/z*: $[M - Br]^+$ calcd for $C_{16}H_{19}BrN_2$ 239.1543, found 239.1542.

2.6 References

1. Wrobleski, A.; Coombs, T. C.; Huh, C. W.; Li, S.-W.; Aubé, J., The Schmidt Reaction. In *Organic Reactions*, John Wiley & Sons, Inc.: 2012; Vol. 78, pp 1-320.

2. Wolff, H., The Schmidt Reaction. In *Organic Reactions*, John Wiley & Sons, Inc.: 1946; Vol. 3, pp 307-332.

3. Smith, P. A. S. Schmidt Reaction: Experimental Conditions and Mechanism. *J. Am. Chem. Soc.* **1948**, *70*, 320-323.

4. Motiwala, H. F.; Fehl, C.; Li, S.-W.; Hirt, E.; Porubsky, P.; Aubé, J. Overcoming Product Inhibition in Catalysis of the Intramolecular Schmidt Reaction. *J. Am. Chem. Soc.* **2013**, *135*, 9000-9009.

5. Aube, J.; Milligan, G. L. Intramolecular Schmidt Reaction of Alkyl Azides. *J. Am. Chem. Soc.* **1991**, *113*, 8965-8966.

6. Nishiyama, K.; Wang, C.; Lebel, H., Azidotrimethylsilane. In *Encyclopedia of Reagents for Organic Synthesis*, John Wiley & Sons, Ltd: 2001.

7. Motiwala, H. F.; Charaschanya, M.; Day, V. W.; Aubé, J. Remodeling and Enhancing Schmidt Reaction Pathways in Hexafluoroisopropanol. *J. Org. Chem.* **2016**, *81*, 1593-1609.

8. Gawley, R. E., The Beckmann Reactions: Rearrangements, Elimination–Additions, Fragmentations, and Rearrangement–Cyclizations. In *Organic Reactions*, John Wiley & Sons, Inc.: 2004; Vol. 35, pp 1-420.

9. Grob, C. A.; Fischer, H. P.; Raudenbusch, W.; Zergenyi, J. Fragmentation Reactions. VII. Beckmann Rearrangement and Fragmentation. *Helv. Chim. Acta.* **1964**, *47*, 1003-1021.

10. Heldt, W. Z. Beckmann Rearrangement. III. Rearrangement of Oxime p-Toluenesulfonates in Chloroform, Acetic acid, and Methanol. *J. Org. Chem.* **1961**, *26*, 1695-1702.

11. Huitric, A. C.; Nelson, S. D., Jr. Beckmann Rearrangement and Fission of 2-Arylcyclohexanone Oxime Tosylates. Trapping of Carbonium Ion Intermediates as Pyridinium Cations. *J. Org. Chem.* **1969**, *34*, 1230-1233.

12. Sato, T.; Wakatsuka, H.; Amano, K. Beckmann Rearrangement of α,β-Unsaturated Ketoximes in Cyclic Systems: Migratory Aptitude of Olefinic Groups. *Tetrahedron* **1971**, *27*, 5381-5390.

13. Maruoka, K.; Miyazaki, T.; Ando, M.; Matsumura, Y.; Sakane, S.; Hattori, K.; Yamamoto, H. Organoaluminum-Promoted Beckmann Rearrangement of Oxime Sulfonates. *J. Am. Chem. Soc.* **1983**, *105*, 2831-2843.

14. Schinzer, D.; Bo, Y. Synthesis of Heterocycles by Tandem Reactions: Beckmann Rearrangements/Allylsilane Cyclizations. *Angew. Chem. Int. Ed.* **1991**, *30*, 687-688.

15. Schinzer, D.; Langkopf, E. Beckmann Rearrangements/Allylsilane Cyclizations: Approach to the Pentacyclic Cephalotaxine-Framework and the Influence of the Terminating Silicon Group. *Synlett* **1994**, *1994*, 375-377.

16. Schinzer, D.; Abel, U.; Jones, P. G. Asymmetric Tandem Reaction: Beckmann Rearrangements/ Allylsilane Cyclizations: Approach to the Optically Active Cephalotaxine-Framework. *Synlett* **1997**, *1997*, 632-634.

17. Sakane, S.; Matsumura, Y.; Yamamura, Y.; Ishida, Y.; Maruoka, K.; Yamamoto, H. Olefinic Cyclizations Promoted by Beckmann Rearrangement of Oxime Sulfonate. *J. Am. Chem. Soc.* **1983**, *105*, 672-674.

18. Kang, K.-T.; Sung, T.-M.; Jung, H.-C.; Lee, J.-G. Facile Synthesis of Various 1-Azabicyclo[n.4.0]alkanes via Beckmann Rearrangement/Allylsilane Cyclization. *Bull. Korean Chem. Soc.* **2008**, *29*, 1669-1670.

19. Litkei, G.; Patonay, T. Flavonoids. XXXVII. Ring Contraction and Ring Enlargement Reactions with Trimethylsilyl Azide in the Field of Flavonoids. *Acta Chim. Hung.* **1983**, *114*, 47-56.

20. Pramanik, S.; Ghorai, P. Trapping of Azidocarbenium Ion: A Unique Route for Azide Synthesis. *Org. Lett.* **2014**, *16*, 2104-2107.

21. Zhang, F.-L.; Wang, Y.-F.; Lonca, G. H.; Zhu, X.; Chiba, S. Amide Synthesis by Nucleophilic Attack of Vinyl Azides. *Angew. Chem. Int. Ed.* **2014**, *53*, 4390-4394.

22. Grant, T. N.; Rieder, C. J.; West, F. G. Interrupting the Nazarov Reaction: Domino and Cascade Processes Utilizing Cyclopentenyl Cations. *Chem. Commun.* **2009**, 5676-5688.

23. West, F. G.; Scadeng, O.; Wu, Y. K.; Fradette, R. J.; Joy, S., The Nazarov Cyclization. In *Comprehensive Organic Synthesis II* Elsevier: 2014; Vol. 5, pp 827-866.

24. Bender, J. A.; Blize, A. E.; Browder, C. C.; Giese, S.; West, F. G. Highly Diastereoselective Cycloisomerization of Acyclic Trienones. The Interrupted Nazarov Reaction. *J. Org. Chem.* **1998**, *63*, 2430-2431.

25. Britten, A. Z.; Bardsley, W. G.; Hill, C. M. Furano- and Pyrano-idolines-model Compounds for Indole Alkaloid Studies. *Tetrahedron* **1971**, *27*, 5631-5639.

26. Rosenmund, P.; Gektidis, S.; Brill, H.; Kalbe, R. Isoeserin Und Homoisoeserin, Darstellung Und Strukturaufklärung Des Indolo-1, 3-diazepin-systems. *Tetrahedron Lett.* **1989**, *30*, 61-62.

27. Schammel, A. W.; Chiou, G.; Garg, N. K. Synthesis of (+)-Phenserine Using an Interrupted Fischer Indolization Reaction. *J. Org. Chem.* **2012**, *77*, 725-728.

28. Boal, B. W.; Schammel, A. W.; Garg, N. K. An Interrupted Fischer Indolization Approach toward Fused Indoline-Containing Natural Products. *Org. Lett.* **2009**, *11*, 3458-3461.

29. Schammel, A. W.; Chiou, G.; Garg, N. K. Interrupted Fischer Indolization Approach toward the Communesin Alkaloids and Perophoramidine. *Org. Lett.* **2012**, *14*, 4556-4559.

30. Nishiyama, K.; Watanabe, A. Addition Reaction of Trimethylsilyl Azide towards Ketones and Facile Formation of Tetrazole Derivatives. *Chem. Lett.* **1984**, *13*, 455-458.

31. Yadav, J. S.; Reddy, B. V. S.; Reddy, U. V. S.; Praneeth, K. Azido-Schmidt Reaction for the Formation of Amides, Imides and Lactams from Ketones in the Presence of FeCl3. *Tetrahedron Lett.* **2008**, *49*, 4742-4745.

32. Khaksar, S. Fluorinated Alcohols: A Magic Medium for the Synthesis of Heterocyclic Compounds. *J. Fluorine Chem.* **2015**, *172*, 51-61.

33. Wu, L. Synthesis and Biological Evaluation of Novel 1,2-Naphthoquinones Possessing Tetrazolo[1,5-a]pyrimidine Scaffolds as Potent Antitumor Agents. *RSC Adv.* **2015**, *5*, 24960-24965.

34. Voitekhovich, S. V.; Lyakhov, A. S.; Ivashkevich, L. S.; Gaponik, P. N. Acid-Mediated Cycloalkylation of C-Aminoazoles with 2,5-Dimethylhexane-2,5-diol. *Tetrahedron Lett.* **2012**, *53*, 419-421.

35. Herbst, R. M.; Roberts, C. W.; Harvill, E. J. The Synthesis of 5-Aminotetrazole Derivatives. *J. Org. Chem.* **1951**, *16*, 139-149.

36. Finnegan, W. G.; Henry, R. A.; Lieber, E. Preparation and Isomerization of 5-Alkylaminotetrazoles. *J. Org. Chem.* **1953**, *18*, 779-91.

37. Boyer, J. H.; Miller, E. J. The Tetrazole-Azidoazomethine Equilibrium. *J. Am. Chem. Soc.* **1959**, *81*, 4671-4673.

38. Cacchi, S.; Palmieri, G.; Misiti, D. Reaction of 2[Prime or Minute]-hydroxychalcone with Hydrazoic Acid. *J. Chem. Soc., Perkin Trans. 1.* **1976**, 2371-2374.

39. Gracias, V.; Milligan, G. L.; Aube, J. Efficient Nitrogen Ring-Expansion Process Facilitated by in situ Hemiketal Formation. An Asymmetric Schmidt Reaction. *J. Am. Chem. Soc.* **1995**, *117*, 8047-8048.

40. Gracias, V.; Frank, K. E.; Milligan, G. L.; Aubé, J. Ring Expansion by in situ Tethering of Hydroxy Azides to Ketones: The Boyer Reaction. *Tetrahedron* **1997**, *53*, 16241-16252.

41. Aube, J.; Milligan, G. L.; Mossman, C. J. Titanium Tetrachloride-mediated Reactions of Alkyl Azides with Cyclic Ketones. *J. Org. Chem.* **1992**, *57*, 1635-1637.

42. Desai, P.; Schildknegt, K.; Agrios, K. A.; Mossman, C.; Milligan, G. L.; Aubé, J. Reactions of Alkyl Azides and Ketones as Mediated by Lewis Acids: Schmidt and Mannich Reactions Using Azide Precursors. *J. Am. Chem. Soc.* **2000**, *122*, 7226-7232.

43. Forsee, J. E.; Aubé, J. Hydrolysis of Iminium Ethers Derived from the Reaction of Ketones with Hydroxy Azides: Synthesis of Macrocyclic Lactams and Lactones. *J. Org. Chem.* **1999**, *64*, 4381-4385.

44. Vekariya, R. H.; Aubé, J. Hexafluoro-2-propanol-Promoted Intermolecular Friedel–Crafts Acylation Reaction. *Org. Lett.* **2016**, *18*, 3534-3537.

45. Motiwala, H. F.; Vekariya, R. H.; Aubé, J. Intramolecular Friedel–Crafts Acylation Reaction Promoted by 1,1,1,3,3,3-Hexafluoro-2-propanol. *Org. Lett.* **2015**, *17*, 5484-5487.

46. Carbery, D. R. Enamides: Valuable Organic Substrates. *Org. Biomol. Chem.* **2008**, *6*, 3455-3460.

47. Courant, T.; Dagousset, G.; Masson, G. Enamide Derivatives: Versatile Building Blocks for Total Synthesis. *Synthesis* **2015**, *47*, 1799-1856.

48. Forsee, J. E.; Aubé, J. Hydrolysis of Iminium Ethers Derived from the Reaction of Ketones with Hydroxy Azides: Synthesis of Macrocyclic Lactams and Lactones. *J. Org. Chem.* **1999**, *64*, 4381-4385.

Chapter 3

Enabling Chemistry Technologies:

High Temperature and High Pressure Continuous Flow Chemistry

3.1 Introduction

3.1.1 Advantages and Challenges in Flow Technology

Ongoing innovations in flow chemistry and continuous processing have emerged as tools that can significantly impact organic synthesis. Flow chemistry is an enabling technology that surpasses benchtop chemistry in many ways (Table 3.1).[1-8] Some advantages are attributed to the high surface-to-volume ratio within micro- and meso-structured flow systems. The small dimensions of a flow reactor permit the precise control of reaction variables and access to unprecedented process windows (e.g., high temperatures, pressures, concentrations)[2], which are challenging regimes to accomplish concomitantly in traditional chemistry. Continuous processing enables organic chemistry by providing additional opportunities that include the ability to perform multiple functions on a single integrated device (e.g., synthesis, purification, analysis, biological screening), accelerate the pace of discovery to production (e.g., automated reaction optimization, high-throughput library development, production-scale synthesis), and sustain green protocols of chemical synthesis (e.g., use of green solvents, reduction of material consumption and waste generation).[1-7] These innovative technologies have enhanced efficiency and improved safety profiles of chemical synthesis, essentially providing new approaches for performing organic chemistry.

Table 3.1. Advantages of continuous-flow processing.[1-7]

• Efficient mixing (micromixing)
• Efficient heat transfer and precise control of temperature (due to high surface-to-volume ratio)
• Process intensification: high-temperature and high-pressure capabilities
• Novel process window: access to a wider range of temperatures, pressures, and concentrations
• Control over multiple reaction variables (e.g., residence time, flow rate, reactor volume)
• Immobilization of catalysts and reagents
• Safer use of hazardous reagents, gases, and reactive intermediates
• Use of green solvents, low-boiling solvents, and access to supercritical fluid states
• Increased photon flux in photochemical reactions
• Reproducibility
• Integration of in-line purification, analytical techniques, and automation
• Multistep reactions in a continuous sequence
• Telescoping of reaction and purification processes
• Ease of scale-ups (e.g., increase the number of reactors or the reactor dimensions)

However, there are many challenges hampering the application of continuous-flow technologies toward routine organic synthesis.[1, 4, 6, 8-11] For example, many researchers are unfamiliar with flow techniques, and effective application of such techniques demands the understanding of both synthetic chemistry and engineering principles. Secondly, there are fundamental differences between batch and flow processes. The use of flow reactors is not straightforward, and has many challenges associated with technology maintenance including dissolution (managing solids), integration of reactor components (e.g., pumps, reactors, back-pressure regulators), and integration of multi-step processes (e.g., in-line analysis, purification, automation). The relative value of flow application should be evaluated by case and depends on various factors including reaction kinetics (e.g., Curtin-Hammett principle), safety (e.g., use of hazardous reagents, heat exchange, pressurized reactions), scalability, and others.[1, 8, 11] Principally, selecting the appropriate flow system requires a critical evaluation of factors governing the reaction of interest that would ultimately make the applications of flow processing impactful and advantageous over batch chemistry.

3.1.2 High-Temperature Chemistry

There is long-standing evidence that high-temperature chemistry using oil baths, hot plates, or reflux-apparatus speeds up synthetic transformations when compared to room temperature chemistry. In principle of the Arrhenius equation ($k = Ae^{-Ea/RT}$), the reaction rate increases exponentially as the absolute temperature is increased. However, under traditional heating conditions, reactions can still take up to days or weeks to complete and experiments are often limited by the solvent's boiling point. The introduction of microwave irradiation to organic synthesis has provided alternative means to rapidly heat reaction mixtures.[12-14] As a result of the microwave technology, there have been a plethora of protocols demonstrating reduced reaction times in comparison to traditional heating sources. Particularly, protocols that rapidly heat in sealed vessels to permit low boiling point solvents for high-temperature reactions, and synthetic transformations that require several hours to reach completion within minutes. As shown in Table 3.2, microwave technology offers several advantages over traditional chemistry, which includes rapid heating and experimentation above the boiling point of some solvents (limited by pressure <30 bar).[12-14] It has also become an essential tool in solvent-free and water-mediated reactions, whereby microwave-irradiation facilitates high-temperature homogeneity. Despite the wide adoption of microwave technology, there are some drawbacks compared to flow technology.[12-14] Similar to benchtop chemistry, syntheses developed in the laboratory often cannot become translated to large-scale production without substantial optimization. Specifically, heating and cooling profiles on small-scale microwave reactors cannot easily become duplicated on larger scale; microwave preparative quantities are generally limited to 30 mL reaction volumes.[8] Additionally, microwave-assisted reactions depend on the ability of the reaction mixture, particularly the solvent, to efficiently absorb microwave energy. Consequently, microwave

processing can become inefficient in cases of low absorptivity. Lastly, the low-pressure threshold (i.e., headspace limitations) of this technology impedes genuine high-temperature–high-pressure processing, which in turn, restricts the options of low-boiling solvents. Pressurized flow reactors eliminate headspace, thereby maintaining uniform reagent concentrations and efficiency with low-boiling reagents. As a consequence of the drawbacks in both traditional and microwave processing, efforts have been made toward high-temperature and high-pressure continuous-flow processing.

Table 3.2. Comparison of traditional heating, microwave reactor, and flow reactor.[8, 12-14]

Traditional heating	Microwave reactor	Flow reactor
+ High temperature (<200 ˚C; limited by the bp of solvent) – Atmospheric pressure – Not as efficient for either rapid heating or cooling	+ High temperature (<250 ˚C) + High pressure (<30 bar) + Rapid heating – Limited headspace (explosion possibility & reduced efficiency with low-boiling solvents)	+ High temperature (<450 ˚C) + High pressure (<200 bar) + Rapid heating + Back-pressure regulator + No headspace limitations
+ Heterogeneous reaction mixtures	+ Heterogeneous reaction mixtures	– Difficulties w/ heterogeneous reaction mixtures
+ Scalable w/ optimization	– Not scalable (limited to 30 mL)	+ Directly scalable

Thus, flow technology is a major advance towards high-temperature–high-pressure processing.[2, 7, 13] Applying a continuous-flow regime not only facilitates the replication of temperatures and pressures in traditional and microwave experimentations, but also provides many other advantages (as highlighted in Tables 3.1 and 3.2).[2, 7] Flow chemistry has an edge over conventional batch chemistry due to the smaller temperature gradients derived from the reactors' large surface-to-volume, which may play a role in heat transfer efficiency. In turn, reactors promoting efficient heat exchange are conducive to high-pressure conditions. This new mode of operation has significant appeal because it is an approach towards chemical space that has yet to be extensively explored and demonstrated. For example, high-pressure capabilities of flow devices has enabled possibilities to work with low-boiling solvents well beyond their boiling points,

replace solvents with liabilities, exploit reaction telescoping (e.g., simplifications in reaction work-up by evaporation of low-boiling solvents, eliminate isolation/purification sequences), and explore solvent reactivity near or in its supercritical state (i.e., changes in the physical properties of solvent under extreme conditions). A particularly important advantage of flow compared to conventional devices is the direct scalability with minimal optimization through the operation of multiple systems in parallel or related strategies. In fact, preparative scale high-temperature–high-pressure reactions are much safer in flow. Finally, additional to the intensifications of reaction conditions, flow technologies are amendable to integration with multiple devices facilitating the incorporation of various chemistry techniques and high-throughput chemical synthesis.

3.1.3 Examples of High-Temperature and High-Pressure Flow Chemistry

Common continuous-flow technologies for organic synthesis are commercially available (Figure 3.1). The majority of commercial reactors use either direct electric heating of a metallic coil (ThalesNano X-Cube Flash), or an Al heating block (Uniqsis Flow Syn). Alternatively, gas-heated or cooled chambers that accommodate a tube reactor have been incorporated in flow systems as well (Vapourtec R Series). Additionally, the standard use of back-pressure regulators in combination with HPLC or syringe pumps allows reaction mixtures to be processed safely at high pressures (typically 70–180 bar).[7, 13] In our investigations, we utilized the Phoenix Flow Reactor™ commercially available from ThalesNano.

(a)  (b) 

(c) 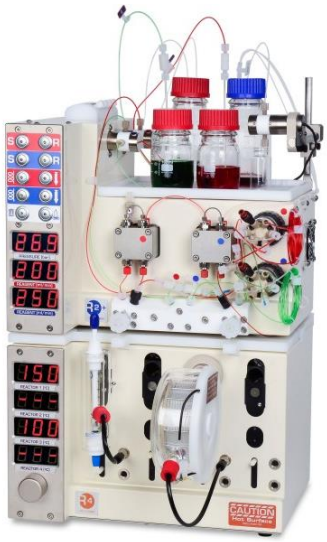

Figure 3.1. Commercially available continuous flow reactors for high-temperature organic synthesis. (a) ThalesNano X-Cube Flash™ (350 ˚C, 180 bar). (b) Uniqsis FlowSyn (260 ˚C, 70 bar). (c) Vapourtec R4 Reactor (250 ˚C, 50 bar). Images adapted from commercial websites.[15-17]

There are many aspects of synthesis and stages in medicinal chemistry that can be accomplished in flow devices in the pharmaceutical industry: (1) synthesis of a few milligrams or multigram scale of compound for drug discovery, (2) synthesis of building blocks for parallel synthesis in drug discovery, (3) multi-step reaction sequences in flow, (4) preparation of kilogram quantities of drug candidate for clinical research, and (5) production of drug molecules for marketing.[2-3, 5-6] Ultimately, process improvements in either of the above noted points have the potential to reduce manufacturing cost and cycle time, as well as, streamline the journey from early discovery to production.

3.1.4 Instrumentation: The Phoenix Flow Reactor™ Platform

In our investigations, we modified a commercially available high-temperature and high-pressure Phoenix Flow Reactor™ from ThalesNano. This commercial flow reactor is a coil consisting of a stainless steel tubing (Hastelloy, 1.0 mm in diameter) of variable length (variable

volume) that is wrapped around a metallic housing tube placed inside an insulated chamber (Figure 3.2a). In our set-up, a stainless steel tubing of 8-mL volume was used. The coil directly heats across the full length and can achieve temperatures as high as 450 ˚C. Within the reactor body, we added a temperature probe outside the coil in order to better monitor the reaction temperature. Further, we realized equilibration to the desired temperature of the reactor (approximately 30 minutes) was necessary prior to experimentations and only for the first run each day. The platform operated through 4 main components: (1) the Phoenix Flow Reactor™, (2) a manual injection valve, (3) a JASCO PU-2085 Plus HPLC pump, and (4) a JASCO BP-2080 Plus back-pressure regulator (Figure 3.2b). The HPLC pump allowed for a continuous-flow of reaction mixtures into the coil with variable flow rates from 0.01 to 4.00 mL/min. The back-pressure regulator allowed the flow system to achieve a pressure maximum of 140 bar. This modified flow platform readily accessed a wide range of temperatures, pressures, and residence times. Additionally, the platform could be modified to incorporate an automated sample processor, as well as, alternative back-pressure regulators, valve injector volume, and stainless steel tubing of variable volumes (2–16 mL volumes). Thereby, through the configuration of individual components into a flow platform, we designed a system that was flexible and amendable to integration with other devices.

In general, the Phoenix system was flushed with a solvent of choice, and then pressurized and set to the desired temperature. Substrates were dissolved in solvent and loaded into the 1 mL-injection loop, which would then inject into the Phoenix system at a specific flow rate. Samples were collected at the outlet of the reactor in scintillation vials, which were concentrated under a nitrogen sample concentrator and analyzed either by analytical HPLC/MS or UPLC/MS. Samples were either characterized following purification using either automated chromatography or preparative HPLC, or characterized without further purification.

(a)

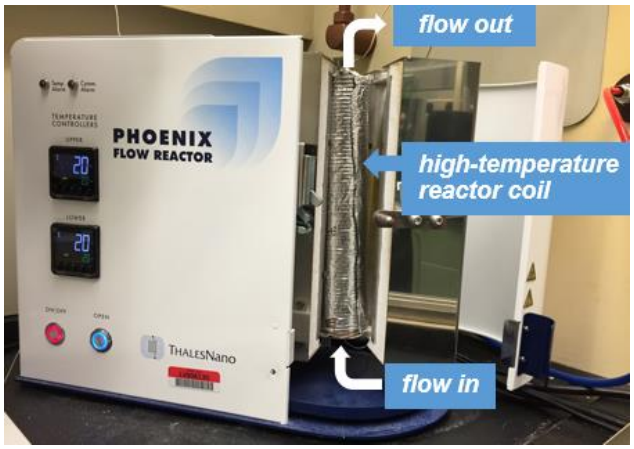

(b)

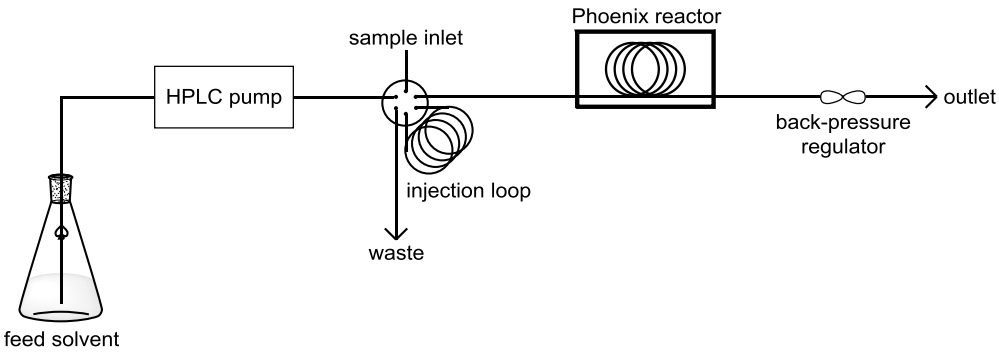

Figure 3.2. The Phoenix Flow Reactor™ platform. (a) Picture of the high-temperature Phoenix flow reactor. (b) Schematic diagram of the Phoenix flow platform configuration. The figure was adapted from Charaschanya et al.[18] and Bogdan et al.[19].

With a modified Phoenix Flow Reactor™ platform in hand, my externship at AbbVie comprised: (a) evaluation of this Phoenix platform for synthesis, (b) development of organic methodologies in unconventional reaction space (>250 ˚C and >20 bar), and (c) demonstration of the flow platform towards medicinal chemistry efforts. During this endeavor, organic chemistry investigated focused on the improvements of heterocycle synthesis and C–N bond formations, which are both important facets in pharmaceutical development of small-molecules. In this work, I collaborated with Dr. Andrew Bogdan, Dr. Jennifer Tsoung, and Dr. Amanda W. Dombrowski

from the high-throughput chemistry group of AbbVie, who contributed to the study design, research, interpretation, and review of data.

3.2 Synthesis of Nitrogen Heterocycles

The U.S. FDA approved drug database reveals that 59% of small-molecule drugs contain a nitrogen heterocycle.[20] Nitrogen heterocycles are among the most important structural components of pharmaceutical agents, and for this reason, heterocyclic formations are commonly utilized chemical transformations in the medicinal and pharmaceutical communities.[21-22] New methodologies and technologies that augment the rapid generation of diverse nitrogen heterocycles are desirable as they hold significant impact in this area. In this section, I discuss a flow chemistry investigation on the Gould-Jacobs reaction (Scheme 3.1). The Gould-Jacobs reaction is a well-known synthetic transformation for the construction of 4-quinolones from anilines (or heteroaromatic amines) and alkylidene diesters (or malonic ester derivatives).[23] Traditionally, the reaction proceeds via a two-step mechanism; condensation of the amine with an alkylidene diester to form the enamine intermediate is followed by a high-temperature ring closure. Typically, the intramolecular cyclization step requires prolonged heating at temperatures >200 °C in high-boiling solvents (e.g., diphenyl ether (DPE), Dowtherm™, tetraglyme).[24-26] Accordingly, preparations of such heterocyclic cores via the Gould-Jacobs reaction are uncommon mainly because reaction work-up is tedious due to difficulties in the removal or uncontrolled precipitation of high-boiling solvents. In rare circumstances, flash vacuum pyrolysis has been applied to synthesize quinolones.[27-28] However, current flash vacuum pyrolysis devices are not suitable for continuous-flow or scale-up operations. In general, this thermal cyclization reaction is underutilized in medicinal chemistry research. These restrictive high-temperature and high-boiling solvent

requirements marked this chemical transformation as an ideal opportunity to explore in a high-temperature–high-pressure flow system. Flow technologies could enable milder reaction conditions and unprecedented solvent states for this transformation. Thus, we relied on flow chemistry to provide a practical solution with better synthetic tractability and prospects of high-throughput library development of such heterocyclic scaffolds. In this context, Lengyel and coworkers have developed a flow protocol for the intramolecular thermal cyclization of the Gould-Jacobs reaction[29], which we selected as the model to study, compare and contrast with our flow platform and potentially extend the scope of this chemistry. The substrates used in the following studies have been published.[30]

Scheme 3.1. The Gould-Jacobs reaction.

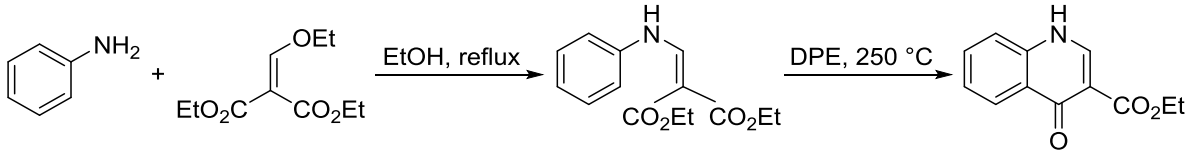

Quinolone, quinoline and related heterocycles (e.g., pyrimidinones) are important synthetic intermediates and scaffolds prominent in lead chemical series and marketed drugs.[31-32] For example, this heterocyclic core is observed in quinolone antibiotics, such as fluoroquinolones (e.g., norfloxacin), nalidixic acid and oxolinic acid, as well as in non-steroidal anti-inflammatory drugs such as floctafenine and glafenine (Figure 3.3). The biological activities associated with such heterocycles represents one of the most important classes of anti-infective agents[32], and thus underscores the need to improve synthetic methodologies that enrich diversification in the field of heterocycles.

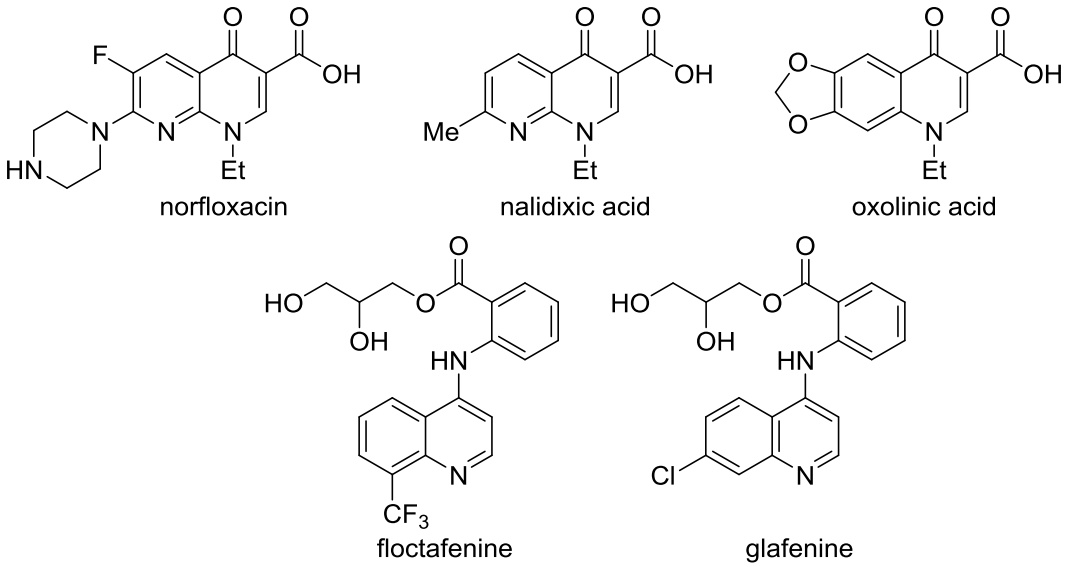

Figure 3.3. Quinolone and quinoline pharmacophores in marketed drugs.

3.2.1 Exploration of Reaction Conditions for the Gould-Jacobs Reaction

In this investigation, the intramolecular thermal cyclization of the Gould-Jacobs reaction was used as a model to evaluate the configuration of the Phoenix flow platform. Our initial attempts to reproduce the cyclization results of compound **3.1** reported by Lengyel and coworkers were unsuccessful (Scheme 3.2a).[29] They carried out the thermal cyclization in a flow system at temperature and pressure in the ranges of 300–360 ˚C and 100–160 bar, with short residence times (0.45–4.5 minutes) in tetrahydrofuran (THF). In our hands, when the transformation was carried out in the Phoenix reactor two product types were consistently observed from the two substrates tested (Scheme 3.2b), which was distinctive from Lengyel et al.'s work. While Lengyel and coworkers carried out the cyclization reaction in the X-Cube Flash flow system, the system still operated by direct electric heating of a metallic coil similar to that of the Phoenix system. This suggested that other variables were responsible for the product outcomes. For the specific transformation highlighted in Scheme 3.2a, Lengyel and coworkers reported a 70% isolated yield of only the ester-product **3.2**. To synthesize **3.2**, the authors used a flow reactor with steel tubing

of 4.5 mL volume at a flow rate of 4.0 mL/min (residence time 1.13 minute), pressure of 130 bar, and temperature of 360 ˚C. In contrast, we utilized a flow reactor with steel tubing of 8.0 mL volume at a flow rate of 4.0 mL/min (2 minutes residence time), pressure of 100 bar, and temperature of 360 ˚C. Under our process window, a separable mixture of ester-product **3.2** and decarboxylated-product **3.3** were synthesized. To further substantiate this mixture, the reaction was carried out with a second substrate **3.4**, which indeed gave two separable product types, ester-product **3.5** and decarboxylated-product **3.6**. Additionally, we sought out an alternative scaffold **3.7**, which was readily prepared by refluxing aniline and diethyl ethoxymethylenemalonate in ethanol (EtOH); analogous to the preparation of the other substrates **3.1** and **3.4**. With the flow conditions at hand, the outcome observed was a conversion only to the decarboxylated-product **3.8**, while the ester-containing heterocycle in either tautomeric forms **3.9a** or **3.9b** was not observed by analytical HPLC/MS (Scheme 3.3). It was evident from the differences between the two flow systems that product outcomes were significantly dependent on the pressure and residence time (i.e., time that the reaction mixture spends in the reactor, which is determined by the tubing volume and flow rate).

Although the product selectivities were not as anticipated, these results were informative about our flow configuration. First, the ability to form two products from one common precursor is potentially attractive if the yields of each scaffold could be optimized. Secondly, variation of reaction parameters such as residence time, flow rate, pressure, and temperature may have significant influence on product selectivities. Thirdly, the formation of the decarboxylated-products (**3.3**, **3.6** or **3.8**) under these preliminary conditions is interesting and possibly useful. The traditional synthesis of **3.3** requires multiple sequential steps of cyclization, hydrolysis, and decarboxylation from the ester-containing heterocycle or synthesis from an alternative starting

material.[33-34] Interestingly, the heterocycle **3.8** is reported in the literature, however only reported as the ester-containing heterocycle synthesized by heating substrate **3.7** in DPE at 240–250 ˚C for an extended period.[34-35]

Scheme 3.2. Model reaction: intramolecular thermal cyclization reaction of the Gould-Jacobs reaction. (a) Work by Lengyel and coworkers.[29] (b) This work.

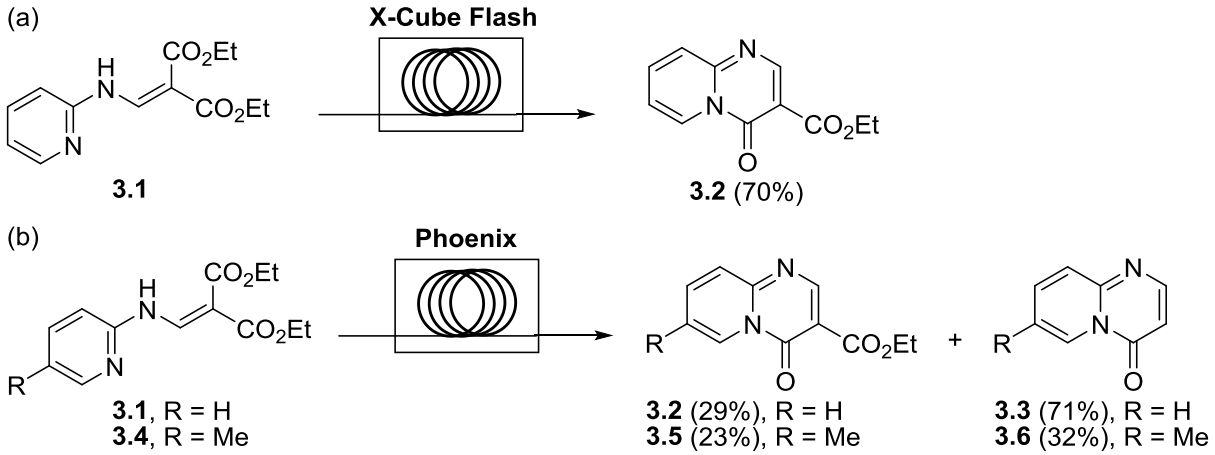

Scheme 3.3. Intramolecular thermal cyclization using the Phoenix flow platform.

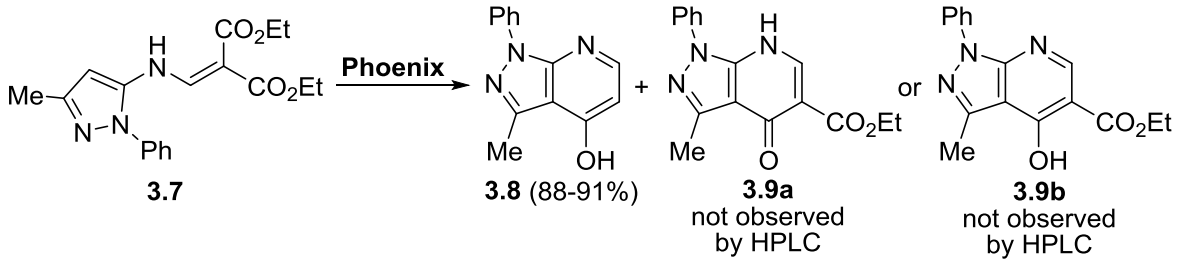

Following the investigations of the thermal intramolecular cyclization, we sought to determine if the entire sequence of the Gould-Jacobs reaction, amidation followed by cyclization, could be carried out in the Phoenix reactor (Table 3.3). Here, we examined a reaction between diethyl phenylmalonate and 4-methyl aniline to form 4-hydroxy-6-methyl quinolinone **3.10** in

flow. We first utilized the Conjure flow system to systematically screen solvents for the reaction sequence. The Accendo Conjure flow system relies on a segmented flow approach as opposed to continuous flow, which uses an immiscible florous spacer to create segments in flow. Specifically, using this approach multiple reactions can flow through the reactor at any one time, which maximizes the reaction optimization process.[36] Table 3.3 describes the reaction in solvents that afforded identifiable products by analytical HPLC/MS. Unfortunately, the desired product **3.10** was minimally formed under all conditions tested. In the best scenario, reaction in dimethylacetamide (DMA) gave 33% of **3.10** by HPLC/MS (entry 4), whereas, in most cases, a range of amidated-products **3.11**–**3.13** were observed by HPLC/MS. Although conversion to **3.10** in DMA was not optimal in the Conjure flow system, we attempted the reaction sequence in the Phoenix system anyway. Unfortunately, the desired product **3.10** was not observed, and instead amidated-product **3.11** and DMA-fragmentation product **3.14** were observed by HPLC/MS (not reported in the table because it was not quantified). In the Phoenix as well, the reaction sequence was carried out in 1,4-dioxane and similarly amidated-product **3.11** was observed (entry 6). It was clear from this investigation that execution of this tandem reaction sequence in flow is difficult. Moreover, the results obtained from the Conjure system do not necessarily translate well with the Phoenix system. Despite this lack of success, this investigation provided meaningful insights about re-designing experiments and the flow configuration. In this light, we learned that the Phoenix could execute amide-bond formations using activated esters without added reagents (e.g., formation of HPLC/MS observed compounds **3.11**–**3.13**). Secondly, the system readily favored the decarboxylation of esters in a tandem sequence of ester hydrolysis and decarboxylation. This inferred to the possibility of conducting certain types of tandem reaction sequences in flow, but would warrant optimization of product selectivities. Thirdly, reaction with solvent itself is highly

possible when subjected to unconventional conditions and could obstruct reaction development. However, there is discussion in the literature that certain solvents in it supercritical state (i.e., as solvent approaches temperature and pressure above its critical point, the properties of its gas and liquid phases converge) may enhance chemical transformations.[2, 7] Finally, different flow reactor configurations can result in variable chemical transformations and product outcomes. Thus, the synthetic abilities of each flow system may require a thorough experimentation in order to execute challenging chemical transformations. In fact, during our preliminary investigations we learned that the Phoenix reactor required an equilibration time period in order to achieve the set temperature of study. Specifically, we determined that approximately 30 minutes was necessary to equilibrate the reactor at the set temperature. Unfortunately, because at the time we lacked knowledge about this reactor design, the reactions carried out in this section did not achieve temperature equilibration (this is not the case with experiments carried out in the following sections).

Table 3.3. Preliminary investigation of the Gould-Jacobs reaction in flow.[a-d]

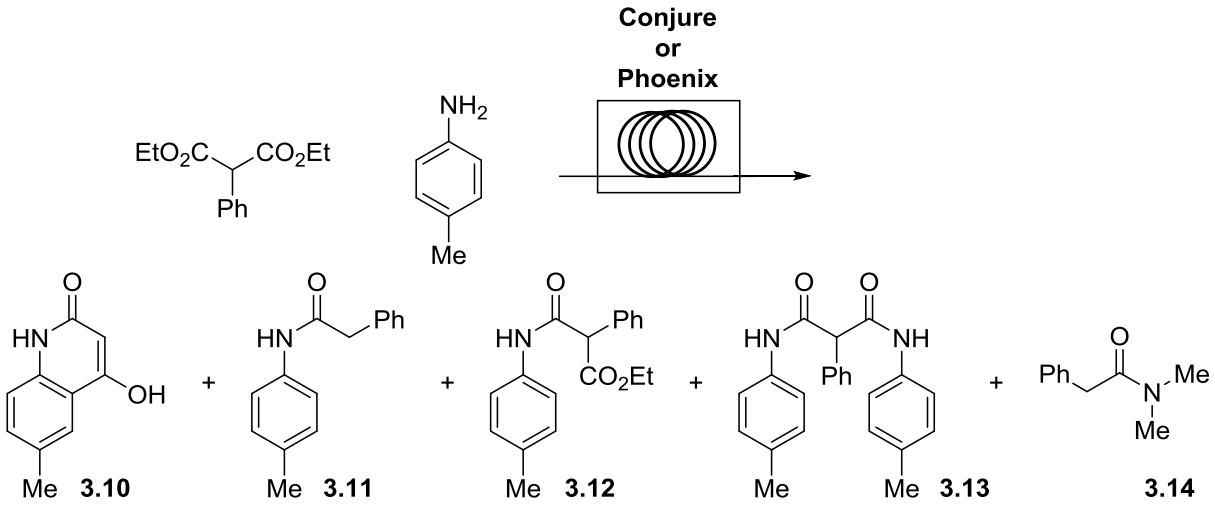

entry	flow system	solvent	3.10	3.11	3.12	3.13	3.14
1	Conjure	toluene	>1	72	16	10	-
2	Conjure	DPE	>1	3	8	39	-
3	Conjure	THF	4	41	22	15	-
4	Conjure	DMA	33	35	11	9	-
5	Conjure	dioxane	-	72	2	1	-
6	Phoenix	dioxane	-	19	-	-	-

[a]The Accendo Conjure flow reactor relies on segmented flow, and uses an immiscible florous spacer to create discrete reaction segments in flow.[36] [b]The Phoenix was flushed with solvent and the system pressurized to 100 bar. The temperature was set to 275 ˚C. Substrates were dissolved in THF (0.1 M) and loaded into the 1 mL-injection loop. The flow rate was set 4.0 mL/min, and the sample injected into the Phoenix system. Samples were collected at the outlet of the reactor, concentrated under a nitrogen sample concentrator, and analyzed by analytical HPLC/MS without any further purification. [c]The Phoenix system was not allowed to equilibrate to the set temperature, because at the time we were unaware that the reactor required equilibration. [d]Conversion by UV trace of the HPLC/MS after solvent removal.

3.2.2 Conclusions and Future Directions

Our preliminary investigation of the Gould-Jacobs reaction in flow was informative. We realized the challenges associated with executing chemical transformations in flow, and the necessity of understanding reactor concept to effectively apply the flow regime towards organic synthesis. Though we were unable to reproduce the original results of the intramolecular thermal cyclization by Lengyel and coworkers, we identified the possibility of optimizing two scaffolds in

flow. Interestingly, decarboxylation of esters is highly favorable under these unconventional conditions, which gave rise to a new scaffold that traditionally required alternative sequences to access. Although we were unable to carry out the two-step sequence of the Gould-Jacobs reaction, we were able to carry out the intramolecular cyclization from fixed starting materials (i.e., pre-coupled amide). It appeared that a tandem amidation-thermal cyclization sequence is less straightforward, and thus requires a thorough investigation of several reaction parameters in flow.

The preliminary investigations carried out during my externship provided a foundation for a detailed study carried out at AbbVie following the completion of my internship. Dr. Jennifer Tsoung and Dr. Andrew Bogdan successfully optimized conditions that selectively and exclusively accessed in high yields both the ester- and decarboxylated-scaffolds (Scheme 3.4).[30] Correlations between increasing pressure and residence time were key determinants to increase the conversion of decarboxylated products. Another important factor that was unaccounted for in our preliminary investigation was the effect of concentration on the reaction outcome. They found that high concentration favored the decarboxylation process, and is most likely attributed to catalysis by the presence of minimal water in the solvent. Confirming this, Tsoung and coworkers were able to utilize a mixture of THF and water to optimize and accelerate the decarboxylation process. In this paper, published in early 2017 in the *Journal of Organic Chemistry*[30], they employed Design-of-Experiments (DoE) software (Stat-Ease Design Expert 7) to rapidly facilitate the synthesis of a heterocyclic library (this optimization approach is further described in section 3.3). In this work, the Phoenix was modified to allow for robotic liquid handling and rapid injections featuring automation onto the Phoenix platform. Moreover, using the automated platform, they demonstrated the application of the cyclization reaction on a preparative scale of approximately 18.2 g/h. Advantageous to this protocol as well was the combination of a low-boiling solvent (e.g.,

THF) with high conversions that streamlined work-up and isolation of products unlike traditional methods.

Scheme 3.4. Synthesis of two scaffolds using the automated Phoenix system. The scheme was adapted from Tsoung et al.[30]

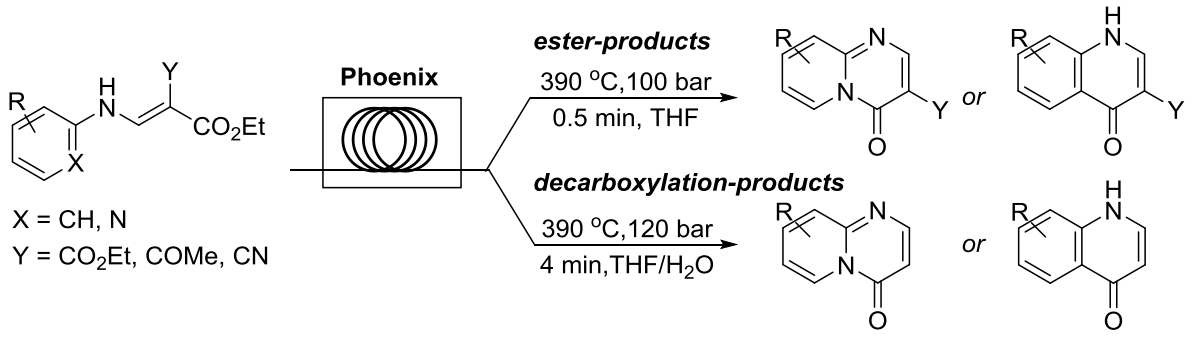

In future directions, this general approach could be adapted to various heterocyclic amines, especially the application of customized monomers could give rise to new chemical series for pharmaceutical developments. The combination of DoE and automated flow provides an approach for the rapid synthesis of therapeutic agents.

3.3 C–N Bond Formation thru Nucleophilic Aromatic Substitution

The nucleophilic aromatic substitution (S_NAr) of aryl compounds and heterocycles is a synthetically valuable and versatile chemical transformation that is widely used in both pharmaceutical and industrial communities. The reaction is guided by three basic principles: an electron deficient aromatic system, the nature of the leaving group to be displaced, and the reactivity of the nucleophile.[37-38] Generally, electron-deficient arenes will proceed through S_NAr in an addition-elimination sequence; aryl halides (particularly fluorides) and diazonium arenes have shown to be the most successful in the literature.[37-38] In this section, I focus on the displacement of aza-substituted aryl halides with nitrogen nucleophiles. A number of synthetic

methods have been developed to install nitrogen functionalities on aryl rings, including transition-metal catalyzed reactions[39-40] such as the Buchwald-Hartwig coupling reaction, Ullmann reaction, Chan-Lam coupling, as well as, metal-free reactions[41] such as the S_NAr reaction. In comparison to transition-metal catalyzed reactions, the classic S_NAr reactions are limited by poor scope and high temperature requirements.[39] However, the classic S_NAr reaction remains fundamental because it is cost-effective, atom economical, and avoids the requirement of designer ligands and the removal of trace metal impurities.[40-41] Recently published, perspectives in the *Journal of Medicinal Chemistry* cited the S_NAr reaction as the most frequently used chemical transformation in current medicinal chemistry.[20-22] Thus, despite its shortcomings, the S_NAr remains a fundamental reaction in the synthetic community.

Traditionally, standard heating is used to conduct S_NAr reactions on electron-deficient aryl halides. In contrast, unactivated substrates require more forcing conditions, such as highly elevated temperatures or microwave-assisted heating. For example, aminations of 2-chloroquinazoline can occur in refluxing 1-pentanol or isopropyl alcohol, heating in EtOH in sealed tubes at 150 ˚C until reaction completion, and heating in high-boiling solvents (e.g., in *N*-methyl-2-pyrrolidone (NMP) heated at 110 ˚C) for an extended period. Alternatively, microwave-assisted heating in acetonitrile (MeCN) has been employed to lower reaction times.[42] A few examples of using flow chemistry to promote S_NAr transformations have been reported in the literature; for example, (1) 2-chloropyridine and piperidine were heated in NMP at 260 ˚C to afford desired product in 20 minutes[43], and (2) a step-wise S_NAr of activated difluorobenzene to monoamidated products was achieved in the X-Cube flash reactor[44].

The classic S_NAr reaction is an attractive candidate for high-temperature–high-pressure continuous-flow processing because of its need for high-temperature. Accordingly, we sought to

develop a protocol for S_NAr reactions in flow (Scheme 3.5). As noted above, high-temperature–high-pressure flow reactors can execute synthesis in solvents above their boiling points without pressure and solvent limitations. The Phoenix flow platform provided a new spectrum of reaction conditions, as well as, the opportunity to incorporate green solvents, minimize reaction time, broaden substrate scope, and maximize yield of the classic S_NAr reaction. The studies carried out in the following sections have been published.[18]

Scheme 3.5. Metal-free strategies for the S_NAr reaction of nitrogen nucleophiles. (a) Classical approach. (b) Example of a S_NAr reaction in flow.[7] (c) This work.

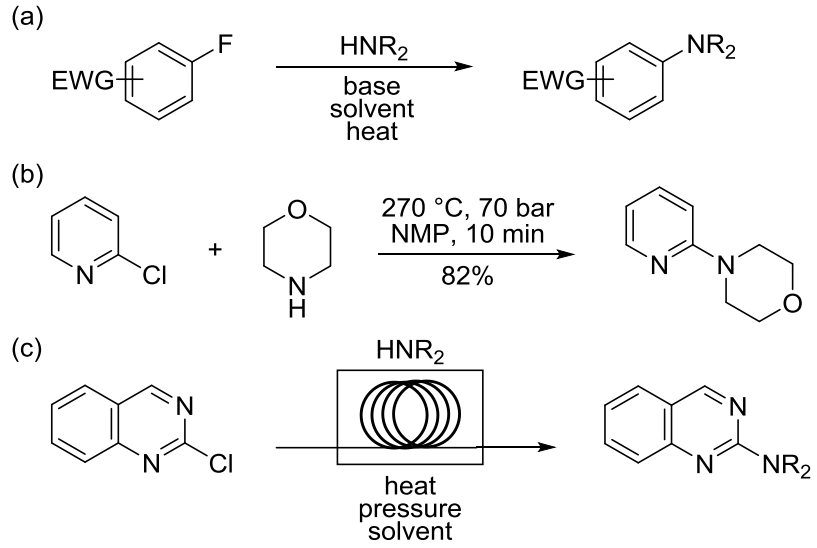

In this study, we evaluated the S_NAr reaction of 2-chloroquinazoline with nitrogen nucleophiles to afford 2-aminopyrimidine-like structures. Aminopyrimidines are found in many drug-like compounds, such as Rosuvastatin and Imatinib (Figure 3.4).[20]

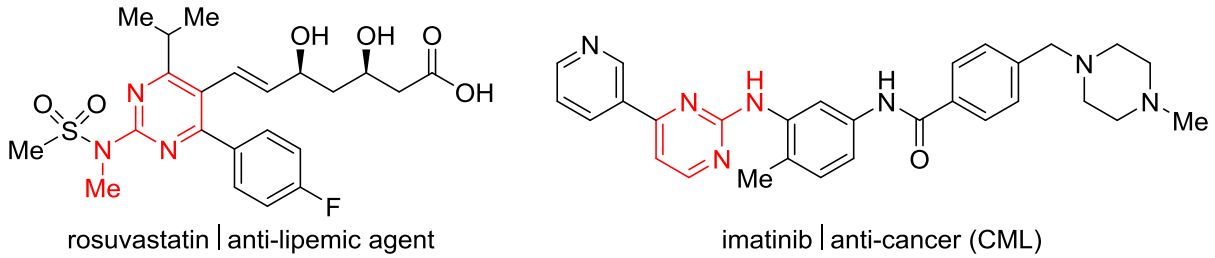

Figure 3.4. Aminoquinazolines with biological activities.

3.3.1 Optimization of Reaction Conditions

We utilized a DoE software, Stat-Ease Design Expert 7, to develop a general approach for the direct amination of heterocycles in continuous-flow. Statistical DoE is a powerful optimization approach because the software provides the ability to quickly determine how multiple parameters and interactions between them can affect product yield.[45] Essentially, this multi-parameter optimization procedure uses mathematical modeling to determine optimal conditions, which must be verified experimentally to validate the results. In this work, the S_NAr reaction between 2-chloroquinazoline and benzylamine was optimized using a DoE approach. A comprehensive evaluation of three reaction parameters was carried out, which included temperature, pressure, and flow rate (Table 3.4). In this study, EtOH was selected as the solvent of choice because of its green facet[46] and its wide application in S_NAr chemistry. With the aid of DoE, a series of reactions were designed involving all three selected variables; these test points used are shown in Table 3.4. Subsequently, 17 reaction conditions were carried out on the Phoenix, and the crude reaction mixtures were analyzed by analytical HPLC/MS to obtain theoretical values of the product yield (Table 3.5). The resulting data were worked into the DoE software for plot analysis, which illustrated the relationship between temperature, pressure, and flow rate on the reaction outcome in the form of three-dimensional response surfaces.

Table 3.4. DoE-designed reaction test points for the optimization of the S_NAr reaction in flow.

parameters	reaction test points
temperature (˚C)	250, 325, 400
pressure (MPa)	8, 10, 12
flow rate (mL/min)	1.0, 2.5, 4.0

Table 3.5. DoE optimization of the S_NAr reaction conditions of 2-chloroquinazoline and benzylamine in a flow reactor.[a]

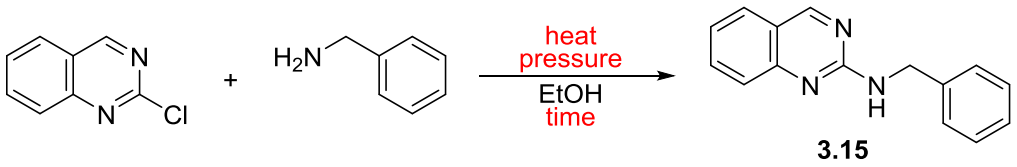

3.15

entry	temperature (˚C)	pressure (bar)	flow rate (mL/min)	3.15 (%)[b]
1	250	80	2.5	46
2	250	100	4.0	29
3	250	100	1.0	75
4	250	120	2.5	42
5	325	80	1.0	37
6	325	80	4.0	20
7	325	100	2.5	34[c]
8	325	120	1.0	62
9	325	120	4.0	47
10	400	80	2.5	25
11	400	100	1.0	37
12	400	100	4.0	27
13	400	120	2.5	37

[a]The Phoenix system was flushed with EtOH at 0.5 mL/min and the system pressurized to the desired test point. The temperature was set and allowed to equilibrate for 30 minutes. Substrates were dissolved in EtOH (0.1 M) and loaded into the 1mL-injection loop. The flow rate was set, and the sample injected into the Phoenix system. Samples were collected at the outlet of the reactor, concentrated under a nitrogen sample concentrator, and analyzed by analytical HPLC/MS without any further purification. [b]Percent product determined by UV trace of the HPLC/MS. [c]Center point, average of 4 runs. (1 MPa = 10 bar)

Upon plot analysis of DoE results (Table 3.5), data revealed that the reaction has considerable dependence on all three variables. In Figure 3.5a, the plot indicated that lower temperatures and higher pressures gave higher percentages of desired product **3.15**. While conversions were reasonable in all cases, significant decomposition and side-reactions were observed at temperatures of 325 ˚C and above. In comparison, reactions performed at 250 ˚C afforded cleaner conversions and recovery of **3.15**. For this reason, reaction temperatures less than 250 ˚C were deemed optimal for the S_NAr reaction.

In Figure 3.5b, data revealed higher percentages of **3.15** when a slower flow rate was used. This suggested that increasing the residence time of the reaction mixture in the flow reactor favored more product formation. Figure 3.5b also confirmed that higher pressures in this flow system gave higher percentages of desired product **3.15**. Based on the 17 reactions carried out, optimal conditions were predicted by Design Expert: flow reactor temperature of 225 ˚C or lower, pressure of 120 bar, and flow rate of 0.5 mL/min (equivalent to a 16 minute residence time). The predicted conditions were carried out, and indeed a complete conversion to **3.15** was observed by analytical HPLC/MS leading to an isolated yield of 97% (Scheme 3.6). It is worth noting that no EtOH adducts were observed while running these reactions.

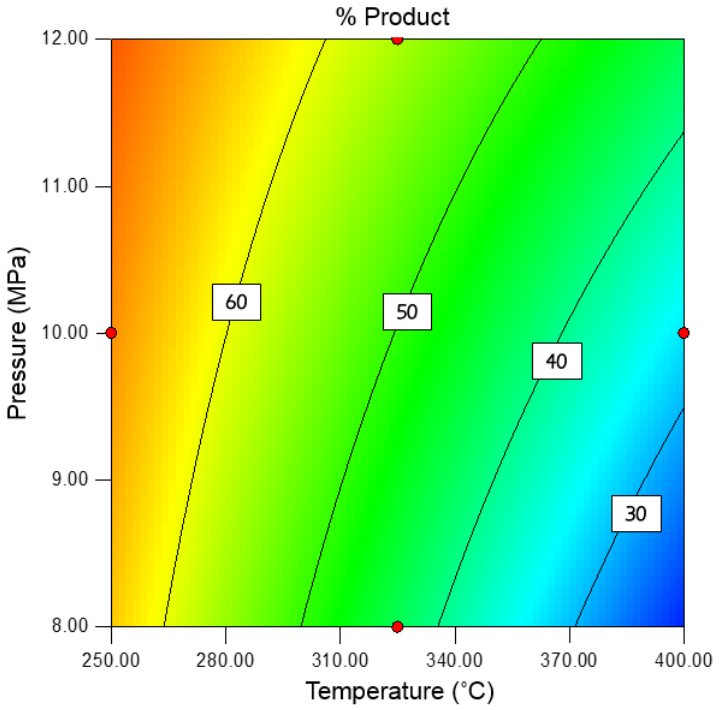

(a)

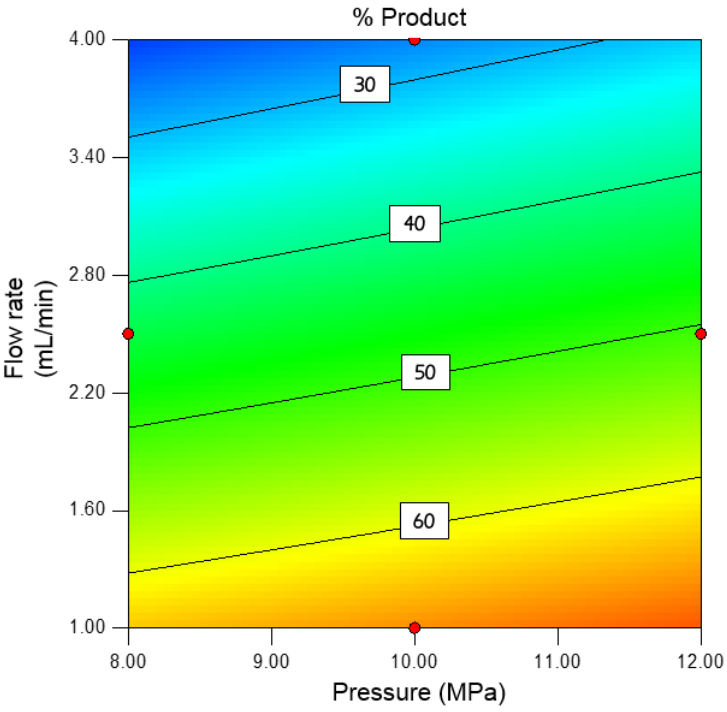

(b)

Figure 3.5. DoE contour plots. (a) The relationship between temperature and pressure at 1.0 mL/min. (b) The relationship between flow rate and pressure at 250 ˚C. Product conversion is indicated in the white box; contour color changes from blue to red resembles that of low to high product conversion, respectively. The figure was adapted from Charaschanya et al.[18] (1 MPA = 10 bar)

Scheme 3.6. DoE-suggested optimal reaction condition and isolated yield of **3.15**.

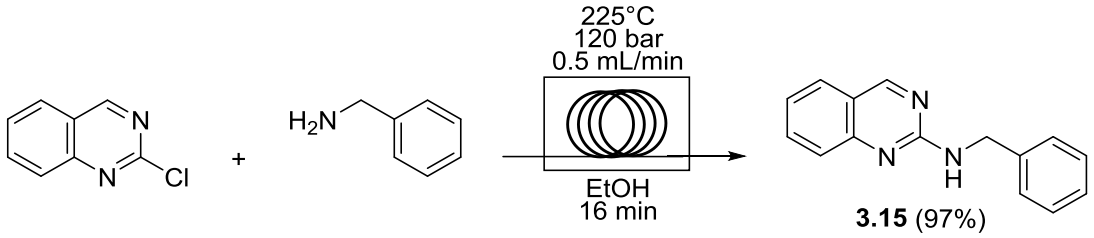

3.3.2 Substrate Scope

Utilizing the optimal conditions, a range of nucleophiles was screened to demonstrate the scope of the S_NAr methodology in flow. The S_NAr of 2-chloroquinazoline with primary amines gave desired products in excellent yields (Figure 3.6, **3.16**–**3.21**). A practical use of a low molecular weight amine in flow was demonstrated; for example, the reaction of 2-chloroquinazoline with methylamine to afford **3.16** in a high yield. Presumably, due to the use of the diamine as a hydrochloride salt, compound **3.19** was isolated in a low yield in comparison to other compounds. Moreover, examples with secondary amines afforded desired products in modest to high yields (compounds **3.22**–**3.27**).

Nucleophilic amines such as imidazole and substituted benzylamines were examined, and the resultant products were isolated in modest yields (compounds **3.15** and **3.28**–**3.29**). Both electron-rich and electron-poor anilines were examined as well (compounds **3.30**–**3.32**). Electron-poor anilines afforded desired products in low yields compared to other nucleophiles. Although, the electron-rich aniline, 4-methoxyaniline, gave **3.31** in a modest yield comparable to other isolated compounds. It should be noted that anilines are weaker nucleophiles than primary amines, and as such may demand more forcing conditions to efficiently participate in S_NAr chemistry. Perhaps, the scope of anilines requires separate optimization studies in order to realize its S_NAr potential in flow.

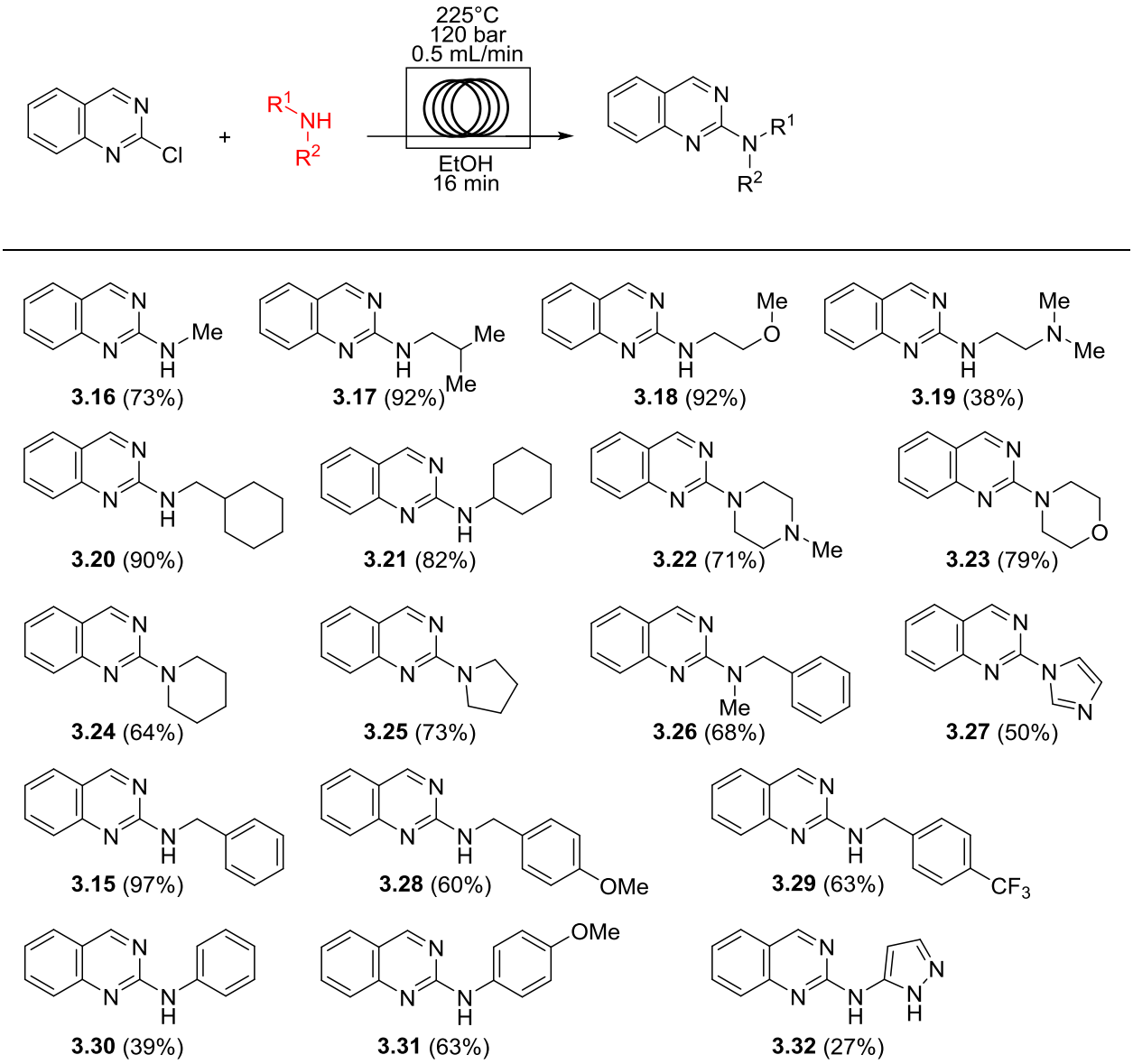

Figure 3.6. Substrate scope for the S_NAr of 2-chloroquinazoline with nitrogen nucleophiles.

From the substrate scope evaluated so far, it can be seen that this methodology is a general approach to the direct amination of heterocycles in flow. The methodology works well with primary and secondary amines, though modestly with anilines. Of note is that all reactions were completed in 16 minutes and only required the removal of solvent under a stream of nitrogen prior to preparative HPLC purification. We sought to extend the scope to related heterocycles such as

quinoxaline and benzimidazole. In Figure 3.7, the S_NAr reactions of both 2-chloroquinoxaline and 2-chlorobenzimidazole with primary and secondary amines afforded the desired products in modest yields (compounds **3.33**–**3.38**). The ability to apply this protocol with ease to other heterocycles further reinforced this methodology as practical approach for direct aminations and heterocyclic synthesis in flow.

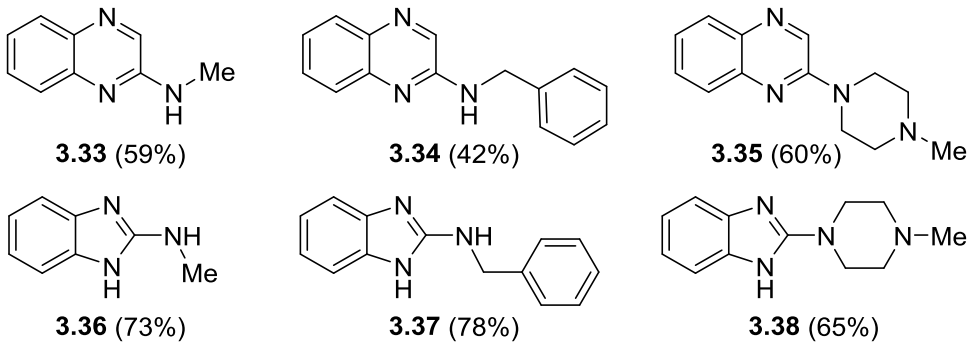

Figure 3.7. Additional evaluation of substrate cope using 2-chloroquinoxaline and 2-chlorobenzimidazole with nitrogen nucleophiles.

3.3.3 Conclusions and Future Directions

In conclusion, we have developed a general approach in flow to carry out the S_NAr reaction of heterocycles with nitrogen nucleophiles. The methodology demonstrated good scope with primary and secondary amines. However, the method can be improved for weaker nucleophiles and the scope could be extended by further investigation. Perhaps, optimization of reaction conditions with aniline substrates would be a good starting point prior to development with oxygen- and sulfur-based nucleophiles. Regardless, this platform has been validated an alternative method to microwave-assisted and traditional heating S_NAr protocols. In comparison to conventional means, this set-up is advantageous because it permitted the efficient use of EtOH, a green and low-boiling solvent, well beyond it is boiling point. Further, the protocol allowed for

shorter reaction times, as well as, lacked the need for added base or catalysts which is distinctive from traditional C–N formation methods. More significantly, the application of the flow platform in conjunction with the Design Expert software demonstrated unusual efficiency in optimization and synthesis of amino-substituted heterocycles. This straightforward and easily assembled flow platform may have significant impact on streamlining the preparation of heterocycle libraries for pharmaceutical interests.

3.4 Thermal Boc Deprotection

The Boc group (*tert*-butoxycarbonyl) is one of the most commonly used protection groups for amines and is extensively used in peptide and heterocyclic synthesis.[21-22, 47] A recent perspective in the *Journal of Medicinal Chemistry* noted that Boc protection-deprotection is one of the five most frequently occurring reactions in medicinal chemistry literature in 2014.[21] This is due to the importance of carbon-heteroatom bonds in the field of medicinal chemistry, especially reductive aminations and amide-bond formations.[21-22] Other advantages for this protecting group include the broad availability of Boc-protected reagents, simple protection–deprotection protocols, and the easily removable by-products (*t*-BuOH, isobutylene, and CO_2) The Boc group is inert to many nucleophilic reagents and considered non-hydrolysable under basic conditions.[47] However, it is usually cleaved with strong acids, typically via concentrated hydrochloric acid (HCl) or trifluoroacetic acid (TFA).[47] We chose to investigate a thermal deprotection of the Boc group in flow because this could serve as an alternative methodology to the widely used acidic methods, as well as, appeal to substrates that are deleterious (i.e., functional group incompatibility, work-up complications, or instability) under acidic Boc removal conditions.

Traditional heating and microwave-assisted conditions for the Boc group are reported in the literature. The most standard reagent-free, thermolytic removal conditions involve heating the substrate neat or in high-boiling solvent, for example, in DPE at 180–185 ˚C for 20–30 minutes.[47-48] Under microwave-assisted heating, substrates are dissolved in mildly acidic solvents, such as 2,2,2-trifluoroethanol, hexafluoro-2-isopropanol, water, or silica gel/dichloromethane in sealed microwave vials, and then heated at 100–170 ˚C or at a specified wattage between a time period of 1 minute to 5 hours, depending on substrate.[47, 49-51] Though these traditional and microwave-assisted methods are facile, quantitative, and in some cases green (i.e., neat or in water), these conditions are only optimal when performed on a small-scale due to the high temperature requirements and the vigorous off-gassing of reaction mixtures.

To augment the current protocols in Boc removal, a high-temperature–high-pressure continuous flow methodology would remove the need for reagents and reaction work-up altogether, as well as, appeal for functional group compatibilities and substrates deleterious under acidic conditions. Under a reagent-free flow condition, the amines are isolated in free base form, which would enable immediate use in multi-step reaction sequences without adding features such as in-line extractions or purifications. Additionally, flow methodology could permit the transition to large-scale processing more readily and safely. The studies carried out in the following sections have been published.[19]

3.4.1 Optimization of Reaction Conditions

We began the optimization by screening a range of temperatures for the deprotection of Boc-L-phenylalanine ester in MeCN (Table 3.6). No conversion to the desired product **3.39** was observed at 200 ˚C (entry 1). However, when the temperature was increased to 300 ˚C a complete

conversion to the deprotected amine **3.39** was observed, and HPLC/MS of this reaction gave a reasonable yield of **3.39** (entry 3). However, the mass trace showed more than one peak indicating possible decomposition occurring when the reaction was exposed to a high temperature for an extended period of time. For this reason, the residence time of the reaction mixture in the flow reactor was explored, and particularly shortened by increasing the flow rate via the HPLC pump (entries 4–6). In entry 6, we found that a complete conversion was still retained using the system's maximum flow rate of 4.0 mL/min. Moreover, the mass trace of this HPLC run showed a much higher percentage of **3.39** formation. A direct comparison to microwave-assisted heating at 200 ˚C (recommended maximum temperature for MeCN applications under microwave heating) was carried out, which gave no conversion to **3.39** (entry 7).

Table 3.6. Optimization of reaction conditions for the thermal removal of Boc-protected L-phenylalanine ester in a flow reactor.[a]

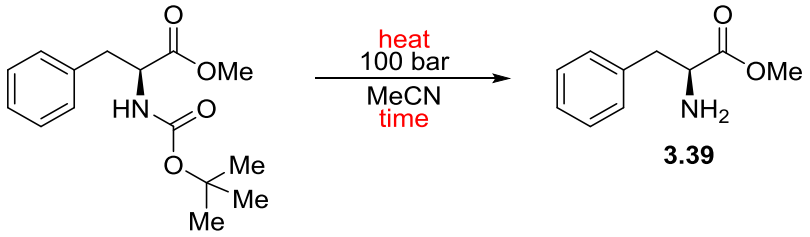

3.39

entry	temperature (˚C)	flow rate (mL/min)	residence time (min)	conversion (%)[b]	3.39 (%)[c]
1	200	1.0	8.0	0	-
2	250	1.0	8.0	49	-
3	300	1.0	8.0	>99	52
4	300	2.0	4.0	>99	68
5	300	3.0	2.7	>99	77
6	300	4.0	2.0	>99	80
7[d]	200	-	8.0	0	-

[a]The Phoenix system was flushed with MeCN at 0.5 mL/min and pressurized to 100 bar. The temperature was set and allowed to equilibrate for 30 minutes. Substrates were dissolved in MeCN (0.1 M) and loaded into the 1mL-injection loop. The flow rate was set, and the sample was injected into the Phoenix system. Samples were collected at the outlet of the reactor, concentrated under a nitrogen sample concentrator, and analyzed by analytical HPLC/MS without any further purification. [b]Conversion was determined by UV trace of the HPLC/MS. [c]Product yield was determined by the MS ion count of the HPLC/MS. [d]Sample was carried out in a Biotage microwave at 200 ˚C for 8 minutes.

For the reaction of entry 6, MeCN was removed under nitrogen, and crude proton and carbon NMR of **3.39** were taken. The resulting spectra indicated that the product was >95% pure with very minor baseline peaks; this suggested that subjecting the material to the high-temperature–high-pressure flow reactor did not cause any appreciable material decomposition. Additionally, work-up was not necessary to utilize the crude material. Furthermore, confirmation by analytical chiral chromatography indicated that the stereochemistry of the amine is retained during this process. To finalize the optimization of reaction conditions, we screened additional low-boiling solvents such as EtOH, methanol, THF, and 2-methyltetrahydrofuran. However, reactions carried out in these solvent conditions were not promising, because HPLC/MS traces and crude NMR spectra showed considerable amounts of impurities. In the case of EtOH, transesterification was observed, and so characterization of byproducts during solvent screenings was not further carried out.

3.4.2 Substrate Scope

With optimal conditions in hand, a series of Boc-protected amines were subjected to thermal deprotection using the Phoenix (Figure 3.8). The data showed that high temperature-high-pressure flow processing is a suitable and general methodology for the deprotection of a variety of amines. Illustrating this, a series of primary and secondary amines were quantitatively deprotected (**3.40**–**3.46**). Aniline **3.47**, indolines **3.48**–**3.49**, related heterocycles, indole **3.50** and imidazole **3.51**, as well as, lactam **3.52** were also readily deprotected. In this series, we showed that a number of functional groups were tolerated which included alcohols, amides, esters, aryl halides, ketones, and amines. It is noteworthy that all the substrates in this Figure were completed within a 2-minute residence time in the flow reactor. However, in the cases of amines **3.48** and **3.49**, products were

observed as a mixture of desired product and the oxidized-product (i.e., indole). It was determined by LC/MS that crude samples prior to solvent removal showed no traces of the starting material or indole, and thus elimination was not due to the flow condition but probably the instability of the products towards oxidation.

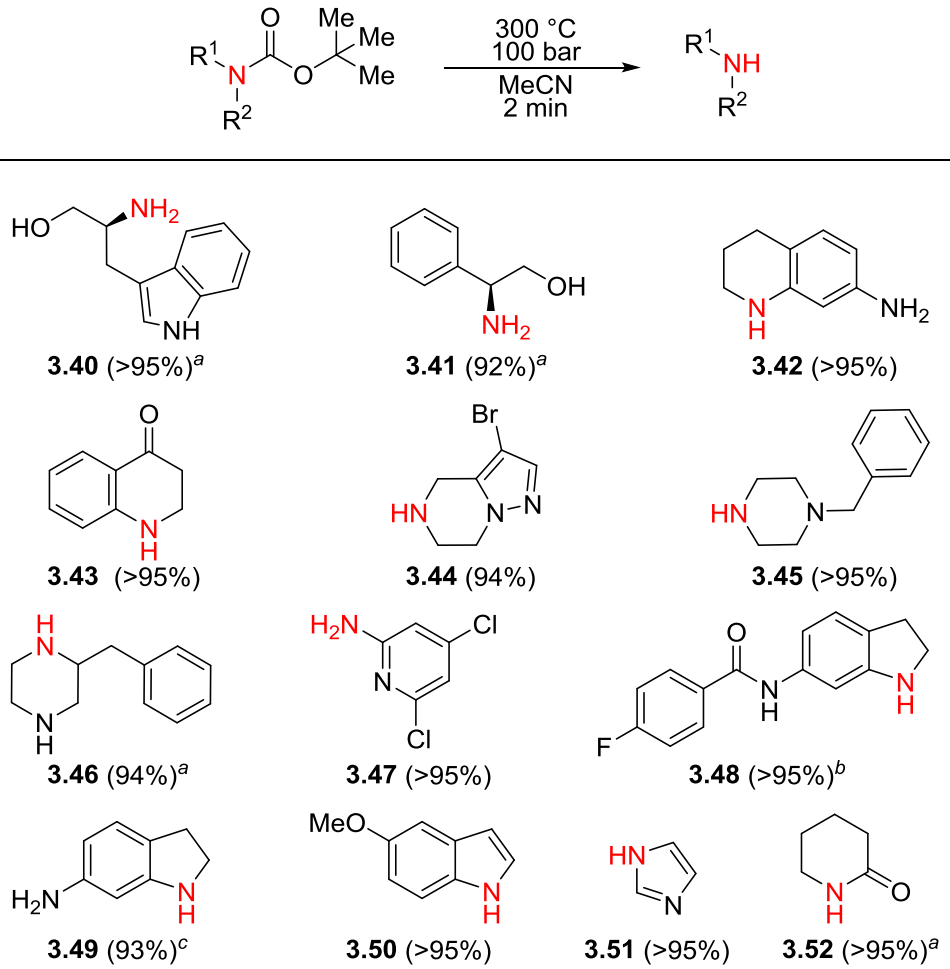

Figure 3.8. Substrate scope for the thermal Boc deprotection of amines in a flow reactor. The red nitrogen indicates the amine that has been deprotected; isolated yields were recorded after solvent removal, and compounds were characterized without further purification. All reactions were run at 0.1 M substrate, unless otherwise noted. [a]Reactions were run at 0.2 M of substrate. [b]Approximately 10% indole was observed after solvent removal. [c]Approximately 15% indole was observed after solvent removal.

In collaborative efforts with Dr. Andrew Bogdan and Dr. Amanda Dombrowski, another set of substrates specifically designed to encompass additional protecting groups were synthesized. We aimed to demonstrate selective removal of Boc over other protecting groups and determine tolerance of functionalities when subjected to the flow reactor. In Figure 3.9, we illustrated that protecting groups such as *tert*-butyldimethylsilyl ethers, tosyl, and carboxybenzyl-group were not affected during the thermal deprotection of Boc, and afforded nearly quantitative yields of the desired amine. Acetal (first example in the Figure) was observed to be the most sensitive protecting group towards flow conditions employed, but still afforded a good yield of the corresponding amine. Noteworthy, the Boc groups were selectively cleaved over other protecting groups, and acid-labile functional groups were well tolerated under flow conditions. To take this a step further, substrates in Figure 3.9 were treated with TFA in order to directly compare our protocol with a standard acidic deprotection method. Crude NMR showed desired removal of Boc amines in combination with considerable impurities as well as mixtures of products. In contrast, the optimal high-temperature–high-pressure flow condition afforded desired products with a greater level of purity.

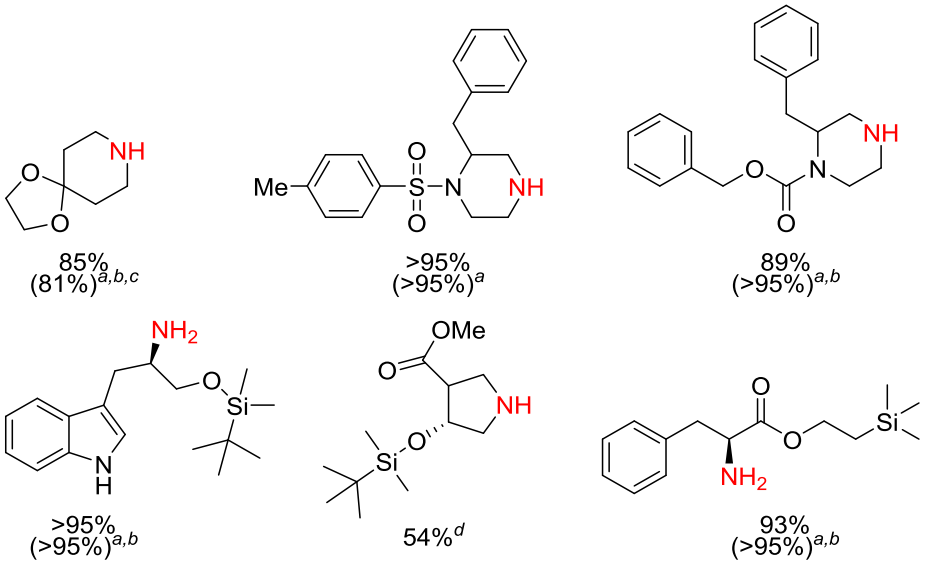

Figure 3.9. Substrate scope for the thermal Boc deprotection of bis-protected substrates in a flow reactor. The red nitrogen indicates the amine that has been deprotected. Isolated yields were recorded after solvent removal, unless otherwise noted. [a]Isolated yield after treatment with TFA. [b]A mixture of products were observed by ^{1}H NMR. [c]10% of piperdin-4-one was observed by ^{1}H NMR. [d]Isolated yield after normal phase chromatography purification.

3.4.3 Conclusions and Future Directions

In conclusion, a methodology utilizing a high-temperature–high-pressure flow reactor to deprotect Boc-amines has been developed. In this work, temperature, solvent, and flow rates were screened to determine the optimal condition (i.e., heating at 300 ˚C and pressurized at 100 bar in MeCN at a flow rate of 4.0 mL/min (2-minute residence time)). The protocol demonstrated broad scope, functional group tolerance, and selective cleavage over multiple protecting groups. In most cases, final products were afforded in excellent yields and high purity. In fact, the protocol only required the removal of solvent without further purification of the free-amines.

Having validated this methodology, Dr. Andrew Bogdan and Dr. Amanda Dombrowski sought to use this thermal deprotection in a multi-step reaction sequence towards medicinal chemistry efforts. The advantages of this thermolytic protocol include avoiding the use of in-line extractors to work-up reaction steps and excessive reagents such as TFA or HCl. As shown in

Schemes 3.7 and 3.8, our collaborators demonstrated the application of this protocol in two different multi-step reaction sequences highly prevalent in medicinal chemistry, and essentially, streamlined 3 batch chemistry processes into one continuous process. Both examples demonstrated high-throughput preparation of small-molecules, where analogs were generated within minutes and in large quantities.

In medicinal chemistry, the ability to functionalize scaffolds efficiently and orthogonally during SAR campaigns is highly desirable. Additionally, a high-throughput approach to chemical synthesis is impactful because compound libraries can be generated within days/weeks for screening. The preliminary examples developed here are particularly attractive not only because amination and Boc-deprotection reactions are common in medicinal chemistry efforts, but also because this methodology is suitable for both small-scale and large-scale synthesis. Essentially, this type of continuous-flow processing can provide advantages at many stages in medicinal chemistry ranging from hit-to-lead development to large-scale production.

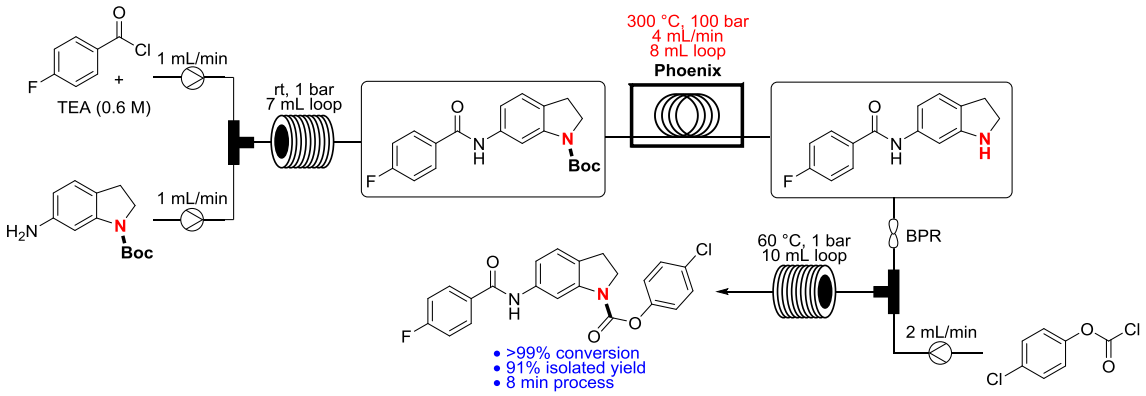

Scheme 3.7. Acylation–deprotection–carbamate formation multi-step reaction sequence in flow via an in-line high-temperature–high-pressure Boc deprotection. The scheme was adapted from Bogdan et al.[19].

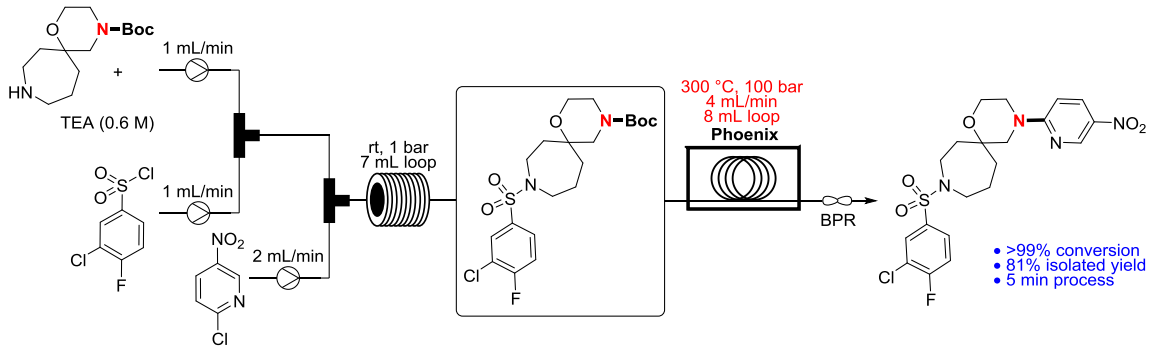

Scheme 3.8. Sulfonylation–deprotection–S_NAr multi-step reaction sequence in flow via an in-line high-temperature–high-pressure Boc deprotection. The scheme was adapted from Bogdan et al.[19].

3.5 Experimental Section

3.5.1 General Information

Reactions were performed in the Phoenix Flow Reactor™ from ThalesNano. The flow platform was set up to operate through four main components: (1) the Phoenix Flow Reactor™, (2) a manual injection valve, (3) a JASCO PU-2085 Plus HPLC pump, and (4) a JASCO BP-2080 Plus back-pressure regulator. All starting materials were commercially available reagents, and were used without further purification unless otherwise noted. Purification was carried out by an automated flash chromatography/medium-pressure liquid chromatography system (Teledyne ISCO Combi*flash*® Rf system) using normal phase silica flash columns (Redi*Sep*® Rf Gold silica columns). Preparative HPLC was performed on either an automated preparative-scale purification system equipped with a Waters Sunfire C8 5m column (150 × 30 mm) or on a Phenomenex Luna C8 5m 100 Å AXIA column (50 × 21.2 mm). A gradient of acetonitrile and 0.1% TFA in water was used at a flow rate of 30 mL/min. Proton nuclear magnetic resonance spectra (^{1}H NMR, 400 or 500 MHz) and proton decoupled carbon nuclear magnetic resonance spectra (^{13}C NMR, 100 or 125 MHz) were obtained in deuterated chloroform ($CDCl_3$) or deuterated dimethylsulfoxide (DMSO-d_6), unless otherwise noted. Chemical shifts are in parts per million (ppm), and are

reported in the order of multiplicity, coupling constants (*J*, Hz) and integration. Chemical shifts are referenced to the center line of solvent (for $CDCl_3$, δ 7.26 ppm for ^1H NMR and 77.16 ppm for ^{13}C NMR; and for DMSO-d_6, δ 2.50 ppm for ^1H NMR and 39.52 ppm for ^{13}C NMR). MS data were obtained by ionizing samples via electron spray ionization (ESI) or desorption chemical ionization (DCI) with a time-of-flight (TOF) as the mass analyzer. Infrared spectra (IR) were obtained with attenuated total reflectance Fourier transform midinfrared spectroscopy (ATR/FT-MIR) using a diamond internal reflection element (IRE). Spectroscopic data for the known compounds prepared according to methodologies described in this chapter match with those reported in the literature. Lastly, the compounds were characterized according the experimental standards at AbbVie pharmaceuticals, which primarily included yield, ^1H NMR, and MS.

General procedure A for the Gould-Jacobs thermal cyclization reaction. The Phoenix system was flushed with THF. The system flow rate was set to 4.0 mL/min, back-pressure regulator to 100 bar, and temperature to 360 ˚C. The Phoenix reactor did not equilibrate at the set temperature (because at the time of this study we were unaware that it was necessary for the system). Substrates were dissolved in THF (0.1 M), loaded into the 1.0 mL-injection loop, and injected into the Phoenix system. The crude reaction mixtures were collected at the outlet of the reactor in 20 mL scintillation vials, which were concentrated under a nitrogen sample concentrator. All compounds were analyzed by analytical HPLC/MS and characterized without any further purification.

General procedure B for the SNAR reaction of nitrogen nucleophiles. The Phoenix system was flushed with EtOH. The system flow rate was set to 0.5 mL/min, back-pressure

regulator to 120 bar, and temperature to 225 ˚C. The Phoenix reactor was allowed to equilibrate for 30 minutes; equilibration of the reactor temperature was only required for the first run each day. Substrates (2-chloroquinazoline, 2-chloroquinoxaoline, or 2-chlorobenzaimidazole, 0.075 mmol) and amines (0.150 mmol, used as 0.3 M solutions in EtOH) were premixed, and loaded into the 1.0 mL-injection loop. Samples were injected into the Phoenix system. The crude reaction mixtures were collected at the outlet of the reactor in 20 mL scintillation vials, which were concentrated under a nitrogen sample concentrator. All compounds were purified by mass-triggered reverse phase HPLC.

General procedure C for the thermal removal of Boc-protected amino group. The Phoenix system was flushed with MeCN. The system flow rate was set to 4.0 mL/min, back-pressure regulator to 100 bar, and temperature to 300 °C. The Phoenix reactor was allowed to equilibrate for 30 minutes; equilibration of the reactor temperature was only required for the first run each day. Substrates were dissolved in MeCN (0.1 or 0.2 M), loaded into the 1.0 mL-injection loop, and injected into the Phoenix system. The crude reaction mixtures were collected at the outlet of the reactor in 20-mL scintillation vials, which were concentrated under a nitrogen sample concentrator. Samples were characterized without further purification, unless otherwise noted.

3.5.2 Experimental Section for 3.2

Preparation of Starting Materials 3.1, 3.4, and 3.7. The aminomethylene adducts were prepared using literature procedures with commercially available starting materials. Characterization data was consistent with that reported in the literature.[24-25, 29, 34]

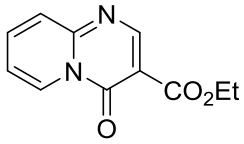

3.2

Ethyl 4-Oxo-4*H*-pyrido[1,2-a]pyrimidine-3-carboxylate, 3.2. Compound **3.2** was prepared from diethyl 2-((pyridin-2-ylamino)methylene)malonate **3.1** according to general procedure A. Characterization data were consistent with reported data.[25, 28-29]

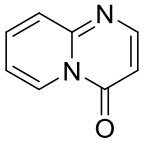

3.3

4*H*-Pyrido[1,2-a]pyrimidin-4-one, 3.3. Compound **3.3** was prepared from diethyl 2-((pyridin-2-ylamino)methylene)malonate **3.1** according to general procedure A. Characterization data were consistent with reported data.[29]

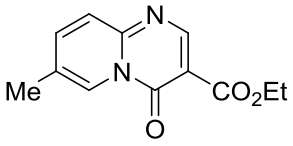

3.5

Ethyl 7-Methyl-4-oxo-4*H*-pyrido[1,2-a]pyrimidine-3-carboxylate, 3.5. Compound **3.5** was prepared from diethyl 2-(((5-methylpyridin-2-yl)amino)methylene)malonate **3.4** according to general procedure A. The product was isolated as an off-white powder in 23% yield. ^{1}H NMR (500 MHz, $CDCl_3$) δ 9.10 (app dt, J = 2.1, 1.0 Hz, 1H), 9.03 (s, 1H), 7.81 (dd, J = 8.9, 2.1 Hz, 1H), 7.72 (d, J = 8.9 Hz, 1H), 4.43 (q, J = 7.1 Hz, 2H), 2.51 (s, 3H), 1.42 (t, J = 7.1 Hz, 3H). ^{13}C NMR (100 MHz, $CDCl_3$) δ 164.9, 158.8, 154.8, 152.3, 141.9, 128.0, 126.6, 126.4, 105.2, 61.1, 18.6, 14.5. HRMS (ESI) m/z: $[M + Na]^+$ calcd for $C_{12}H_{12}N_2O_3Na$ 255.0740, found 255.0741.

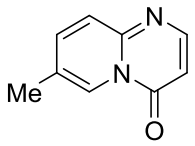

3.6

7-Methyl-4H-pyrido[1,2-a]pyrimidin-4-one, 3.6. Compound **3.6** was prepared from diethyl 2-(((5-methylpyridin-2-yl)amino)methylene)malonate **3.4** according to general procedure A. The product was isolated as a cream-colored powder in 32% yield. ^{1}H NMR (400 MHz, DMSO-d_6) δ 8.87 (d, J = 2.1 Hz), 8.30 (d, J = 6.6 Hz, 1H), 7.97 (dd, J = 9.0, 2.1 Hz, 1H), 7.70 (d, J = 9.0 Hz, 1H), 6.41 (d, J = 6.6 Hz, 1H), 2.42 (s, 3H); ^{13}C NMR **(**100 MHz, DMSO-d_6) δ 156.3, 151.7, 149.3, 141.6, 127.4, 124.8, 123.7, 103.3, 17.7. HRMS (ESI/TOF-Q) m/z: $[M+H]^+$ calcd for $C_9H_9N_2O$ 161.0709, found 161.0714.

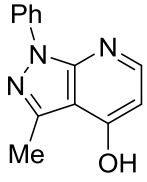

3.8

3-Methyl-1-phenyl-1H-pyrazolo[3,4-b]pyridin-4-ol, 3.8. Compound **3.8** was prepared from diethyl 2-(((3-methyl-1-phenyl-1H-pyrazol-5-yl)amino)methylene)malonate **3.7** according to general procedure A. The product was isolated as a beige powder in 88–91% yield. ^{1}H NMR (400 MHz, DMSO-d_6) δ 8.28–8.19 (m, 3H), 7.61–7.45 (m, 2H), 7.31–7.22 (m, 1H), 6.60 (d, J = 5.5 Hz, 1H), 2.63 (s, 3H); ^{13}C NMR (100 MHz, DMSO -d_6) δ 161.4, 152.6, 150.2, 142.2, 139.4, 128.9, 125.1, 120.0, 107.6, 103.6, 14.3. HRMS (ESI/TOF-Q) m/z: $[M+H]^+$ calcd for $C_{13}H_{12}N_3O$ 226.0975, found 226.0979.

3.5.3 Experimental Section for 3.3

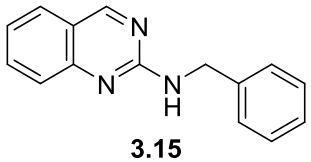

3.15

***N*-Benzylquinazolin-2-amine, 3.15.**[42, 52] The title compound **3.15** was prepared according to general procedure B as the TFA salt in 97% yield. ^{1}H NMR (400 MHz, DMSO-d_6) δ 9.27 (br s, 1H), 7.92 (br s, 1H), 7.80 (br s, 1H), 7.56 (d, J = 8.5 Hz, 1H), 7.37–7.27 (m, 5H), 7.22 (m, 1H), 4.67 (br s, 2H). MS (ESI$^+$) m/z: 236.0 $(M + H)^+$.

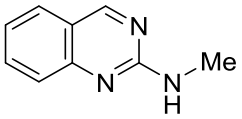

3.16

***N*-Methylquinazolin-2-amine, 3.16.** The title compound **3.16** was prepared according to general procedure B as the TFA salt in 73% yield. ^{1}H NMR (500 MHz, DMSO-d_6) δ 9.34 (s, 1H), 7.99 (dd, J = 7.9 Hz, 1H), 7.89 (t, J = 7.8 Hz, 1H), 7.70 (m, 1H), 7.44 (t, J = 7.5 Hz, 1H), 3.03 (s, 3H). MS (ESI$^+$) m/z: 160.0 $(M + H)^+$.

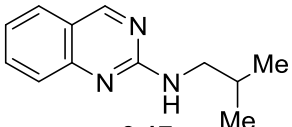

3.17

***N*-Isobutylquinazolin-2-amine, 3.17.** The title compound **3.17** was prepared according to general procedure B as the TFA salt in 92% yield. ^{1}H NMR (400 MHz, DMSO-d_6) δ 9.33 (br s, 1H), 7.93 (m, 2H), 7.67 (m, 1H), 7.43 (m, 1H), 3.29 (m, 2H), 1.97 (m, 1H), 0.95 (d, J = 6.7 Hz, 6H). MS (ESI$^+$) m/z: 202.0 $(M + H)^+$.

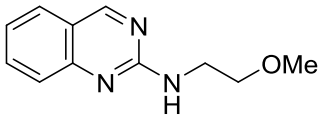

3.18

***N*-(2-Methoxyethyl)quinazolin-2-amine, 3.18.** The title compound **3.18** was prepared according to general procedure B as the TFA salt in 92% yield. ^{1}H NMR (400 MHz, DMSO-d_6) δ 9.32 (br s, 1H), 7.92 (m, 2H), 7.64 (m, 1H), 7.43 (m, 1H), 3.65 (m, 2H), 3.57 (m, 2H), 3.29 (s, 3H). MS (ESI$^+$) m/z: 204.0 $(M + H)^+$.

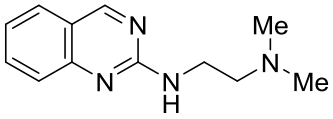

3.19

***N*^{1},*N*^{1}-Dimethyl-*N*^{2}-(quinazolin-2-yl)ethane-1,2-diamine, 3.19.** The title compound **3.19** was prepared according to general procedure B as the TFA salt in 38% yield. ^{1}H NMR (400 MHz, DMSO-d_6) δ 9.70 (br s, 1H), 7.83 (m, 2H), 7.55 (d, J = 8.4 Hz, 1H), 7.33 (m, 1H), 3.76 (m, 2H), 3.36 (t, J = 5.9 Hz, 2H), 2.88 (s, 6H). MS (ESI$^+$) m/z: 217.0 $(M + H)^+$.

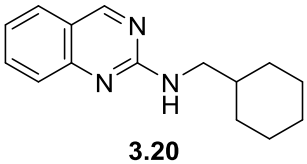

3.20

***N*-(Cyclohexylmethyl)quinazolin-2-amine, 3.20.**[52] The title compound **3.20** was prepared according to general procedure B as the TFA salt in 90% yield. ^{1}H NMR (500 MHz, DMSO-d_6) δ 9.39 (br s, 1H), 7.96–7.86 (m. 2H), 7.67 (m, 1H), 7.42 (m, 1H), 3.35 (m, 2H), 1.79–1.60 (complex, 6H), 1.24–1.10 (complex, 3H), 0.98 (m, 2H). MS (ESI$^+$) m/z: 242.0 $(M + H)^+$.

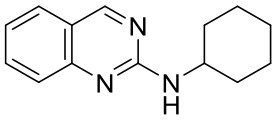

3.21

***N*-Cyclohexylquinazolin-2-amine, 3.21.**[52] The title compound **3.21** was prepared according to general procedure B as the TFA salt in 82% yield. ^{1}H NMR (500 MHz, DMSO-d_6) δ 9.36 (br s, 1H), 8.00 (d, J = 7.9 Hz, 1H), 7.91 (m, 1H), 7.68 (m, 1H), 7.47 (t, J = 7.5 Hz, 1H), 3.84 (m, 1H), 1.94 (m, 2H), 1.74 (m, 2H), 1.62 (m, 1H), 1.40–1.20 (complex, 4H), 1.16 (m, 1H). MS (ESI$^+$) m/z: 228.0 $(M + H)^+$.

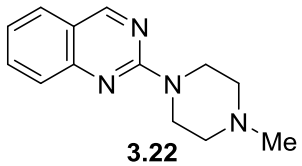

3.22

2-(4-Methylpiperazin-1-yl)quinazoline, 3.22.[53] The title compound **3.22** was prepared according to general procedure B as the TFA salt in 71% yield. ^{1}H NMR (400 MHz, DMSO-d_6) δ 9.31 (s, 1H), 7.92 (dd, J = 8.1, 1.4 Hz, 1H), 7.80 (ddd, J = 8.5, 6.9, 1.5 Hz, 1H), 7.58 (d, J = 8.5 Hz, 1H), 7.36 (m, 1H), 4.89 (m, 2H), 3.55 (m, 2H), 3.35 (m, 2H), 3.10 (m, 2H), 2.85 (s, 3H). MS (ESI$^+$) m/z: 229.0 $(M + H)^+$.

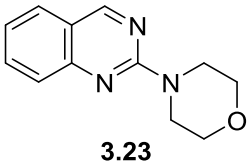

3.23

4-(Quinazolin-2-yl)morpholine, 3.23.[53] The title compound **3.23** was prepared according to general procedure B as the TFA salt in 79% yield. ^{1}H NMR (500 MHz, DMSO-d_6) δ 9.00 (s, 1H), 7.88 (m, 1H), 7.77 (m, 1H), 7.55 (m, 1H), 7.32 (m, 1H), 3.83 (m, 4H), 3.69 (m, 4H). MS (ESI$^+$) m/z: 216.0 $(M + H)^+$.

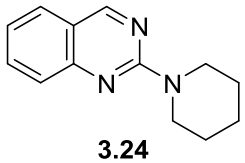

3.24

2-(Piperidin-1-yl)quinazoline, 3.24.[42] The title compound **3.24** was prepared according to general procedure B as the TFA salt in 64% yield. ^{1}H NMR (400 MHz, DMSO-d_6) δ 9.33 (br s, 1H), 7.96 (dd, J = 8.0, 1.4 Hz, 1H), 7.86 (ddd, J = 8.5, 7.1, 1.5 Hz, 1H), 7.65 (dd, J = 8.5, 0.9 Hz, 1H), 7.42 (ddd, J = 8.0, 7.0, 1.0 Hz, 1H), 3.89 (m, 4H), 1.64 (complex, 6H). MS (ESI$^+$) m/z: 214.0 $(M + H)^+$.

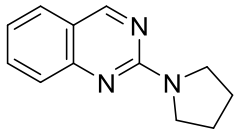

3.25

2-(Pyrrolidin-1-yl)quinazoline, 3.25.[53] The title compound **3.25** was prepared according to general procedure B as the TFA salt in 73% yield. ^{1}H NMR (400 MHz, DMSO-d_6) δ 9.45 (s, 1H), 8.06 (dd, J = 8.0, 1.3 Hz, 1H), 7.95 (m, 1H), 7.77 (d, J = 8.4 Hz, 1H), 7.51 (t, J = 7.5 Hz, 1H), 3.57 (m, 2H), 2.00 (m, 6H). MS (ESI$^+$) m/z: 200.0 $(M + H)^+$.

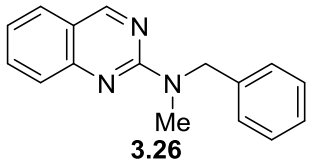

3.26

***N*-Benzyl-*N*-methylquinazolin-2-amine, 3.26.** The title compound **3.26** was prepared according to general procedure B as the TFA salt in 68% yield. ^{1}H NMR (500 MHz, DMSO-d_6) δ 9.37 (s, 1H), 7.98 (d, J = 8.0 Hz, 1H), 7.87 (t, J = 7.9 Hz, 1H), 7.70 (m, 1H), 7.42 (m, 1H), 7.34–7.25 (m, 5H), 5.05 (s, 2H), 3.23 (s, 3H). MS (ESI$^+$) m/z: 250.0 $(M + H)^+$.

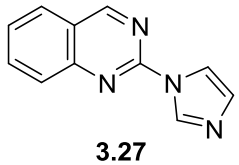

3.27

2-(1*H*-Imidazol-1-yl)quinazoline, 3.27. The title compound **3.27** was prepared according to general procedure B as the TFA salt in 50% yield. ^{1}H NMR (400 MHz, DMSO-d_6) δ 9.83 (s, 1H), 9.83 (s, 1H), 8.39 (m, 1H), 8.31 (dd, J = 8.3, 1.3 Hz, 1H), 8.15 (ddd, J = 8.4, 6.8, 1.5 Hz, 1H), 8.07 (m, 1H), 7.84 (ddd, J = 8.0, 6.0, 1.1 Hz, 1H), 7.65 (s, 1H). MS (ESI$^+$) m/z: 197.0 (M + H)$^+$.

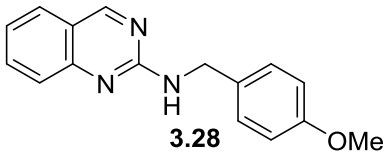

3.28

***N*-(4-Methoxybenzyl)quinazolin-2-amine, 3.28.** The title compound **3.28** was prepared according to general procedure B as the TFA salt in 60% yield. ^{1}H NMR (400 MHz, DMSO-d_6) δ 9.24 (br s, 1H), 7.83 (m, 2H), 7.56 (d, J = 8.4 Hz, 1H), 7.33 (m, 3H), 6.89 (m, 2H), 4.61 (m, 2H), 3.72 (s, 3H). MS (ESI$^+$) m/z: 266.0 (M + H)$^+$.

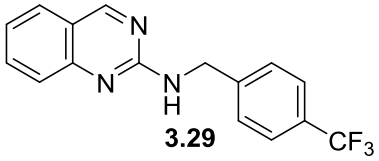

3.29

***N*-(4-(Trifluoromethyl)benzyl)quinazolin-2-amine, 3.29.**[52] The title compound **3.29** according was prepared to general procedure B as the TFA salt in 63% yield. ^{1}H NMR (400 MHz, DMSO-d_6) δ 9.24 (br s, 1H), 7.88 (m, 1H), 7 .76 (m, 1H), 7.68 (d, J = 8.1 Hz, 1H), 7.60 (d, J = 8.1 Hz, 1H), 7.51 (m, 1H), 7.33 (m, 1H), 4.75 (br s, 2H). MS (ESI$^+$) m/z: 304.0 (M + H)$^+$.

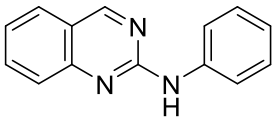

3.30

***N*-Phenylquinazolin-2-amine, 3.30.**[42] The title compound **3.30** was prepared according to general procedure B as the TFA salt in 39% yield. ^{1}H NMR (400 MHz, DMSO-d_6) δ 9.87 (s, 1H), 9.31 (s, 1H), 7.98 (m, 2H), 7.92 (dd, J = 8.1, 1.3 Hz, 1H), 7.81 (m, 1H), 7.66 (d, J = 8.5 Hz, 1H), 7.39 (t, J = 7.5 Hz, 1H), 7.33 (m, 2H), 6.99 (t, J = 7.5, 1H). MS (ESI$^+$) m/z: 222.1 (M + H)$^+$.

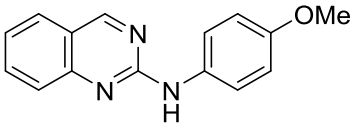

3.31

***N*-(4-Methoxyphenyl)quinazolin-2-amine, 3.31.** The title compound **3.31** was prepared according to general procedure B as the TFA salt in 63% yield. ^{1}H NMR (400 MHz, DMSO-d_6) δ 9.88 (br s, 1H), 9.29 (s, 1H), 7.91 (dd, J = 8.0, 1.4 Hz, 1H), 7.80 (m, 3H), 7.62 (m, 1H), 7.37 (ddd, J = 8.0, 6.9, 1.1 Hz, 1H), 6.94 (m, 2H), 3.75 (s, 3H). MS (ESI$^+$) m/z: 252.0 (M + H)$^+$.

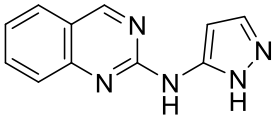

3.32

***N*-(1*H*-Pyrazol-5-yl)quinazolin-2-amine, 3.32.** The title compound **3.32** was prepared according to general procedure B as the TFA salt in 27% yield. ^{1}H NMR (500 MHz, DMSO-d_6) δ 9.54 (s, 1H), 8.49 (d, J = 2.7 Hz, 1H), 8.11 (dd, J = 8.1, 1.4 Hz, 1H), 7.97 (ddd, J = 8.5, 6.9, 1.5 Hz, 1H), 7.87 (d, J = 8.4 Hz, 1H), 7.61 (ddd, J = 8.1, 6.8, 1.1 Hz, 1H), 5.96 (d, J = 2.8 Hz, 1H). MS (ESI$^+$) m/z: 212.0 (M + H)$^+$.

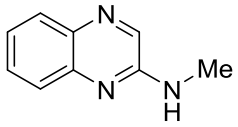

3.33

***N*-Methylquinoxalin-2-amine, 3.33.** The title compound **3.33** was prepared according to general procedure B as the TFA salt in 59% yield. ^{1}H NMR (400 MHz, DMSO-d_6) δ 8.45 (s, 1H), 7.82 (m, 1H), 7.62 (m, 2H), 7.41 (m, 3H), 7.36 (m, 2H), 7.29 (m, 1H), 4.65 (s, 2H). MS (ESI$^+$) m/z: 159.9 $(M + H)^+$.

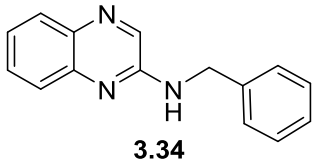

3.34

***N*-Benzylquinoxalin-2-amine, 3.34.** The title compound **3.34** was prepared according to general procedure B as the TFA salt in 42% yield. ^{1}H NMR (500 MHz, DMSO-d_6) δ 8.39 (s, 3H), 7.81 (dd, J = 8.2, 1.3 Hz, 1H), 7.63 (m, 2H), 7.39 (ddd, J = 8.3, 6.9, 1.6 Hz, 1H), 2.98 (s, 3H). MS (ESI$^+$) m/z: 236.0 $(M + H)^+$.

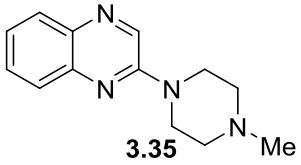

3.35

2-(4-Methylpiperazin-1-yl)quinoxaline, 3.35. The title compound **3.35** was prepared according to general procedure B as the TFA salt in 60% yield. ^{1}H NMR (400 MHz, DMSO-d_6) δ 8.83 (s, 1H), 7.87 (m, 1H), 7.65 (m, 2H), 7.48 (m, 1H), 4.66 (m, 2H), 3.54 (m, 2H), 3.33 (m, 2H), 3.15 (m, 2H), 2.84 (s, 3H). MS (ESI$^+$) m/z: 229.0 $(M + H)^+$.

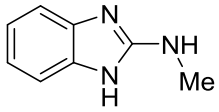

3.36

***N*-Methyl-1*H*-benzo[d]imidazol-2-amine, 3.36.** The title compound **3.36** was prepared according to general procedure B as the TFA salt in 73% yield. ^{1}H NMR (500 MHz, DMSO-d_6) δ 7.35 (m, 2H), 7.23 (m, 2H), 2.97 (s, 3H). MS (ESI$^+$) m/z: 148.0 $(M + H)^+$.

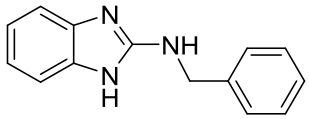

3.37

***N*-Benzyl-1*H*-benzo[d]imidazol-2-amine, 3.37.** The title compound **3.37** was prepared according to general procedure B as the TFA salt in 78% yield. ^{1}H NMR (400 MHz, DMSO-d_6) δ 7.38 (m, 6H), 7.23 (m, 3H), 4.59 (s, 1H). MS (ESI$^+$) m/z: 224.0 $(M + H)^+$.

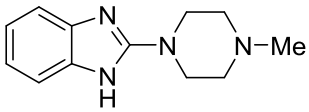

3.38

2-(4-Methylpiperazin-1-yl)-1*H*-benzo[d]imidazole, 3.38. The title compound **3.38** was prepared according to general procedure B as the TFA salt in 65% yield. ^{1}H NMR (400 MHz, DMSO-d_6) δ 7.44 (m, 2H), 7.26 (m, 2H), 3.87–3.44 (complex, 8H), 2.85 (m, 3H). MS (ESI$^+$) m/z: 217.0 $(M + H)^+$.

3.5.4 Experimental Section for 3.4

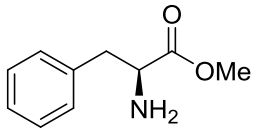

3.39

Methyl *L*-Phenylalaninate, 3.39.[54-55] Prepared according to general procedure C using methyl (*tert*-butylcarbonyl)-*L*-phenylalaninate, (55.8 mg, 0.201 mmol) to afford **3.39** as an oil (34.8 mg, >95% yield). ^{1}H NMR (500 MHz, 9:1 v/v DMSO-d_6:D_2O) δ 7.33–7.25 (m, 2H), 7.25–7.20 (m, 1H), 7.20–7.13 (m, 2H), 3.62–3.55 (m, 4H), 2.85 (qd, J = 13.4, 6.7 Hz, 2H); ^{13}C NMR (101 MHz, DMSO-d_6:D_2O) δ 175.7, 138.0, 129.6, 128.7, 126.9, 55.9, 51.9, 41.0. MS (ESI$^+$) m/z: 180.2 $(M + H)^+$.

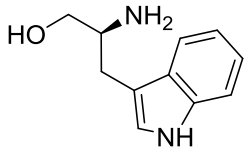

3.40

(*S*)-2-Amino-3-(1*H*-indol-3-yl)propanol, 3.40. Prepared according to the general procedure C using *tert*-butyl (*S*)-(1-hydroxy-3-(1*H*-indol-3-yl)propan-2-yl)carbamate (0.2 M, 800 µL, 0.16 mmol) to afford **3.40** (30.6 mg, >95% yield). ^{1}H NMR (400 MHz, 9:1 v/v DMSO-d_6:D_2O) δ 7.56 (d, J = 7.8 Hz, 1H), 7.37 (d, J = 8.1 Hz, 1H), 7.15 (s, 1H), 7.09 (t, J = 7.5 Hz, 1H), 6.99 (t, J = 7.4 Hz, 1H), 3.38 (dd, J = 10.6, 4.7 Hz, 1H), 3.26 (dd, J = 10.6, 6.7 Hz, 1H), 2.98 (td, J = 6.7, 4.7 Hz, 1H), 2.81 (dd, J = 14.1, 6.3 Hz, 1H), 2.63 (dd, J = 14.2, 7.0 Hz, 1H); ^{13}C NMR (101 MHz, 9:1 v/v DMSOd_6:D_2O) δ 136.5, 127.9, 123.7, 121.4, 118.9, 118.8, 111.74, 111.73, 65.7, 53.6, 29.4. MS (ESI$^+$) m/z: 191.2 $(M + H)^+$.

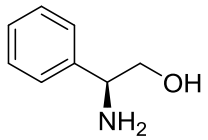

3.41

(*S*)-2-Amino-2-phenylethanol, 3.41.[56] Prepared according to the general procedure C using *tert*-butyl (*S*)-(2-hydroxy-1-phenylethyl)carbamate (0.2 M, 800 μL, 0.16 mmol) to afford **3.41** (20.5 mg, 93% yield). ^{1}H NMR (400 MHz, 9:1 v/v DMSO-d_6:D_2O) δ 7.39–7.19 (m, 5H), 3.86 (dd, J = 7.9, 4.7 Hz, 1H), 3.47 (dd, J = 10.5, 4.8 Hz, 1H), 3.33 (dd, J = 10.4, 8.0 Hz, 1H); ^{13}C NMR (101 MHz, 9:1 v/v DMSO-d_6:D_2O) δ 143.9, 128.5, 127.3, 127.2, 67.9, 57.4. MS (ESI+) m/z: 138.2 $(M + H)^+$.

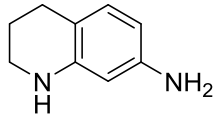

3.42

1,2,3,4-Tetrahydroquinolin-7-amine, 3.42. Prepared according to the general procedure C using *tert*-butyl (1,2,3,4-tetrahydroquinolin-7-yl)carbamate to afford **3.42** (29.2 mg, >95% yield). ^{1}H NMR (400 MHz, 9:1 v/v DMSO-d_6:D_2O) δ 6.47 (d, J = 7.8 Hz, 1H), 5.74 (dd, J = 7.9, 2.3 Hz, 1H), 5.69 (d, J = 2.2 Hz, 1H), 3.10–3.01 (m, 2H), 2.46 (t, J = 6.3 Hz, 2H), 1.69 (dd, J = 6.6, 4.8 Hz, 2H). ^{13}C NMR (101 MHz, 9:1 v/v DMSO-d_6:D_2O) δ 147.0, 146.0, 129.7, 109.7, 103.9, 99.9, 41.4, 26.5, 22.8. MS (ESI^+) m/z: 149.2 $(M + H)^+$.

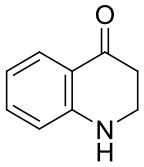

3.43

2,3-Dihydroquinolin-4(1*H*)-one, 3.43. Prepared according to the general procedure C using *tert*-butyl 4-oxo-3,4-dihydroquinoline-1(2*H*)-carboxylate to afford **3.43** (27.9 mg, >95% yield). ^{1}H NMR (400 MHz, 9:1 v/v DMSO-d_6:D_2O) δ 7.59 (dd, J = 8.0, 1.7 Hz, 1H), 7.29 (ddd, J = 8.5, 7.0, 1.7 Hz, 1H), 6.77 (dd, J = 8.4, 1.0 Hz, 1H), 6.62 (ddd, J = 8.0, 7.0, 1.1 Hz, 1H), 3.42 (dd, J = 7.8, 6.6 Hz, 2H), 2.59–2.48 (m, 2H); ^{13}C NMR (101 MHz, 9:1 v/v DMSO-d_6:D_2O) δ 194.1, 153.4, 135.5, 127.1, 118.2, 116.7, 116.5, 41.2, 37.8. MS (ESI$^+$) m/z: 148.1 $(M + H)^+$.

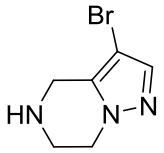

3.44

3-Bromo-4,5,6,7-tetrahydropyrazolo[1,5-*a*]pyrazine, 3.44. Prepared according to the general procedure C using *tert*-butyl 3-bromo-6,7-dihydropyrazolo[1,5-*a*]pyrazine-5(4*H*)-carboxylate to afford **3.44** (38.1 mg, 94% yield). ^{1}H NMR (400 MHz, 9:1 v/v DMSO-d_6:D_2O) δ 7.50 (s, 1H), 3.97 (t, J = 5.6 Hz, 2H), 3.79 (s, 2H), 3.09 (t, J = 5.5 Hz, 2H); ^{13}C NMR (101 MHz, 9:1 v/v DMSO-d_6:D_2O) δ 138.1, 136.7, 88.1, 48.1, 42.8, 41.5. MS (ESI$^+$) m/z: 204.0 $(M + H)^+$.

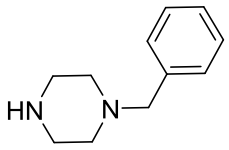

3.45

1-Benzylpiperazine, 3.35.[57-58] Prepared according to the general procedure C using *tert*-butyl 4-benzylpiperazine-1-carboxylate to afford **3.35** (33.5 mg, >95% yield). ^{1}H NMR (400 MHz, 9:1 v/v DMSO-d_6:D_2O) δ 7.41–7.21 (m, 5H), 3.42 (s, 2H), 2.75–2.65 (m, 4H), 2.47–2.14 (m, 4H); ^{13}C NMR (101 MHz, 9:1 v/v DMSO-d_6:D_2O) δ 138.3, 129.5, 128.6, 127.4, 63.2, 53.9, 45.4. MS (ESI+) m/z: 177.2 $(M + H)^+$.

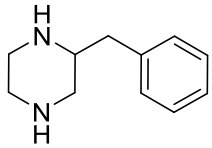

3.46

2-Benzylpiperazine, 3.46. Prepared according to the general procedure C using *tert*-butyl 3-benzylpiperazine-1-carboxylate (0.2 M, 800 μL, 0.16 mmol) to afford **3.46** (28.2 mg, >95% yield). ^{1}H NMR (400 MHz, 9:1 v/v DMSO-d_6:D_2O) δ 7.38–7.25 (m, 2H), 7.25–7.13 (m, 3H), 2.88–2.59 (m, 4H), 2.59–2.34 (m, 4H), 2.30–2.19 (m, 1H); ^{13}C NMR (101 MHz, 9:1 v/v DMSO-d_6:D_2O) δ 139.2, 129.6, 128.8, 126.5, 56.9, 51.0, 46.2, 45.6, 40.5. MS (ESI$^+$) m/z: 177.2 $(M + H)^+$.

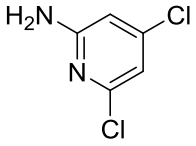

3.47

4,6-Dichloropyridin-2-amine, 3.47. Prepared according to the general procedure C using *tert*-butyl (4,6-dichloropyridin-2-yl)carbamate to afford **3.47** (30.8 mg, >95% yield). ^{1}H NMR (400 MHz, 9:1 v/v DMSO-d_6:D_2O) δ 6.66 (d, J = 1.5 Hz, 1H), 6.49 (d, J = 1.5 Hz, 1H); ^{13}C NMR (101 MHz, 9:1 v/v DMSO-d_6:D_2O) δ 160.7, 149.8, 145.1, 110.6, 106.0. MS (ESI$^+$) m/z: 163.0 $(M + H)^+$.

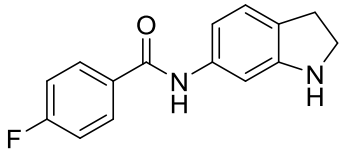

3.48

4-Fluoro-*N*-(indolin-6-yl)benzamide, 3.48. Prepared according to the general procedure C using *tert*-butyl 6-(4-fluorobenzamido)indoline-1-carboxylate to afford **3.48** (48.6 mg, >95% yield). ^{1}H NMR (400 MHz, DMSO-d_6) δ 8.02-7.95 (m, 2H), 7.37–7.30 (m, 2H), 7.05–6.97 (m,

2H), 6.87 (dd, J = 7.9, 1.9 Hz, 1H), 3.41 (t, J = 8.4 Hz, 2H), 2.88 (t, J = 8.4 Hz, 2H); ^{13}C NMR (101 MHz, DMSO-d_6) δ 164.8, 164.3 (d, J = 251.5 Hz), 153.2, 138.3, 130.7 (d, J = 9.1 Hz), 125.2, 124.4, 115.8 (d, J = 21.8 Hz), 110.1, 102.1, 47.2, 29.2. MS (ESI$^+$) m/z: 257.1 $(M + H)^+$.

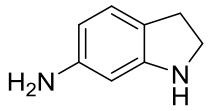

3.49

Indolin-6-amine, 3.49. Prepared according to the general procedure C using *tert*-butyl 6-aminoindoline-1-carboxylate to afford **3.49** (24.8 mg, 93% yield). After the dry-down, a ~15% impurity that is presumed to be the corresponding indole, 1*H*-indol-6-amine, was observed by ^{1}H NMR. ^{1}H NMR (400 MHz, DMSO-d_6) δ 6.69 (d, J = 7.8 Hz, 1H), 5.90–5.81 (m, 2H), 3.31 (t, J = 8.2 Hz, 2H), 2.73 (d, J = 8.3 Hz, 2H); ^{13}C NMR (101 MHz, DMSO-d_6) δ 153.6, 148.0, 124.7, 117.4, 104.2, 96.7, 47.2, 29.0. MS (ESI$^+$) m/z: 135.2 $(M + H)^+$.

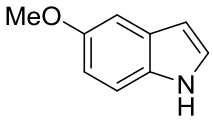

3.50

5-Methoxy-1*H*-indole, 3.50.[59-60] Prepared according to the general procedure C using *tert*-butyl 5-methoxy-1*H*-indole-1-carboxylate to afford **3.50** (29.4 mg, >95% yield). ^{1}H NMR (400 MHz, 9:1 v/v DMSO-d_6:D_2O) δ 7.35–7.25 (m, 2H), 7.05 (d, J = 2.4 Hz, 1H), 6.74 (dd, J = 8.8, 2.5 Hz, 1H), 6.36 (dd, J = 3.1, 1.0 Hz, 1H), 3.75 (s, 3H); ^{13}C NMR (101 MHz, 9:1 v/v DMSO-d_6:D_2O) δ 153.7, 131.3, 128.4, 126.0, 112.4, 111.6, 102.2, 101.4, 55.8. MS (ESI$^+$) m/z: 148.1 $(M + H)^+$.

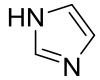

3.51

Imidazole, 3.51.[61] Prepared according to the general procedure C using *tert*-butyl 1*H*-imidazole-1-carboxylate to afford **3.51** (13.4 mg, >95% yield). ^{1}H NMR (400 MHz, 9:1 v/v DMSO-d_6:D_2O) δ 7.67 (s, 1H), 7.04 (s, 2H); ^{13}C NMR (101 MHz, 9:1 v/v DMSO-d_6:D_2O) δ 135.5, 121.7.

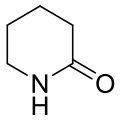

3.52

Piperidin-2-one, 3.52.[62-63] Prepared according to the general procedure C using *tert*-butyl 2-oxopiperidine-1-carboxylate (0.2 M, 800 μL, 0.16 mmol) to afford **3.52** (15.1 mg, >95% yield). ^{1}H NMR (400 MHz, 9:1v/v DMSO-d_6:D_2O) δ 3.13 (t, J = 5.6 Hz, 2H), 2.14 (t, J = 6.3 Hz, 2H), 1.73–1.58 (m, 4H); ^{13}C NMR (101 MHz, 9:1 v/v DMSO-d_6:D_2O) δ 171.6, 41.6, 31.6, 22.2, 20.9. MS (ESI$^+$) m/z: 100.2 $(M + H)^+$.

3.6 References

1. McQuade, D. T.; Seeberger, P. H. Applying Flow Chemistry: Methods, Materials, and Multistep Synthesis. *J. Org. Chem.* **2013**, *78*, 6384-6389.

2. Hessel, V.; Kralisch, D.; Kockmann, N.; Noël, T.; Wang, Q. Novel Process Windows for Enabling, Accelerating, and Uplifting Flow Chemistry. *ChemSusChem* **2013**, *6*, 746-789.

3. Wegner, J.; Ceylan, S.; Kirschning, A. Flow Chemistry – A Key Enabling Technology for (Multistep) Organic Synthesis. *Adv. Synth. Catal.* **2012**, *354*, 17-57.

4. Mason, B. P.; Price, K. E.; Steinbacher, J. L.; Bogdan, A. R.; McQuade, D. T. Greener Approaches to Organic Synthesis Using Microreactor Technology. *Chem. Rev.* **2007**, *107*, 2300-2318.

5. Newman, S. G.; Jensen, K. F. The Role of Flow in Green Chemistry and Engineering. *Green Chem.* **2013**, *15*, 1456-1472.

6. Malet-Sanz, L.; Susanne, F. Continuous Flow Synthesis. A Pharma Perspective. *J. Med. Chem.* **2012**, *55*, 4062-4098.

7. Razzaq, T.; Kappe, C. O. Continuous Flow Organic Synthesis under High-Temperature/Pressure Conditions. *Chem. Asian J.* **2010**, *5*, 1274-1289.

8. Plutschack, M. B.; Pieber, B.; Gilmore, K.; Seeberger, P. H. The Hitchhiker's Guide to Flow Chemistry. *Chem. Rev.* **2017**, *117*, 11796-11893.

9. Hartman, R. L.; McMullen, J. P.; Jensen, K. F. Deciding Whether To Go with the Flow: Evaluating the Merits of Flow Reactors for Synthesis. *Angew. Chem. Int. Ed.* **2011**, *50*, 7502-7519.

10. Jensen, K. F. Flow Chemistry—Microreaction Technology Comes of Age. *AIChE J.* **2017**, *63*, 858-869.

11. Valera, F. E.; Quaranta, M.; Moran, A.; Blacker, J.; Armstrong, A.; Cabral, J. T.; Blackmond, D. G. The Flow's the Thing…Or Is It? Assessing the Merits of Homogeneous Reactions in Flask and Flow. *Angew. Chem. Int. Ed.* **2010**, *49*, 2478-2485.

12. Gawande, M. B.; Shelke, S. N.; Zboril, R.; Varma, R. S. Microwave-Assisted Chemistry: Synthetic Applications for Rapid Assembly of Nanomaterials and Organics. *Acc. Chem. Res.* **2014**, *47*, 1338-1348.

13. Glasnov, T. N.; Kappe, C. O. The Microwave-to-Flow Paradigm: Translating High-Temperature Batch Microwave Chemistry to Scalable Continuous-Flow Processes. *Chem. Eur. J.* **2011**, *17*, 11956-11968.

14. Damm, M.; Glasnov, T. N.; Kappe, C. O. Translating High-Temperature Microwave Chemistry to Scalable Continuous Flow Processes. *Org. Process Res. Dev.* **2010**, *14*, 215-224.

15. John Morris. http://www.johnmorris.com.au/X-Cube.aspx?pd=3694 (accessed February 02, 2018).

16. Uniqsis. http://www.uniqsis.com/paProducts.aspx (accessed February 02, 2018).

17. Vapourtec. https://www.vapourtec.com/products/r-series-flow-chemistry-system-overview/ (accessed February 02, 2018).

18. Charaschanya, M.; Bogdan, A. R.; Wang, Y.; Djuric, S. W. Nucleophilic Aromatic Substitution of Heterocycles Using a High-Temperature and High-Pressure Flow Reactor. *Tetrahedron Lett.* **2016**, *57*, 1035-1039.

19. Bogdan, A. R.; Charaschanya, M.; Dombrowski, A. W.; Wang, Y.; Djuric, S. W. High-Temperature Boc Deprotection in Flow and Its Application in Multistep Reaction Sequences. *Org. Lett.* **2016**, *18*, 1732-1735.

20. Vitaku, E.; Smith, D. T.; Njardarson, J. T. Analysis of the Structural Diversity, Substitution Patterns, and Frequency of Nitrogen Heterocycles among U.S. FDA Approved Pharmaceuticals. *J. Med. Chem.* **2014**, *57*, 10257-10274.

21. Brown, D. G.; Boström, J. Analysis of Past and Present Synthetic Methodologies on Medicinal Chemistry: Where Have All the New Reactions Gone? *J. Med. Chem.* **2016**, *59*, 4443-4458.

22. Roughley, S. D.; Jordan, A. M. The Medicinal Chemist's Toolbox: An Analysis of Reactions Used in the Pursuit of Drug Candidates. *J. Med. Chem.* **2011**, *54*, 3451-3479.

23. Gould, R. G.; Jacobs, W. A. The Synthesis of Certain Substituted Quinolines and 5,6-Benzoquinolines. *J. Am. Chem. Soc.* **1939**, *61*, 2890-2895.

24. Smith, R. B.; Faki, H.; Leslie, R. Limitations of the Jacobs–Gould Reaction Using Microwave Irradiation. *Synth. Commun.* **2011**, *41*, 1492-1499.

25. Mane, U. R.; Li, H.; Huang, J.; Gupta, R. C.; Nadkarni, S. S.; Giridhar, R.; Naik, P. P.; Yadav, M. R. Pyrido[1,2-a]pyrimidin-4-ones as Antiplasmodial Falcipain-2 Inhibitors. *Bioorg. Med. Chem.* **2012**, *20*, 6296-6304.

26. Price, C. C.; Roberts, R. M. 4,7-Dichloroquinoline. *Org. Synth.* **1948**, *28*, 38-41.

27. Lengyel, L. C.; Sipos, G.; Sipőcz, T.; Vágó, T.; Dormán, G.; Gerencsér, J.; Makara, G.; Darvas, F. Synthesis of Condensed Heterocycles by the Gould–Jacobs Reaction in a Novel Three-Mode Pyrolysis Reactor. *Org. Process Res. Dev.* **2015**, *19*, 399-409.

28. Prager, R.; Singh, Y. The Chemistry of 5-Oxodihydroisoxazoles. IX. Annelated Pyrimidines by Flash Vacuum Pyrolysis. *Aust. J. Chem.* **1994**, *47*, 1263-1270.

29. Lengyel, L.; Nagy, T. Z.; Sipos, G.; Jones, R.; Dormán, G.; Ürge, L.; Darvas, F. Highly Efficient Thermal Cyclization Reactions of Alkylidene Esters in Continuous Flow to Give Aromatic/Heteroaromatic Derivatives. *Tetrahedron Lett.* **2012**, *53*, 738-743.

30. Tsoung, J.; Bogdan, A. R.; Kantor, S.; Wang, Y.; Charaschanya, M.; Djuric, S. W. Synthesis of Fused Pyrimidinone and Quinolone Derivatives in an Automated High-Temperature and High-Pressure Flow Reactor. *J. Org. Chem.* **2017**, *82*, 1073-1084.

31. Musiol, R. An Overview of Quinoline as a Privileged Scaffold in Cancer Drug Discovery. *Expert Opin. Drug Discov.* **2017**, *12*, 583-597.

32. Bisacchi, G. S. Origins of the Quinolone Class of Antibacterials: An Expanded "Discovery Story". *J. Med. Chem.* **2015**, *58*, 4874-4882.

33. Molnár, A.; Mucsi, Z.; Vlád, G.; Simon, K.; Holczbauer, T.; Podányi, B.; Faigl, F.; Hermecz, I. Ring Transformation of Unsaturated N-Bridgehead Fused Pyrimidin-4(3H)-ones: Role of Repulsive Electrostatic Nonbonded Interaction. *J. Org. Chem.* **2011**, *76*, 696-699.

34. Kendre, D. B.; Toche, R. B.; Jachak, M. N. Synthesis of Pyrazolo[3,4-b]pyridines and Attachment of Amino Acids and Carbohydrate as Linkers. *J. Heterocycl. Chem.* **2008**, *45*, 1281-1286.

35. Bernardino, A. M. R.; Ferreira, V. F.; Fontoura, G. A. T.; Frugulhetti, I. C. P. P.; Lee, M. Y.; Romeiro, G. A.; Souza, M. C. B.; Sa, P. M. Synthesis of 4-Anilino-1H-pyrazolo[3,4-b]pyridine Derivatives and their In Vitro Antiviral Activities. *J. Braz. Chem. Soc.* **1996**, *7*, 273-277.

36. Bogdan, A. R.; Sach, N. W. The Use of Copper Flow Reactor Technology for the Continuous Synthesis of 1,4-Disubstituted 1,2,3-Triazoles. *Adv. Synth. Catal.* **2009**, *351*, 849-854.

37. Caron, S.; Ghosh, A., Nucleophilic Aromatic Substitution. In *Practical Synthetic Organic Chemistry*, John Wiley & Sons, Inc.: 2011; pp 237-253.

38. Terrier, F., The SNAr Reactions: Mechanistic Aspects. In *Modern Nucleophilic Aromatic Substitution*, Wiley-VCH Verlag GmbH & Co. KGaA: 2013; pp 1-94.

39. Hartwig, J. F. Discovery and Understanding of Transition-Metal-Catalyzed Aromatic Substitution Reactions. *Synlett* **2006**, 1283-1294.

40. Torborg, C.; Beller, M. Recent Applications of Palladium-Catalyzed Coupling Reactions in the Pharmaceutical, Agrochemical, and Fine Chemical Industries. *Adv. Synth. Catal.* **2009**, *351*, 3027-3043.

41. Sun, C.-L.; Shi, Z.-J. Transition-Metal-Free Coupling Reactions. *Chem. Rev.* **2014**, *114*, 9219-9280.

42. Henriksen, S. T.; Sørensen, U. S. 2-Chloroquinazoline. Synthesis and Reactivity of a Versatile Heterocyclic Building Block. *Tetrahedron Lett.* **2006**, *47*, 8251-8254.

43. Hamper, B. C.; Tesfu, E. Direct Uncatalyzed Amination of 2-Chloropyridine Using a Flow Reactor. *Synlett* **2007**, *2007*, 2257-2261.

44. Lengyel, L.; Gyóllai, V.; Nagy, T.; Dormán, G.; Terleczky, P.; Háda, V.; Nógrádi, K.; Sebők, F.; Ürge, L.; Darvas, F. Stepwise Aromatic Nucleophilic Substitution in Continuous Flow. Synthesis of an Unsymmetrically Substituted 3,5-Diamino-Benzonitrile Library. *Mol. Diversity* **2011**, *15*, 631-638.

45. Weissman, S. A.; Anderson, N. G. Design of Experiments (DoE) and Process Optimization. A Review of Recent Publications. *Org. Process Res. Dev.* **2015**, *19*, 1605-1633.

46. Jessop, P. G. Searching for Green Solvents. *Green Chem.* **2011**, *13*, 1391-1398.

47. Wuts, P. G. M.; Greene, T. W., Protection for the Amino Group. In *Greene's Protective Groups in Organic Synthesis*, John Wiley & Sons, Inc.: 2006; pp 696-926.

48. Rawal, V. H.; Cava, M. P. Thermolytic Removal of t-Butyloxycarbonyl (BOC) Protecting Group on Indoles and Pyrroles. *Tetrahedron Lett.* **1985**, *26*, 6141-6142.

49. Thaqi, A.; McCluskey, A.; Scott, J. L. A Mild Boc Deprotection and the Importance of a Free Carboxylate. *Tetrahedron Lett.* **2008**, *49*, 6962-6964.

50. Choy, J.; Jaime-Figueroa, S.; Jiang, L.; Wagner, P. Novel Practical Deprotection of N-Boc Compounds Using Fluorinated Alcohols. *Synth. Commun.* **2008**, *38*, 3840-3853.

51. Siro, J. G.; Martin, J.; Garcia-Navio, J. L.; Remuinan, M. J.; Vaquero, J. J. Easy microwave-assisted deprotection of N-Boc derivatives. *Synlett* **1998**, 147-148.

52. Li, F.; Chen, L.; Kang, Q.; Cai, J.; Zhu, G. Regioselective N-Alkylation with Alcohols for the Preparation of 2-(N-Alkylamino)quinazolines and 2-(N-Alkylamino)pyrimidines. *New J. Chem.* **2013**, *37*, 624-631.

53. Huang, X.; Yang, H.; Fu, H.; Qiao, R.; Zhao, Y. Efficient Copper-Catalyzed Synthesis of 2-Amino-4(3H)-quinazolinone and 2-Aminoquinazoline Derivatives. *Synthesis* **2009**, *2009*, 2679-2688.

54. Gynther, M.; Laine, K.; Ropponen, J.; Leppänen, J.; Mannila, A.; Nevalainen, T.; Savolainen, J.; Järvinen, T.; Rautio, J. Large Neutral Amino Acid Transporter Enables Brain Drug Delivery via Prodrugs. *J. Med. Chem.* **2008**, *51*, 932-936.

55. Chang, Y.-H.; Chen, C.-Y.; Singh, G.; Chen, H.-Y.; Liu, G.-C.; Goan, Y.-G.; Aime, S.; Wang, Y.-M. Synthesis and Physicochemical Characterization of Carbon Backbone Modified [Gd(TTDA)(H2O)]2− Derivatives. *Inorg. Chem.* **2011**, *50*, 1275-1287.

56. Anakabe, E.; Vicario, Jose L.; Badía, D.; Carrillo, L.; Yoldi, V. Asymmetric Synthesis of Arylglycines and Their Use as Chiral Templates for the Stereocontrolled Synthesis of 7,8-Disubstituted 3-Aryl-1,2,3,4-tetrahydroisoquinolin-4-ols. *Eur. J. Org. Chem.* **2001**, *2001*, 4343-4352.

57. Tyagi, V.; Gupta, A. K. One-Pot, Two-Step Direct Conversion of Alkenes to Amines Through Tandem Ozonolysis and Ammonia-Borane in Water. *Synth. Commun.* **2014**, *44*, 493-499.

58. Zhang, C.; Tan, C.; Zu, X.; Zhai, X.; Liu, F.; Chu, B.; Ma, X.; Chen, Y.; Gong, P.; Jiang, Y. Exploration of (S)-3-Aminopyrrolidine as a Potentially Interesting Scaffold for Discovery of Novel Abl and PI3K Dual Inhibitors. *Eur. J. Med. Chem.* **2011**, *46*, 1404-1414.

59. Wu, J.; Talwar, D.; Johnston, S.; Yan, M.; Xiao, J. Acceptorless Dehydrogenation of Nitrogen Heterocycles with a Versatile Iridium Catalyst. *Angew. Chem. Int. Ed.* **2013**, *52*, 6983-6987.

60. Coowar, D.; Bouissac, J.; Hanbali, M.; Paschaki, M.; Mohier, E.; Luu, B. Effects of Indole Fatty Alcohols on the Differentiation of Neural Stem Cell Derived Neurospheres. *J. Med. Chem.* **2004**, *47*, 6270-6282.

61. Kohn, H.; Sawhney, K. N.; Bardel, P.; Robertson, D. W.; Leander, J. D. Synthesis and Anticonvulsant Activities of α-Heterocyclic α-Acetamido-N-benzylacetamide Derivatives. *J. Med. Chem.* **1993**, *36*, 3350-3360.

62. Jin, X.; Kataoka, K.; Yatabe, T.; Yamaguchi, K.; Mizuno, N. Supported Gold Nanoparticles for Efficient α-Oxygenation of Secondary and Tertiary Amines into Amides. *Angew. Chem. Int. Ed.* **2016**, *55*, 7212-7217.

63. Khusnutdinova, J. R.; Ben-David, Y.; Milstein, D. Oxidant-Free Conversion of Cyclic Amines to Lactams and H2 Using Water As the Oxygen Atom Source. *J. Am. Chem. Soc.* **2014**, *136*, 2998-3001.